BPS black hole counting in Calabi-Yau spaces

Pierre Descombes

Thèse pour obtenir le grade de docteur de Sorbonne Université

En Physique théorique

École doctorale 564 (EDPIF)

Unité de recherche 5789

Comptage d'états BPS sur les espaces de Calabi-Yau

Présentée par Pierre Descombes
le 26 Juin 2023

Sous la direction de Boris Pioline
et Olivier Schiffmann

Devant le jury composé de

Andrea BRINI, professeur associé Université de Sheffield	**Rapporteur**
Dominic JOYCE, professeur, Université d'Oxford	**Rapporteur**
Soheyla FEYZBAKHSH, Docteure, Imperial College of London	**Examinatrice**
Amir Kian KASHANI-POOR, Maître de conférences, Ecole normale supérieure de Paris	**Examinateur**
Emanuele MACRI, professeur, Université Paris-Saclay	**Examinateur**
Boris Pioline, Directeur de recherche, Sorbonne Université	**Co-directeur**
Olivier Schiffmann, Directeur de recherche, Université Paris-Saclay	**Co-directeur**

A Mamine,
Même si tu ne comprenais pas grand chose au comptage d'états BPS,
Tu connaissais le secret du chant des oiseaux,
Celui de la recette de la meilleur soupe du monde,
Et de l'amour de tes petits enfants.

Contents

Chapter 1

Résumé

Cette thèse se situe aux interfaces entre les mathématiques, en particulier la géométrie énumérative et algébrique, et la physique théorique, en particulier la théorie des cordes. Le contexte physique est le comptage des états BPS en théorie des champs supersymétriques $N = 2$, $D = 4$ (c'est à dire avec 2 supersymétries, et trois dimensions spatiales et une temporelle). Mathématiquement, cela s'exprime par la théorie de Donaldson-Thomas, qui donne le comptage virtuel de faisceaux sur des variétés de Calabi-Yau tridimensionnelles, ou de représentations de carquois avec potentiel.

Ce lien entre physique et mathématiques s'est tout d'abord incarné dans le phénomène de la symétrie miroir homologique. Ce phénomène suggère que les variétés de Calabi-Yau 3D apparaissent par paires $(X, \check{X})$, telles que les propriétés symplectiques de X soient reliées aux propriétés complexes de $\check{X}$, et vice versa. Physiquement, cela provient du fait que la théorie des champs supersymétrique $N = 2$, $D = 4$ obtenue en compactifiant la théorie des cordes de type IIA sur X est équivalente à celle obtenue en compactifiant la théorie de type IIB sur $\check{X}$, et vice versa. Nous serons en particulier intéressés par une formulation mathématique de cette symétrie, proposée par Kontsevich dans [Kon95], appelée la conjecture de symétrie miroir. On interprétera physiquement cette conjecture comme une équivalence entre la catégorie des A branes topologiques sur X (mathématiquement, la catégorie dérivée des faisceaux cohérents sur X), et celle des B branes topologiques sur $\check{X}$ (mathématiquement, la catégorie de Fukaya dérivée de Lagrangiens dans $\check{X}$); les A/B branes topologiques étant des conditions aux bords pour une version topologique de la théorie de type IIA/B.

Nous décrirons ensuite les états BPS des théories supersymétriques $N = 2$, $D = 4$ obtenues plus haut, c'est-à-dire les états préservant une des deux supersymétries. Notamment, grâce à la supersymétrie, le comptage de ces états est invariant par changement de couplage de la théorie. Ils sont décrits comme des branes stables: la donnée spécifiant le spectre des branes stables à l'intérieur de la catégorie des branes topologiques est formalisée mathématiquement par la notion de condition de stabilité de Bridgeland, introduite dans [Bri07]. On motivera physiquement cette définition, et présentera une partie des mathématiques luxuriantes sous-jacentes à l'étude de l'espace des conditions de stabilité sur les catégories dérivées. On présentera en particulier les techniques de constructions de conditions de stabilité, et l'étude des transitions géométriques dans l'espace des conditions de stabilité.

Nous présenterons ensuite le cas spécifique de la théorie de type IIA compactifiée sur une singu-

larité CY3. Nous présentons les résolutions crépantes de singularités, et leurs analogues noncommutatifs, les résolutions noncommutatives crépantes (NCCR), introduites dans [VdB04]. Dans le cas CY3, ces NCCR sont décrites par des carquois avec potentiel. Une région de l'espace des conditions de stabilité est alors décrite par les conditions de stabilité de King sur ces carquois avec potentiel. On présentera alors les exemples majeurs de constructions de NCCR sur lesquels nous avons travaillé, notamment les pavages de branes pour les singularités toriques, les carquois de Mckay pour les singularités d'orbifold, et les collections exceptionnelles pour les cônes sur les surfaces del Pezzo.

Nous introduirons enfin la théorie de Donaldson-Thomas numérique (respectivement cohomologique), qui donne un nombre d'Euler virtuel (respectivement un polynôme de Hodge virtuel) pour l'espace de modules des branes stables. Nous motiverons et expliquerons la construction du faisceau pervers de Donaldson-Thomas présentée dans [BBD$^+$15], dont le polynôme de Hodge donne les invariants DT cohomologiques. Nous présenterons ensuite la formule de wall crossing de Kontsevich-Soibelman, qui relie les séries génératrices d'invariants DT pour différentes conditions de stabilité. Nous expliquerons aussi comment extraire des séries génératrices DT les invariants BPS, qui sont supposément intégraux, et devraient physiquement donner le comptage des états BPS, la puissance de y dans le polynôme de Hodge donnant le double du spin de l'état BPS.

Finalement, nous esquisserons le lien établi par la théorie des cordes entre le comptage des états BPS et le problème de l'entropie des trous noirs en gravité quantique. Nous présenterons comment cette description des états BPS en tant que trous noirs à plusieurs centres apporte un éclairage nouveau sur le phénomène du wall crossing, et comment elle suggère une formule très puissante pour calculer les invariants DT, la formule des arbres de flots. Dans le cas des carquois avec potentiel, cette formule est complètement explicite mathématiquement, et a été prouvée dans [AB21]; les données initiales requises sont alors appelées les invariants BPS attracteurs que nous introduirons plus bas.

Une fois ces notions introduites et motivées, nous présenterons le résultat du travail de recherche de ce doctorat, qui s'articule autour de quatre articles:

Le premier, 'Hyperbolic localization of the Donaldson-Thomas sheaf' [Des22], est un article de mathématiques soumis au 'Journal of Algebraic Geometry'. Il traite du problème de localisation torique en théorie de Donaldson-Thomas. On considère un espace de module d'objets BPS X munis d'une action torique, et on essaie d'exprimer les invariants de Donaldson-Thomas de X en fonction de ceux des composantes fixées X^0_π par le tore. Une telle formule est bien connue depuis [GP97] pour les invariants DT numériques. Toutefois, dans le cas des invariants DT cohomologiques, le problème semblait plus épineux: une formule existait dans la littérature physique depuis [NO16], mais semblait difficile à relier au formalisme du faisceau pervers de Donaldson-Thomas de [BBD$^+$15], et les résultats de cette formule semblaient eux même dépendre de certains choix. J'ai alors prouvé une formule de localisation torique pour les invariants DT cohomologiques dans [Des22], qui peut s'exprimer comme une version virtuelle de la décomposition de Bialinicky-Birula, et qui coïncide avec la formule de [NO16] lorsque l'espace de modules est projectif. Cela permet d'exprimer les invariants DT cohologiques de la partie attractrice X^+ comme une somme des invariants DT cohomologiques des parties fixées X^0_π, avec un décalage cohomologique facilement calculable.

Le second article, 'Cohomological DT invariants from localization' [Des21], est un article de mathématiques publié au 'Journal of the London Mathematical Society'. Dans cet article, j'ai présenté une application concrète de la formule de localisation évoquée plus haut, dans le cadre des carquois à potentiel torique, qui donnent des résolutions noncommutatives crépantes des singularités

CY3 toriques. On étudie les séries génératrices d'invariants DT comptant des représentations encadrées de carquois toriques. Leur version numérique a été calculée par localisation dans [MR08], en se ramenant à une énumération de généralisations de partitions planes appelées partitions de pyramides. Notamment, dans le cas de $\mathbb{C}^3$, on retrouve la série de MacMahon, qui énumère les partitions planes. Les calculs de la version cohomologique de ces séries génératrices de localisation effectués dans la littérature physique ne coïncidaient alors pas avec les calculs mathématiques, comme remarqué dans [BBS13]. J'ai expliqué cette différence par le fait que le calcul par localisation ne donne que les invariants DT de la partie attractrice, et donc ne permet que de compter les représentations encadrées avec certaines contraintes de nilpotence. J'ai alors donné une formule explicite pour corriger le calcul par localisation afin d'obtenir les vraies séries génératrices, en incluant des contributions de D0 branes (ou faisceaux gratte-ciel) supportées en dehors de la partie attractrice, et de D2 branes (ou faisceaux supportés sur des courbes) qui résolvent des singularités étendues de type A. Cela donne une formule complètement algorithmique, qui permet de calculer ces séries génératrices uniquement à partir de la donnée du diagramme torique.

Le troisième article, 'On the existence of scaling multi-centered black holes', est un article de physique mathématiques coécrit avec Boris Pioline, publié aux 'Annales Henri Poincaré'. Nous avons établi dans cet article des contraintes sur l'appariement de Dirac imposées par l'existence de solutions conformes de trous noirs à plusieurs centres, dans une théorie de la supergravité $N = 2$, $D = 4$. Ces conditions généralisent les inégalités triangulaires trouvées dans [DM11a] nécessaires à l'existence de trous noirs à trois centres. Les trous noirs à plusieurs centres représentent les états BPS à fort couplage de la théorie, et les états BPS à faible couplage sont donnés par les représentations stables d'un carquois avec un potentiel générique. Nous avons montré des contraintes similaires pour l'existence de représentations attracteurs stables pour les carquois avec potentiel générique, utilisant des estimations de dimension d'espaces de modules. Cela donne un indice mathématique supplémentaire de la pertinence du lien entre description de carquois et description de trous noirs à plusieurs centres.

Le quatrième article, 'BPS Dendroscopy on Local $\mathbb{P}^2$', est un article de physique mathématiques coécrit avec Pierrick Bousseau, Bruno Le Floch et Boris Pioline. Nous avons étudié la formule d'arbres de flots dans le cas du plan projectif local. L'espace de module de Kähler est alors donné par le demi plan de Poincaré $\mathbb{H}$, modulo l'action du groupe modulaire $\Gamma_1(3)$, ce qui donne une sphère avec trois points marqués. La limite supérieure du plan de Poincaré correspond à la limite de grand volume, où les conditions de stabilité se rapprochent des conditions de Gieseker. Le second point, situé sur la ligne réelle, est le point de conifold, ou une brane devient de masse nulle. Le dernier point est le point d'orbifold, où la géométrie de $\mathbb{P}^2$ local dégénère en $\mathbb{C}^3/\mathbb{Z}_3$, et autour duquel les conditions de stabilité sont décrites par la stabilité de King du carquois de McKay. Nous avons étudié la formule d'arbres de flots sur $\mathbb{H}$: les données initiales correspondent à des branches émanant des points de conifold. Nous avons tout d'abord étudié le comportement des arbres de flots autour des points d'orbifold, et montré que les données initiales dans le voisinage du point d'orbifold correspond aux nœuds du carquois de McKay. Nous avons ensuite étudié la structure globale des arbres qui vont dans la région de grands volume, montré qu'ils sont en nombre fini, et ont des données initiales très particulières.

Chapter 2

Acknowledgements

I first want to thank warmly my PhD advisors, Boris Pioline and Olivier Schiffmann, for their constant help during my PhD. Boris was at the origin of the project and was always present at the LPTHE for long informal discussions of various topics between physics and mathematics, from which I always came away with tons of bibliographical references to feed my curiosity. His patience in explaining to me the subtleties of S duality, administrative duties, and English grammar had no limit. His energy and enthusiasm to build bridges between physicists and mathematicians by organizing the Darboux seminar, various conferences, and reading groups on hardcore math papers to extract from them some physical intuition, has inspired me in this PhD at the interface. Our long blackboard discussions with Olivier in Jussieu or Orsay have helped to shape my mathematical intuitions and my general knowledge on beers, African art, and metal. He has explained kindly to me the subtle art of writing mathematical papers and giving mathematical talks, without sounding like an infiltrated physicist. His various invitations to summer schools and conferences in Diderot and IHES and seminars and working groups in Orsay (with always some good food and drinks as an option) have helped me grasp some ideas of geometric representation theory.

I also thank Andrea Brini and Dominic Joyce, the referees of my PhD manuscript, for having accepted this mission, and for their judicious remarks. I also thank Soheyla Feyzbakhsh, Amir Kashani-Poor, and Emanuele Macri for having accepted to take part in the jury for my defense. I also thank Emanuele Macri and Gregory Schehr for having taken part in my 'comité de suivi'.

I thank Pierrick Bousseau, Bruno Le Floch, and Boris Pioline for our collaboration on the paper [BDLFP22], and David Jaramillo Duque Amir Kashani-Poor, and Thorsten Schimannek, the other members of the 'reading group on DT theory and everything else', for really inspiring discussions on various topics. I also thank all the mathematicians and physicists with whom I have discussed during my PhD, especially Noah Arbesfeld, Guillaume Beaujard, Marc Bellon, Andrea Brini, Tristan Bozec, Tom Bridgeland, Carlo Bussisano, Alessandro Chiodo, Ben Davison, Maxime Fairon, Soheyla Feyzbakhsh, Lucien Hennecart, Benjamin Hennion, Dominic Joyce, Thibault Jullliard, Wei Li, Emanuele Macri, Sasha Minets, Sergej Monavari, Anne Moreau, Sergey Mozgovoy, Riccardo Ontani, Marco Roballo, Richard Thomas, Tanguy Vernet, Dimtri Wyss, Tony Yue Yu and Menelaos Zikidis.

I thank especially Richard Thomas, who has inspired me for the article [Des22], and has supported me for my postdoc applications. I will be very proud to do my postdoc under his supervision!

I thank all my colleagues at LPTHE with whom I have shared these three years: Osmin,

Gaëtan and Damien, for the explosive debates of the first year, Grégoire for the article we will definitely write together, Carlo for the Sicilian energy in the office, Simon for having taught me many things on Mathematica, juggling, and ant reproduction, Yehudi, Jordan, and Greivin for sharing an office full of positivity, Anthony, a good enough student representative, Vincent, Diyar, and Jules, for my political education, Wenqi for her Lagrangian, Francesco for his incredible cocktails, and Maximilian, Andriani, Andrei, Yann, Vincent, Thorsten and Jordan, for the movie nights when we have discovered together some true masterpieces.

Je remercie aussi mes amis, qui m'ont supporté pendant ces trois années. Etienne, Bora, Nathan et Raphaël, les membres du gang de Bourg La Reine; Arnaud, pour tous les films qu'on a fait et qu'on fera ensemble; Wilson et Théo pour les soirées parisiennes et bretonnes; Etienne, Simon et Thomas, pour nos randos et nos lectures au coin du feu; Tangui pour les qg du LKB au buisson ardent, Ruben pour les weekend à Amterdam, Edouard pour les vacances à vélo; Mathias et Pierre, pour nos explorations souterraines; et Gaëtan, Clément, Alcime, Geoffroy, Marin, Antoine et tous les autres, pour le temps qu'on a passé à gérer une quarantaine d'adolescents turbulents, mais attachants quand même.

Je remercie enfin ma famille pour tout le temps qu'on a passé ensemble, en particulier ces derniers temps, Papa, Maman, François-Nicolas, Louis et Jeanne, et mes grands parents, pour tout leur amour.

Chapter 3

Introduction

This thesis is situated at the interface between mathematics, in particular enumerative and algebraic geometry, and theoretical physics, in particular string theory. The main physical background is the counting of BPS states in $\mathcal{N} = 2$, $D = 4$ supersymmetric field theory. Mathematically, this is expressed through Donaldson-Thomas theory, the virtual counting of sheaves on Calabi-Yau threefolds, or representations of quivers with potentials. In this introduction, we will introduce the physical and mathematical background to understand and motivate this Donaldson-Thomas theory.

In the first section, we will present the phenomenon of homological mirror symmetry, which was first observed by physicists and then studied by mathematicians. It suggests that Calabi-Yau threefolds come in pair $(X, \check{X})$, such that properties of the symplectic geometry of X are related to properties of the complex geometry of $\check{X}$, and vice versa. Physically, it says that the $\mathcal{N} = 2$, $D = 4$ supersymmetric field theory obtained by compactifying type IIA string theory on X is equivalent to those obtained by compactifying type IIB string theory on $\check{X}$. We will be particularly interested in a mathematical formulation of this symmetry, provided by Kontsevich in [Kon95], called the homological mirror symmetry conjecture. We will interpret physically this conjecture as an equality of categories of topological A branes on X (mathematically, the derived category of coherent sheaves on X) and topological B branes on $\check{X}$ (mathematically, the derived Fukaya category of Lagrangians on $\check{X}$), i.e. boundary conditions for a topological version of type IIA and type IIB superstring theories.

In the second section, we will describe the BPS states of the $\mathcal{N} = 2$, $D = 4$ supersymmetric field theories obtained above, i.e. states preserving one supersymmetry over the two. They are described as stable branes: the data giving the spectrum of stable branes inside the category of topological branes is formalized mathematically by the notion of Bridgeland stability condition, introduced in [Bri07]. We will motivate physically this definition, and also present a part of the rich mathematics behind the study of the space of stability conditions of a derived category. We will in particular present the techniques for the construction of stability conditions, and the study of geometric transitions in the space of stability conditions.

In the third section, which is more mathematical, we will present the specific case of type IIA string theory compactified on a Calabi-Yau three singularity. We will present crepant resolutions of singularities, and their noncommutative analogue, the noncommutative crepant resolutions (NCCR), introduced in [VdB04]. In the Calabi-Yau three case, the NCCRs are described as quivers

with potential. In a region of the space of stability conditions on the category of topological A branes, stability is described by King stability on such quivers with potential, for which one can sometimes use very powerful combinatorial techniques. We will present the three main constructions of NCCR, namely the brane tiling technique for toric CY3 singularities, the McKay quiver technique for orbifold, and the method of exceptional collections, for cones over weak del Pezzo surfaces.

In the fourth section, more mathematical, we will introduce numerical (resp cohomological) Donaldson-Thomas theory, which defines a virtual Euler characteristic (resp Hodge polynomial) for the moduli space of stable branes. The mathematics are quite technical here, so we will begin with a presentation of the main objects in use, namely perverse sheaves. We will then motivate the definition and explain the constructions in [BBD+15] of the Donaldson-Thomas perverse sheaf, whose Hodge polynomial gives the cohomological DT invariants. We will then present and motivate the Kontsevich-Soibelman wall crossing formula, which relates generating series of DT invariants for different stability conditions, and express how to extract from the DT generating series the BPS invariants, which are conjectured to be integral, and gives physically a count of BPS states, the power of y in the Hodge polynomial corresponding to twice the spin of the BPS state.

In the fifth section, which is more physical, we will draw the link in string theory between the counting of BPS states and the problem of black hole entropy. We will present how this description of BPS states as multi-centered black holes sheds new light on the phenomenon of wall crossing, and how it suggests a very powerful formula to compute DT invariants, the flow tree formula. In the case of quivers with potential, this formula is completely explicit mathematically, and was proven in [AB21], and the initial data that one needs are the so-called attractor BPS invariants that we will introduce.

Finally, we will present the results obtained during this PhD. The first two articles, [Des22], provided in Chapter 6, and [Des21], provided in Chapter 7, are mathematical papers (the second being published in the Journal of the London mathematical Society). I have developed in Chapter , a toric localization formula to compute cohomological DT invariants. I have adapted it in Chapter , provided in chapter 9, to the seminal case of toric quivers with potentials, refining the computation of numerical DT invariants from [MR08]. It helped to solve a puzzle in the literature between the computations of physicists and mathematicians.

The papers [DP22], provided in Chapter 8, and [BDLFP22], provided in Chapter 9, are mathematical physics papers (the first being published at the Annales Henri Poincaré), written respectively with Boris Pioline, and with Pierrick Bousseau, Bruno Le Floch, and Boris Pioline. In Chapter 8, we have given constraints for quivers with generic potentials to admit conformal multi-centered black holes and similar constraints to have nontrivial attractor invariants. In Chapter 9, we have worked on the flow tree for local $\mathbb{P}^2$, where the space of stability condition has rich modular structure.

3.1 Homological mirror symmetry and branes

3.1.1 Mirror Calabi-Yau threefolds

We consider the content of a $\mathcal{N} = 2$ supersymmetric field theory in $4 = 3 + 1$ dimension (three dimensions of space and one dimension of time). It contains two supersymmetric spinors Q_1, Q_2 which generate two supersymmetries. Supersymmetry is a symmetry which exchanges bosons and

fermions of spins $n, n+1/2$ with $n \in \frac{1}{2}\mathbb{Z}$. Hence, in the presence of 2 supersymmetries, each particle comes in a quadruplet, with 1 particle of spin n, two of spin $n+1/2$, and one of spin $n+1$. Because we suppose that the maximal spin of a physical particle is 2:

- If the theory contain gravity, ie is $\mathcal{N}$=2, D=4 supergravity, there is one graviton multiplet, with one graviton (spin=2) mediating gravity, two gravitinos (spin=3/2) generating the two supersymmetry, mediating 2 supersymmetry, and one gauge boson (spin=1).
- If the theory doesn't contain gravity (it is said to be rigid), there are two gravitino multiplets, with either a gravitino generating a supersymmetry, a gauge boson and a spin 1/2 spinor.
- There can be an arbitrary number of vector multiplets, each containing one gauge boson (generating a gauge symmetry), two spin 1/2 spinors, and one complex scalar (spin 0).
- There can be an arbitrary number of hyper-multiplets, each containing two spin 1/2 spinors and two complex scalars.

Of particular interest are massless scalars, because they determine the moduli of the theory: because the vacuum expectation value of a massless scalar is not constrained, we will consider two theories with different ground states as two theories on a moduli space $\mathcal{M}$ of theories. In fact, the massless scalars give only the tangent space to this moduli space, i.e. this picture of the moduli space is accurate only in a small neighborhood of the theory we are considering, giving deformations to it. We expect that the global topology of the moduli space should be more complex: indeed, there are boundary points and monodromy, as we will see in examples. The moduli are then given by the scalars coming from the n_V massless vector multiplets and the n_H massless hyper-multiplets. Because these scalars give a parametrization of the moduli space in the vicinity of a point, this space is locally a product of a vector multiplet moduli space $\mathcal{M}_V$ and an hyper-multiplet moduli space $\mathcal{M}_H$. Because there are 2 complex scalars in each hypermultiplet, $\mathcal{M}_H$ is of real dimension $4n_H$: it is in fact a quaternionic Kähler manifold when the theory has supergravity and an Hyperkähler manifold for rigid theories. The structure of $\mathcal{M}_H$ is quite complicated, we will not speak a lot about it; see [AMPP13] for a review on its construction in the case that interests us.

Because there is 1 complex scalar in each vector multiplet, $\mathcal{M}_V$ is of real dimension $2n_V$: it is in fact a projective (resp rigid) special Kähler manifold for a supergravity (resp rigid) theory. We will review this geometry here; see [Fre97] for a complete presentation. There is a local system of electromagnetic charges Γ on $\mathcal{M}_V$, which is an integral lattice with a pairing $\langle \cdot, \cdot \rangle$, pairing electric with magnetic charges. Each state of the theory has a particular charge $\gamma \in \Gamma$.

- In the supergravity case, the lattice Γ has rank $2n_V+2$, and its pairing is non-degenerate. $\mathcal{M}_V$ is moreover Hodge, i.e. its symplectic form ω is integral: consider the Hodge bundle $\mathcal{L}_V$, the line bundle with first Chern class $-\omega$, and the $\mathbb{C}^*$-bundle $\hat{\mathcal{M}}_V$ obtained from $\mathcal{L}_V$ by removing the zero section. There is a central charge Z defined on $\hat{\mathcal{M}}_V$, which is a $\mathbb{C}^*$-equivariant section of $Hom(\Gamma, \mathbb{C})$, which embedds locally $\hat{\mathcal{M}}_V$ as a Lagrangian submanifold of $Hom(\Gamma, \mathbb{C})$ with respect to the pairing.
- In the rigid case, Γ is given by an extension:

$$0 \to \Gamma_f \to \Gamma \to \Gamma_g \to 0 \tag{3.1.1}$$

Where Γ_f is a constant local system of lattices of rank n_f (i.e. invariant under monodromy) called the lattice of flavor charges, and Γ_g is a local system of lattices of rank $2n_V$ with non-degenerate pairing called the lattice of gauge charges. There is a central charge defined on $\mathcal{M}_V$, which is a section of $Hom(\Gamma, \mathbb{C})$, which is constant on Γ_f and embedds locally $\mathcal{M}_V$ as an isotropic submanifold of $Hom(\Gamma, \mathbb{C})$ with respect to the pairing.

We will be interested in two types of $D = 4$, $\mathcal{N} = 2$ supersymmetric field theory obtained by compactification of two 10-dimensional superstring theories on Calabi-Yau threefolds, type IIA and type IIB theories. These two theories are superstring theories, so sigma models on a complex curve Σ with a spin structure (i.e. a choice of the square root $K^{1/2}$ of its canonical bundle K) with value in a 10-dimensional Kähler target space X. The Lagrangian is given by:

$$S = 2t \int_\Sigma d^2z \{ g_{IJ} \partial_z \phi^I \partial_{\bar{z}} \phi^J \partial_{\bar{z}} + i g_{i\bar{j}} \psi_-^{\bar{j}} D_z \psi_-^i + i g_{i\bar{j}} \psi_+^{\bar{j}} D_{\bar{z}} \psi_+^i + R_{i\bar{i}j\bar{j}} \psi_+^i \psi_+^{\bar{i}} \psi_-^j \psi_-^{\bar{j}} \} \tag{3.1.2}$$

where g_{IJ} is the compactifying manifold's Kählerian metric. ϕ^i and $\phi^{\bar{j}}$ are the holomorphic and anti-holomorphic coordinates of the map from the worldsheet Σ to the Kähler manifold X, and ψ_+ and ψ_- are their left-moving and right-moving fermionic superpartners, with value in the respective bundle of Σ (D denote their covariant derivatives as elements of these bundles):

$$\psi_+^i \in \Gamma(K^{1/2} \otimes \phi^* T_X^{1,0}) \tag{3.1.3}$$

$$\psi_+^{\bar{j}} \in \Gamma(K^{1/2} \otimes \phi^* T_X^{0,1}) \tag{3.1.4}$$

$$\psi_-^i \in \Gamma(\bar{K}^{1/2} \otimes \phi^* T_X^{1,0}) \tag{3.1.5}$$

$$\psi_-^{\bar{j}} \in \Gamma(\bar{K}^{1/2} \otimes \phi^* T_X^{0,1}) \tag{3.1.6}$$

Here T_X is the complex tangent bundle of X, with holomorphic and anti-holomorphic parts $T_X^{(1,0)}$and $T_X^{(0,1)}$. It gives a $D = 2$ conformal field theory on the complex curve Σ, which is quantized using the ghost system with a central charge -15. Each dimension of X gives a boson ϕ_i and a fermion ψ contributing respectively 1 and 1/2 to the central charge of the CFT; hence the dimension of X is fixed to be 10 to obtain a vanishing central charge and then to cancel the gauge anomaly. The quantification of this theory gives a tower of string excitation with a state of negative square mass, a tachyon, signaling some instability. This tachyon is removed by choosing only certain periodicity conditions for the fermions ψ on Σ, a choice called a GSO projection. There are only two consistent choices, giving respectively type IIA and type IIB theory.

We can consider the target space $M = X \times \mathbb{R}^{1,3}$, with X a smooth complete Kähler manifold and $\mathbb{R}^{1,3}$ the Minkowski spacetime, with signature $(-+++)$. Following the physicist's convention, we call X compact when it is smooth and projective and noncompact when it is smooth, complete, and quasi-projective but not projective. If X is compact and its diameter is far smaller than the scale of observations, one will obtain an effective supergravity theory in $D = 4$ dimension, where oscillations in the directions of X will be interpreted as states of the $D = 4$ theory. If X is noncompact, we will obtain a rigid supersymmetric theory in $D = 4$ dimensions. A second supersymmetry is conserved, hence one obtains an $\mathcal{N} = 2$ $D = 4$ theory, if a spinor is conserved by parallel transport, i.e. the holonomy of X is $SU(3) \subset U(3)$, or equivalently, the Kählerian metric of X is Ricci flat. Thanks to Yau's proof of the Calabi theorem, X admits a Ricci flat Kählerian metric if and only if the first Chern class of its tangent bundle vanishes, in which case X is called a Calabi-Yau manifold. In this

case, one obtain a $D = 4$, $\mathcal{N} = 2$ supersymmetric supergravity or rigid theory by compactifying type IIA or type IIB string theory on X.

We consider type IIB compactified on a compact CY3 X, giving $\mathcal{N} = 2$ $D = 4$ supergravity. The lattice Γ is then the lattice $H_3(X, \mathbb{Z})$ of 3-cycles with its intersection pairing. The position in the hypermultiplet moduli space fixes the symplectic geometry of X. The vector multiplet moduli space is given exactly (with no quantum corrections when X is small compared to the Plank scale) by the moduli space $\mathcal{M}_C$ of smooth complex structures of X. Indeed, vector multiplets are given by $H^1(X, T_X) = H^{2,1}(X, \mathbb{C})$ parametrizing deformations of the complex structure, and, by the Bogomolov-Tian-Todorov theorem, these deformations are unobstructed, hence $\mathcal{M}_C$ is of complex dimension $h^{2,1}$. The $\mathbb{C}^*$ bundle $\hat{\mathcal{M}}_V$ on $\mathcal{M}_C$ corresponds to the extra data of a holomorphic three form $\Omega \in H^3(X, \mathbb{C})$, the central charge is then defined by integrating Ω on any three cycle. The Griffith transversality theorem says exactly that the central charge embeds $\hat{\mathcal{M}}_V$ locally as a Lagrangian in $Hom(\Gamma, \mathbb{C})$, which is defined by Picard-Fuchs equations. The boundary of $\mathcal{M}_C$ contains exceptional divisors where the holomorphic volume of some three-cycles vanishes, and then X becomes singular, and there is some monodromy for Γ around these divisors.

Consider now type IIA compactified on a compact (resp noncompact) CY3 X. The lattice of charge is the lattice $\bigoplus_{p=0}^{3} H^{p,p}(X, \mathbb{C})$ (resp $\bigoplus_{p=0}^{3} H_c^{p,p}(X, \mathbb{C})$) of even-dimensional (compact) cycles with its intersection pairing. If X is noncompact, the lattice Γ_f is given by cycles with compact support with vanishing intersection with all the cycles with compact support: in particular, the charge of the points and in general several classes of curves are in Γ_f. The position in the hypermultiplet moduli space fixes the complex geometry of X. Near the large volume limit, i.e. when X (or its compact cycles) is large compared to the string length l, the vector multiplet moduli space is given by the complexified Kähler cone, parametrized by $K = B + i\omega$, with $B \in H^{1,1}(M, \mathbb{C})$ the B field, and ω in the Kähler cone. This description is not valid away from the large volume limit, because there are quantum corrections. The true vector multiplet moduli space, of complex dimension $h^{1,1}$, denoted $\mathcal{M}_K$, is called the stringy Kähler moduli space, and seems really interesting mathematically: it links the Kähler cones of birational Calabi-Yau threefolds, as in the minimal model program, and contains regions described by noncommutative geometry, as we will see below. In the large volume, where $\mathcal{M}_K$ is identified with a neighborhood of the infinity in the complexified Kähler cone, the central charge map is given by $Z : K \mapsto exp(K)$. The true central charge is determined by equations involving corrections by tree level topological string, i.e. the genus zero Gromov-Witten invariants counting rational curves.

In the 1980s, some dualities relating different superstring theories were predicted. One of the most famous is T duality: type IIA compactified on a torus of radius l/R gives the same theory as type IIB compactified on a torus of radius lR, where l is the typical string length. During the 1990s, a higher-dimensional version of this duality was discovered and named mirror symmetry. Namely, Calabi-Yau threefolds seem to come in pairs $(X, \check{X})$, where type IIA compactified on X is equivalent to type IIB compactified on $\check{X}$, and vice versa. In particular, the complex and stringy Kähler moduli spaces of X and $\check{X}$ are exchanged under this duality. It is particularly interesting because it relates the genus zero Gromov-Witten invariants of X with Picard-Fuchs equations on $\check{X}$, and gives a way to count rational curves on X and obtain closed formulas in certain cases like the quintic, which seems unreachable by classical methods.

3.1.2 Category of topological branes

We will now see how mirror symmetry has been interpreted by Maxim Kontsevich in terms of branes. In order to study type IIA and type IIB string theories, Witten has defined simplified versions of them, the type A and type B topological string theories. In particular, these theories depend only on the hypermultiplet moduli space, and not on the vector multiplet moduli space. Hence, type A theory depends on the complex geometry of X, and type B depends on the symplectic geometry of X. We will consider objects in this theory, which are called branes, and give boundary conditions for the conformal field theory on Σ. Beware that a brane preserving one supersymmetry in type A is called a B brane, and in type B, an A brane. We consider for the moment that X is compact, i.e. smooth and projective.

In a first approximation, a brane is a closed subvariety of $M = X \times \mathbb{R}^{1,3}$ on which a boundary of a string can end. The branes extended in the Minkowski space are extended objects of high mass, which do not interest us here: we are interested in branes that are pointlike in the $4D$ space and then wrap X. In order to preserve one of the two supersymmetries, B branes must be complex subspaces, and A branes must be Lagrangian subspaces. Notice that the complex structure fixes an orientation on a complex submanifold, but not on a Lagrangian submanifold. Hence, two orientations are possible for an A brane: given an A brane, we call the brane with the opposite orientation its antibrane. We must consider gauge invariance on boundary conditions; for this reason, N coincident branes on the same closed subvariety S must be given by the data of a $U(N)$ vector bundle with connection on S. The preservation of the supersymmetry imposes for the B branes that this connection is holomorphic and for the A branes that this connection is flat. Moreover, two holomorphic connections on the same holomorphic vector bundles give gauge equivalent B branes, and two Hamiltonian isotopic Lagrangians give gauge equivalent A branes.

To conclude, in a first approximation:

- B branes are holomorphic vector bundles supported on complex subvarieties.
- A branes are oriented Lagrangians with $U(N)$ flat connections.

Consider now strings stretched between branes. Between two branes E, F, there is a spectrum of strings with different masses. They form a complex $\mathbf{Hom}(E, F)$ with differential m_1, with homology $Ext^i(E, F)$ giving strings with increasing masses, namely:

- $Ext^{\leq 0}(E, F)$ gives tachyons, i.e. unstable strings: A string $f \in Ext^0(E, F)$ signals the possibility of a tachyonic condensation decomposing F into E and a brane $Cone(F)$.
- $Ext^1(E, F)$ gives massless strings, i.e. deformations: Given $f \in Ext^1(E, F)$, there exists a bound state of F and E, linked together by the massless string f
- $Ext^{\geq 2}(E, F)$ gives massive states, providing obstructions.

There is a kind of composition law for strings: if f is a string stretched between E and F, and g is a string stretched between F and G, then there is a natural way to define a string $m_2(f, g)$ stretched between E and G. One then has a graded map:

$$m_2 : \mathbf{Hom}(E, F) \times \mathbf{Hom}(F, G) \to \mathbf{Hom}(E, G) \tag{3.1.7}$$

This map is associative on the cohomology $Ext^{\cdot}$, signaling that the physical states of strings can be glued naively, but in general is not associative at the level of the complexes **Hom**: The default

of associativity is encoded in a tower of maps $(m_n)_{n>0}$, providing the data of an A_∞ category $\mathcal{D}$ of branes. In general, we can always kill the higher m_n by taking an homotopy-equivalent model where the $(m_n)_{n>2}$ vanish, hence $\mathcal{D}$ is a dg category, but the A_∞ description is sometimes more natural, as we will see for A branes.

For any brane $E \in \mathcal{D}$, there must be an antibrane $E[1] \in \mathcal{D}$: This defines a shift functor $[1] : \mathcal{D} \to \mathcal{D}$, which is an autoequivalence of category, whose powers are denoted by $[m], m \in \mathbb{Z}$. It must shift the string spectrum, namely $\mathbf{Hom}^\cdot(E[n], F[m]) = \mathbf{Hom}^{\cdot+m-n}(E, F)$. In particular, we don't need to have $[2] = Id$, hence the brane/antibrane relation is not an involution: we have upgraded a $\mathbb{Z}_2$ parity symmetry to a $\mathbb{Z}$-symmetry. Notice that a tachyonic string $f \in Ext^0(E, F)$, giving a tachyonic condensation $E \xrightarrow{f} F \to G$, is the same thing as a massless string in $Ext^1(E[1], F)$, giving a bound state $F \to G \to E[1]$. One obtains the usual cross ratio relations, expressing the fact that a decay $F \implies E + G$ is the same as a decay $G \implies F + E[1]$. The data of the possible brane decays is then axiomatized into the data of a triangulated category:

Definition 3.1.1. A triangulated category is an A_∞ (or dg)-category with a shift functor [1] and a collection of exact triangles, stable by isomorphism:

$$E \to F \to G \to E[1] \tag{3.1.8}$$

This collection is subject to the axioms:

- TR1: The triangle $E \xrightarrow{id} E \to 0 \to E[1]$ is exact (it gives the trivial tachyonic condensation $E \implies E$).
- TR2: For any $f : Ext^0(E, F)$, there is a triangle $E \xrightarrow{f} F \to G \to E[1]$, G being called a cone of f (existence of tachyonic condensation).
- TR3: A triangle $E \to F \to G \to E[1]$ is exact if and only if the rotated triangle $F \to G \to E[1] \to F[1]$ is exact (the data of a decay $F \implies E + G$ is equivalent to the data of a decay $G \implies F + E[1]$, i.e. it is CPT invariance).
- Given two exact triangle with morphisms forming a commuting diagram:

$$\begin{array}{ccccccc} E & \longrightarrow & F & \longrightarrow & G & \longrightarrow & E[1] \\ \downarrow{\scriptstyle \alpha} & & \downarrow{\scriptstyle \beta} & & & & \downarrow{\scriptstyle \alpha[1]} \\ E' & \longrightarrow & F' & \longrightarrow & G' & \longrightarrow & E'[1] \end{array}$$

  There is a unique vertical arrow $\gamma : G \to G'$ such that the diagram is commutative (this axiom describes how strings evolves after a tachyonic condensation of branes).
- The "octaedral axiom": a technical axioms that expresses the fact that one can compose decay.

Given a triangulated category $\mathcal{D}$, one can consider its Grothendieck group $K_0(\mathcal{D})$, the free Abelian group generated by its elements, divided by the relations $[F] = [E] + [G]$ for each $E \to F \to G \to E[1]$ exact triangle. It is the group of conserved charges of the branes. It has a bilinear pairing:

$$\langle E, F \rangle = \sum_{i \in \mathbb{Z}} \dim(\mathrm{Ext}^i(E, F)) \tag{3.1.9}$$

Notice that it descendsto the Grothendieck group by using long exact sequences in cohomology obtained from the exact triangles. The quotient of $K_0(\mathcal{D})$ by the kernel of $\langle \cdot, \cdot \rangle$ is then a lattice Γ, which is a lattice of electromagnetic charge for the $D = 4$, $\mathcal{N} = 2$ theory, the Euler pairing giving the electromagnetic pairing.

For B branes, the spectrum of strings is provided by the usual complex $\mathbf{Hom}(E, F)$ obtained by resolving the bifunctor $Hom(E, F)$, which is not exact. One replaces E by a projective resolution and F by an injective resolution, and one obtains $\mathbf{Hom}(E, F)$ as the complex of morphisms between these two complexes. An injection of holomorphic vector bundles $E \mapsto F$ is then a tachyon in $Ext^0(E, F)$, and then one has to consider its quotient F/E as a brane. Then one has to consider that any coherent sheaf on X is a B brane. The Abelian category of coherent sheaves is not sufficient to describe B branes, because it has no shift, hence cannot describe antibrane, and it has cone only for injective morphisms. In it, the brane decays are described by short exact sequences $0 \to E \to F \to G \to 0$. There is a standard construction to obtain a triangulated category $D^b(\mathcal{A})$ from an Abelian category $\mathcal{A}$: one takes the derived category, the category of complexes modulo quasi-isomorphism, i.e. morphisms of complexes that are isomorphisms on the cohomology. We denote by $D^b(X)$ the derived category of coherent sheaves on X. It was proposed by Kontsevich in [Kon95] and further checked physically by Douglas in [Dou01] and Aspinwall in [Asp04] that it is the true category of B branes. Its Grothendieck group is the K-theory group $K_0(X)$, which has in general complicated torsion. But, by Grothendieck-Riemann-Roch, the Euler pairing factors into the intersection pairing through the Mukai vector:

$$\begin{aligned} v : & K_0(X) \to \bigoplus H_{2k}(X, \mathbb{Q}) \\ & [E] \mapsto v(E) := ch(E)\sqrt{td(TX)} \end{aligned} \tag{3.1.10}$$

Here $ch(E)$ denotes the Chern character, and $td(TX)$ the Todd class of the tangent bundle of X. The lattice of electromagnetic charges of B branes is then $\bigoplus H_{2k}(M, \mathbb{Q})$ with its intersection form.

The category of A branes is the Fukaya category $Fuk(X)$, which can be built for any symplectic manifold X of dimension $2n$. To define the spectrum of strings between two A branes given by two Lagrangians L, L' with $U(1)$ connection, one must perturb them by a Hamiltonian isotopy (then, without changing the physical class of the A brane) such that they intersect transversely at isolated points (recall that they are middle-dimensional). The complex $\mathbf{Hom}(L, L')$ is defined by Floer theory. The points of intersections forms a basis of $\mathbf{Hom}(L_0, L_1)$, but the grading is quite difficult to define. For this, one must have an extra data on branes called a grading, lifting the $\mathbb{Z}_2$ data of the orientation to a $\mathbb{Z}$-data, and such that there is a shift [1] shifting the grading, which reverses the orientation. The degree of a point of intersection $x \in L_0 \cap L_1$ is then defined by using the Darboux lemma to give a local symplectic presentation of the intersection of L and L' as an intersection of two linear Lagrangians in $\mathbb{R}^{2n}$. The Fukaya category is then naturally built naturally as an A_∞ category. Namely, consider oriented Lagrangians $L_0, ..., L_d$ which intersect transversely two by two, and intersection points $x_{i,i+1} \in L_i \cap L_{i+1}$. One defines:

$$m_d(x_{01}, ..., x_{d-1,d}) = \sum_{x_{0,d} \in L_0 \cap L_d} n(x_{01}, ..., x_{d-1,d}; x_{0,d}) x_{0,d} \in \mathbf{Hom}(L_0, L_d) \tag{3.1.11}$$

Here $n(x_{01}, ..., x_{d-1,d}; x_{0,d})$ counts J-holomorphic polygons (for a choice of quasi-complex structure J) in X with vertex on $x_{i,i+1}$ and edges mapped to $L_0, ..., L_d$. The degenerations in the space

of J-holomorphic disks give the A_∞ relations. Notice that this definition is really difficult to set rigorously, because of the transversality assumption. The shift is derived naturally in the Fukaya category, but cones are in general not defined, hence the category of A branes is expected to be the twisted derived category $D^bFuk(X)$ of the Fukaya category (an analogue of derived categories for A_∞ category). By construction, intersection points of positive intersections are in even degrees of $\mathbf{Hom}(L_0, L_1)$, and intersection points of negative intersections are in odd degrees, hence $\langle L_0, L_1\rangle$ is the classical intersection form; the electromagnetic lattice of charges of A branes is then $H_3(X, \mathbb{Q})$ with its intersection form.

We can now formulate the homological mirror conjecture of Kontsevich from [Kon95]:

Conjecture 3.1.2. *Smooth, projective Calabi-Yau threefolds come in pair $(X, \check{X})$ such that the derived category of coherent sheaves on X is triangulated equivalent to the derived Fukaya category of $\check{X}$ (and vice versa).*

All mirror symmetry phenomena are expected to result from this equivalence of triangulated categories. In particular, we will see in the next section how we can read from it the isomorphism between the stringy Kähler moduli space of X and the complex moduli space of $\check{X}$, by interpreting the two as spaces of stability condition on the same triangulated category. We will also consider type IIA compactified on a noncompact X: the branes must then have compact support, and the category of topological branes is $D^b_c(X)$, the category of complexes of coherent sheaves with homology having compact support.

3.2 Bridgeland stability conditions

3.2.1 Stability of A branes

We now consider the full type IIA and type IIB theory, and not only their topological truncation. We will consider the BPS branes of the theory, branes that conserve one supersymmetry. We will see that the physical branes of those theories are a subset of the topological B branes and A branes, which are stable under a stability condition. This stability depends on the vector multiplet moduli space, i.e. on the stringy Kähler moduli space for B branes and on the complex moduli space for A branes.

Consider a $D = 4$, $\mathcal{N} = 2$ string theory, with supersymmetry generated by the spinors Q^1, Q^2. Then, following [BBS07, Chapter 8], on the space of branes of charge γ and mass M, the spinors Q^J verify:

$$\{Q^I_\alpha, Q^{\dagger J}_\beta\} = 2M\delta^{IJ}\delta_{\alpha\beta} + 2iZ^{IJ}(\gamma)\Gamma^0_{\alpha\beta} \tag{3.2.1}$$

Here the Γ^i are the spinor matrices, and $Z(\gamma)$ a 2×2 matrice, depending on the electromagnetic charge γ, called the central charge matrice. By (3.2.1), Z must be antisymmetric, so, by a unitary base change of the supercharges, have the form:

$$Z = \begin{pmatrix} 0 & Z(\gamma) \\ -Z(\gamma) & 0 \end{pmatrix} \tag{3.2.2}$$

with $Z \in Hom(\Gamma, \mathbb{C})$ the central charge discussed above. Equation (3.2.1) guarantees also the positivity of the matrix:

$$B = \begin{pmatrix} M & Z \\ -Z & M \end{pmatrix} \tag{3.2.3}$$

which is equivalent to the BPS bound:

$$M \geq |Z(\gamma)| \tag{3.2.4}$$

A state of mass M preserve a supersymmetry if it is annihilated by a combination Q of the Q^I; in this case $\{Q, Q^\dagger\} = 0$, hence B has an null vector. Finally, we find that, to be a BPS state, a particle must saturate the BPS bound:

$$M = |Z(\gamma)| \tag{3.2.5}$$

By denoting $Z(\gamma) = Me^{i\pi\phi}$, ϕ determines which supersymmetry is conserved and is called the phase of the BPS brane. Then a map Z from the vector multiplet space to $\mathrm{Hom}(\Gamma, \mathbb{C})$ determines the set of BPS branes.

For A branes, recall that the vector multiplet moduli space is the moduli space of complex structures $\mathcal{M}_C$, and that the central charge $Z : \hat{\mathcal{M}}_V \to H^3(M, \mathbb{C}) = \mathrm{Hom}(H_3(M, \mathbb{Q}), \mathbb{C})$ is given by integrating the holomorphic three form Ω:

$$Z(L) = \int_L \Omega \tag{3.2.6}$$

Notice that at each point $x \in L$ we have $\Omega = e^{i\pi\phi(x)} vol_L$. The data of the graded Lagrangian is exactly the data that allows to lift canonically ϕ to a continuous function $\phi : L \to \mathbb{R}$. The mass of the A brane is the volume of the Lagrangian L. The BPS bound in this case is then given by:

$$|Z(L)| = |\int_L e^{i\pi\phi} vol| \leq \int_L |e^{i\pi\phi}| vol = M(L) \tag{3.2.7}$$

with equality if and only if ϕ is constant, i.e. $\Omega = e^{i\pi\phi} vol$ on L. In this case, the BPS brane L is said to be a special Lagrangian of phase ϕ. In particular, note that such a Lagrangian minimize volume in its homotopy class. The Thomas-Yau uniqueness result [TY01, Theorem 4.3] shows that each Hamiltonian isotopy class (which corresponds to objects of the Fukaya category) contains at most one special Lagrangian: if this object is simple, we call such an object stable of phase ϕ. The subcategories $(\mathcal{P}(\phi))_{\phi\in\mathbb{R}}$ generated by stable A branes of phase ϕ, whose objects are called semistable A branes of phase ϕ, defines then a slicing of $D^b Fuk(X)$, according to the following definition:

Definition 3.2.1. A slicing is a collection of thick subcategories $(\mathcal{P}(\phi))_{\phi\in\mathbb{R}}$ such that:

i) $\mathcal{P}(\phi)[1] = \mathcal{P}(\phi + 1)$.

ii) $Ext^0(\mathcal{P}(\phi), \mathcal{P}(\phi')) = 0$ if $\phi' > \phi$.

Assumption *i)* is immediate from the definition of graded Lagrangians, and *ii)* is immediate from the definition of the grading on $\mathbf{Hom}(L, L')$. The simple objects of $\mathcal{P}(\phi)$ are the stable ones: the physical idea is that an object of $\mathcal{P}(\phi)$ which is not simple will decay with no energetic cost into its simple constituents, which is expressed mathematically by a Jordan-Hölder decomposition. A semisimple object of the category $\mathcal{P}(\phi)$ polystable object, and we say that two semistable objects are S-equivalent if they have the same stable decomposition. In general, it is possible to form some coarse moduli space for the stack of objects of $\mathcal{P}(\phi)$, whose points correspond to S-equivalence classes of semistable objects.

Consider now two special Lagrangians L_1, L_2 of the same phase ϕ for an holomorphic three-form Ω, intersecting at a point $x \in \mathbf{Hom}^1(L_2, L_1)$.One can use local holomorphic symplectic isomorphism with an open neighborhood of 0 in $\mathbb{C}^m$ with $L_2 = \{(x_1, ..., x_m)|x_i \in \mathbb{R}\}$ and $L_1 = \{(e^{i\pi\phi_1}x_1, ..., e^{i\pi\phi_m}x_m)|x_i \in \mathbb{R}\}$ with $0 < \phi_i < 1$, and the grading of x says that $\sum \phi_i = 1$. In this case, Lawlor has built in [Law89] a special Lagrangian of phase ϕ asymptotic to $L_1 \cup L_2$. In [Joy03, Section 9], Joyce has glued this local picture to associate with an element of $a \in \mathrm{Ext}^1(L_2, L_1)$ a special Lagrangian $L_1 \looparrowright L_2$, called a connected sum of L_1 and L_2, such that there is an exact triangle given by $a \in \mathrm{Ext}^1(L_2, L_1)$:

$$L_1 \to L_1 \looparrowright L_2 \to L_2 \to L_1[1] \tag{3.2.8}$$

Consider now the space of complex structures on X, which is smooth: in the neighborhood of the complex structure ω, the isotopy classes of L_1, L_2 are still stable of phase ϕ_1, ϕ_2. There is a real codimenion 1 wall through Ω on which $\phi_1 = \phi_2$. Then [Joy03, Theorem 9.10] says that on the side $\phi_1 < \phi_2$ of the wall, there exists a special Lagrangian in the isotopy class of $L_1 \looparrowright L_2$ and there is no such object on the other side of the wall. In physical terms, it is an instance of wall crossing: the bound state of $L_1 \looparrowright L_2$ decays on the wall into L_1 and L_2 because L_1 becomes destabilizing. One says that on the other side of the wall, $L_1 \looparrowright L_2$ has an Harder-Narasimhan decomposition into the semistable objects L_1, L_2 of phase $\phi_1 > \phi_2$. This motivates the following definition by Bridgeland [Bri07]:

Definition 3.2.2. Consider a triangulated category $\mathcal{D}$, and a finite dimension quotient Γ of the Grothendieck group. A stability condition on $\mathcal{D}$ is the data of a central charge $Z \in Hom(\Gamma, \mathbb{C})$ with a slicing $(\mathcal{P}(\phi))_{\phi\in\mathbb{R}}$ such that:

- An object $E \in \mathcal{P}(\phi)$ satisfies $Z(E) = Me^{i\pi\phi}$ with $M \in \mathbb{R}_{>0}$ (M being the mass of E).
- For a norm $|\cdot|$ on Γ, one has $C > 0$ such that for any semistable E, $|E| \leq C|Z(E)|$ (support condition).
- Any object $E \in \mathcal{D}$ has a (necessarily unique from the axioms of a slicing) Harder-Narasimhan decomposition:

$$\begin{array}{ccccccccccc} 0 = E_0 & & \longrightarrow & & E_1 & & \longrightarrow & E_2 \to \ldots \to & E_{n-1} & & \longrightarrow & & E_n = E \\ & \nwarrow \swarrow & & & & \nwarrow \swarrow & & & & \nwarrow \swarrow & & & \\ & A_1 & & & & A_2 & & & & A_n & & & \end{array} \tag{3.2.9}$$

  with $A_j \in \mathcal{P}(\phi_j)$ for all j, and $\phi_1 > \phi_2 > ... > \phi_n$.

The support condition was added in further works, and suggested by Kontsevich and Soibelman in [KS]: it expresses the fact that semistable objects cannot have arbitrary small mass, otherwise it would give a singularity in the space of stability condition (a massless object giving an extra moduli). The Harder-Narasimhan condition corresponds to the idea that an arbitrary brane will decompose into semistable branes. Notice that there is a natural action of the autoequivalences of $\mathcal{D}$ on stability conditions, and also an action of $\mathbb{C}$ on stability conditions, accounting for the ambiguity in the scaling of the central charge, given by:

$$c \cdot (Z, (\mathcal{P}(\phi))) \mapsto (e^{i\pi c}Z, (\mathcal{P}(\phi - \Re(c)))) \tag{3.2.10}$$

This led to the Thomas-Yau-Joyce conjecture of [TY01], [Joy14] (which is inspired by the stability of B branes), namely that each complex structure on X and holomorphic three-form Ω defines a stability condition on $D^bFuk(X)$, with central charge $L \to \int_L \Omega$, and the slicing defined above. The support property is verified, but the Harder-Narasimhan decomposition is really difficult to show. It is conjectured that it can be obtained from the mean curvature flow with some surgery, maybe by including some singular Lagrangian. See the review [Li22] for a recent account.

For a stability condition σ, we denote in $\phi_{\min}(E), \phi_{\max}(E)$ respectively the minimal and maximal slope appearing in the Harder-Narasimhan decomposition of E. A topology on the set of stability conditions, giving a space $\mathrm{Stab}(\mathcal{D})$ was defined in [Bri07], from the distance:

$$d(\sigma, \sigma') = \max(|Z - Z'|_\infty, \sup_{E \in \mathcal{D}} (\max(|\phi_{\min}(E) - \phi'_{\min}(E)|, |\phi_{\max}(E) - \phi'_{\max}(E)|))) \tag{3.2.11}$$

Hence two stability conditions are close by if their central charges and the slopes of their Harder-Narasimhan decompositions are close. There is a continuous map $Z : Stab(\mathcal{D}) \to Hom(\Gamma, \mathbb{C})$. The main result of [Bri07] is then:

Theorem 3.2.3. *([Bri07]) The map $Z : Stab(\mathcal{D}) \to Hom(\Gamma, \mathbb{C})$ given by the central charge is a homeomorphism on its image.*

Hence deformations of a stability condition correspond locally with deformations of the central charge. Applying this result to the derived Fukaya category $D^bFuk(X)$, we obtain that the central charge gives a local homeomorphism $Z : Stab(D^bFuk(X)) \to H^3(M, \mathbb{C})$. But the space of holomorphic 3-forms was only a Lagrangian in $H^3(M, \mathbb{C})$. The total space $\mathrm{Stab}(D^bFuk(X))$ is expected to correspond to noncommutative deformations of X in the sense of Kontsevich-Rosenberg: it must parameterize deformations of the derived category of coherent sheaves $D^b(X)$, which outside L are no longer described as a derived category of a complex deformation of X.

3.2.2 Stability of B branes

We will now study the mirror picture, namely the study of B branes. The description of stable A branes as special Lagrangian was exact physically, because the space of complex structures and the equations of stability in type IIB received no quantum corrections. On the other hand, the theory is really hard analytically: the construction of the derived Fukaya category and a general proof of the Thomas-Yau conjecture are far from complete. B branes on X are described by the derived category $D^b(X)$ which is a far more classical object, and live in the world of algebraic geometry, where we can hope to have very powerful techniques. However, the A model suffers from quantum corrections, hence the physically accessible definition of stability of B branes is only valid in the large volume limit. We will then use insight from homological mirror symmetry, namely that the stringy Kähler moduli space must be a Lagrangian subspace of $\mathrm{Stab}(D^b(X))$, the central charge being described by mirror symmetry. Notice that everything that we will say on the stability of B branes also holds when X is noncompact, one must then only replace $D^b(X)$ by $D^b_c(X)$, and consider the lattice of charge given by compact even-dimensional cycles.

Consider an asymptotic direction $K_t = B + t\omega$ in the complexified Kähler cone, with $t \gg 0$. The central charge $Z(E)$ is given asymptotically by:

$$Z_t(E) = t^n r(E) \int_M \omega^n + it^{n-1}\omega^{n-1} \cdot c_1(E) + o(t^{n-1}) \tag{3.2.12}$$

Here, $r(E)$ denotes the rank and $c_1(E)$ the first Chern class. Asymptotically, the phases ϕ of vector bundles E on X are ordered as the slopes:

$$\mu_\omega(E) := \frac{c_1(E)\cdot\omega^{n-1}}{r(E)} \tag{3.2.13}$$

We say then that a vector bundle F is slope-(semi)stable if for each nontrivial exact sequence $0 \to E \to F \to G \to 0$, one has $\mu_\omega(E) < (\leq)\mu(F) < (\leq)\mu(G)$. As before, semistable objects have a (generally non-unique) Jordan-Hölder decomposition into stable objects of the same slope, and a semistable object is called polystable if it is the direct sum of its simple factors. From Noetherianity of the Abelian category $Coh(X)$, each vector bundle has a unique Harder-Narasimhan filtration, whose successive quotients are semistable objects of strictly decreasing slope. If we had taken all the asymptotic expansion of $Z_t(E)$, we would have obtained a finer notion of semistability called Gieseker stability and a finer Harder-Narasimhan decomposition, which would allow to decompose any elements of $Coh(X)$, and not only vector bundles, into simple factors.

We now consider the asymptotic versions of the BPS bound in the asymptotic direction $K_t = B + t\omega$. In this limit, as we have seen, the simplest B branes are holomorphic vector bundles with hermitian connections, whose curvature will be denoted F_A. The mass of such a brane is then given by $\int_M |F_A|^2 dvol_M$, and BPS, i.e. stable B branes, will be branes that minimize this mass. By variational calculus, the minimization of the mass is equivalent to the Yang-Mills equation $d_A^* F_A$, which can be rephrased in this Kählerian context as the Hermite-Yang-Mills equation:

$$F_A \wedge \omega^{n-1} = \mu(E)\frac{\omega^n}{\int_M \omega^n} \tag{3.2.14}$$

This equation can be seen as a Nonabelian analogue of the Kähler-Einstein equation. A Nonabelian analogue of the Calabi-Yau theorem is provided by the theorem of Donaldson-Uhlenbeck-Yau (also called Hitchin-Kobayashi correspondence):

Theorem 3.2.4. *A holomorphic vector bundle on a Kählerian manifold carries a (necessarily unique) Hermite-Yang-Mills connection if and only if it is slope polystable.*

The necessity part is quite easy to prove, but the converse proof is analytically very hard. It builds a geometric flow, the Hermite-Yang-Mills flow, which flows to a Hermitian-Yang-Mills connection unless there is some destabilizing subbundle, in which case the flow breaks at a finite time. As the mean curvature flow for A branes, it can be interpreted physically as the process by which an unstable brane decays into polystable ones. This deep theorem allows to replace the analytic notion of stability by an algebraic notion, which is far simpler, and in particular extends at finite volume through the notion of Bridgeland stability condition.

We will now explain the link with Bridgeland stability condition. Using Gieseker stability, an arbitrary object of $Coh(X)$ has a unique Harder-Narasimhan decomposition into Gieseker-semistable branes, which are then branes that are stable in the large volume limit. To decompose arbitrary objects of the derived category $D^b(X)$, one has to first consider the decomposition given by the homology of the complex in order to write an arbitrary complex as an extension of shifts of objects in $Coh(X)$, and then decompose the homology according to Harder-Narasimhan decomposition in $Coh(X)$. This kind of construction is the most usual way to define a stability condition on a triangulated category, so we will axiomatize it.

Definition 3.2.5. A t-structure in a triangulated category $\mathcal{D}$ is a pair $(\mathcal{D}^{\geq 0}, \mathcal{D}^{\leq 0})$ of full subcategories, stable under isomorphisms, such that (we denote $\mathcal{D}^{\overset{\leq}{>}n} := \mathcal{D}^{\overset{\leq}{>}0}[-n]$):

- $Ext^0(\mathcal{D}^{\leq 0}, \mathcal{D}^{\geq 1}) = 0$.
- $\mathcal{D}^{\leq -1} \subset \mathcal{D}^{\leq 0}$ and $\mathcal{D}^{\geq 1} \subset \mathcal{D}^{\geq 0}$.
- If $F \in \mathcal{D}$, there is a (necessarily unique up to isomorphism) triangle $E \to F \to G \to E[1]$, with $E \in \mathcal{D}^{\leq 0}$ and $G \in \mathcal{D}^{\geq 1}$

We call $\mathcal{A} := \mathcal{D}^{\geq 0} \cap \mathcal{D}^{\leq 0}$ the Abelian heart of the t-structure.

A t-structure is then the structure one needs to obtain for each E a (necessarily unique up to isomorphism) decomposition:

$$\begin{array}{ccccccccccc} 0 = E_n & & \longrightarrow & & E_{n-1} & & \longrightarrow & & E_{n+2} \to \ldots \to E_{m+1} & & \longrightarrow & & E_m = E \\ & \nwarrow & & \swarrow & & \nwarrow & & \swarrow & & \nwarrow & & \swarrow & \\ & A_{n-1}[n-1] & & & & A_{n-2} & & & & A_m & & & \end{array} \tag{3.2.15}$$

with exact triangles, and $A_r \in \mathcal{A}$ are called the cohomology with respect to the heart $\mathcal{A}$. Suppose that we have:

Definition 3.2.6. A stability function on an Abelian category $\mathcal{A}$ (with Γ a finite dimensional quotient of its Grothendieck group) is a central charge $Z \in Hom(\Gamma, \mathbb{C})$ satisfying:

- $Z(E) = me^{i\pi\phi(E)}$, $m > 0$ and $0 < \phi(E) \leq 1$
- We have $C > 0$ such that for any ϕ-stable object $E \in \mathcal{A}$, $|E|\text{`}C|Z(E)|$ (support property).
- There exists a Harder-Narasimhan filtration with respect to ϕ.

Given the heart of a t-structure and a stability condition Z on it, we define the slicing $\mathcal{P}(\phi)$ such that, for $0 < \phi \leq 1$, $\mathcal{P}(\phi)$ is the full subcategory of ϕ-semistable objects of $\mathcal{A}$ of phase ϕ, and $\mathcal{P}(\phi + n) = \mathcal{P}(\phi)[n]$. The support property is direct, and one obtains the Harder-Narasimhan decomposition on $\mathcal{D}$ by combining the homology decomposition with respect to the heart and Harder-Narasimhan filtration on $\mathcal{A}$. One obtains:

Theorem 3.2.7. *There is a bijection between the stability condition on $\mathcal{D}$ and pairs $(\mathcal{A}, Z)$ of hearts of t-structures and a stability function on it.*

Slope or Gieseker stability conditions are not stability conditions in this sense on $Coh(X)$ (unless if X is a curve), so we have not built true stability conditions on $D^b(X)$, but only an asymptotic version of them corresponding to a large volume limit in the stringy Kähler moduli space. We will now see how to build true stability conditions that correspond to the interior of the stringy Kähler moduli space.

3.2.3 Construction of stability conditions

We will explain the case of the construction of Bridgeland stability conditions on a smooth projective surface X, which is well understood, and explain after how to extend this construction to the threefold case. We consider a complexified Kähler class $K = B + i\omega$, with ω in the ample cone. A standard procedure to build a new heart from an old one is given by tilting the heart with respect to a t-structure:

Definition 3.2.8. A torsion pair of an Abelian category $\mathcal{A}$ is a pair of subcategories $(\mathcal{T}, \mathcal{F})$ such that $Ext^0(\mathcal{T}, \mathcal{F}) = 0$, and any object $E \in \mathcal{A}$ admits a (necessarily unique up to isomorphism) decomposition by an exact triangle $T \to E \to F \to T[1]$ with $T \in \mathcal{T}$ and $F \in \mathcal{F}$

Suppose now that $\mathcal{A}$ is the heart of a t-structure $(\mathcal{D}^{\geq 0}, \mathcal{D}^{\leq 0})$ in the triangulated category $\mathcal{D}$. Then, given a torsion pair $(\mathcal{T}, \mathcal{F})$, $\mathcal{D}'^{\geq 0} := \langle \mathcal{D}^{\geq 0}, \mathcal{F}[1] \rangle$ and $\mathcal{D}'^{\leq 0} := \langle \mathcal{D}^{\leq -1}, \mathcal{T} \rangle$ defines a new t-structure, whose heart is $\langle \mathcal{F}[1], \mathcal{T} \rangle$, called the tilted heart.

We follow here the presentation of [Moz22], adapting the constructions of [Bri03] originally made for K surfaces. We consider as above the slope μ_ω. We then define, for $s \in \mathbb{R}$:

- $Coh_{\omega,>s}$ is the full subcategory of $Coh(X)$ generated by μ_ω semistable vector bundles of slope $> s$ and torsion sheaves.
- $Coh_{\omega,\leq s}$ is the full subcategory of $Coh(X)$ generated by μ_ω semistable vector bundles of slope $\leq s$

It is automatically a torsion pair by the general property of slope stability, and we consider the tilted heart:

$$\mathcal{A}_K := \langle Coh_{\omega,\leq B\cdot\omega}[1], Coh_{\omega,>B\cdot\omega} \rangle \tag{3.2.16}$$

Theorem 3.2.9. *([Moz22, Theorem 6.5], generalization of [Bri03, Lemma 6.2]) The central charge $Z_K : E \mapsto (e^{B+i\omega}, ch(E))$ is a stability function $\mathcal{A}_{B,\omega}$, hence $(Z_K, \mathcal{A}_K)$ defines a stability condition on $D^b(X)$.*

Proof (sketch): The existence of Harder-Narasimhan filtration is a technical result using the Noetherianity property. We claim that $Z(E) = me^{i\pi\phi}$ with $m > 0$, $0 < \phi \leq 1$ for any $E \in \mathcal{A}_K$. Recall the formula:

$$Z(E) = (\frac{r(E)}{2}(\omega^2 - B^2) + c_1(E)\cdot B - ch_2(E)) + i(c_1(E) - r(E)B)\cdot\omega \tag{3.2.17}$$

By construction, $\Im(Z(E)) \geq 0$ for $E \in \mathcal{A}_K$. It remains to be proved that one cannot have $Z(E) \in \mathbb{R}_+$. It suffices to show it in the cases:

- If E is torsion, then either E is supported in dimension 0, in which case $Z(E) = -ch_2(E) < 0$, or $\Im(Z(E)) = c_1(E)\cdot\omega > 0$ because ω is ample.
- If E is μ_ω-stable of slope $> B\cdot\omega$, then $\Im(Z(E)) > 0$

- If $E = F[1]$, with F μ_ω-stable of slope $\leq B \cdot \omega$, either $\Im(Z(E)) > 0$, or $\Im(Z(E) = 0$, F is stable of slope $B \cdot \omega$, and:

$$\begin{aligned}\Re(Z(E)) &= \frac{r(F)}{2}(B^2 - \omega^2) - c_1(F) \cdot B + ch_2(F) \\ &\leq \frac{r(F)}{2}(B^2 - \omega^2) - c_1(F) \cdot B + \frac{c_1(F)^2}{2r(F)} \\ &= \frac{1}{2r(F)}(r(F)B - c_1(F))^2 - r(F)\frac{\omega^2}{2} \end{aligned} \tag{3.2.18}$$

  Here we have used in the second line the Bogomolov-Gieseker inequality for the μ_ω-stable bundle F. Remark that, because $\mu_\omega(F) = B \cdot \omega$, $(r(F)B - c_1(F)) \cdot \omega = 0$, and, because $\omega^2 = 0$, from the Hodge index theorem, $(r(F)B - c_1(F))^2 \leq 0$, hence:

$$\Re(Z(E)) \leq -r(F)\frac{\omega^2}{2} < 0 \tag{3.2.19}$$

  which concludes the proof in this case.

Because any element of $\mathcal{A}_K$ is an extension of elements as above, it completes the proof of the claim. Then one can also prove the support property from Bogomolov-Gieseker inequality. □

We have then built stability conditions on X, embedding the complexified Kähler cone of X into the space of Bridgeland stability condition. The central charge on the stringy Kähler moduli space is determined by mirror symmetry, and the formula $Z_K : E \mapsto (e^{B+i\omega}, ch(E))$ is only an asymptotic approximation: we can otherwise expect that it is possible to build a stability condition from the central charges from mirror symmetry in the vicinity of the large volume limit using this tilting procedure (as it is the case for example for local $\mathbb{P}^2$). Remark that the Bogomolov-Gieseker inequality is a crucial ingredient. As analyzed in [BM11] for local $\mathbb{P}^2$, the boundary of the space of stability condition is itself determined by the sharp Bogomolov-Gieseker inequality of [DLP85]. Notice that the Bogomolov-Gieseker inequality can be proven using the Hitchin-Kobayashi correspondence, a further indication of their deep links with brane stability.

We will now explain why the tilting procedure is so important to build stability conditions. Consider a smooth projective complex variety X of dimension n. We will fix a part of the $\mathbb{C}$-action on $\mathrm{Stab}(X)$, by defining $\mathrm{Stab}^0(X)$ as the closed subspace of stability condition such that $Z(\mathcal{O}_x) = -1$ for any $x \in M$ (denoting by $\mathcal{O}_x$ the skyscraper sheaf on X). This restriction only reduces the action of $\mathbb{C}$ to an action of $2\mathbb{Z}$. We define then $\mathrm{Stab}_0^g(X) \subset Stab_0(X)$, the space of geometric stability condition, i.e. stability conditions such that the skyscraper sheaves are stable of phase 1. From the general arguments of [Bri03, section 9], $\mathrm{Stab}_0^g(X)$ is an open subset of $\mathrm{Stab}_0(X)$ delimited by a finite number of codimension one walls, where some skyscraper sheaves are destabilized by some objects. Consider $\sigma \in \mathrm{Stab}_0^g(X)$: we will now compare the heart $Coh(X)$ and the heart $\mathcal{A}$ obtained by taking extensions of semistable objects of phase $0 < \phi \leq 1$ (such that σ is defined equivalently by $(Z, \mathcal{A})$).

Proposition 3.2.10. *([Bri03, Lemma 10.1]) Each object of $\mathcal{A}$ has cohomology in dimensions $[-n+1, 0]$.*

Proof: Consider $E \in \mathcal{A}$. Then for each $x \in M$, $Hom(E, \mathcal{O}_x[i]) = 0$ for $i < 0$ by stability, and $Hom(\mathcal{O}_y[i], E) = Hom(E, \mathcal{O}_y[n+i]) = 0$ (using Serre duality) for $i \geq 0$. Then from [BM99, Prop

5.4], E is quasi-isomorphic to a n-terms complex of locally free sheaves $E^{-n+1} \xrightarrow{d^{-n+1}} E^{-n+2} \to ... \to E^0$. □

For a curve, we find that $\mathcal{A} = Coh(X)$, hence any geometric stability condition has the usual heart. For a surface, $\mathcal{A}$ and $Coh(X)$ must be tilted hearts of the same torsion pair, implying that any geometric stability condition must be built using the above procedure and a similar type of torsion pair. If X is a threefold, which is the case which interest us, it is quite tricky: $\mathcal{A}$ has homological length three. In nice cases, one can built $\mathcal{A}$ by double tilt. It is the construction used in [BMT11]: corresponding to the central charge $Z_K : E \mapsto (e^{B+i\omega}, ch(E))$, the authors have built a heart $\mathcal{A}_K$ by double tilt, on which $\Im(Z(E)) \geq 0$. As for the surface case, the main technical point is to show that one cannot have $Z(E) \in \mathbb{R}_+$ on $\mathcal{A}_K$: this requirement is equivalent to inequalities, which are the only obstruction for proving that $(Z_K, \mathcal{A}_K)$ is a stability condition, and are dubbed 'generalized Bogomolov-Gieseker inequality. They have been shown for $\mathbb{P}^3$ in [Mac12], the quintic threefold in [Li18], and for several other examples, see the references in [BM22, page 15].

3.2.4 Geometric transitions

As we noticed, the constructions using tilts allow for building geometric stability conditions. We will now try to describe the stability conditions on the other side of a wall destabilizing some skyscraper sheaves. Suppose that, on the other side of the wall, we have a smooth projective moduli space Y of stable objects of phase 1 of the same dimension as X, and write $\mathcal{P} \in D^b(X \times Y)$ the tautological sheaf. Denote by p_X, p_Y the projections $X \times Y \to X, Y$, and consider the Fourier-Mukai transform:

$$F := (p_X)_*(\mathcal{P} \otimes (p_Y)^*(\cdot)) : D^b(Y) \to D^b(X) \tag{3.2.20}$$

Then we have the following result from Bondal-Orlov and Bridgeland:

Theorem 3.2.11. *([Bri98, Theorem 1.1] F is an equivalence of category if $Ext^0(\mathcal{P}_y, \mathcal{P}_y) = \mathbb{C}$ for any $y \in Y$, and $Ext^i(\mathcal{P}_y, \mathcal{P}_{y'}) = 0$ for any $y \neq y' \in Y$ and $i \in \mathbb{Z}$, and $\mathcal{P}_y \otimes \omega_X = \mathcal{P}_y$ (this last condition is trivially verified if X is Calabi-Yau).*

In this case, stability conditions across the wall can be interpreted as geometric stability conditions on Y. Sometimes, $Y \simeq X$, hence F is a derived equivalence and corresponds often to a monodromy transform in the stringy Kähler moduli space: the autoequivalence F can then be seen as a 'stringy symmetry', which is not seen by classical geometry, probed by points, but seen by 'stringy geometry', probed by strings and branes. Sometimes one can have $Y \neq X$, hence the wall corresponds to a topology change, and one can say that string theory has interpolated between two geometries that are different classically. If skyscraper sheaves on an open subset of X remain stable (if they are destabilized by objects supported on a closed subset of X), this autoequivalence is associated with a birational transformation between X and Y. Notice that some phases can be more complicated, for example described by an orbifold of a Landau-Ginsburg model.

Natural examples of such walls correspond to extremal contractions in the minimal model program. Any stability condition $\sigma \in \text{Stab}_0(X)$ has a central charge of the form:

$$Z(E) = -v_n(E) + (B + i\omega) \cdot v_{n-1}(E) + ... \tag{3.2.21}$$

If $\sigma \in \text{Stab}_0^g(X)$, a vector bundle $\mathcal{O}_C(D)$ supported on a curve C is automatically in the subcategory $\mathcal{A}((0,1))$ generated by stable objects of phase $0 < \phi < 1$ from the same types of arguments as in

the proof of Proposition 3.2.10, hence one has $\omega \cdot C > 0$, and, because $\mathrm{Stab}_0^g(X)$ is open, ω is ample. When Z varies and ω reaches a codimensional one wall of the nef cone, where $\omega \cdot C = 0$ for a curve C in an extremal ray of the cone of effective 2-cycles, some objects $\mathcal{O}_C(D)$ enters the category $\mathcal{P}(1)$ and destabilize skyscraper sheaves of points of C. We have then, as a particular case of the very general result of [BM12]:

Theorem 3.2.12. *([BM12, Theorem 4.1]) On the boundary of the geometric chambers, two general points of a curve C are S-equivalent if and only if $C \cdot \omega = 0$.*

The general idea (which must be checked in details in concrete cases) is that, on the wall, the normalization of the coarse moduli space is Mori's cone contraction associated with the corresponding wall of the nef cone, and that across the wall one will obtain the flopped manifold. Two birational Calabi-Yau threefolds are related by a sequence of flops, and it was the analysis of such phenomena that led to the proof in [Bri00] of the fact that birational Calabi-Yau threefolds have equivalent derived categories.

Another type of wall is provided by the destabilization of skyscraper sheaves by a spherical object. A spherical object $E \in D^b(X)$ with X of dimension n is an object such that $\mathbf{Hom}(E, E)$ has the homology of a sphere, namely:

$$Ext^i(E, E) = \begin{cases} \mathbb{C} & \text{if } i = 0, n \\ 0 & \text{else} \end{cases} \tag{3.2.22}$$

The mirror of E is then a Lagrangian sphere. The divisor where a Lagrangian sphere has vanishing mass is an exceptional divisor in the complex moduli space of $\check{X}$, and the monodromy around this divisor is given by Dehn twist. In [ST00], the authors described the mirror of this Dehn twist as an autoequivalence of $D^b(X)$ called spherical twist ST_E: For each object F, $T_E(F)$ is in an exact triangle:

$$\mathbf{Hom}(E, F) \otimes E \to F \to T_E(F) \to \mathbf{Hom}(E, F) \otimes E \tag{3.2.23}$$

The first morphism being given by evaluation. In $\mathrm{Stab}_0(X)$, there is a codimension 1 wall where $E \in \mathcal{P}(1)$, and across this wall, skyscraper sheaves $\mathcal{O}_x$ gets destabilized by E and recombine with E to give new stable objects $T_E(\mathcal{O}_x)$. In a compactification of the stringy Kähler moduli space, this codimension 1 wall ends on a codimension 2 divisor, called a conifold divisor, where $Z(E) = 0$, and the monodromy around this divisor is given by T_E. If X is Calabi-Yau, $\mathcal{O}_X$ is spherical, and the conifold divisor of $\mathcal{O}_X$ is often of special importance.

A more general picture was drawn by Szendroï in [Sze01] and Horja in [Hor01] in order to understand more generally the mirror of monodromy of the complex moduli space, where one allows more general objects to have vanishing mass, see [AHK02] for a physically oriented presentation

3.3 Calabi-Yau three singularities

3.3.1 Noncommutative crepant resolutions

Consider a Gorenstein variety X. A crepant resolution of X is a proper birational map $Y \to X$ from a smooth variety Y such that $f^*\omega_X = \omega_Y$. In some sense, it is the 'most economical" resolution because we don't add any new components to the canonical divisor. Crepant resolutions

of a 2-dimensional singularity are isomorphic, and the only 2-dimensional singularities admitting a crepant resolution are singularities $\mathbb{C}^2/G$, with G a finite (hence ADE) subgroup of $SL_2(\mathbb{C})$, which are resolved by an ADE system of (-2) rational curves. In dimension 3, crepant resolutions of a singularity are not all isomorphic but are birational variety; in particular, different crepant resolutions of a CY3 singularity are related by flops. As we have seen above, the space of stability conditions can connect geometric chambers for the different crepant resolutions of a single singularity. We will now see how some regions of the space of stability conditions can also be described by noncommutative geometry as the space of King stability conditions on a quiver with relations.

The notion of noncommutative crepant resolution was introduced in [VdB04], in order to introduce a noncommutative analogue of crepant resolutions. Consider an affine Gorenstein singularity $X = Spec(R)$.

Definition 3.3.1. ([VdB04, Definition 4.1]) A noncommutative crepant resolution of R is a homologically homogeneous R-algebra of the form $A = End_R(M)$ where M is a reflexive R-module.

We try to follow the explanations of Van den Bergh below [VdB04, Definition 4.1]. There is an injection $R \hookrightarrow Z(A)$ into the center of A, which represents the intuitive idea that the 'noncommutative space' with coordinates A surjects on $Spec(R)$. The homological homogeneity condition is a form of smoothness condition for noncommutative rings. The other conditions are the noncommutative analogues of birationnality and crepancy. Birationality is expressed algebraically by the fact that varieties $Spec(R)$ and $Spec(R')$ are birational if and only if their function fields K, K' are isomorphic. As usual in noncommutative geometry, the category of module is a substitute for the spectrum, and hence we must ask that K and $A \otimes_R K$ are Morita equivalents, hence $A \otimes_R K = M_n(K)$. The analogue of crepancy is to ask that the dualizing module $\omega_A = Hom_R(A, \omega_R)$ is generated by ω_R. According to Van den Bergh, this condition is satisfied if and only if A is a maximal order in $A \otimes_R K = M_n(K)$. According to [AG60], all the maximal orders of $M_n(K)$ are of the form $A = End_R(M)$ for R a reflexive R-module, which motivates the definition.

We can write the decomposition of M into indecomposable modules $M = \bigoplus_{i \in Q_0} M_i$, with M_i of dimension δ_i. According to [VdB04, Section 6.3], we can always change M such that A is replaced by a Morita equivalent algebra, in such a way that the M_i are all distinct, and the dimension vector $\delta = (\delta_i)_{i \in Q_0} \in \mathbb{N}^{Q_0}$ is primitive, hence has no nontrivial divisor. In particular, A is basic, and there is then a Gabriel quiver $Q = (Q_0, Q_1)$, an oriented graph with nodes $i \in Q_0$ and arrows $(a : i \to j) \in Q_1$, and an ideal I of the path algebra $\mathbb{C}Q$ of the quiver, the algebra of pah with multiplication given by concatenation, such that $A = \mathbb{C}Q/I$: this construction comes from [Gab72]. We will consider the derived category $D^b(A)$ of finitely generated representations of A and the subcategory $D^b_{fd}(A)$ of complexes whose cohomology is finite-dimensional. The left A-module M_i corresponds to the projective object at i of the quiver Q. Finite dimensional representations of A are then graded by dimension vector $d \in \mathbb{N}^{Q_0}$, a d-dimensional representation of A being equivalent to the data of d_i-dimensional vector spaces V_i for each $i \in Q_0$ and linear maps $\phi_a : V_i \to V_j$ for each $(a : i \to j) \in Q_1$, satisfying the relations of I. In particular, $\Gamma = \mathbb{Z}^d$ is a finite dimensional quotient of the Grothendieck group of $D^b_{fd}(A)$. We are particularly interested in representations of dimension vector δ.

Given $\theta \in \delta^\perp = \{\theta \in \mathbb{R}^{Q_0} | \theta \cdot \delta = 0\}, \rho \in (\mathbb{R}^*_+)^{Q_0}$, we can consider the stability function $Z(d) = -\sum_{i \in Q_0} \theta_i d_i + i \sum_{i \in Q_0} d_i$ on the abelian category $Rep(A)$ of finite dimensional representations of A. It defines a stability condition $(Z, Rep(A))$ on $D^b_{fd}(A)$. We call $\sigma_{\theta,\rho} = (Z_{\theta,\rho}, \mathcal{P}_{\theta,\rho}(\phi))$ its rotation

by a phase $1/2$, with central charge:

$$Z_{\theta,\rho}(d) = -\sum_{i\in Q_0} \rho_i d_i - i\sum_{i\in Q_0} \theta_i d_i + i \tag{3.3.1}$$

$\mathcal{P}_{\theta,\rho}(1)$ does not depend on ρ and is the subcategory of θ-semistable representations of A in the common sense: namely, representations of dimension vector d such that $\theta(d) = 0$, and such that for any subobject of dimension d', $\theta(d') \leq 0$. There is a map $f_d : X_d^{\theta,s} \to X = Spec(R)$ from the fine moduli space of θ-stable representations of A, as proven in [VdB04, Proposition 6.21]. At the level of points, notice that from the Schur lemma, a stable representation has only scalar endomorphisms, hence the action of R on a stable representation V specify the coordinates of the point $p(V) \in Y$.

The dimension vector δ is primitive, and then there is a decomposition of $\mathbb{R}^{Q_0}$ into a finite number of conical chambers, with a finite number of codimension 1 walls, such that inside chambers all δ-dimensional θ-semistable representations are θ-stable, and stay stable inside chambers, hence there is a fine moduli space X_δ^C of stable objects of dimension δ for each chamber. Van den Bergh proves that over the open locus X_1 where M is locally free, $(f_\delta^C)^{-1}(X_1) \to X_1$ is an isomorphism. Consider now the irreducible component Y^C of X_δ^C containing $(f_\delta^C)^{-1}(X_1)$. It is proven a posteriori in [VdB04, Remark 6.6.1] that Y^C is in fact a connected component of X_δ^C, but it is not clear if there can be other connected components. The main result of [VdB04] is:

Theorem 3.3.2. *([VdB04, Theorem 6.3.1]) If X is of dimension ≤ 3, then the $Y^C \to X$ are crepant resolutions, and there is for each chamber a natural derived equivalence $D^b(A) \simeq D^b(Y^C)$.*

This derived equivalence is built using Fourier-Mukai transform. It restricts to a derived equivalence $D^b_{fd}(A) \simeq D^b_c(Y^C)$ with the category of complexes whose cohomology has compact support. The proof is a generalization of the proof of [BK01] in the case of the McKay correspondence, which we will expose below. It is a justification a-posteriori of the interest of the definition of noncommutative crepant resolutions: they give a procedure to build (commutative) crepant resolutions. Moreover, the derived equivalence fits with the Bondal-Orlov conjecture that crepant resolutions must be derived equivalents and with the Kontsevich-Rosenberg philosophy of expressing noncommutative geometry using derived categories. A converse direction, allowing to build noncommutative crepant resolutions from commutative ones, works for small crepant resolutions of affine singular threefolds from [VdB04, Theorem 5.1]. It does not work in full generality, even for CY3; counterexamples were given in [Dao10]: In particular, $\mathbb{C}[x_0, x_1, x_2, x_3]/(x_0^4 + x_1^3 + x_2^3 + x_3^3)$ admits a commutative crepant resolution but no noncommutative ones.

We will denote $\mathrm{Stab}(Y^C) := \mathrm{Stab}(D^b_c(Y^C))$, with central charges factoring through homology with compact support. Using $D^b_{fd}(A) \simeq D^b_c(Y^C)$, we have built an open immersion:

$$\sigma : \delta^\perp \times (\mathbb{R}_+^*)^{Q_0} \to \mathrm{Stab}_0(Y^C) \tag{3.3.2}$$

Which sends $Y^C \times (\mathbb{R}_+^*)^{Q_0}$ to $\mathrm{Stab}_0^g(Y^C)$, and the walls of Y^C correspond to some walls of $\mathrm{Stab}_0^g(Y^C)$, inducing topological transitions between Y^C and $Y^{C'}$, for C' the adjacent chamber. Noncommutative crepant resolutions give a way to describe some parts of the space of stability conditions of crepant resolutions by King stability on quivers with relations. Using the wall crossing relations that we will introduce below, it allows going go back and forth between counting of sheaves and counting of quiver representations.

We will now be interested in noncommutative crepant resolutions of affine singular CY3, whose most salient classes of examples will be developed in the next sections (remark that local $\mathbb{P}^2$ will fit in each of these classes). As we will explain below, the Serre duality imposes that the derived category of a smooth CY3 variety is a CY3 category, hence that A is a CY3 algebra. It imposes constraints on the relations I, namely that these relations must be derived from a potential, at least in a formal sense, from [VdB04]. A potential W on a quiver Q is a (potentially formal) linear combination of oriented cycles of Q, where cycles are considered up to cyclic permutations. Alternatively, a potential is an element $W \in \mathbb{C}Q/[\mathbb{C}Q, \mathbb{C}Q]$ of the commutant of the path algebra (or its completion). The cyclic derivative of an oriented cycle w is defined by

$$\partial_a w = \sum_{i:a_i=a} a_{i+1}...a_n a_1...a_{i-1} \tag{3.3.3}$$

This formula is extended to $\mathbb{C}Q/[\mathbb{C}Q, \mathbb{C}Q]$ by linearity. The cyclic derivatives of the potential define the ideal $(\partial W) = ((\partial_a W)_{a\in Q_1})$. The Jacobian algebra is the quotient $J_{Q,W} = \mathbb{C}Q/(\partial W)$ (or the quotient of the completed path algebra) and is isomorphic with A (or its completion). We will consider here for simplicity that the potential is a finite sum of cycles, hence we don't have to pass to the completions, which is the case in the examples that we will present.

Singularities with crepant resolutions exist in at least two codimensions; hence, in an affine CY3 singularity with a crepant resolution, there is a singularity at the origin, and there can be affine lines of extended singularities of the form $\mathbb{C}^* \times \mathbb{C}^2/G$, with G an ADE subgroup of $SL_2(\mathbb{C})$. These extended singularities are resolved by $\mathbb{C}^* \times (\tilde{\mathbb{C}^2/G})$, with $(\tilde{\mathbb{C}^2/G})$ the CY2 resolution of $\mathbb{C}^2/G$ by an ADE system of (-2) rational curves.

3.3.2 Toric singularities

Toric singularities are classified by their toric cone in a lattice $M^\vee$. For a toric CY3 singularity, one has a splitting $M^\vee = L^\vee \times \mathbb{Z}$, and the toric cone is necessarily the three-dimensional cone $\mathbb{N}(\{1\} \times D)$, with D a polygon of the two dimensional lattice $L^\vee$, called the toric diagram. We denote by $M^+ \subset M$ the dual cone. Extremal rays of the dual cone are in correspondence with sides z of the toric diagram D and correspond to toric coordinates x_z, and the equations satisfied by these coordinates can be read from the dual cone. More precisely, we have $X = Spec(\mathbb{C}[M^+])$. We denote by K_z the number of subdivisions of the edge z of the toric diagram: one has in particular:

$$X - x_z^{-1}(0) \simeq \mathbb{C}^* \times \mathbb{C}^2/\mathbb{Z}_{K_z} \tag{3.3.4}$$

They are the only extended singularities of X, and they are of type A (which is logical because type D and E singularities are not toric). Interior nodes of the toric diagram will correspond to a compact divisor, resolving the singularity in a crepant resolution.

Noncommutative crepant resolutions by quiver with potentials can be associated with a toric CY3 singularity by a procedure called the 'fast inverse algorithm', described by Hanany and Vegh in [HV07]. [Boc11] and [Bro11] proved that this procedure furnishes indeed a NCCR. Namely, one considers the two-dimensional torus $L \otimes \mathbb{R}/L$, and one draws K_z rays of direction $l_z \in L$ (the direction dual to z) for each side z of D, in general position. Different choices of position would lead to quivers with potentials linked by mutations. The complement of these lines determines polygonal domains, or tiles, with oriented edges. We color those tiles white, dark gray, or light gray according to the orientations of their edges:

- If the edges of the tile are oriented in a clockwise direction around the tile, we color the tile dark gray.
- If the edges of the tile are oriented in a counter-clockwise direction around the tile, we color the tile light gray.
- If the orientations of the different edges of the tile do not agree, we color the tile in white

We define a brane tiling on the torus by putting a black node in each dark gray tile, a white node in each light gray tile, and connecting a black node and a white node if the corresponding tiles are connected at one of their corners. The white tiles are then in correspondence with tiles of the brane tiling.

Definition 3.3.3. The quiver with potential (Q, W) associated with a brane tiling is defined as the dual of this brane tiling, i.e. :

- The set of nodes Q_0 of the quiver is the set of tiles of the brane tiling.
- The set of arrows Q_1 of the quiver is the set of edges of the brane tiling. An edge of the tiling between two tiles gives an arrow of the quiver between the two corresponding nodes, oriented such that the black node is at the left of the arrow.
- Denote by Q_2 the set of nodes of the brane tiling, and Q_2^+ (resp. Q_2^-) the subset of white (resp. black) nodes. To a node $F \in Q_2$ one associates the cycle w_F of Q composed by arrows surrounding this node. We define:

$$W = \sum_{F \in Q_2^+} w_F - \sum_{F \in Q_2^-} w_F \tag{3.3.5}$$

We give below an example of this procedure in the cases of $Y = \mathbb{C}^3$, $\mathbb{C}^2/\mathbb{Z}_2 \times \mathbb{C}$ and local $\mathbb{P}^2$

$\mathbb{C}^3$:

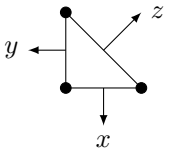

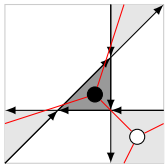

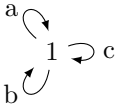

$W = abc - acb$

$\mathbb{C}^2/\mathbb{Z}_2 \times \mathbb{C}$:

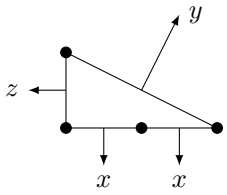

Hypersurface $x^2 - yz = 0$ in $\mathbb{C}^3$.

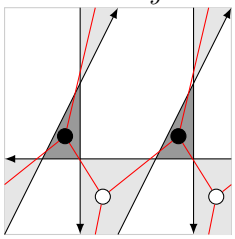

Local $\mathbb{P}^2$ / $\mathbb{C}^3/\mathbb{Z}_3$:

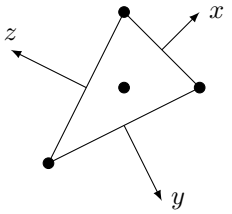

Hypersurface $xyz = w^3$ in $\mathbb{C}^4$.

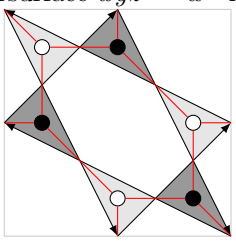

For $\mathbb{C}^3$ we find that the Jacobi algebra of this quiver with potential is:

$$J_{Q,W} = \mathbb{C}\langle x, y, z\rangle/([x, y], [y, z], [z, x]) = \mathbb{C}[x, y, z] = \mathbb{C}[\mathbb{C}^3] \tag{3.3.6}$$

The noncommutative resolution seems trivial because there is no singularity to resolve: one has trivially $Coh(\mathbb{C}^3) = Rep(\mathbb{C}[x, y, z])$ because $\mathbb{C}^3$ is affine. But this representation allows presenting the moduli space of sheaves on $\mathbb{C}^3$ globally as the critical locus of the function $\mathrm{Tr}(W)$ in the moduli space of representations of Q, which will be of special interest to study DT invariants.

For $\mathbb{C}^2/\mathbb{Z}_2\times\mathbb{C}$, we observe that the edge z has two subdivisions, corresponding to the $\mathbb{Z}_2$ extended singularity in the direction z. Notice that the two lines with direction l_z divide the torus into two strips. The dimension vector corresponding to the indicator function of such strips will be denoted as $\alpha^z_{[k,k'[}$, and is the dimension vector of curves resolving the type A extended singularities, which will carry Donaldson-Thomas invariants of particular importance in the localization computation of Chapter 7.

The case of $\mathbb{C}^3/\mathbb{Z}_3$, resolved by the local $\mathbb{P}^2$ is particularly interesting, its space of stability condition was studied in [BM11]. It is the simplest case with a compact divisor, where the DT invariants are not known to be expressible by a closed formula. Moreover, it fits also in the class of cones over a del Pezzo surface and in the class of orbifolds (the singularity is $\mathbb{C}^3/\mathbb{Z}_3$), which will be studied in the next section.

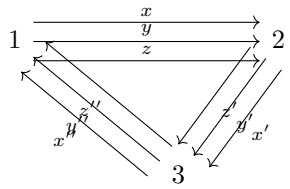

$$W = z''y'x + x''y'x + y''x'z - z''x'y - y''z'x - x''y'z$$

For a general toric quiver, the dimension vector δ that will give skyscraper sheaves of crepant resolutions is $\delta = (1)_{i\in Q_0}$. As said in the last section, there is a chamber decomposition of $\mathbb{R}^{Q_0}$ such that in each chamber C, the moduli space Y^C of δ-dimensional stable representations provides a crepant resolution of X (here there are no other connected components). It was shown in [IU16], elaborating on [CI02], that each crepant resolution arises in this way, hence that a single noncommutative resolution produces all the commutative resolutions. It is likely to be a general fact for noncommutative crepant resolutions of CY3 singularities. Alternatively, crepant resolutions Y of X are in correspondence with triangulations of the toric diagram. The dual of a triangulation, called the string web, gives all the information about the orbits of the torus $(\mathbb{C}^*)^3$ in Y. There is a 3-dimensional orbit; interior (resp exterior) faces of the string web correspond to compact (resp noncompact) divisors; the lines correspond to lines; and trivalent intersection points correspond to fixed points of the torus action. Incomplete triangulations, with some faces that are not triangles, give incomplete resolutions. Flipping an edge inside a square corresponds to a flop. Each orbit corresponds to a subset of arrows that vanishes in the δ-dimensional representations corresponding to the skyscraper sheaves of the orbit; see [Moz09]. The procedure consisting of finding the data of the toric diagram from a toric quiver with potential is called the fast forward algorithm.

3.3.3 McKay correspondence

We are now interested in CYn singularities of the form $X = \mathbb{C}^n/G$, with $G \subset SL(\mathbb{C}^n)$. This example is [VdB04, Example 1.1]. We have $X = Spec(R)$ with $R = \mathbb{C}[x_1, ..., x_n]^G$. Then $S = \mathbb{C}[x_1, ..., x_n]$ is a reflexive R-module, and $A = End_R(S)$ is a noncommutative crepant resolution of X. This was in fact the case where the authors of [BK01] proves a theorem similar to Theorem 3.3.2, which inspired the notion of noncommutative crepant resolution. They were also studied by physicists before the formalization of the concept of Bridgeland stability conditions in [DM96]: physicists have found that in compactifications of type IIA string theory on CY $X = \mathbb{C}^n/G$, in some part of the stringy Kähler moduli space, the 'D0 branes', i.e. the skyscraper sheaves, were decaying, being replaced by 'fractional branes' corresponding to irreducible representations of G.

We will now give a description of the Gabriel quiver of such a resolution, which was given by McKay for $SL_n(\mathbb{C})$ and Auslander in the general case. This quiver is called the McKay quiver of G. We consider the twisted algebra $S\#G$: there is an obvious morphism $S\#G \to End_R(S) = A$ which extends S-linearly the action of G on S. Auslander proves in [Aus62] that this gives an isomorphism $S\#G \to End_R(S)$ if $G \subset SL_n(\mathbb{C})$. There is then a bijection between indecomposable summands of S as a R module, i.e. nodes of the Gabriel quiver, and indecomposable summands of $S\#G$ as a $S\#G$-module. We can associate to each finite dimensional representation V of G a $S\#G$-module $S \otimes G$, and to each $S\#G$-module P a finite dimensional representation $P/\mathfrak{n}P$ of G, where $\mathfrak{n} = (x_1, ..., x_n) \subset \mathbb{C}[x_1, ..., x_n]$. It establishes a bijection between indecomposable summands of $S\#G$ and irreducible representations of G. Hence the nodes of the Gabriel quiver correspond with irreducible representations of G (including the trivial representation).

Using this correspondence, the number of arrows $i \to j$ from the node corresponding to ρ_i to the node corresponding to ρ_j is the number of summands isomorphic to ρ_i in $\rho_j \otimes V$, where $V = \mathbb{C}^n$ is the fundamental representation. We can associate to each arrow $a : i \to j$ and element ψ_a of a basis of $Hom_G(\rho_j \otimes V, \rho_i)$. It defines a surjection $\mathbb{C}Q \to A$. A general description of its kernel I defining $A = \mathbb{C}Q/I$ is provided in [BSW08, Theorem 3.2].

For $n = 2$, we have $G \subset SL_2(\mathbb{C})$ is an ADE subgroup, and A is the preprojective algebra associated with the affine Dynkin quiver associated with G. Namely, the extended Dynkin quiver is an unoriented graph, and we associate to each node of this graph a node of the McKay quiver Q, and to each edge a couple of arrows going in the opposite direction. The relations are quadratic and are the preprojective relations.

For $n = 3$, we will give the formula of [BSW08, Theorem 3.2]. The relations come from a potential $W = \sum_w \nu_w w$, where the sum is made over the oriented cycle of length 3 considered modulo permutations, and we will give a formula for ν_w. For a path $v : i \to j$ of length l, we consider the morphism $\phi_l^* : \rho_i \to \rho_j \otimes V^{\otimes n}$ obtained by composing the $\psi_a^* : \rho_k \to \rho_{k'} \otimes V$ for each arrow $a : k \to k'$ in the path. For $w : i \to i$ a cycle of length 3, we consider the morphism:

$$\rho_i \overset{\psi_w^*}{\to} \rho_i \otimes V^{\otimes 3} \overset{Id_{\rho_i} \otimes \alpha^3}{\to} \rho_i \otimes \Lambda^3 V \simeq \rho_i \tag{3.3.7}$$

Where $\alpha^3 : V^{\otimes 3} \to \Lambda^3 V$ is the symmetrizer, and we have used in the last isomorphism the fact that $G \subset SL_3(\mathbb{C})$. From the Schur lemma, this morphism is a scalar that we denote by c_w, and we define $\nu_w := dim(\rho_i) c_w$. One can check that this number does not depend on the basepoint i.

We will now explain how to construct the McKay quiver and its potential for the orbifold $\mathbb{C}^3/\mathbb{Z}^3$, with the diagonal action (ω, ω, ω) of $\mathbb{Z}_3$ (we denote $\omega = e^{2i\pi/3}$). The group is abelian, and has three

one-dimensional representations: $\rho_1, \rho_\omega, \rho_{\omega^2}$. We have that $Hom(\rho_{\omega^{n+1}} \otimes \mathbb{C}^3, \rho_\omega)$ is 3 dimensional, and is generated by the 3 projections x, y, z. Hence the McKay quiver that we obtain is the same quiver as the one obtained by brane tiling, considering $\mathbb{C}^3/\mathbb{Z}^3$ as a toric singularity, and one can easily check using the above procedure that one finds the same 'antisymmetrized' potential.

3.3.4 Cones over (weak) del Pezzo surfaces

This case was discussed in [VdB04, Section 7].Consider a weak del Pezzo surface S, the homogeneous coordinate ring $R := \bigoplus i \in \mathbb{N}\Gamma(S, \omega_S^{-n})$, and the Calabi-Yau cone $X_S = Spec(R)$ over S. Because ω_Z is big and nef, X_S is a singular CY3, which admits a crepant resolution $Y_S \to X_S$ by the total space of ω_Z^{-1}. We have the following diagram:

$$\begin{array}{ccc} Y_S & \xrightarrow{\pi} & S \\ \downarrow f & & \\ X_S & & \end{array}$$

If S is del Pezzo, hence ω_Z^{-1} is ample, there is only a singularity at 0, resolved by S. In the general case, effective curves on S with vanishing intersections with the anticanonical divisors form disjoint ADE systems of (-2) rational curves. They produce extended singularities of ADE type in the cone X_S, which are resolved in Y.

Consider now a tilting sequence of sheaves on S, i.e. a collection $(E_1, ..., E_n)$ such that $\mathrm{Ext}^k(E_i, E_j) = 0$ for $k \neq 0$ which generates $D^b(S)$. There is a quiver Q with relations I and set of nodes $Q_0 = \{1, ..., n\}$, such that the endomorphism algebra $End(\bigoplus_{i=1}^n E_i)$ is isomorphic to $\mathbb{C}Q/I$. There is an equivalence of categories:

$$\mathbf{Hom}(\bigoplus_{i=1}^{n} E_i, \cdot) : D^b(S) \to D^b(\mathbb{C}Q/I) \tag{3.3.8}$$

If one supposes moreover that E is a full strongly exceptional collection, i.e. that $\mathrm{Ext}^0(E_i, E_j) = 0$ for $i > j$, then there are only arrows $i \to j$ for $i \leq j$ in $\bar{Q}$: $\bar{Q}$ is a quiver without oriented loop. The simplest full strongly exceptional collection is the Beilinson sequence $(\mathcal{O}, \mathcal{O}(1), \mathcal{O}(2))$ on $\mathbb{P}^2$, with the corresponding quiver:

$$1 \;\begin{array}{c}\xrightarrow{x}\\ \xrightarrow{y}\\ \xrightarrow{z}\end{array}\; 2 \;\begin{array}{c}\xrightarrow{x'}\\ \xrightarrow{y'}\\ \xrightarrow{z'}\end{array}\; 3 \qquad\qquad I = (x'y - y'x, y'z - z'y, z'x - x'z)$$

The relations gives the commutation of x, y, z. Strongly exceptional full collections were built on any del Pezzo surface in [KO95], and it was shown that any two such collections on a del Pezzo surface are linked by mutations. For construction of exceptional collections on weak del Pezzo surfaces, see [Per08].

Now, consider the collection $(\pi^* E_1, ..., \pi^* E_n)$ of $D_c^b(Y_S)$, which generates $D^b(Y_S)$. The algebra $End(\bigoplus_{i=1}^n \pi^* E_i)$ is then the Jacobi algebra $J_{Q,W}$ of a quiver with potential (Q, W) with set of nodes $Q_0 = \bar{Q}_0$. We have an equivalence:

$$\mathbf{Hom}(\bigoplus_{i=1}^{n} \pi^* E_i, \cdot) : D^b(Y) \to D^b(J_{Q,W}) \tag{3.3.9}$$

which restricts to an equivalence $D^b_c(Y_S) \to D^b_{fd}(J_{Q,W})$. It was shown in [VdB04, Proposition 7.2] that $J_{Q,W}$ gives a noncommutative crepant resolution of X_S when S is del Pezzo, and we expect that this is still true when S is weak del Pezzo.

There is a nice relation between (Q, W) and $(\bar{Q}, I)$ We remark that π^* injects $End(\bigoplus_{i=1}^n E_i)$ into $End(\bigoplus_{i=1}^n \pi^* E_i)$, hence Q is obtained from $\bar{Q}$ by adding arrows. Namely, there is a set of arrows $J \subset Q_1$, such that $\bar{Q}$ is obtained from Q by removing the arrows of J, i.e. $\bar{Q} = (Q_0, Q_1 - J)$, and such that the relations of I are the relations imposed by the arrows of J, namely $I = (\partial_a W)_{a \in J}$. More precisely, the potential is of the form $W = \sum_{a \in J} a \partial_a W$. The construction of (Q, W) from $(\bar{Q}, I)$ is a noncommutative analogue of taking the Calabi-Yau cone over a surface. This procedure can in fact be done at the level of triangulated categories and is called a Calabi-Yau completion. For the case of $\mathbb{P}^2$, we obtain the McKay quiver that we have seen above.

3.4 Donaldson-Thomas theory

3.4.1 Perverse sheaves and enumerative geometry

We consider a (possibly singular) algebraic variety X. A Whitney stratification of X is a locally finite partition $\mathcal{S}$ of X into locally closed smooth subschemes $S \in \mathcal{S}$ called strata, such that the frontier $\partial S = \bar{S} - S$ of any strata is a finite union of strata, and with some technical assumptions expressing the fact that the strata have in some sense the same type of singularity. A Whitney stratification provides a way to separate the different levels of singularity in a scheme. A fundamental result of Whitney says that every algebraic variety has a Whitney stratification. A constructible sheaf on X is then a sheaf on X whose stalk at each point is finitely generated and such that there exists a Whitney stratification $\mathcal{S}$ of X, with $F|_S$ a local system for each strata $S \in \mathcal{S}$. The derived category $D^b_{cons}(X)$ is then the derived category of complexes of sheaves whose homology is constructible. In a rough sense, a constructible complex in $D^b_{cons}(X)$ is obtained by gluing shifts of local systems on locally closed subvarieties of X.

Now, it is possible to define a t-structure $({}^p(D^b_{cons})^{\leq 0}, {}^p(D^b_{cons})^{\geq 0})$ on $D^b_{cons}(X)$, called the perverse t-structure, whose Abelian heart $Perv(X)$ will be of great interest and behaves better than the heart of constructible sheaves when X is singular. ${}^p(D^b_{cons})^{\leq 0}$ consists of complexes F whose j-th cohomology has support of dimension $\leq -j$, and ${}^p(D^b_{cons})^{\geq 0}$ is given dually by complexes F whose Verdier dual $\mathbb{D}F$ satisfies the same condition. Perverse sheaves are then objects adapted to stratifications of X.

The simple objects of $Perv(X)$ are easy to describe. Consider a locally closed subset Y and an irreducible local system $\mathcal{L}$ on Y. There is a unique way to extend $\mathcal{L}[dim(Y)]$ to a simple perverse sheaf on $\bar{Y}$, and by pushforwarding it into X, we obtain a perverse sheaf $\mathcal{IC}(Y, \mathcal{L}) \in Perv(X)$. A fundamental property of $Perv(X)$ is that any perverse sheaf has a Jordan-Hölder filtration into simple perverse sheaves, and that the simple objects of $Perv(X)$ are exactly the $\mathcal{IC}(Y, \mathcal{L})$ for $\mathcal{L}$ irreducible. This can be thought of as a kind of continuity property: a simple perverse sheaf is determined by its value on a dense open subset of its support. Now, if a perverse sheaf is moreover pure in the sense of Deligne theory of weights, it is semisimple, and then a sum of simple objects. The main tool to deal with perverse sheaves is the decomposition theorem of [BBDG83]

Theorem 3.4.1. *Given a proper map $f : X \to Y$ and a pure perverse sheaf $F \in Perv(X)$, then $f_*(F)$ is pure and then a direct sum of shifts of simple perverse sheaves in $Perv(Y)$*

When X is smooth and Y is possibly singular, hence f is a resolution of singularity, and we apply this result to $\mathbb{Q}_X[dim(X)] \in Perv(X)$, the shifted structure sheaf, this decomposition gives the stratification of Y according to the type of fiber. Hence perverse sheaves, combined with purity, are the good objects to feel stratification of singular spaces and singular fibrations.

We will now try to understand the relevance of perverse sheaves from two different points of view. The first is the Riemann-Hilbert correspondence. For a presentation aimed at physicists, see [xHKK20, Section 3.4]. There is correspondence between differential equations on X with regular singularities and local systems on dense open subsets of X, obtained by taking the solutions. Now, a differential equation can be encoded by a D-module. Consider the sheaf D_X of differential operators on X, which is a sheaf of $\mathcal{O}_X$-algebras generated by vector fields. A D-module is then a coherent sheaf on X with a structure of D_X-module. Considering a differential operator P on X, it gives a D-module $F = D_X/P \cdot D_X$. Higher-dimensional D-modules correspond to differential systems with several unknowns. Local solutions of the differential equations $P(X) = 0$ (or of the system encoded by the D-module F) correspond to sections of the sheaf $Hom(\mathcal{O}_X, F)$. We restrict now to regular holonomic D-modules, which form an Abelian heart of the derived category of D-modules, and generalize the notion of differential equation with regular singularities. The sheaf of local sections $Hom(\mathcal{O}_X, F)$ forgets some useful homological information, which is reflected by the fact that the equation has no solution at singular points. For this reason, it is better to consider the homological resolution of Hom in the derived category of sheaves:

$$Sol(F) := \mathbf{Hom}(\mathcal{O}_X, F) \tag{3.4.1}$$

Then $Sol(F)$ is a constructible complex, and one has:

Theorem 3.4.2. *(Riemann-Hilbert correspondence) The functor Sol induces an equivalence of categories between the Abelian category of holonomic D-modules and the Abelian category $Perv(X)$ of perverse sheaves (over $\mathbb{C}$).*

A perverse sheaf can then be thought of as an holonomic D-module; in particular, the interpretation of $\mathcal{IC}(Y, \mathcal{L})$ is simpler in this category: it is the holonomic D-module whose local solutions on Y are given by the local system $\mathcal{L}$. The decomposition theorem can then be seen as a decomposition of holonomic D-modules into simple ones.

We give now the second point of view on perverse sheaves, Grothendieck's function-sheaves correspondence, which is of interest for enumerative geometry. It takes its roots in the proof of the Weil conjectures. For X an algebraic variety defined over $\mathbb{Z}$, the Weil conjectures link the counting of points of X over finite fields and the cohomology of X over $\mathbb{C}$. It has been a guiding motivation in the introduction by Grothendieck and its school of the notion of scheme in order to treat on an equal footing varieties over finite fields and on $\mathbb{C}$. A second step was to create a cohomology theory for algebraic varieties over any base field, which coincides with usual cohomology over $\mathbb{C}$. It was provided with étale cohomology, a sheaf cohomology arising from the topology where sheaves are glued using étale maps. In order to be as interesting over finite fields as they are over $\mathbb{C}$, the coefficient fields of this topology must be the non-Archimedean fields $\mathbb{Q}_l$, for l a prime different from the characteristic of the finite fields. We work then in the derived category $D^b_{cons}(X, \mathbb{Q}_l)$ of $\mathbb{Q}_l$-constructible complexes. Consider now a variety X over the finite fields $\mathbb{F}_q$, with closure $\mathbb{F}_{\bar{q}}$, and consider the Frobenius $F : X \to X$, acting on coordinates by $x \mapsto x^q$. The points $X(\mathbb{F}_q)$ of X over $\mathbb{F}_q$ corresponds to fixed points of F in $\bar{X} := X \times_{\mathbb{F}_q} \mathbb{F}_{\bar{q}}$. The Grothendieck-Lefschetz formula is then

the central ingredient to the proof of the Weil conjectures:

$$|X(\mathbb{F}_q)| = \sum_i (-1)^n \mathrm{Tr}(F^*, H_c^i(X, \mathbb{Q}_l) \tag{3.4.2}$$

(3.4.2) is in fact a particular case of the very general Grothendieck function-sheaf dictionary, which we will present now. For a constructible complex $K \in D^b_{cons}(X, \mathbb{Q}_l)$, consider the function on $X(\mathbb{F}_q)$:

$$t_K : x \mapsto \sum_i (-1)^i \mathrm{Tr}(F^*, \mathcal{H}^i(K_x)) \tag{3.4.3}$$

Here K_x denotes the stalk of K at x. It is a constructible function $t_K \in \mathcal{C}(X(\mathbb{F}_q), \mathbb{Q}_l)$. Let $f : X \to Y$ be a morphism of varieties over $\mathbb{F}_q$. Then we can define the pullback:

$$\begin{aligned} f^* :& \mathcal{C}(Y(\mathbb{F}_q), \mathbb{Q}_l) \to \mathcal{C}(X(\mathbb{F}_q), \mathbb{Q}_l) \\ & f^* t(x) = t \circ f(x)) \end{aligned} \tag{3.4.4}$$

And the proper pushforward (integration over the fibers):

$$\begin{aligned} f_! :& \mathcal{C}(X(\mathbb{F}_q), \mathbb{Q}_l) \to \mathcal{C}(Y(\mathbb{F}_q), \mathbb{Q}_l) \\ & f^* t(y) = \sum_{x \in X(\mathbb{F}_q) | f(x) = y} t(x) \end{aligned} \tag{3.4.5}$$

Now we have the fundamental result:

Theorem 3.4.3. *(Grothendieck trace formulas) The map $K \to t_K$ intertwines the pullback and proper pushforward of constructible complexes and functions.*

Applies this now to the constant sheaf $\mathbb{Q}_l$ on X: we have $t_{\mathbb{Q}_l} = 1$, and consider the map $f : X \to pt$ to a point. Clearly $f_! t_{\mathbb{Q}_l} = |X(\mathbb{F}_q)|$, and $f_*(\mathbb{Q}_l)$ is the cohomology with compact support of X, i.e. $t_{f_*(\mathbb{Q}_l)}$ is the right hand side of (3.4.2), hence one recover the Grothendieck Lefschetz formula as a special case of the Grothendieck trace formula.

We have thus seen that to translate an arithmetic problem over finite fields to a geometrical problem over $\mathbb{C}$, it is useful to use the function-sheaf dictionary and to replace a function t by a constructible complex K such that $t_K = t$. To have some multiplicity, one must restrict oneself to some Abelian heart of $D^b_{cons}(X, \mathbb{Q}_l)$. It is a very deep result than the map

$$t. : Perv(X) \to \mathcal{C}(X(\mathbb{F}_q), \mathbb{Q}_l) \tag{3.4.6}$$

is injective. Given a function of arithmetical interest over a finite field, it is then interesting to search to see if there is a (necessarily unique) perverse sheaf representing it. The results of the decomposition theorem appear then as a kind of continuity result for functions, as we have seen above.

3.4.2 The Donaldson-Thomas perverse sheaf

We are now interested in constructing invariants counting (semistable) branes in type II theory compactified on a CY3-fold, or, analogously, (semistable) objects in a CY3 dg category. We will

first introduce (quite informally) derived algebraic geometry, which is the good language to deal with moduli spaces (or stacks) of such objects. See [Toë14] for a nice introduction to derived algebraic geometry.

Scheme theory applies the fundamental idea of differential geometry—namely, defining a manifold as a topological space with local coordinates and changes of coordinates—to algebraic geometry. Namely, a scheme is a topological space that is locally homeomorphic to the spectrum of a ring with 'change of coordinates rules'. These data are encoded into a locally ringed space, a topological space with a sheaf of rings that is locally the natural ringed space over the spectrum of a ring. One can then do locally algebraic constructions with rings and glue them together to obtain scheme constructions. A common construction is the intersection $Y \cap Z$ of two closed subschemes Y, Z of a scheme X. Locally, one has $X = Spec(R), Y = Sec(S), Z = Spec(T)$, and one has surjective ring morphisms $S \to R$, $T \to R$ corresponding to the closed embeddings. One defines locally:

$$Y \cap Z = Spec(S \otimes_R T) \tag{3.4.7}$$

Hence, intersections (and more generally, fiber products) are locally modeled on tensor products of rings. Even if X, Y, Z are smooth, if Y and Z do not intersect transversely, this intersection is not smooth and does not well take into account multiplicities of intersection. We want to build an intersection theory by counting the homology classes of the intersection, which would be constant under deformations of Y and Z, and would give the class of $Y \cap Z$ when Y, Z intersect transversely. This is done by the classical intersection theory; see [Ful98]. The theory is really technical, but the main idea is that it is not always possible to perturb X, Y in a geometrical way to have a transverse intersection, but it is possible to perturb them homologically. Hence, homological techniques seem to be very important to deal with singular phenomena in algebraic geometry.

The main idea of derived algebraic geometry is to place these homological techniques at the heart of the definition of the spaces themselves. Namely, instead of considering rings of coordinates, one should consider dg-algebra of coordinates, where the complex gives a resolution of the ring of coordinates. The change of coordinates must be given by the quasi-isomorphism of dg-algebra. More formally, a derived scheme is a topological space with a sheaf of dg-algebra (i.e. with value in the ∞-category of dg-algebra modulo isomorphism) that is locally isomorphic to the spectrum of a dg-algebra. The topology of a derived scheme depends only on the 0-th homology of the sheaf of dg-algebra; hence, one can define a functor of classical truncation from derived schemes to schemes. A derived scheme is then a scheme with some extra structure, giving information about the obstructions. Now, all the operations of algebraic geometry can be done on a derived scheme, but they are translated in a derived way. For example, the derived intersection of derived schemes will be defined by:

$$Y \overset{L}{\cap} Z = Spec(S \overset{L}{\otimes}_R T) \tag{3.4.8}$$

where we have taken the derived tensor product of the dg-algebras S, T over R. Now, the derived structure of $Y \overset{L}{\cap} Z$ encodes all the homological data of classical intersection theory.

In general, when one tries to classify objects in algebraic geometry, one obtains not a scheme but a stack, or a higher stack. Such objects are described as functors of points. The idea is that in a moduli problem, there is a natural way of defining a family of objects over a base M (which can be taken to be affine) and restricting such a family. Hence, to a first approximation, a moduli problem

can be seen as a presheaf $(Sch^{aff})^{op} \to set$ on the category Sch^{aff} of affine schemes, which is by definition the opposite of the category of commutative rings. Now, if we incorporate the data of the automorphisms of the objects, we obtain a presheaf of groupoid, and if we classify objects in a *dg*-category, which have higher automorphisms classified by negative Ext, we obtain a presheaf of ∞-groupoid. The fact that we can glue families of objects is expressed by the fact that this presheaf is a sheaf for the faithfully flat and locally of finite presentation topology (ffpf). Hence, a (higher) stack is defined as a sheaf of (∞) groupoid for the ffpf topology on Sch^{aff}. In derived algebraic geometry, one wants to consider families on derived affine schemes; hence, a (higher) derived stack is defined as a sheaf of (∞) groupoids for the ffpf topology on $d - Sch^{aff}$, the category of affine derived schemes, which is opposite to the category of dg-algebras. The nicest (derived) stacks are representable by (derived schemes). A larger, but still manageable, class is the class of Artin, or algebraic (higher, derived) stacks, which are in some sense stacks with some covering by a smooth scheme.

Given a higher derived stack X, derived algebraic geometry naturally builds a tangent obstruction complex $\mathbb{T}_X$, which carries all the information about local deformations of X at each point. Namely:

- $H^0(\mathbb{T}_X)$ is the tangent space of the classical truncation of X, which gives the infinitesimal deformations of each point.
- $H^i(\mathbb{T}_X)$, for $i < 0$, is the 'stacky' part: $H^{-1}(\mathbb{T}_X)$ gives the tangent space of the group of automorphisms at each point, and smaller homology corresponds to higher automorphisms.
- $H^i(\mathbb{T}_X)$, for $i > 0$, is the 'derived' part, i.e. the obstruction theory of X: $H^1(\mathbb{T}_X)$ gives the obstruction to extend infinitesimal deformations to higher order, and the higher homology gives higher obstructions.

This complex has a physical incarnation as the BRST-BV complex used to quantize gauge systems with obstructions, namely negative homology corresponds to the ghosts, and positive homology to the anti-fields.

According to [TV05], the objects of a dg-category with some reasonable assumptions (which are verified for the derived category of a smooth quasi-projective scheme or the derived category of a quiver with potential, which are the cases that interest us), form an Artin higher derived stack $\mathcal{M}$. Its tangent obstruction complex is just a shift of 1 of the **Hom** complex, namely:

$$(\mathbb{T}_M)_E = \mathbf{Hom}(E, E)[1] \tag{3.4.9}$$

We find a formalization picture that we developed above: $\mathrm{Ext}^{\leq 0}(E, E)$ gives tachyonic strings, hence (higher) automorphisms; $\mathrm{Ext}^1(E, E)$ gives massless strings, hence deformations; and $\mathrm{Ext}^{\geq 2}(E, E)$ gives massive strings, hence obstructions. Consider now a Bridgeland stability condition $\sigma = (Z, (\mathcal{P}(\phi))_{\phi \in \mathbb{R}}$, and a slope ϕ. The condition of being semistable is open, hence, using the technical result [STV11, Prop 2.1], there is an open derived substack $\mathcal{M}_\phi^{\sigma-ss}$ of semistable of phase ϕ. From stability, negative Ext vanishes in $\mathcal{P}(\phi)$, hence $\mathcal{M}_\phi^{\sigma-ss}$ is a derived stack (there are no higher automorphisms).

We consider now the dg category $D_c^b(X)$, with X a smooth quasi-projective CYn. The Serre duality in this case gives a non-degenerate pairing:

$$\mathbf{Hom}(E, F) \times \mathbf{Hom}(F, E[n]) \to \mathbb{C} \tag{3.4.10}$$

We call more generally a CYn category a dg-category with such a Serre functor. It induces a non-degenerate pairing:

$$\mathbb{T}_{\mathcal{M}} \times \mathbb{T}_{\mathcal{M}}[n-2] \to \mathbb{C} \tag{3.4.11}$$

Such a pairing is called a $2-n$-shifted symplectic structure, as introduced in [PTVV13]. It was then proven in [BD21, Prop. 3.3] that $\mathcal{M}_\phi^{\sigma-ss}$ are $2-n$-shifted symplectic stacks. In particular, the fine moduli space $M_\phi^{\sigma-s}$ of stable objects is a $2-n$-shifted symplectic scheme.

- When $n=2$, hence in a CY2 category, the 0-shifted symplectic structure induces a non-degenerate pairing of the tangent space with itself, hence an holomorphic symplectic, i.e. Hyperkähler structure. One finds again the fact that moduli spaces of stable sheaves on K3 surfaces, or of stable representations of preprojective algebras, are Hyperkähler.
- When $n=3$, hence in a CY3 category, the -1 shifted symplectic structure induces a non-degenerate pairing of the tangent space and obstructions. Moreover, because $M_\phi^{\sigma-s}$ is a scheme, there are no (higher) automorphisms, and then, dually, there are no higher obstructions. The cotangent complex provides then a symmetric perfect obstruction theory and the virtual dimension is 0.

We are particularly interested in the case of CY3 categories, which are categories of branes in mirror symmetry. Using intersection theory, [BF96] builds virtual classes for a proper scheme with perfect obstruction theory, which, when the obstruction theory is symmetric, i.e. when the virtual dimension is 0, gives a virtual count of points. This construction was used in [Tho98] by Thomas, as suggested by Donaldson, to define a virtual count of sheaves on CY3-folds, which are now called the numerical Donaldson-Thomas invariants. The symmetric obstruction theory was built using gauge theory but coincides with the one defined by derived geometry.

We will not explain the construction of the virtual class, but we will explain an equivalent definition found in [Beh09], which has motivated the definition of a refining of numerical Donaldson-Thomas invariants, the cohomological Donaldson-Thomas invariants. Namely, Behrend has built a constructible function $\nu_X : X \to \mathbb{Z}$ on any scheme X. The function $\nu_X(x)$ counts in some sense the multiplicity of the point $x \in X$: it is defined using embeddings into smooth space, but the number is independent of the embedding. We have $\nu_X(x) = (-1)^{dim(M)}$ on a smooth space M, ν is invariant under étale maps and is multiplicative under the product of spaces. Then [Beh09, Theorem 4.18] shows that, when X is proper and has perfect symmetric obstruction theory, the numerical DT invariant is the weighted characteristic:

$$\chi(X, \nu_X) := \sum_{n \in \mathbb{Z}} n\chi(\nu_X^{-1}(n)) \tag{3.4.12}$$

We will use this as a definition of the numerical DT invariant when X is not proper.

Now, remark that the moduli space of stable holomorphic bundles on a CY3 can be described, using the Donaldson-Uhlenbeck-Yau theorem and gauge theory, as complex bundles with hermitian Yang-Mills connections. Such connections form the critical locus of the Chern-Simons functional in an infinite-dimensional moduli space. Consider the critical locus $X = Crit(f)$ of a regular function $f : U \to \mathbb{C}$ on a smooth space. It has a natural derived structure, whose tangent obstruction complex is:

$$0 \to T_U|_X \overset{hess_f}{\to} T^*U|_X \to 0 \tag{3.4.13}$$

where $hess_f$ denotes the Hessian of f. There is an obvious non-degenerate pairing between $\mathbb{T}_X$ and $\mathbb{T}_X[1]$: derived critical loci are then natural examples of -1-shifted symplectic space. One can then expect to have an algebraic version of the gauge-theoretic description of moduli spaces as critical loci. Namely, for scheme X, we define a critical chart (R, U, f, i) as the data of an open set $R \subset X$, a closed embedding $i : R \to U$ into a smooth scheme U, and a regular function $f : U \to \mathbb{R}$ such that $i(R) = Crit(f)$. The fundamental 'shifted symplectic Darboux lemma' of [BBJ19] gives then:

Theorem 3.4.4. *([BBJ19]) A -1 shifted symplectic scheme's classical truncation has a natural d-critical structure, resulting in a natural collection of critical charts covering X.*

The d-critical structures were defined in [Joy13]. For a closed embedding $i : R \to U$ of an open subset of X into a smooth scheme U, we denote by $I_{R,U}$ the ideal of functions of U vanishing on R. Then a d-critical structure on X gives a consistent choice $s_{R,U}$ of classes of regular function $f + I^2_{R,U} : U \to \mathbb{C}$ such that $i(R) \subset Crit(f)$ for each such embedding $i : R \to U$, and, up to shrinking R, one can choose a function f in this class with $i(R) = Crit(f)$. Hence, a d-critical structure gives a restriction on the critical charts that we can use but also gives a very practical recipe for building critical charts.

Now, on a critical chart (R, U, f, i), the Behrend function ν_R has a very concrete expression. Consider $x \in R$, then $i(x) \in Crit(f)$. Replace U by its analytification, denote $c = f(i(x))$, and consider $f_x : y \to f(y) - c$. Then, consider $\epsilon > 0$ small enough and S_ϵ the real sphere of radius ϵ in U centered on $i(x)$. Consider now the Milnor map:

$$\begin{aligned} M :& S_\epsilon - S_\epsilon \cap f_c^{-1}(0) \to S^1 \\ & y \mapsto \frac{f_c(y)}{|f_c(y)|} \end{aligned} \tag{3.4.14}$$

Here S^1 is the unit circle. For $\epsilon > 0$ small enough, this map is a fibration and does not depend on ϵ: It is called the Milnor fibration, and its fiber $MF_f(x)$ is called the Milnor fiber. According to [Beh09], one has:

$$\nu_X(x) = \nu_R(x) = (-1)^{dim(U)}(1 - \chi(MF_f(x))) \tag{3.4.15}$$

In the case $f = z^{n+1} : \mathbb{C} \to \mathbb{C}$, the Milnor fiber is a set of $n + 1$ points, hence one finds $\nu_X(x) = n$, as expected because x has then multiplicity n. In general, one can understand the number $\nu_X(x)$ as a kind of quantification: quantum mechanically, the state brane is not exactly at the critical locus of the potential f, but can probe a small neighborhood of it. Now that we have found a 'critical Euler number' for critical spaces, we can try to find a 'critical cohomology. According to Grothendieck's function-sheaf dictionary, we want to search for a perverse sheaf $P_{U,f} \in Perv(R)$ whose Euler number at each point is $\nu_R(x)$. A natural cohomological refining of (3.4.15) would be to ask that at each point $x \in R$ the cohomology $H(P_{U,f}|_x)$ of the stalk at x would be obtained from the cohomology of the Milnor fiber. Those properties are verified by the perverse sheaf of vanishing cycles, which we will denote by $P_{U,f}$.

We will now quickly explain the construction of $P_{U,f}$. We consider first that $Crit(f) \subset U_0 := f^{-1}(0)$ We consider the analytification U^{an} of U and the following diagram, whose squares are cartesian commutative:

$$\begin{array}{ccccc} U_0^{an} & \xrightarrow{i} & U^{an} & \xleftarrow{\pi} & \tilde{U}^{an} \\ \downarrow 0 & & \downarrow f & & \downarrow \tilde{f} \\ \{0\} & \longrightarrow & \mathbb{C} & \longleftarrow & \tilde{\mathbb{C}}^* \end{array}$$

where $\tilde{\mathbb{C}}^*$ is the universal cover of $\mathbb{C}^*$: $\tilde{U}^{an} \to U^{an} - U_0^{an}$ is then a $\mathbb{Z}$-cover where the monodromy has been 'delooped' around U_0. Then, one defines the nearby cycle functor:

$$\psi_f : i^*\pi_*\pi^* D^b_{cons}(U^{an}) \to D^b_{cons}(U_0^{an}) \tag{3.4.16}$$

This functor is a kind of categorification of the Milnor fiber: namely, the stalk of $\psi_f F$ at a point of $x \in U_0^{an}$ computes the cohomology of F on the Milnor fiber $MF_f(x)$. We have a natural morphism $i^* \to \psi_f$, and then ϕ_f is isomorphic to a cone $\phi_f = Cone(i^* \to \psi_f)$. This formula provides a categorification of (3.4.15): one removes the contribution of the cohomology of F at x to its cohomology on the Milnor fiber. A nontrivial result is that ϕ_f induce a morphism of perverse sheaves $\phi_f : Perv(U) \to Perv(U_0)$, whose images are supported on $Crit(f) = i(R)$, hence one obtains a functor $i^*\phi_f : Perv(U) \to Perv(R)$. In some sense, $i^*\phi_f F$ 'computes the cohomology of F on the Milnor fiber, minus F itself'. We apply then this functor to $\mathbb{Q}_U[dim(U)] \in Perv(U)$, the shift of the structure sheaf centered on 0:

$$P_{U,f} := i^*\phi_f \mathbb{Q}_U[dim(U)] \in Perv(R) \tag{3.4.17}$$

If f has several critical values $c \in \mathbb{C}$, one sum the contributions for each shift f_c. $\phi_{U,f}$ is then a good categorification of the Milnor function ν_R. An other way to motivate this, maybe closer to the physicist's intuition, comes from the fact that $P_{U,f}$ is quasi-isomorphic in $D^b_{cons}(R)$ to the twisted de Rahm complex introduced in [Wit82], which is the complex centered on 0, whose spaces are the spaces of forms, and whose derivative is $d + df\wedge$. It is a deformation of the usual de Rahm complex, which localizes on the critical locus, and which is motivated from supersymmetric quantum field theory, see [Wit82, Section 4].

Now, notice that the value of ν_R does not depend on the presentation of R as a critical locus, and then glue to define a global function ν_X on X. Likewise, we would like to glue the locally defined $P_{U,f} \in Perv(R)$ into a global perverse sheaf $P_X \in Perv(X)$, for X a -1-shifted symplectic scheme. A refining of (3.4.12) would be to define the cohomological Donaldson-Thomas invariant as the cohomology with compact support $H_c(X, P_X)$ with value in this perverse sheaf; in particular, its Euler number would be the numerical Donaldson-Thomas invariant defined above. One has to glue objects in the Abelian category of perverse sheaves; hence, one has to define local restrictions of P_X on charts (this is provided by the $P_{U,f}$), define gluing isomorphisms on intersections of charts, and check cocycle conditions. It was done in [BBD+15], and we will review this construction.

Given a finite-dimensional vector space E and a non-degenerate quadratic form $q : E \to \mathbb{C}$, one can define an action by stabilization on critical charts:

$$(E, q) : (R, U, f, i) \mapsto (R, U \times E, f \boxplus q, i \times \{0\}) \tag{3.4.18}$$

We consider here $f \boxplus q : (x, u) \to f(x) + q(u)$. According to [Joy13, Section 2.3], this action is transitive on critical charts of a d-critical scheme. It means that, considering two critical charts (R, U, f, i) and (S, V, g, j) intersecting at $x \in R \cap S$, one can, up to restricting the charts to a neighborhood of x, find $(E, q), (E', q')$ and an isomorphism of critical charts:

$$(R, U \times E, f \boxplus q, i \times \{0\}) \simeq (S, V \times E', g \boxplus q', j \times \{0\}) \tag{3.4.19}$$

Hence, to define the gluing isomorphisms, it suffices to define isomorphisms $P_{U,f} \simeq P_{U\times E, f\boxplus q}$. Suppose that we have chosen an orientation on E. We have:

$$P_{E,q} = H^{n-1}(MF_q(0), \mathbb{Q}) \otimes \mathbb{Q}_{\{0\}} \simeq \mathbb{Q}_{\{0\}} \tag{3.4.20}$$

where $MF_q(0)$ denotes the Milnor fiber of q at 0, which is T^*S^{n-1}, and the second isomorphism comes from the orientation of S^{n-1} coming from the chosen orientation of E. One has then a natural isomorphism in $Perv(R)$:

$$P_{U\times E, f\boxplus q} \simeq P_{U,f} \boxtimes P_{E,q} \simeq P_{U,f} \tag{3.4.21}$$

Where the first isomorphism is the Thom-Sebastiani isomorphism $\mathcal{TS}_{U,f,E,q}$, and the second comes from the chosen orientation of E. The opposite orientation would give the isomorphism with the opposite sign. A consistent choice of orientations is equivalent to the data of a square root of the determinant $det(\mathbb{L}_X)$ of the cotangent complex $\mathbb{L}_X = (\mathbb{T}_X)^{-1}$ of X: Indeed, on a critical chart, the tangent complex is given by:

$$0 \to i^*(TU) \overset{i^*(hess_f)}{\to} i^*(T^*U) \to 0 \tag{3.4.22}$$

As said before, hence one have:

$$det(\mathbb{L}_X)|_R := i^*(K_U)^{\otimes 2} \tag{3.4.23}$$

Hence, a choice of square root $det(\mathbb{L}_X)^{1/2}$ is equivalent to a consistent choice of orientation for the critical charts. The main result of [BBD+15] is then that, given such a choice, the cocycle conditions are satisfied:

Theorem 3.4.5. *([BBD+15, Theorem 6.9]) For a -1-shifted symplectic scheme with orientation $det(\mathbb{L}_X)^{1/2}$, the locally defined perverse sheaves $P_{U,f}$ glues canonically into a globally defined $P_X \in Perv(X)$*

We will call P_X the Donaldson-Thomas perverse sheaf. In fact, it is possible to upgrade this construction to the construction of a monodromic mixed Hodge module, such that one can define the cohomological DT invariants to be a Hodge polynomial, still denoted $H(X, P_X)$, in the diagonal variable y, identified as a square root of the Tate motive, and the parameter t. In [BBBBJ15], the authors have extended this construction to -1-shifted symplectic stacks X with orientation $det(\mathbb{L}_X)^{1/2}$. Consider now a reasonable $CY3$ category with orientation data on its stack of objects, which we will ask to be compatible with extensions. As said before, given a Bridgeland stability condition σ, the stacks $\mathcal{M}_{\phi,\gamma}^{\sigma-ss}$ of semistable objects of phase ϕ and dimension vector $\gamma \in \Gamma$ are -1 shifted symplectic and have an orientation; hence, one can define a DT perverse sheaf $P_{\mathcal{M}_{\phi,\gamma}^{\sigma-ss}}$. We consider the ring R, which is the Grothendieck ring of monodromic mixed Hodge structures. We introduce the noncommutative ring, called the quantum affine space:

$$R\langle (x^\gamma)_{\gamma\in\Gamma}\rangle / (x^\gamma x^{\gamma'} - (-y)^{\langle\gamma,\gamma'\rangle} x^{\gamma+\gamma'}) \tag{3.4.24}$$

Here $R\langle x\rangle$ denotes the free R-module generated by x, and $\langle\cdot,\cdot\rangle$ denotes the Euler pairing introduced in (3.1.9). All the generating series that we will consider will be elements of this ring. We consider the generating series of stacky invariants:

$$\mathcal{A}_\phi^{\sigma-ss} := \sum_{\gamma\in\Gamma} H(\mathcal{M}_{\phi,\gamma}^{\sigma-ss}, P_{\mathcal{M}_{\phi,\gamma}^{\sigma-ss}}) x^\gamma \tag{3.4.25}$$

Here $H(M,P) \in R$, with $P \in MMHM(M)$ denotes the class in the Grothendieck group of the monodromic mixed Hodge structure given by the hypercohomology of the monodromic mixed Hodge module P.

We will now end this section with a discussion on the construction of orientation data. On the derived category $D^b_{fd}(Q,W)$ of finite-dimensional representations of quiver with potential, the moduli spaces are globally a critical locus of a potential, and there is no orientation issue. It can be used to easily build canonical orientation data on local CY3 which are derived equivalent to a quiver with potential. The case of compact CY3 is far more complicated, because one has to use all the gluing technology introduced above. A canonical orientation data compatible with extensions was built for projective smooth CY3 X in [JU21b]. We will give a (very rough) picture of this construction. First, notice that, in some homotopy sense, extensions retract on direct sums; hence, it suffices to show consistency of orientation data for direct sums. Now, notice that any object in $D^b(X)$ is quasi-isomorphic to a complex of holomorphic vector bundles; hence, still by some homotopy-theoretic arguments, it suffices to build an orientation data on the moduli stack of holomorphic vector bundles, which is isomorphic to the moduli stack of complex vector bundles with holomorphic connections, where one can use gauge theory. The idea is then to fix a vector bundle E and define an orientation (called in this context a spin structure) on the moduli stack M of holomorphic connections. Now, a choice of spin structure, i.e. a choice of square root of the determinant of a kind of cotangent complex of M defined using gauge theory, corresponds to a choice of orientation, i.e. a trivialization of the cotangent complex, on its loop space ΩM. But the loop space ΩM is the stack of G_2 connections on the bundle E on $X \times S^1$. One is thus led to the question of finding an orientation on the moduli stack of G_2 connections on a complex vector bundle E' on a G_2 manifold X'.

This question was dealt with in [JU21a]: the idea is that E' is trivializable outside an associative threefold $Y \hookrightarrow X'$, such that this embedding is infinitesimally isomorphic with an embedding $Y \to S^7$ into the 7-sphere. According to an excision theorem, orientations on the moduli stack of G2-connections on E correspond then to orientations of G2-connections on a complex vector bundle on S^7. But complex vector bundles on S^7 are stably trivial, hence this moduli space is orientable: a choice of orientation corresponds to a choice of orientation on S^7. The result [JU21a, Theorem 1.2] says that a choice of flag structure on X', i.e. a choice of orientations for associative threefolds with some consistency condition, is determines by the above procedure an orientation data on the moduli spaces of G_2 connections that is consistent with direct sums. On G_2 manifolds of the form $X \times S^1$, for X CY3, there is a canonical choice of flag structure, obtained by considering the class of associative threefolds of the form $C \times S^1$, where C is a holomorphic curve in X. Unrolling everything, this choice of flag structure provides a choice of orientation data on the moduli stack of objects of $D^b(X)$.

The physical meaning of this construction seems to be that one has to consider the equivalence between type IIA string theory compactified on X and M theory compactified on $X \times S^1$, and that the construction of orientation data must come from M theory. Associative threefolds of a G_2 manifold X' form M2 branes of M theory compactified on X', and they seem to play an important role here. The physical meaning of a flag structure is quite obscure in the general case, but it seems to be quite logical, in the case $X' = X \times S^1$, that it must be determined from the distinguished set of M2 branes $C \times S^2$, which reduced to D2 branes of type IIA under compactification of S^1.

3.4.3 Wall crossing and integrality

Wall crossing

Consider a reasonable CY3 triangulated category $\mathcal{D}$ with an orientation, like $D^b_c(X)$ with X smooth and quasi-projective or $D^b(Q,W)$ with (Q,W) a quiver with potential. The formulas that we will give are expected to hold in this general context, but are now proven only for $D^b(Q,W)$, because of the difficulties linked with the gluing studied above.

The wall crossing formula was introduced in [KS], and is expected to relate the DT invariants for different stability conditions. Consider a stability condition σ, and an interval (ϕ,ψ) of length < 1. Then, consider the subcategory $\mathcal{P}((\phi,\psi))$ whose objects have Harder-Narasimhan filtration has phase $\phi < \phi' < \psi$. Its objects have no negative Ext from stability, hence they form an oriented -1-shifted symplectic stack $\mathcal{M}^{\sigma}_{(\phi,\psi)}$, with DT generating series:

$$\mathcal{A}^{\sigma}_{(\phi,\psi)} := \sum_{\gamma\in\Gamma} H_c(\mathcal{M}^{\sigma}_{(\phi,\psi),\gamma}, P_{\mathcal{M}^{\sigma-ss}_{(\phi,\psi,\gamma}})x^{\gamma} \tag{3.4.26}$$

Here H_c denotes the cohomology with compact support. Now, it is claimed in [KS] that the Harder-Narasimhan decomposition induces at the level of generating series:

$$\mathcal{A}^{\sigma}_{(\phi,\psi)} = \prod_{\phi'=\phi}^{\psi} \mathcal{A}^{\sigma}_{\phi'} \tag{3.4.27}$$

Here the noncommutativity rule:

$$x^{\gamma}x^{\gamma'} = (-y)^{\langle\gamma,\gamma'\rangle}x^{\gamma+\gamma'} \tag{3.4.28}$$

accounts for the fact that there are many F fitting in an exact triangle $E\to F\to G\to E[1]$, with E and G fixed. If we denote $\mathcal{M}^{\sigma}_{\gamma,\gamma'}$ the stack of such extensions with $E\in\mathcal{M}^{\sigma-ss}_{\gamma,\phi'}$ and $G\in\mathcal{M}^{\sigma-ss}_{\gamma',\phi''}$, then one has a map:

$$\mathcal{M}^{\sigma}_{\gamma,\gamma'} \to \mathcal{M}^{\sigma-ss}_{\gamma,\phi'} \times \mathcal{M}^{\sigma-ss}_{\gamma',\phi''} \tag{3.4.29}$$

This map can be thought of as being a vector bundle of virtual dimension $\langle\gamma',\gamma\rangle$, hence there is a term $(-y)^{\langle\gamma',\gamma\rangle}$ in the product, which is cancelled by the noncommutativity rule (3.4.28).

Now, consider σ,σ' two stability conditions linked by a path in the space of stability conditions. Suppose that there are no semistable objects of phase ϕ or ψ along this path. Then the subcategory $\mathcal{P}((\phi,\psi))$ is constant on this path, and then (3.4.27) gives:

$$\prod_{\phi'=\phi}^{\psi} \mathcal{A}^{\sigma}_{\phi'} = \prod_{\phi'=\phi}^{\psi} \mathcal{A}^{\sigma'}_{\phi'} \tag{3.4.30}$$

This formula is called the wall crossing formula and allows, in principle, to compute DT invariants at a stability condition from the knowledge of DT invariants at another stability condition. In particular, it can relate DT invariants for birational CY3, or DT invariants counting sheaves and DT invariants counting representations of quivers with potentials. Because of the gluing issues mentioned above, it has been shown rigorously only for quivers with potentials in [Dav17]. In

particular, if we consider the stability condition $\sigma_{\theta,\rho}$ defined from a stability parameter θ at (3.3.1), the interval of phase $(1/2, 3/2)$ satisfies the above condition, and one can apply the above formalism to obtain the usual wall crossing formula for quivers with potentials as formulated in [Dav17].

In practical situations, in particular on projective CY3, it is unreasonable to ask that there be no semistable objects of phases ϕ and ψ on a path in the space of stability conditions because the phases of semistable objects are expected to be dense. It is possible to modify the wall crossing formula above by considering an equality up to high dimension vectors, but we will not write a precise formula here.

Integrality

We have now expressed the Harder-Narasimhan decomposition as a factorization of the DT generating series. We will now express the Jordan-Hölder decomposition of a semistable object into its stable components as a plethystic exponential. Indeed, the stacky generating series $\mathcal{A}^\sigma_\phi$ are not satisfying physically, because they count semistable representations, but semistable representations must physically be identified up to S-equivalence, as can be seen from the Donaldson-Uhlenbeck-Yau theorem, and because the recombination of a semistable brane into an S-equivalent brane costs no energy. Suppose that the stability condition σ and the phase ϕ are generic in the sense that dimension vectors γ, γ' of σ-semistable objects of phase ϕ have vanishing brackets $\langle \gamma, \gamma' \rangle$. It means that the recombination of S-equivalence implies trivial wall crossing, or, in physical language, that it implies mutually nonlocal objects. It is expected then that this recombination phenomenon is expressed by a multiple cover formula:

$$\mathcal{A}^\sigma_\phi = \mathrm{Exp}\Big(\sum_{\gamma\in\Gamma} \frac{\Omega_{\sigma,\gamma}}{-y+y^{-1}} x^\gamma\Big) \tag{3.4.31}$$

Here Exp denotes the plethystic exponential:

$$\mathrm{Exp}(f(x)) := \exp\Big(\sum_{k=1}^{\infty} \frac{f(x^k)}{k}\Big) \tag{3.4.32}$$

The $\Omega_{\sigma,\gamma}$, which are defined formally by this formula, are expected to be integers, and to give the right count of σ-semistable branes of charge γ. This integrality conjecture was proven for quiver with potentials in [DM16], and is expected to hold in the more general context that we present here.

We will now sketch the proof of the integrality conjecture of [DM16], in the case of quiver with potentials. The idea is to use the Jordan-Hölder map projecting on the coarse moduli space:

$$JH : \mathcal{M}^{\sigma-ss}_\phi \to M^{\sigma-ss}_\phi \tag{3.4.33}$$

This map is not proper but has some 'hidden properness' properties, coming from the fact that it can be approximated in some sense by proper maps, defined using framed representations. The authors of [DM16] consider:

$$\begin{aligned} \mathcal{BPS}^\sigma_{\phi,\gamma} &:= \mathcal{H}^1 P_{\mathcal{M}^{\sigma-ss}_\phi} \in Perv(M^{\sigma-ss}_\phi) \\ \Omega_{\sigma,\gamma} &:= H_c(M^{\sigma-ss}_{\phi,\gamma}, \mathcal{BPS}^\sigma_\phi) \end{aligned} \tag{3.4.34}$$

Here $\mathcal{H}^{\cdot}$ denotes the perverse filtration, and H_c denotes the cohomology with compact support. The authors of [DM16] considered then some CoHa-like product in $Perv(M_\phi^{\sigma-ss})$ obtained by considering extensions. They show then:

$$\mathcal{H}^{\cdot}(JH_* P_{\mathcal{M}_\phi^{\sigma-ss}}) = Sym(\mathcal{BPS}_\phi^\sigma \otimes H(B\mathbb{C}^*)_{vir}) \tag{3.4.35}$$

Here the term $B\mathbb{C}^*$ comes from the scaling automorphism of semistable objects (recall that $\mathcal{M}_\phi^{\sigma-ss}$ is a $\mathbb{C}^*$-gerbe over the stable locus). Taking the cohomology, the right-hand side gives:

$$\mathrm{Exp}(\sum_{\gamma\in\Gamma} \frac{\Omega_{\sigma,\gamma}}{-y+y^{-1}} x^\gamma) \tag{3.4.36}$$

where the term $(-y+y^{-1})$ correspond to $H(B\mathbb{C}^*)_{vir}$. Concerning the left-hand side, the 'hidden properness' allows to show that taking the perverse cohomology commutes with taking the cohomology, hence it gives $\mathcal{A}_\phi^\sigma$, which proves the formula (3.4.31).

Notice that the coarse moduli space $M^{\sigma-ss}$, classifying semistable objects up to S-equivalence, is not -1-shifted symplectic, unless all semistable objects are stable. Indeed, in the case of $D^b(Q,W)$, this coarse moduli space is the critical locus of $\mathrm{Tr}(W)$ on the coarse moduli space of semistable representations of Q, which is not necessarily smooth, so we cannot apply directly the construction of [BBD+15] to $M^{\sigma-ss}$ to define $\Omega_{\sigma,\gamma}$. It is shown in [DM16] that $\mathcal{BPS}_\phi^\sigma$ can also be obtained by applying the vanishing cycle functor $\phi_{Tr(W)}$ to the intersection cohomology of this coarse moduli space.

It appears to be possible to extend the construction of [DM16] to the more general context of CY3 categories. Namely, according to [Tod18], the Jordan-Hölder map in any reasonable CY3 category can be locally described using quivers with (formal) potentials. Hence, one can try to define the objects as in [DM16], and work locally using quivers with potentials to conclude. Unfortunately, one has to deal with gluing issues in ∞-categories of constructible complexes; hence, a general proof of the integrality conjecture does not exist at the moment. Notice that all the perverse sheaves in DT theory are in fact upgraded to monodromic mixed Hodge modules; in particular, they carry a canonical self-duality isomorphism. If we have built like that a perverse sheaf $\mathcal{BPS}_\phi^\sigma$, when X is projective, the coarse moduli space is projective, and the cohomology of $\mathcal{BPS}_\phi^\sigma$ will be self-Poincaré dual, hence $\Omega_{\sigma,\gamma}$ will be self dual under $y \to y^{-1}$.

Some formulas are better expressed by using the rational BPS invariants $\bar{\Omega}_{\sigma,\gamma}$ obtained by taking the classical (rather than plethystic) logarithm of the stacky invariants:

$$\mathcal{A}_\phi^\sigma = \exp(\sum_{\gamma\in\Gamma} \frac{\bar{\Omega}_{\sigma,\gamma}}{-y+y^{-1}} x^\gamma) \tag{3.4.37}$$

Here exp denotes the classical exponential. Integers and rational BPS invariants are related by a simple multiple cover formula:

$$\bar{\Omega}_{\sigma,\gamma}(y) = \sum_{k|\gamma} \frac{1}{k} \frac{y^{-1}-y}{y^{-k}-y^k} \Omega_{\sigma,\gamma/k}(y^k) \tag{3.4.38}$$

Unframed and framed representations of quivers with potential

Consider a quiver with potential (Q, W). We can consider the moduli stack $\mathfrak{M}_{Q,W,d}$ of d-dimensional representations of (Q, W), and the generating series of DT invariants:

$$\mathcal{A}(x) = \sum_{d \in \mathbb{N}^{Q_0}} H_c(\mathfrak{M}_{Q,W,d}, P_{\mathfrak{M}_{Q,W,d}}) x^d \tag{3.4.39}$$

Consider a stability condition θ with $\theta \cdot \gamma = 0$, and which is generic for γ (i.e. all dimension vectors d', d'' with $\theta(d') = \theta(d'') = 0$ satisfies $\langle d', d'' \rangle = 0$. We denote $\Omega_{\theta,\gamma} := \Omega_{\sigma,\gamma}$ the BPS invariant for the corresponding stability condition $\sigma_{\theta,\rho}$ for any choice of positive ρ, which counts d-dimensional θ-semistable representations of (Q, W) with the right multiplicity, and is integral from [DM16].

Consider now a node $i \in Q_0$. We consider d-dimensional i-framed representations of this quiver, which are doublets (V, v), with V a d-dimensional representation of Q, and $v \in V_i$ a vector generating V. In fact, such representations are θ-stable $(d, 1)$ dimensional representations of the quiver with potential (Q_i, W) obtained by adding a node ∞ and an arrow $f : \infty \to i$, and by taking $\theta_\infty > 0$ and $\theta_i < 0$ for $i \in Q_0$. We denote by $\mathcal{M}_{i,d}$ the moduli space of i-framed representations of (Q, W), and consider the generating series of i-framed DT invariants:

$$Z_i(x) = \sum_{d \in \mathbb{N}^{Q_0}} H_c(\mathcal{M}_{i,d}, P_{\mathcal{M}_{i,d}}) x^d \tag{3.4.40}$$

When the quiver with potential is an NCCR, and then is derived equivalent to a crepant resolution Y of a CY3 singularity, framed representations are noncommutative analogue of framed sheaves, i.e. surjective morphisms $\mathcal{O}_Y \twoheadrightarrow F$, with $F \in D^b_c(Y)$. By applying the Kontsevich-Soibelman wall crossing formula to (Q_i, W), one obtains a wall crossing formula relating the DT invariants of (Q, W) with the i-framed DT invariants. Namely, considering the automorphisms of the quantum affine space:

$$S_{\pm i} : x^d \mapsto (-y)^{\pm d_i} x^d \tag{3.4.41}$$

The following formula is proven in [Mor12] and [Moz13]:

$$Z_i(x) = S_i(\mathcal{A}(x)) S_{-i}(\mathcal{A}(x)^{-1}) \tag{3.4.42}$$

It allows to relate the framed generating series and the BPS invariants $\Omega_{\theta,d}$, using the Kontsevich-Soibelman wall crossing formula and integrality.

3.5 Extremal black holes and flow tree formula

3.5.1 Black holes entropy and branes

We will now discuss a seemingly unrelated subject: the entropy of black holes, which we will relate below to DT theory. The second principle of thermodynamics suggests that black holes should have an entropy; indeed, when matter with some entropy is falling into a black hole, the entropy of the universe should not decrease. Indeed, explicit computations of Christodoulou and Bekenstein in the 1960s show that by performing some energy balance sheet during such processes, one can find:

$$dM = \Omega dJ + \Phi dQ + \frac{\kappa}{8\pi} dA \tag{3.5.1}$$

with M the masses (energy) of the black hole, Ω its angular velocity, J its angular momentum, Φ its electric potential, Q its electric charge, κ its surface gravity, i.e. the curvature of its horizon, and A the area of its horizon. It is tempting to see in this formula a "first law of black hole thermodynamics", with some multiple of A being the entropy, and some multiple of κ the temperature. A result of Bardeen, Carter and Hawking in [BCH73] shows that κ is constant at the horizon surface, suggesting a "zeroth law of black hole thermodynamics" saying that the "temperature" of the black hole is constant as its horizon. What's more, Hawking showed that the area of a black hole cannot decrease in classical gravity, and even that the sum of black hole areas cannot decrease in classical processes involving black hole interactions, suggesting a "second law of black hole thermodynamics".

All these considerations lead Bekenstein to predict in [Bek19] that black holes have temperature and entropy:

$$T_{BH} = \frac{\kappa}{2\pi} \qquad S_{BH} = \frac{A}{4} \tag{3.5.2}$$

in Planck units. The seemingly crazy fact that black holes have a nonzero temperature at the horizon leads Hawking to study this question in [Haw75] using quantum field theory in curved spacetime. Based on the works of Unruh, he shows that a vacuum state in some referential is seen as a thermal state for uniformly accelerated observers. Because the geometry near the horizon looks like a uniformly accelerated frame for a static observer outside the black hole, what is a vacuum state for the falling observer is a thermal state for the static observer outside the horizon with exactly the Bekenstein-Hawking temperature. The black hole is radiating according to the black body law, and this 'Hawking radiation' can be seen as coming from quantum fluctuations on the horizon. Due to this radiation, black holes will evaporate until they reach zero temperature, which happens when they have the mass of an extremal Reissner-Nordström black hole. In supersymmetric spacetime, such extremal black holes would become BPS states, which preserve one half of the supersymmetry.

In statistical physics, the entropy is expressed in enumerative terms: the entropy of a system with a given state at a macroscopic level is the logarithm of the number of microscopic states admitting this macroscopic description. This leads to the problem of the microscopic origin of black holes entropy: the huge entropy of black holes must correspond to a huge number of microscopic states giving the same macroscopic description. In classical relativity, results from Carter and Hawking show the 'No-hair theorem': a classical black hole has its mass, electromagnetic charges, and kinetic momentum (or spin), which are macroscopic, as its only parameter. So in classical gravity, there are no microscopic degrees of freedom corresponding with the Bekenstein-Hawking entropy. Such microscopic degrees of freedom must come from a quantization of spacetime inside the black hole; hence, comparing the asymptotic behavior of these numbers of microstates in any given theory of quantum gravity with Bekenstein-Hawking entropy is a good check for the theory.

We will study such a check for superstring theory, in particular type IIB and type IIA compactified on a smooth projective Calabi-Yau threefold, which gives a $D = 4$ $\mathcal{N} = 2$ supergravity theory. We will be interested only in BPS black holes, which conserve one supersymmetry, for reasons that will appear below. Consider a BPS brane which is pointlike in space, hence supported on the CY3. At low string coupling, it admits the description that we gave above, as complexes of coherent sheaves in type IIA and as Lagrangians in type IIB, i.e. σ-semistable objects in a CY3 triangulated category of branes, σ corresponding to the vector-multiplet moduli. More precisely, following quantum mechanics, a BPS brane is an unit vector in an Hilbert space, with the dimension of this Hilbert space giving the number of microstates. The Hilbert space of BPS states is expected to correspond to the hypercohomology of the perverse sheaf $\mathcal{BPS}^{\sigma}_{\phi,\gamma}$ defined as in [DM16] on the

coarse moduli space of σ-semistable objects. In 4 dimensions, the charge γ gives physically the electromagnetic charge of the brane, and the pairing $\langle \cdot, \cdot \rangle$ on Γ giving the electro-magnetic pairing. The cohomological dimension, i.e. the power of y in $\Omega_{\sigma,\gamma}$, corresponds to twice the spin of the brane. In supergravity, X is assumed to be projective, i.e. , as seen above, $\Omega_{\sigma,\gamma}$ is expected to be self-dual under $y \to y^{-1}$, hence the BPS Hilbert space splits as a direct sum of spin representations of $SU(2)$. Finally, the generating series of the BPS indices $\Omega_{\sigma,\gamma}$ will then provide partition functions of BPS branes with various electromagnetic charges and spins (the mass being fixed by the BPS condition).

Several computations suggest that when one increases the string coupling in this theory, a BPS brane begins to curve spacetime, and at high coupling, the spacetime must be the spacetime of an extremal/BPS black hole (with the same charge and spin). Here the BPS condition is very important: even if the physics changes significantly, the protection of supersymmetry ensures that the Witten index, i.e. the number of bosonic states minus the number of fermionic states, is unchanged. This Witten index will be in this case the numerical BPS invariant $\Omega_{\sigma,\gamma}(y = 1, t = 1)$ that we will introduce below, giving a virtual Euler characteristic for moduli spaces of BPS objects. The data of the spin of BPS states is encoded in the cohomological BPS invariant $\Omega_{\sigma,\gamma}$ that we will introduce below, giving a virtual cohomology for moduli spaces of BPS objects. Unlike the numerical invariants, the cohomological BPS invariants are not protected by supersymmetry, unless there is some R-charge. In type II superstring theory compactified on a projective CY3, the partition function of BPS black holes must then correspond to the generating series of $\Omega_{\sigma,\gamma}$ counting BPS branes obtained from DT theory. In some simple geometries, it has been shown that the asymptotic expansion of the DT generating series gives the first terms of the Bekenstein-Hawking entropy, which is a very nontrivial check of string theory, see [Pio06] for a review. On the other hand, this physical interpretation gives very interesting mathematical conjectures on the behavior of DT invariants.

3.5.2 Flow tree formula

Moreover, this supergravity picture gives a third point of view on the stability of BPS states and wall crossing, which fits well with the slope stability of B branes and the special Lagrangian condition on A branes. We explain now the work of Denef in [Den00]. The idea is to search for a static supergravity solution corresponding to a BPS black hole of charge γ, for a parameter σ_∞ in the vector multiplet moduli space $\mathcal{M}_V$. Consider the normalized central charge Z from $\mathcal{M}_V$ to $Hom(\Gamma, \mathbb{C})$, and consider the Kähler metric g of $\mathcal{M}_V$. The spacetime is then topologically given by $\mathbb{R} \times (\mathbb{R}^3 - \{0\})$, $\{0\}$ corresponding to the singularity. One searches for a metric ds^2 on $\mathbb{R}^4 - \{0\}$, and an electromagnetic field F on $\mathbb{R}^4 - \{0\}$ with total charge γ. Moreover, the value of the vector multiplet moduli is allowed to vary in spacetime, with σ_∞ corresponding only to the value measured by an observer at space infinity; hence, there is a map:

$$\sigma : \mathbb{R}^3 - \{0\} \to \mathcal{M} \tag{3.5.3}$$

so that $\sigma(x) = \sigma_i nfty$ when x reaches spatial infinity. Moreover, if one assumes that the solution is spherically symmetric, the equations can be solved explicitly. In particular, we can write everything in terms of $\tau = 1/r$, where r is the radial coordinate. The solution depends only on 2 functions of τ, U and σ. The metric is given by:

$$ds^2 = -e^{2U} dt^2 + e^{-2U}(dr^2 + r^2 d^2\Omega_2) \tag{3.5.4}$$

The electromagnetic field is given by:

$$\mathcal{F} = \frac{c}{\sqrt{4\pi}}(sin\theta d\theta \wedge d\phi \otimes \Gamma + e^{2U} d\tau \wedge dt \otimes \hat{\Gamma}) \tag{3.5.5}$$

with c an irrelevant constant and Γ (resp $\hat{\Gamma}$) being the electric (resp magnetic) part of the electromagnetic charge γ. The two functions U and σ are then subject to the evolution equation (σ is written in local coordinates z^a):

$$\frac{dU}{d\tau} = -\, e^U |Z_\sigma(\gamma)| \tag{3.5.6}$$

$$\frac{dz^a}{d\tau} = -\, 2e^U g^{a\bar{b}} \bar{\partial}_{\bar{b}} |Z_\sigma(\gamma)| \tag{3.5.7}$$

Hence the variation of σ is given by descending the gradient of $|Z_{\sigma(\tau)}(\gamma)|$ with speed $2e^U$, hence $|Z_{\sigma(\tau)}(\gamma)|$ decreases strictly from spatial infinity where $\sigma(0) = \sigma_\infty$ to the horizon where it must reach a local minimum. So the moduli at the horizon depend on the moduli at spatial infinity only through a choice of basin of attraction. This is called the attractor mechanism, and stability conditions σ_* minimizing $|Z_{\sigma(\tau)}(\gamma)|$ are called attractor stability conditions.

Now, recalling that a stability condition cannot have a semistable object of vanishing mass $|Z(\gamma)|$ (otherwise it would give a new modulus, hence a singularity of the vector multiplet moduli space), there are two possibilities:

- $|Z| \to |Z|_{min} > 0$: This case is not pathological, and the first attractor equation 3.5.6 gives the metric up to first order near the horizon. We obtain:

  $$e^{-U} = |Z|_{min}\tau + cste \tag{3.5.8}$$

  By doing an affine transformation to τ (possible because $|Z|_{min} > 0$, and we are near the horizon $\tau = \infty$), we can obtain $e^{-U} = \tau = 1/r$, and obtain the near-horizon metric:

  $$ds^2 \approx (-r^2 d\tau^2 + \frac{1}{r^2}) + d\Omega_2^2 \tag{3.5.9}$$

  So the near horizon geometry is $AdS_2 \times S_2$, exactly like extremal black holes. In fact, we find that we have exactly the Reissner-Nordström metric, the metric of extremal black holes, when there is no flow, i.e. when the moduli at spatial infinity are at a minimum of $|Z|$.

- $|Z| \to 0$ and the moduli reach a singular point in the moduli space (a conifold point): the black hole solution is an 'empty hole', as described by Denef in [Den00]. It does not correspond physically to a true black hole. In fact, if we extend the attractor equation to the case of compactification on a local CY3 (where gravity decouples), only this case occurs. Indeed, Z is holomorphic on $\mathcal{M}$ in this case, and then $|Z(\gamma)|$ has no nonvanishing minima.

Unfortunately, we are describing only a tiny subset of the spectrum of BPS black holes with such a description. In [Den00], Denef removed the assumption of spherical symmetry and tried to describe black holes with multiple centers. Namely, we fix the electromagnetic charges of the centers to be $(\gamma_1, ..., \gamma_n)$ such that $\sum_i \gamma_i = \gamma$: the supergravity equations near each center are then approximated by the attractor mechanism, hence the moduli near each center must be an attractor

stability condition σ_i^* for γ_i. One fixes the positions $x_1, ..., x_n \in \mathbb{R}^3$ of the centers and considers the static solutions of supergravity with spacetime topologically given by $\mathbb{R}(\mathbb{R}^3\{x_1, ..., x_n\})$. One needs then to describe the metric, the electromagnetic field of charge γ, and the local value of the vector multiplet moduli:

$$\sigma : \mathbb{R}^3 - \{x_1, ..., x_n\} \to \mathcal{M}_V \tag{3.5.10}$$

Denef proves that such supergravity solutions depends only on σ, and that such a σ must satisfy that at each point x, $\Im(Z_{\sigma(x)})$ is proportional to (up to rotating Z, we assume here that $Z_{\sigma_\infty}(\gamma) \in \mathbb{R}_-$):

$$\sum_{i=1}^{n} \frac{\langle \gamma_i, \cdot \rangle}{|x - x_i|} + \Im(Z_{\sigma_\infty}) \tag{3.5.11}$$

Notice in particular that $\Im(Z_{\sigma_i^*}(x_i) = 0$, hence by evaluating on the x_j, we obtain the constraints on the positions of the center:

$$\sum_{i \neq j} \frac{\langle \gamma_i, \gamma_j \rangle}{|x_i - x_j|} = -\Im(Z_{\sigma_\infty}(\gamma_j)) \tag{3.5.12}$$

In particular, if one considers two charges γ_1, γ_2, there is a solution to Denef equations, hence a bound state of γ_1 and γ_2, if and only if $arg(Z_{\sigma_\infty}(\gamma_1)) - arg(Z_{\sigma_\infty}(\gamma_2))$ is of the same sign as $\langle \gamma_1, \gamma_2 \rangle$. When the arguments of the central charge get closer, the centers get farther, until the distance becomes infinite and the bound state disappears: It is a primitive instance of wall crossing.

The map σ has an amoeba-like shape, with limit points corresponding to σ_∞ and the σ_i^*. On the more degenerate boundary points of the Denef's solutions, these amoebas degenerate to an oriented binary tree with root at σ_∞, with each branch carrying a charge γ' which is the sum of the charges of its two children, and the flow of σ being defined on the branch by:

$$\Im(Z_{\sigma_\infty}) = cste + \langle \gamma', \cdot \rangle \tag{3.5.13}$$

Using some partition of unity, it is argued that the cohomology of the moduli space of Denef's solutions is a sum of contributions corresponding to each of those binary trees; this gives the flow tree formula. More precisely, the flow tree formula expresses the rational BPS invariant $\bar{\Omega}_{\sigma_\infty,\gamma}$ in terms of the rational BPS invariants $\bar{\Omega}_{\sigma_i^*,\gamma_i}$ at the attractor stability conditions, giving a sum of the form:

$$\bar{\Omega}_{\sigma_\infty,\gamma} = \sum_{\gamma_1+...+\gamma_n=\gamma} \sum_{\sigma_1^*,...,\sigma_n^*} F_{\gamma_1,\sigma_1^*,...,\gamma_n,\sigma_n^*} \prod_{i=1}^{n} \bar{\Omega}_{\sigma_i^*,\gamma_i} \tag{3.5.14}$$

where $F_{\gamma_1,\sigma_1^*,...,\gamma_n,\sigma_n^*}$ is given by a sum over binary tree as above, with combinatorially defined coefficients. One uses the rational DT invariants $\bar{\Omega}$ instead of the integral one ω because their statistical behavior is simpler.

This formula can be a priori proven mathematically from the Kontsevich-Soibelman wall crossing formula, as was attempted in [KS13], but in this general context the analysis is quite complicated, and, as said before, because of the gluing issues in DT theory, the Kontsevich-Soibelman wall crossing formula itself is not formally proven in full generality.

In the supergravity case, the attractor invariants are expected to have exponential growth. We can extend the flow tree formula to the rigid case: in this case, the central charge is holomorphic, hence $|Z_\sigma(\gamma)|$ has no minimum inside $\mathcal{M}_V$: the attractor stability conditions can only correspond to boundary points of the vector multiplet moduli space, when some BPS objects become massless. In particular, the attractor invariants are expected to be very simple initial data. In Chapter 9, we have studied this formula for the case of local $\mathbb{P}^2$, as we will explain below.

3.5.3 Attractor invariants for quivers with potential

Consider now a quiver with potential (Q, W): King stability defines an open subset of the space $\mathrm{Stab}(Q, W)$ of stability conditions on $D^b_{f.d}(Q, W)$. The flow tree formula can be expressed completely explicitly on this open set using King stability. Given a dimension vector $d \in \mathbb{N}^{Q_0}$, one defines an attractor stability condition to be a small perturbation $\theta_\gamma \in \mathbb{R}^{Q_0}$ of $\langle \gamma, \cdot \rangle$ which is generic in $\gamma^\perp$. One defines the attractor invariant as:

$$\Omega_{*,\gamma} := \Omega_{\theta_\gamma,\gamma} \tag{3.5.15}$$

It was proven in [MP20, Theorem 3.7], using the wall crossing formula, that this definition is independent of the perturbation. The attractor flow tree formula then becomes:

$$\bar{\Omega}_{\theta,\gamma} = \sum_{\gamma_1+\ldots+\gamma_n=\gamma} F_{\gamma_1,\ldots,\gamma_n} \prod_{i=1}^{n} \bar{\Omega}_{*,\gamma_i} \tag{3.5.16}$$

Where the $F_{\gamma_1,\ldots,\gamma_n}$ are defined by summing combinatorial terms for each binary tree as above. This formula is now completely explicit and was proven in [AB21], using the wall crossing formula in a crucial way. Notice that the notion of attractor invariants is equivalent to the notion of initial data of scattering diagrams as developed in [Bri17], and that the flow tree formula can be seen as an efficient way to build a scattering diagram from its initial data.

In general situations, one hopes that the attractor invariants for a quiver with potential are simple, such that one can use the flow tree formula to effectively compute the BPS spectrum of the theory. In the simple case of an acyclic quiver, the only nonvanishing attractor invariants are in fact:

$$\Omega_{*,e_i} = 1 \tag{3.5.17}$$

for e_i the dimensions vectors of the nodes of the quiver. According to [Mou19], one can relate the attractor invariants of quivers related by mutations, from which one deduces that the attractor invariants of a quiver with potential, which is mutation-equivalent to an acyclic one, are also given by (3.5.17). In the language of scattering diagrams of [Bri17], the only incoming walls correspond to the nodes of the quiver, hence the stability scattering diagram coincides with the cluster scattering diagram.

The attractor invariants can be very complicated for a quiver with an arbitrary high number of arrows. However, in many cases, for quivers with potentials corresponding to $\mathcal{N} = 2$ $D = 4$ rigid supersymmetric field theory, one observes (or conjectures) that the only attractor invariants correspond to the nodes of the quiver or are supported on dimension vectors in $\Gamma_f = ker(\langle \cdot, \cdot \rangle)$, and in particular do not appear in the flow tree formula. In the language of scattering diagrams,

one says that the stability scattering diagram and the cluster scattering diagrams differ from an element that commutes with wall crossing. This is the case for quivers with potentials associated with triangulations of punctured surfaces, or class S theories in physical language, as was proven in [PYK21, Theorem 1.4].

For quivers with potentials arising from noncommutative crepant resolutions of CY3 singularities, it seems reasonable to suppose that this is also the case, in particular that the only attractor invariants correspond to nodes of the quivers, skyscraper sheaves (or D0 branes) (on dimension vectors $n\delta$), and dimension vectors of curves in the intersection of the Euler form. Some arguments in this direction were given, using estimation of the dimensions of moduli spaces, for cones over del Pezzo surfaces in [BMP20], and explicit computations in this direction for more general toric quivers were given in [MP20]. A general conjectural formula for the attractor invariants of toric quivers is given in Conjecture 7.3.9, and this formula was proven for local $\mathbb{P}^2$ in Theorem 9.1.1, using ideas from [BMP20].

Chapter 4

Summary of results

4.1 Hyperbolic localization of the Donaldson-Thomas sheaf

In Chapter 6, I developed a localization formula for cohomological DT invariants. Namely, consider a scheme or stack X with a $\mathbb{C}^*$-action. We can consider the fixed components $X^0 = \bigsqcup_{\pi\in\Pi} X^0_\pi$s, and the attracting locus X^+, which is a disjoint union $X^+ = \bigsqcup_{\pi\in\Pi} X^+_\pi$ of components flowing to fixed components when $t \to 0$. There is a diagram:

$$X \xleftarrow[\eta]{} X^+ \xrightarrow{p} X^0$$

where η denotes the inclusion, and p the projection given by the limit $p \to 0$. One then considers the hyperbolic localization functor:

$$p_!\eta^* : D^b_c(X) \to D^b_c(X^0) \tag{4.1.1}$$

Suppose now that X is smooth, and for $\pi \in \Pi$ denote by d^+_π the number of contracting weights in $T_x|_{X^0_\pi}$. The Białynicki-Birula decomposition of [BB73] says that p is an affine fiber bundle of dimension d^+_π. It can be expressed using Hyperbolic localization as an isomorphism:

$$p_!\eta^*\mathbb{Q}_X \simeq \bigoplus_{\pi\in\Pi} \mathbb{Q}_{X^0_\pi}[-2d^+_\pi] \tag{4.1.2}$$

Here $\mathbb{Q}_Y$ denotes the structure sheaf of Y. By taking the hypercohomology with compact support, one obtains an equality in the Grothendieck ring R of monodromic mixed Hodge structures:

$$H_c(X) = \sum_{\pi\in\Pi} (-y)^{2d^+_\pi} H_c(X^0_\pi) + H_c(X - \eta(X^+) \tag{4.1.3}$$

One can then obtain the cohomological DT invariants of X from the cohomological DT invariants of the fixed components, and the cohomology of the complement of the attracting variety, which are in general simpler than X itself.

I have established a similar localization formula when X is a -1-shifted symplectic scheme (resp stack), and the $\mathbb{C}^*$-action leaves the potential invariant. One needs a technical assumption, namely

that this action is étale-locally linearizable (resp lisse étale-locally linearizable), i.e. that X is covered by $\mathbb{C}^*$-equivariant affine étale charts which are affine (resp by a $\mathbb{C}^*$-equivariant smooth atlas being étale-locally linearizable). For schemes, (or algebraic spaces), this assumption is quite weak, and is satisfied if X is a quasi-separated algebraic space which is locally of finite type from [AHR19]. In this case, X^0 has a natural -1-shifted symplectic structure, and, a choice of orientation of X determines naturally a choice of orientation of X^0. Denoting by Ind_π the number of contracting weights in $\mathbb{T}_X|_{X^0_\pi}$, I have proven:

Theorem 4.1.1. *(Theorem 6.1.1) For X an oriented -1-shifted symplectic scheme or stack with an étale-locally linearizable $\mathbb{C}^*$ action leaving the shifted symplectic structure invariant. One has a natural isomorphism:*

$$p_!\eta^* P_X \simeq \bigoplus_{\pi\in\Pi} P_{X^0_\pi}[-\mathrm{Ind}_\pi] \tag{4.1.4}$$

By taking the cohomology with compact support:

$$H_c(X, P_X) = \sum_{\pi\in\Pi} (-y)^{\mathrm{Ind}_\pi} H_c(X^0_\pi, P_{X^0_\pi}) + H_c(X - \eta(X^+, P_X) \tag{4.1.5}$$

One can then reduce the computation of the cohomological Donaldson-Thomas invariants of X to the computation of the cohomological DT invariants of the fixed components and the complementary of the attracting locus. By taking the numerical limit, i.e. specializing to $t = y = 1$, one finds the usual localization result of [GP97] for numerical DT invariants, or its reformulation by Behrend [Beh09]:

$$\chi(X, \nu_X) = \sum_{\pi\in\Pi} \pm\chi(X, \nu_{X^0_\pi}) \tag{4.1.6}$$

The isomorphism (4.1.4) is first built for a critical chart (R, U, f, i). The idea is to shift by the dimensions of the localization formula (4.1.2), giving:

$$(p_U)!(\eta_U)^* \mathcal{IC}_U \simeq \bigoplus_{\pi\in\Pi} \mathcal{IC}_{U^0_\pi}[-\mathrm{Ind}_\pi] \tag{4.1.7}$$

and then to use the commutation of hyperbolic localization with vanishing cycles proven in [Ric16] to obtain:

$$(p_R)!(\eta_R)^* P_{U,f} \simeq \bigoplus_{\pi\in\Pi} P_{U^0_\pi, f^0_\pi}[-\mathrm{Ind}_\pi] \tag{4.1.8}$$

Finally, one has to use the gluing technology of [BBD+15] to show that these isomorphisms on critical charts glue together into in a global isomorphism (4.1.4), in particular that they are compatible with stabilization by quadratic forms: in this step, one has to check the functoriality property of all the isomorphisms that we considered, and to take care of the orientation issues.

4.2 Cohomological DT invariants from localization

4.2.1 Main result

In Chapter 7, I have applied my localization Theorem 4.1.1 to the case of quivers with potentials introduced above. Consider (Q, W) a toric quiver with potential arising from a brane tiling, as

presented above. The three-dimensional torus $\mathbb{T}^3$ acting on X acts also on (Q, W) by scaling the arrows, leaving the potential homogeneous. The two-dimensional subtorus $\mathbb{T}^2$ fixing the Calabi-Yau form on X corresponds to a two-dimensional subtorus leaving the potential W invariant. In particular, for $i \in Q_0$, it induces a torus action on the -1-shifted symplectic space $\mathcal{M}_{i,d}$ of i-framed representations, which leaves invariant the -1-shifted symplectic structure. One can then try to apply localization formulas for DT invariants to compute $Z_i(x)$ or its numerical limit. The advantage of working with framed representations is that the fixed components of the $\mathbb{T}^2$ action are isolated points, which have a nice combinatorial description, given in [MR08]. Namely, for the case of $\mathbb{C}^3$, fixed points are in correspondance with plane partitions. In general, fixed points corresponds to some generalisation of plane partitions called pyramid partitions, which are simple to enumerate given the data of the brane tiling. They form some sub-poset of an infinite poset, called the pyramid with atom i on the top, or the empty room configuration, which is given by all the $\mathbb{T}^3$-weights of paths beginning at i. Each element of the poset, corresponding to a path $v : i \to j$, is called an atom, and is said to have color j.

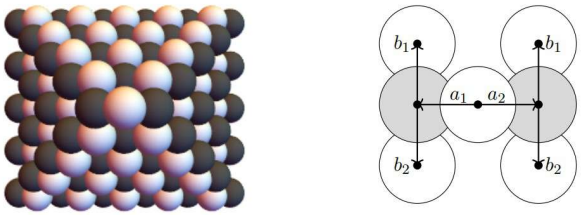

Figure 4.1: Empty room configuration for the toric quiver of the conifold, from [GY20]

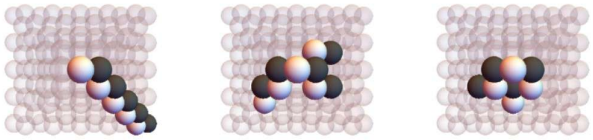

Figure 4.2: Empty room configuration for the toric quiver of the conifold, from [GY20]

We denote by Π_i the set of pyramid partitions with atom i on the top, and, for $\pi \in \Pi_i$, by d_π the corresponding dimension vector. Then, applying the localization formula for numerical DT invariants of [GP97], the authors of [MR08] obtained the result:

$$Z_i(x, y = 1, t = 1) = \sum_{\pi \in \Pi_i} \pm x^{d_\pi} \tag{4.2.1}$$

Here the sign is given by the parity of the dimension of the space of framed representations of Q (without considering the potential). It was a long-standing problem to refine this localization formula to a formula for cohomological DT invariants. To apply the localization result 4.1.1 one

must first choose a generic one dimensional subtorus $\mathbb{C}^* \subset \mathbb{T}^2$, such that the fixed components of $\mathbb{C}^*$ are also fixed by $\mathbb{T}^2$, and hence corresponds to pyramid partitions. This choice corresponds to a choice of slope s, i.e. a choice of a plane in the toric fan, which divides the extremal rays, i.e. the toric coordinates, into two sets, namely the set of toric coordinates which are expanded by the torus action, denoted by $\mathcal{Z}^s$, and the set of toric coordinates which are contracted by the torus action. We denote then by Ind_π^s the number of contracting weights in the tangent obstruction complex of $\mathcal{M}_{i,d_\pi}$. The main result that I have obtained in Chapter 7 is the following formula for generating series of framed invariants for toric quivers:

Theorem 4.2.1. *For a generic slope s, denoting by $\mathcal{Z}^s$ the set of expanded toric coordinates, one has:*

$$Z_i(x) = S_{-i}[\mathrm{Exp}\left(\textstyle\sum_d \Delta^s\Omega_d \frac{(-y)^{2d_i}-1}{-y+y^{-1}} x^d\right)] \sum_{\pi\in\Pi_i} (-y)^{\mathrm{Ind}_\pi^s} x^{d_\pi} \tag{4.2.2}$$

using the correction term:

$$\begin{aligned}\Delta^s\Omega(x) =&(-y^3 - (\textstyle\sum_{z\in\mathcal{Z}^s} K_z - 2)y + (\sum_{z\in Z} K_z - 1)y^{-1}) \sum_{n\geq 1} x^{n\delta} \\ &+ (-y+y^{-1}) \sum_{z\in\mathcal{Z}^s} \sum_{k\neq k'} \sum_{n\geq 0} x^{n\delta+\alpha^{\tilde{z}}_{[k,k'[}}\end{aligned} \tag{4.2.3}$$

This localization formula is particularly useful in the case of non-small crepant resolutions, where there are some compact divisors resolving the singularity, and the quiver is not symmetric. In this case, no closed formula is known, and this formula is the first one for cohomological DT invariants. It has been implemented on Mathematica for some toric geometries. The formula is completely algorithmic, and one can in principle write a program expressing these generating series from the simple data of the toric diagram, by building the toric quiver with potential using the fast forward algorithm

4.2.2 Sketch of proof

The proof goes as follows. The attracting variety of the $\mathbb{C}^*$ action is $\mathcal{M}_{i,d}^{Z:N}$, the closed subset of representations for which the cycles corresponding to the expanded toric coordinates in Z are nilpotent. We can form the generating series of the DT invariants with this nilpotency condition:

$$Z_i^{Z:N}(x) := \sum_{d\in\mathbb{N}^{Q_0}} H_c(\mathcal{M}_{i,d}^{Z:N}, P_{\mathcal{M}_{i,d}^{Z:N}}) x^d \tag{4.2.4}$$

The representations of Q with nilpotency constraints form a Serre subcategory of the category of representations of Q, namely an extension of two representations satisfy the nilpotency constraints if and only if the two representations satisfy those constraints. In this framework, the wall crossing and integrality formulas of [DM16] continue to hold. Then one can relate $Z_i^{Z:N}(x)$ with BPS invariants $\Omega_{\theta,d}^{Z:N}$ counting unframed semistable representations with the same nilpotency constraints.

The main interest of passing to unframed BPS invariants is that at this level invertible/nilpotent decomposition holds; in particular, for z a toric coordinate, one has the decomposition formula:

$$\Omega_{\theta,d} = \Omega_{\theta,d}^{z:N} + \Omega_{\theta,d}^{z:I} \tag{4.2.5}$$

where $\Omega_{\theta,d}^{z:N}$ (resp $\Omega_{\theta,d}^{z:I}$) is the BPS invariant counting representations where the cycle associated to z is nilpotent (resp invertible). But the representations with some cycles being invertible have very specific dimension vectors, which are in the kernel of the Euler form $\langle\cdot,\cdot\rangle$. The idea is that representations of (Q,W) with the cycles associated to z being nilpotent are representations of a localization of $J_{Q,W}$, which is a NCCR of:

$$X - x_z^{-1}(0) \simeq \mathbb{C}^* \times \mathbb{C}^2/\mathbb{Z}_{K_z} \tag{4.2.6}$$

This localization is isomorphic to a localization of the Jacobi algebra of the tripled quiver with potential resolving $\mathbb{C}\times\mathbb{C}^2/\mathbb{Z}_{K_z}$. Its DT invariants were computed in [Moz11], and are supported on dimension vectors $\alpha^z_{[k,k'[}$ corresponding to rational curves resolving the $\mathbb{C}^2/\mathbb{Z}_{K_z}$ singularity. Using several applications of the invertible/nilpotent decomposition formula (4.2.5), one obtains

$$\begin{aligned}\Delta^s\Omega(x) :=& \Omega_{\theta,d} - \Omega_{\theta,d}^{\mathcal{Z}^s:N}\\ =&(-y^3 - (\textstyle\sum_{z\in\mathcal{Z}^s} K_z - 2)y + (\sum_{z\in\mathcal{Z}^s} K_z - 1)y^{-1}) \displaystyle\sum_{n\geq 1} x^{n\delta}\\ &+ (-y+y^{-1}) \sum_{z\in\mathcal{Z}^s}\sum_{k\neq k'}\sum_{n\geq 0} x^{n\delta+\alpha^z_{[k,k'[}}\end{aligned} \tag{4.2.7}$$

The dimension vectors appearing in $\Delta^s\Omega(x)$ are in the kernel of the Euler form, hence $\Delta^s\Omega(x)$ does not depend on θ, and commutes with wall crossing. Using the formulas relating $Z_i(x)$ and $\Omega_{\theta,d}$, and the formulas relating $Z_i^{Z:N}(x)$ and $\Omega_{\theta,d}^{Z:N}$, one can complete the square and obtains:

$$Z_i(x) = S_{-i}[\mathrm{Exp}\left(\textstyle\sum_d \Delta^s\Omega_d \frac{(-y)^{2d_i}-1}{-y+y^{-1}} x^d\right)] Z_i^{\mathcal{Z}^s:N}(x) \tag{4.2.8}$$

Injecting (4.2.4), one obtains the main formula (4.2.2).

4.2.3 The case of $\mathbb{C}^3$ and MacMahon

This procedure is particularly enlightening for $\mathbb{C}^3$, which was studied in [BBS13]. Here there is just one node, so we call $Z(x)$ the generating series of framed DT invariants. The fixed points correspond to plane partitions, and then using toric localization, the generating series of numerical DT invariants is the MacMahon generating series:

$$Z(x) = \sum_{n\in\mathbb{N}} \mathrm{Pl}(n) x^n \tag{4.2.9}$$

Here $\mathrm{Pl}(n)$ denotes the number of plane partitions of n. This generating series was computed by MacMahon:

$$Z(x, y=1, t=1) = \mathrm{Exp}(\sum_{n\in\mathbb{N}} n x^n) = \prod_{n=1}^{\infty} \frac{1}{(1-x^n)^n} \tag{4.2.10}$$

In fact, the wall crossing formula between Z and Ω gives:

$$Z(x) = S_{-i}(\mathrm{Exp}(\sum_{n\in\mathbb{N}} \frac{(-y)^{2n}-1}{-y+y^{-1}} \Omega_n x^n)) \tag{4.2.11}$$

One then wants the numerical limit $\Omega_n(y=1,t=1)=-1$. This can be achieved in several ways. In [BBS13], it was shown that the correct refining is $\Omega_n=-y^3$: this result was obtained by computing directly $Z(x)$, by doing motivic decompositions on the space of framed representations. In this case, the localization computation can also be carried out completely. Namely, there are two nonequivalent choice of slopes: a choice s^+ in which one toric coordinates (say x) is expanded, and two are contracted, and a choice s^- in which two coordinates (say x,y) are expanded, and one is contracted. One can then compute the generating series:

$$Z^{s^\pm}(x)=\sum_{\pi\in\Pi}(-y)^{\mathrm{Ind}_\pi^{s^\pm}}x^{d_\pi} \tag{4.2.12}$$

which are two different refinings of the MacMahon generating series. In this case, the computation of the index is very simple: because of many cancellations between the terms of the tangent-obstruction complex, it is only a sum of elementary contributions for each atom of the plane partition. The computation was then done in [NO16], and one obtains:

$$Z^{s^\pm}(x)=S_{-i}(\mathrm{Exp}(\sum_{n\in\mathbb{N}}\frac{(-y)^{2n}-1}{-y+y^{-1}}(-y)^{\pm 1}x^n)) \tag{4.2.13}$$

It gives precisely $\Omega_n^{x:N}=-y$ and $\Omega_n^{\{x,y\}:N}=-y^{-1}$. Our formula (4.2.1) gives exactly:

$$\Delta^{s^\pm}\Omega_n=-y^3+y^{\pm 1} \tag{4.2.14}$$

Then, using either of the two choices of localization, one obtains the correct refining $\Omega_n=-y^3$.

4.2.4 Computation of Ind_π^s

I will now explain precisely how to compute Ind_π^s. To obtain a localisation formula, we will study the $\mathbb{T}^3$-equivariant tangent space of a component $\mathcal{M}_{i,\pi}^0$ of the $\mathbb{T}^3$ fixed locus, in the moduli space

$$\mathcal{M}_{i,d_\pi}$$

of i-cyclic representations of the framed quiver of dimension d_π. Because the moduli space is a derived scheme, in particular the critical loci of a scheme, we will consider the virtual tangent/obstruction complex considered in appendix E of [CDM+14], and its $\mathbb{T}^3$ equivariant refinement. We denote by κ the weight of the superpotential W. For the framed quiver with potential (Q_i,W), this can be computed from the sequence [CDM+14]

$$0\to S_\pi^0\xrightarrow{\delta_0}S_\pi^1\xrightarrow{\delta_1}S_\pi^2\xrightarrow{\delta_2}S_\pi^3\to 0 \tag{4.2.15}$$

We denote by V_i the $\mathbb{T}^3$-equivariant vector space of paths of V ending on the node i (recall that V, as a $\mathbb{T}^3$ fixed point, admits a L_T grading: the $\mathbb{T}^3$ equivariant structure is given by the fact that V_λ is scaled by $t^{-\lambda}$). The various parts of the exact sequence are defined as follows:

- The space S_π^0 is the space of infinitesimal gauge transformations δg_i (we denote for convenience $\delta g_i=0$ for i a framing node):

$$S_\pi^0=\bigoplus_{i\in Q_0}\mathrm{Hom}_{\mathbb{C}}(V_{i,\pi},V_{i,\pi}) \tag{4.2.16}$$

- The differential δ_0 is the linearization of gauge transformations (taking care of the fact that framing nodes are not gauged):

$$\delta_0 : (\delta g_i)_{i\in Q_0} \mapsto (\delta g_j a - a\delta g_i)_{a:i\to j\in(Q_f)_1} \tag{4.2.17}$$

- S^1_π is the tangent space, i.e. the space of infinitesimal deformations of the arrows (δa):

$$S^1_\pi = \bigoplus_{(a:i\to j)\in(Q_f)_1} \mathrm{Hom}_{\mathbb{C}}(V_{i,\pi}, V_{j,\pi}) \otimes t_a \tag{4.2.18}$$

- The differential δ_1 is the linearization of the superpotential relations $r_a = \partial_a W_f = 0$:

$$\delta_1 : (\delta_a)_{a\in(Q_f)_1} \mapsto ((\partial r_b/\partial a).\delta_a)_{b\in(Q_f)_1} \tag{4.2.19}$$

- S^2_π is the space of obstructions, given by the superpotential relations $r_a = \partial_a W$: for $a : k \to j$, it is a relation between paths $v_i : j \to k$ such that av_i are cycles of the superpotential of weight κ, so the v_i have weight κt_a^{-1}, so:

$$S^2_\pi = \bigoplus_{(r_a:j\to k)\in\bar{R}} \mathrm{Hom}_{\mathbb{C}}(V_{j,\pi}, V_{k,\pi}) \otimes \kappa t_a^{-1} = \bar{S^1_\pi} \otimes \kappa \tag{4.2.20}$$

- δ_2 is linearization of relations between relations of the superpotential corresponding to each gauged node i:

$$\delta_2 : (r_a)_{a\in(Q_f)_1} \mapsto (\sum_{a:i\to j} r_a.a - \sum_{a:j\to i} a.r_a)_{i\in Q_0} \tag{4.2.21}$$

  Indeed, we can show for each gauged node i:

$$\delta_2(\partial_a W_f)) = 0 \tag{4.2.22}$$

  when we multiply a relation $\partial_a W_f$ by a, we obtain a relation between cycles of the superpotential. In fact, for each time that a given cycle v of the superpotential passes by the node i, there will be an arrow $a : j \to i$, so v will appear in $\partial_a W_f.a$, i.e. in $\delta_2(\partial_a W_f)_i$ with a $+$ sign; and an arrow $a : i \to j$, so v will appear in $a.\partial_a W_f$, so in $\delta_2(\partial_a W_f)_i$ with a $-$ sign; i.e. all these contributions cancels and $\delta_2(\partial_a W_f)_i = 0$ as claimed.

- Finally, S^3_π is the space of relations between relations of the superpotential. For each gauged node i it is a sum of cycles of the superpotential, i.e. of weights κ, so:

$$S^3_\pi = \bigoplus_{i\in Q_0} \mathrm{Hom}_{\mathbb{C}}(V_{i,\pi}, V_{i,\pi}) \otimes \kappa = \bar{S^0_\pi} \otimes \kappa \tag{4.2.23}$$

While the proposition below derives from deeper principles and was already implicit in [CDM+14], we shall outline a proof in order to gain more intuition:

Proposition 4.2.2. *The sequence (4.2.15) is a complex, self-dual up to a twist by κ. Its cohomology is supported in rank 1 and rank 2: the rank 1 cohomology corresponds to the first order deformations, and the rank two to higher order obstructions. In particular, deformations are dual to obstructions.*

Sketch of the proof: We have shown the self duality for the spaces S^i_π up to a twist by κ in the equations (4.2.20) and (4.2.23). The self duality for the morphisms δ_i follows from formal manipulations from the definition, and we refer to [CDM+14] for the proof.

The injectivity of d_0 corresponds informally to the fact that the framing rigidifies the representations. Consider an infinitesimal gauge transformation $(\delta g_i)_i$ in the kernel of d_0. Consider a rooted path v formed by $\infty_i \overset{a_1}{\to} i_1...i_{n-1} \overset{a_n}{\to} i_n$. We have:

$$\begin{aligned}\delta g_i v =&(\delta g_{i_n} a_n - a_n \delta g_{i_{n-1}}) a_{n-1}...a_1 + ... + a_n...(\delta g_{i_2} a_{i_2} - a_{i_2}\delta g_{i_1})a_{i_1} \\ &+ a_n...a_2(\delta g_{i_1} a_1 - a_1.0) = 0\end{aligned} \tag{4.2.24}$$

But rooted paths with target the node i generate V_i in the cyclic representation V, i.e. $\delta g_i = 0$, i.e. δ_0 is injective, as claimed.

The fact that $\delta_1 \circ \delta_0 = 0$ follows from the invariance of the superpotential relations under small gauge transformations: if we consider a relation $r_a : i_1 \to i_0$ coming from an arrow $a : i_0 \to i_1$, a cycle $i_0 \overset{a}{\to} i_1 \overset{b_1}{\to} i_2...i_{n-1} \overset{b_n}{\to} i_0$ of the superpotential will give a term $b_n...b_2\delta b_1 + b_n...\delta b_2 b_1 + ... + \delta b_n...b_2 b_1$ in $(\delta_1(\delta b_i))_a$. If $\delta b_i = \delta g_{i+1} b_i - b_i \delta g_i$, i.e. the deformation of the arrows is an infinitesimal gauge variation, there will be successive cancellations, and we will keep only $\delta g_0 b_n...b_1 - b_n...b_1 \delta g_1$. When summing over all cycle of the superpotential, we obtain $(\delta_1(\delta b_i))_a = \delta g_0 \partial W/\partial a|_\pi - \partial W/\partial a|_\pi \delta g_1 = 0$ because π satisfy the superpotential relations.

The fact that $\delta_2 \circ \delta_1 = 0$, and the surjectivity of δ_2, can be obtained by duality, respectively from the relation $\delta_1 \circ \delta_0 = 0$, and the injectivity of δ_0. In fact, $\delta_2 \circ \delta_1 = 0$ can also be obtained by linearizing (8.3.8).

Because of the injectivity of δ_0 and the surjectivity of δ_2, the exact sequence can have non-trivial cohomology only in S^1_π and S^2_π. The interpretation of the cohomology at S^1_π is clear: it corresponds to first order deformations of the arrows that respect the relations of the superpotential up to infinitesimal gauge transformation, i.e. it is the tangent space to the moduli scheme of framed representations. According to the generic principles of deformation theory, S^2_π are the obstructions to have higher order deformations. There is no higher obstructions, and the obstructions are dual to the first order deformations up to a factor κ, i.e. the virtual dimension of the moduli scheme is zero. This property of the Tangent Obstruction complex is generic for critical loci of a superpotential; and corresponds to the notion of $[-1]$-shifted symplectic structure in derived geometry.□

So we have the virtual tangent/obstruction class, given in $\mathbb{T}^3$ equivariant K-theory by:

$$\begin{aligned}T^{vir}_\pi &= \text{Deformations} - \text{Obstructions} \\ &= -S^0_\pi + S^1_\pi - S^2_\pi + S^3_\pi \\ &= -S^0_\pi + S^1_\pi - \kappa(-\bar{S^0_\pi} + \bar{S^1_\pi})\end{aligned} \tag{4.2.25}$$

where ω^π_i denotes the toric weights of $-S^0_\pi + S^1_\pi$.

The non-equivariant tangent/obstruction complex is self-dual, but its $\mathbb{T}^3$-equivariant version of is not, unless $\kappa = 1$. Henceforth, we shall restrict to the torus $\mathbb{T}^2$ leaving the superpotential W invariant, so that $\kappa = 1$. We denote d^0_+ (resp d^1_+) the number of contracting weights in S^0_π (resp in S^1_π), d^0_- (resp d^1_-) the number of repelling weights in S^0_π (resp S^1_π), and d^0_0 (resp d^1_0) the number of weights in n S^0_π (resp in S^1_π) that are invariants with this choice of slope. Ind^s_π is then given by the

count with sign, for a connected part π of the $\mathbb{T}^3$-fixed locus, the number of weights of T^{vir} that become contracting when $t \to 0$ in $\mathbb{C}^*$. This count is given, according to (4.2.25), by:

$$\mathrm{Ind}^s_\pi = -d^0_+ + d^1_+ - d^1_- + d^0_- \tag{4.2.26}$$

Consider now a pyramid π, and denotes, for $j \in Q_0$, by π_j the set of $\mathbb{T}^3$ weights of atoms of color j in the pyramid. For a $\mathbb{T}^3$ weight , define $\mathrm{sgn}^s(\lambda)$ to be:

- $+1$ if λ is contracting with respect to the slope s .
- -1 if λ is repelling contracting with respect to the slope s.
- 0 if λ is neutral contracting with respect to the slope s.

Then one obtains (recall that i is the framing node):

$$\mathrm{Ind}^s_\pi = \sum_{(a:j\to k)\in Q_1} \sum_{\lambda\in\pi_j} \sum_{\mu\in\pi_k} \mathrm{sgn}^s(\mu-\lambda-a) + \sum_{\lambda\in\pi_i} \mathrm{sgn}^s(\lambda) \tag{4.2.27}$$

This formula must then be inserted into (4.2.2). To obtain this formula from (4.2.26), remark that the first term comes from the contributions of arrows of Q in S^1_π, the second term comes from the contribution of the framing arrow to S^1_π, and that by symmetry the terms $d^0_\pm$ coming from the contribution of S^0_π cancel each others. For particular examples of such index computations with pictures, see [Cir20].

4.3 On the existence of scaling multi-centered black holes (with Boris Pioline)

In Chapter 8, we have studied the existence of particular types of BPS states in the strong, i.e. supergravity, limit and in the small coupling limit of $\mathcal{N}=2$, $D=4$ supersymmetric fields theory. Consider in such a theory some elementary electromagnetic charges γ_i for $i \in Q_0$, with electromagnetic pairing $\kappa_{ij} = \langle \gamma_i, \gamma_j \rangle$. In the small coupling limit, the BPS states with charge $\sum_i \gamma_i$ of such a theory are described by θ-stable Abelian (i.e. of dimension vector $(1,...,1)$) representations of a quiver with potential (Q,W). The quiver has no loops nor 2-cycles, and there are $\max(\kappa_{ij},0)$ arrows with source i and target j. We consider that W is a generic linear combination of the simple oriented cycles, i.e. oriented cycles which are not the product of two nontrivial oriented cycles. We assume furthermore that Q admits an R-charge, i.e. an assignment $R \in \mathbb{R}^{Q_1}$ such that W is homogeneous of R-charge 2: it is the condition to have a conformal limit in the infrared. Not every quiver has an R-charge, but we have obtained also some constraints for quivers without R-charges. Notice that in particular, the existence of an R-charge is equivalent to the existence of a cut, a set of arrows $I \subset Q_1$ such that each cycle of W contains exactly one arrow of I.

In the supergravity limit, we have seen that BPS states for a stability parameter θ are multi-centered black holes, i.e. 3-dimensional configurations of points $(x_i) \in (\mathbb{R}^3)^{Q_0}$ satisfying Denef's equations:

$$\sum_{j\neq i} \frac{\kappa_{ij}}{|x_i - x_j|} = \theta_i \quad \forall i \in Q_0 \tag{4.3.1}$$

The moduli space of multi-centered black holes can be noncompact when there are some asymptotic directions in it. Such asymptotic directions correspond to scaling solutions, solutions of Denef's equations with stability parameter $\theta = 0$

$$\sum_{j \neq i} \frac{\kappa_{ij}}{|x_i - x_j|} = 0 \quad \forall i \in Q_0 \tag{4.3.2}$$

Notice that this equation is conformal in the sense that its solutions can be scaled arbitrarily. This equation can be interpreted as a 'current conservation' at the nodes of the quiver: namely, to each arrow $(a : i \to j) \in Q_0$, we associate a strictly positive current $\lambda_a^0 := \frac{1}{|x_i - x_j|}$, and (8.1.3) expresses the fact that the current entering at each node is equal to the current outgoing at each node.

In the low coupling limit, we are interested in θ-stable Abelian representations of (Q, W) . According to [Kin94a], such representations are equivalently described by $(\phi_a)_{a \in Q_1} \in \mathbb{C}^{Q_1}$ satisfying the equations of the potential (also called the F-term equations), and the stability equation (also called the D-term equations):

$$\sum_{(a:i \to j) \in Q_1} |\phi_a|^2 - \sum_{(a:j \to i) \in Q_1} |\phi_a|^2 = \theta_i \quad \forall i \in Q_0 \tag{4.3.3}$$

In particular an attractor stability condition θ can always be written as:

$$\theta_i = \sum_{(a:j \to i) \in Q_1} (1 + \delta_a) - \sum_{(a:i \to j) \in Q_1} (1 + \delta_a) \tag{4.3.4}$$

with $\delta \ll 1$, hence we can rewrite the attractor stability equation as:

$$\sum_{(a:i \to j) \in Q_1} (1 + |\phi_a|^2 + \delta_a) = \sum_{(a:j \to i) \in Q_1} (1 + |\phi_a|^2 + \delta_a) \quad \forall i \in Q_0 \tag{4.3.5}$$

Hence this equation expresses the conservation of the positive current $\lambda_a^* := 1 + |\phi_a|^2 + \delta_a$ at the nodes of the quiver.

There is a first constraint for the existence of scaling solutions or Abelian attractor stable representations: the quiver Q must be strongly connected, hence it cannot be separated into two parts with arrows flowing only in one direction between the two parts. Indeed, if it were the case, there would be a strictly positive current flowing between the two parts, which would contradict current conservation.

The main result that we have obtained in Chapter 8 is a set of numerical constraints on the κ_{ij} for the existence of scaling solutions, or attractor stable Abelian representations. Such equations were well known in the case of a quiver with three centers, since [DM11a]. Consider a triangular quiver $Q : 1 \to 2 \to 3 \to 1$: scaling solutions are then triangles with sides of lengths $\lambda\kappa_{12}, \lambda\kappa_{23}, \lambda\kappa_{31}$, with $\lambda > 0$. Hence the κ_{ij}'s must satisfy the triangular inequalities:

$$\kappa_{12} \leq \kappa_{23} + \kappa_{31} \tag{4.3.6}$$

and circular permutations. We have generalized these types of inequalities to quivers with an arbitrary number of nodes. To understand this generalization, observe that the arrows with source

1 and target 2 (and permutations) form a cut I of Q, hence the triangular inequalities can be reformulated by saying that for any cut I, one has:

$$|I| \leq |Q_1 - I| \tag{4.3.7}$$

In fact, we have proven this for any quiver:

Theorem 4.3.1. *Consider a quiver Q admitting some scaling solutions, then for each cut $I \subset Q_1$, one has:*

$$|I| \leq |Q_1 - I| \tag{4.3.8}$$

If one supposes moreover that the quiver Q is biconnected, i.e. cannot be disconnected by removing a node, such an equality is saturated if and only if the scaling solutions are collinear. The proof of this theorem uses triangular inequalities in a crucial way. Namely, the idea is to express the positive conserved current λ as a sum of positive constant currents μ_w circulating on the oriented cycles w of the quiver. By definition, each cycle w contains a single arrow $a \in I$. The idea is to sum the generalized triangular inequalities with respect to a in the polygon defined by w in $\mathbb{R}^3$, with weight μ_w, and a simple computation gives (4.3.8).

It was noticed in [DM11a] that similar kinds of inequalities can be obtained for the existence of Abelian attractor stable representations in the three nodes quiver Q: $1 \to 2 \to 3 \to 1$, up to some assumptions. It was assumed here that any Abelian stable representation must lie in a 'branch' where one set of arrows vanish. Consider the branch in which the κ_{31} arrows with source 3 and target 1 vanish. The moduli space of stable representations of (Q, W) in this branch is cut out by κ_{31} relations of the potential inside the moduli space of Abelian representations of the quiver $1 \to 2 \to 3$, which is smooth of dimension $\kappa_{12} + \kappa_{23} - 2$. Assuming that the relations are transverse, the moduli space of Abelian attractor stable representations of (Q, W) is smooth of dimension $\kappa_{12} + \kappa_{23} - 2 - \kappa_{31} \geq 0$; if it in not empty we have then the inequality:

$$\kappa_{31} \leq \kappa_{12} + \kappa_{23} - 2 \tag{4.3.9}$$

Now, the attractor stability condition selects automatically the branch having the lowest expected dimension, hence giving the strongest constraints. Modulo the above assumptions, if Q has an Abelian attractor stable representation, then

$$\kappa_{31} \leq \kappa_{12} + \kappa_{23} - 2 \tag{4.3.10}$$

and its circular permutations holds.

In Chapter 8, we have proven the assumptions in this reasoning, using Bertini's theorem, assuming in a crucial way that the potential W is generic, and have generalized these inequalities to any quiver:

Theorem 4.3.2. *Consider a quiver with generic potential (Q, W) admitting an Abelian attractor stable representation, then for each cut $I \subset Q_1$, one has:*

$$|I| \leq |Q_1 - I| - |Q_0| + 1 \tag{4.3.11}$$

We have proven that for W generic, each stable Abelian representation lies in a branch where a set of arrows vanish, and we have proven a dimension estimate for each branch as presented above. The delicate part was to show that the attractor stability condition is the one which selects the branch having the lower expected dimension, ensuring that the inequality (4.3.11) holds for any cut. It was done using the formalism of conserved currents introduced above.

4.4 BPS Dendroscopy on Local $\mathbf{P^2}$ (with Pierrick Bousseau, Bruno Le Floch and Boris Pioline)

In Chapter 9, we have studied the flow tree formula on the stringy Kähler moduli space of local $\mathbb{P}^2$. This moduli space is given by the upper half plane $\mathbb{H}$, and is embedded in $\mathrm{Stab}_0(Y_{\mathbb{P}^2})$. The central charge is given as an holomorphic function of $\tau \in \mathbb{H}$:

$$Z_\tau(\gamma) = -rT_D(\tau) + dT(\tau) - ch_2 \tag{4.4.1}$$

Here T and T_D are given by periods of an holomorphic curve with $\Gamma_1(3)$ level structure. The embedding $\mathbb{H} \hookrightarrow \mathrm{Stab}_0(Y_{\mathbb{P}^2})$ corresponding to this central charge was described in [BM11]. The index 4 subgroup $\Gamma_1(3) \subset SL_2(\mathbb{Z})$ generated by $T : \tau \to \tau + 1$ and $V : \tau \to \tau/(1-3\tau)$ acts on $\mathbb{H}$. This action corresponds to an action by derived equivalence on $Y_{\mathbb{P}^2}$, with T being given by the tensor product with $\mathcal{O}(1)$, and V by the spherical twist $ST_{\mathcal{O}}$ (here $\mathcal{O}$ denotes the structure sheaf of the zero section $\mathbb{P}^2$). The fundamental chambers are presented in the following picture:

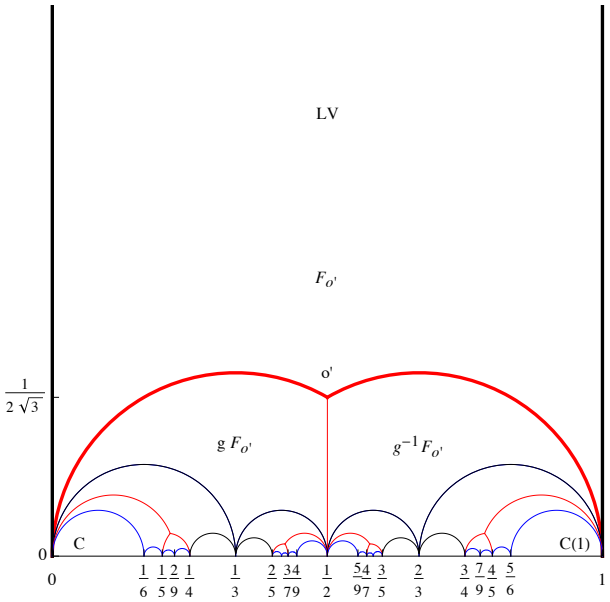

Figure 4.3: Fundamental domain of $\Gamma_1(3)$ centered around the orbifold point $\tau_{o'} = 1/2 + i/2\sqrt{3}$, and some of its images

The cusp at $\tau = i\infty$ corresponds to the large volume limit, i.e. Gieseker stability condition. In the fundamental domain $F_{O'}$ and its translated by T, the stability condition is geometric, i.e. skyscraper sheaves (or $D0$ branes) are stable. The point of intersection of three chambers corresponds to orbifold points (like o'), in the vicinity of which the stability condition is given by King stability condition on a quiver with potential, which is the McKay quiver of $\mathbb{C}^3/\mathbb{Z}_3$ introduced above. The corners of the chambers on the real line are called conifold points: in this point, some stable object becomes massless, e.g. $\mathcal{O}(m)$ becomes massless at $\tau = m$.

The scattering diagram underlying the flow tree formula was studied for local $\mathbb{P}^2$ in [Bou19], in a different slice of $\mathrm{Stab}_0(Y_{\mathbb{P}^2})$, which is an approximation of $\mathbb{H}$ near the large volume limit. It was then proven that the attractor flow tree formula is valid here, and amounts to counting finitely many binary trees with leaves corresponding to objects $\mathcal{O}(m)$ and $\mathcal{O}(m)[1]$.

In Chapter 9, we have generalized this analysis to the scattering diagram on the true stringy Kähler moduli space $\mathbb{H}$. The flow tree formula near an orbifold point corresponds to the flow tree formula for the Mckay quiver with potential as studied in [AB21]. In Chapter 9, we have obtained a description of the initial data, i.e. the attractor BPS invariants, for the Mckay quiver of $\mathbb{C}^3/\mathbb{Z}_3$:

Theorem 4.4.1. *(Theorem 9.1.1) For the McKay quiver with potential of $\mathbb{C}^3/\mathbb{Z}_3$, the attractor invariant $\Omega_{*,\gamma}$ vanishes for all dimension vectors γ except for*

$$\begin{aligned}\Omega_{*,\gamma_i} &= 1\\ \Omega_{*,k\delta} &= -y^3 - y - y^{-1}\end{aligned} \tag{4.4.2}$$

The proof uses a Nonabelian version of the proof of Theorem 4.3.2, using some dimension estimate. This proof was suggested in [BMP20], but we have removed some holes in the proof here.

Now, the scattering diagram on $\mathbb{H}$ is in principle built using initial rays emanating from all the conifold points, which are dense on the real line. Hence, the attractor invariant at the leaf of the trees appearing in the flow tree formula could in principle be any of the corresponding massless objects, and not only $\mathcal{O}(m)$ and $\mathcal{O}(m)[1]$, as in [Bou19]. We have shown that this is not the case, and that the attractor invariants appearing in the flow tree formula are really simple. Namely, consider $\tau \in \mathbb{H}$ in the geometric chamber, and a phase $\phi \in (0,1]$, and the flow trees giving the BPS states of phase ϕ at τ. We have first shown that there is a finite number of flow trees appearing in the flow tree formula. We have shown also that there is a critical phase ϕ_{crit} such that, for $|\phi - 1/2| \leq \phi_{crit}$, the attractor invariants appearing at the leaves of the flow trees giving the BPS states of phase ϕ are only the objects $\mathcal{O}(m)$ and $\mathcal{O}(m)[1]$, and are the same as in the scattering diagram of [Bou19]. For $|\phi - 1/2| > \phi_{crit}$, there are an accumulation of topological transitions at critical phases, where the flow tree gets more and more complicated, as in the following figure:

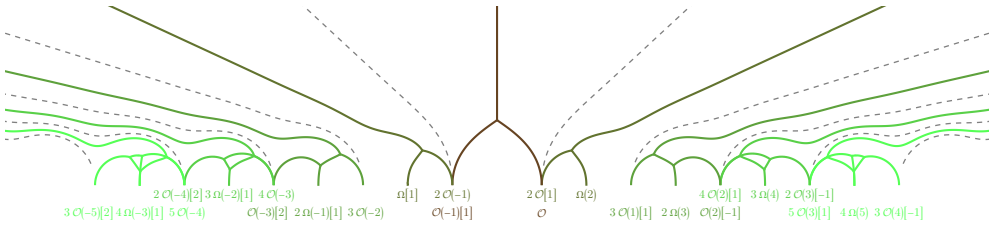

Figure 4.4: Trees contributing to $\gamma = (0, 1, -1/2) =$ for ϕ varying from 0 (right) to 1 (left). The dashed lines corresponding to the incoming rays for the different critical values of ϕ.

However, these flow trees are of a rather specific form. A vicinity of the large volume limit in $\mathbb{H}$ can be divided into 'orbifold regions' near the orbifold points at $\tau = m + 1/2 + i/2\sqrt{3}$, and a 'large volume region' above. The scattering diagram in the 'orbifold regions' are the scattering diagrams of the Mckay quiver, and the scattering diagrams in the 'large volume region' have initial data given

by rays outgoing from the orbifold regions. Hence the flow trees for $|\phi - 1/2| > \phi_{crit}$ have branches corresponding to flow trees for the McKay quiver. A precise expression of these results is given in Theorem 9.1.3.

This work provides the first treatment of the flow tree formula on the true stringy Kähler moduli space of a noncompact CY3, which exhibits a very rich behaviour. It would be interesting to pursue this work to study more complicated examples, such as other local del Pezzo surfaces.

Chapter 5

Conclusion and open directions

In this thesis, we have studied some aspects of BPS states counting in $\mathcal{N}=2$, $D=4$ supersymmetric fields theories obtained from compactification of type II superstring theories on a CY3-fold. The main computational tools developed and studied here, namely the toric localization formula and the flow tree formula, have been applied to rigid theories, originating from compactifications on local CY3-folds, or theories described by a quiver with potential. The case of BPS states counting for supergravity theories, as compactifications on compact CY3-folds, is more complicated. One mathematical difficulty in this case comes from the fact that the moduli spaces of BPS objects in this case are not further given by global critical charts, hence one must use the whole gluing technology of [BBD+15] to define the DT invariants counting BPS states. We present here some open directions to pursue this work.

Other applications of toric localization

In Chapter 7, I have applied my toric localization formula for cohomological DT invariants of Chapter 6 to the classical problem of counting framed representations of toric quiver with potentials. Given a toric CY3-fold X, one can also count framed sheaves in various chambers. The localization computation of numerical DT invariants is then given by the topological vertex formalism of [AKMV05], which share similarities with the enumeration of pyramid partitions of [MR08]. A K-theoretic version of these computations was provided in [IKV09], under the name of the refined topological vertex. As in Chapter 7, the refined topological vertex must compute the cohomological DT invariants of the attracting variety, and one must multiply the generating series of the refined topological vertex by some contribution of BPS invariants supported outside the attracting variety of X. It would be interesting to write this out concretely.

It would be also interesting to apply the localization formula of Chapter 6 to non-toric setting, for example for CY3-folds with action of a two dimensional torus, with a one dimensional subtorus $\mathbb{C}^*$ leaving the CY3-form invariant. In this case, the fixed components of this $\mathbb{C}^*$-action should not be isolated points, but have bigger dimension. However, one can hope that the localization problem is still tractable in this case.

Attractor BPS invariants of quiver with potentials

In Chapter 7, I have conjectured the formula 7.3.9 for the attractor BPS invariants of toric quivers. The conjecture is that the only dimension vectors supporting nontrivial attractor BPS invariants are:

- Dimension vectors e_i of simple objects/ fractional branes.
- Dimension vectors $n\delta$ of skyscraper sheaves/ D0 branes.
- Tower of dimension vectors $n\delta + \alpha^a_{[k,k'[}$ corresponding to line bundles on curves/D2 branes resolving extended A_n singularities.

We have proven this formula for the McKay quiver of $\mathbb{C}^3/\mathbb{Z}_3$ in Theorem 9.1.1, formalizing some arguments of [BMP20].

In fact, using the formalism of geometric stability conditions, it is possible to prove that, for any quiver with potential (Q, W) providing a noncommutative crepant resolution of a CY3 singularity, attractor invariants must be supported on walls between geometric chambers. Attractor BPS invariants must then come in towers $\Omega_{*,n\delta+k\alpha}$, with $\alpha < \delta$ and $\Omega*, \alpha \neq 0$. Hence, one has finally to find attractor invariants supported on dimension vectors $\alpha < \delta$, thereby destabilizing skyscraper sheaves/D0 branes. Using brane tiling techniques and arguments inspired by [BMP20] and Chapter 8, the proof of the conjecture 7.3.9 is almost complete and will hopefully be the subject of a future article. It seems possible that this conjecture is in fact a particular case of a formula holding for any quiver (Q, W) coming from a noncommutative crepant resolution of a CY3 singularity, and that in this generality the attractor BPS invariants are supported on dimension vectors e_i of fractional branes, $n\delta$ of D0 branes, and $n\delta+\alpha$ of D2-D0 branes wrapping extended ADE singularities. However, the proof of this conjecture outside the toric case seems far more complicated.

Flow tree formula for local del Pezzo surfaces

In Chapter 9, we have studied the flow tree formula on the stringy Kähler moduli space of local $\mathbb{P}^2$. It could be interesting to study this formula for other examples of local del Pezzo surfaces. One must begin with a study of the embedding of the stringy Kähler moduli space as a moduli space of Bridgeland stability conditions, as was done in [BM11]. This embedding is understood for the large volume approximation of the stringy Kähler moduli space, see [Moz22], but there is still some work to do for the exact stringy Kähler moduli space. It could be interesting to see if the phenomena appearing for local $\mathbb{P}^2$ were specific to this geometry or not.

Gluing structures in DT theory

In [BBD+15], the authors work to glue the perverse sheaves of vanishing cycles defined locally on critical charts to define a global perverse sheaf on any -1-shifted scheme or stack with orientation data. In Chapter 6, I have used this formalism to glue localization isomorphisms for perverse sheaves of vanishing cycles. Many structures in cohomological Donaldson-Thomas theory are currently only defined for quiver with potential, like the cohomological Hall algebra, the BPS lie algebra of Davison and Meinhardt, or the proof of the integrality of BPS invariants. These structures are expected to

exist for any reasonable CY3 category with suitable orientation data, but in this case one has to deal with gluing issues, as for the definition of the perverse sheave of [BBD+15]. In particular, one has to glue objects in ∞-categories, and not only the Abelian category of perverse sheaves, hence one must use homotopy coherent techniques.

Modularity of DT generating series

The S-duality is a conjectural duality relating type IIB string theory at low and large coupling: it is provided by an action of $SL_2(\mathbb{Z})$ on the axio-dilaton $\tau = c^0 + i/g_s$, with g_s the string coupling. When one compactifies type IIB on a compact CY3 X, $SL_2(\mathbb{Z})$ acts then on the quaternionic Kähler hypermultiplet moduli space $\mathcal{M}_H$. $\mathcal{M}_H$ is a complex integrable system fibered over the stringy Kähler moduli space $\mathcal{M}_K$. Its metric receives nonperturbative corrections from instantons, which correspond with B branes on X. The contribution of D6-D4-D2-D0 branes is subleading compared to contributions of D4-D2-D0 branes, using that the authors of [AP19b] have obtained from the $SL_2(\mathbb{Z})$-invariance of the metric some information about the action of $SL_2(\mathbb{Z})$ on generating series of D4-D2-D0 branes. Specifically, define Ω_γ^{MSW} to be the BPS invariant of γ in the large volume limit, or anti-attractor chamber. Consider that we fix the D4 brane charge p and consider the D2 brane charge μ up to spectral flow, and the D0 brane charge q_0. The main result of [AP19b] is that the numerical limit of the generating series:

$$h_{p,\mu}(\tau) := \sum_{q_0} \Omega^{MSW}_{(0,p,\mu,q_0)}) e^{-2\pi i q_0 \tau} \tag{5.0.1}$$

forms a vector valued higher depth mock modular forms. In [AMP20], it is conjectured that, taking into account the cohomological refinement, they form a higher depth mock Jacobi form. It means that, when p is irreducible, $(h_{p,\mu})_\mu$ forms a vector-valued Jacobi form, and, when p is reducible, one has a precise formula determining nonholomorphic completions $\hat{h}_{p,\mu}$ transforming as vector-valued Jacobi forms. $\hat{h}_{p,\mu}$ is expressed in terms of $h_{p',\mu'}$ for lower D4 brane charge p'. These modularity properties are really interesting for obtaining precise information on the entropy of BPS black holes.

Physically, the Kontsevich-Soibelman wall crossing formula can be derived from the continuity of the quaternionic Kähler metric on $\mathcal{M}_H$; see [AMPP13] for a review. As sketched above, cohomological Hall algebras arguments allow (up to some gluing issues) to prove this formula mathematically. It would be very nice to obtain a mathematical proof of the modularity properties of $h_{p,\mu}$, in order to have a mathematical check of S duality.

One other physical approach to proving physically the modularity of the D4-D2-D0 generating series is by using S duality between type IIA theory and M theory: Given a divisor p on a CY3 X, there is a 2D SCFT corresponding to an $M5$ wrapping p, whose characters must correspond to $h_{p,\mu}$. Mathematically, this SCFT must correspond to a vertex operator algebra, which one can build from the cohomological Hall algebra. This has been done for Hilbert schemes of points on surfaces, or CY2 quivers, by Nakajima; see [Nak16] for a review. One can then hope to derive the mock modular properties of the characters of this vertex operator algebra from some arguments similar to [Zhu95]. Another approach to proving mathematically these modularity properties is by using Noether-Lefschetz theory, as sketched in [FT20]. We hope to explore these interesting connections in future work.

Chapter 6

Hyperbolic localization of the Donaldson-Thomas sheaf

In this chapter we prove a toric localization formula in cohomological Donaldson Thomas theory. Consider a -1-shifted symplectic scheme or stack with a $\mathbb{C}^*$ action leaving the -1-shifted symplectic form invariant. This includes the moduli stack of sheaves or complexes of sheaves on a Calabi-Yau threefold with a $\mathbb{C}^*$-invariant Calabi-Yau form, or the intersection of two $\mathbb{C}^*$-invariant Lagrangians in a symplectic space with a $\mathbb{C}^*$-invariant symplectic form. In this case we express the restriction of the Donaldson-Thomas perverse sheaf defined by Joyce et al. to the attracting variety as a sum of cohomological shifts of the DT perverse sheaves on the $\mathbb{C}^*$ fixed components. This result can be seen as a -1-shifted version of the Białynicki-Birula decomposition for smooth schemes.

6.1 Introduction

Overview

A -1 shifted symplectic space or stack X, like the moduli stack of sheaves, or complexes of sheaves, on a Calabi-Yau threefold, or an intersection of two Lagrangians, is, informally, a space or stack where the obstruction space is dual to the tangent space. Building from ideas of Kontsevich-Soibelman, Joyce and collaborators have defined a perverse sheaf $P_{X,s}$ (and furthermore a monodromic mixed Hodge module on this perverse sheaf) on such X with a d-critical structure s and an orientation. The Euler number of the cohomology of this so-called Donaldson Thomas sheaf gives the numerical Donaldson-Thomas invariants defined by Thomas. The numerical DT invariant localizes under torus action leaving the shifted symplectic structure invariant as the Euler number of a smooth space, i.e. the numerical DT invariant of a space or stack X with an action of a torus $\mathbb{C}^*$ is the signed sum of the invariants of the $\mathbb{C}^*$-fixed components. On a smooth space, the Białynicki-Birula decomposition gives a refinement of the localization formula of the Euler number, which can be expressed using the hyperbolic localization functor as:

$$p_!\eta^*\mathbb{Q}_X \simeq \bigoplus_{\pi\in\Pi} \mathbb{L}^{\frac{d^+_\pi}{2}}\mathbb{Q}_{X^0_\pi} \tag{6.1.1}$$

where $\mathbb{Q}_Y$ denotes the constant sheaf on Y, $\mathbb{L}^{1/2}$ denotes the shift $[-1]$ of a complex (or the underlying monodromic mixed Hodge structure), η is the inclusion of the attracting variety X^+ of X, p is the projection of the attracting variety on the $\mathbb{C}^*$-fixed locus with connected components decomposition $X^0 := \bigsqcup_{\pi\in\Pi} X^0_\pi$ and d^+_π is the number of contracting weights in the action of $\mathbb{C}^*$ on the tangent space of X in X^0_π. For an algebraic space or stack X with a $\mathbb{C}^\star$-invariant d-critical structure s and orientation, the fixed components X^0_π carry natural d-critical structures s^0_π and orientation. In this chapter we prove a similar hyperbolic localization formula for the Donaldson-Thomas perverse sheaf (and monodromic mixed Hodge module) defined using those oriented d-critical structures:

$$p_!\eta^* P_{X,s} \simeq \bigoplus_{\pi\in\Pi} \mathbb{L}^{\mathrm{Ind}_\pi/2} P_{X^0_\pi, s^0_\pi} \tag{6.1.2}$$

where Ind_π is the signed number of contracting weights in the tangent obstruction complex of X on the component X^0_π. Hence, to compute the virtual class $[X]^{vir} := H_c(X, P_{X,s})$ of X in the Grothendieck group of monodromic mixed Hodge structures, one is reduced to the computation of the cohomological DT invariants of the fixed components (which in nice are cases isolated fixed points), and the cohomological DT invariants of the open complement $X - \eta(X^+)$ of the attracting locus (which in nice cases is simpler than the whole moduli space):

$$[X]^{vir} = \sum_{\pi\in\Pi} \mathbb{L}^{\mathrm{Ind}_\pi/2} [X^0_\pi]^{vir} + [X - \eta(X^+)]^{vir} \tag{6.1.3}$$

An example where this procedure can be carried out completely is given by framed invariants of toric quivers, as studied in [Des21]. When X is projective, or more generally when each point of X is in the attracting locus of a fixed component (one says that the $\mathbb{C}^*$-action is circle-compact), we obtain a formula similar to the localization formula for K-theoretic invariants:

$$[X]^{vir} = \sum_{\pi\in\Pi} \mathbb{L}^{\mathrm{Ind}_\pi/2} [X^0_\pi]^{vir} \tag{6.1.4}$$

The Donaldson-Thomas perverse sheaf

Donaldson-Thomas theory was first designed to count sheaves on Calabi-Yau threefolds. In [Tho98], Thomas defined the numerical Donaldson-Thomas invariants, giving the virtual Euler number of the moduli space of stable coherent sheaves on a Calabi-Yau threefold, using the perfect obstruction theory given by Serre duality on the Ext spaces of the sheaves. In [Beh09], Behrend gave a new interpretation of these invariants: expressing the moduli space locally as the critical locus of a potential, the numerical Donaldson-Thomas invariant is given by an Euler number weighted at each point by the Milnor number. In [KS] and [KS10], Kontsevich and Soibelman have sketched the definition of a cohomological refinement of this counting, with value in the abelian category of monodromic mixed Hodge modules (MMHM), using the functor of vanishing cycles of this potential, in a partially conjectural framework.

In papers [Joy13], [BBJ19],[BBD+15] and [BBBBJ15], Joyce and collaborators have developed a rigorous cohomological Donaldson-Thomas theory, using the language of $[-1]$ shifted symplectic structures in derived geometry introduced in [PTVV13]. Informally, derived geometry replaces the notion of tangent space T_X by a tangent complex $\mathbb{T}_X$, where $(\mathbb{T}_X)_0$ gives the tangent directions, $(\mathbb{T}_X)_1$ gives the obstructions, $(\mathbb{T}_X)_2$, $(\mathbb{T}_X)_3$, ... give the higher obstructions, and $(\mathbb{T}_X)_{-1}$ gives the

infinitesimal automorphisms. A $[-1]$-shifted symplectic structure gives a pairing between $\mathbb{T}_X$ and $\mathbb{T}_X[-1]$: in particular, it pairs tangent directions with obstructions. In [PTVV13], it was shown that moduli stack of complexes on a Calabi-Yau 3-fold, and intersections of two Lagrangians in a symplectic space, carry naturally a $[-1]$-shifted symplectic structure.

In [BBJ19] and [BBBBJ15], it was shown that $[-1]$-shifted derived schemes (resp. stacks) can be written locally as the critical locus of a functional on a smooth scheme, i.e. can be covered by critical charts of the form (R, U, f, i), where $R \subset X$ is open, U is a smooth scheme, $f : U \to \mathbb{C}$ a regular map, and $i : R \to U$ a closed embedding such that $i(R) = \mathrm{Crit}(f)$, and there is a way to compare intersecting critical charts. More formally, such a scheme (resp. stack) carries a d-critical structure s, a notion that we will introduce below. In [BBD+15], Joyce and collaborators has constructed the Donaldson-Thomas perverse sheaf $P_{X,s}$ carrying a monodromic mixed Hodge module for a d-critical scheme or stack (X, s), with extra data called orientation $K_X^{1/2}$. Its restriction to a critical (R, U, f, i) is given by $\mathcal{PV}_{U,f}$, the perverse sheaf (or monodromic mixed Hodge module) of vanishing cycles defined by applying the vanishing cycles functor ϕ_f of f to $\mathcal{IC}_U$, the intersection cohomology complex of U with its natural mixed Hodge module structure, and then restricting to R. The orientation is used to glue the perverse sheaves on intersections of critical charts. The numerical Donaldson-Thomas invariant defined in [Tho98] is then, as expected, the Euler number of the cohomology of this perverse sheaf. We will use the formalism of d-critical structures in the present article, but we shall not use the formalism of derived geometry and shifted symplectic structures.

Hyperbolic localization

The aim of this work is to provide a way to compute the cohomological Donaldson-Thomas invariants by localization, namely, given a d-critical scheme (or stack) X with a $\mathbb{C}^*$-action and a $\mathbb{C}^*$-invariant d-critical structure, express the invariants of X in terms of the invariants of the $\mathbb{C}^*$-fixed scheme (or stack) X^0. Graber and Pandharipande have proven a torus localization formula for numerical Donaldson-Thomas invariants in [GP97]. An analogue formula was derived in [BF08] using the alternative definition as weighted Euler numbers: the numerical Donaldson-Thomas invariants of X are the sum of those of each components of X^0 weighted by a sign given by the parity of the dimension of the normal space to the component. Hence numerical Donaldson-Thomas invariants localize under torus action exactly like the Euler numbers of smooth spaces.

In [BB73], Białynicki-Birula proved that, on a smooth scheme X with $\mathbb{C}^*$ action, the attracting subset of X (i.e. the subset of points $x \in X$ such that $\lim_{t\to 0} t.x$ exists) admits a sort of cellular decomposition. Each cell of this so-called Białynicki-Birula decomposition is an affine fiber bundle on a component of the fixed variety X^0, whose dimension is given by the number of contracting $\mathbb{C}^*$-weights in the tangent space of X^0. Hence one can compute the cohomology of the attracting subset of X in terms of the cohomology of X^0. In [Bra02] and [Dri13], Braden and Drinfeld gave a functorial reformulation of the Białynicki-Birula decomposition, which can be extended to singular algebraic spaces or stacks. For any algebraic space (resp. stack) X with $\mathbb{C}^*$-action one can define the $\mathbb{C}^*$-fixed space (resp. stack) X^0 and also the contracting (resp. repelling) space (resp. stack) $X^\pm$ using the functor of points in an obvious way. There is then the so-called hyperbolic localization diagram:

$$X \xleftarrow{\eta_X^\pm} X^\pm \xrightarrow{p_X^\pm} X^0$$

where $\eta_X^\pm$ is the inclusion of the attracting (resp. repelling) subset, and p_X^+ (resp. p_X^-) sends x to

$\lim_{t\to 0} x$ (resp. $\lim_{t\to\infty} x$). This diagram is easy to describe when X is an affine scheme: therefore it suffices to find $\mathbb{C}^*$-equivariant covering of X by affine spaces. The existence of such covering is not obvious at all, and is far too restrictive in the Zariski topology. Fortunately, a deep result of [AHR20] and [AHR19] shows that quasi-separated algebraic spaces locally of finite type have a $\mathbb{C}^*$-equivariant étale cover by affine spaces. For an algebraic stack $\mathcal{X}$ with a $\mathbb{C}^*$-action, consider $\mathcal{Y} := [\mathcal{X}/T]$; for $x \in \mathcal{X}$, considering the corresponding point $y \in \mathcal{Y}$, there is an exact sequence:

$$1 \longrightarrow G_x \longrightarrow G_y \longrightarrow T_x \longrightarrow 1$$

where G_x, G_y are the stabilizer groups of x, y and $T_x \subset T$ is the subgroup fixing x. Now according to [AHR20], a quasi-separated algebraic stack locally of finite type with affine stabilizers, such that the above exact sequence is split for all $x \in \mathcal{X}$, has a smooth $\mathbb{C}^*$-equivariant presentation from an affine scheme with $\mathbb{C}^*$-action. Under those assumptions, X^0 and $X^\pm$ are then algebraic spaces (resp. stacks). The functors $(p_X^\pm)_!(\eta_X^\pm)^*$ are called hyperbolic localization functors. From [Dri13] there is a natural morphism build from morphisms of the six-functor formalism in the derived category of constructible sheaves, or the derived category of monodromic mixed Hodge modules:

$$S_X : \mathbb{D}(p_X^-)_!(\eta_X^-)^*\mathbb{D} \to (p_X^+)_!(\eta_X^+)^* \tag{6.1.5}$$

This is by [Dri13] and [Ric16] an isomorphism when those functors are applied to $\mathbb{C}^*$-equivariant complexes, i.e. complexes equivariant under the action of $\mathbb{C}^*$, in a sense which we will explain below.

Assume now that X is smooth, and denote by Π the cocharacters of $\mathbb{C}^*$, and for $\pi \in \Pi$ X^0_π the union of the connected components of X^0 where the $\mathbb{C}^*$-action on T_{X^0} has cocharacter π. For $\pi \in \Pi$, denote by $d^0_\pi, d^+_\pi, d^-_\pi$ the number of invariants, resp. contracting, resp. repelling weights in π, and define $\mathrm{Ind}_\pi := p^+_\pi - p^-_\pi$. The Białynicki-Birula decomposition for smooth scheme says that $X^\pm$ is a disjoint union of affine fiber bundles $X^\pm_\pi$ of dimension $d^\pm_\pi$ over X^0_π. Using the hyperbolic localization functors, this can be reformulated as:

$$\begin{aligned}(p_X^\pm)_!(\eta_X^\pm)^*\mathbb{Q}_U &= \bigoplus_{\pi\in\Pi} \mathbb{L}^{d^\pm_\pi}\mathbb{Q}_{U^0_\pi}\\ \Rightarrow (p_X^\pm)_!(\eta_X^\pm)^*\mathcal{IC}_U &= \bigoplus_{\pi\in\Pi} \mathbb{L}^{\pm\mathrm{Ind}_\pi/2}\mathcal{IC}_{U^0_\pi}\end{aligned} \tag{6.1.6}$$

where $\mathbb{Q}_Y$ and $\mathcal{IC}_Y$ are respectively the constant sheaf and the intersection complex of Y, or their natural mixed Hodge modules. This isomorphism sends S_X to the self-duality isomorphism of the intersection complex.

The main result

For a $\mathbb{C}^*$-equivariant oriented d-critical scheme or stack X satisfying the assumptions under which the hyperbolic localization functors were defined, we will prove that X^0 carries a natural d-critical structure s^0, and a natural orientation $K_{X^0}^{1/2}$ on (X^0, s^0) induced by $K_X^{1/2}$. The aim of this article is to prove that an analogue of (6.1.6) holds for the Donaldson-Thomas perverse sheaf (resp. monodromic mixed Hodge module) on a d-critical oriented algebraic space (theorem 6.4.2) or stack (theorem 6.5.3):

Theorem 6.1.1. *For X a quasi-separated locally of finite type algebraic space (resp. a quasi-separated locally of finite type algebraic stack with affine stabilizers such that the exact sequence 6.1 is split for each $x \in X$) with an action of a one dimensional torus $\mathbb{C}^*$ and $\mathbb{C}^*$-equivariant d-critical structure s and orientation, there are natural isomorphisms of perverse sheaves and monodromic mixed Hodge modules:*

$$\beta^{\pm}_{X,s} : (p^{\pm}_X)_!(\eta^{\pm}_X)^* P_{X,s} \xrightarrow{\simeq} \bigoplus_{\pi\in\Pi} \mathbb{L}^{\pm \mathrm{Ind}_\pi/2} P_{X^0_\pi, s^0_\pi} \tag{6.1.7}$$

where Ind_π denotes the signed number of contracting weights in the $\mathbb{C}^*$ action on the tangent obstruction complex of X at X^0_π.

Sketch of the proof

The main ingredient of the proof of this theorem is the commutation of the hyperbolic localization and vanishing cycles functor proven in [Ric16]. On a critical chart (R, U, f, i), denoting (R^0, U^0, f^0, i^0), combining this with the classical Białynicki-Birula decomposition of U (6.1.6), one obtains isomorphisms in the derived category of constructible sheaves with monodromy, or of monodromic mixed Hodge modules:

$$\beta^{\pm}_{U,f} : (p^{\pm}_R)_!(\eta^{\pm}_R)^* \mathcal{PV}_{U,f} \to \bigoplus_{\pi\in\Pi} \mathbb{L}^{\pm \mathrm{Ind}_\pi/2} \mathcal{PV}_{U^0_\pi, f^0_\pi} \tag{6.1.8}$$

This is the content of proposition 6.3.3. We must show that these isomorphisms behave well with respect to the pullback by étale (resp. smooth) maps of critical locus: this is the content of proposition 6.3.4. We must also show that they behave well with respect to the Thom-Sebastiani isomorphism from [Mas01]:

$$\mathcal{TS}_{U,f,V,g} : \mathcal{PV}_{U\times V, f\boxplus g} \simeq \mathcal{PV}_{U,f} \boxtimes \mathcal{PV}_{S,g} \tag{6.1.9}$$

This is the content of proposition 6.3.5.

Now, consider a d-critical oriented algebraic space (X, s). The isomorphism $\beta^{\pm}_{X,s}$ is an isomorphism in the abelian category $\bigoplus_\pi \mathrm{Perv}(X^0_\pi)[-\mathrm{Ind}_\pi]$ of shifted perverse sheaves, or the abelian category $\bigoplus_\pi \mathrm{MMHM}(X^0_\pi)[-\mathrm{Ind}_\pi]$ of monodromic mixed Hodge modules, which forms stacks for the étale topology on X, hence it suffices to define them to be $\beta^{\pm}_{U,f}$ on each critical chart (R, U, f, i), and to show that they agree on intersections of critical charts, the compatibility with monodromy and self-duality can be checked on critical charts. Notice that the tangent obstruction complex of X on R is quasi-isomorphic with $0 \to T_U \to T^*_U \to 0$, hence Ind_π is the signed number of contracting weights in the tangent-obstruction complex of X at X^0_π.

For d-critical algebraic spaces, one can glue the Donaldson-Thomas perverse sheaf on intersecting critical charts by embedding them étale-locally into a single critical chart. To show that the isomorphisms $\beta^{\pm}_{U,f}$ glue into a single isomorphism, one must show that they are compatible with embedding. Etale-locally, an embedding of critical charts is of the form $(U, f) \hookrightarrow (U \times E, f \oplus q)$ where q is a non-degenerate $\mathbb{C}^*$-invariant quadratic form on a $\mathbb{C}^*$-equivariant vector space E, and one glues the perverse sheaves using the isomorphism:

$$\mathcal{PV}_{U\times E, f\boxplus q} \xrightarrow{\mathcal{TS}_{U,f,E,q}} \mathcal{PV}_{U,f} \boxtimes \mathcal{PV}_{E,q} \xrightarrow{\simeq} \mathcal{PV}_{U,f}$$

where we have used the isomorphism $\mathcal{PV}_{E,q} \simeq \mathbb{Q}$, using a choice of orientation on E (this choice is at the root of orientation issues in cohomological DT theory). The proof of the compatibility of the isomorphisms $\beta^{\pm}$ with embeddings is then obtained using the compatibility with étale pullback and Thom-Sebastiani isomorphism proven above, and dealing with orientation issues.

For a d-critical oriented algebraic stack $(\mathcal{X}, s)$, an isomorphism $\beta^{\pm}_{\mathcal{X},s}$ in the abelian category $\bigoplus_{\pi} \mathrm{Perv}(\mathcal{X}^0_{\pi})[-\mathrm{Ind}_{\pi}]$ of shifted perverse sheaves can be defined by giving its pullback $\beta^{\pm}_{Y,y^\star(s)}$ by smooth 1-morphisms $y : Y \to \mathcal{X}$ from d-critical oriented algebraic space $(Y, y^\star(s))$, and by checking that for each smooth 2-morphism (ϕ, η) between 1-morphisms $y : Y \to \mathcal{X}$, $z : Z \to \mathcal{X}$, with $\phi : Y \to Z$ a smooth morphism of d-critical oriented algebraic spaces, one has:

$$\phi^*(\beta^{\pm}_{Z,z^\star(s)}) = \beta^{\pm}_{Y,y^\star(s)} \tag{6.1.10}$$

This is done in proposition 6.4.4.

In this chapter, we use the functorial properties of the six-functor formalism in the derived categories $D^b_c(Y)$ of bounded constructible complex over various algebraic spaces (or stacks) Y, or, more formally, an $(\infty, 1)$-categorical enhancement of them. When we say that a diagram commutes from the naturality of the six-functor formalism, we imply that it commutes up to a natural 2-isomorphism. Because the final diagrams lie in the abelian heart $\bigoplus_{\pi} \mathrm{Perv}(\mathcal{X}^0_{\pi})[-\mathrm{Ind}_{\pi}]$ of $D^b_c(X^0)$, which is a classical category, they truly commute. Moreover, without specification, all the algebraic spaces are assumed to be quasi-separated and locally of finite type, and all algebraic stacks are assumed to be quasi-separated, locally of finite type, and with affine stabilizers.

For X an algebraic space, the category $\mathrm{MHM}(X)$ of mixed Hodge modules is an abelian category with a faithful and exact functor $rat : \mathrm{MHM}(X) \to \mathrm{Perv}(X)$. In particular, because rat is faithful, the commutativity of a diagram can be checked at the level of perverse sheaves. Moreover, because a mixed Hodge module M is the data of filtrations on the $\mathcal{D}$-module associated to the complexification of the perverse sheaf $rat(M)$ by the Riemann-Hilbert correspondence, a morphism of mixed Hodge modules is an isomorphism if the underlying morphism of perverse sheaves is an isomorphism. There is a six-functor formalism on the derived category of mixed Hodge modules, which projects under rat on the six-functor formalism on $D^b_c(X)$, the derived category of constructible complexes. Furthermore, because rat is exact, a morphism between complexes of mixed hodge modules is an isomorphism in the derived category if the underlying morphism of constructible complexes is an isomorphism in the derived category. Hence the extension of our results to monodromic mixed Hodge modules is straightforward: our morphisms being defined easily using the six-functor formalism, so we used the same definition to extend them to morphisms in the derived category of monodromic mixed Hodge modules. The hard work consists in checking that these morphisms are isomorphisms, or that they gives commutative diagrams, but this can be checked at the level of perverse sheaves as explained above.

Analytic version

In [BBD+15], there is also an analytic version of cohomological Donaldson-Thomas theory, for analytic oriented d-critical analytic spaces, which are locally the critical locus of an holomorphic function. These constructions can also be extended to d-critical oriented analytic stacks using an analytic version of the constructions of [BBBBJ15]. Unfortunately we are missing crucial results on $\mathbb{C}^*$-action on analytic spaces or stacks. When an analytic space (resp. stack) with $\mathbb{C}^*$-action has a $\mathbb{C}^*$-equivariant analytic (resp. smooth) cover by an affine analytic space, we show that the fixed

and attracting/repelling variety are algebraic spaces (resp. stack), hence the hyperbolic localization functors, and the morphism S_X, are defined. However, we do not know under which generality such a $\mathbb{C}^*$-equivariant cover exists, and, according to David Rydh (private communication), the main techniques of [AHR20] does not apply directly to the analytic setting. Moreover, we need an analytic version of [Ric16, Theo B] saying that S_X is an isomorphism when applied to $\mathbb{C}^*$-equivariant complexes. Furthermore, according to [BBD+15, Remark 2.20], the six-functor formalism is not fully defined for mixed Hodge modules in the analytic case, hence it could be difficult to lift a localization result from the level of perverse sheaves to the level of mixed Hodge modules. Once such results are available, the whole results of this article should extend directly to the analytic case.

Relations to other works

The idea of using hyperbolic localization to obtain a localization formula in cohomological DT theory was first formulated by Balazs Szendroi section 8.4 of [Sze15]. It was applied in section 6 of [Nak16] and in the section 8.3 [RSYZ19], where it was used in a specific example of framed representations of quiver with potential. In [Ric16], Timo Richarz proved the commutativity of the hyperbolic localization with the vanishing cycles functor in greater generality. We have used this result to establish the formula (6.1.3) for any critical locus of a potential in [Des21], and the extension of this result to d-critical structures was suggested to us by Richard Thomas.

In [BJM19], the authors defined a Donaldson-Thomas motive, gluing the motive of vanishing cycles defined using arc spaces. Motives glue in the Zariski topology and not in the étale topology, hence to prove a localization formula one must a priori restrict to d-critical schemes admitting Zariski $\mathbb{C}^*$-equivariant critical charts. According to [Joy13, Prop 2.43], the existence of such charts is equivalent to the existence of a $\mathbb{C}^*$-equivariant Zariski cover (such a $\mathbb{C}^*$-action is then called 'good'), which holds for normal spaces from Sumihiro's theorem [S+74], but not in greater generality (see example 2.46 of [Joy13]). Davesh Maulik has proven a formula similar to (6.1.4) for motivic DT invariants on d-critical schemes with a good circle-compact $\mathbb{C}^*$-action, as explained in section 5.3 of [BBBBJ15], in an unpublished preprint (private communication). A generalization of this result for non-Archimedean geometry was proven after in [Jia17, Theo 7.17]. For non circle-compact actions one can compute the DT motive of the attracting variety, which is by definition circle-compact, by this way.

A toric localization similar to (6.1.4) exists also for K-theoretic DT invariants as defined in [NO16]. The K-theoretic DT invariants are a refinement of numerical DT invariants defined for projective moduli spaces with symmetric obstruction theories, which was developed parallel to the motivic and cohomological refinement of Kontsevich-Soibelman and Joyce and collaborators. One expect in general that they correspond to the χ_y genus of the Hodge polynomial of cohomological DT theory, hence in particular one replace $\mathbb{L}^{1/2}$ by $-y$ in K-theoretic formulas. When the moduli space X is non compact, but has a $\mathbb{C}^*$-action with compact fixed components, it was suggested in [NO16] to use the equation (6.1.4) to define the K theoretic invariants of X. However, this definition depends on the choice of the $\mathbb{C}^*$-action (this choice is called a choice of slope). The equation (6.1.3) in the non-projective case explains the origin of this ambiguity: one computes by toric localization only the virtual cohomology of the attracting variety, which is not the whole moduli space and depends on the chosen $\mathbb{C}^*$-action.

This dependency on the slope was studied explicitly in [Arb19] for the moduli space of framed representations of a toric quiver, and this was related to the ambiguity in the refined topological

vertex of [IKV09]. In this case, there is a two dimensional torus invariant acting on the moduli space of framed representations, scaling the arrows of the quiver by leaving the potential invariant, hence the space of slopes is $\mathbb{P}^1_{\mathbb{R}}$. The fixed points can be described as molten crystals from [MR08]. In [Arb19, Prop 3.3], it was established that there is a wall and chamber structure on the space of slopes, with the generating functions of framed invariants being constant in a chamber and jumping at a wall, the wall corresponding to slopes where the weight of an elementary cycle of the quiver becomes attracting or repelling. This is quite strange at first sight, because inside a given chamber the cohomological weight of a given molten crystal does changes on many walls, but the final result does not change: those walls are 'invisible'. In [Des21] it was established that the attracting variety is the subspace of representations where the cycles with repelling weights are nilpotent, hence the attracting variety changes exactly on the walls defined in [Arb19], i.e. (6.1.3) give an explanation of this wall and chamber structure. Moreover, using a nilpotent/invertible decomposition for unframed representation and a wall-crossing relation between framed and unframed invariants, [Des21] obtained the full framed generating series by multiplying the one obtained by localization by a generating series of framed invariants where some cycles are imposed to be invertible. The latter is simple to compute and has a universal closed formula for all toric quivers. Notice that in this case the moduli space is the critical locus of the potential of the quiver, hence one does not need all the subtleties of the gluing, i.e. one needs only proposition 6.3.3.

6.2 Classical Białynicki-Birula decomposition

6.2.1 Hyperbolic localization

Consider an algebraic space S, and X be an algebraic space over S with a relative $\mathbb{C}^*$ over S.

Definition 6.2.1. An algebraic space X over an algebraic space S with a relative $\mathbb{C}^*$ over S is said to be étale locally (resp. analytical locally) linearizable if there is a $\mathbb{C}^*$-equivariant étale (resp. analytical) covering family $\{U_i \to X\}_i$ where the U_i are affine S-algebraic spaces with $\mathbb{C}^*$-action.

According to [AHR19, Cor 20.2], an algebraic space X is then étale locally linearizable over S when X and S are quasi-separated, and X is locally of finite type over S, and we expect similarly that the fact of being analytic locally linearizable is not too restrictive. We will here adapt the setting of [Ric16] to the complex analytic case. Consider the following functors on the category of S-algebraic spaces:

$$\begin{aligned} X^0 :& Y \mapsto \mathrm{Hom}_S^T(Y, X) \\ X^+ :& Y \mapsto \mathrm{Hom}_S^T((\mathcal{A}^1_Y)^+, X) \\ X^- :& Y \mapsto \mathrm{Hom}_S^T((\mathcal{A}^1_Y)^-, X) \end{aligned} \tag{6.2.1}$$

where the superscript $\mathbb{C}^*$ denotes the $\mathbb{C}^*$-equivariant morphism, and $T, (\mathcal{A}^1_Y)^+, (\mathcal{A}^1_Y)^-$ has the trivial, resp. usual, resp. opposite $\mathbb{C}^*$-action.

The structure morphism $(\mathcal{A}^1_S)^\pm \to S$ is $\mathbb{C}^*$-equivariant and defines then a morphism:

$$\zeta^\pm : X^0 \to X^\pm \tag{6.2.2}$$

The zero section of $(\mathcal{A}^1_S)^\pm \to S$ defines a morphism:

$$p^\pm : X^\pm \to X^0 \tag{6.2.3}$$

such that $p^{\pm} \circ \zeta^{\pm} = \mathrm{Id}_{X^0}$. Finally, the unit section of $(\mathcal{A}^1_S)^{\pm} \to S$ defines a morphism:

$$\eta^{\pm} : X^{\pm} \to X \tag{6.2.4}$$

such that $\xi := \eta^+ \circ \zeta^+ = \eta^- \circ \zeta^-$ is the inclusion of the subfunctor $X^0 \subset X$. Hence it defines the hyperbolic localization diagram as in [Ric16]:

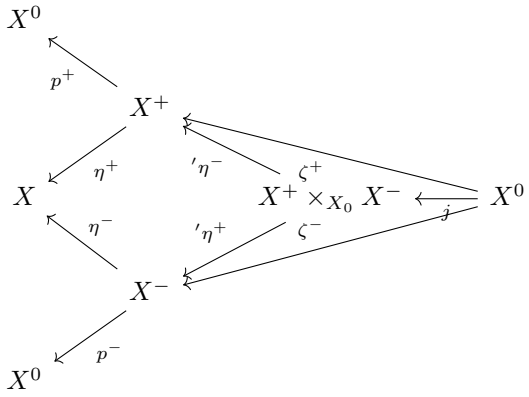

Proposition 6.2.2. *For X an S algebraic space with an étale (resp. analytical)-locally linearizable $\mathbb{C}^*$-action, X^0 is representable by a closed algebraic (resp. analytic) subspace of X, and $X^{\pm}$ are representable as X^0-affine algebraic (resp. algebraic) spaces, and j is open and closed.*

Proof: The version for algebraic spaces is [Ric16, Prop 1.17]. We give a similar proof in the complex analytic space. The proof of the proposition when X is affine goes exactly the same as in [Ric16, Lem 1.9], namely X^0, X^+, X^- are represented by the closed subscheme defined by the ideal of homogeneous elements of degree zero (resp. strictly negative, resp. strictly positive positive degree), and $X^0 = X^+ \times_{X_0} X^-$.

Suppose now the $U \to X$ is the embedding of a $\mathbb{C}^*$-invariant open subset of X in the analytic topology. One can adapt [Ric16, Lem 1.10]: for Y/S a complex analytic space, an element $\phi \in (U \times_X X_0)(Y)$ corresponds to a commutative diagram:

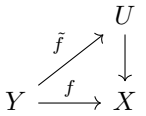

and, because $U \to X$ is an open immersion, $\tilde{f}$ is $\mathbb{C}^*$-equivariant, hence $\phi \in U^0(T)$. Then $U^0 = U \times_X X^0$ a functors, and then, taking a $\mathbb{C}^*$-equivariant analytic covering family $\{U_i \to X\}_i$ where the U_i are S-affine, one obtains a Cartesian commutative diagram:

$$\begin{array}{ccc} \bigsqcup_i U_i^0 & \longrightarrow & X^0 \\ \downarrow & & \downarrow \\ \bigsqcup_i U_i & \longrightarrow & X \end{array}$$

Because the top left element is representable, and the vertical left arrow is a closed immersion, one obtains that X^0 is representable as a close analytic subspace of X.

For $U \to X$ the embedding of a $\mathbb{C}^*$-invariant open subset of X in the analytic topology, one can adapt [Ric16, Lem 1.11]: for Y/S a complex analytic space, an element $\phi \in (U^0 \times_{X_0} X^{\pm})(Y)$ corresponds to a commutative diagram of $\mathbb{C}^*$-equivariant morphisms:

$$\begin{array}{ccc} Y & \xrightarrow{f|_Y} & U \\ \downarrow & & \downarrow \\ (\mathbb{A}^1_Y)^{\pm} & \xrightarrow{f} & X \end{array}$$

where $Y \to (\mathbb{A}^1_Y)^{\pm}$ is the zero section. The open subset $f^{-1}(U)$ contains Y and is $\mathbb{C}^*$ invariant in $\mathbb{A}^1_Y$, hence is the whole $\mathbb{A}^1_Y$, i.e. $\phi \in U^{\pm}(Y)$. Hence $U^{\pm} = U^0 \times_{X_0} X^{\pm}$ as functors, and taking a $\mathbb{C}^*$-equivariant analytic covering family $\{U_i \to X\}_i$ where the U_i are S-affine, one obtains a Cartesian commutative diagram:

$$\begin{array}{ccc} \bigsqcup_i U_i^{\pm} & \longrightarrow & X^{\pm} \\ \downarrow & & \downarrow \\ \bigsqcup_i U_i^0 & \longrightarrow & X^0 \end{array}$$

Because the top left element is representable, and the vertical left arrow is affine, one obtains that X^0 is representable as an affine analytic space on X^0. Moreover, $X^0 = X^+ \times_{X_0} X^-$ is an open and closed immersion because it is the case analytical locally.□

There is a natural transformation $\mathbb{D}(\eta^-)_!(p^-)^*\mathbb{D} \simeq (\eta^-)_*(p^-)^! \to (\eta^+)_!(p^+)^*$ built using the six-functor formalism between derived functors $D^b_c(X) \to D^b_c(X^0)$, as explained in [Ric16, Section 2.2], and we can define the same similar transformation at the level of mixed Hodge modules. We change slightly the terminology of [Ric16], replacing the term 'monodromic' by 'equivariant' to avoid future confusions with monodromic mixed Hodge modules. Let $a, p : T \otimes_S X \to X$ denote the action (resp. projection). We say that a constructible complex $A \in D^b_c(X)$ is naively $\mathbb{C}^*$-equivariant if there exists an isomorphism $a^*A \simeq p^*A$ in $D^b_c(T \otimes_S)$. Let us define $D^b_c(X)^{\mathbb{C}^*-eq}$ to be the full subcategory strongly generated by naively $\mathbb{C}^*$-equivariant complexes, i.e. generated by a finite iteration of taking the cone of a morphism in $D^b_c(X)$. The objects in $D^b_c(X)^{\mathbb{C}^*-eq}$ are called $\mathbb{C}^*$-equivariant. The result [Ric16, Theo B] can then be rephrased as:

Proposition 6.2.3. *For X an algebraic space with $\mathbb{C}^*$ action, the natural morphism of constructible complexes (or complexes of mixed Hodge modules) $S_X(A) : \mathbb{D}(\eta_X^-)_!(p_X^-)^*\mathbb{D}(A) \to (\eta_X^+)_!(p_X^+)^*(A)$ is an isomorphism when A is a $\mathbb{C}^*$-equivariant constructible complex.*

where we have used the fact that a morphism of complexes of mixed Hodge modules is an isomorphism if the underlying morphism of constructible is an isomorphism.

6.2.2 Compatibility with smooth morphisms

The hyperbolic localization diagram is functorial, namely for $\phi : X \to Y$ there are $\mathbb{C}^*$-equivariant morphisms $\phi^{\pm} : X^{\pm} \to Y^{\pm}$ and morphisms $\phi^0 : X^0 \to Y^0$, obtained by composition with ϕ using

the functor description, such that all the squares commutes in the following diagram:

$$\begin{array}{ccccc} X & \xleftarrow[\eta_X^{\pm}]{} & X^{\pm} & \underset{\zeta_X^{\pm}}{\overset{p_X^{\pm}}{\rightleftarrows}} & X^0 \\ \downarrow{\scriptstyle \phi} & & \downarrow{\scriptstyle \phi^{\pm}} & & \downarrow{\scriptstyle \phi^0} \\ Y & \xleftarrow[\eta_Y^{\pm}]{} & Y^{\pm} & \underset{\zeta_Y^{\pm}}{\overset{p_Y^{\pm}}{\rightleftarrows}} & Y^0 \end{array}$$

Proposition 6.2.4. *For a smooth $\mathbb{C}^*$-equivariant morphism $\phi : X \to Y$, $\phi^{\pm}$ and ϕ^0 are also smooth, and the natural map $X^{\pm} \to X^0 \times_{Y^0} Y^{\pm}$ is an affine fibre bundle.*

Proof: Consider first that ϕ is étale (resp. the embedding of an open subset in the analytic topology): then [Ric16, Lem 1.10, 1.11] (resp. our proof of the representability of $X^0, X^{\pm}$) shows respectively that $X^0 = X \times_Y Y^0$ and that $X^{\pm} = X^0 \times_{Y^0} Y^{\pm}$: in particular, ϕ^0, and therefore $\phi^{\pm}$, are étale (resp. the embedding of an open subset in the analytic topology) by base change.

Consider now the case of an affine $\mathbb{C}^*$-equivariant fibration $\phi : Y \times_S \mathbb{A}^d_S \to Y$ where the fiber has a linear $\mathbb{C}^*$ action. Then $\phi^0 : Y^0 \times_S (\mathbb{A}^d_S)^0 \to Y^0$ and $\phi^{\pm} : Y^{\pm} \times_S (\mathbb{A}^d_S)^{\pm} \to Y^{\pm}$ are smooth, and:

$$\begin{aligned} &(Y \times_S \mathbb{A}^d_S)^{\pm} = Y^{\pm} \times_S (\mathbb{A}^d_S)^{\pm} \\ \to &(Y \times_S \mathbb{A}^d_S)^0 \times_{Y^0} Y^{\pm} = Y^{\pm} \times_S (\mathbb{A}^d_S)^0 \end{aligned} \tag{6.2.5}$$

is affine.

Suppose now that ϕ is smooth. For $x \in X^0$, we can restricts to a $\mathbb{C}^*$-invariant étale (resp. open in the analytic topology) neighborhood of $\phi(x)$ in which Y is affine, and further restricts to a $\mathbb{C}^*$-invariant étale (resp. open in the analytic topology) neighborhood of x in X which is affine. As argued in the proof of proposition 2.43 of [Joy13, Prop 2.43], because $\mathbb{C}^*$ is a torus, an affine $\mathbb{C}^*$-equivariant space can be written as $Spec(R[x_1, ..., x_n]/(h_1, ..., h_r))$ where the x_i are $\mathbb{C}^*$-equivariant coordinates, and the h_i are $\mathbb{C}^*$-equivariant polynomial. Then the $\mathbb{C}^*$-equivariant smooth map $\phi : X \to Y$ is étale locally given by the dual of the map of rings:

$$\tilde{R}[x_1, ..., x_n]/(h_1, ..., h_r) \to \tilde{R}[y_1, ..., y_m]/(k_1, ..., k_s) \tag{6.2.6}$$

where we replace the ring of polynomial in n variables by the ring of holomorphic functions in n variables i the analytic setting, which can be rewritten:

$$R \to R[y_1, ..., y_m]/(l_1, ..., l_{r+s}) \tag{6.2.7}$$

where $R := \tilde{R}[x_1, ..., x_n]/(h_1, ..., h_r)$ and the l_i are the $\mathbb{C}^*$-equivariant polynomials (resp. holomorphic functions) $k_1, ..., k_r, x_1 - \phi'(x_1), ..., x_n - \phi'(x_n)$. Denote by c the rank of the matrix $(\frac{\partial l_i}{\partial y_j}|_x)_{ij}$ in the neighborhood of x, and up to reordering suppose that $(\frac{\partial l_i}{\partial y_j}|_x)_{0 \leq i,j \leq c}$ is invertible at x, hence in the neighborhood of x it is still invertible, i.e. $R[y_{c+1}, ..., y_m] \to R[y_1, ..., y_m]/(l_1, ..., l_{r+s})$ is étale (resp. a local homeomorphism) and $R[y_1, ..., y_m]/(l_1, ..., l_c) \to R[y_1, ..., y_m]/(l_1, ..., l_{r+s})$ is a local homeomorphism, hence ϕ can be étale locally written as a composition of $\mathbb{C}^*$-equivariant morphisms:

$$R \to R[y_{c+1}, ..., y_m] \to S[y_1, ..., y_m]/(l_1, ..., l_{r+s}) \tag{6.2.8}$$

where the second map is étale (resp. a local homeomorphism). Because $X^0 \to Y^0$, $X^\pm \to Y^\pm$ and $X^\pm \to X^0 \times_{Y^0} Y^\pm$ are smooth for $X \to Y$ $\mathbb{C}^*$-equivariant and étale (resp. open embeddings in the analytic topology) and for $X \to Y$ affine fibrations with $\mathbb{C}^*$-linear fibers, then it is true for smooth maps because the property of being smooth can be checked étale locally.

In order to show that the smooth morphism $q : X^\pm \to X^0 \times_{Y^0} Y^\pm$ is an affine fibre bundle, one can take $X = X^\pm$, $Y = Y^\pm$. We provide here a relative version of the proof of [J19, Lem 7.2]. Consider the sheaf of ring $\mathcal{B}_0$ of Y^0 (resp. $\mathcal{C}_0$ of X^0). Because $Y^\pm \to Y$ (resp. $X^\pm \to X$) is affine, it corresponds to a sheaf of $\mathbb{Z}$-graded $\mathcal{B}_0$- (resp. $\mathcal{C}_0$)-) algebra $\mathcal{B} = \bigoplus_{i\geq 0} \mathcal{B}_i$ (resp. $\mathcal{C} = \bigoplus_{i\geq 0} \mathcal{C}_i$). The morphism q is dual to $\mathcal{B} \otimes_{\mathcal{B}_0} \mathcal{C}_0 \to \mathcal{C}$. Consider a point $z \in \mathcal{B} \otimes_{\mathcal{B}_0} \mathcal{C}_0$ with residue field $\kappa(x)$, and consider a minimal system $f_1, ..., f_r$ of homogeneous generators of the ideal $\mathcal{C}_{>0}/(\mathcal{B}_{>0}) \otimes \kappa(z)$ of $\mathcal{C}/(\mathcal{B}_{>0}) \otimes \kappa(z)$. Shrink $X^0 \times_{Y^0} Y^\pm$ to an affine neighborhood z so that those generators lift to generators $F_1, ..., F_r$ of $\mathcal{C}_{>0}/(\mathcal{B}_{>0})$. On the one hand, we have a natural morphism $p : \mathcal{B} \otimes_{\mathcal{B}_0} \mathcal{C}_0[F_1, ..., F - r] \to \mathcal{C}$. Since $F_1, ..., F_r$ are homogeneous and generate the ideal $\mathcal{C}/(\mathcal{B}_{>0})$, the morphism p is surjective by induction on the degrees.

On the other hand, note that $f_1, ..., f_r$ are linearly independent in the relative cotangent space of q. As the fibers are smooth, we have $r \leq \dim(q^{-1}(z)) = \dim(Spec(\mathcal{C} \otimes \kappa(z)))$. Since q is flat, we have:

$$\mathcal{C} \otimes \kappa(z) = (\mathcal{B} \otimes_{\mathcal{B}_0} \mathcal{C}_0[F_1, ..., F - r]/\ker(p)) \otimes \kappa(z) = \frac{\kappa(z)[F_1, ..., F_r]}{\ker(p) \otimes \kappa(z)} \tag{6.2.9}$$

The right hand side has dimension r only if $\ker(p) \otimes \kappa(z) = 0$. Thus (after possibly shrinking $X^0 \times_{Y^0} Y^\pm$ again), we have $\ker(p) = 0$ and $\mathcal{C} \simeq \mathcal{B} \otimes_{\mathcal{B}_0} \mathcal{C}_0[F_1, ..., F - r]$, so $X^\pm = \mathbb{A}^r \times X^0 \times_{Y^0} Y^\pm$ locally on $X^0 \times_{Y^0} Y^\pm$, hence $X^\pm \to X^0 \times_{Y^0} Y^\pm$ is an affine fibre bundle.□

Denote now by Π the set of cocharacters of $\mathbb{C}^*$, and for a given cocharacter $\pi \in \Pi$, by $d_\pi^+, d_\pi^0, d_\pi^-$ respectively the number of $\mathbb{C}^*$-contracting, resp. $\mathbb{C}^*$-invariants, resp. $\mathbb{C}^*$-repelling weights, and by $\mathrm{Ind}_\pi = d_\pi^+ - d_\pi^-$. For a smooth $\mathbb{C}^*$-equivariant morphism $\phi : X \to Y$, denote by ϕ_π^0 the morphism ϕ^0 restricted to the locus of X^0 where the $\mathbb{C}^*$-action on X induces an action of cocharacter π on $T_{X/Y}$ (in particular it is smooth of relative dimension d_π^0). It induces a decomposition into connected components, hence $\phi^0 = \bigsqcup_{\pi\in\Pi} \phi_\pi^0$, and similarly $\phi^+ = \bigsqcup_{\pi\in\Pi} \phi_\pi^+$.

Proposition 6.2.5. *For a smooth $\mathbb{C}^*$-equivariant morphism $\phi : X \to Y$ of relative dimension d there are natural isomorphisms in the six-functor formalism for constructible complexes:*

$$(p_X^\pm)_!(\eta_X^\pm)^*\phi^*[d] \simeq \bigoplus_{\pi\in\Pi} \mathbb{L}^{\pm \mathrm{Ind}_\pi/2}(\phi_\pi^0)^*[d_\pi^0](p_Y^\pm)_!(\eta_Y^\pm)^* \tag{6.2.10}$$

moreover, they commute with the duality S_X and S_Y in an obvious way.

In particular if ϕ is étale (resp. a local biholomorphism), $T_{X/Y}$ is trivial, hence one has a natural isomorphism:

$$(p_X^\pm)_!(\eta_X^\pm)^*\phi^*[d] \simeq (\phi^0)^*[d](p_Y^\pm)_!(\eta_Y^\pm)^* \tag{6.2.11}$$

Proof: Consider the following commutative diagram:

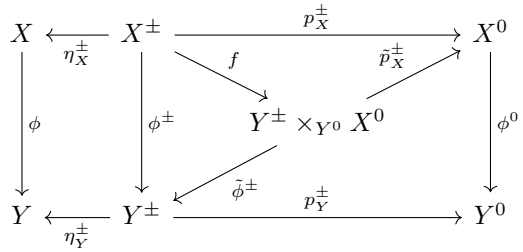

One has the following sequence of isomorphisms:

$$\begin{aligned}(p_X^\pm)_!(\eta_X^\pm)^*\phi^*[d] \simeq & (p_X^\pm)_!(\phi^\pm)^*[d](\eta_Y^\pm)^* \\ \simeq & (\tilde{p}_X^\pm)_! f_! f^*(\tilde{\phi}^\pm)^*[d](\eta_Y^\pm)^* \end{aligned} \tag{6.2.12}$$

where we have used the commutativity of the left square in the first line, and the commutativity of the two small triangles in the second line. The right square of the above diagram admits an decomposition as a disjoint union of those diagrams:

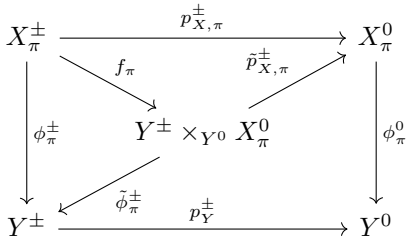

hence one obtains:

$$\begin{aligned}(\tilde{p}_{X,\pi}^\pm)_!(f_\pi)_!(f_\pi)^*(\tilde{\phi}_\pi^\pm)^*[d](\eta_Y^\pm)^* \simeq & (\tilde{p}_{X,\pi}^\pm)_![-2d_\pi^\pm](\tilde{\phi}_\pi^\pm)^*[d_\pi^+ + d_\pi^0 + d_\pi^-](\eta_Y^\pm)^* \\ \simeq & \mathbb{L}^{\pm \mathrm{Ind}_\pi/2}\phi_\pi^0[d_\pi^0](p_Y^\pm)_!(\eta_Y^\pm)^* \end{aligned} \tag{6.2.13}$$

where we have used the fact that f_π is an affine fibration with $d_\pi^\pm$-dimensional fiber in the first line and the base change in the down right Cartesian triangle in the second line. Summing on the connected components decomposition, one obtains a natural isomorphism in the six-functor formalism:

$$(p_X^\pm)_!(\eta_X^\pm)^*\phi^*[d] \simeq \bigoplus_{\pi\in\Pi} \mathbb{L}^{\pm \mathrm{Ind}_\pi/2}(\phi^0)^*[d_\pi^0](p_Y^\pm)_!(\eta_Y^\pm)^* \tag{6.2.14}$$

□

Now considering U a smooth S-algebraic space with $\mathbb{C}^*$-action, one can consider the smooth $\mathbb{C}^*$-equivariant morphism $\phi : U \to S$, where S has the trivial $\mathbb{C}^*$-action. The hyperbolic localization functor is then trivial on S, and:

$$\mathcal{IC}_U = \phi^*[d]\mathcal{IC}_S = \phi^![-d]\mathcal{IC}_S \tag{6.2.15}$$

in particular $\mathcal{IC}_S$ is $\mathbb{C}^*$-equivariant, hence $\mathcal{IC}_U$ is also $\mathbb{C}^*$-equivariant, and self-Verdier dual, hence the natural arrow $\mathbb{D}(p_U^-)_!(\eta_U^-)^*\mathcal{IC}_U \to (p_X^+)_!(\eta_X^+)^*\mathcal{IC}_U$ is an isomorphism. Moreover, there is then an open and closed decomposition $U^0 = \bigsqcup_{\pi\in\Pi} U^0_\pi$, and:

$$\mathcal{IC}_{U^0_\pi} = (\phi^0_\pi)^*[d^0_\pi]\mathcal{IC}_S = (\phi^0_\pi)^![-d^0_\pi]\mathcal{IC}_S \tag{6.2.16}$$

hence an absolute version of the last proposition gives:

Corollary 6.2.6. *For a smooth $\mathbb{C}^*$-equivariant S-algebraic (resp. analytic) space U there are natural isomorphisms in the six-functor formalism such that the following diagram commutes:*

$$\begin{array}{ccc} \mathbb{D}(p_U^-)_!(\eta_U^-)^*\mathcal{IC}_U & \xrightarrow{\simeq} & \\ \Big\downarrow{\scriptstyle s_U} & & \bigoplus_{\pi\in\Pi} \mathbb{L}^{\mathrm{Ind}_\pi/2}\mathcal{IC}_{U^0_\pi} \\ (p_U^+)_!(\eta_U^+)^*\mathcal{IC}_U & \xrightarrow{\simeq} & \end{array}$$

6.3 Critical Białynicki-Birula decomposition

In this section and in the rest of the chapter, all the algebraic spaces will be assumed to be quasi-separated and locally of finite type over $\mathbb{C}$: in particular, all the $\mathbb{C}^*$-actions will then be étale locally linearizable, the proper pullback and proper pushout of any functor, and the hyperbolic localization diagram, will be defined.

6.3.1 The functor of vanishing cycles

Consider an algebraic space U with a regular function $f : U \to \mathbb{C}$. We give a definition of the functor of vanishing cycles ϕ_f, which is equivalent to those exposed in definition 2.10 of [BBD+15]. Consider the following commutative diagram of complex analytic spaces, where U^{an} is the analytification of U, and the square are Cartesian:

$$\begin{array}{ccccc} U_0^{an} & \xrightarrow{\iota} & U^{an} & \xleftarrow{j_\theta} & \tilde{U}_\theta^{an} \\ \downarrow{\scriptstyle f} & & \downarrow{\scriptstyle f} & & \downarrow{\scriptstyle f} \\ \{0\} & \longrightarrow & \mathbb{C} & \longleftarrow & e^{i\theta}\{v\in\mathbb{C} | \Re(v) \le 0\} \end{array}$$

We define the functors:

$$\phi_f^\theta := \iota^*(j_\theta)_!(j_\theta)^! : D(X) \to D(X_0) \tag{6.3.1}$$

There are natural isomorphisms $\tilde{T}_f^\theta : \phi_f^0 \to \phi_f^\theta$ induced by rotating $\mathbb{C}$ counterclockwise by an angle θ around the origin. One defines the vanishing cycles functor $\phi_f := \phi_f^0$, and the natural isomorphism $\tilde{T}_f^{2\pi} : \phi_f \to \phi_f$ is the monodromy of vanishing cycle. Because ϕ_f is constructed using maps of analytic spaces and not maps of $\mathbb{C}$-schemes, it is not direct that they maps constructible complex of

U to constructible complex of U_0, but it is the case, as explained in definition 2.10 of [BBD+15], i.e. it defines a functor $\phi_f : D^b_c(U) \to D^b_c(U_0)$, and it even defines functors $\phi_f : \mathrm{Perv}(U) \to \mathrm{Perv}(U_0)$.

Massey defines in [Mas16] a natural isomorphism giving the commutation of the vanishing cycles functor (considered as a functor $\phi_f : D^b_c(U) \to D^b_c(U_0)$) with the Verdier duality $\mathbb{D}\phi_f \simeq \phi_f\mathbb{D}$. Consider the Cartesian diagram of closed subspaces:

$$\begin{array}{ccccc} U_0^{an} & & & & \\ & \searrow^{q} & & & \\ & & \tilde{U}_0^{an} \cap \tilde{U}_\pi^{an} & \xrightarrow{\hat{j}_\pi} & \tilde{U}_0^{an} \\ & & \downarrow{\scriptstyle \hat{j}_0} & \searrow^{m} & \downarrow{\scriptstyle j_0} \\ & & \tilde{U}_\pi^{an} & \xrightarrow{j_\pi} & U \end{array}$$

Then Massey defines the following sequence of isomorphisms:

$$\begin{aligned} \mathbb{D}\phi_f \simeq & \mathbb{D}q^* m^* (j_0)_! (j_0)^! \\ \simeq & \mathbb{D}q^! m^* (j_0)_! (j_0)^! \\ \simeq & \mathbb{D}q^! (\hat{j}_0)^! (j_\pi)^* \\ \simeq & q^* (\hat{j}_0)^* (j_\pi)^! \mathbb{D} \\ \simeq & q^* m^* (j_\pi)_! (j_\pi)^! \mathbb{D} \\ \simeq & \phi_f^\pi \mathbb{D} \end{aligned} \tag{6.3.2}$$

where in the first and last line we have used the fact that $\iota = m \circ q$, in the second line [Mas16, Lem 2.1] which proves that the natural morphism $q^! m^* (j_0)_! (j_0)^! \to q^* m^* (j_0)_! (j_0)^!$ is an isomorphism and in the third and fifth line the isomorphisms built in [Mas16, Lem 2.2] using the six-functor formalism in the Cartesian square of closed subspace of X, Using the fact that $U^{an} = \tilde{U}_0^{an} \cup \tilde{U}_\pi^{an}$. The Massey isomorphism is then defined by the composition:

$$\mathbb{D}\phi_f \xrightarrow{\simeq} \phi_f^\pi \mathbb{D} \xrightarrow{(\tilde{T}_f^\pi)^{-1}} \phi_f \mathbb{D}$$

and it commutes with the monodromy operator $\tilde{T}_f^{2\pi}$.

For two algebraic spaces X, Y with projections $\pi_1 : X \times Y \to X, \pi_2 : X \times Y \to Y$, for $F \in D^b_c(X), G \in D^b_c(Y)$, one denotes:

$$F \boxtimes G := \pi_1^*(F) \otimes \pi_2^* G \tag{6.3.3}$$

For $f; X \to \mathbb{C}, g : Y \to \mathbb{C}$, denote by $f \boxplus g := f \circ \pi_1 + g \circ \pi_2 : X \times Y \to \mathbb{C}$. For $j : Y \to X$ a closed embedding, denote $R\Gamma_Y := j_! j^! : D^b_c(X) \to D^b_c(X)$.

Consider two algebraic spaces U, V with a regular function $f : U \to \mathbb{C}, g : V \to \mathbb{C}$, denote by $k : U_0 \times V_0 \to (U \times V)_0$ the embedding into the zero locus of $f \boxplus g$. Massey defines in [Mas01] a natural Thom-Sebastiani isomorphism:

$$\phi_f \boxtimes \phi_g \simeq k^* \phi_{f \boxplus g} \tag{6.3.4}$$

denote by $\iota : U_0 \to U, \jmath : V_0 \to V, q : (U \times V)_0 \to U \times V$ the closed embeddings of the zero set of $f, g, f \boxplus g$. One has the closed embedding $\tilde{U}_0 \times \tilde{V}_0 \to (U \tilde{\times} V)_0$, and [Mas01, lem 1.2] shows that the natural arrow of the six-functor formalism $R\Gamma_{\tilde{U}_0 \times \tilde{V}_0} \to R\Gamma_{(U \tilde{\times} V)_0}$ is an isomorphism. The Thom-Sebastiani isomorphism is then defined by the composition of natural isomorphisms of the six-functor formalism:

$$\begin{aligned} \phi_f \boxtimes \phi_g =& \iota^* R\Gamma_{\tilde{U}_0} \boxtimes \jmath^* R\Gamma_{\tilde{V}_0} \\ \simeq& (\iota \times \jmath)^* R\Gamma_{\tilde{U}_0 \times \tilde{V}_0} \\ \xrightarrow{\simeq}& k^* q^* R\Gamma_{U \tilde{\times} V_0} \\ =& k^* \phi_{f \boxplus g} \end{aligned} \tag{6.3.5}$$

it is shown in [Mas01] that this isomorphism commutes with monodromy and it can be shown that it commutes with duality.

There is a theory of vanishing cycles functor for mixed Hodge modules, which projects under *rat* to the above theory for perverse sheaves, as exposed in [BBD+15, sec 2.10]. There is a vanishing cycle functor:

$$\phi_f^H : \mathrm{MHM}(U) \to \mathrm{MMHM}(U_0) \tag{6.3.6}$$

It sends a mixed Hodge module on U to a monodromic mixed Hodge module on U_0, i.e. a mixed Hodge module with commuting actions of a unipotent operator T_s and a nilpotent operator N, giving respectively the semisimple part and the logarithm of the unipotent part of the monodromy operator. There is also a self duality isomorphism and a Thom-Sebastiani isomorphism, and it is checked in [BBD+15, appendix A] that *rat* sends them to the corresponding isomorphisms of perverse sheaves. When a mixed Hodge module $M \in \mathrm{MHM}(U)$ is polarized, i.e. is provided with an isomorphism $\sigma : \mathbb{D}M \simeq M$, the self-duality isomorphism of ϕ_f^H provides them $\phi_f^H M$ with a strong polarization, i.e. an isomorphism with its dual commuting with monodromy.

6.3.2 Functoriality of the vanishing cycles

The vanishing cycles functor has some functoriality properties. Consider a map of algebraic spaces $\Phi : U \to V$, and a regular functions $f : V \to \mathbb{C}$, $f = g \circ \Phi : U \to \mathbb{C}$, and denote by $\Phi_0 : U_0 \to V_0$ the induced map on the zero locus.

Proposition 6.3.1. *There are natural morphisms built using the six-functor formalism for constructible complexes or complexes of mixed Hodge modules:*

$$\begin{aligned} (\Phi_0)^* \phi_g^\theta &\to \phi_f^\theta \Phi^* \\ (\Phi_0)_! \phi_f^\theta &\to \phi_g^\theta \Phi_! \end{aligned} \tag{6.3.7}$$

They are compatible with monodromy and Thom-Sebastiani isomorphism, and are compatible with composition and base change of Φ.

Proof: We consider then the commutative diagram, where all the squares are Cartesian:

$$\begin{array}{ccccc}
U_0^{an} & \xrightarrow{\iota_U} & U^{an} & \xleftarrow[j_{\theta,U}]{} & \tilde{U}_\theta^{an} \\
\downarrow{\scriptstyle \Phi_0} & & \downarrow{\scriptstyle \Phi} & & \downarrow{\scriptstyle \tilde{\Phi}_\theta} \\
V_0^{an} & \xrightarrow{\iota_V} & V^{an} & \xleftarrow[j_{\theta,V}]{} & \tilde{V}_\theta^{an} \\
\downarrow{\scriptstyle g} & & \downarrow{\scriptstyle g} & & \downarrow{\scriptstyle g} \\
\{0\} & \longrightarrow & \mathbb{C} & \longleftarrow & e^{i\theta}\{v \in \mathbb{C} | \Re(v) \leq 0\}
\end{array}$$

In the following of the proof, the superscript "an" will be implicit for readability. Then one has the following sequence of natural morphisms of the six-functor formalism:

$$\begin{aligned}
(\Phi_0)^* \phi_g^\theta =& \Phi_0^* (\iota_V)^* (j_{\theta,V})_! (j_{\theta,V})^! \\
\simeq& (\iota_U)^* \Phi^* (j_{\theta,V})_! (j_{\theta,V})^! \\
\simeq& (\iota_U)^* (j_{\theta,U})_! \tilde{\Phi}^* (j_{\theta,V})^! \\
\to& (\iota_U)^* (j_{\theta,U})_! (j_{\theta,U})^! \Phi^* \\
=& \phi_f^\theta \Phi^*
\end{aligned} \tag{6.3.8}$$

where the first and last lines are the definitions, the second line follows from the commutativity of the left square, the third from the Cartesianity of the right square, and then fourth from the commutativity of the right square.

$$\begin{aligned}
(\Phi_0)_! \phi_f^\theta =& (\Phi_0)_! (\iota_U)^* (j_{\theta,U})_! (j_{\theta,U})^! \\
\simeq& (\iota_V)^* \Phi_! (j_{\theta,U})_! (j_{\theta,U})^! \\
\simeq& (\iota_V)^* (j_{\theta,VU})^! \\
\to& (\iota_V)^* (j_{\theta,V})_! (j_{\theta,V})^! \Phi_! \\
=& \phi_g^\theta \Phi_!
\end{aligned} \tag{6.3.9}$$

where the first and last lines are the definitions, the second line follows from the Cartesianity of the left square, the third from the commutativity of the right square, and then fourth from the fact that the right square is Cartesian.

Because $f = g \circ \Phi$ these morphisms are compatible with the isomorphisms $\tilde{T}^\theta$, namely the following squares are commutative:

$$\begin{array}{ccc}
(\Phi_0)^* \phi_g & \longrightarrow & \phi_f \Phi^* \\
\downarrow{\scriptstyle (\Phi_0)^* \tilde{T}_g^\theta} & & \downarrow{\scriptstyle \tilde{T}_f^\theta \Phi^*} \\
(\Phi_0)^* \phi_g^\theta & \longrightarrow & \phi_f^\theta \Phi^*
\end{array} \qquad
\begin{array}{ccc}
(\Phi_0)_! \phi_f & \longrightarrow & \phi_g \Phi^* \\
\downarrow{\scriptstyle (\Phi_0)_! \tilde{T}_f^\theta} & & \downarrow{\scriptstyle \tilde{T}_g^\theta \Phi_!} \\
(\Phi_0)_! \phi_f^\theta & \longrightarrow & \phi_g^\theta \Phi_!
\end{array}$$

in particular these morphisms are compatible with the monodromy.

Consider now U, U', V, V' algebraic spaces with regular functions to $\mathbb{C}$ f, f', g, g' and maps $\Phi : U \to U'$, $\Psi : V \to V'$. Considering the Cartesian diagram, where the horizontal maps are closed embeddings:

$$\begin{array}{ccccc} U \times V & \longleftarrow & (U \tilde{\times} V)_0 & \longleftarrow & \tilde{U}_0 \times \tilde{V}_0 \\ \downarrow{\scriptstyle \Phi\times\Psi} & & \downarrow{\scriptstyle \Phi\times\Psi} & & \downarrow{\scriptstyle \Phi\times\Psi} \\ U' \times V' & \longleftarrow & (U' \tilde{\times} V')_0 & \longleftarrow & \tilde{U'}_0 \times \tilde{V'}_0 \end{array}$$

One has then commutative squares of morphisms from the six-functor formalism:

$$\begin{array}{cccc} (\Phi\times\Psi)^* R\Gamma_{\tilde{U'}_0\times\tilde{V'}_0} & \longrightarrow & R\Gamma_{\tilde{U}_0\times\tilde{V}_0}(\Phi\times\Psi)^* & \qquad (\Phi\times\Psi)_! R\Gamma_{\tilde{U}_0\times\tilde{V}_0} \longrightarrow R\Gamma_{\tilde{U'}_0\times\tilde{V'}_0}(\Phi\times\Psi)_! \\ \downarrow\simeq & & \downarrow\simeq & \qquad \downarrow\simeq \quad\quad \downarrow\simeq \\ (\Phi\times\Psi)^* R\Gamma_{(U'\tilde{\times}V')_0} & \to & R\Gamma_{(U\tilde{\times}V)_0}(\Phi\times\Psi)^* & \qquad (\Phi\times\Psi)_! R\Gamma_{(U\tilde{\times}V)_0} \to R\Gamma_{(U'\tilde{\times}V')_0}(\Phi\times\Psi)_! \end{array}$$

Consider now the Cartesian diagram:

$$\begin{array}{ccccc} U_0 \times V_0 & \xrightarrow{k} & (U\times V)_0 & \xrightarrow{q} & U\times V \\ \downarrow{\scriptstyle \Phi_0\times\Psi_0} & & \downarrow{\scriptstyle (\Phi\times\Psi)_0} & & \downarrow{\scriptstyle \Phi\times\Psi} \\ U'_0 \times V'_0 & \xrightarrow{k} & (U'\times V')_0 & \xrightarrow{q} & U'\times V' \end{array}$$

One has then commutative squares of morphisms from the six-functor formalism:

$$\begin{array}{cccc} (\Phi_0\times\Psi_0)^*(\iota'\times\jmath')^* & \to & (\iota\times\jmath)^*(\Phi\times\Psi)^* & \qquad (\Phi_0\times\Psi_0)_!(\iota\times\jmath)^* \to (\iota'\times\jmath')^*(\Phi\times\Psi)_! \\ \downarrow\simeq & & \downarrow\simeq & \qquad \downarrow\simeq \quad\quad \downarrow\simeq \\ k^*((\Phi\times\Psi)_0)^*(q')^* & \to & (\iota\times\jmath)^*(\Phi\times\Psi)^* & \qquad k^*((\Phi\times\Psi)_0)_! q^* \longrightarrow (\iota'\times\jmath')^*(\Phi\times\Psi)_! \end{array}$$

And one obtains then finally commutative square of morphisms:

$$\begin{array}{ccccc} (\Phi_0\times\Psi_0)^*(\iota'\times\jmath')^* R\Gamma_{\tilde{U'}_0\times\tilde{V'}_0} & \tilde{\Rightarrow} & (\iota\times\jmath)^*(\Phi\times\Psi)^* R\Gamma_{\tilde{U'}_0\times\tilde{V'}_0} & \to & (\iota\times\jmath)^* R\Gamma_{\tilde{U}_0\times\tilde{V}_0}(\Phi\times\Psi)^* \\ \downarrow\simeq & & \downarrow\simeq & & \downarrow\simeq \\ k^*(\Phi\times\Psi)_0^*(q')^* R\Gamma_{\tilde{U'}_0\times\tilde{V'}_0} & \tilde{\Rightarrow} & (\iota\times\jmath)^*(\Phi\times\Psi)^* R\Gamma_{\tilde{U'}_0\times\tilde{V'}_0} & \to & (\iota\times\jmath)^* R\Gamma_{\tilde{U}_0\times\tilde{V}_0}(\Phi\times\Psi)^* \\ \downarrow\simeq & & \downarrow\simeq & & \downarrow\simeq \\ k^*(\Phi\times\Psi)_0^*(q')^* R\Gamma_{\tilde{U'}_0\times\tilde{V'}_0} & \tilde{\Rightarrow} & (\iota\times\jmath)^*(\Phi\times\Psi)^* R\Gamma_{\tilde{U'}_0\times\tilde{V'}_0} & \to & (\iota\times\jmath)^* R\Gamma_{\tilde{U}_0\times\tilde{V}_0}(\Phi\times\Psi)^* \end{array}$$

And similarly:

$$\begin{array}{ccccc} (\Phi_0\times\Psi_0)_!(\iota\times\jmath)^* R\Gamma_{\tilde{U}_0\times\tilde{V}_0} & \tilde{\Rightarrow} & (\iota'\times\jmath')^*(\Phi\times\Psi)_! R\Gamma_{\tilde{U}_0\times\tilde{V}_0} & \to & (\iota'\times\jmath')^* R\Gamma_{\tilde{U'}_0\times\tilde{V'}_0}(\Phi\times\Psi)_! \\ \downarrow\simeq & & \downarrow\simeq & & \downarrow\simeq \\ (k')^*((\Phi\times\Psi)_0)_! q^* R\Gamma_{\tilde{U}_0\times\tilde{V}_0} & \tilde{\Rightarrow} & (\iota'\times\jmath')^*(\Phi\times\Psi)_! R\Gamma_{\tilde{U}_0\times\tilde{V}_0} & \to & (\iota'\times\jmath')^* R\Gamma_{\tilde{U'}_0\times\tilde{V'}_0}(\Phi\times\Psi)_! \\ \downarrow\simeq & & \downarrow\simeq & & \downarrow\simeq \\ (k')^*((\Phi\times\Psi)_0)_! q^* R\Gamma_{\tilde{U}_0\times\tilde{V}_0} & \tilde{\Rightarrow} & (\iota'\times\jmath')^*(\Phi\times\Psi)_! R\Gamma_{\tilde{U}_0\times\tilde{V}_0} & \to & (\iota'\times\jmath')^* R\Gamma_{\tilde{U'}_0\times\tilde{V'}_0}(\Phi\times\Psi)_! \end{array}$$

Hence the following diagrams are commutative:

$$\begin{array}{ccc} (\Phi_0\times\Psi_0)^*(\phi_{f'}\boxtimes\phi_{g'}) & \to & (\phi_f\boxtimes\phi_g)(\phi\times\Psi)^* \\ \downarrow\simeq & & \downarrow\simeq \\ k^*((\Phi\times\Psi)_0)^*\phi_{f'\boxplus g'} & \longrightarrow & \phi_{f\boxplus g}(\Phi\times\Psi)^* \end{array} \qquad \begin{array}{ccc} (\Phi_0\times\Psi_0)_!(\phi_f\boxtimes\phi_g) & \to & k^*(\phi_{f'}\boxtimes\phi_{g'})(\phi\times\Psi)_! \\ \downarrow\simeq & & \downarrow\simeq \\ (k')^*((\Phi\times\Psi)_0)_!\phi_{f\boxplus g} & \longrightarrow & k^*\phi_{f'\boxplus g'}(\Phi\times\Psi)_! \end{array}$$

i.e. the morphisms of the proposition are compatible with the Thom-Sebastiani isomorphism.

Consider now U, V, W algebraic spaces, with three regular maps to $\mathbb{C}$, and maps $\Phi : U \to V, \Psi : V \to W$ such that $f = g \circ \Phi, g = h \circ \Psi$. Considering the naturality of the six-functor formalism in the Cartesian diagram:

$$\begin{array}{ccccc} U_0 & \xrightarrow{\iota_U} & U & \xleftarrow[j_{\theta,U}]{} & \tilde{U}_\theta \\ \downarrow{\scriptstyle\Phi_0} & & \downarrow{\scriptstyle\Phi} & & \downarrow{\scriptstyle\tilde{\Phi}_\theta} \\ V_0 & \xrightarrow{\iota_V} & V & \xleftarrow[j_{\theta,V}]{} & \tilde{V}_\theta \\ \downarrow{\scriptstyle\Psi_0} & & \downarrow{\scriptstyle\Psi} & & \downarrow{\scriptstyle\tilde{\Psi}_\theta} \\ W_0 & \xrightarrow{\iota_W} & W & \xleftarrow[j_{\theta,W}]{} & \tilde{W}_\theta \\ \downarrow{\scriptstyle h} & & \downarrow{\scriptstyle h} & & \downarrow{\scriptstyle h} \\ \{0\} & \longrightarrow & \mathbb{C} & \longleftarrow & e^{i\theta}\{v\in\mathbb{C}|\Re(v)\leq 0\} \end{array}$$

one obtains directly that the following diagrams of morphisms are commutative:

$$\begin{array}{ccccc} & & (\Phi_0)^*\phi_g\Psi^* & & \\ & \nearrow & & \searrow & \\ ((\Psi\circ\Phi)_0)^*\phi_h = (\Phi_0)^*(\Psi_0)^*\phi_h & & \longrightarrow & & \phi_f\Phi^*\Psi^* = \phi_f(\Psi\circ\Phi)^* \end{array}$$

$$\begin{array}{ccccc} & & (\Psi_0)_!\phi_g\Phi_! & & \\ & \nearrow & & \searrow & \\ ((\Psi\circ\Phi)_0)_!\phi_f = (\Psi_0)_!(\Phi_0)_!\phi_f & & \longrightarrow & & \phi_f\Psi_!\Phi_! = \phi_f(\Psi\circ\Phi)_! \end{array}$$

hence the morphisms of the proposition are compatible with the composition.

Consider now a Cartesian square of morphisms between algebraic spaces:

$$\begin{array}{ccc} U\times_W V & \xrightarrow{\Phi'} & V \\ \downarrow{\scriptstyle\Psi'} & & \downarrow{\scriptstyle\Psi} \\ U & \xrightarrow{\Phi} & W \end{array}$$

and a regular function $f : W \to \mathbb{C}$. Consider now the following commutative diagram, where all

the squares are Cartesian:

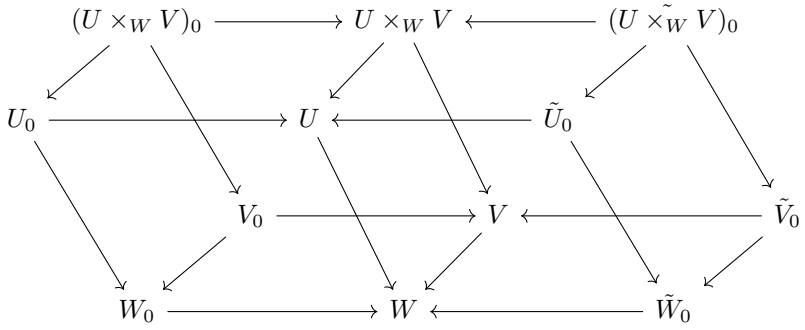

Hence from the naturality of the isomorphisms expressing the functoriality and base change of the six-functor formalism, one obtains that the following diagram of morphisms is commutative:

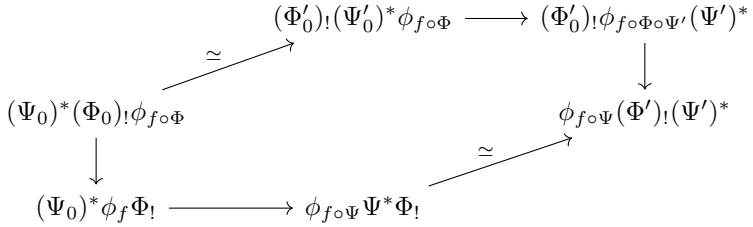

where the diagonal arrows are the isomorphisms from the base change and the vertical and horizontal arrows are the morphisms from the proposition. Then the morphisms of the proposition are compatible with base change.

The functoriality of functor of vanishing cycles for mixed Hodge modules shows that the morphisms of the proposition are defined at the level of mixed Hodge modules. Because of the compatibility results of [BBD+15, Appendix A], the functor *rat* sends the various squares expressing the compatibility conditions in this proposition to the corresponding squares at the level of perverse sheaves, which are commutative, hence they commute at the level of mixed Hodge modules. □

Now, for Φ smooth of relative dimension d (resp. Ψ proper), observing that $\mathbb{D}\Phi^*[d]\mathbb{D} = \Phi^*[d]$ (resp. $\mathbb{D}\Psi_!\mathbb{D} = \Psi_!$ and then also $\mathbb{D}(\Phi_0)^*[d]\mathbb{D} = (\Phi_0)^*[d]$ because Φ_0 is smooth of codimension d (resp. $\mathbb{D}(\Psi_0)_!\mathbb{D} = (\Psi_0)_!$ because Ψ_0 is proper), consider the following diagrams:

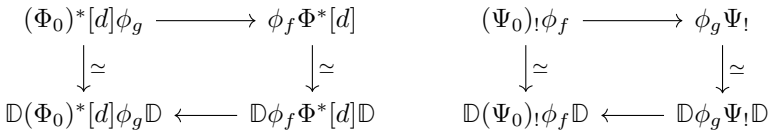

where the vertical arrows comes from the self-duality of the vanishing cycles functor. It is not hard to show that these squares are commutative, and we find again the standard fact that for Φ smooth

of relative dimension d, and Ψ proper, there are natural isomorphisms:

$$\begin{aligned}(\Phi_0)^*[d]\phi_g &\simeq \phi_f \Phi^*[d] \\ (\Psi_0)_!\phi_f &\simeq \phi_g \Psi_!\end{aligned} \tag{6.3.10}$$

commuting with the monodromy and the duality of the vanishing cycles.

Consider now a $\mathbb{C}^*$ action on U such that f is $\mathbb{C}^*$ invariant, i.e. U is can be considered as an algebraic space over $\mathbb{A}^1_{\mathbb{C}}$. In particular U is locally of finite type and quasi-separated over a quasi-separated base, hence the $\mathbb{C}^*$-action on it is étale-locally linearizable, and then the $\mathbb{C}^*$-action on U^{an} (and also on any base change of U^{an}) is analytic-locally linearizable over $\mathbb{C}$, hence the hyperbolic localization diagram of U^{an} and all its base change exists as diagrams of analytic spaces. Consider a $\mathbb{C}^*$-equivariant constructible complex A. The functor ϕ_f is defined using the morphisms of the six-functor formalism defined $\mathbb{C}^*$-equivariant functions, hence $\phi_f(A)$ is $\mathbb{C}^*$-equivariant. We will use the idea of [Ric16] to prove the commutation of the hyperbolic localization with the vanishing cycle:

Proposition 6.3.2. *For $A \in D^b_c(U)^{T-mon}$, the natural morphism $(p^{\pm}_{U_0})_!(\eta^{\pm}_{U_0})^*\phi_f \simeq \phi_{f^0}(p^{\pm}_U)_!(\eta^{\pm}_U)^*(A)$ is an isomorphism, compatible with monodromy and duality, in the sense that the following diagram is commutative:*

$$\begin{array}{ccc} (p^+_{U_0})_!(\eta^+_{U_0})^*\phi_f\mathbb{D}(A) & \xrightarrow{\simeq} & \phi_{f^0}(p^+_U)_!(\eta^+_U)^*\mathbb{D}(A) \\ \simeq\uparrow & & \simeq\uparrow \\ \mathbb{D}(p^-_{U_0})_!(\eta^-_{U_0})^*\phi_f\mathbb{D}(A) & \xleftarrow{\simeq} & \mathbb{D}\phi_{f^0}(p^-_U)_!(\eta^-_U)^*\mathbb{D}(A) \end{array}$$

where the vertical arrows are given by the isomorphisms of the vanishing cycles with its dual and the isomorphism of proposition 6.2.3, and commutes with Thom-Sebastiani isomorphism and pullback by smooth maps.

Proof: It follows directly from proposition 6.3.1 that the isomorphism of the proposition is compatible with monodromy. To show that the natural morphism is an isomorphism, we need only to show that the diagram of the proposition is commutative. In fact, the following diagram of $\mathbb{C}^*$-equivariant spaces:

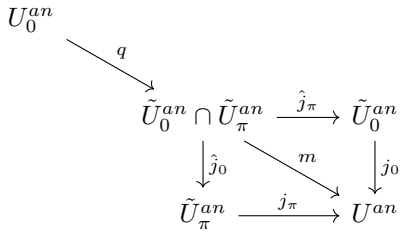

it is obtain by base change from the space $U^{an} \to 0$, hence the hyperbolic localisation diagram of all the spaces in this diagram are also obtained by base change from the hyperbolic localization diagram. Hence all the squares are Cartesian in the diagram obtained by superposing the hyperbolic localization diagrams of those spaces. hence the natural isomorphisms of the six-functor formalism

gives that the following square of isomorphisms is commutative:

$$\begin{array}{ccc} (p^+_{U_0})_!(\eta^+_{U_0})^*\phi^\pi_f\mathbb{D} & \longrightarrow & \phi^\pi_{f^0}(p^+_U)_!(\eta^+_U)^*\mathbb{D} \\ \uparrow & & \uparrow \\ \mathbb{D}(p^-_{U_0})_!(\eta^-_{U_0})^*\phi_f\mathbb{D}(A) & \longleftarrow & \mathbb{D}\phi_{f^0}(p^-_U)_!(\eta^-_U)^*\mathbb{D}(A) \end{array}$$

where the vertical arrow are given by Richarz morphism S_U and Massey's isomorphism $\mathbb{D}\phi_f \simeq \phi^\pi_f\mathbb{D}$. Because the isomorphism of the proposition is compatible with the monodromy, hence the following square is commutative:

$$\begin{array}{ccc} (p^+_{U_0})_!(\eta^+_{U_0})^*\phi_f\mathbb{D} & \longrightarrow & \phi_{f^0}(p^+_U)_!(\eta^+_U)^*\mathbb{D} \\ \downarrow{\scriptstyle (p^+_{U_0})_!(\eta^+_{U_0})^*\tilde{T}^\pi_f} & & \downarrow{\scriptstyle \tilde{T}^\pi_{f^0}} \\ (p^+_{U_0})_!(\eta^+_{U_0})^*\phi^\pi_f\mathbb{D} & \longrightarrow & \phi^\pi_f(p^+_U)_!(\eta^+_U)^*\mathbb{D} \end{array}$$

and then gluing vertically the two last squares we obtain that the square of the proposition is commutative.

Consider now U, V two algebraic spaces with $\mathbb{C}^*$ action, $\mathbb{C}^*$-invariants regular functions $f : U \to \mathbb{C}, g : V \to \mathbb{C}$, and a smooth map $\Phi : U \to V$ of relative dimension d. Applying the compatibility of the morphisms of proposition 6.3.1 with composition and base change to the morphisms in the following commutative diagram 6.2.2, one obtains that the following diagram is commutative:

$$\begin{array}{ccccc} & & \bigoplus_{\pi\in\Pi}\mathbb{L}^{\pm\mathrm{Ind}_\pi/2}(\Phi^0_{0,\pi})^*[d^0_\pi](p^\pm_{V_0})_!(\eta^\pm_{V_0})^*\phi_g & \longrightarrow & \bigoplus_{\pi\in\Pi}\mathbb{L}^{\pm\mathrm{Ind}_\pi/2}(\Phi^0_{0,\pi})^*[d^0_\pi]\phi_{g^0}(p^\pm_V)_!(\eta^\pm_V)^* \\ & \nearrow{\scriptstyle\simeq} & & & \downarrow{\scriptstyle\simeq} \\ (p^\pm_{U_0})_!(\eta^\pm_{U_0})^*(\Phi_0)^*[d]\phi_g & & & & \phi_{f^0}\bigoplus_{\pi\in\Pi}\mathbb{L}^{\pm\mathrm{Ind}_\pi/2}(\Phi^0_{0,\pi})^*[d^0_\pi](p^\pm_V)_!(\eta^\pm_V)^* \\ \downarrow{\scriptstyle\simeq} & & & \searrow{\scriptstyle\simeq} & \\ (p^\pm_{U_0})_!(\eta^\pm_{U_0})^*\phi_f\Phi^*[d] & \longrightarrow & \phi_{f^0}(p^\pm_U)_!(\eta^\pm_U)^*\Phi^*[d] & & \end{array}$$

hence this isomorphism is compatible with pullbacks by smooth maps.

Consider two smooth spaces U, V with a $\mathbb{C}^*$ action. The product space $U \times V$ is itself provided with a $\mathbb{C}^*$ action, and functors $X^0, X^\pm$ are obviously compatible with products, hence the hyperbolic localization diagram of $U \times V$ is the product of the hyperbolic localization diagrams of U and V. In particular:

$$\begin{aligned} (p_{U\times V})_!(\eta_{U\times V})^* &= (p_U \times p_V)_!(\eta_U \times \eta_V)^* : D^b_c(U \times V) \to D^b_c(U^0 \times V^0 = (U \times V)^0) \\ (p_{U_0\times V_0})_!(\eta_{U_0\times V_0})^* &= (p_{U_0} \times p_{V_0})_!(\eta_{U_0} \times \eta_{V_0})^* : D^b_c(U_0 \times V_0) \to D^b_c(U^0_0 \times V^0_0 = (U_0 \times V_0)^0) \end{aligned} \tag{6.3.11}$$

Denote now by $k : U_0 \times V_0 \to (U \times V)_0$ the natural closed embedding closed embedding. Using the two commutative diagram of 6.3.2, one obtains that the following diagram is commutative:

$$\begin{array}{ccccc} (p^\pm_{U_0} \times p^\pm_{V_0})_!(\eta^\pm_{U_0} \times \eta^\pm_{V_0})^*(\phi_f \boxtimes \phi_g) & \longrightarrow & (p^\pm_{U_0} \times p^\pm_{V_0})_!(\phi_{f^+} \boxtimes \phi_{g^+})(\eta^\pm_U \times \eta^\pm_V)^* & \longrightarrow & (\phi_{f^0} \boxtimes \phi_{g^0})(p^\pm_U \times p^\pm_V)_!(\eta^\pm_U \times \eta^\pm_V)^* \\ \downarrow{\scriptstyle\simeq} & & \downarrow{\scriptstyle\simeq} & & \downarrow{\scriptstyle\simeq} \\ (k^0)^*(p^\pm_{U_0} \times p^\pm_{V_0})_!(\eta^\pm_{U_0} \times \eta^\pm_{V_0})^*\phi_{f\boxplus g} & \longrightarrow & (k^0)^*(p^\pm_{U_0} \times p^\pm_{V_0})_!\phi_{f^+\boxplus g^+}(\eta^\pm_U \times \eta^\pm_V)^* & \longrightarrow & (k_0)^*\phi_{f^0\boxplus g^0}(p^\pm_U \times p^\pm_V)_!(\eta^\pm_U \times \eta^\pm_V)^* \end{array}$$

hence the isomorphism is compatible with Thom-Sebastiani isomorphism.

Again the same compatibility results can be lifted at the level of complexes of mixed Hodge modules.□

6.3.3 Hyperbolic localization of the perverse sheaf of vanishing cycles

Consider a critical chart (R,U,f,i), i.e. a smooth algebraic space U with a regular function $f : U \to \mathbb{C}$ with $i : R \to U$ denoting the embedding of the critical locus. The image of ϕ_f is supported on R, hence denoting $i_c : R_c := R \cap U_c \to U_c$ the embedding, $(i_c)^*\phi_f \simeq (i_c)^!\phi_f$ is a functor from $\mathrm{Perv}(U)$ to $\mathrm{Perv}(R_c)$. One defines in particular the perverse sheaf on R:

$$\mathcal{PV}_{U,f} := \bigoplus_{c\in f(R)} i_c^*\phi_{f-c}\mathcal{IC}_U \tag{6.3.12}$$

with a monodromy operator $\tau_{U,f} := \mathcal{PV}_{U,f} \to \mathcal{PV}_{U,f}$ defined by:

$$\tau_{U,f} = \bigoplus_{c\in f(R)} \tilde{T}^{2\pi}_{f-c}|_{R_c} \tag{6.3.13}$$

and a polarization operator $\sigma_{U,f} : \mathcal{PV}_{U,f} \xrightarrow{\simeq} \mathbb{D}\mathcal{PV}_{U,f}$ defined by the composition of isomorphisms:

$$\begin{array}{ccc} \mathcal{PV}_{U,f} = \bigoplus_{c\in f(R)} i_c^*\phi_{f-c}\mathcal{IC}_U & \xrightarrow{\simeq} & \bigoplus_{c\in f(R)} i_c^*\phi_{f-c}\mathbb{D}\mathcal{IC}_V \\ & & \downarrow\simeq \\ \mathbb{D}\mathcal{PV}_{U,f} = \mathbb{D}\bigoplus_{c\in f(R)} i_c^*\phi_{f-c}\mathcal{IC}_U & \xleftarrow{\simeq} & \bigoplus_{c\in f(R)} i_c^*\mathbb{D}\phi_{f-c}\mathcal{IC}_U \end{array}$$

where we have used first the self-duality of the intersection complex, secondly Massey's isomorphism, and thirdly the fact that $(i_0)^*\phi_f = (i_0)^!\phi_f$.

This perverse sheaf is given the structure of strongly polarized a monodromic mixed Hodge module in [BBD+15, sec 2.10], using the polarized mixed Hodge module on $\mathcal{IC}_U$, the strongly polarized monodromic mixed Hodge module obtained by applying ϕ_f^H, and then using i^* at the level of mixed Hodge modules. The functor *rat* sends then the monodromy automorphism to $\tau_{U,f}$, and the strong polarization to $\sigma_{U,f}$.

Proposition 6.3.3. *For a $\mathbb{C}^*$-equivariant critical chart (U,R,f,i), there are natural isomorphisms in the abelian category $\bigoplus_{\pi\in\Pi}\mathrm{MMHM}(R^0_\pi)[-\mathrm{Ind}_\pi]$:*

$$\beta^{\pm}_{U,f} : (p^{\pm}_R)_!(\eta^{\pm}_R)^*\mathcal{PV}_{U,f} \to \bigoplus_{\pi\in\Pi} \mathbb{L}^{\pm\mathrm{Ind}_\pi/2}\mathcal{PV}_{U^0_\pi,f^0_\pi} \tag{6.3.14}$$

compatible with the strong polarization, i.e. such that the following square is commutative:

$$\begin{array}{ccc} (p^+_R)_!(\eta^+_R)^*\mathcal{PV}_{U,f} & \xrightarrow{\beta^+_{U,f}} & \bigoplus_{\pi\in\Pi}\mathbb{L}^{\mathrm{Ind}_\pi/2}\mathcal{PV}_{U^0_\pi,f^0_\pi} \\ \downarrow{\scriptstyle B_R^{-1}\circ\sigma_{U,f}} & & \downarrow{\scriptstyle \oplus_{\pi\in\Pi}\sigma_{U^0_\pi,f^0_\pi}} \\ \mathbb{D}(p^-_R)_!(\eta^-_R)^*\mathcal{PV}_{U,f} & \xrightarrow{\beta_{U,f}} & \bigoplus_{\pi\in\Pi}\mathbb{L}^{-\mathrm{Ind}_\pi/2}\mathbb{D}\mathcal{PV}_{U^0_\pi,f^0_\pi} \end{array}$$

Proof: Consider the following commutative diagram:

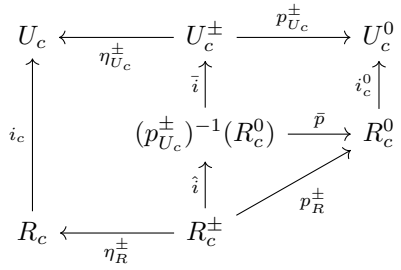

where $\hat{i}$ and $\bar{i}$ are the obvious inclusions, and $\bar{p} := p^{\pm}_{U_c}|_{(p^{\pm}_{U_c})^{-1}(R_c^0)}$. The upper right square is Cartesian. One can define the following isomorphisms:

$$\begin{aligned}(p^{\pm}_{R_c})_!(\eta^{\pm}_{R_c})^*(i_c)^* &\simeq \bar{p}_!\hat{i}_!\hat{i}^*\bar{i}^*(\eta^{\pm}_{U_c})^* \\ &\simeq \bar{p}_!\bar{i}^*(\eta_{U_c})^* \\ &\simeq (i_c^0)^*(p^{\pm}_{U_c})_!(\eta^{\pm}_{U_c})^* \end{aligned} \tag{6.3.15}$$

where we have used the fact that $\hat{i}_!\hat{i}^* = \mathrm{Id}$ because $\hat{i}$ is a closed embedding in the second line, and the base change theorem in the upper right square in the last line. Moreover, because these isomorphism, and also the isomorphisms S_R, S_{U_c} are built using the natural morphisms of the six-functor formalism in the above diagram, the following diagram is commutative, for $A \in D^b_c(U_c)^{\mathbb{C}^*-eq}_{R_c}$:

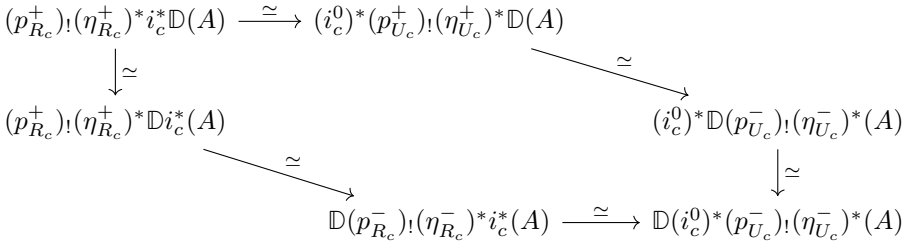

Then one obtains isomorphisms:

$$\beta^{\pm}_{U,f} : (p^{\pm}_R)_!(\eta^{\pm}_R)^*\mathcal{PV}_{U,f} \simeq \bigoplus_{\pi\in\Pi} \mathbb{L}^{\pm \mathrm{Ind}_\pi/2} PV_{U^0_\pi, f^0_\pi} \tag{6.3.16}$$

by the following composition of isomorphisms:

$$\begin{array}{ccc} (p^{\pm}_R)_!(\eta^{\pm}_R)^*\mathcal{PV}_{U,f} := (p^{\pm}_R)_!(\eta^{\pm}_R)^* \bigoplus_{c\in f(R)} i_c^*\phi_{f-c}\mathcal{IC}_U & \xrightarrow{\simeq} & \bigoplus_{c\in f(R)} (i_c^0)^*(p^{\pm}_{U_c})_!(\eta^{\pm}_{U_c})^*\phi_{f-c}\mathcal{IC}_U \\ & & \downarrow \simeq \\ \bigoplus_{\pi\in\Pi} \mathbb{L}^{\pm \mathrm{Ind}_\pi/2} PV_{U^0_\pi, f^0_\pi} := \bigoplus_{c\in f(R)} i_c^*\phi_{f-c} \bigoplus_{\pi\in\Pi} \mathbb{L}^{\pm \mathrm{Ind}_\pi/2}\mathcal{IC}_{U^0_\pi} & \xleftarrow{\simeq} & \bigoplus_{c\in f(R)} i_c^*\phi_{f-c}(p^{\pm}_U)_!(\eta^{\pm}_U)^*\mathcal{IC}_U \end{array}$$

where the first isomorphism is (6.3.15), the second from proposition 6.3.2 where one has remaked that $\mathcal{IC}_U$ is $\mathbb{C}^*$-equivariant, and the third from corollary 6.2.6.

Using the commutativity of the diagram 6.3.2, one obtains that the following square is commutative:

$$\begin{array}{ccc} (p^{\pm}_{U_0})_!(\eta^{\pm}_{U_0})^*\phi_f\mathcal{IC}_U & \xrightarrow{\simeq} & \bigoplus_{\pi\in\Pi}\mathbb{L}^{\pm\mathrm{Ind}_\pi/2}\phi_{f^0_\pi}\mathcal{IC}_{U^0_\pi} \\ \downarrow{\scriptstyle (p^{\pm}_{U_0})_!(\eta^{\pm}_{U_0})^*(\tilde{T}_f^{2\pi})} & & \downarrow{\scriptstyle \oplus_{\pi\in\Pi}\tilde{T}_{f^0_\pi}^{2\pi}} \\ (p^{\pm}_{U_0})_!(\eta^{\pm}_{U_0})^*\phi_f\mathcal{IC}_U & \xrightarrow{\simeq} & \bigoplus_{\pi\in\Pi}\mathbb{L}^{\pm\mathrm{Ind}_\pi/2}\phi_{f^0_\pi}\mathcal{IC}_{U^0_\pi} \end{array}$$

the compatibility with the monodromy results then by applying $(i_0)^*$ to this diagram, applying the functorial isomorphism (6.3.15), and finally writing the definition of $\tau_{U,f}$ by noticing that $(-1)^{\dim(U)} = (-1)^{\pm\mathrm{Ind}_\pi+\dim(U^0_\pi)}$.

The proof of the compatibility with $\sigma_{U,f}$ is slightly more technical. In fact $\beta^{\pm}_{U,f}$ and $\sigma_{U,f}$ are both defined by composing three isomorphisms expressing the commutation of the hyperbolic localization and Verdier duality with i_c^*, with ϕ_f and with $\mathcal{IC}_U$, and then one should divide the square expressing the compatibility into nine sub-squares:

$$\begin{array}{ccccc} 11 & \longrightarrow & 12 & \longrightarrow & 13 & \longrightarrow & 14 \\ \downarrow & & \downarrow & & \downarrow & & \downarrow \\ 21 & \longrightarrow & 22 & \longrightarrow & 23 & \longrightarrow & 24 \\ \downarrow & & \downarrow & & \downarrow & & \downarrow \\ 31 & \longrightarrow & 32 & \longrightarrow & 33 & \longrightarrow & 34 \\ \downarrow & & \downarrow & & \downarrow & & \downarrow \\ 41 & \longrightarrow & 42 & \longrightarrow & 43 & \longrightarrow & 44 \end{array}$$

Where the objects are:

$$
\begin{aligned}
&11 : (p_R^+)_!(\eta_R^+)^*(i_0)^*\phi_f\mathcal{IC}_U\\
&12 : (i_0^0)^*(p_{U_0}^+)_!(\eta_{U_0}^+)^*\phi_f\mathcal{IC}_U\\
&13 : (i_0^0)^*\phi_{f^0}(p_U^+)_!(\eta_U^+)^*\mathcal{IC}_U\\
&14 : (i_0^0)^*\phi_{f^0}\bigoplus_{\pi\in\Pi}\mathbb{L}^{\mathrm{Ind}_\pi/2}\mathcal{PV}_{U_\pi^0,f_\pi^0}\\
&21 : (p_R^+)_!(\eta_R^+)^*(i_0)^*\phi_f\mathbb{D}\mathcal{IC}_U\\
&22 : (i_0^0)^*(p_{U_0}^+)_!(\eta_{U_0}^+)^*\phi_f\mathbb{D}\mathcal{IC}_U\\
&23 : (i_0^0)^*\phi_{f^0}(p_U^+)_!(\eta_U^+)^*\mathbb{D}\mathcal{IC}_U = (i_0^0)^*\phi_{f^0}\mathbb{D}(p_U^-)_!(\eta_U^-)^*\mathcal{IC}_U\\
&24 : (i_0^0)^*\phi_{f^0}\bigoplus_{\pi\in\Pi}\mathbb{D}\mathbb{L}^{-\mathrm{Ind}_\pi/2}\mathcal{PV}_{U_\pi^0,f_\pi^0}\\
&31 : (p_R^+)_!(\eta_R^+)^*(i_0)^*\mathbb{D}\phi_f\mathcal{IC}_U\\
&32 : (i_0^0)^*(p_{U_0}^+)_!(\eta_{U_0}^+)^*\mathbb{D}\phi_f\mathcal{IC}_U = (i_0^0)^*\mathbb{D}(p_{U_0}^-)_!(\eta_{U_0}^-)^*\phi_f\mathcal{IC}_U\\
&33 : (i_0^0)^*\phi_{f^0}(p_U^+)_!(\eta_U^+)^*\mathbb{D}\mathcal{IC}_U = (i_0^0)^*\mathbb{D}\phi_{f^0}(p_U^-)_!(\eta_U^-)^*\mathcal{IC}_U\\
&34 : (i_0^0)^*\mathbb{D}\phi_{f^0}\bigoplus_{\pi\in\Pi}\mathbb{L}^{-\mathrm{Ind}_\pi/2}\mathcal{PV}_{U_\pi^0,f_\pi^0}\\
&41 : (p_R^+)_!(\eta_R^+)^*\mathbb{D}(i_0)^*\phi_f\mathcal{IC}_U = \mathbb{D}(p_R^-)_!(\eta_R^-)^*(i_0)^*\phi_f\mathcal{IC}_U\\
&42 : \mathbb{D}(i_0^0)^*(p_{U_0}^+)_!(\eta_{U_0}^+)^*\phi_f\mathcal{IC}_U = (i_0^0)^*\mathbb{D}(p_{U_0}^-)_!(\eta_{U_0}^-)^*\phi_f\mathcal{IC}_U\\
&43 : \mathbb{D}(i_0^0)^*\phi_{f^0}(p_U^+)_!(\eta_U^+)^*\mathcal{IC}_U = (i_0^0)^*\mathbb{D}\phi_{f^0}(p_U^-)_!(\eta_U^-)^*\mathcal{IC}_U\\
&44 : \mathbb{D}(i_0^0)^*\phi_{f^0}\bigoplus_{\pi\in\Pi}\mathbb{L}^{-\mathrm{Ind}_\pi/2}\mathcal{PV}_{U_\pi^0,f_\pi^0}
\end{aligned}
\tag{6.3.17}
$$

The down left square commutes because it is the diagram 6.3.3 with $A = \phi_f\mathcal{IC}_U$. The central square commutes because 6.3.2 commutes, and the upper right square commutes because it is $(i_0^0)^*\phi_{f^0}$ applied to the commutative diagram in corollary 6.2.6. The squares which are not off the down-left/up right diagonal are commutative because the isomorphisms constructed are functorial. Then the whole diagram is commutative, and, summing over $c \in f(R)$, one obtains the commutativity of the diagram expressing the compatibility with the polarization.

Again the same compatibility results can be directly lifted to the derived category of monodromic mixed Hodge modules.□

6.3.4 Compatibility with smooth maps

Consider two critical charts $(R, U, f, i), (S, V, g, j)$ and $\Phi : U \to V$ a smooth map of relative dimension d with $f = g \circ \Phi$. Joyce defines then in [BBBBJ15] the isomorphism

$$\Xi_\Phi : (\Phi|_R)^*[d]\mathcal{PV}_{V,g} \simeq \mathcal{PV}_{U,f} \tag{6.3.18}$$

by the following composition of isomorphisms:

$$\begin{array}{ccc} (\Phi|_R)^*[d]\mathcal{PV}_{V,g} = (\Phi|_R)^*[d]\bigoplus_{c\in g(S)} j_c^*\phi_{g-c}\mathcal{IC}_V & \xrightarrow{\simeq} & \bigoplus_{c\in f(R)} i_c^*(\Phi_c)^*[d]\phi_{g-c}\mathcal{IC}_V \\ & & \downarrow\simeq \\ \mathcal{PV}_{U,f} = \bigoplus_{c\in f(R)} i_c^*\phi_{f-c}\mathcal{IC}_U & \xleftarrow[\simeq]{} & \bigoplus_{c\in f(R)} i_c^*\phi_{f-c}\Phi^*[d]\mathcal{IC}_V \end{array}$$

identifying $(\Phi|_R)^*[d](\sigma_{V,g})$ with $\sigma_{U,f}$ and $(\Phi|_R)^*[d](\tau_{V,g})$ with $\tau_{U,f}$ according to proposition 4.3 of [BBBBJ15].

Proposition 6.3.4. *The isomorphisms $\beta^{\pm}_{U,f}$ commute with pullback of smooth maps of $\mathbb{C}^*$-equivariant critical charts, i.e. for $\Phi : U \to V$ a $\mathbb{C}^*$ equivariant and smooth map of relative dimension d and critical charts (R, U, f, i) and (S, V, g, j) with $f = g \circ \Phi$ one has the commutative diagram:*

$$\begin{array}{ccc} \bigoplus_{\pi\in\Pi} \mathbb{L}^{\pm\mathrm{Ind}_\pi/2}(\Phi^0_\pi|_{R^0})^*[d^0_\pi](p^\pm_S)_!(\eta^\pm_S)^*\mathcal{PV}_{V,g} & \xrightarrow{\beta^\pm_{V,g}} & \bigoplus_{\pi,\pi'\in\Pi} \mathbb{L}^{(\pm\mathrm{Ind}_{\pi'})/2}(\Phi^0_\pi|_{R^0})^*[d^0_\pi]\mathcal{PV}_{V^0_{\pi'-\pi},g^0_{\pi'-\pi}} \\ \uparrow\simeq & & \\ (p^\pm_R)_!(\eta^\pm_R)^*(\Phi|_R)^*[d]\mathcal{PV}_{V,g} & & \downarrow \Xi_{\Phi^0} \\ \downarrow \Xi_\Phi & & \\ (p^\pm_R)_!(\eta^\pm_R)^*\mathcal{PV}_{U,f} & \xrightarrow{\beta^\pm_{U,f}} & \bigoplus_{\pi\in\Pi} \mathbb{L}^{\pm\mathrm{Ind}_{\pi'}/2}\mathcal{PV}_{U^0_{\pi'},f^0_{\pi'}} \end{array}$$

In particular, one obtains that $\beta^{\pm}_{U,f}$ commute with the restriction on an étale neighborhood.

Proof: Consider now the following diagram, where we denote $G = \phi_g\mathcal{IC}_V$:

$$\begin{array}{ccc} (p_R)_!(\eta_R)^*(\Phi|_R)^*(j_0)^*G = (\Phi|_{R^0})^*(p_S)_!(\eta_S)^*(j_0)^*G & \longrightarrow & (\Phi|_{R^0})^*(j^0_0)^*(p_{V_0})_!(\eta_{V_0})^*G \\ \downarrow & & \downarrow \\ (p_R)_!(\eta_R)^*(i_0)^*(\Phi_0)^*G & \longrightarrow & (i^0_0)^*(p_{U_0})_!(\eta_{U_0})^*(\Phi_0)^*G = (i^0_0)^*(\Phi^0_0)^*(p_{V_0})_!(\eta_{V_0})^* \end{array}$$

where the horizontal isomorphisms are those of (6.3.15) applied to V and U: it is a diagram of isomorphisms between objects in an abelian category, and the isomorphisms are built from the

natural isomorphisms of the six-functor formalism in the diagram:

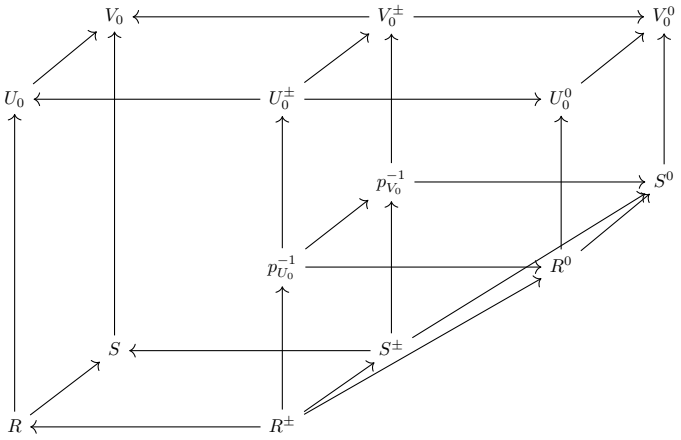

hence this diagram commutes. Finally, consider the diagram:

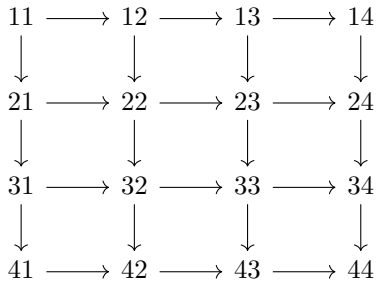

Where the objects are:

$$
\begin{aligned}
&11 : (p_R)_!(\eta_R)^*(\Phi|_R)^*[d](j_0)^*\phi_g\mathcal{IC}_V = (\Phi|_{R^0})^*[d](p_S)_!(\eta_S)^*(j_0)^*\phi_g\mathcal{IC}_V\\
&12 : (\Phi|_{R^0})^*[d](j_0^0)^*(p_{V_0})_!(\eta_{V_0})^*\phi_g\mathcal{IC}_V\\
&13 : (\Phi|_{R^0})^*[d](j_0^0)^*\phi_{g^0}(p_V)_!(\eta_V)^*\mathcal{IC}_V\\
&14 : (\Phi|_{R^0})^*[d](j_0^0)^*\phi_{g^0}\bigoplus_{n\in\mathbb{Z}}\mathbb{L}^{n/2}\mathcal{PV}_{V_n^0,g_n^0}\\
&21 : (p_R)_!(\eta_R)^*(i_0)^*(\Phi_0)^*[d]\phi_g\mathcal{IC}_V\\
&22 : (i_0^0)^*(p_{U_0})_!(\eta_{U_0})^*(\Phi_0)^*[d]\phi_g\mathcal{IC}_V = (i_0^0)^*(\Phi_0^0)^*[d](p_{V_0})_!(\eta_{V_0})^*\phi_g\mathcal{IC}_V\\
&23 : (i_0^0)^*(\Phi_0^0)^*[d]\phi_{g^0}(p_V)_!(\eta_V)^*\mathcal{IC}_V\\
&24 : (i_0^0)^*(\Phi_0^0)^*[d]\phi_{g^0}\bigoplus_{n\in\mathbb{Z}}\mathbb{L}^{n/2}\mathcal{PV}_{V_n^0,g_n^0}\\
&31 : (p_R)_!(\eta_R)^*(i_0)^*\phi_f\Phi^*[d]\mathcal{IC}_V\\
&32 : (i_0^0)^*(p_{U_0})_!(\eta_{U_0})^*\phi_f\Phi^*[d]\mathcal{IC}_V\\
&33 : (i_0^0)^*\phi_{f^0}(p_U)_!(\eta_U)^*\Phi^*[d]\mathcal{IC}_V = (i_0^0)^*\phi_{f^0}(\Phi^0)^*[d](p_V)_!(\eta_V)^*\mathcal{IC}_V\\
&34 : (i_0^0)^*\phi_{f^0}(\Phi^0)^*[d]\bigoplus_{n\in\mathbb{Z}}\mathbb{L}^{n/2}\mathcal{PV}_{V_n^0,g_n^0}\\
&41 : (p_R)_!(\eta_R)^*(i_0)^*\phi_f\mathcal{IC}_U\\
&42 : (i_0^0)^*(p_{U_0})_!(\eta_{U_0})^*\phi_f\mathcal{IC}_U\\
&43 : (i_0^0)^*\phi_{f^0}(p_U)_!(\eta_U)^*\mathcal{IC}_U\\
&44 : (i_0^0)^*\phi_{f^0}\bigoplus_{n\in\mathbb{Z}}\mathbb{L}^{n/2}\mathcal{PV}_{U_n^0,f_n^0}
\end{aligned}
\tag{6.3.19}
$$

the three diagonal squares of the above diagram are respectively the commutative diagrams 6.3.4, 6.3.2 and the commutative diagram expressing the fact that the isomorphism giving the commutation of the hyperbolic localization and pullback by smooth maps in proposition 6.2.5 is compatible with composition of smooth maps, and the off diagonal squares commute because the functoriality of the isomorphism. Then the whole diagram is commutative. According to the definition of Ξ_Φ, Ξ_{Φ^0} and $\beta_{U,f}, \beta_{V,g}$, the diagram 6.3.4 is the direct sum of the above diagram with f replaced by $f - c$ for $c \in f(R)$, hence it is also commutative. □

6.3.5 Compatibility with Thom-Sebastiani isomorphism

Consider two critical charts (U, R, f, i) and (S, V, g, j). Notice that because U and V are smooth $\mathrm{Crit}(f \boxplus g) = \mathrm{Crit}(f) \times \mathrm{Crit}(g)R \times S$. Consider the sequence of closed embeddings:

$$R \times S \xrightarrow{i_c \times j_d} U_c \times V_d \xrightarrow{k_{c,d}} (U \times V)_{c+d}$$

In [BBD+15], Joyce defined the Thom-Sebastiani isomorphism:

$$\mathcal{TS}_{U,f,V,g} : \mathcal{PV}_{U\times V, f\boxplus g} \simeq \mathcal{PV}_{U,f} \boxtimes \mathcal{PV}_{S,g} \tag{6.3.20}$$

By the following sequence of isomorphisms:

$$\begin{aligned}\mathcal{PV}_{U\times V,f\boxplus g} =& \bigoplus_{e\in f\boxplus g(R\times S)} ((i\times j)_e)^*\phi_{f\boxplus g-e}\mathcal{IC}_{U\times V}\\ \simeq& \bigoplus_{c\in f(R),d\in g(S)} (i_c\times j_d)^*k_{c,d}^*\phi_{(f-c)\boxplus(g-d)}\mathcal{IC}_{U\times V}\\ \simeq& \bigoplus_{c\in f(R),d\in g(S)} (i_c\times j_d)^*(\phi_{f-c}\boxtimes\phi_{g-d})\mathcal{IC}_{U\times V}\\ \simeq& (\bigoplus_{c\in f(R)} (i_c)^*\phi_{f-c}\mathcal{IC}_U)\boxtimes(\bigoplus_{d\in g(S)} (j_d)^*\phi_{g-d}\mathcal{IC}_V)\\ =& \mathcal{PV}_{U,f}\boxtimes\mathcal{PV}_{S,g}\end{aligned} \tag{6.3.21}$$

where the third line is the Thom-Sebastiani isomorphism of [Mas01].

Proposition 6.3.5. *The isomorphism $\beta_{U,f}$ commutes with Thom-Sebastiani isomorphism, namely for $\mathbb{C}^*$-equivariant critical chart (U,R,f,i) and (S,V,g,j), one has the commutative diagram:*

$$\begin{array}{ccc}(p_R^\pm\times p_S^\pm)_!(\eta_R^\pm\times\eta_S^\pm)^*(\mathcal{PV}_{U\times V,f\boxplus g}) & \xrightarrow{\beta_{U\times V}^\pm} & \oplus_{\pi,\pi'\in\Pi}\mathbb{L}^{\pm(\mathrm{Ind}_\pi+\mathrm{Ind}_{\pi'})/2}\mathcal{PV}_{U_\pi^0\times V_{\pi'}^0,f_\pi^0\boxplus g_{\pi'}^0}\\ \downarrow{\scriptstyle (p_R^\pm\times p_S^\pm)_!(\eta_R^\pm\times\eta_S^\pm)^*\mathcal{TS}_{U,f,V,g}} & & \downarrow{\scriptstyle \oplus_{\pi,\pi'\in\Pi}\mathbb{L}^{\pm(\mathrm{Ind}_\pi+\mathrm{Ind}_{\pi'})/2}\mathcal{TS}_{U_\pi^0,f_\pi^0,V_{\pi'}^0,g_{\pi'}^0}}\\ ((p_R^\pm)_!(\eta_R^\pm)^*\mathcal{PV}_{U,f})\boxtimes((p_S^\pm)_!(\eta_S^\pm)^*\mathcal{PV}_{S,g}) & \xrightarrow{\beta_U\times\beta_V} & \begin{array}{l}\oplus_{\pi\in\mathbb{Z}}\mathbb{L}^{\pm\mathrm{Ind}_\pi/2}\mathcal{PV}_{U_\pi^0,f_\pi^0})\\ \oplus_{\pi'\in\Pi}\mathbb{L}^{\pm\mathrm{Ind}_{\pi'}/2}\mathcal{PV}_{V_{\pi'}^0,g_{\pi'}^0})\end{array}\end{array}\boxtimes$$

Proof: Consider the following diagram:

$$\begin{array}{ccccccc}11 & \longrightarrow & 12 & \longrightarrow & 13 & \longrightarrow & 14\\ \downarrow & & \downarrow & & \downarrow & & \downarrow\\ 21 & \longrightarrow & 22 & \longrightarrow & 23 & \longrightarrow & 24\end{array}$$

Where the objects are:

$$\begin{aligned}&11: (p_R^\pm\times P_S^\pm)_!(\eta_R^\pm\times\eta_S^\pm)^*(i_0\times j_0)^*k^*\phi_{f\boxplus g}\mathcal{IC}_{U\times V}\\ &12: (i_0^0\times j_0^0)^*(p_{U_0}^\pm\times p_{V_0}^\pm)_!(\eta_{U_0}^\pm\eta_{V_0}^\pm)^*k^*\phi_{f\boxplus g}\mathcal{IC}_{U\times V} = (i_0^0\times j_0^0)^*(k^0)^*(p_{(U\times V)_0}^\pm)_!(\eta_{(U\times V)_0}^\pm)^*\phi_{f\boxplus g}\mathcal{IC}_{U\times V}\\ &13: (i_0^0\times j_0^0)^*(k^0)^*\phi_{f^0\boxplus g^0}(p_U^\pm\times p_V^\pm)_!(\eta_U^\pm\times\eta_V^\pm)^*\mathcal{IC}_{U\times V}\\ &14: (i_0^0\times j_0^0)^*(k^0)^*\phi_{f^0\boxplus g^0}\bigoplus_{\pi,\pi'\in\Pi}\mathbb{L}^{(\mathrm{Ind}_\pi+\mathrm{Ind}_{\pi'})/2}\mathcal{IC}_{U_\pi^0\times V_{\pi'}^0}\\ &21: (p_R^\pm\times P_S^\pm)_!(\eta_R^\pm\times\eta_S^\pm)^*(i_0\times j_0)^*(\phi_f\boxtimes\phi_g)\mathcal{IC}_{U\times V}\\ &22: (i_0^0\times j_0^0)^*(p_{U_0}^\pm\times p_{V_0}^\pm)_!(\eta_{U_0}^\pm\eta_{V_0}^\pm)^*(\phi_f\boxtimes\phi_g)\mathcal{IC}_{U\times V}\\ &23: (i_0^0\times j_0^0)^*(\phi_{f^0}\boxtimes\phi_{g^0})(p_U^\pm\times p_V^\pm)_!(\eta_U^\pm\times\eta_V^\pm)^*\mathcal{IC}_{U\times V}\\ &24: (i_0^0\times j_0^0)^*(\phi_{f^0}\boxtimes\phi_{g^0})\bigoplus_{\pi,\pi'\in\Pi}\mathbb{L}^{(\mathrm{Ind}_\pi+\mathrm{Ind}_{\pi'})/2}\mathcal{IC}_{U_\pi^0\times V_{\pi'}^0}\end{aligned} \tag{6.3.22}$$

the left and the right squares commutes from the functoriality of the corresponding isomorphisms, and the central square commutes because it is the diagram 6.3.2, which commutes, hence the whole diagram commutes. Identifying $\mathcal{IC}_{U\times V}$ with $\mathcal{IC}_U \boxtimes \mathcal{IC}_V$ and $\mathcal{IC}_{U^0_\pi \times V^0_{\pi'}}$ with $\mathcal{IC}_{U^0_\pi} \boxtimes \mathcal{IC}_{V^0_{\pi'}}$, and summing over $c \in f(R), d \in g(S)$, one obtains the commutative square of the proposition. □

As explained in example 2.14 of [BBD+15], for q a non-degenerate quadratic form on an n-dimensional vector space E, one has $\mathrm{Crit}(q) = \{0\}$, and then:

$$\mathcal{PV}_{E,q} = H^{n-1}(MF_q(0), \mathbb{Q}) \otimes \mathbb{Q}_{\{0\}} \simeq \mathbb{Q}_{\{0\}} \tag{6.3.23}$$

where $MF_q(0)$ denotes the Milnor fiber of q at 0, which is T^*S^{n-1}, and the second isomorphism comes from the orientation of S^{n-1} coming from an orientation of E. Consider now E with a linear $\mathbb{C}^*$-action and a $\mathbb{C}^*$-invariant non-degenerate quadratic form q. We can decompose $E = E^0 \oplus E^+ \oplus E^-$ according to the $\mathbb{C}^*$-weights, and the non-degenerate invariant quadratic form q gives a natural isomorphism $E^- = (E^+)^\vee$, hence a natural isomorphism $K_E = K_{E^0}$, i.e. a natural bijection between orientations of E and orientations of E^0. Denoting $q^0 := q|_{E^0}$, one obtains directly the commutativity of the following square:

$$\begin{array}{ccc} \mathcal{PV}_{E,q} & \xrightarrow{\beta^{\pm}_{E,q}} & \mathcal{PV}_{E^0,q^0} \\ \downarrow\simeq & & \downarrow\simeq \\ \mathbb{Q}_{\{0\}} & \xrightarrow{\simeq} & \mathbb{Q}_{\{0\}} \end{array}$$

where the vertical arrows comes from consistent orientations of V and V^0.

6.4 Białynicki-Birula decomposition on a d-critical algebraic space

6.4.1 D-critical algebraic space

We recall here the notions and results of [Joy13] and [BBD+15] about d-critical structures and the Donaldson-Thomas sheaf. Joyce and his collaborators have developed the theory of d-critical schemes and build the perverse sheaf on it using the Zariski topology, mainly in order to define also motivic Donaldson-Thomas invariants, which can be glued in the Zariski topology, but not in the étale topology. But because coherent sheaves and perverse sheaves glue in the étale topology, and the perverse sheaf of vanishing cycles transforms naturally under étale maps, the same formalism can be developed in the étale topology. We will then work in the étale topology, and consider d-critical algebraic spaces.

In [Joy13, Theo 2.1], Joyce constructs sheaves $\mathcal{S}_X$ and $\mathcal{S}^0_X$ on any algebraic space X. Given an étale map $R \to X$ and a closed embedding $i : R \hookrightarrow U$ into a smooth scheme U, denote by $I_{R,U}$ the sheaf of ideal in $i^{-1}(\mathcal{O}_U)$ of functions on U near $i(R)$ which vanishes on $i(R)$. There is then an exact sequence of sheaves on R defining locally $\mathcal{S}_X$:

$$0 \to \mathcal{S}_X|_R \xrightarrow{\iota_{R,U}} \frac{i^{-1}(\mathcal{O}_U)}{I^2_{R,U}} \xrightarrow{d} \frac{i^{-1}(T^*U)}{I_{R,U}.i^{-1}(T^*U)} \tag{6.4.1}$$

One has a decomposition $\mathcal{S}_X = \mathcal{S}_X^0 \oplus \mathbb{C}$, and $\mathcal{S}_X^0 \subset \mathcal{S}_X$ is the kernel of the composition:

$$\mathcal{S}_X \to \mathcal{O}_X \to \mathcal{O}_{X^{red}} \tag{6.4.2}$$

with X^{red} the reduced subspace of X. This construction is functorial, i.e. for $\Phi : X \to Y$ a morphism of scheme there is a sheaf morphism $\Phi^\star : \mathcal{S}_Y^0 \to \mathcal{S}_X^0$.

A d-critical structure on X is a section s of $\mathcal{S}_X^0$ such that for each $x \in X$ there exist an étale neighborhood R of x, and embedding $i : R \hookrightarrow U$ into a smooth algebraic space U, and a regular function $f : U \to \mathbb{C}$ such that $i(R) = \mathrm{Crit}(f)$ and $\iota_{R,U}(s|_R) = i^{-1}(f) + I^2_{R,U}$. Informally, the data of s precise the functional f of critical charts up to second order terms, and one has $f|_{R^{red}} = 0$. We deal then with critical charts (R, U, f, i): considering an étale map $U' \to U$, one can consider a subchart $(R' := R \times_U U', U', f' := f|_{U'}, i' := i|_{R'}) \to (R, U, f, i)$.

One can also consider embeddings of charts $\Phi : (R, U, f, i) \hookrightarrow (S, V, g, j)$ for $R \to S \to X$ étale maps, i.e. a locally closed embedding $\Phi : U \to V$ such that $\Phi \circ i = j|_R : R \to V$ and $f = g \circ \Phi : U \to \mathbb{C}$. According to [Joy13, Theo 2.20], one can compare two critical charts using embeddings: namely, for (R, U, f, i) and (S, V, g, j) two critical charts and $x \in R \cap S$, there exist subcharts $(R', U', f', i') \subset (R, U, f, i)$ and $(S', V', g', j') \subset (S, V, g, j)$ such that $x \in R' \cap S'$, a critical chart (T, W, h, k) and embeddings $\Phi : (R', U', f', i') \hookrightarrow (T, W, h, k)$ and $\Psi(S', V', g', j') \hookrightarrow (T, W, h, k)$.

For a $[-1]$-shifted symplectic structure, on a d-critical chart (R, U, f, i), the tangent-obstruction complex $\mathbb{L}_X|_{R^{red}}$ is quasi-isomorphic with $0 \to TU \to T^*U \to 0$, and then $det(\mathbb{L}_X)|_{R^{red}} = i^*(K_U^{\otimes 2})|_{R^{red}}$, i.e. the sheaves $i^*(K_U^{\otimes 2})|_{R^{red}}$ glue in a sheaf on X^{red} For a general d-critical scheme and an embedding $\Phi : (R, U, f, i) \to (S, V, g, j)$, from definition 2.26 of [Joy13], one has a natural isomorphism:

$$J_\Phi : i^*(K_U^{\otimes^2})|_{R^{red}} \to j^*(K_V^{\otimes^2})|_{R^{red}} \tag{6.4.3}$$

Using the fact that two maps can be locally embedded in a single map, it is shown in [Joy13, Theo 2.28] that these sheaves glue together into a single sheaf $K_{X,s}$ on X^{red} called the canonical sheaf, with natural local isomorphisms:

$$\begin{aligned} &\iota_{R,U,f,i} : K_{X,s}|_{R^{red}} \to i^*(K_U^{\otimes^2})|_{R^{red}} \\ &J_\Phi \circ \iota_{R,U,f,i} = \iota_{S,V,g,j} \end{aligned} \tag{6.4.4}$$

6.4.2 Gluing the Donaldson-Thomas sheaves

Given a d-critical scheme, one could try naively to define a perverse sheaf and strongly polarized monodromic mixed Hodge modules modeled locally on $\mathcal{PV}_{U,f}$ for each critical charts (R, U, f, i), gluing these sheaves and strongly polarized monodromic mixed Hodge modules by constructing isomorphisms on intersections of critical charts, satisfying the cocycle conditions. This is complicated by the orientations issue seen above. The construction of $\mathcal{PV}_{U,f}$ is natural with respect to étale restriction of maps, and étale locally two intersecting critical charts are related by stabilization i.e. embedding of the form $\Phi : (R, U, f, i) \hookrightarrow (S, U \times E, g \boxplus q, j \times 0)$, with E a vector space and q a non-degenerate quadratic form. As seen above, the descent data to define the orientation $K_{X,s}^{1/2}$ is equivalent to give a natural orientation on E for any such stabilization. We can then consider the chain of isomorphisms in $\mathrm{Perv}(X)$ (or $MMHM(X)$):

$$\Theta(\Phi) : \mathcal{PV}_{U\times E, f\boxplus q} \simeq \mathcal{PV}_{U,f} \boxtimes \mathcal{PV}_{E,q} \simeq \mathcal{PV}_{U,f} \tag{6.4.5}$$

Where the first isomorphism is the Thom-Sebastiani isomorphism $\mathcal{TS}_{U,f,E,q}$, and the second comes from the natural orientation of E. The technical work of [BBD+15] is to check that $(\mathcal{PV}_{U,f}, \Theta(\Phi))$ defines a descent data, namely that the $\Theta(\Phi)$ glue on intersections of critical charts to define comparison isomorphisms, and that the cocycle relations are verified.

We are here interested in building an isomorphism between perverse sheaves, so we have to work one categorical level below: namely, we must define these isomorphisms locally, and check that this isomorphism commutes with the gluing isomorphisms. We will then use only the above presentation $(\mathcal{PV}_{U,f}, \Theta(\Phi))$ for $P_{X,s}$, and will not use the equivalent, but more technical, presentation of [BBD+15].

6.4.3 Białynicki-Birula decomposition

An action $\mu : T \times X \to X$ of a one dimensional torus $\mathbb{C}^*$ on a d-critical scheme X is said to leave invariant the d-critical structure s (resp. the orientation $K_{X,s}^{1/2}$) if $\mu(\gamma)^\star(s) = s$ (resp. $\mu(\gamma)^* K_{X,s}^{1/2} = K_{X,s}^{1/2}$) for $\gamma \in T$. In particular, the d-critical structure of the classical truncation of a (-1)-shifted symplectic scheme with a $\mathbb{C}^*$-action leaving the (-1)-shifted symplectic structure invariant is $\mathbb{C}^*$-invariant. If the action is étale locally linearizable, then translating [Joy13, Prop 2.43, 2.44] from the Zariski to the étale topology, we can then work with $\mathbb{C}^*$-equivariant critical charts. Namely, we can cover X in the étale topology by charts (R, U, f, i) such that U has a $\mathbb{C}^*$-action for which i is equivariant and f is invariant. Moreover, considering (R, U, f, i) and (S, V, g, j) two $\mathbb{C}^*$-equivariant critical charts, and $x \in R \cap S$, one has étale restrictions $(R', U', f', i') \to (R, U, f, i)$ and $(S', V', g', j') \to (S, V, g, j)$ with $x \in R' \cap S'$, and $\mathbb{C}^*$-equivariant critical chart (T, W, h, k) and $\mathbb{C}^*$-equivariant embeddings $\Phi : (R', U', f', i') \hookrightarrow (T, W, h, k)$ and $\Psi(S', V', g', j') \hookrightarrow (T, W, h, k)$.

As explained in [Joy13, Cor 2.45], considering the closed embedding $\xi_X : X^0 \hookrightarrow X$, X^0 admits a natural d-critical structure $(X^0, s^0 := \xi_X^\star(s))$. Indeed, for (R, U, f, i) a $\mathbb{C}^*$-equivariant d-critical chart, denoting by R^0, U^0 the $\mathbb{C}^*$-fixed locus of R,U, and $f^0 = f|_{U^0}$, $i^0 = i|_{R^0}$, (R^0, U^0, f^0, i^0) is a d-critical chart of X^0 such that $s^0_{R^0,U^0} = f^0 + I^2_{R^0,U^0}$, and then X^0 is covered by d-critical charts.

Consider now the orientation issue. Suppose first that (X, s) is the classical truncation of a -1-shifted symplectic space with a $\mathbb{C}^*$-action. Then the tangent-obstruction complex $\mathbb{L}_X|_{X^0}$ splits as a direct sum:

$$\mathbb{L}_X|_{X^0} = \mathbb{L}_{X^0} \oplus \mathbb{L}^+_{X^0} \oplus \mathbb{L}^-_{X^0} \tag{6.4.6}$$

Here $\mathbb{L}^+_{X^0}$ (resp $\mathbb{L}^-_{X^0}$) denotes the part of contracting (resp repelling) weight under the $\mathbb{C}^*$-action. The -1-shifted symplectic structure provides then a canonical isomorphism between $\mathbb{L}^+_{X^0}$ and $(\mathbb{L}^-_{X^0})^\vee[1]$, hence, taking:

$$\begin{aligned} det(\mathbb{L}_X)|_{X^0} &= det(\mathbb{L}_{X^0}) \otimes det(\mathbb{L}^+_{X^0})^2 \\ \Longrightarrow K_{X^0,s^0} &= K_{X,s} \otimes det(\mathbb{L}^+_{X^0})^{-2} \end{aligned} \tag{6.4.7}$$

Hence, given an orientation $K_{X,s}^{1/2}$ on X, we can define canonically an orientation on X^0:

$$K^{1/2}_{X^0,s^0} := K^{1/2}_{X,s} \otimes det(\mathbb{L}^+_{X^0})^{-1} \tag{6.4.8}$$

Such construction is still possible if (X, s) is a d critical space with $\mathbb{C}^\star$ action, not necessarily coming from a -1-shifted symplectic space:

Lemma 6.4.1. *If (X,s) is a d critical space with $\mathbb{C}^\star$ action, there is a natural bijection between orientations of (X,s) and orientations of (X^0,s^0).*

Proof: We can define an orientation $K_{X,s}^{1/2}$ (resp $K_{X^0,s^0}^{1/2}$) by descent: we define $(K_{X,s}^{1/2})_R := K_U$ (resp $(K_{X^0,s^0}^{1/2})_{R^0} := K_{U^0}$) for each critical chart (R,U,f,i) (resp (R^0,U^0,f^0,i^0), and gluing isomorphisms on double intersections which satisfies cocycle on triple intersections. Using [Joy13, Prop 2.43], we can use $\mathbb{C}^*$-equivariant critical charts, and, using [Joy13, Prop 2.44] and Lemma 6.6.1, it suffice to define gluing isomorphisms for $\mathbb{C}^*$-equivariant embeddings of charts of the form $(R,U,f,i)\hookrightarrow(R,U\times E,f\boxplus q,i\times 0)$, where E is a finite dimensional vector space with linear $\mathbb{C}^*$ action and q is a $\mathbb{C}^*$-invariant non-degenerate quadratic form. As seen above (6.3.5), an orientation on E, which defines a descent isomorphism for $K_{X,s}^{1/2}$ for the embedding $(R,U,f,i)\hookrightarrow(R,U\times E,f\boxplus q,i\times 0)$, provides then naturally an orientation of V^0, which is a descent isomorphism for $K_{X^0,s^0}^{1/2}$ and the embedding $(R^0,U^0,f^0,i^0)\hookrightarrow(R^0,U^0\times E^0,f^0\boxplus q^0,i^0\times 0)$. The isomorphisms for $K_{X^0,s^0}^{1/2}$ glue on triple intersections if and only if those for $K_{X,s}^{1/2}$ glue also. □

Consider the decomposition of X^0 into connected components $X^0=\bigsqcup_{\pi\in\Pi}X^0_\pi$: one can further consider the oriented d-critical schemes $(X^0_\pi,s^0_\pi,K^{1/2}_{X^0_\pi,s^0_\pi})$. Denote by Ind_π the number of contracting weight in the tangent-obstruction complex of X at X^0_π. In a critical chart (R,U,f,i), the tangent-obstruction complex is given by $0\to TU\to T^*U\to 0$, and then, denoting by d_+,d_0,d_- respectively the number of contracting, invariant and repelling weights in TU at $i(X^0_\pi\cap R)$, one has $\mathrm{Ind}_\pi = d_+-d_-$, i.e. this definition is consistent with the previous definition on a critical chart.

Theorem 6.4.2. *For X an oriented d-critical algebraic space X with an étale linearizable $\mathbb{C}^*$ action leaving the d-critical structure and the orientation invariant, one has natural isomorphisms of perverse sheaves and monodromic mixed Hodge modules on X^0 (with its orientation defined in Lemma 6.4.1):*

$$\beta^\pm_{X,s}:(p^\pm_X)_!(\eta^\pm_X)^*P_{X,s}\xrightarrow{\simeq}\bigoplus_{\pi\in\Pi}\mathbb{L}^{\pm\mathrm{Ind}_\pi/2}P_{X^0_\pi,s^0_\pi} \tag{6.4.9}$$

which are compatible with polarization, in the sense that the following diagram is commutative:

$$\begin{array}{ccc}(p^+_X)_!(\eta^+_X)^*P_{X,s} & \xrightarrow{\beta^+_{X,s}} & \bigoplus_{\pi\in\Pi}\mathbb{L}^{\mathrm{Ind}_\pi/2}P_{X^0_\pi,s^0_\pi}\\ \downarrow{\scriptstyle S_X^{-1}\circ(p^+_X)_!(\eta^+_X)^*(\Sigma_{X,s})} & & \downarrow{\scriptstyle\bigoplus_{\pi\in\Pi}\mathbb{L}^{\mathrm{Ind}_\pi/2}\Sigma_{X^0_\pi,s^0_\pi}}\\ \mathbb{D}(p^-_X)_!(\eta^-_X)^*P_{X,s} & \xleftarrow[\mathbb{D}\beta^-_{X,s}]{} & \mathbb{D}\bigoplus_{\pi\in\Pi}\mathbb{L}^{-\mathrm{Ind}_\pi/2}P_{X^0_\pi,s^0_\pi}\end{array}$$

Proof: We can cover X^0 by critical charts of the form (R^0,U^0,f^0,i^0), which are the $\mathbb{C}^*$-fixed part of $\mathbb{C}^*$-equivariant charts (R,U,f,i), and the relate them by the transitive action of stabilization, i.e. embedding of the form $\Phi^0:(R^0,U^0,f^0,i^0)\hookrightarrow(R^0,U^0\times E^0,f^0\boxplus q^0,i^0\times 0)$, which are the $\mathbb{C}^*$-fixed part of $\mathbb{C}^*$-equivariant embedding $\Phi:(R,U,f,i)\hookrightarrow(R,U\times E,f\boxplus q,i\times 0)$. Hence $\mathrm{Perv}(X^0)$ (or $MMHM(X^0)$) can be defined by descent datum with these charts and embeddings. Namely, P_{X^0,s^0} is defined as said before by the descent datum $(\mathcal{PV}_{U,f},\Theta(\Phi^0))$. Because hyperbolic localization commutes with étale restriction, $(p^\pm_X)_!(\eta^\pm_X)^*P_{X,s}$ can be defined by the descent datum $((p^\pm_R)_!(\eta^\pm_R)^*\mathcal{PV}_{U,f},(p^\pm_R)_!(\eta^\pm_R)^*\Theta(\Phi))$.

On a chart (R^0, U^0, f^0, i^0), we consider the isomorphism built in Proposition 6.3.3:

$$\beta^{\pm}_{U,f} : (p^{\pm}_R)_!(\eta^{\pm}_R)^*\mathcal{PV}_{U,f} \to \bigoplus_{\pi\in\Pi} \mathbb{L}^{\pm \mathrm{Ind}_\pi/2}\mathcal{PV}_{U^0_\pi, f^0_\pi} \tag{6.4.10}$$

We have to check he compatibility of these isomorphisms with stabilization. Consider as above $\Phi^0 : (R^0, U^0, f^0, i^0) \hookrightarrow (R^0, U^0 \times E^0, f^0 \boxplus q^0, i^0 \times 0)$, and consider the natural orientation on E and E^0 defined by $K^{1/2}_{X,s}$ and $K^{1/2}_{X^0,s^0}$. consider now the following diagram:

$$\begin{array}{ccc}
(p^{\pm}_R)_!(\eta^{\pm}_R)^*(\mathcal{PV}_{U\times E, f\boxplus q}) & \xrightarrow{\beta^{\pm}_{U\times E}} & \oplus_{\pi\in\Pi} \mathbb{L}^{\pm(\mathrm{Ind}_\pi} \mathcal{PV}_{U^0_\pi \times E^0, f^0_\pi \boxplus q^0} \\
\downarrow{\scriptstyle (p^{\pm}_R)_!(\eta^{\pm}_R)^*\mathcal{TS}_{U,f,E,q}} & & \downarrow{\scriptstyle \oplus_{\pi\in\Pi}\mathbb{L}^{\pm(\mathrm{Ind}_\pi)/2}\mathcal{TS}_{U^0_\pi, f^0_\pi, E^0, q^0}} \\
((p^{\pm}_R)_!(\eta^{\pm}_R)^*\mathcal{PV}_{U,f}) \boxtimes (\mathcal{PV}_{E,q}) & \xrightarrow{\beta^{\pm}_U \times \beta^{\pm}_E} & \oplus_{\pi\in\mathbb{Z}} \mathbb{L}^{\pm \mathrm{Ind}_\pi/2}\mathcal{PV}_{U^0_\pi, f^0_\pi}) \boxtimes \mathcal{PV}_{E^0,q^0}) \\
\downarrow{\scriptstyle \simeq} & & \downarrow{\scriptstyle \simeq} \\
(\eta^{\pm}_R)^*\mathcal{PV}_{U,f}) & \xrightarrow{\beta^{\pm}_U} & \oplus_{\pi\in\mathbb{Z}} \mathbb{L}^{\pm \mathrm{Ind}_\pi/2}\mathcal{PV}_{U^0_\pi, f^0_\pi})
\end{array}$$

The above square is the commutative square of Proposition 6.3.5 expressing the commutation of hyperbolic localization with Thom-Sebastiani isomorphism, and the square below is the tensor product of the commutative square 6.3.5 with $(\eta^{\pm}_R)^*\mathcal{PV}_{U,f})$. Hence the above diagram is commutative, and is equal to:

$$\begin{array}{ccc}
(p^{\pm}_R)_!(\eta^{\pm}_R)^*(\mathcal{PV}_{U\times E, f\boxplus q}) & \xrightarrow{\beta^{\pm}_{U\times E}} & \oplus_{\pi\in\Pi} \mathbb{L}^{\pm(\mathrm{Ind}_\pi} \mathcal{PV}_{U^0_\pi \times E^0, f^0_\pi \boxplus q^0} \\
\downarrow{\scriptstyle (p^{\pm}_R)_!(\eta^{\pm}_R)^*\Theta(\Phi)} & & \downarrow{\scriptstyle \oplus_{\pi\in\Pi}\mathbb{L}^{\pm(\mathrm{Ind}_\pi)/2}\Theta(\Phi^0_\pi)} \\
(\eta^{\pm}_R)^*\mathcal{PV}_{U,f}) & \xrightarrow{\beta^{\pm}_U} & \oplus_{\pi\in\mathbb{Z}} \mathbb{L}^{\pm \mathrm{Ind}_\pi/2}\mathcal{PV}_{U^0_\pi, f^0_\pi})
\end{array}$$

Hence the $\beta^{\pm}_U$ are compatible with stabilization, and then by descent glue to give an isomorphism on X^0. for each $\mathbb{C}^*$-equivariant critical chart (R, U, f, i) compatible with the monodromy and the duality. From Proposition 6.3.3, the $\beta^{\pm}_U$ are compatible with polarization and monodromy, hence by descent $\beta^{\pm}_X$ are also compatible (the commutativity of the corresponding squares can be checked locally).

6.4.4 Compatibility with smooth pullbacks

Consider a smooth map of d-critical algebraic spaces $\phi : (X, s) \to (Y, t)$ of relative dimension d (i.e. a smooth map such that $\phi^\star(t) = s$). [BBBBJ15, Cor 3.8] shows that:

$$K_{X,s} = K_{Y,t} \otimes (\Lambda^{top} T^*_{X/Y})^{\otimes 2}|_{X^{red}} \tag{6.4.11}$$

A smooth map of oriented d-critical scheme $\phi : (X, s, K_{X,s}^{1/2}) \to (Y, t, K_{Y_t}^{1/2})$ is then the data a smooth map $\phi : (X, s) \to (Y, t)$ of oriented d-critical scheme together with the data of an isomorphism:

$$K_{X,s}^{1/2} = \phi^*(K_{Y,t}^{1/2}) \otimes (\Lambda^{top} T^*_{X/Y})|_{X^{red}}. \tag{6.4.12}$$

which is a square root of the above isomorphism. Given such a map, [BBBBJ15, Prop 4.5] built an isomorphism:

$$\Delta_\phi : \phi^*[d]P_{Y,t} \simeq P_{X,s} \tag{6.4.13}$$

Consider now a $\mathbb{C}^*$-equivariant smooth map of oriented d-critical schemes $\phi : (X, s, K_{X,s}^{1/2}) \to (Y, t, K_{Y_t}^{1/2})$ of relative dimension d. From Lemma 6.6.2, X is covered by $\mathbb{C}^*$-equivariant critical charts (R, U, f, i) such that there is a $\mathbb{C}^*$-equivariant critical chart and (S, V, g, j) of Y with a smooth map $\Phi : U \to V$ of relative dimension d such that $f = g \circ \Phi$ and $\Phi \circ i = j \circ \phi$. Hence sheaves and perverse sheaves on X^0 can be defined by descent with a definition on each critical chart (R^0, U^0, f^0, i^0) coming from a chart of this form, and comparison on charts coming from simultaneous stabilization of (S, V, g, j) and (R, U, f, i).

Lemma 6.4.3. *If $\phi : (X, s, K_{X,s}^{1/2}) \to (Y, s, K_{Y,t}^{1/2})$ is a smooth $\mathbb{C}^*$ morphism of oriented d-critical loci, then $\phi^0 : (X^0, s^0, K_{X^0,s^0}^{1/2}) \to (Y^0, t^0, K_{Y^0,t^0}^{1/2})$ is aloso a smooth morphism of oriented d-critical loci.*

Proof: The induced morphism $\phi^0 : X^0 \to Y^0$ is smooth of dimension d. One has:

$$\begin{aligned}(\phi^0)^\star(t^0) &= (\phi^0)^\star \xi_Y^\star(t) \\ &= \xi_X^\star \phi^\star(t) \\ &= \xi_X^\star(s) \\ &= s^0\end{aligned} \tag{6.4.14}$$

where the first and the last line are the definition of t^0 and s^0, the second line follows from the functoriality of * and the fact that $\xi_Y \phi^0 = \phi \xi_X$, and the third line follows from the fact that ϕ is a morphism of d-critical structure. Then ϕ^0 is a morphism of d-critical algebraic space.

We will now prove that:

$$K_{X^0,s^0}^{1/2} = (\phi^0)^*(K_{Y^0,t^0}^{1/2}) \otimes (\Lambda^{top} T^*_{X^0/Y^0})|_{(X^0)^{red}} \tag{6.4.15}$$

We prove this equality by descent: this equality holds by the definitions $K_{X^0,s^0}^{1/2}|_{R^0} = K_{U^0}$ and $K_{Y^0,t^0}^{1/2} = K_{V^0}$ for each pair of critical charts of X, Y of the form described above. Now, considering a stabilization for a pair of critical charts of X, Y, the compatibility of the descent isomorphisms on X with (6.4.12) implies the compatibility of the descent isomorphisms on X^0 with (6.4.15), which proves (6.4.15). □

We can in particular consider the isomorphism:

$$\Delta_{\phi^0} : (\phi^0)^*[d]P_{Y^0,t^0} \to P_{X^0,s^0} \tag{6.4.16}$$

Proposition 6.4.4. *The hyperbolic localization isomorphism commutes with smooth pullbacks, namely for $\phi : (X, s, K_{X,s}^{1/2}) \to (Y, t, K_{Y,t}^{1/2})$ a $\mathbb{C}^*$-equivariant smooth map of oriented critical algebraic space of relative dimension d, the following diagram of isomorphisms commutes:*

$$\begin{array}{ccc}
(\bigoplus_{\pi\in\Pi} \mathbb{L}^{\pm \mathrm{Ind}_\pi/2}(\phi_\pi^0)^*[d_\pi^0](p_Y^\pm)_!(\eta_Y^\pm)^* P_{Y,t})|_{R^0} & \xrightarrow{\oplus_{\pi\in\Pi} \mathbb{L}^{\pm \mathrm{Ind}_\pi/2}(\phi_\pi^0)^*[d_\pi^0]\beta_{Y,t}^\pm} & \bigoplus_{\pi,\pi'\in\Pi} \mathbb{L}^{\pm \mathrm{Ind}_{\pi'}/2}(\phi_\pi^0)^*[d_\pi^0] P_{Y^0_{\pi'-\pi}, t^0_{\pi'-\pi}} \\
\simeq \uparrow & & \\
((p_X^\pm)_!(\eta_X^\pm)^*\phi^*[d]P_{Y,t}))|_{R^0} & & \oplus_{\pi,\pi'\in\Pi} \mathbb{L}^{\pm \mathrm{Ind}_{\pi'}/2}\Delta_{\phi_\pi^0} \downarrow \\
\Delta_\phi \downarrow & & \\
((p_X^\pm)_!(\eta_X^\pm)^* P_{X,s})|_{R^0} & \xrightarrow{\beta_{X,s}^\pm} & \bigoplus_{\pi'\in\Pi} \mathbb{L}^{\pm \mathrm{Ind}_{\pi'}/2} P_{X^0_{\pi'}, s^0_{\pi'}}
\end{array}$$

Proof: It suffices to show that this square commutes étale locally on X^0. According to lemma 6.6.2, we can then choose $\mathbb{C}^*$-equivariant critical charts (R, U, f, i) and (S, V, g, j) of X and Y containing x and y with a smooth map $\Phi : U \to V$ of relative dimension d such that $f = g \circ \Phi$ and $\Phi \circ i = j \circ \phi$. On such charts, the commutation of the proposition is given by Proposition 6.3.4. □

6.5 Hyperbolic localization on a d-critical algebraic stack

6.5.1 Hyperbolic localization on an algebraic stack

Definition 6.5.1. An algebraic stack $\mathcal{X}$ with an action of a 1-dimensional torus $\mathbb{C}^*$ is said to be lisse-étale locally linearizable if for every point x there is a $\mathbb{C}^*$-equivariant smooth affine neighborhood (X, u) of $(\mathcal{X}, x)$ inducing an isomorphism of stabilizers of u and x .

According to [AHR20, Theo 20.1], a quasi-separated algebraic stack with affine stabilizers locally of finite presentation over $\mathbb{C}$ is lisse-étale locally linearizable over each point $x \in \mathcal{X}$ such that, denoting by G_x the stabilizer subgroup of x, G_y the stabilizer subgroup of the image y of x in $\mathcal{Y} := \mathcal{X}/T$, and $T_x \subset T$ the subgroup stabilizing x, the following exact sequence is split:

$$1 \to G_x \to G_y \to T_x \to 1 \tag{6.5.1}$$

Consider now the functors of groupoids:

$$\begin{aligned}
\mathcal{X}^0 &: Y \mapsto \mathrm{Hom}_S^T(Y, \mathcal{X}) \\
\mathcal{X}^+ &: Y \mapsto \mathrm{Hom}_S^T((\mathcal{A}_Y^1)^+, \mathcal{X}) \\
\mathcal{X}^- &: Y \mapsto \mathrm{Hom}_S^T((\mathcal{A}_Y^1)^-, \mathcal{X})
\end{aligned} \tag{6.5.2}$$

where the superscript $\mathbb{C}^*$ denotes the $\mathbb{C}^*$-equivariant morphism, and $T, (\mathcal{A}_Y^1)^+, (\mathcal{A}_Y^1)^-$ has the trivial, resp. usual, resp. opposite $\mathbb{C}^*$-action. We can define the whole hyperbolic localization diagram by the same way than for algebraic spaces, and we have:

Proposition 6.5.2. *For $\mathcal{X}$ an S algebraic stack with a lisse-étale locally linearizable $\mathbb{C}^*$-action, $\mathcal{X}^0$ and $\mathcal{X}^\pm$ are representable as algebraic stacks, and for any smooth $\mathbb{C}^*$-equivariant 1-morphism $Y \to \mathcal{X}$, $Y^0 \to \mathcal{X}^0$ and $Y^\pm \to \mathcal{X}^\pm$ are also smooth and the natural morphism of algebraic spaces $Y^\pm \to Y^0 \times_{\mathcal{X}_0} \mathcal{X}^\pm$ is an affine fiber bundle.*

Proof: $\mathcal{X}^0$ and $\mathcal{X}^\pm$ are stacks because the above functors satisfy descent. Two $\mathbb{C}^*$-equivariant 1-morphisms $Y \to \mathcal{X}$ are 2-isomorphic if and only if they are 2-isomorphic to a single 1-morphism, hence as functors of groupoids the diagonal $\mathcal{X}^0 \to \mathcal{X}^0 \times \mathcal{X}^0$ is the pullback of the diagonal $\mathcal{X} \to \mathcal{X} \times \mathcal{X}$, hence it is representable because $\mathcal{X}$ is an algebraic stack. Similarly, two $\mathbb{C}^*$-equivariant morphisms $y, y' : \mathbb{A}^1_Y$ are 2-isomorphic if and only if their restriction to 0 and to 1 are 2-isomorphic to single 1-morphisms, hence as functors of groupoids the diagonal $\mathcal{X}^\pm \to \mathcal{X}^\pm \times \mathcal{X}^\pm$ is the pullback of the diagonal of $\mathcal{X}^0 \times \mathcal{X}$, hence it is representable because $\mathcal{X}$ and $\mathcal{X}^0$ has representable diagonal.

Consider a smooth $\mathbb{C}^*$-equivariant 1-morphism $Y \to \mathcal{X}$ from an algebraic space Y. Then $Y^0 \to Y \to X$ is $\mathbb{C}^*$-equivariant, and then factorize as a morphism $Y^0 \to X^0$. Consider a 1-morphism $U \to \mathcal{X}^0$ from an algebraic space, and the following commutative cube:

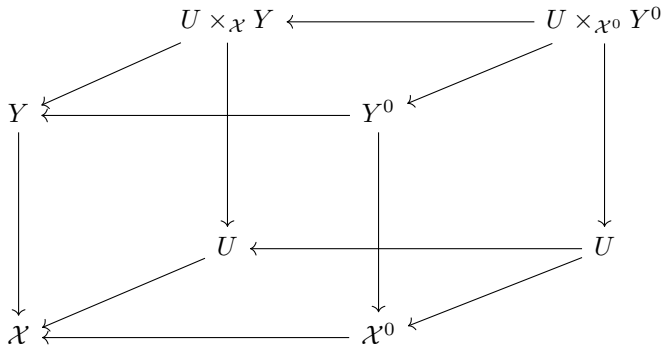

the above, below, left and right squares are Cartesian and in the front and back squares the right vertical arrow is the restriction of the left vertical arrow on the $\mathbb{C}^*$-fixed domains and codomains. Because $Y \to \mathcal{X}$ is presentable and the left square is Cartesian, then $U \times_{\mathcal{X}} Y$ is an algebraic space, and then because the above square is Cartesian $U \times_{\mathcal{X}^0} Y^0$ is an algebraic space. Because $Y \to \mathcal{X}$ is smooth and the left square is Cartesian, $U \times_{\mathcal{X}} Y \to U$ is smooth, and then proposition 6.2.4 applied to the back square, which is a square of algebraic spaces, gives that $U \times_{\mathcal{X}^0} Y^0 \to U$ is smooth. Hence $Y^0 \to \mathcal{X}^0$ is smooth. As morphism of functors of groupoids $Y^\pm \to \mathcal{X}$ factorize as a morphism $Y^\pm \to \mathcal{X}^\pm$. Exactly the same proof as above, replacing the superscripts ^{0} by $^\pm$ gives that $Y^\pm \to \mathcal{X}^\pm$ is smooth.

Consider the smooth and surjective $\mathbb{C}^*$-equivariant presentation Y of $\mathcal{X}$ obtained by taking the disjoint union of $\mathbb{C}^*$-equivariant smooth affine neighborhood (Y_x, y_x) inducing an isomorphism of stabilizers for each point x of X. A point $x \in \mathcal{X}^0$ has stabilizer $\mathbb{C}^*$, and then the point y_x has stabilizer $\mathbb{C}^*$, hence $y_x \in Y^0$, i.e. $Y^0 \to \mathcal{X}^0$ is surjective, and smooth from above. Then $\mathcal{X}^0$ is an algebraic stack. Consider a point $x \in \mathcal{X}^\pm$, i.e. a $\mathbb{C}^*$-equivariant morphism $x : (\mathbb{A}^1)^\pm \to \mathcal{X}$. Consider the smooth $\mathbb{C}^*$-equivariant morphism of algebraic spaces $Y \times_{\mathcal{X}} (\mathbb{A}^1)^\pm \to (\mathbb{A}^1)^\pm$ obtained by base change from $Y \to \mathcal{X}$. As any smooth $\mathbb{C}^*$-equivariant morphism of algebraic spaces can be étale-locally written as a $\mathbb{C}^*$-equivariant fibration with $\mathbb{C}^*$-linear affine fiber, then it admits étale locally a smooth $\mathbb{C}^*$-equivariant section. Any $\mathbb{C}^*$-equivariant étale neighborhood of 0 in $(\mathbb{A}^1)^\pm$ is $(\mathbb{A}^1)^\pm$ itself, there is a $\mathbb{C}^*$-invariant section s of $Y \times_{\mathcal{X}} (\mathbb{A}^1)^\pm \to (\mathbb{A}^1)^\pm$, giving a $\mathbb{C}^*$-equivariant morphism $y : (\mathbb{A}^1)^\pm \to Y$ lifting $x : (\mathbb{A}^1)^\pm \to \mathcal{X}$, i.e. a point of $y \in Y^\pm$ above $x \in \mathcal{X}^\pm$. Hence $Y^\pm \to \mathcal{X}^\pm$ is surjective, and smooth from above, i.e. $\mathcal{X}^\pm$ is an algebraic stack.

The proof of the fact that $Y^\pm \to Y^0 \times_{\mathcal{X}_0} \mathcal{X}^\pm$ is an affine fiber bundle is similar to the proof of the corresponding fact in proposition 6.2.4.□

For a smooth $\mathbb{C}^*$-equivariant 1-morphism $\phi : Y \to \mathcal{X}$ from an algebraic space, denote by ϕ^0_π the component of ϕ^0 where the cocharacter induced by the action of $\mathbb{C}^*$ on the relative tangent complex is π. Exactly the same manipulations than in the proof of proposition 6.2.5 gives the natural functor in the six-functor formalism:

$$(p_Y^\pm)_!(\eta_Y^\pm)^*\phi^*[d] \simeq \bigoplus_{\pi\in\Pi} \mathbb{L}^{\pm \mathrm{Ind}_\pi/2}(\phi^0_\pi)^*[d^0_\pi](p^\pm_{\mathcal{X}})_!(\eta^\pm_{\mathcal{X}})^* \tag{6.5.3}$$

The smooth 1-morphisms $\phi^0 : Y^0 \to \mathcal{X}^0$ coming from a smooth $\mathbb{C}^*$-equivariant 1-morphism $\phi : Y \to \mathcal{X}$ from an algebraic space covers X, hence a sheaf on X^0 is determined by its pullback by such ϕ^0. In particular, the morphisms S_Y of proposition 6.2.3 glue into a morphism:

$$S_{\mathcal{X}} : \mathbb{D}(p^-_{\mathcal{X}})_!(\eta^-_{\mathcal{X}})^*\mathbb{D} \to (p^+_{\mathcal{X}})_!(\eta^+_{\mathcal{X}})^* \tag{6.5.4}$$

which is an isomorphism on $\mathbb{C}^*$-equivariant sheaves.

6.5.2 D-critical stack

As defined in section 2.8 of [Joy13], a d-critical structure on an algebraic stack X is equivalent to the data of d-critical structure $y^\star(s)$ on the scheme Y for each smooth 1-morphism $y : Y \to X$ such that for each 2-morphism (ϕ, η) between the 1-morphism $y : Y \to X$ and $z : Z \to X$, $\phi^\star z^\star(s) = y^\star(s)$. In particular, [BBBBJ15, Theo 3.18] shows that a (-1)-shifted symplectic algebraic stack has a canonical d-critical structure. On a d-critical stack X, Joyce built its canonical sheaf K_X, which is the determinant of the tangent complex if X is the classical truncation of a (-1)-shifted symplectic stack. An orientation $K_X^{1/2}$ is then a square root of K_X, and [Joy13, Lem 2.57] shows that an orientation $K_X^{1/2}$ determines an orientation of $(Y, y^\star(s))$ for each scheme Y and 1-morphism $y : Y \to X$. In particular, a smooth 2-morphism (ϕ, η) of relative dimension d gives then a smooth morphism of oriented critical scheme $\phi : (X, y^\star(s), K_Y^{1/2}) \to (Y, z^\star(s); K_Z^{1/2})$ of relative dimension d.

A perverse sheaf $\mathcal{P}$ (and an underlying strongly polarized mixed Hodge module) on an algebraic stack X is given by the data:

- For each smooth 1-morphism $y : Y \to X$ from a scheme Y, a perverse sheaf $y^*\mathcal{P}$ on Y.
- For each commutative diagram in the 2-category of $\mathbb{C}$-algebraic stacks:

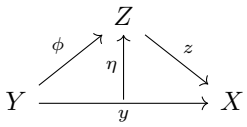

  with Y, Z being schemes, and y, z smooth and ϕ smooth of relative dimension d, an isomorphism $\mathcal{P}(\phi, \eta) : \phi^*[d]z^*\mathcal{P} \to y^*\mathcal{P}$.

with a compatibility condition on composition of 2-morphisms, see definition 4.6 of [BBBBJ15]. A morphism of perverse sheaf$\beta : \mathcal{P} \to \mathcal{Q}$ is then given by the data of a morphism of perverse sheaves $y^*\beta : y^*\mathcal{P} \to y^*\mathcal{Q}$ for each smooth 1-morphism $y : Y \to X$ from a scheme Y. The compatibility

condition is that for of the above diagram, the following diagram is commutative:

$$\begin{array}{ccc} \phi^*[d]z^*\mathcal{P} & \xrightarrow{\mathcal{P}(\phi)} & y^*\mathcal{P} \\ \downarrow{\scriptstyle \phi^*[d]z^*\beta} & & \downarrow{\scriptstyle y^*\beta} \\ \phi^*[d]z^*\mathcal{Q} & \xrightarrow{\mathcal{Q}(\phi,\eta)} & y^*\mathcal{Q} \end{array}$$

In [BBBBJ15, Theo 4.8], the authors show that for an oriented d-critical stack $(X, s, K_{X,s}^{1/2})$ the data P_{Y,y^*} and $\Delta_\phi : \phi^*[d](P_{Z,z^\star(s)}) \to P_{Y,y^\star(s)}$ defines a perverse sheaf $P_{X,s}$ on X.

When $(X, s, K_{X,s}^{1/2})$ is a $\mathbb{C}^*$-equivariant d-critical algebraic stack with a lisse-étale linearizable $\mathbb{C}^*$-action, the smooth 1-morphisms $y^0 : Y^0 \to \mathcal{X}^0$ and 2-morphisms $(\phi^0, \eta^0) : y^0, Y^0 \to z^0, Z^0$ arising from a smooth $\mathbb{C}^*$-equivariant 1-morphism $y : Y \to \mathcal{X}$ or 2-morphism $(\phi, \eta) : y, Y \to z, Z$ cover $\mathcal{X}^0$, hence a sheaf or a morphism of sheaf on $\mathcal{X}^0$ can be defined using those 1-morphisms and 2-morphisms. For each $y^0 : Y^0 \to \mathcal{X}^0$ arising from a smooth $\mathbb{C}^*$-equivariant 1-morphism $y : Y \to \mathcal{X}$, $(y^0)^\star(\xi_\mathcal{X})^\star(s) = (\xi_Y)^\star y^\star(s)$ defines a d-critical structure on Y^0, and $K_{X^0,s^0}^{1/2}$ gives an orientation on X^0. According to Lemma 6.4.3, these d-critical structures and orientations glues to gives an oriented d-critical stack $\mathcal{X}^0, s^0, H_{\mathcal{X},s}^{1/2}$.

According to proposition 6.4.4 and equation (6.5.3), the isomorphisms $\beta_{Y,y^\star(s)}$ glue into an isomorphism $\beta_{\mathcal{X},s}^{\pm}$ commuting with monodromy and duality:

Theorem 6.5.3. *For $\mathcal{X}$ an oriented d-critical algebraic stack with a lisse-étale linearizable $\mathbb{C}^*$-action leaving the d-critical structure and the orientation invariant, one has natural isomorphisms of perverse sheaves and monodromic mixed Hodge modules on $\mathcal{X}^0$:*

$$\beta_{\mathcal{X},s}^{\pm} : (p_\mathcal{X}^{\pm})_!(\eta_\mathcal{X}^{\pm})^* P_{\mathcal{X},s} \to \bigoplus_{\pi\in\Pi} \mathbb{L}^{\pm \mathrm{Ind}_\pi/2} P_{\mathcal{X}_\pi^0, s_\pi^0} \tag{6.5.5}$$

Which are compatible with strong polarization in the sense that the following diagram is commutative:

$$\begin{array}{ccc} (p_\mathcal{X}^+)_!(\eta_\mathcal{X}^+)^* P_{\mathcal{X},s} & \xrightarrow{\beta_{\mathcal{X},s}^+} & \bigoplus_{\pi\in\Pi} \mathbb{L}^{\mathrm{Ind}_\pi/2} P_{\mathcal{X}_\pi^0, s_\pi^0} \\ \downarrow{\scriptstyle S_\mathcal{X}^{-1}\circ(p_\mathcal{X}^+)_!(\eta_\mathcal{X}^+)^*(\Sigma_{\mathcal{X},s})} & & \downarrow{\scriptstyle \bigoplus_{\pi\in\Pi} \mathbb{L}^{\mathrm{Ind}_\pi/2}\Sigma_{\mathcal{X}_\pi^0,s_\pi^0}} \\ \mathbb{D}(p_\mathcal{X}^-)_!(\eta_\mathcal{X}^-)^* P_{\mathcal{X},s} & \xleftarrow[\mathbb{D}\beta_{\mathcal{X},s}^-]{} & \mathbb{D}\bigoplus_{\pi\in\Pi} \mathbb{L}^{-\mathrm{Ind}_\pi/2} P_{\mathcal{X}_\pi^0, s_\pi^0} \end{array}$$

6.6 Technical lemmas

6.6.1 Trivialization of torus-equivariant embeddings

Lemma 6.6.1. *Let $\Phi : (R, U, f, i) \to (S, V, g, j)$ be a $\mathbb{C}^*$-equivariant embedding of $\mathbb{C}^*$-equivariant critical charts. For $x \in i(R^0)$, there are smooth $\mathbb{C}^*$-equivariant algebraic space U', V', $x' \in U'$, $\mathbb{C}^*$-equivariant morphisms $\iota : U' \to U$ with $\iota(x') = x$, $\jmath : V' \to V$, $\Phi' : U' \to V'$, $\alpha : V' \to U$ and $\beta : V' \to E$ with E a vector space with $\mathbb{C}^*$ action, with ι, $\jmath$ and $\alpha \otimes \beta$ being étale, such that the following square commutes:*

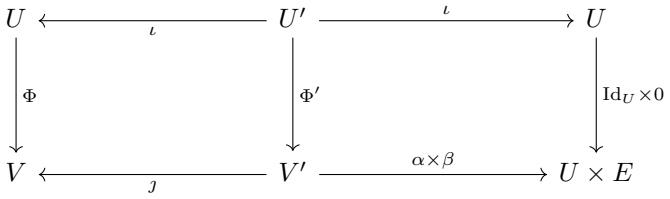

and $g \circ \jmath = f \circ q \circ \alpha : V' \to \mathbb{C}$*, with* q *a non-degenerate* $\mathbb{C}^*$*-invariant quadratic form on* E*.*

Proof: We follow here closely the proof of [Joy13, Prop 2.22, 2.23], adapting it to the equivariant case: we take care to consider at each step only étale cover with $\mathbb{C}^*$ action, and to keep $\mathbb{C}^*$-equivariant functions and coordinates. The map $\Phi : U \to V$ is a $\mathbb{C}^*$-equivariant embedding of smooth schemes of respective dimension $\dim(U) = m, \dim(V) = m + n$. We can then find $\mathbb{C}^*$-equivariant étale coordinates $(\dot{y}_1, ..., \dot{y}_m, \dot{z}_1, ..., \dot{z}_n)$ on a $\mathbb{C}^*$-equivariant Zariski open neighborhood $\dot{V}$ of $j(x)$ in V such that $j(x) = (0, ..., 0)$ and $\Phi(U) \cap \dot{V}$ is the locus $\dot{z}_1 = ... = \dot{z}_n = 0$ in $\dot{V}$. Set $\dot{U} = \Phi^{-1}(\dot{V})$ and $\dot{x}_a = \dot{y}_a \circ \Phi|_{\dot{U}}$ for $a = 1, ..., m$. Then $\dot{U}$ is an open neighborhood of $i(x)$ in U , and $(\dot{x}_1, ..., \dot{x}_m)$ are étale coordinates on $\dot{U}$ with $i(x) = (0, ..., 0)$. Then the ideal $I_{R,U} = I_{(df)}$ is on $\dot{U}$ the ideal generated by the $\mathbb{C}^*$-equivariant functions $\frac{\partial f}{\partial \dot{x}_a}$ for $a = 1, ..., m$, and the ideal $I_{S,V} = I_{(dg)}$ is on $\dot{V}$ the ideal generated by the $\mathbb{C}^*$-equivariant functions $\frac{\partial g}{\partial \dot{y}_a}$ for $a = 1, ..., m$ and $\frac{\partial g}{\partial \dot{z}_b}$ for $b = 1, ..., n$. Since Φ maps U to $\dot{z}_1 = ... = \dot{z}_n = 0$ and $i(R)$ to $j(R) \subset j(S)$, we have $I_{(df)} \simeq I_{(dg)}|_{\dot{z}_1=...=\dot{z}_n=0}$, that is:

$$\begin{aligned}(\frac{\partial f}{\partial \dot{x}_a}(\dot{y}_1, ..., \dot{y}_m) : a = 1, ..., m) = (&\frac{\partial g}{\partial \dot{y}_a}(\dot{y}_1, ..., \dot{y}_m, 0, ..., 0) : a = 1, ..., m, \\ &\frac{\partial g}{\partial \dot{z}_b}(\dot{y}_1, ..., \dot{y}_m, 0, ..., 0) : b = 1, ..., n)\end{aligned} \tag{6.6.1}$$

this holds provided each $\frac{\partial g}{\partial \dot{z}_b}(\dot{y}_1, ..., \dot{y}_m, 0, ..., 0)$ lies in $(\frac{\partial g}{\partial \dot{y}_a}(\dot{y}_1, ..., \dot{y}_m, 0, ..., 0) : a = 1, ..., m$. Thus, making $\dot{U}, \dot{V}$ smaller if necessary, we can suppose there exist étale locally $\mathbb{C}^*$-equivariant functions $A_{ab}(\dot{y}_1, ..., \dot{y}_m)$ on $\dot{U}$ for $a = 1, ..., m, b = 1, ..., n$ such that for each b:

$$\frac{\partial g}{\partial \dot{z}_b}(\dot{y}_1, ..., \dot{y}_m, 0, ..., 0) = \sum_{a=1}^{m} A_{ab}(\dot{y}_1, ..., \dot{y}_m) \frac{\partial g}{\partial \dot{y}_a}(\dot{y}_1, ..., \dot{y}_m, 0, ..., 0) \tag{6.6.2}$$

Defining the $\mathbb{C}^*$-equivariant functions $\tilde{y}_a = \dot{y}_a - \sum_{a=1}^{m} A_{ab}(\dot{y}_1, ..., \dot{y}_m)\dot{z}_b$, and $\tilde{z}_b = \dot{z}_b$, they give $\mathbb{C}^*$-equivariant étale coordinates on a $\mathbb{C}^*$-invariant neighborhood $\tilde{V}$ of $j(x)$. We also define the $\mathbb{C}^*$-invariant subspace $\tilde{U} = \Phi^{-1}(\tilde{V})$, and define on it the $\mathbb{C}^*$-equivariant étale coordinates $\tilde{x} = \dot{x}|_{\tilde{U}}$: then $\tilde{y}_a \circ \Phi|_{\tilde{U}} = \tilde{x}_a$ and $\tilde{z}_b \circ \Phi|_{\tilde{U}} = 0$. Then:

$$\begin{aligned}\frac{\partial g}{\partial \tilde{z}_b}(\tilde{y}_1, ..., \tilde{y}_m, 0, ..., 0) =& \sum_{a=1}^{m} \frac{\partial g}{\partial \dot{y}_a}(\dot{y}_1, ..., \dot{y}_m, 0, ..., 0).\frac{\partial \dot{y}_a}{\partial \tilde{z}_b} + \sum_{c=1}^{n} \frac{\partial g}{\partial \dot{z}_c}(\dot{y}_1, ..., \dot{y}_m, 0, ..., 0).\frac{\partial \dot{z}_c}{\partial \tilde{z}_b} \\ =& \sum_{a=1}^{m} \frac{\partial g}{\partial \dot{y}_a}(\dot{y}_1, ..., \dot{y}_m, 0, ..., 0)(-A_{ab}(\dot{y}_1, ..., \dot{y}_m)) \\ &+ \sum_{c=1}^{n}(\sum_{a=1}^{n} A_{ac}(\dot{y}_1, ..., \dot{y}_m)).\frac{\partial g}{\partial \dot{y}_a}(\dot{y}_1, ..., \dot{y}_m, 0, ..., 0).\delta_{bc} \\ =& 0\end{aligned} \tag{6.6.3}$$

We define the $\mathbb{C}^*$-equivariant space $\check{V}$ and the $\mathbb{C}^*$-equivariant étale morphisms $\check{\jmath}, \check{\alpha}, \check{\beta}$ by the $\mathbb{C}^*$-equivariant Cartesian square:

$$\begin{array}{ccc} \check{V} & \xrightarrow{\check{\jmath}} & \tilde{V} \\ \downarrow{\scriptstyle \check{\alpha}\times\check{\beta}} & & \downarrow{\scriptstyle (\tilde{y}_1,\dots,\tilde{y}_m,\tilde{z}_1,\dots,\tilde{z}_n)} \\ \tilde{U}\times\mathbb{C}^n & \xrightarrow{(\tilde{x}_1,\dots,\tilde{x}_m)\times \mathrm{Id}_{\mathbb{C}^n}} & \mathbb{C}^{m+n} \end{array}$$

where $\mathbb{C}^{m+n}$ is provided with the $\mathbb{C}^*$-action induced from the action of $\mathbb{C}^*$ on the étale coordinates. There is a unique $\check{v} \in \check{V}$ with $\check{\alpha}(\check{v}) = i(x)$, $\check{\beta}(\check{v}) = (0,...,0)$ and $\check{\jmath}(\check{v}) = j(x)$.). We can regard $\check{\jmath} : \check{V} \to \tilde{V} \subset V$ as an étale $\mathbb{C}^*$-invariant open set in V. Define $\mathbb{C}^*$-equivariant étale coordinates $(\check{y}_1,...,\check{y}_m,\check{z}_1,...,\check{z}_n) : \check{V} \to \mathbb{C}^{m+n}$ by $\check{y}_a = \tilde{y}_a \circ \check{\jmath}, \check{z}_b = \tilde{z}_b \circ \check{\jmath}$, and define the $\mathbb{C}^*$-invariant functions $\check{f}, \check{g} : \check{V} \to \mathbb{C}$ by $\check{f} = f \circ \check{\alpha}, \check{g} = g \circ \check{\jmath}$, and $\check{h} = \check{g} - \check{f} : \check{V} \to \mathbb{C}$. The previous argument now shows that on the smooth subscheme $\check{U} \subset \check{V}$ defined by $\check{z}_1 = ... = \check{z}_n = 0$ we have $\check{h}|_{\check{U}}$ and $\frac{\partial \check{h}}{\partial \check{z}_b}|_{\check{U}} = 0$ for $b = 1,...,n$. Therefore the $\mathbb{C}^*$ invariant function $\check{h}$ lies in the ideal $(\check{z}_1,...,\check{z}_n)^2$ generated by $\mathbb{C}^*$-equivariant functions on $\check{V}$. So making $\check{U}, \check{V}, \tilde{U}, \tilde{V}$ smaller but still $\mathbb{C}^*$-invariant, we may write $\check{h} = \sum_{b,c=1}^n \check{z}_b \check{z}_c Q_{bc}$ for some $\mathbb{C}^*$-invariant $Q_{bc} : \check{V} \to \mathbb{C}$ with $Q_{bc} = Q_{cb}$. Up to a $\mathbb{C}^*$-equivariant linear change of coordinates $\check{z}$, we can write:

$$\sum_{b,c=1}^n \check{z}_b \check{z}_c Q_{bc}(0,...,0) = 2\sum_{b=1}^r \check{z}_{2b-1}\check{z}_{2b} + \sum_{b=2r+1}^n \check{z}_b^2 \tag{6.6.4}$$

with $n_{2i-1} = -n_{2i} > 0$ for $i \le r$ and $n_i = 0$ for $i \ge 2r+1$. Suppose that $n \ge 2r+1$: the $\mathbb{C}^*$-invariant function $Q_{nn}(\check{y}_1,...\check{y}_m,\check{z}_1,...,\check{z}_n)$ is invertible near $\check{v}$, we can take a double étale cover of $\check{V} - Q_{nn}^{-1}(0)$ such that Q_{nn} has a square root $Q_{nn}^{1/2}$. Because Q_{nn} is $\mathbb{C}^*$-invariant, $\check{V} - Q_{nn}^{-1}(0)$ is stable under $\mathbb{C}^*$, hence we can extend the $\mathbb{C}^*$ action to the double cover, such that the cover is $\mathbb{C}^*$-equivariant. We replace then $\check{V}$ by this étale neighboorhood of $\check{v}$, and all the coordinates and Q_{bc}, and $Q_{nn}^{1/2}$, are still $\mathbb{C}^*$-equivariant. We can then write:

$$\begin{aligned} h &= \sum_{b,c=1}^n \check{z}_b \check{z}_c Q_{bc} \\ &= \sum_{b,c=1}^{n-1} \check{z}_b \check{z}_c (Q_{bc} - Q_{nn}^{-1} Q_{bn} Q_{cn}) + (Q_{nn}^{1/2}\check{z}_n + \sum_{b=1}^{n-1} Q_{nn}^{-1/2} Q_{bn}\check{z}_b)^2 \\ &= \sum_{b,c=1}^{n-1} \check{z}_b \check{z}_c \hat{Q}_{bc} + z_n^2 \end{aligned} \tag{6.6.5}$$

where $\hat{Q}_{bc} = Q_{bc} - Q_{nn}^{-1} Q_{bn} Q_{cn}$ is $\mathbb{C}^*$ equivariant of character $-n_b - n_c$ and $z_n = Q_{nn}^{1/2}\check{z}_n + \sum_{b=1}^{n-1} Q_{nn}^{-1/2} Q_{bn}\check{z}_b$ is $\mathbb{C}^*$-invariant, with $\frac{\partial z_n}{\partial \check{z}_b}(\check{v}) = \delta_{nb}$ and $\hat{Q}_{bc}(0,...,0) = \delta_{bc}$. By recursion we can find an étale open neighborhood of $\check{v}$ in $\check{V}$, $\mathbb{C}^*$-invariant functions on it z_b for $b \ge 2r+1$ with $\frac{\partial z_b}{\partial \check{z}_c}(\check{v}) = \delta_{bc}$, and $\mathbb{C}^*$-equivariant functions on it $\check{Q}_{bc}$ for $b, c \ge 2r$ with $\check{Q}_{bc}(0,...,0) = Q_{bc}(0,...,0)$,

such that:

$$h = \sum_{b,c=1}^{2r} \check{z}_b \check{z}_c \check{Q}_{bc} + \sum_{b=2r+1}^{n} z_b^2 \tag{6.6.6}$$

On a $\mathbb{C}^*$-invariant open neighborhood of $\check{v}$ such that $\check{Q}_{2r-1,2r}$ is invertible:

$$\begin{aligned} h &= \sum_{b,c=1}^{2r-2} \check{z}_b \check{z}_c (\check{Q}_{bc} - \sum_{b,c=1}^{2r-2} \check{Q}^{-1}_{2r-1,2r} \check{Q}_{b,2r} \check{Q}_{2r-1,c}) + \sum_{b=2r+1}^{n} z_b^2 \\ &+ 2(\check{z}_{2r-1} + \sum_{b=1}^{2r-2} \check{Q}^{-1}_{2r-1,2r} \check{Q}_{b,2r} \check{z}_b)(\check{Q}_{2r-1,2r} \check{z}_{2r} + \sum_{c=1}^{2r-2} \check{Q}_{2r-1,c} \check{z}_c) \\ &= \sum_{b,c=1}^{2r-2} \check{z}_b \check{z}_c \tilde{Q}_{bc} + 2 z_{2r-1} z_{2r} + \sum_{b=2r+1}^{n} z_b^2 \end{aligned} \tag{6.6.7}$$

where $\tilde{Q}_{bc} = \check{Q}_{bc} - \sum_{b,c=1}^{2r-2} \check{Q}^{-1}_{2r-1,2r} \check{Q}_{b,2r} \check{Q}_{2r-1,c}$ is $\mathbb{C}^*$-equivariant of character $-n_b - n_c$ with $\tilde{Q}_{bc}(0,...,0) = Q_{bc}(0,...,0)$, $z_{2r-1} = \check{z}_{2r-1} + \sum_{b=1}^{2r-2} \check{Q}^{-1}_{2r-1,2r} \check{Q}_{b,2r} \check{z}_b$ is $\mathbb{C}^*$ equivariant of character n_{2r-1} with $\frac{\partial z_{2r-1}}{\partial \check{z}_b}(\check{v}) = \delta_{2r-1,b}$, and $z_{2r} = \check{Q}_{2r-1,2r} \check{z}_{2r} + \sum_{c=1}^{2r-2} \check{Q}_{2r-1,c} \check{z}_c$ is $\mathbb{C}^*$-equivariant of weight n_{2r} with $\frac{\partial z_{2r}}{\partial \check{z}_b}(\check{v}) = \delta_{2r,b}$. By recursion, there is then on an a $\mathbb{C}^*$-invariant étale open neighborhood $\jmath' : V' \to \check{V}$ of $\check{v}$ and $\mathbb{C}^*$-equivariant functions z_b with $\frac{\partial z_b}{\partial \check{z}_c}(\check{v}) = \delta_{bc}$ (i.e. by restricting V' to a $\mathbb{C}^*$-invariant open neighborhood of $\check{v}$, $(y_1 := y_1 \circ \jmath', ..., y_m := y_m \circ \jmath', z_1, ..., z_n$ forms a system of étale coordinates of $V')$, such that:

$$h = 2 \sum_{b=1}^{r} z_{2b-1} z_{2b} + \sum_{b=2r+1}^{n} z_b^2 \tag{6.6.8}$$

Define the $\mathbb{C}^*$-invariant subset $U' = \{v' \in V' : z_1(v') = ... = z_n(v') = 0$. Define the $\mathbb{C}^*$-equivariant maps $\iota : U' \to U, \jmath : V' \to V, \Phi' : U' \to V', \alpha : V' \to U, \beta : V' \to \mathbb{C}^n$ by $\iota := \check{\alpha} \circ \jmath'|'_U$, $\jmath := \check{\jmath} \circ \jmath'$, $\Phi' = \mathrm{Id}_{U'}$, $\alpha = \check{\alpha} \circ \jmath'$ and $\beta = (z_1, ..., n_n)$. As $\jmath' : V' \to \check{V}$ is an étale open neighborhood of $\check{v}$ in $\check{V}$, there exists $u' \in V'$ with $\jmath'(u') = \check{v}$, and $z_b(u' = 0$ for $b = 1, ..., n$ as $\check{z}_b(\check{v}) = 0$, so $u' \in U$ with $\iota(u') = \check{\alpha} \circ \jmath'(u') = \check{\alpha}(\check{v}) = i(x)$. Also $\iota, \jmath, \alpha \times \beta$ are étale as $\check{alpha} \times \check{\beta}, \check{\jmath}, \jmath'$ are. The same computations as in the proof of [Joy13, Prop 2.23] show that in a neighborhood of u', which can be taken to be $\mathbb{C}^*$-invariant, we have $\Phi \circ \iota = \jmath \circ \Phi$, so this making u' smaller and still $\mathbb{C}^*$-invariant it holds on U'. The equations $\alpha \circ \Phi' = \iota, \beta \circ \Phi' = 0$ are immediate, and $g \circ \jmath = f \circ \alpha + (2 \sum_{b=1}^{r} z_{2b-1} z_{2b} + \sum_{b=2r+1}^{n} z_b^2) \circ \beta$ follows from (6.6.8). □

6.6.2 Smooth torus-equivariant morphism of d-critical scheme

Lemma 6.6.2. *Consider a smooth morphism of d-critical scheme $\phi : (X, s) \to (Y, t)$ of relative dimension d. For $x \in X$, we can then choose two $\mathbb{C}^*$-equivariant critical charts (R, U, f, i) and (S, V, g, j) of X and Y containing x and $y := f(x)$ with a smooth map $\Phi : U \to V$ of relative dimension d such that $f = g \circ \Phi$ and $\Phi \circ i = j \circ \phi$.*

Proof: This is a $\mathbb{C}^*$-equivariant version of the result used in the proof of [BBBBJ15, Prop 4.5]: as before, we check that we can do each step in a $\mathbb{C}^*$-equivariant way. As in the proof of [Joy13, Prop

2.43], because the $\mathbb{C}^*$ action on Y is étale-locally linearizable, we can find an étale neighborhood S' of y with a closed $\mathbb{C}^*$-equivariant embedding into a smooth algebraic space with $\mathbb{C}^*$-action V', with $\dim(V') = \dim(T_yY)$. According to the proof of the proposition 6.2.4, the $\mathbb{C}^*$-equivariant smooth map $\phi^{-1}(S') \to S'$ is étale locally a $\mathbb{C}^*$-equivariant affine fibration, hence we can find a $\mathbb{C}^*$-equivariant étale neighborhood S of y, $\mathbb{C}^*$-equivariant embeddings $i : R := \phi^{-1}(S) \to U$, $j : S \to V$ into smooth algebraic spaces with $\mathbb{C}^*$-action U, V with dimension $\dim(U) = \dim(T_xX)$, $\dim(V) = \dim(T_yY)$, with a $\mathbb{C}^*$-equivariant smooth map of relative dimension d $\Phi : U \to V$ such that $\Phi \circ i = j \circ \phi|_R$. Hence as in the proof of [Joy13, Prop 2.43], up to shrinking S, V (and then R, U) to a $\mathbb{C}^*$-invariant open subspace we can find a $\mathbb{C}^*$ invariant regular function $g : V \to \mathbb{C}$ such that $\iota_{S,V}(t|_S) = j^{-1}(g) + I^2_{S,V}$, and $S = \mathrm{Crit}(g)$, i.e. (S, V, g, j) is a $\mathbb{C}^*$-equivariant critical chart of Y near y. Defining the $\mathbb{C}^*$-equivariant regular function $f := g \circ \Phi : U \to \mathbb{C}$, because $s = \phi^\star(t)$, one has $\iota_{R,U}(s|_R) = i^{-1}(f) + I^2_{R,U}$. Also $\Phi \circ i = j \circ \phi|_R$ and Φ, ϕ are smooth of relative dimension d, then $i(R) = \Phi^{-1}(j(S))$ in a neighborhood of $i(x)$: taking the union of all these neighborhood, one can shrink U (and then R) to $\mathbb{C}^*$-invariant open neighborhood satisfying $i(R) = \Phi^{-1}(j(S))$. Because Φ is smooth, one has:

$$\mathrm{Crit}(f) = \Phi^{-1}(\mathrm{Crit}(g)) = \Phi^{-1}(j(S)) = i(R) \tag{6.6.9}$$

i.e. (R, U, f, i) is a $\mathbb{C}^*$-equivariant critical chart near x. We have then build $\mathbb{C}^*$-equivariant critical charts (R, U, f, i) and (S, V, g, j) of X and Y near x and y with a smooth map $\Phi : U \to V$ of relative dimension d such that $f = g \circ \Phi$ and $\Phi \circ i = j \circ \phi$. □

Chapter 7

Cohomological DT invariants from localization

7.1 Introduction

Donaldson-Thomas (DT) invariants are the mathematical counterpart of the BPS invariants counting supersymmetric bound states in type II string compactifications. On a non-compact toric Calabi-Yau threefold X, the study of DT invariants can be translated into a representation-theoretic problem using an equivalence between the bounded derived category of coherent sheaves on X and the bounded derived category of representations of a quiver with potential (Q, W), encoded in a brane tiling. We denote by Q_0 (resp Q_1) the set of nodes (resp arrows) of the quiver. We will consider cohomological DT invariants as defined by Davison in [Dav17] and Davison-Meinhardt in [DM16] following ideas of Kontsevich-Soibelman in [KS10]. The prime object of interest is the generating series of the cohomological DT invariants $\mathcal{A}(x)$, or BPS monodromy, first defined in [KS10]: it is a generating series in the Grothendieck ring of monodromic mixed Hodge structures (MMHS). The cohomological BPS invariants $\Omega_{\theta,d}$ defined in [DM16, Theo A], for dimension vector $d \in \mathbb{N}^{Q_0}$ and generic King stability parameter $\theta \in \mathbb{R}^{Q_0}$ are valued in the Grothendieck ring of MMHS, and give a virtual version of the cohomology with compact support of the moduli space of θ-semistable d-dimensional representations. The Harder-Narasimhan decomposition, expressing a general quiver representation as an extension of semistable representations with increasing slope $\mu = \theta.d/\sum_{i\in Q_0} d_i$, and then the Jordan-Hölder filtration, expressing a semistable representation as an extension of stable objects with the same slope, can be expressed by the formula [DM16, eq 7]:

$$\mathcal{A}(x) = \prod_{l}^{\curvearrowright} \mathrm{Exp}\left(\sum_{d\in l} \frac{\Omega_{\theta,d}}{\mathbb{L}^{1/2} - \mathbb{L}^{-1/2}} x^d\right) \tag{7.1.1}$$

Here $\mathbb{L}^{1/2}$ denotes the square root of the Tate motive, Exp denotes the plethystic exponential defined in [DM16, eq 6], and the product ranges over rays l with increasing slope. Denoting by $\langle\cdot,\cdot\rangle$ the anti-symmetrized Euler form of the quiver introduced below, the attractor invariants $\Omega_{*,d}$ defined in [MP20, sec. 3.6] are special instances of $\Omega_{\theta,d}$ for θ a small generic deformation of the self-stability (or attractor) condition $\langle\cdot, d\rangle$, subject to the constraint $\theta(d) = 0$. The attractor invariants correspond with initial data of the stability scattering diagram introduced in [Bri17], and

one can extract from them all the DT invariants using the recently proven attractor and flow tree formulas, see [Moz21] and [AB21]. We denote by $\Omega_\theta(x) := \sum_d \Omega_{\theta,d} x^d$ and $\Omega_*(x) := \sum_d \Omega_{*,d} x^d$ the corresponding generating series. These series are in general hard to compute, and there is to our knowledge no general closed formula unless X has no compact divisors.

One way to compute these BPS invariants is to consider i-cyclic representations, i.e. representations with a vector generating the whole representation at the node i. Equivalently, one considers DT invariants for the framed quiver with potential (Q_i, W) (with a single framing node ∞ and a single framing arrow $f : \infty \to i$) in the non-commutative stability chamber. Defining the automorphisms $S_{\pm i}(x^d) = \mathbb{L}^{\pm d_i/2} x^d$, the generating series of cohomological framed invariants $Z_i(x)$ is related to the generating series of unframed invariants $\mathcal{A}(x)$ by a wall crossing formula [Mor12, Moz13],

$$Z_i(x) = S_i(\mathcal{A}(x)) S_{-i}(\mathcal{A}(x)^{-1}) \tag{7.1.2}$$

For D a non-compact divisor of X, corresponding to a corner of the toric diagram, one can also consider D-cyclic representations, as defined in [NYY14, sec 3.2]. The corresponding framed quiver (Q_D, W_D) has a single framing node ∞ and a pair of arrows $\infty \to i$ and $j \to \infty$ with an additional potential term (see section 7.2.3 below for details). We denote by $Z_D(x)$ their cohomological generating series. An i-cyclic (resp. D-cyclic) representation can be viewed as a noncommutative analogue of a sheaf with a map from the structure sheaf $\mathcal{O}_X$ (resp. $\mathcal{O}_D$). In physics, framed DT invariants count framed BPS states with a D6-brane or non-compact D4-brane charge. Accordingly, we shall refer to the two types of framings as D6- and D4-brane framing, respectively.

The moduli space of i-cyclic (resp. D cyclic) representations admits a maximal torus action rescaling the arrows of Q_i (resp. Q_f), leaving the potential W (resp. W_D) equivariant, i.e. invariant up to a scalar: we denote by Λ the character lattice of the torus. We further denote by Δ_i (resp. Δ_D) the subset of Λ (called the Empty Room Configuration, or ERC) given by weights of paths starting at the framing node which are non vanishing in an i-cyclic (resp D-cyclic) representation of (Q_i, W) (resp Q_D, W_D) : Δ_i can be interpreted a pyramid with an atom of type i on the top, whose facets are given by Δ_D, for D running over the corners of the toric diagram.

In Lemma 7.4.3 we show that the i-cyclic (respectively, D-cyclic) representations which are fixed under the maximal torus leaving the potential invariant are in bijection with the set Π_i of subpyramids of Δ_i (respectively, the set Π_D of subfacets of Δ_D). This allows to translate the computation of the numerical limit of the generating series $Z_i(x)$ (resp. $Z_D(x)$) into a purely combinatoric problem, as proven in [MR08, Cor 5.7]. The formalism of K-theoretic localization, developed in [NO16] allows to compute by toric localization a refinement of the numerical Donaldson-Thomas invariants, known as the K-theoretic DT invariants (which are expected to agree with the χ_y genus evaluation of the cohomological DT invariants), provided the moduli space of framed representations is compact. This formalism therefore applies when the ERC is finite (for example in [CKK14] in the PT chamber, or in [Cir20] for finite pyramids of the conifold). In our situation, the moduli space is non-compact, and the invariants obtained naively by applying the K-theoretic localization formula in the non-compact setting differ from the the cohomological invariants. It can be seen by comparing the computations for the Hilbert scheme of points on $\mathbb{C}^3$ in the K-theoretic setting in [NO16, sec 8.3], and in the cohomological setting in [BBS13].

For a one dimensional torus $\mathbb{C}^*$ acting on a smooth scheme, the Bialynicki-Birula decomposition allows to express the cohomology of the attracting variety, i.e. the subvariety of points flowing onto a fixed point when $t \to 0$, as a sum of the cohomology of the fixed points components, shifted

by the number of contracting weights in the $\mathbb{C}^*$-equivariant tangent space of the fixed locus. The moduli space of cyclic representations of a framed quiver with potential (Q_f, W_f) is not smooth: it is the critical locus of the functional $\mathrm{Tr}(W_f)$, but the general philosophy of derived geometry allows to think about it as a smooth scheme, provided that one replaces the tangent space by the full tangent-obstruction complex. We establish then a derived version of Bialynicki-Birula decomposition. Namely, consider a moduli space M which is the critical locus of a potential on a smooth ambient scheme with a $\mathbb{C}^*$-action leaving the potential invariant. A choice of such a $\mathbb{C}^*$-action is called a choice of slope, and is denoted by s. Denotes by M^+ the attracting variety, and by M^0_π for $\pi \in \Pi$ the fixed components of the torus action. For $\pi \in \Pi$, denotes by $\mathrm{Ind}^s_p i$ the signed number of contracting weight in the restriction to M^0_π of the tangent-obstruction complex of M. Then we prove (7.4.31):

$$[M^+]^{vir} = \sum_{\pi \in \Pi} \mathbb{L}^{\mathrm{Ind}^s_\pi/2} [M^0_\pi]^{vir} \tag{7.1.3}$$

This formula holds also when M is a $[-1]$-shifted symplectic scheme or stack, i.e. can only be described locally as the critical locus of a potential, as proven in [Des22]. It explains the observed discrepancy between K-theoretic and cohomological/motivic computations: the K-theoretic computations provides only the refined invariants of the attracting variety of the $\mathbb{C}^*$-action given by the slope s.

We apply this result to D6 and D4 brane framings. The fixed components are then isolated points corresponding to pyramids $\pi \in \Pi_i$ (resp $\pi \in \Pi_D$), hence $[M^0_\pi]^{vir} = 1$. A choice of slope is then equivalent to a choice of a generic line separating the brane tiling lattice L, into two half planes $L^{>0}$ and $L^{<0}$, corresponding to contracting (resp. repelling) weights in the $t \to 0$ limit. According to Lemma 7.4.1, the attracting variety of the moduli space of framed representations is then given by representations in which the cycles with repelling weights are nilpotent. To a side z of the toric diagram one associates a vector $l_z \in L$, given by the outward normal to one subdivision of this side, which corresponds to the L-weight of a particular cycle of (Q, W) denoted by v^z. Those cycles generate all the cycles of (Q, W) (precisely, for w a cycle of Q, one has a power $n \in \mathbb{N}$ such that w^n can be written as a product of v^z), and correspond to the toric coordinates on X when one views the Jacobian algebra of (Q, W) as a noncommutative crepant resolution of the coordinate ring of X. The attracting variety is then the set of framed representations such that for $l_z \in L^{<0}$, v^z is nilpotent.

Imposing nilpotency and invertibility of various cycles of Q amounts to restricting to a Serre subcategory of the category of critical representations of the quiver. Consequently, the formalism of cohomological Hall algebra and wall crossing still applies. For two disjoint sets of sides of the toric diagram Z_I and Z_N, we use the superscript $Z_I : I, Z_N : N$ to denotes the invariants computed by restricting to the representations such that for $z \in Z_I$ (resp. $z \in Z_N$), v^z is invertible (resp. nilpotent). We denotes for convenience by $[z, z']$ the set of sides of the toric diagram between z and z' in the clockwise order, and use the superscript I (resp N) to denotes fully invertible (resp fully nilpotent) invariants, i.e. invariants counted by considering only representations where all the cycles are invertible (resp nilpotent). For D4 brane framing, we can choose a generic slope s such that for z, z' the sides of the toric diagram adjacent to the corner corresponding to D, $l_z, l_{z'} \in L^{>0}$. For a D6 brane framing, there must be always some cycles v^z with repelling weights, hence for a generic slope s we denotes by $[z, z']$ the set of sides $\tilde{z}$ of the toric diagram such that $\tilde{z} \in L^{<0}$. We

obtains then:

$$Z_D(x) = \sum_{\pi \in \Pi_D} \mathbb{L}^{\mathrm{Ind}^s_\pi/2} x^{d_\pi}$$
$$Z_i^{[z,z']:N}(x) = \sum_{\pi \in \Pi_i} \mathbb{L}^{\mathrm{Ind}^s_\pi/2} x^{d_\pi} \tag{7.1.4}$$

We must then relate the generating series $Z_i^{[z,z']:N}(x)$ of partially nilpotent i-cyclic representations with the full generating series $Z_i(x)$. It is done using an invertible/nilpotent decomposition of BPS invariants, namely from Proposition 7.3.3:

$$\Omega_\theta(x) = \Omega^{z:I}(x) + \Omega_\theta^{z:N}(x) \tag{7.1.5}$$

We use also the fact that, from Lemma 7.3.1, partially invertible representations exists for dimensions vectors in the kernel of the anti-symmetrized Euler form, hence $\Omega^{z:I}(x)$ is in the center of the quantum affine plane and is insensitive to wall crossing. When some cycles are invertible in a representation, we can use the isomorphisms given by the arrows of the cycle to identify the nodes of the cycle, and we obtain a representations of a reduced quiver. Partially invertible BPS invariants of a quiver can then be expressed as BPS invariants of a simpler quiver, and we obtain then universal formulas for them in Section 7.3.3. We provide some notations for dimensions vectors supporting invertible BPS invariants: to a side z of the toric diagram with K_z subdivisions, one associates zig-zag paths, which are special paths on the brane tiling dividing the torus into K_z parallel strips: for $k \neq k' \in \mathbb{Z}/K_z\mathbb{Z}$, we denote by α_k^z the dimension vector with 1 on nodes of Q inside the k-th strip of the torus, $\alpha^z_{[k,k'[} = \alpha^z_k + \alpha^z_{k+1} + ... + \alpha^z_{k'-1}$, and δ the dimension vector with 1 on each node. We use these expressions and invertible/nilpotent decompositions to express $\Omega_\theta(x)$ in terms of $\Omega_\theta^{[z,z']:N}(x)$ in Proposition 7.3.7. Using the formula (7.1.2) and (7.1.1) relating framed invariants and BPS invariants, we obtain then:

Theorem 7.1.1. *(Theorem 7.4.5)*

i) For D a non-compact divisor of X, corresponding to the corner p of the toric diagram lying between the two sides z, z', and a generic slope s such that $l_z, l_{z'} \in L^{>0}$ (such slopes always exist, because the angle between l_z and $l_{z'}$ is smaller than π), we have:

$$Z_D(x) = \sum_{\pi \in \Pi_D} \mathbb{L}^{\mathrm{Ind}^s_\pi/2} x^{d_\pi} \tag{7.1.6}$$

ii) For a generic slope s such that $l_{\tilde{z}} \in L^{<0} \iff \tilde{z} \in [z, z']$, one has:

$$Z_i(x) = S_{-i}[\mathrm{Exp}\left(\textstyle\sum_d \Delta^s \Omega_d \frac{\mathbb{L}^{d_i}-1}{\mathbb{L}^{1/2}-\mathbb{L}^{-1/2}} x^d\right)] \sum_{\pi \in \Pi_i} \mathbb{L}^{\mathrm{Ind}^s_\pi/2} x^{d_\pi} \tag{7.1.7}$$

Using the correction term:

$$\begin{aligned}\Delta^s\Omega(x) =& (\mathbb{L}^{3/2} + (\textstyle\sum_{\tilde{z}\in[z,z']} K_{\tilde{z}} - 2)\mathbb{L}^{1/2} - (\sum_{\tilde{z}\in[z,z']} K_{\tilde{z}} - 1)\mathbb{L}^{-1/2}) \sum_{n\geq 1} x^{n\delta} \\ &+ (\mathbb{L}^{1/2} - \mathbb{L}^{-1/2}) \sum_{\tilde{z}\in[z,z']} \sum_{k\neq k'} \sum_{n\geq 0} x^{n\delta + \alpha^{\tilde{z}}_{[k,k'[}}\end{aligned} \tag{7.1.8}$$

This localization formula can be easily implemented on a computer to calculate the framed cohomological DT invariants explicitly for any brane tiling and reasonably small dimension vectors.

The invertible/nilpotent decomposition allows also to give a general result about BPS invariants of toric quiver. Namely, we relate in Proposition 7.3.7 $\Omega_\theta(x)$, and $\Omega_\theta^N(x)$, the fully nilpotent the BPS invariants. But the Corollary 7.3.1 shows that $\Omega_\theta^N(x)$ is the Poincaré dual of $\Omega_\theta(x)$, hence we prove an universal formula for BPS invariants of toric quivers up to a self Poincaré dual contribution, where we denote by b: the number of points on the boundary of the toric diagram and by i the number of points in the interior of the toric diagram:

Theorem 7.1.2. *(Theorem 7.3.8)*

$$\Omega_\theta(x) = (\mathbb{L}^{3/2} + (b-3+i)\mathbb{L}^{1/2} + i\mathbb{L}^{-1/2}) \sum_{n\geq 1} x^{n\delta} + \mathbb{L}^{1/2} \sum_{z} \sum_{k\neq k'} \sum_{n\geq 0} x^{n\delta + \alpha^z_{[k,k'[}} + \Omega_\theta^{sym}(x) \tag{7.1.9}$$

with $\Omega_\theta^{sym}(x)$ self Poincaré dual, and supported on dimension vectors $d \notin \langle\delta\rangle$. The same formula holds for attractor invariants.

For toric Calabi-Yau threefolds without compact divisors (also known as local curves, corresponding to toric diagrams with no internal points), the quiver Q is symmetric, and consequently the unframed DT invariants do not exhibit wall-crossing. They are known in most cases, see [BBS13, MMNS12, MN15] and [MP20, sec 5] for a review. We check that Theorem 7.3.8 is consistent with these results: in some cases, including the simplest case of the conifold, there exists infinite towers of dimension vectors d with $\Omega_\theta(d) = 1$, associated to rational curves with normal bundle $\mathcal{O}(-1) + \mathcal{O}(-1)$, whose contributions are included in $\Omega^{sym}(x)$. In contrast, the dimension vectors with $\Omega_\theta(d) = \mathbb{L}^{1/2}$ appearing in Theorem 7.3.8 are associated to rational curves with normal bundle $\mathcal{O}(-2) + \mathcal{O}(0)$. In some cases one can find 'preferred slopes' (as shown in [Arb19, sec 4.3]) where many cancellations occur in the index, and obtain a closed formula for the full BPS invariants from the cohomological localization: we check that it agrees with the cohomological computations for $\mathbb{C}^3$, the conifold and $\mathbb{C}^2/(\mathbb{Z}/2\mathbb{Z}) \times \mathbb{C}$ in Section 7.5.1.

For Calabi-Yau threefolds with compact divisors, corresponding to asymmetric quivers, there is no closed formula to our knowledge for numerical invariants, let alone for the cohomological ones. In particular BPS invariants depend on the King stability parameter θ, and the symmetric contribution $\Omega_\theta^{sym}(x)$ is quite intricate for arbitrary θ. In [BMP20], toric quivers associated to toric Fano surfaces (i.e. toric diagrams with one interior point and no interior boundary points) are studied. It is conjectured in [BMP20, p. 21], [MP20, Conj 1.2] that in this case the only attractor invariants are those supported on dimension vectors e_i for $i \in Q_0$, corresponding to simple representations, and those supported on the dimensions vectors $\mathbb{N}^*\delta$, corresponding to D0 branes, i.e. Hilbert schemes of points. In [MP20] weak toric Fano surfaces (i.e. toric diagrams with one interior point and interior boundary points) are considered: it is observed that there can be additional dimension vectors with non-vanishing attractor invariants, but it is conjectured ([MP20, Conj 1.1]) that they lie in the kernel of the anti-symmetrized Euler form. We shall formulate a refinement of these conjectures:

Conjecture 7.1.3. *(Conjecture 7.3.9) For toric diagram with $i \geq 1$ internal lattice points, the attractor invariants are given by:*

$$\Omega_*(x) = \sum_i x_i + (\mathbb{L}^{3/2} + (b-3+i)\mathbb{L}^{1/2} + i\mathbb{L}^{-1/2}) \sum_{n\geq 1} x^{n\delta} + \mathbb{L}^{1/2} \sum_z \sum_{k\neq k'} \sum_{n\geq 0} x^{n\delta + \alpha^z_{[k,k'[}} \quad (7.1.10)$$

The attractor invariants associated to simple representations and Hilbert scheme of points are known. When there are $K_z - 1$ lattice points on a side z of the toric diagram, the toric threefold X exhibits a $\mathbb{C}^2/\mathbb{Z}_{K_z} \times \mathbb{C}^*$ singularity away from the zero locus of the toric coordinate corresponding to z, as recalled in the proof of Proposition 7.3.6. The conjecture then predicts that the only additional attractor invariants correspond to D2-branes wrapped on rational curves in this extended singularity.

The rest of this article is organized as follows:

- In section 2 we review known results on Donaldson-Thomas theory on toric threefolds, and introduce the basic definitions and notations. In section 2.1, we introduce the moduli spaces of representations associated to unframed and framed quiver, their cohomological DT invariants and generating series thereof. In section 2.2 we recall how the quiver with potential for toric Calabi-Yau threefolds can be deduced from brane tiling, and emphasize the utility of zig-zag paths. In section 2.3 we introduce the D6- and D4-framing.

- In section 3, using invertible/nilpotent decompositions of unframed representations, we relate generating series of BPS invariants with various nilpotency constraints. In section 3.1 we introduce the notion of partially invertible/nilpotent representations, and define their generating series and BPS invariants. In section 3.2 we show that the invertible/nilpotent decomposition on unframed representations implies a decomposition of BPS invariants. In section 3.3, we compute BPS invariants for partially invertible representations. In section 3.4 we orchestrate previous results, express the BPS invariants in terms of the partially nilpotent BPS invariants accessible by toric localization, and prove the Theorem 7.3.8.

- In section 4, we study toric localization for framed quivers. In section 4.1 we describe the fixed locus and the attracting locus of the toric action scaling the arrows of D4- and D6-framed representations. In section 4.2, we describe the $\mathbb{C}^*$-equivariant tangent-obstruction complex at a $\mathbb{C}^*$-fixed component of the moduli space. In section 4.3, we prove the 'derived Bialynicki-Birula decomposition' 7.4.5 for D4- and D6-framed invariants. In section 4.4, we relate our localization result to the localization of K-theoretic DT invariants.

- In section 5 we illustrate our formula and formulate our Conjecture for the complete set of attractor invariants. In section 5.1 we compare our results with the known formulas for local curves, and explains on specific examples the discrepancy between K-theoretic and cohomological computations. In section 5.2 we compare our Theorem 7.3.8 and Conjecture 7.3.9 with the computations in [BMP20, MP20] for toric threefolds with one compact divisor. In order to facilitate comparison with future computations, we spell out our Conjecture for the canonical bundle over toric weak Fano surfaces, using the brane tilings listed in [HS12].

7.2 Basic notions on Donaldson-Thomas theory and toric quivers

7.2.1 Invariants of quivers with potential

Representations and cohomological DT invariants

Consider a quiver with potential (Q,W), with Q_0 (resp. Q_1) the set of nodes (resp. arrows) of Q, the source and target of an arrow a being denoted respectively $s(a)$ and $t(a)$, and W a linear combination of cycles of Q (we follow the notations of [MR08] whenever possible). The path algebra of the quiver Q, denoted by $\mathbb{C}Q$, is the free algebra generated by arrows of the quiver, such that $ba=0$ if $s(b)\neq t(a)$. A cycle is a path $w=a_1...a_n$ with $s(a_n)=t(a_1)$. The cyclic derivative is defined by

$$\partial_a w = \sum_{i:a_i=a} a_{i+1}...a_n a_1...a_{i-1} \tag{7.2.1}$$

and extended to $\mathbb{C}Q$ by linearity. The cyclic derivatives of the potential define the ideal $(\partial W)=((\partial_a W)_{a\in Q_1})$. The Jacobian algebra is the quotient $J_{Q,W}=\mathbb{C}Q/(\partial W)$. We shall usually identify a path with its image in $J_{Q,W}$, i.e. paths which differ by derivatives of the potential will be identified.

Consider a framed quiver with potential (Q_f,W_f) obtained from (Q,W) by adding a single framing node ∞, (possibly multiple) framing arrows between the framing node and nodes of Q, and (when allowed) additional cycles in the potential, corresponding to path starting and ending at the framing node. One consider the projective $\mathbb{C}Q_f$ module $\mathfrak{P}_f$ generated by paths of Q_f starting at the framing node. One can also consider the Jacobian algebra $J_{Q_f,W_f}:=\mathbb{C}Q_f/(\partial W_f)$ and the left J_{Q_f,W_f} module $P_f:=\mathfrak{P}_f/((\partial W_f)\cap\mathfrak{P}_f)$.

For any dimension vector $d\in\mathbb{N}^{Q_0}$, we denote by $\mathfrak{M}_{Q,d}$ the moduli stack of d-dimensional representations of the unframed quiver Q (without imposing the potential relations), i.e. the moduli stack of left $\mathbb{C}Q$ modules, which can be expressed more explicitly by:

$$\mathfrak{M}_{Q,d}=\frac{\prod_{(a:i\to j)\in Q_1}\mathrm{Hom}(\mathbb{C}^{d_i},\mathbb{C}^{d_j})}{\prod_{i\in Q_0}GL_{d_i}} \tag{7.2.2}$$

Here the gauge group $G_d=\prod_{i\in Q_0}GL_{d_i}$ acts on $a\in Hom(\mathbb{C}^{d_i},\mathbb{C}^{d_j})$ by $a\mapsto g_j a g_i^{-1}$. For a stability parameter θ, we denote by $\mathcal{M}_{Q,d}^{\theta,ss}$ (resp $\mathcal{M}_{Q,d}^{\theta,s}$) the moduli space of θ-semistable representations (resp the smooth open subset of θ-stable representations), obtained by geometric invariant theory as in [Kin94b].

Similarly, for any dimension vector $d\in\mathbb{N}^{Q_0}$ we denote by $\mathcal{M}_{Q_f,d}$ the moduli space of f-cyclic representations of the framed quiver Q_f with dimension vector $d'=(d,1)\in\mathbb{N}_0^{Q_f}$, i.e. representations with dimension 1 on the framing node, such that the subrepresentation generated by the framing node is the whole representation:

$$\mathcal{M}_{Q_f,d}=\frac{(\prod_{(a:i\to j)\in(Q_f)_1}\mathrm{Hom}(\mathbb{C}^{d'_i},\mathbb{C}^{d'_j}))^{\mathrm{cycl}}}{\prod_{i\in Q_0}GL_{d_i}} \tag{7.2.3}$$

Here the subscript 'cycl' denotes the open subset of f-cyclic representations. f-cyclic representations are θ-stable representations of Q_f, for a stability parameter $\theta \in \mathbb{R}^{(Q_f)_0}$ such that $\theta.d = 0$, $\theta_\infty > 0$ and $\theta_i < 0$ for $i \in Q_0$, hence from geometric invariant theory $\mathcal{M}_{Q_f,d}$ is a smooth scheme. Equivalently, $\mathcal{M}_{Q_f,d}$ is the scheme which corresponds to d-dimensional quotients of the module of paths $\mathfrak{P}_f$, i.e. quotient by a $\mathbb{C}Q_f$ submodule ρ of codimension d.

We consider the functional $\mathrm{Tr}(W)$ on $\mathfrak{M}_{Q,d}$ and $\mathcal{M}^{\theta,ss}_{Q,d}$ (resp. $Tr(W_f)$ on $\mathcal{M}_{Q_f,d}$), and their critical locus $\mathfrak{M}_{Q,W,d}$ and $\mathcal{M}^{\theta,ss}_{Q,W,d}$ (resp. $\mathcal{M}_{Q_f,W_f,d}$). Representations in the critical locus are called critical representations, and correspond to left $J_{Q,W}$ modules (resp. quotients of P_f). One denotes by ϕ_W (resp. ϕ_{W_f}) the vanishing cycle functor of $Tr(W)$ (resp. $\mathrm{Tr}(W_f)$), having support on critical representations: it is a functor with source the category of mixed Hodge modules on $\mathfrak{M}_{Q,d}$ (resp. $\mathcal{M}^{\theta,ss}_{Q,d}$, resp. on $\mathcal{M}_{Q_f,d}$), and target the category of monodromic mixed Hodge modules on $\mathfrak{M}_{Q,d}$ and $\mathcal{M}^{\theta,ss}_{Q,d}$ (resp. on $\mathcal{M}_{Q_f,d}$) with support on $\mathfrak{M}_{Q,W,d}$ and $\mathcal{M}^{\theta,ss}_{Q,W,d}$ (resp. $\mathcal{M}_{Q_f,W_f,d}$).

Consider a constructible substack $\mathfrak{M}^S_{Q,d}$ of $\mathfrak{M}_{Q,d}$ (resp. a constructible subscheme $\mathcal{M}^{\theta,ss,S}_{Q,d}$ of $\mathcal{M}^{\theta,ss}_{Q,d}$, resp. $\mathcal{M}^S_{Q_f,d}$ of $\mathcal{M}_{Q_f,d}$). In this work we shall consider substacks or subschemes that are attracting varieties of a toric action, or giving representations with nilpotency and invertibility constraints on particular cycles. Following the general formalism of cohomological Donaldson-Thomas invariants developed in [KS10],[Dav17] and [DM16], one defines the cohomological DT invariants of critical representations in the Grothendieck group of monodromic mixed Hodge structures:

$$\begin{aligned}[\mathfrak{M}^S_{Q,W,d}]^{vir} =& H^\bullet_c(\mathfrak{M}^S_{Q,d}, \phi_W \mathcal{IC}_{\mathfrak{M}_{Q,d}})\\ [\mathcal{M}^S_{Q_f,W_f,d}]^{vir} =& H^\bullet_c(\mathcal{M}^S_{Q_f,d}, \phi_{W_f} \mathcal{IC}_{\mathcal{M}_{Q_f,d}})\end{aligned} \tag{7.2.4}$$

denoting by $H^\bullet_c(M,F)$ the Grothendieck class of the cohomology with compact support of the complex of the monodromic mixed Hodge module F on M and by $\mathcal{IC}_M$ the intersection complex of M, or more precisely the corresponding mixed Hodge module. We omit the superscript S when we consider the entire stack or scheme of representations.

In [DM16], Davison and Meinhardt introduce the BPS sheaf on $\mathcal{M}^{\theta,ss}_{Q,d}$:

$$\mathcal{BPS}^\theta_{W,d} := \begin{cases} \phi_W \mathcal{IC}_{\mathcal{M}^{\theta,ss}_{Q,d}} & \text{if } \mathcal{M}^{\theta,st}_{Q,d} \neq \emptyset \\ 0 & \text{otherwise} \end{cases} \tag{7.2.5}$$

The BPS invariants are then defined by:

$$\Omega^S_{\theta,d} = H^\bullet_c(\mathcal{M}^{\theta,ss,S}_{Q,d}, \mathcal{BPS}^\theta_{W,d}) \tag{7.2.6}$$

For a dimension vector d, considering a small deformation θ_d of the self stability condition $\langle -, d\rangle$, generic such that $\theta_d(d) = 0$, we define the attractor invariants:

$$\Omega^S_{*,d} = \Omega^S_{\theta_d,d} \tag{7.2.7}$$

Then [MP20, Theo 3.7], based on the theory of cluster scattering diagrams developed in [GHKK18], states that attractors invariants $\Omega_{*,d}$ are well defined, i.e. they do not depend on the small generic deformation θ_d. Since the formalism of cluster scattering diagram also applied when restricting to a Serre subcategory of the category of representations of a quiver, the same arguments ensure that $\Omega^S_{*,d}$ are also well defined.

Remark 7.2.1. We will interpret previous computations in the motivic setting as formulas in this Grothendieck ring of MMHS, using the realization map from monodromic motives to MMHS (the compatibility between the motivic and cohomological definitions was checked in [Dav19, Appendix A]). We replace the multiplication by the square root $\mathbb{L}^{1/2}$ of the Tate motive by the cohomological shift $[-1]$ at the level of perverse sheaves, or by the tensor product with the MMHS given by the vanishing cycles of $z \to z^2 : \mathbb{C} \to \mathbb{C}$ as in [DM16, p. 19], which is a square root of the MMHS of the affine line. In particular, when we compute the Hodge polynomial associated to the monodromic mixed Hodge structure, we replace $\mathbb{L}^{1/2}$ by $(-y)$, and by -1 in the numerical limit, in agreement with [BBS13].

Remark 7.2.2. In [Dav17] and [DM16], Davison and Meinhardt use Borel-Moore homology, i.e. the dual of the cohomology with compact support, hence their invariants are the Poincaré dual of our invariants. Here we follow the convention of [MP20], which is also the convention used in the literature about motivic invariants of quivers with potential.

Quantum affine space and generating series

For $d, d' \in \mathbb{Z}^{Q_0}$, the Euler form χ_Q and its anti-symmetrized version $\langle , \rangle$ are defined by:

$$\begin{aligned} \chi_Q(d,d') &= \sum_{i \in Q_0} d_i d'_i - \sum_{(a:i\to j)\in Q_1} d_i d'_j \\ \langle d, d' \rangle &= \chi_Q(d,d') - \chi_Q(d',d) \end{aligned} \tag{7.2.8}$$

The quantum affine space $\hat{\mathbb{A}}$ is the algebra generated by elements x^d, for $d \in \mathbb{N}^{Q_0}$, with coefficients in the Grothendieck group (having a ring structure) of monodromic mixed Hodge structures, and relations:

$$x^d x^{d'} = \mathbb{L}^{\langle d,d' \rangle/2} x^{d+d'} \tag{7.2.9}$$

We introduce the algebra automorphism $S_{\pm i}$ of the quantum affine space $\hat{\mathbb{A}}$ (denoting P a class of the Grothendieck group of monodromic mixed Hodge structure):

$$S_{\pm i} : P x^d \mapsto \mathbb{L}^{\pm d_i/2} P x^d \tag{7.2.10}$$

Consider S, a Serre subcategory of the Abelian category of representations of Q, i.e. a full subcategory such that for each exact sequence:

$$0 \to V_1 \to V \to V_2 \to 0 \tag{7.2.11}$$

$V \in S$ if and only if $V_1 \in S$ and $V_2 \in S$. We denote by $\mathfrak{M}^S_{Q,d}$, $\mathcal{M}^{\theta,ss,S}_{Q,d}$ and $\mathcal{M}^S_{Q_f,d}$ the substack and subschemes of representations lying in S (resp such that the induced representation of Q lies in S). The generating series of unframed or framed invariants restricted to the Serre subcategory

S, with values in the quantum affine space $\hat{\mathbb{A}}$, are defined by:

$$\begin{aligned}\mathcal{A}^S(x) &= \sum_d [\mathfrak{M}^S_{Q,W,d}]^{vir} x^d \\ Z^S_f(x) &= \sum_d [\mathcal{M}^S_{Q_f,W_f,d}]^{vir} x^d \\ \Omega^S_\theta(x) &= \sum_d \Omega^S_{\theta,d} x^d \\ \Omega^S_*(x) &= \sum_d \Omega^S_{*,d} x^d \end{aligned} \tag{7.2.12}$$

As recalled in the introduction, the Harder-Narasimhan decomposition express a general quiver representation as an extension of semistable representations with increasing slope $\mu = \theta.d/\sum_{i\in Q_0} d_i$, and the Jordan-Hölder filtration, express a semistable representation as an extension of stable objects with the same slope. Consider a stability condition θ which is generic, i.e. such that if d, d' have the same slope then $\langle d - d', \bullet\rangle = 0$. The Harder-Narasimhan and Jordan-Hölder decompositions can then be expressed by the formula [DM16, eq 7]:

$$\mathcal{A}^S(x) = \prod_l^{\curvearrowright} \mathrm{Exp}\left(\sum_{d\in l} \frac{\Omega^S_{\theta,d}}{\mathbb{L}^{1/2} - \mathbb{L}^{-1/2}} x^d\right) \tag{7.2.13}$$

Here Exp denotes the plethystic exponential defined in [DM16, eq 6], and the product ranges over rays l with increasing slope.

7.2.2 Unframed quivers associated to toric threefolds

From toric diagrams to quivers with potential

Let us consider a toric Calabi Yau threefold X. The fast inverse algorithm described in [HV07, sec 5] gives a brane tiling on the two- dimensional torus from the toric diagram of X, i.e. a bipartite graph with white and black vertex and edges between a white and a black vertex. In fact, it can give different brane tilings that are related by toric mutations.

We consider the toric diagram of X, which is a convex polygon in a two dimensional free lattice $L^\vee$. We denote by n the number of corners of the toric diagram, and the corners themselves by p_i for $i \in \mathbb{Z}/n\mathbb{Z}$ in the clockwise order. The side of the toric diagram between two adjacent corners p_i and p_{i+1} will be denoted by $z_{i+1/2}$. We denote by K_z the number of subdivisions of the edge z, i.e. the number of the lattice points on that edge (counting the endpoints) minus one. We denote by $l_z \in L$ the primitive vector generating the dual of the side z in L. As an example, for $\mathbb{C}^3$, the toric diagram and vectors l_z are given by Figure 7.1.

Let us now describe the fast inverse algorithm. On the real two dimensional torus obtained by dividing $\mathbb{R}^2$ by the lattice L, we draw for each edge z of the toric diagram K_z generic oriented lines directed along l_z, in generic position such that two lines intersect only in one point and three lines do not intersect. The different choices in the relative arrangement of lines will correspond to different quivers with potential related by toric mutations. The complement of these lines determines polygonal domains, or tiles, with oriented edges. We color those tiles in white, dark grey or light grey, according to the orientations of their edges:

Figure 7.1: Toric diagram of $\mathbb{C}^3$

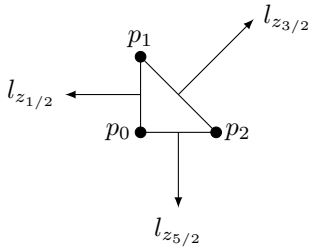

- If the edges of the tile are oriented in the clockwise order around the tile, we color the tile in dark grey
- if the edges of the tile are oriented in the counter-clockwise order around the tile, we color the tile in light grey
- if the orientations of the different edges of the tile do not agree, we color the tile in white

We define a brane tiling on the torus by putting a black node in each dark grey tile, a white node in each light grey tile, and connecting a black node and a white node if the corresponding tiles are connected at one of their corners. The white tiles are then in correspondence with tiles of the brane tiling.

Definition 7.2.3. The quiver with potential (Q, W) associated of a brane tiling is defined as the dual of this brane tiling, i.e. :

- The set of nodes Q_0 of the quiver is the set of tiles of the brane tiling.
- The set of arrows Q_1 of the quiver is the set of edges of the brane tiling. An edge of the tiling between two tiles gives an arrow of the quiver between the two corresponding nodes, oriented such that the black node is at the left of the arrow.
- Denote by Q_2 the set of nodes of the brane tiling, and Q_2^+ (resp. Q_2^-) the subset of white (resp. black) nodes. To a node $F \in Q_2$ one associate the cycle w_F of Q composed by arrows surrounding this node. We define:

$$W = \sum_{F \in Q_2^+} w_F - \sum_{F \in Q_2^-} w_F \tag{7.2.14}$$

By definition, the quiver with potential (Q, W) is drawn on a torus: the unfolding of this quiver to the universal cover $\mathbb{R}^2$ of the torus is called the periodic quiver. In the case of $\mathbb{C}^3$, this procedure is described in Figure 7.2.

Definition 7.2.4. A zig-zag path of a brane tiling is a sequence of edges turning alternatively maximally right and maximally left at each node of the toric diagram.

Figure 7.2: The fast inverse algorithm for $\mathbb{C}^3$

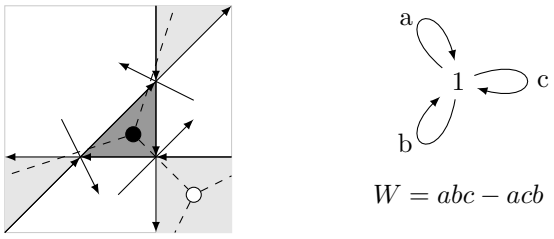

Figure 7.3: Zig-zag paths and the fast inverse algorithm

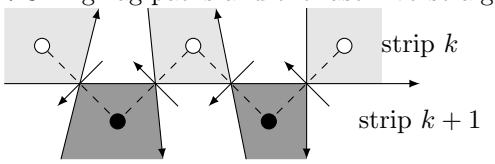

The set of edges intersecting one of the K_z lines with direction l_z forms a zig-zag path, following the general picture of Figure 7.3. These zig-zag paths divide then the torus into K_z parallel strips.

As in the literature about toric quivers, we will consider general brane tiling on the torus with a consistency conditions. The consistency condition can then be expressed as the existence of an R-charge as in [Moz09, Def 2.4], or equivalently by the following conditions [IU09, Def 5.1] on zig-zag paths:

- There is no homologically trivial zigzag path.
- No zigzag path has a self-intersection on the universal cover.
- No pair of zigzag paths on the universal cover intersect each other in the same direction more than once.

Not every consistent brane tiling come from the fast inverse algorithm, but one can associate to a such a brane tiling a toric diagram by considering its perfect matching as described in the next subsection. The Jacobian algebra of the quiver with potential associated to this brane tiling gives then a noncommutative crepant resolution of the corresponding toric Calabi-Yau threefold, and all the brane tiling associated to a toric diagram are related by toric mutations. There are then still K_z parallel zig-zag paths with homology l_z associated to a side z of the toric diagram, dividing the torus into K_z strips, which we can label by $k \in \mathbb{Z}/K_z\mathbb{Z}$.

The cyclic ordering is given by the orientation in the Figure 7.3, i.e. the k-th strip lies to the left of the zig-zag path and the $k+1$-th strip lies to the right. We call Zig_k (resp. Zag_k) the set of arrows crossing the zig-zag path, going from the k-th strip to the $k+1$-th strip (resp. from $k+1$-th strip to the k-th strip). We denote by α_k^z the dimension vector with component 1 on the nodes inside the k-th strip, and 0 on the other nodes. We further define

$$\alpha^z_{[k,k'[} = \alpha^z_k + \alpha^z_{k+1} + ... + \alpha^z_{k'-1} \tag{7.2.15}$$

We keep in mind that the index k lives in $\mathbb{Z}/K_z\mathbb{Z}$. The dimension vector $\alpha^z_{[k,k'[}$ is supported between the k-th and the k'-th zig-zag path. In particular, $\alpha^z_{[k,k[} = \delta$ is the dimension vector with entries 1 on each node of Q_0, associated to points on X.

Perfect matchings and lattices of paths

Following [Moz09, sec 2.2], consider the complex of Abelian groups:

$$\mathbb{Z}^{Q_2} \xrightarrow{d_2} \mathbb{Z}^{Q_1} \xrightarrow{d_1} \mathbb{Z}^{Q_0} \tag{7.2.16}$$

such that $d_2(F) = \sum_{a\in F} a$ and $d_1(a) = t(a) - s(a)$. We define:

$$\Lambda = \mathbb{Z}^{Q_1}/\langle d_2(F) - d_2(G) | F, G \in Q_2\rangle \tag{7.2.17}$$

and denotes by $\kappa \in \Lambda$ the image of $d_2(F)$ in the quotient Λ for any $F \in Q_2$. The lattice Λ (resp. its quotient $\Lambda/\mathbb{Z}\kappa = \mathbb{Z}^{Q_1}/d_2(\mathbb{Z}^{Q_2})$) is then the character lattice of the maximal torus scaling the arrows of Q by leaving the potential W equivariant (resp. invariant), and κ is the Λ weight of the potential. According to [MR08, Prop 4.8], two paths with the same source agree in $J_{Q,W}$ if and only if they have the same Λ-weight.

The map d_1 descends to a map $d_1 : \Lambda \to \mathbb{Z}^{Q_0}$, and we define $M = ker(d)$: M (resp. $M/\mathbb{Z}\kappa$) is the sublattice of Λ (resp. $\Lambda/\mathbb{Z}\kappa$) giving the weights of cycles of Q, i.e. M (resp. $M/\mathbb{Z}\kappa$) gives the weight lattice of the quotient of the maximal torus scaling the arrows of the quiver leaving the potential equivariant (resp. invariant) by the gauge torus T_G scaling the nodes of the quiver.

Definition 7.2.5. A perfect matching is a subset I of the edges of the brane tiling such that each node of the brane tiling is adjacent to exactly one edge of I. By duality, a perfect matching is equivalent to a cut I of the quiver with potential (Q, W), i.e. a subset of Q_1 such that each cycle w_F of the potential W contains exactly one arrow of I.

We define the linear map $\chi_I : \mathbb{Z}^{Q_1} \to \mathbb{Z}$ sending $a \in Q_1$ to 1 if $a \in I$ and 0 either. Since $\chi_I(d_2(F)) = 1$ for $F \in Q_2$ by definition of a perfect matching, χ_I descends to a map $\chi_I : \Lambda \to \mathbb{Z}$ such that $\chi_I(\kappa) = 1$, and restricts to $\bar{\chi_I} \in M^\vee$. Let $\sigma \in M^\vee_{\mathbb{Q}}$ be the cone generated by the $\bar{\chi_I}$. According to [Moz09, Remark 4.16], σ gives then the fan of X, and the intersection of σ with the hyperplane $\{f \in M^\vee_{\mathbb{Q}} | f(\kappa) = 1\}$ gives the toric diagram of X: in particular, the lattice $L^\vee$ of the toric diagram is identified with $(M/\mathbb{Z}\kappa)^\vee$. The lattice L of the brane tiling torus can then be identified as $L = M/\mathbb{Z}\kappa$.

As was first noticed in [HV07, sec 4.2], $\bar{\chi_I}$ gives a node of the toric diagram: the map sending a perfect matching to the corresponding node of the toric diagram is surjective but not injective in general. However, there is a unique perfect matching associated to any corner of the toric diagram. We shall consider only such perfect matchings, and denote by I_i the cut associated to the corner p_i.

When the two perfect matchings correspond to two adjacent corners p_i and p_{i+1} that are endpoints of the same side $z = z_{i+1/2}$, their union gives the zig-zag paths with direction $l_z \in L$. Removing the arrows of the two cuts I_i, I_{i+1}, one obtains a quiver which is a union of connected parts supported on the K_z strip separated by the zig-zag paths: we denote by Q^k the quiver supported on the k-th strip. We can then distinguish four types of arrows:

- Arrows that are not in any cuts I_i, I_{i+1} are the arrows of one connected part Q^k of the remaining quiver for a $k \in \mathbb{Z}/K_z\mathbb{Z}$.
- Arrows that are in the intersection of the two cuts lie outside the zig-zag paths, i.e. they connect nodes inside the same connected component Q^k, for a $k \in \mathbb{Z}/K_z\mathbb{Z}$; we denote the set of those arrows by J_k.
- Arrows in $I_i - I_{i+1}$ lie inside zig zag paths. With our conventions, they go from Q^k to Q^{k+1}, for a $k \in \mathbb{Z}/K_z\mathbb{Z}$, i.e. they forms to the above defined set Zig_k
- Arrows in $I_{i+1} - I_i$ are in zig zag paths. With our conventions, they go from Q^{k+1} to Q^k for a $k \in \mathbb{Z}/K_z\mathbb{Z}$; i.e. they forms the above defined set Zag_k.

Let us denote by $M^+ \subset M$ the semigroup generated by weights of cycles of Q. According to [Moz09, Cor 3.3, Cor 3.6], $M^+_{\mathbb{Q}}$ is a cone which is the dual cone of σ, and M^+ is saturated, i.e. :

$$M^+ = \{\lambda \in M | \chi_I(\lambda) \geq 0 \quad \forall\, I\} \tag{7.2.18}$$

We denote by $\mathbb{C}[M^+]$ the ring generated by elements v^λ for $\lambda \in M^+$, with relations $v^{\lambda+\lambda'} = v^\lambda v^{\lambda'}$. Because σ is the fan of X, on has then $X = Spec(\mathbb{C}[M^+])$. By associating to $v^\lambda \in \mathbb{C}[M^+]$ the sum over $i \in Q_0$ of the cycles v_i^λ of weight λ with source and target i (recall that two paths of Q agree in $J_{Q,W}$ if they have the same source and Λ-weight), one obtains an inclusion $\mathbb{C}[M^+] \to J$. It was then proven in [Bro11, Theo 1.4] that $\mathbb{C}[M^+]$ is the center of $J_{Q,W}$. According to [Moz09, Porp 3.13], $J_{Q,W}$ provides then a noncommutative crepant resolution of the coordinate ring of X.

The edges of the cone $M^+_{\mathbb{Q}} = \sigma^\vee$ are dual to sides of the toric diagram. Consider a side $z_{i+1/2}$ between the corners p_i and p_{i+1}: the corresponding edge of $M^+_{\mathbb{Q}}$ lies in the intersection $\chi_{I_i}^{-1}(0) \cap \chi_{I_{i+1}}^{-1}(0)$, i.e. is generated by cycles of Q without arrows of $I_\cup I_{i+1}$. This shows that all the indecomposable cycles of the quivers Q^k have the same M-weight (and equivalently the same Λ weight) denoted by λ_z. In particular, by construction, the projection of λ_z onto $L = M/\mathbb{Z}\kappa$ is l_z. We use then the notation $v^z := v^{\lambda_z} \in J$. We have then the commutation relation, for any path $(w : i \to j) \in J$

$$w v_i^z = v_j^z w \tag{7.2.19}$$

Examples

We illustrate our notations on several examples:

Example 7.2.6 (PdP_{3a})**.** The toric diagram and brane tiling are given by Figure 7.4, where we have drawn the perfect matchings corresponding to the corners p_0, p_1, p_2 in blue, red and green, respectively. An arrow of the cut I_i with source j and target k will be denoted by Φ^i_{jk}.

The zig-zag paths defined by taking the union of two consecutive perfect matchings on the boundary of the toric diagram are as follows:

- $I_0 \cup I_1$: the corresponding zig-zag path corresponding to the side $z_{1/2}$ is given by the succession of blue and red edges. The remaining quiver has one connected component Q^0, i.e. $K_z = 1$ (corresponding to the fact that the associated edge of the toric diagram has one subdivision). It is a simple cyclic quiver with six nodes in the order $(0, 1, 2, 3, 4, 5)$. We have then $Q_1^0 = I_2$, $J_0 = \emptyset$, $\mathrm{Zig}_0 = I_0$ and $\mathrm{Zag}_0 = I_1$ and $\alpha_0^{z_{1/2}} = \delta$.

Figure 7.4: Toric diagram and brane tiling for PdP_{3a}

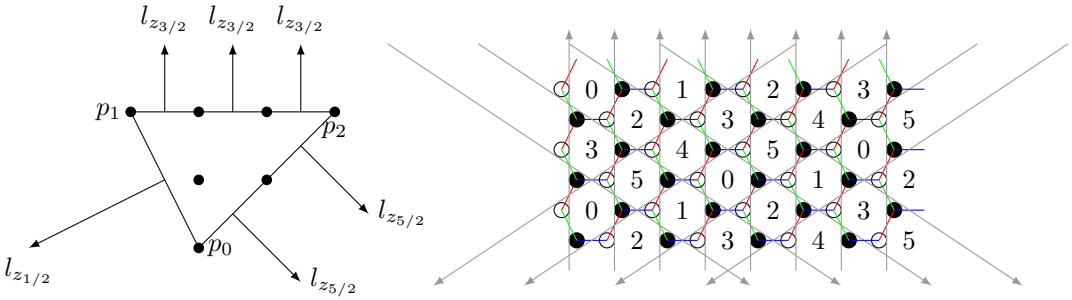

- $I_1 \cup I_2$: the corresponding zig-zag paths corresponding to the side $z_{3/2}$ are given by the succession of red and green edges. The remaining quiver has three connected components Q^0, Q^1 and Q^2, i.e. $K_z = 3$ (corresponding to the fact that the associated edge of the toric diagram has three subdivisions). Q^0, Q^1 and Q^2 are simple two cycles with nodes respectively $(0,3)$, $(1,4)$ and $(2,5)$. We have:

$$\begin{array}{lll} Q_0^0 = \{0,3\} & Q_0^1 = \{1,4\} & Q_0^2 = \{2,5\} \\ Q_1^0 = \{\Phi_{03}^0, \Phi_{30}^0\} & Q_1^1 = \{\Phi_{14}^0, \Phi_{41}^0\} & Q_1^2 = \{\Phi_{25}^0, \Phi_{52}^0\} \\ J_0 = \emptyset & J_1 = \emptyset & J_2 = \emptyset \\ \mathrm{Zig}_0 = \{\Phi_{13}^1, \Phi_{40}^1\} & \mathrm{Zig}_1 = \{\Phi_{24}^1, \Phi_{51}^1\} & \mathrm{Zig}_2 = \{\Phi_{02}^1, \Phi_{35}^1\} \\ \mathrm{Zag}_0 = \{\Phi_{01}^2, \Phi_{34}^2\} & \mathrm{Zag}_1 = \{\Phi_{12}^2, \Phi_{45}^2\} & \mathrm{Zag}_2 = \{\Phi_{23}^2, \Phi_{50}^2\} \\ \alpha_0^{z_{3/2}} = e_0 + e_3 & \alpha_1^{z_{3/2}} = e_1 + e_4 & \alpha_2^{z_{3/2}} = e_2 + e_5 \end{array} \tag{7.2.20}$$

- $I_2 \cup I_0$: the corresponding zig-zag paths corresponding to the side $z_{5/2}$ are given by the succession of green and blue edges. The remaining quiver has two connected components Q^0 and Q^1, i.e. $K_z = 2$ (corresponding to the fact that the associated edge of the toric diagram has two subdivisions). Q^0 and Q^1 are respectively simple three cycles with nodes respectively $0, 2, 4$ and $1, 3, 5$. We have:

$$\begin{array}{ll} Q_0^0 = \{0,2,4\}, & Q_0^1 = \{1,3,5\} \\ Q_1^0 = \{\Phi_{02}^1, \Phi_{24}^1, \Phi_{40}^1\} & Q_1^1 = \{\Phi_{13}^1, \Phi_{35}^1, \Phi_{51}^1\} \\ J_0 = \emptyset & J_1 = \emptyset \\ \mathrm{Zig}_0 = \{\Phi_{12}^2, \Phi_{34}^2, \Phi_{50}^2\} & \mathrm{Zig}_1 = \{\Phi_{01}^2, \Phi_{23}^2, \Phi_{45}^2\} \\ \mathrm{Zag}_0 = \{\Phi_{03}^0, \Phi_{25}^0, \Phi_{41}^0\}, & \mathrm{Zag}_1 = \{\Phi_{14}^0, \Phi_{30}^0, \Phi_{52}^0\} \\ \alpha_0^{z_{5/2}} = e_0 + e_2 + e_4 & \alpha_1^{z_{5/2}} = e_1 + e_3 + e_5 \end{array} \tag{7.2.21}$$

Example 7.2.7 (Suspended pinched point)**.** For The suspended pinched point, one resolution of the toric diagram, and the corresponding brane tiling, are given by Figure 7.5. Here we have drawn the edges of the perfect matching p_1 in red, and the edges of the perfect matching p_2 in blue. The

Figure 7.5: Toric diagram and brane tiling for the suspended pinched point

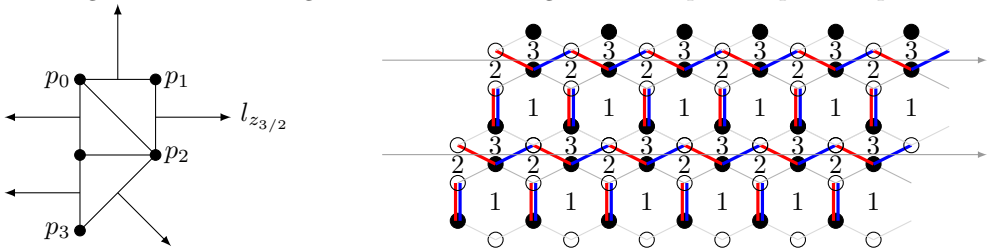

union of these perfect matchings describes zig-zag paths corresponding to the side $z_{3/2}$ of the toric diagram. It divides the brane tiling into strips oriented from the left to the right. In particular, the quiver obtained after the two cuts has one connected component Q^0 (corresponding to the fact that the corresponding edge of the toric diagram has one subdivision). We have then:

$$\begin{aligned} &Q_0^0=\{1,2,3\},\quad Q_1^0=\{\Phi_{12},\Phi_{13},\Phi_{21},\Phi_{31}\}\\ &J_0=\{\Phi_{11}\},\quad \mathrm{Zig}_0=\{\Phi_{32}\},\quad \mathrm{Zag}_0=\{\Phi_{23}\},\quad \alpha_0^{z_{3/2}}=\delta\\ &v_1^z=\Phi_{21}\Phi_{12}=\Phi_{31}\Phi_{13},\quad v_2^z=\Phi_{12}\Phi_{21},\quad v_3^z=\Phi_{13}\Phi_{31} \end{aligned} \tag{7.2.22}$$

7.2.3 Framed quivers associated to toric threefolds

D6-brane framing

We introduce a first type of framed quiver built from an unframed quiver (Q,W) coming from a brane tiling. Choosing $i\in Q_0$ a node of the quiver, we consider the framed quiver Q_i with a framing node ∞, and an arrow $q:\infty\to i$, i.e. $((Q_i)_0,(Q_i)_1)=(Q_0\cup\{\infty\},Q_1\cup\{q\})$. The potential is still W, because there is no cycle passing by the framing node. We will consider i-cyclic representations, i.e. representations V of the framed quiver Q_i such that $d_\infty=1$, and the subrepresentation generated by V_∞ is the whole representation. We denote by $Z_i(x)$ the generating series of the cohomological DT invariants $[\mathcal{M}_{Q_i,W,d}]^{vir}$ of i-cyclic critical representations, following the definitions in (7.2.4) and (7.2.12).

Remark 7.2.8. Such a framing corresponds to adding a D6-brane in physics terminology. Framed i-cyclic representations are a noncommutative analogue of sheaves with compact support on X with a framing by the sheaf $\mathcal{O}_X$: such a complex is then considered as a bound state of a D6 noncompact brane (i.e. a sheaf with support on the whole noncompact threefold X) with a D4-D2-D0 compact brane (i.e. a sheaf with compact support on 2 dimensional, 1 dimensional and 0 dimensional subvarieties).

Consider a Serre subcategory S of the Abelian category of representations of Q. There is a general formula, which is a variant of the wall crossing formula of [KS10], expressing the framed generating series $Z_i^S(x)$ in terms of the generating series $\mathcal{A}^S(x)$ of representations of the unframed quiver (Q,W), developed in [Mor12],[Moz13] and [MMNS12];

$$Z_i^S(x)=S_i(\mathcal{A}^S(x))S_{-i}(\mathcal{A}^S(x)^{-1}) \tag{7.2.23}$$

Figure 7.6: D4 brane framing and the fast inverse algorithm

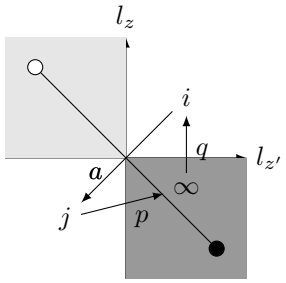

D4-brane framing

We consider a cut I corresponding to a corner p_i of the toric diagram, denoting D the corresponding divisor. The divisor D is in particular noncompact. We now introduce, following [NYY14, sec 3.2], a framed quiver with potential (Q_D, W_D), such that D-cyclic representations are a noncommutative analogue of sheaves with compact support on X with a framing by the sheaf $\mathcal{O}_D$. In physics terminology, such framed sheaves correspond to bound states of a noncompact D4 brane wrapped on D, together with compact D4-D2-D0 branes.

The corner p_i lies between the two sides $z = z_{i-1/2}$ and $z' = z_{i+1/2}$, with K_z and K'_z subdivisions, respectively. We can then choose one of the intersection points of the $K_z, K_{z'}$ oriented lines on the torus with direction $l_z, l_{z'}$ (according to [NYY14, sec 4.4], different intersection points correspond to different choices for the holonomy of the gauge fields at infinity). Following the general procedure of the fast inverse algorithm, the picture at the intersection point is given by Figure 7.6.

Here we have two tiles of the brane tiling, the tile corresponding to the node i of the quiver in the quadrant $(+z, +z')$, the tile corresponding to the node j of the quiver in the quadrant $(-z, -z')$, and an edge between those tiles, corresponding to an arrow $a : i \to j$ of the quiver. The corresponding framed quiver, which we denote by Q_D, has one framing node ∞ and two framing arrows $q : \infty \to i$ and $p : j \to \infty$, i.e. $((Q_D)_0, (Q_D)_1) = (Q_0 \cup \{\infty\}, Q_1 \cup \{p, q\}$. The potential for the frame quiver is obtained by adding the cycle paq to the original unframed potential,

$$W_D = W + paq \tag{7.2.24}$$

We denote by $Z_D(x)$ the generating series of the cohomological DT invariants $[\mathcal{M}_{Q_D,W_D,d}]^{vir}$ of D-cyclic critical representations, following the definitions in (7.2.4) and (7.2.12). To our knowledge, there is no known simple expression of the generating series $Z_D(x)$ in terms of the unframed generating series $\mathcal{A}(x)$ similar to the formula (7.2.23) expressing $Z_i(x)$ in terms of $\mathcal{A}(x)$.

Some general properties of D-cyclic critical representations are proven in [NYY14]. First, in [NYY14, sec 3.7] it is proven that the arrow p always vanishes in such representations. Taking the partial derivative $\partial_p W_D = aq$, the arrow p gives the relation $aq = 0$. Second, in section 3.8 it is shown that this relation imposes that in fact all the arrows of the cut I vanish. This shows that the $\mathbb{C}Q_D/(\partial W_D)$ module of paths with source at a framing node P_D is generated by paths beginning by the framing node q, followed by a paths of the quiver with relation $(Q_I, \partial_I W)$ obtained from Q by removing the arrows of I and imposing the relations $\partial_a W = 0$ for $a \in I$.

Figure 7.7: Facet corresponding to a D4 brane framing

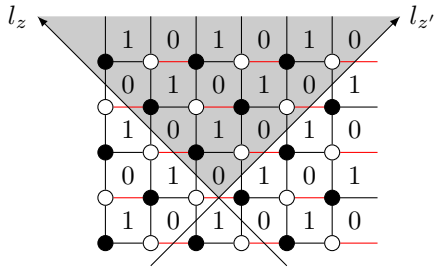

In the periodic quiver plane, the paths of (Q_I, W_I) beginning at the node i extend in the facet between the two half lines directed by l_z, $l_{z'}$ intersecting at i. Indeed, the Zag arrows of the zig-zag paths associated to z are in I, preventing paths of Q' to cross the half line directed by l_z, and the Zig arrows of the zig-zag paths associated to z' are in I, preventing paths of (Q_I, W_I) to cross the half line directed by $l_{z'}$.

As an example, for the conifold, it gives Figure 7.7, where we have drawn the edges of the perfect matching in red and filled in gray the nodes of the periodic quiver that are accessible from the node 0 after having removed the arrows of the cut.

7.3 Invertible and nilpotent BPS invariants

7.3.1 Definition

Let us choose a side z of the toric diagram. We have seen that the sum of cycles $v^z = \sum_{i\in Q_0} v_i^z$ in the center $\mathbb{C}[M^+]$ of the Jacobian algebra $J_{Q,W}$ is identified with the toric coordinate of X associated to z. The noncommutative analogue of sheaves supported on the locus of X where the toric coordinate associated to z is non-vanishing (resp. vanishing) are critical representations V where the endomorphism v^z of V is invertible (resp. nilpotent).

Consider a short exact sequence of d_1, $d = d_1 + d_2$ and d_2 dimensional representations of Q:

$$0 \to V_1 \to V \to V_2 \to 0 \tag{7.3.1}$$

The operator v^z is upper triangular with respect to this block decomposition, with diagonal blocks $v^z|_{V_1}$ and $v^z|_{V_2}$, i.e. v^z is invertible (resp. nilpotent) in V if and only it is invertible (resp. nilpotent) in V_1 and V_2. Hence the subcategory of representations of Q obtained by imposing nilpotency or invertibility to some of the v^z is a Serre subcategory of the category of representations of Q.

For Z_I, Z_N two disjoint subsets of the sides of the toric diagram, we use then the superscript $Z_I : I, Z_N : N$ to denotes the restriction to the Serre subcategories of representations where v^z is invertible for $z \in Z_I$ and nilpotent for $z \in Z_N$. We use the superscript I (resp. N) to denotes the Serre subcategory when all the cycles v^z are invertible (resp nilpotent), and call the corresponding representations and generating series 'totally invertible' (resp. 'totally nilpotent'). Recalling that the sides of the toric diagram are cyclically ordered, we use also intervals notations like $[z, z']$, to denote the set the sides of the toric diagram enumerated in the clockwise order, starting at z and ending at z'.

It is important to stress that not all results of Donaldson-Thomas theory extend to the partially invertible and nilpotent invariants. In particular, purity results does not hold for the BPS invariants $\Omega_{\theta,d}^{Z_I:I,Z_N:N}$, as will become apparent in the formulae of Propositions 7.3.5 and 7.3.6.

7.3.2 Invertible/Nilpotent decomposition

Let us fix a side z of the toric diagram. Consider a representation in $\mathfrak{M}_{Q,W,d}^{z:I}$, i.e. such that the endomorphism v^z is invertible. For each $k \in \mathbb{Z}/K_z\mathbb{Z}$ the connected component Q^k of the quiver between the k-th and the $k+1$-th zig-zag path associated to z is strongly connected: for $i, j \in (Q^k)_0$, there is then paths $v : i \to j$ and $v' : j \to i$ in Q^k, such that $v'v : i \to i$ is a cycle of Q^k, i.e. is equal in $J_{Q,W}$ to a power of v_i^z. It implies that v is invertible, i.e. $d_i = d_j$. Then the dimension vector is constant inside a strip between two zig-zag paths associated to z, hence the dimension vector d is in $\langle(\alpha_k^z)_k\rangle$, the linear span with positive integer coefficients of the $(\alpha_k^z)_k$. We have the useful property:

Lemma 7.3.1. *The dimension vectors α_k^z belong to the kernel of the skew-symmetrized Euler form $\langle\cdot,\cdot\rangle$. For each Z_I, Z_N such that $Z_I \neq \emptyset$, dimensions vectors supporting representations of the Serre subcategory $Z_I : I, Z_N : N$ are then in the kernel of $\langle\cdot,\cdot\rangle$, hence the corresponding BPS invariants are not subject to wall crossing, and we denote them by $\Omega^{Z_I:I,Z_N:N}(x)$, omitting the subscript θ.*

Proof. Consider $i \in Q_0^k$: $\langle\alpha_{k'}^z, e_i\rangle$ gives the number of arrows of the quiver going from the the node i to a node in $Q_0^{k'}$, minus the number of arrows of the quiver going from a node in $Q_0^{k'}$ to the node i. The tile i is bordered by n incoming and n outgoing arrows. If the $k-1$-th (resp the k-th) zig-zag path border the tile i, then there is one incoming and one outgoing arrow adjacent to a node of Q_0^{k-1} (resp Q_0^{k+1}), and the rest of the arrows are incoming and outgoing arrows are adjacent to a node of Q_0^k. By disjunction of case, there is as many incoming and outgoing arrows at i adjacent to a node of $Q_0^{k'}$, hence $\langle\alpha_{k'}^z, e_i\rangle = 0$.

Consider a representation $V \in \mathfrak{M}_{Q,d}^{Z_I:I,Z_N:N}$. Take $z \in Z_I$: v^z is then invertible on V, i.e. $d \in \langle(\alpha_k^z)_k\rangle \subset ker\langle,\rangle$. In particular, the associated term $[\mathfrak{M}_{Q,W,d}^{Z_I:I,Z_N:N}]^{vir}x^d$, and then $\mathcal{A}^{Z_I:I,Z_N:N}(x)$, is in the center of the quantum affine space, i.e. no wall crossing can occur, and BPS invariants do not depend on the stability parameter θ. □

We now show the following Lemma, which is a direct generalization of [Dav16, Lem 4.1] to the case of non-symmetric quivers:

Lemma 7.3.2. *Consider a quiver with potential (Q, W) and an element v central in $J_{Q,W}$, such that representations where v is invertible have a dimension vector in the kernel of the anti-symmetrized Euler form $\langle,\rangle$. Then v acts as a scalar on representations in the support of $\mathcal{BPS}_{W,d}^{\theta}$.*

Proof. We refer to the proof of the Lemma 4.1 of [Dav16] for the details of the arguments: here the major difference is that we consider a quiver which is not symmetric, and then the quantum affine space is not commutative. Considering θ generic, i.e. such that if d, d' have the same slope then $\langle d - d', \bullet\rangle = 0$, and a ray l of the form $d + ker(\langle,\rangle)$. The relative integrality Theorem from [DM16, Theo A] gives:

$$\bigoplus_{d\in l} \mathcal{H}(JH_*\phi_W\mathcal{IC}_{\mathfrak{M}_{Q,d}^{\theta,ss}}) = \mathrm{Sym}_{\boxtimes_\oplus}(H(B\mathbb{C}^*)_{vir} \otimes (\bigoplus_{d\in l} \mathcal{BPS}_{W,d}^{\theta})) \tag{7.3.2}$$

where JH is the Jordan-Hölder map sending a semistable object to the associated polystable object and ϕ_W is the vanishing cycle functor of $\mathrm{Tr}(W)$ on $\mathfrak{M}^{\theta,ss}_{Q,d}$. Consider $V \in \mathrm{Supp}(\mathcal{BPS}^{\theta}_{W,d})$. In particular, V is the polystable object associated with a representation in the support of ϕ_W, hence in the critical locus of $\mathrm{Tr}(W)$, and then V itself is a $J_{Q,W}$-module. Suppose that v, which is central in $J_{Q,W}$, has at least two different eigenvalues, which we denote ϵ_1 and ϵ_2. We choose two disjoints open set $U_1, U_2 \subset \mathbb{C}$ such that the eigenvalues of v lies in $U_1 \cup U_2$, $\epsilon_1 \in U_1, \epsilon_2 \in U_2$. Given an open set $U \subset \mathbb{C}$ we denote by $(\mathcal{M}^{\theta,ss}_{Q,d})^U$ (resp. $(\mathfrak{M}^{\theta,ss}_{Q,d})^U$) the subspace (resp. substack) of representations such that v has all its eigenvalues in U, in particular $V \in (\mathcal{M}^{\theta,ss}_{Q,d})^{U_1\cup U_2} - ((\mathcal{M}^{\theta,ss}_{Q,d})^{U_1} \cup (\mathcal{M}^{\theta,ss}_{Q,d})^{U_2})$. A critical representation $W \in \mathfrak{M}^{U_1\cup U_2}_{Q,W,d}$ splits canonically as a direct sum of representations W_1, W_2 where v has eigenvalues respectively in U_1, U_2, giving:

$$(\mathfrak{M}^{\theta,ss}_{Q,W,d})^{U_1\cup U_2} = \bigsqcup_{d_1+d_2=d} (\mathfrak{M}^{\theta,ss}_{Q,W,d_1})^{U_1} \times (\mathfrak{M}^{\theta,ss}_{Q,W,d_2})^{U_2} \tag{7.3.3}$$

Remark here that necessarily at least one of the two U_i is contained in $\mathbb{C}^*$, say U_1, and then contains only representations where v is invertible, i.e. the d_1 which gives nontrivial terms in the sum lies in the ray $l_0 := ker(\langle , \rangle)$, giving:

$$\begin{aligned}\bigsqcup_{d\in l}(\mathfrak{M}^{\theta,ss}_{Q,W,d})^{U_1\cup U_2} &= \bigsqcup_{d\in l}\bigsqcup_{d_1+d_2=d} (\mathfrak{M}^{\theta,ss}_{Q,W,d_1})^{U_1} \times (\mathfrak{M}^{\theta,ss}_{Q,W,d_2})^{U_2} \\ &= (\bigsqcup_{d_1\in l_0} (\mathfrak{M}^{\theta,ss}_{Q,W,d_1})^{U_1}) \times (\bigsqcup_{d_2\in l} (\mathfrak{M}^{\theta,ss}_{Q,W,d_2})^{U_2})\end{aligned} \tag{7.3.4}$$

By the same argument as in the proof of Lemma 4.1 of [Dav16], it gives:

$$\begin{aligned}&\bigoplus_{d\in l} \mathcal{H}(JH_*\phi_W \mathcal{IC}_{\mathfrak{M}^{\theta,ss}_{Q,d}|_{(\mathfrak{M}^{\theta,ss}_{Q,d})^{U_1\cup U_2}}}) \\ &= \bigoplus_{d_1\in l_0} \mathcal{H}(JH_*\phi_W \mathcal{IC}_{\mathfrak{M}^{\theta,ss}_{Q,d}|_{(\mathfrak{M}^{\theta,ss}_{Q,d})^{U_1}}}) \boxtimes_{\oplus} \bigoplus_{d_2\in l} \mathcal{H}(JH_*\phi_W \mathcal{IC}_{\mathfrak{M}^{\theta,ss}_{Q,d}|_{(\mathfrak{M}^{\theta,ss}_{Q,d})^{U_2}}})\end{aligned} \tag{7.3.5}$$

Applying the relative integrality Theorem of [DM16], we obtain:

$$\begin{aligned}&\mathrm{Sym}_{\boxtimes_\oplus}(H(B\mathbb{C}^*)_{vir} \otimes (\bigoplus_{d\in l} \mathcal{BPS}^{\theta}_{W,d}|_{(\mathcal{M}^{\theta,ss}_{Q,d})^{U_1\cup U_2}}) \\ =&\mathrm{Sym}_{\boxtimes_\oplus}(H(B\mathbb{C}^*)_{vir} \otimes (\bigoplus_{d_1\in l_0} \mathcal{BPS}^{\theta}_{W,d_1}|_{(\mathcal{M}^{\theta,ss}_{Q,d_1})^{U_1}})) \\ &\boxtimes_\oplus \mathrm{Sym}_{\boxtimes_\oplus}(H(B\mathbb{C}^*)_{vir} \otimes (\bigoplus_{d_2\in l} \mathcal{BPS}^{\theta}_{W,d_2}|_{(\mathcal{M}^{\theta,ss}_{Q,d_2})^{U_2}})) \\ =&\mathrm{Sym}_{\boxtimes_\oplus}(H(B\mathbb{C}^*)_{vir} \otimes ((\bigoplus_{d_1\in l_0} \mathcal{BPS}^{\theta}_{W,d_1}|_{(\mathcal{M}^{\theta,ss}_{Q,d_1})^{U_1}}) \oplus (\bigoplus_{d_2\in l} \mathcal{BPS}^{\theta}_{W,d_2}|_{(\mathcal{M}^{\theta,ss}_{Q,d_2})^{U_2}})))\end{aligned} \tag{7.3.6}$$

and then by identification one has:

$$\sum_{d\in l} \mathcal{BPS}^{\theta}_{W,d}|_{(\mathcal{M}^{\theta,ss}_{Q,d})^{U_1\cup U_2}} \simeq (\sum_{d_1\in l_0} \mathcal{BPS}^{\theta}_{W,d_1}|_{(\mathcal{M}^{\theta,ss}_{Q,d_1})^{U_1}}) \oplus (\sum_{d_2\in l} \mathcal{BPS}^{\theta}_{W,d_2}|_{(\mathcal{M}^{\theta,ss}_{Q,d_2})^{U_2}}) \tag{7.3.7}$$

We can then deduce:

$$\mathrm{Supp}(\mathcal{BPS}^{\theta}_{W,d}|_{(\mathcal{M}^{\theta,ss}_{Q,d})^{U_1\cup U_2}}) \subset (\mathcal{M}^{\theta,ss}_{Q,d})^{U_1} \cup (\mathcal{M}^{\theta,ss}_{Q,d})^{U_2} \tag{7.3.8}$$

but $V \in (\mathcal{M}^{\theta,ss}_{Q,d})^{U_1\cup U_2} - ((\mathcal{M}^{\theta,ss}_{Q,d})^{U_1} \cup (\mathcal{M}^{\theta,ss}_{Q,d})^{U_2})$, and so the restriction of $\mathcal{BPS}^{\theta}_{W,d}$ to V is zero. We conclude that if $V \in \mathrm{Supp}(\mathcal{BPS}^{\theta}_{W,d})$, then v has a single eigenvalue. For a stable $J_{Q,W}$-module W, because v is central in $J_{Q,W}$, it defines an element of $\mathrm{Hom}(W,W) = \mathbb{C}$ by stability, and then v acts as a scalar. V is a direct sum of θ-stable representations where v acts as a scalar, and v has a single eigenvalue on V, i.e. acts as a scalar on V. □

We can now prove the invertible/nilpotent decomposition of BPS invariants, considering Z_I, Z_N two subsets of the set of sides of the toric diagram. A particular case of this result was stated and used in [MP20, eq 6.18].

Proposition 7.3.3. *For each Z_I, Z_N, z such that $z \notin Z_I \cup Z_N$, we have:*

$$\Omega^{Z_I:I,Z_N:N}_{\theta}(x) = \Omega^{Z_I:I,Z_N,z:I}(x) + \Omega^{Z_I:I,Z_N:N,z:N}_{\theta}(x) \tag{7.3.9}$$

Proof. Recall that the element v^z is in the center of the Jacobian algebra $J_{Q,W}$, and from the Lemma 7.3.1 the assumptions of Lemma 7.3.2 are satisfied, i.e. v^z acts as a scalar on a representation in the support of $\mathcal{BPS}^{\theta}_{W,d}$. In particular, the support of $\mathcal{BPS}^{\theta}_{W,d}$ is the disjoint union of a locus where the $(v_i^z)_{i\in Q_0}$ are invertible, and a locus where they are nilpotent, i.e. :

$$\begin{aligned}
&\mathrm{Supp}(\mathcal{BPS}^{\theta}_{W,d}) \cap (\mathcal{M}^{\theta,ss}_{Q,d})^{Z_I:I,Z_N:N} \\
=&(\mathrm{Supp}(\mathcal{BPS}^{\theta}_{W,d}) \cap (\mathcal{M}^{\theta,ss}_{Q,d})^{Z_I:I,Z_N:N,z:I}) \sqcup (\mathrm{Supp}(\mathcal{BPS}^{\theta}_{W,d}) \cap (\mathcal{M}^{\theta,ss}_{Q,d})^{Z_I:I,Z_N:N,z:N}) \\
\Rightarrow&\Omega^{Z_I:I,Z_N:N}_{\theta,d} = \Omega^{Z_I:I,Z_N,z:I}_{\theta,d} + \Omega^{Z_I:I,Z_N:N,z:N}_{\theta,d}
\end{aligned} \tag{7.3.10}$$

where the second line holds by taking the induced long exact sequence in cohomology. The result follows by noticing that $\Omega^{Z_I:I,Z_N,z:I}_{\theta,d}$ does not depend on θ, and by taking the generating series. □

Remark 7.3.4. The fact that, for a cycle v^z, the BPS invariants are the sum BPS invariants with v^z invertible and BPS invariants with v^z nilpotent was used in [MP20, eq. 6.18] in some specific examples of toric quivers. It was also remarked in [MP20, eq 6.17] that in those examples the invertible BPS invariants do not suffer wall crossing and are simple to compute. The formula [MP20, eq. 6.18] was proven after dimensional reduction relative to a perfect matching corresponding to a corner p of the toric diagram. After this dimensional reduction, it is then possible to give an invertible/nilpotent decomposition of the cycles $v^z, v^{z'}$ corresponding to the sides z, z' adjacent to p, but the other cycles $v^{z''}$ vanish. Hence to provide the invertible/nilpotent decomposition on various cycles v^z as in Proposition 7.3.3 one must establish this identity without doing a dimensional reduction, hence work with the formalism of vanishing cycles as done in this section.

7.3.3 Computation of the partially invertible part

Proposition 7.3.5. *i) For any toric quiver with potential, denoting by b the number of boundary points of the toric diagram and i is the number of internal points of the toric diagram:*

$$\Omega_{n\delta} = \mathbb{L}^{3/2} + (b-3+i)\mathbb{L}^{1/2} + i\mathbb{L}^{-1/2} \text{ for } n \geq 1 \tag{7.3.11}$$

ii) Consider z, z' two different sides of the toric diagram, we have:

- *if z and z' are adjacent to the same corner, then:*

$$\Omega^{z:I,z':I}(x) = (\mathbb{L}^{3/2} - 2\mathbb{L}^{1/2} + \mathbb{L}^{-1/2}) \sum_{n\geq 1} x^{n\delta} \tag{7.3.12}$$

- *otherwise:*

$$\Omega^{z:I,z':I}(x) = \Omega^{I}(x) = (\mathbb{L}^{3/2} - 3\mathbb{L}^{1/2} + 3\mathbb{L}^{-1/2} - \mathbb{L}^{-3/2}) \sum_{n\geq 1} x^{n\delta} \tag{7.3.13}$$

Proof. *i*) Any generic stability condition θ gives a crepant resolution $X_\theta \xrightarrow{p} X$, by taking the moduli space of θ-stable δ-dimensional critical representations of (Q, W), as proven in [Moz09][Theo 4.5]. Denote by $X_\theta^{Z:I}$ the open locus of representations such that v^z is invertible for $z \in Z$, i.e. $X_\theta^{Z:I} = \cap_{z\in Z}(v^{\lambda_z} p)^{-1}(\mathbb{C}^*)$.

As shown in [Moz09, Theo 4.5], there is an equivalence between the bounded derived category of critical representations of (Q, W) and the bounded derived category of coherent sheaves on X_θ. This derived equivalence restricts to a derived equivalence between the bounded derived category of critical representations such that $\sum_{i\in Q_0} v_i^z$ is invertible for $z \in Z$, and the bounded derived category of sheaves on $X_\theta^{Z:I}$. In particular, the cohomological DT/PT correspondance proven in [Bri10, Theo 1.1], and the wall crossing formula expressing the DT/PT wall crossing in terms of the BPS invariants $\Omega_{\theta,d}$, proven in [Mor12] and [Moz13] applies, giving:

$$\sum_n [(X_\theta^{Z:I})^{[n]}]^{vir} x^{n\delta} = \mathrm{Exp}\left(\sum_n \Omega_{\theta,n\delta}^{Z:I} \frac{\mathbb{L}^{n/2} - \mathbb{L}^{-n/2}}{\mathbb{L}^{1/2} - \mathbb{L}^{-1/2}} x^{n\delta}\right) \tag{7.3.14}$$

with $(X_\theta^{Z:I})^{[n]}$ being the Hilbert scheme of n points on $X_\theta^{Z:I}$. The generating series of the motives of the Hilbert schemes of points on any smooth quasi-projective threefold (as $X_\theta^{Z:I}$) was computed in [BBS13, Theo 3.3]:

$$\sum_n [(X_\theta^{Z:I})^{[n]}]^{vir} = \mathrm{Exp}\left(\mathbb{L}^{-3/2}[X_\theta^{Z:I}] \sum_{n\geq 1} \frac{\mathbb{L}^{n/2} - \mathbb{L}^{-n/2}}{\mathbb{L}^{1/2} - \mathbb{L}^{-1/2}} x^{n\delta}\right) \tag{7.3.15}$$

i.e. we can identify:

$$\Omega_{n\delta}^{Z:I} = \mathbb{L}^{-3/2}[X_\theta^{Z:I}] \quad for\ n \geq 1 \tag{7.3.16}$$

Here we have dropped the dependence on θ because $n\delta$ is in the kernel of the anti-symmetrized Euler form. In particular, the computation of the cohomological class $[X_\theta]$ in [MP20, Lem 4.2] gives the claimed expression for $\Omega_{n\delta}$, as explained in [MP20, Remark 5.2].

ii) Consider a subset Z_I of the sides of the toric diagram containing at least two elements $z \neq z'$. For any representation in $\mathcal{M}_{Q,W,d}^{\theta,ss,Z_I:I}$, v^z and $v^{z'}$ are invertible. Consider d such that $\mathcal{M}_{Q,W,d}^{\theta,ss,Z_I:I} \neq \emptyset$: the dimensions d_i are constant inside the strips delimited by lines directed by l_z, and also inside the strips delimited by lines directed by $l_{z'}$. Since these two sets of lines intersect only at isolated

points of the torus, all the d_i's must then be equal. Hence for $d \notin \langle\delta\rangle$, $\Omega^{Z_I}_{\theta,d}$ vanish, giving:

$$\begin{aligned}\Omega^{Z_I:I}(x) =& \sum_n \Omega^{Z_I:I}_{n\delta} x^{n\delta} \\ =& \mathbb{L}^{-3/2}[X^{Z_I:I}_\theta] \sum_{n\geq 1} x^{n\delta}\end{aligned} \tag{7.3.17}$$

Here we have used equation (7.3.16) in the second line, considering a generic stability condition θ. Recall that we have $X = Spec(\mathbb{C}[M^+])$, and then $X^{Z_I:I} = Spec(\mathbb{C}[M^+, (v^{-\lambda_z})_{z\in Z_I}]$. There are two possible cases:

- $Z_I = \{z, z'\}$ consists of two sides of the toric diagram which are adjacent to the same corner p associated to the cut I. In that case, the subsemigroup of M generated by M^+ and $-\lambda_z, -\lambda_{z'}$ is the half lattice $\{\lambda \in M | \bar{\chi_I}(\lambda) \geq 0\}$, isomorphic with $\mathbb{N}\times\mathbb{Z}^2$. This implies that $X^{Z_I:I} = (\mathbb{C}^*)^2 \times \mathbb{C}$; $X^{Z_I:I}$, which is smooth, i.e. is equal to its crepant resolution $X^{Z_I:I}_\theta$:

$$\begin{aligned}&X^{z:I,z':I}_\theta = (\mathbb{C}^*)^2 \times \mathbb{C} \\ \Rightarrow&\Omega^{z:I,z':I}(x) = (\mathbb{L}^{3/2} - 2\mathbb{L}^{1/2} + \mathbb{L}^{-1/2}) \sum_{n\geq 1} x^{n\delta}\end{aligned} \tag{7.3.18}$$

- Z_I contains two sides of the toric diagram z, z' which are not on the same corner of the toric diagram. In this case the sub semigroup of M generated by L^+ and $-\lambda_z, -\lambda_{z'}$ is the whole lattice M isomorphic with $\mathbb{Z}^3$. This implies that $X^{Z_I:I} = (\mathbb{C}^*)^3$, which is smooth, i.e. is equal to its crepant resolution $X^{Z_I:I}_\theta$:

$$\begin{aligned}&X^{Z_I:I} = X^{z:I,z':I}_\theta = X^I = (\mathbb{C}^*)^3 \\ \Rightarrow&\Omega^{z:I,z':I}(x) = \Omega^I_\theta(x) = (\mathbb{L}^{3/2} - 3\mathbb{L}^{1/2} + 3\mathbb{L}^{-1/2} - \mathbb{L}^{-3/2}) \sum_{n\geq 1} x^{n\delta}\end{aligned} \tag{7.3.19}$$

□

Proposition 7.3.6. *Consider a side z of the toric diagram:*

$$\Omega^{z:I}(x) = (\mathbb{L}^{3/2} + (K_z - 2)\mathbb{L}^{1/2} - (K_z - 1)\mathbb{L}^{-1/2}) \textstyle\sum_{n\geq 1} x^{n\delta} + (\mathbb{L}^{1/2} - \mathbb{L}^{-1/2}) \sum_{k\neq k'} \sum_{n\geq 0} x^{n\delta + \alpha^z_{[k,k'[}} \tag{7.3.20}$$

Proof. The main idea of the proof is to obtain an analogue of the isomorphism $X^{z:I} \cong \mathbb{C}^2/\mathbb{Z}_{K_z} \times \mathbb{C}^*$ at the level of the noncommutative resolution by quivers with potential. We denote by $(\bar{Q}, \bar{W})$ the quiver with potential associated to the toric threefold $\mathbb{C}^2/\mathbb{Z}_{K_z} \times \mathbb{C}$: its nodes are $\bar{Q}_0 = \mathbb{Z}/K_z\mathbb{Z}$, its arrows are $a_k : k \to k$, $b_k : k \to k+1$, $c_k : k+1 \to k$, and its potential is:

$$\bar{W} = \sum_{k\in\mathbb{Z}/K_z\mathbb{Z}} (a_k c_k b_k - a_{k+1} b_k c_k) \tag{7.3.21}$$

We denote by $\bar{z}$ the side of the toric diagram of $\mathbb{C}^2/\mathbb{Z}_{K_z} \times \mathbb{C}$ such that $v^{\bar{z}} = \bigoplus_k a_k$. Starting with a representation V of (Q, W) such that v^z is invertible, one can obtain a representation of $(\bar{Q}, \bar{W})$ such that the a_k's are invertible informally by the following procedure:

Figure 7.8: Contraction of the quiver for PdP_{3a}

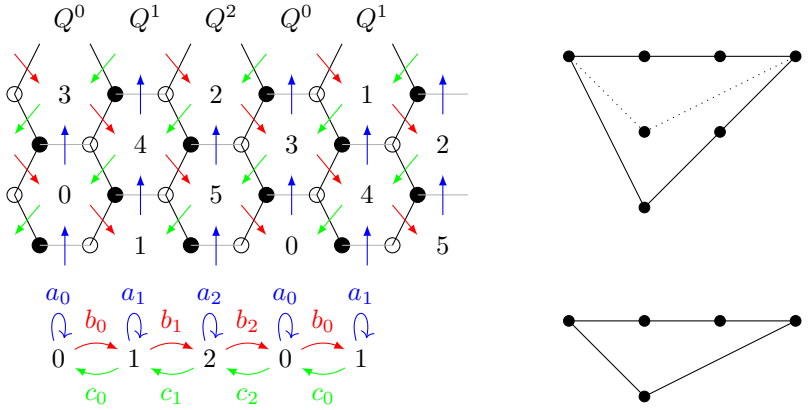

- contract the strips Q^k onto the single node k using the fact that all the arrows of Q^k are isomorphisms.
- Send the invertible cycles v_i^z, for $i \in (Q^k)_0$, to an invertible loop $a_k : k \to k$.
- Send the arrows of $\mathrm{Zig}_k : (Q^k)_0 \to (Q^{k+1})_0$ to $b_k : k \to k+1$
- Send the arrows of $\mathrm{Zag}_k : (Q^{k+1})_0 \to (Q^k)_0$ to $c_k : k+1 \to k$

This contraction, and the corresponding operation on the toric diagrams, are illustrated in Figure 7.8 for the case of the Pseudo-del Pezzo surface PdP_{3a}.

Consider now the toric diagram associated to the toric quiver: from simple convex geometry, it contains a node which is in a line parallel with the line containing the side z and which is at minimal distance from this line: for I a perfect matching associated to this node, one has then $\chi_I(\lambda_z) = 1$, hence each cycle v_i^z contains exactly one arrow of I. We consider then the surjective morphism of path algebras:

$$\begin{aligned}
\Phi :& \mathbb{C}Q \to \mathbb{C}\bar{Q} \\
& \Phi(e_i) := e_k \text{ for } i \in Q_0^k \\
& \Phi(u) := a_k^{\delta_{u\in I}} \text{ for } u \in Q_1^k \\
& \Phi(u) := c_k b_k a_k^{\delta_{u\in I}} \text{ for } u \in J_k \\
& \Phi(u) := b_k a_k^{\delta_{u\in I}} \text{ for } u \in \mathrm{Zig}_k \\
& \Phi(u) : a_k c_k^{\delta_{u\in I}} \text{ for } u \in \mathrm{Zag}_k
\end{aligned} \tag{7.3.22}$$

We evaluate then $\Phi(W)$. Consider a white (resp black) node of the perfect matching on the k-th zig-zag path: the corresponding cycle w of the potential is of the form cbv (resp bcv), for v a path of Q_k (resp Q_{k+1}), $b \in \mathrm{Zig}_k$ and $c \in \mathrm{Zag}_k$. If v contains an arrow of I, then $w = c_k b_k a_k$ (resp $w = b_k c_k a_{k+1}$). Consider the cycle of Q^k (resp Q^{k+1}) going along the k-th zig-zag path: it has weight λ_z, hence contains exactly one arrow of I, and then the k-th zig-zag path contains exactly one white node $w = c_k b_k a_k$ such that the arrow of I adjacent to this node is in Q^k and and one

black node $w = b_k c_k a_{k+1}$ such that the arrow of I adjacent to this node is in Q^{k+1}. If an arrow $b \in \mathrm{Zig}_k$ (resp $c \in \mathrm{Zag}_k$) is in I, then the cycles of the potential corresponding to the black and white node adjacent to this edge in the dimer model are equal to $c_k b_k a_k$, and then cancel each other. The cycles corresponding to the white and black nodes adjacent to an edge in $u \in J_k$ are both equal to $c_k b_k a_k$ and then cancel each others. Finally we obtain:

$$\Phi(W) = \bar{W} \tag{7.3.23}$$

In particular Φ pass to the quotient to a surjective morphism of Jacobi algebra:

$$\Phi : J_{Q,W} \to J_{\bar{Q},\bar{W}} \tag{7.3.24}$$

For each k, choose a node $i_k \in Q_0^k$, and weak paths $(u_k : i_k \to i_{k+1}) = u'^{-1} b u$ (resp $(v_k : i_{k+1} \to i_k) = v'^{-1} c v$) with u, v' paths of Q^k and u', v paths of Q^{k+1}, such that $\chi_I(u_k) = \chi_(v_k) = 0$. We define then a morphism between localized path algebras:

$$\begin{aligned}
\Psi :& \mathbb{C}\bar{Q}[(a_k^{-1})_k] \to \mathbb{Q}[((v_i^z)^{-1})_i] \\
& \Psi(e_k) := e_{i_k} \\
& \Psi(a_k) := v_{i_k}^z \\
& \Psi(b_k) := u_k \\
& \Psi(c_k) := v_k
\end{aligned} \tag{7.3.25}$$

it satisfies $\Phi \circ \Psi = \mathrm{Id}_{\mathbb{C}\bar{Q}[(a_k^{-1})_k]}$, and pass to the quotient to a morphism of Jacobi algebra:

$$\Psi : J_{\bar{Q},\bar{W}}[(a_k^{-1})_k] \to J_{Q,W}[((v_k^z)^{-1})_k] \tag{7.3.26}$$

which is the inverse of Φ, hence Φ gives an isomorphism of localized Jacobi algebras:

$$\Phi : J_{Q,W}[((v_k^z)^{-1})_k] \to J_{\bar{Q},\bar{W}}[(a_k^{-1})_k] \tag{7.3.27}$$

For $\bar{d} \in \mathbb{N}^{\bar{Q}_0}$, denote $d = \sum_k d_k \alpha_k^z$. The morphism Φ of path algebra induces an closed embedding of stacks $\mathfrak{M}_{\bar{Q},\bar{d}}^{\bar{z}:I} \to \mathfrak{M}_{Q,d}^{z:I}$ intertwining the potential, such that the restriction to the critical locus is an isomorphism. It is then an embedding of critical charts in the sense of [Joy13], hence:

$$\begin{aligned}
[\mathfrak{M}_{Q,W,d}^{z:I}]^{vir} &= H_c(\mathfrak{M}_{Q,d}^{z:I}, \phi_W \mathcal{IC}_{\mathfrak{M}_{Q,d}^{z:I}}) \\
&= H_c(\mathfrak{M}_{\bar{Q},\bar{d}}^{\bar{z}:I}, \phi_{\bar{W}} \mathcal{IC}_{\mathfrak{M}_{\bar{Q},\bar{d}}^{\bar{z}:I}}) \\
&= [\mathfrak{M}_{\bar{Q},\bar{W}\bar{d}}^{\bar{z}:I}]^{vir}
\end{aligned} \tag{7.3.28}$$

Here the first and the last lines holds because the definition of the vanishing cycle functor is local, hence commutes with open embeddings, and the second line follows from the isomorphism of [BBD+15, Theo 5.4]. We obtain a relation between the generating series $\mathcal{A}$ of DT invariants of (Q, W) and the generating series $\bar{\mathcal{A}}$ of DT invariants of $(\bar{Q}, \bar{W})$:

$$\mathcal{A}^{z:I}(x) = \bar{\mathcal{A}}^{\bar{z}:I}((x^{\alpha_k^z})_k) \tag{7.3.29}$$

Hence, using the fact that d and $\bar{d}$ are in the kernel of the anti-symmetrized Euler forms, and then that the corresponding BPS invariants Ω of (Q,W) and $\bar{\Omega}$ of $(\bar{Q},\bar{W})$ does not depends on the stability parameter:

$$\begin{aligned} \Omega_d^{z:I} &= \bar{\Omega}_{\bar{d}}^{\bar{z}:I} \\ \Rightarrow \Omega^{z:I}(x) &= \bar{\Omega}^{\bar{z}:I}((x^{\alpha_k^z})_k) \end{aligned} \tag{7.3.30}$$

Then [Moz11, Theo 6.1] gives:

$$\bar{\Omega}((x^{\alpha_k^z})_k) = (\mathbb{L}^{3/2} + (K_z - 1)\mathbb{L}^{1/2}) \sum_{n\geq 1} x^{n\delta} + \mathbb{L}^{1/2} \sum_{k\neq k'} \sum_{n\geq 0} x^{n\delta + \alpha^z_{[k,k'[}} \tag{7.3.31}$$

We could compute $\bar{\Omega}^{z:I}$ by doing a method similar as in [MN15], considering invertible/nilpotent decompositions and Jordan block decompositions. We prefer to show to extract $\bar{\Omega}^{\bar{z}:I}$ from $\bar{\Omega}$ using only formal manipulations, as an illustration of our formalism. We will prove the claim below:

$$\bar{\Omega}^{\bar{z}:I}(x) = \frac{[\mathbb{C}^*]}{[\mathbb{C}]} \bar{\Omega}(x) \tag{7.3.32}$$

This is related with the fact that $\bar{\Omega}^{\bar{z}:I}(x)$ (resp. $\bar{\Omega}(x)$) is the generating series of BPS invariants for a noncommutative crepant resolution of $\mathbb{C}^2/\mathbb{Z}_{K_z} \times \mathbb{C}^*$(resp. of $\mathbb{C}^2/\mathbb{Z}_{K_z} \times \mathbb{C}$). Consider a generic stability θ giving a crepant resolution $(\mathbb{C}^2/\mathbb{Z}_{K_z} \times \mathbb{C})_\theta = (\mathbb{C}^2/\mathbb{Z}_{K_z})_\theta \times \mathbb{C}$, and remark that $(\mathbb{C}^2/\mathbb{Z}_{K_z} \times \mathbb{C})_\theta^{z:I} = (\mathbb{C}^2/\mathbb{Z}_{K_z})_\theta \times \mathbb{C}^*$, using (7.3.16), one obtains for $n \geq 1$:

$$\begin{aligned} \bar{\Omega}^{\bar{z}:I}(n\delta, y) &= \mathbb{L}^{-3/2}[(\mathbb{C}^2/\mathbb{Z}_{K_z})_\theta \times \mathbb{C}^*] \\ \bar{\Omega}(n\delta, y) &= \mathbb{L}^{-3/2}[(\mathbb{C}^2/\mathbb{Z}_{K_z})_\theta \times \mathbb{C}] \\ \Rightarrow \bar{\Omega}^{\bar{z}:I}(n\delta, y) &= \frac{[\mathbb{C}^*]}{[\mathbb{C}]} \bar{\Omega}(n\delta, y) \end{aligned} \tag{7.3.33}$$

We show that the relation of the claim holds also for the other dimension vectors using invertible/nilpotent decompositions and duality properties for $(\bar{Q},\bar{W})$. Denote by $\bar{z}, \bar{z}', \bar{z}''$ the external edges of the toric diagram of $\mathbb{C}^2/\mathbb{Z}_{K_z} \times \mathbb{C}$ considered in the clockwise order. One has:

$$\begin{aligned} \bar{\Omega}^{\bar{z}:I}(x) &= \bar{\Omega}(x) - \bar{\Omega}^{\bar{z}:N}(x) \\ \bar{\Omega}^{\bar{z}:N}(x) &= \mathbb{D}(\bar{\Omega}^{\bar{z}':N,\bar{z}'':N}(x)) \\ \bar{\Omega}^{\bar{z}':N,\bar{z}'':N}(x) &= \bar{\Omega}(x) - \bar{\Omega}^{\bar{z}':I,\bar{z}'':N}(x) - \bar{\Omega}^{\bar{z}'':I}(x) \\ \Rightarrow \bar{\Omega}^{\bar{z}:I}(x) &= \bar{\Omega}(x) - \mathbb{D}(\bar{\Omega}(x)) + \mathbb{D}(\bar{\Omega}^{\bar{z}':I,\bar{z}'':N}(x)) + \mathbb{D}(\bar{\Omega}^{\bar{z}'':I}(x)) \end{aligned} \tag{7.3.34}$$

where $\mathbb{D}$ is the Verdier duality, i.e. the Poincaré duality for mixed Hodge structures. In the first and the third lines we have performed invertible/nilpotent decompositions using Proposition 7.3.3, and in the second line we have used Corollary 7.4.2. We have $K_{\bar{z}'} = K_{\bar{z}''} = 1$, i.e. the BPS invariants $\bar{\Omega}^{\bar{z}':I,\bar{z}'':N}$ and $\bar{\Omega}^{\bar{z}'':I}$ have only terms with dimension vector $n\delta$, giving:

$$\begin{aligned} \bar{\Omega}_d^{\bar{z}:I} &= \bar{\Omega}_d - \Sigma(\bar{\Omega}_d) \quad \forall d \notin \langle\delta\rangle \\ &= \frac{[\mathbb{C}^*]}{[\mathbb{C}]} \bar{\Omega}_d \quad \forall d \notin \langle\delta\rangle \end{aligned} \tag{7.3.35}$$

The last line holds because the BPS invariants are either 0 or $\mathbb{L}^{1/2}$ for $d \notin \langle\delta\rangle$ from (7.3.31). This ends the proof the claim (7.3.32), giving:

$$\begin{aligned}\Omega^{z:I}(x) &= \bar{\Omega}^{\bar{z}:I}((x^{\alpha_k^{\tilde{z}}})_k)\\ &= (\mathbb{L}^{3/2} + (K_z - 2)\mathbb{L}^{1/2} - (K_z - 1)\mathbb{L}^{-1/2}) \textstyle\sum_{n\geq 1} x^{n\delta} + (\mathbb{L}^{1/2} - \mathbb{L}^{-1/2}) \sum_{k\neq k'} \sum_{n\geq 0} x^{n\delta + \alpha^z_{[k,k'[}}\end{aligned} \tag{7.3.36}$$

□

7.3.4 Identities between partially nilpotent attractors invariants

We now have all the necessary ingredients to express the BPS invariants Ω_θ in terms of BPS invariants $\Omega_\theta^{Z_N:N}$ with nilpotency constraints on a given cycle v^z.

Proposition 7.3.7. *We can express, for $[z, z']$ a strict subset of the set of sides of the toric diagram:*

$$\begin{aligned}\Omega_\theta(x) =&(\mathbb{L}^{3/2} + (\textstyle\sum_{\tilde{z}\in[z,z']} K_{\tilde{z}} - 2)\mathbb{L}^{1/2} - (\sum_{\tilde{z}\in[z,z']} K_{\tilde{z}} - 1)\mathbb{L}^{-1/2}) \sum_{n\geq 1} x^{n\delta}\\ &+ (\mathbb{L}^{1/2} - \mathbb{L}^{-1/2}) \sum_{\tilde{z}\in[z,z']} \sum_{k\neq k'} \sum_{n\geq 0} x^{n\delta + \alpha^{\tilde{z}}_{[k,k'[}} + \Omega_\theta^{[z,z']:N}(x)\end{aligned} \tag{7.3.37}$$

$$\begin{aligned}\Omega_\theta(x) =&(\mathbb{L}^{3/2} + (b-3)\mathbb{L}^{1/2} - (b-3)\mathbb{L}^{-1/2} - \mathbb{L}^{-3/2}) \sum_{n\geq 1} x^{n\delta}\\ &+ (\mathbb{L}^{1/2} - \mathbb{L}^{-1/2}) \sum_{z} \sum_{k\neq k'} \sum_{n\geq 0} x^{n\delta + \alpha^{z}_{[k,k'[}} + \Omega_\theta^{N}(x)\end{aligned} \tag{7.3.38}$$

Proof. We use Proposition 7.3.5, which says that for non adjacent z_i and z, $\Omega^{z_i:I,z:I} = \Omega^I$. In particular, for $z \notin [z_{i-1}, z_{i+1}]$ we have:

$$\begin{aligned}&\Omega^{z_i:I,z_{i+1}:N,z:I} = 0\\ \Rightarrow&\Omega^{z_i:I,[z_{i+1},z_{i-1}[:N} = \Omega_\theta^{z_i:I,z_{i+1}:N}\end{aligned} \tag{7.3.39}$$

We have also:

$$\begin{aligned}\Omega^{z_i:I,[z_{i+1},z_i[:N} =&\Omega^{z_i:I,[z_{i+1},z_{i-1}[:N} - \Omega^{z_{i-1}:I,z_i:I,[z_{i+1},z_{i-1}[:N}\\ =&\Omega^{z_i:I,z_{i+1}:N} - \Omega^{z_{i-1}:I,z_i:I} + \Omega^I\end{aligned} \tag{7.3.40}$$

Graphically, the two equations (7.3.39) and (7.3.40) can be written:

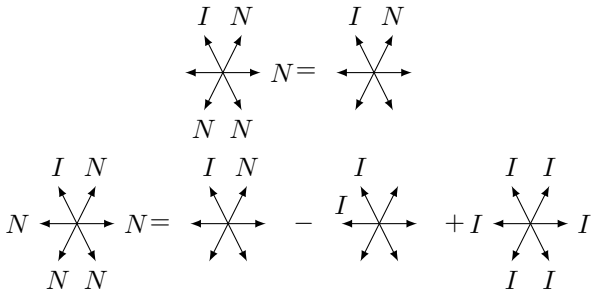

We can combine the formulas of Propositions 7.3.5 and 7.3.6:

$$\begin{aligned}\Omega^{z_l:I,z_{l+1}:N} =&\Omega^{z_l:I} - \Omega^{z_l:I,z_{l+1}:I}\\ =&(\mathbb{L}^{1/2}-\mathbb{L}^{-1/2})\left(K_z\sum_{n\geq 1}x^{n\delta}+\sum_{k\neq k'}\sum_{n\geq 0}x^{\alpha^z_{[k,k'[}+n\delta}\right)\end{aligned} \tag{7.3.41}$$

We decompose successively, denoting for convenience $z=z_i, z'=z_j$:

$$\begin{aligned}\Omega_\theta =&\Omega^{z_j:I}+\sum_{z_l\in[z_i,z_j[}\Omega^{z_l:I,]z_l,z_j]:N}+\Omega_\theta^{[z_i,z_j]:N}\\ =&\Omega^{z_j:I,z_{j+1}:I}+\Omega^{z_j:I,z_{j+1}:N}+\sum_{z_l\in[z_i,z_j[}\Omega^{z_l:I,z_{l+1}:N}+\Omega_\theta^{[z_i,z_j]:N}\\ =&(\mathbb{L}^{3/2}+(\textstyle\sum_{z\in[z_i,z_j]}K_z-2)\mathbb{L}^{1/2}-(\sum_{z\in[z_i,z_j]}K_z-1)\mathbb{L}^{-1/2})\sum_{n\geq 1}x^{n\delta}\\ &+(\mathbb{L}^{1/2}-\mathbb{L}^{-1/2})\sum_{z\in[z_i,z_j]}\sum_{k\neq k'}\sum_{n\geq 0}x^{n\delta+\alpha^z_{[k,k'[}}+\Omega_\theta^{[z_i,z_j]:N}(x)\end{aligned} \tag{7.3.42}$$

Here in the second line we have used (7.3.39), and we have used (7.3.41) and Proposition 7.3.5 in the last line. The manipulations above can be represented graphically as:

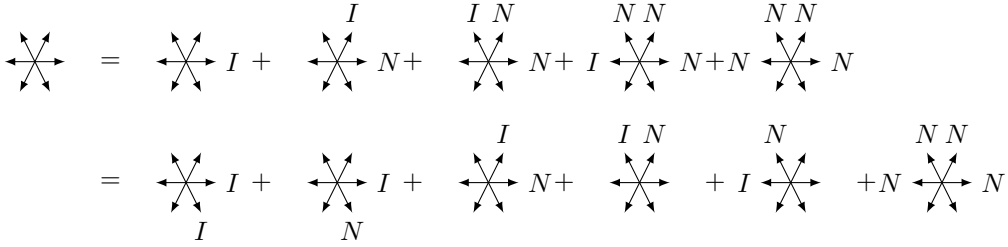

Similarly we can decompose :

$$\begin{aligned}\Omega_\theta =&\Omega^{z_{n-1}:I}+\sum_{z_l\in]z_0,z_{n-1}[}\Omega^{z_l:I,]z_l,z_{n-1}]:N,}+\Omega^{z_0:I,]z_0,z_{n-1}]:N}+\Omega_\theta^N\\ =&\Omega^{z_{n-1}:I,z_0:I}+\Omega^{z_{n-1}:I,z_0:N}+\sum_{z_l\in]z_0,z_{n-1}[}\Omega^{z_l:I,z_{l+1}:N}+\Omega^{z_0:I,z_1:N}-\Omega^{z_{n-1}:I,z_0:I}+\Omega^I+\Omega_\theta^N\\ =&\sum_{z_l\in[z_0,z_{n-1}]}\Omega^{z_l:I,z_{l+1}:N}+\Omega^I+\Omega_\theta^N\\ =&(\mathbb{L}^{3/2}+(b-3)\mathbb{L}^{1/2}-(b-3)\mathbb{L}^{-1/2}-\mathbb{L}^{-3/2})\sum_{n\geq 1}x^{n\delta}\\ &+(\mathbb{L}^{1/2}-\mathbb{L}^{-1/2})\sum_z\sum_{k\neq k'}\sum_{n\geq 0}x^{n\delta+\alpha^z_{[k,k'[}}+\Omega_\theta^N(x)\end{aligned} \tag{7.3.43}$$

Here we have used (7.3.39) and (7.3.40) in the second line, we have simplified in the third line, and (7.3.41) and the formulas of Propositions 7.3.5 in the last line, recalling $b=\sum_z K_z$. Graphically, the manipulations above corresponds to:

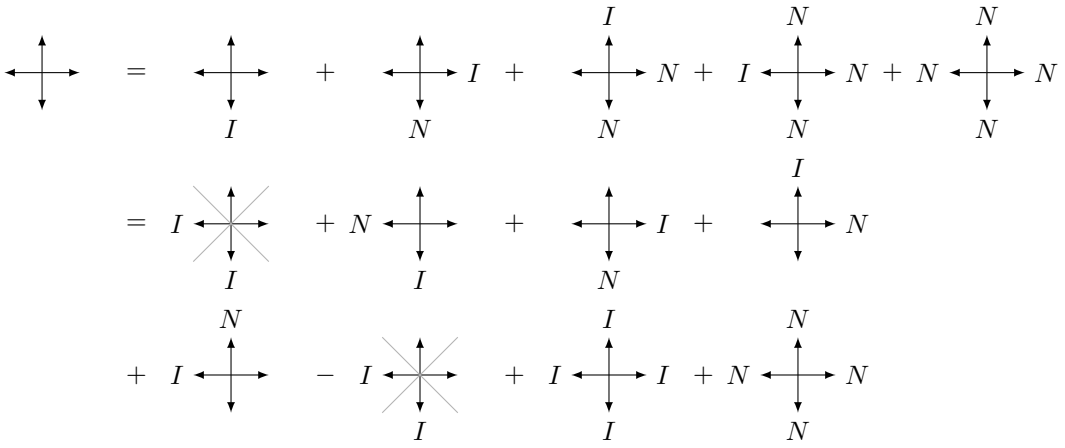

Here the two crossed terms cancel. Notice that the correction between the partially nilpotent invariants lie in the center of the quantum affine space, i.e. they are not subject to wall crossing: in particular, the same relations hold for the BPS invariants Ω_θ at any generic stability θ, an then also for attractor invariants Ω_*. □

Using the duality result of Corollary 7.4.2, we are able to derive a universal formula expressing BPS invariants up to an unknown self-Poincaré dual contribution:

Theorem 7.3.8.

$$\Omega_\theta(x) = (\mathbb{L}^{3/2} + (b-3+i)\mathbb{L}^{1/2} + i\mathbb{L}^{-1/2}) \sum_{n\geq 1} x^{n\delta} + \mathbb{L}^{1/2} \sum_{z} \sum_{k\neq k'} \sum_{n\geq 0} x^{n\delta + \alpha^z_{[k,k'[}} + \Omega^{sym}_\theta(x) \tag{7.3.44}$$

with $\Omega^{sym}_\theta(x)$ self Poincaré dual, and supported on dimension vectors $d \notin \langle\delta\rangle$. The same formula holds for attractor invariants.

Proof. We have from Corollary 7.4.2:

$$\Omega_\theta(x) = \mathbb{D}(\Omega^N_\theta(x)) \tag{7.3.45}$$

We have then, using the formula of Proposition 7.3.7:

$$\begin{aligned}\Omega_\theta(x) - \mathbb{D}(\Omega_\theta(x)) &= (\mathbb{L}^{3/2} + (b-3)\mathbb{L}^{1/2} - (b-3)\mathbb{L}^{-1/2} - \mathbb{L}^{-3/2}) \sum_{n\geq 1} x^{n\delta} \\ &+ (\mathbb{L}^{1/2} - \mathbb{L}^{-1/2}) \sum_{z} \sum_{k\neq k'} \sum_{n\geq 0} x^{n\delta + \alpha^z_{[k,k'[}}\end{aligned} \tag{7.3.46}$$

Hence, introducing:

$$\begin{aligned}&\Omega^{sym}_\theta(x) := \Omega_\theta(x) - \left((\mathbb{L}^{3/2} + (b-3+i)\mathbb{L}^{1/2} + i\mathbb{L}^{-1/2}) \textstyle\sum_{n\geq 1} x^{n\delta} + \mathbb{L}^{1/2} \sum_z \sum_{k\neq k'} \sum_{n\geq 0} x^{n\delta + \alpha^z_{[k,k'[}}\right) \\ &\Rightarrow \Omega^{sym}_\theta(x) = \mathbb{D}(\Omega^{sym}_\theta(x))\end{aligned} \tag{7.3.47}$$

From $i)$ of Proposition 7.3.5, one further obtains that Ω^{sym}_θ is supported on dimension vectors $d \notin \langle\delta\rangle$. The same property follows for $\Omega_*(x)$, by noticing that $\Omega_{*,d} = \Omega_{\theta_d,d}$ for θ_d a specific stability parameter. □

For local curves, i.e. symmetric quivers corresponding to toric diagrams without interior lattice points, the BPS invariants (which does not depend on the stability θ, because the quantum affine space is commutative in this case) have been computed explicitly. We will check as an illustration the compatibility of those results with our formula in Section 7.5.1. It appears that the only contribution to the symmetric part $\Omega^{sym}(x)$ come from dimension vectors d with $\Omega_d = 1$.

For toric diagrams with $i \geq 1$ interior lattice points, the symmetric part $\Omega_\theta^{sym}(x)$ can be quite complicated, and in particular it is subject to wall crossing. The attractor invariants are expected to be simpler than BPS invariants for generic θ. The simple representations, with dimension vectors $e_i, i \in Q_0$, always contribute to the attractor invariants, with $\Omega_{*,e_i} = 1$ because there are no self 1-cycles in this case. A natural question is then whether there exist other dimension vectors for which the attractor invariants have a non-zero symmetric part $\Omega_{*,d}^{sym}$. We conjecture, based on evidence collected in [BMP20] and on computations in [MP20] recalled in Section 7.5.2, that such dimension vectors do not exist:

Conjecture 7.3.9. *For toric diagram with $i \geq 1$ internal lattice points, the attractor invariants are given by:*

$$\Omega_*(x) = \sum_i x_i + (\mathbb{L}^{3/2} + (b-3+i)\mathbb{L}^{1/2} + i\mathbb{L}^{-1/2}) \sum_{n\geq 1} x^{n\delta} + \mathbb{L}^{1/2} \sum_z \sum_{k\neq k'} \sum_{n\geq 0} x^{n\delta + \alpha^z_{[k,k'[}} \quad (7.3.48)$$

7.4 Toric localization for framed quivers with potential

7.4.1 Torus fixed variety and attracting variety

Consider a one dimensional torus $\mathbb{C}^*$ acting on a variety X. We consider as in [Bra02], [Dri13] and [Ric16] the hyperbolic localization diagram:

$$X \xleftarrow{\eta^\pm} X^\pm \xrightarrow{p^\pm} X^0$$

Here X^0 denotes the closed subvariety of $\mathbb{C}^*$-fixed points, and $X^\pm$ the attracting (resp. repelling) variety, i.e. the disjoint union of the components of X flowing to a $\mathbb{C}^*$-fixed component when $t \to 0$ (resp. $t \to \infty$), $\eta^\pm$ gives the disjoint union of the closed embeddings of those components, and $p^\pm$ gives the projection to the $\mathbb{C}^*$-fixed component. The functors of constructible complexes $(p^+)_!(\eta^+)^* : D_c^b(X) \to D_c^b(X^0)$ is called the hyperbolic localization functor.

We consider the torus $(\mathbb{C}^*)^{(Q_f)_1}$ acting on $\mathbb{C}Q_f$, and therefore also on $\mathfrak{P}_f$, by scaling the arrows of Q_f. We consider the subtorus T leaving invariant the relations of the potential W_f, hence such that W_f is homogeneous, with weight denoted by κ: its action on $\mathcal{M}_{Q_f,d}$ restricts to an action on $\mathcal{M}_{Q_f,W_f,d}$. The gauge torus $T_G = (\mathbb{C}^*)^{Q_0}$ acts on $(\mathbb{C}^*)^{(Q_f)_1}$ by adjunction $(t_a)_{(a:i\to j)\in(Q_f)_1} \mapsto (t_i t_a t_j^{-1})_{(a:i\to j)\in(Q_f)_1}$, where we denote $t_\infty = 1$. The action of T on $\mathcal{M}_{Q_f,d}$ and $\mathcal{M}_{Q_f,W_f,d}$ descends to an action of T/T_G. The scaling of the framing arrow $p : \infty \to i$ p can be cancelled by the action of T_G, and for the $D4$ brane framing, the condition that the cycle paq has weight κ determines the weight of the relation arrow $q : j \to \infty$. Hence the torus acting on $\mathcal{M}_{Q_f,d}$ by leaving the potential homogeneous is the three dimensional torus $\mathbb{T}^3$ with weight lattice M, and the subtorus leaving the potential invariant is the two dimensional subtorus $\mathbb{T}^2$ with weight lattice $M/\kappa\mathbb{Z} = L$.

To study toric localization we will the consider a one dimensional subtorus $\mathbb{C}^* \subset \mathbb{T}^2$ leaving the potential invariant. This data is called a choice of slope in K-theoretic Donaldson-Thomas theory, because such a torus is determined by the data of line passing through the origin of L, separating this lattice into two half planes $L^{>0}$ (resp $L^{<0}$), the half space of positive (resp negative) weights. In the following Lemma, we consider the more general case of a subtorus $\mathbb{C}^* \subset \mathbb{T}^3$, which is then determined by the separation of M into the half spaces $M^{>0}$ (resp $M^{<0}$) of positive (resp negative) weights:

Lemma 7.4.1. *i) For D the divisor corresponding to the corner p of the toric diagram lying between the two sides z, z', if $\lambda_z \in M^{>0}$ and $\lambda_{z'} \in M^{>0}$:*

$$\mathcal{M}^+_{Q_D,W_D,d} = \mathcal{M}_{Q_D,W_D,d} \tag{7.4.1}$$

ii) If $\lambda_{\tilde{z}} \in M^{<0} \iff \tilde{z} \in [z, z']$, then:

$$\begin{aligned} \mathcal{M}^{\theta,ss,+}_{Q,W,d} &= \mathcal{M}^{\theta,ss,[z,z'[:N}_{Q,W,d} \\ \mathcal{M}^{+}_{Q_i,W,d} &= \mathcal{M}^{[z,z']:N}_{Q_i,W,d} \end{aligned} \tag{7.4.2}$$

Proof. Consider the set C of cycles of Q (resp Q_f) of length less than $\sum_{i\in Q_0} d_i$, and consider the map:

$$\begin{aligned} Tr :& \mathcal{M}^{\theta,ss}_{Q,d} \to \mathbb{C}^C \\ & V \hookrightarrow (Tr(w))_{w\in C} \end{aligned} \tag{7.4.3}$$

and the same map for $\mathcal{M}_{Q_f,d}$. From general geometric invariant theory (see [Kin94b]), these maps are projective, hence:

$$\begin{aligned} \mathcal{M}^{\theta,ss,\pm}_{Q,d} &= Tr^{-1}(\mathbb{C}^C)^{\pm} \\ \mathcal{M}^{\pm}_{Q_f,d} &= Tr^{-1}(\mathbb{C}^C)^{\pm} \end{aligned} \tag{7.4.4}$$

i.e. the attracting (resp repelling) variety is the variety of representations where the cycles in $M^{<0}$ are nilpotent.

From [Moz09, Corrolary 3.6], M^+, the lattice of weights of cycles of Q, is saturated in the cone $M^+_{\mathbb{Q}}$ which is the convex hull of the rays with direction $\lambda_{\tilde{z}}$, for $\tilde{z}$ a side of the toric diagram. For $w \in M^+$, there are then sides of the toric diagram z_i and integers $n, n_i \in \mathbb{N}^*$ such that $w^n = \prod_i (v^z)^{n_i}$. In particular, $w \in M^{<0}$ if and only if there is a z_i such that $\lambda_{z_i} \in M^{<0}$, and w is nilpotent in a critical representation if and only if there is a z_i which is nilpotent. Then in a critical representation the property "$w \in M^{<0} \iff w$ is nilpotent" is equivalent to "$\lambda_z \in M^{<0} \iff v^z$ is nilpotent". Hence if $l_{\tilde{z}} \in M^{<0} \iff \tilde{z} \in [z, z']$, one has *ii)*:

$$\begin{aligned} \mathcal{M}^{\theta,ss,+}_{Q,W,d} &= \mathcal{M}^{\theta,ss,[z,z']:N}_{Q,W,d} \\ \mathcal{M}^{+}_{Q_i,W,d} &= \mathcal{M}^{[z,z']:N}_{Q_i,W,d} \end{aligned} \tag{7.4.5}$$

Because each arrow of I acts trivially on P_D, only the subcone $M^+_{\mathbb{Q}} \cap \bar{\chi_I}^{-1}(0)$ acts non-trivially in a framed representation of (Q_D, W_D), hence $v^{z''}$ acts trivially for $z'' \neq z, z'$, from which we deduce *i)*. □

Corollary 7.4.2. *For any dimension vector d and stability parameter θ, one has:*

$$\Omega_{\theta,d}^{[z,z'[:N} = \mathbb{D}(\Omega_{\theta,d}^{[z',z[:N}) \tag{7.4.6}$$

Here $\mathbb{D}$ denotes the Poincaré duality at the level of monodromic mixed Hodge structures.

Proof. Consider a $\mathbb{C}^*$ action scaling all the arrows of the quiver, such that $\lambda_{\tilde{z}} \in M^{<0} \iff \tilde{z} \in [z, z'[$ (such an action exists because M^+ is convex). Hence from Corollary 7.4.2:

$$\begin{aligned} \mathcal{M}_{Q,d}^{\theta,ss,+} &= \mathcal{M}_{Q,d}^{\theta,ss,[z,z'[:N} \\ \mathcal{M}_{Q,d}^{\theta,ss,-} &= \mathcal{M}_{Q,d}^{\theta,ss,[z',z[:N} \end{aligned} \tag{7.4.7}$$

Then denoting by $q : \mathcal{M}_{Q,d}^{\theta,ss,0} \to *$ the projection to a point, one obtains (similar arguments were used in [Dav16, Prop 7.9]):

$$\begin{aligned} \mathbb{D}(\Omega_{\theta,d}^{[z',z[:N}) &= \mathbb{D}H_c(\mathcal{M}_{Q,d}^{\theta,ss,-}, \phi_W \mathcal{IC}_{\mathcal{M}_{Q,d}^{\theta,ss}}) \\ &= \mathbb{D}q_!(p^-)_!(\eta^-)^* \phi_W \mathcal{IC}_{\mathcal{M}_{Q,d}^{\theta,ss}} \\ &= q_!(p^+)_!(\eta^+)^* \mathbb{D}\phi_W \mathcal{IC}_{\mathcal{M}_{Q,d}^{\theta,ss}} \\ &= q_!(p^+)_!(\eta^+)^* \phi_W \mathcal{IC}_{\mathcal{M}_{Q,d}^{\theta,ss}} \\ &= H_c(\mathcal{M}_{Q,d}^{\theta,ss,+}, \phi_W \mathcal{IC}_{\mathcal{M}_{Q,d}^{\theta,ss}}) \\ &= \Omega_{\theta,d}^{[z,z'[:N} \end{aligned} \tag{7.4.8}$$

Here we have used the definitions of the BPS invariants and the characterization of the attracting and repelling varieties in the first and last lines, the fact that $q_! = q_*$ because q is projective, and Braden's contraction Lemma of [Bra02] in its form [Ric16, Theo B] using the fact that $\phi_W \mathcal{IC}_{\mathcal{M}_{Q,d}^{\theta,ss}}$ is $\mathbb{C}^*$-equivariant in the third line, and the self-duality of the vanishing cycles functor and the intersection complex in the fourth line. □

We will now describe the fixed points of the action of $\mathbb{T}^2$, the torus leaving the potential invariant, on $\mathcal{M}_{Q_f,W_f,d}$. The action of the torus $\mathbb{T}^3$ scaling the arrows of the quiver by leaving the potential invariant induces a Λ-grading on J_{Q_f,W_f}, and P_f has a Λ-grading as an J_{Q_f,W_f}-module, i.e.

$$a.(P_f)_\lambda \subset (P_f)_{\lambda + \mathrm{wt}(a)} \ , \quad \text{for } \lambda \in \Lambda \tag{7.4.9}$$

A path which does not vanish in P_i (resp. P_D) is of the form vp, with v a path of Q, and two paths with he same Λ-weights agree in $J_{Q,W}$, then $(P_i)_\lambda$ (resp. $(P_D)_\lambda$) is at most one dimensional for $\lambda \in \Lambda$. We define the Empty Room (ERC) Configuration Δ_f as the subset of Λ such that $(P_f)_\lambda$ is not empty, hence one dimensional. One calls the elements of $\lambda \in \Delta_f$ such that $d_1(\lambda) = i$ the atoms of color i of the ERC. One denotes $\lambda \leq \mu$ for $\lambda, \mu \in \Lambda$ if there exist $v \in \mathbb{C}Q_f$ such that $\mu = \lambda + \mathrm{wt}(v)$. The relation $\leq$ is manifestly reflexive and transitive. If $\lambda \leq \mu \leq \lambda$, then there are paths $v, w \in \mathbb{C}Q_f$ such that $\mathrm{wt}(v) + \mathrm{wt}(w) = 0$, i.e. wv has Λ weight 0, then from [MR08, Prop 4.8] wv is trivial in $\mathbb{C}Q$, and then $w : j \to i$ is trivial in $\mathbb{C}Q_f$, giving $\lambda = \mu$: $\leq$ is then anti-symmetric. Thus $\leq$ defines a poset structure on Δ_f.

We denote by Π_f the set of finite ideals of Δ_f, i.e. subsets $\pi \subset \Delta_f$ such that $x \leq y, y \in \pi \Rightarrow x \in \pi$. For $\pi \in \Pi_f$ we denote by $d_\pi \in \mathbb{N}^{Q_0}$ the dimension vector such that $(d_\pi)_i$ gives the number of atoms of color i in π. Those posets can be visualized in three dimension by choosing a quasi-inverse $\Lambda \to M$ of the embedding $M \hookrightarrow \Lambda$. In the D6 brane framing case, Δ_i can be seen as a three-dimensional pyramid with atom i on the top which is the dual of the toric fan of X, with each atom being obtained by a path of the quiver. In the D4-brane framing case, the action of the relation arrow $q : j \to \infty$ and of all the arrows of I are trivial on P_D: consider the quiver with relations $(Q_I, \partial_I W)$, where one has removed the arrows of I and enforced the relations $\partial_a W$ for $a \in I$. Hence Δ_D can be seen as a facet of the pyramid Δ_i, which is the dual of the ray of the toric fan supporting the corner of the toric diagram corresponding to d, obtained by considering only paths of $(Q_I, \partial_I W)$ starting at i.

Lemma 7.4.3. *The $\mathbb{T}^2$-fixed variety $\mathcal{M}^{\mathbb{T}^2}_{Q_f,W_f,d}$ is an union of isolated points, which are in natural bijection with the set of d-dimensional pyramids in Π_f.*

Proof. As in [MR08, Theo 2.4], f-cyclic representations fixed by a torus actions are quotients of P_f by an ideal ρ which i homogeneous under this torus action, hence the elements of $\mathcal{M}^{\mathbb{T}^2}_{Q_f,W_f,d}$ are the quotients P_f/ρ for ρ $\Lambda_f/\mathbb{Z}\kappa$-homogeneous.

It was shown in [MR08, Rem 4.10] that any path $v : i \to \iota$ of Q can be written in $\mathbb{C}Q/\partial W$ as $w^n v_0$, for $v_0 : i \to \iota$ a minimal path of the unframed quiver, $w : \iota \to \iota$ an arbitrary cycle of the potential W, and $n \in \mathbb{N}$. Recall that any cycle of W contains an arrow of I, and then has a trivial action on P_D. Then for $\iota \in Q_0$, $l \in \Lambda/\mathbb{Z}\kappa$ (resp. $l \in \Lambda/\mathbb{Z}\kappa$) such that $(P_i)_l$ (resp. $(P_D)_l$) is not empty, one has:

$$\begin{aligned}(P_D)_l &= \langle v_0 p \rangle \\ (P_i)_l &= \langle (w^n v_0 p)_{n\in\mathbb{N}} \rangle \end{aligned} \tag{7.4.10}$$

with $v_0 : i \to \iota$ a minimal path of the periodic quiver and $w : \iota \to \iota$ a cycle of W. Consider $\rho = \bigoplus_l \rho_l$ a $\Lambda/\mathbb{Z}\kappa$ homogeneous submodule of P_i (resp. of P_D) with finite codimension. For a 'D4 brane' framing ρ_l is automatically $\mathbb{Z}\kappa$-homogeneous, and then $\rho = \bigoplus_l \rho_l$ is Λ-homogeneous. For z a side of the toric diagram, $Tr((v^z)^n)$ is scaled by $\mathbb{T}^2$, hence vanish on a $\mathbb{T}^2$-fixed point, i.e. v^z is nilpotent on a $\mathbb{T}^2$-fixed point. Because M^+ is saturated in $M_{\mathbb{Q}}$, there is an $n \in \mathbb{N}^*$ such that w^n can be expressed as a product of v^z, then w is itself nilpotent on a $\mathbb{T}^2$-fixed point. In particular $\rho_l = \langle (w^n v_0 p)_{n \geq N} \rangle$ for $N \in \mathbb{N}$, hence it is $\kappa\mathbb{Z}$-homogeneous, therefore ρ,is Λ-homogeneous. Hence:

$$\mathcal{M}^{\mathbb{T}^2}_{Q_f,W_f,d} = \mathcal{M}^{\mathbb{T}^3}_{Q_f,W_f,d} \tag{7.4.11}$$

and $\mathbb{T}^2$-fixed points corresponds to quotients P_f/ρ with ρ Λ-homogeneous. A Λ-homogeneous submodule ρ with codimension $(1, d)$ of P_f is then a sum of graded components of P_f (recall that $(P_f)_\lambda$ is at most one dimensional):

$$\rho = \bigoplus_{\lambda \notin \pi} (P_f)_\lambda \tag{7.4.12}$$

The condition that ρ is a submodule is equivalent, by construction of the poset structure on Δ_f, to the condition that π is an ideal of Δ_f, and we have $d_\pi = d$. There is then a natural bijection between the set of Λ_f-homogeneous submodule of P_f with finite codimension (which by *iii*) in the assumption is equal to the set of $\Lambda/\mathbb{Z}\kappa$-homogeneous submodule of P_f with finite codimension) and Π_f. □

7.4.2 The tangent-obstruction complex

We have seen that representations in $\mathcal{M}^{\mathbb{T}^3}_{Q_f,d}$ are Λ-graded. For $i \in Q_0$, there is a tautological sheaf V_i on the moduli space of representations, whose stalk at each points corresponding to a representation V is the vector space V_i at the node i. The restriction of these tautological sheaves on $\mathcal{M}^{\mathbb{T}^3}_{Q_f,d}$ are then Λ-graded. The restriction $T_{\mathcal{M}_{Q_f,d}}|_{\mathcal{M}^{\mathbb{T}^3}_{Q_f,d}}$ of the tangent space of $\mathcal{M}_{Q_f,d}$ at $\mathcal{M}^{\mathbb{T}^3}_{Q_f,d}$ as a $\mathbb{T}^3$-equivariant structure. Denoting by t^a the $\mathbb{T}^3$-equivariant line bundle with weight a, the $\mathbb{T}^3$-equivariant tangent space on $\mathcal{M}^{\mathbb{T}^3}_{Q_f,\pi}$ is the cokernel of the map of fiber bundles:

$$S^0_\pi \xrightarrow{\delta_0} S^1_\pi \tag{7.4.13}$$

Where:

- The fiber bundle S^0_π is the space of infinitesimal gauge transformations δg_i (we denote for convenience $\delta g_i = 0$ for i a framing node):

$$S^0_\pi = \bigoplus_{i \in Q_0} \mathrm{Hom}_{\mathbb{C}}(V_i, V_i) \tag{7.4.14}$$

- S^1_π is the space of infinitesimal deformations of the arrows (δa):

$$S^1_\pi = \bigoplus_{(a:i\to j)\in(Q_f)_1} \mathrm{Hom}_{\mathbb{C}}(V_i, V_j) \otimes t^a \tag{7.4.15}$$

- The differential δ_0 is the linearization of gauge transformations (taking care of the fact that framing nodes are not gauged):

$$\delta_0 : (\delta g_i)_{i\in Q_0} \mapsto (\delta g_j a - a \delta g_i)_{(a:i\to j)\in(Q_f)_1} \tag{7.4.16}$$

Notice that this complex is in fact M-graded.

For a torus $\mathbb{C}^* \subset \mathbb{T}^2$ leaving the potential invariant, the attracting and repelling behaviour of the action near the fixed component can be studied using this complex. The signed number of weights in $L^{>0}$ (resp in L^0, resp in $L^{<0}$) in this complex gives the number d^+_π (resp d^0_π, resp d^-_π) of contracting (resp invariant, resp repelling) weights in $T_{\mathcal{M}_{Q_f,d}}|_{\mathcal{M}^{\mathbb{T}^3}_{Q_f,d}}$. We define then, following the notations used in K-theoretic Donaldson-Thomas theory:

$$\mathrm{Ind}^s_\pi := d^+_\pi - d^-_\pi \tag{7.4.17}$$

here we have insisted on the dependency on the slope s. Notice that the $\mathbb{T}^3$-equivariant structure of S^0_π is self-dual, hence the number of contracting and repelling weights in S^0_π are equal: to compute Ind^s_π, it suffice then to compute the difference between the number of contracting and repelling weights in S^1_π.

Remark 7.4.4. The weights of the cycles given by the subtorus $\mathbb{C}^* \subset \mathbb{T}^2$ must be integers, hence the line separating L^0 must be directed by an element of the lattice L. The general procedure to obtain a localization result is, for a given dimension vector, to choose a slope generic for this dimension vector, i.e. such that the only weight of L^0 appearing in the tangent complex is 0, and then such that the fixed points of $\mathbb{C}^*$ are the fixed points of $\mathbb{T}^2$. Then rigorously to compute the generating series of framed invariants one must consider a family of slope $(s_d)_d$, one for each dimension vector. To avoid heavy notations, we consider slopes s with irrational coefficients, hence such that $L^0 = \{0\}$, which we call generic slopes. For a given dimension vector d, we establish then the localization result by choosing a rational slope s_d generic for d and approximating s, i.e. such that all the weights appearing in the tangent space, and also the weights l_z of the cycles v^z, have the same contracting and repelling behaviour under the slopes s and s_d.

$\mathcal{M}_{Q_f,W_f,d}$ is the critical locus of the potential $Tr(W_f)$ inside the smooth scheme $\mathcal{M}_{Q_f,d}$. The derivative of $Tr(W_f)$ gives then a duality between the tangent directions and the obstructions of $\mathcal{M}_{Q_f,W_f,d}$, it is then a $[-1]$-shifted symplectic scheme in the language of derived geometry. The Hessian of $Tr(W_f)$ defines then the tangent-obstruction complex:

$$0 \to T_{\mathcal{M}_{Q_f,d}} \to T^*_{\mathcal{M}_{Q_f,d}} \to 0 \tag{7.4.18}$$

One of the main idea of derived geometry is to replace the tangent space, which behaves not very well for singular spaces, by the tangent-obstruction complex, which behaves here far better. The tangent-obstruction complex of $\mathcal{M}_{Q_f,W_f,d}$ restricted to $\mathcal{M}^0_{Q_f,W_f,d}$ has also a $\mathbb{T}^3$-equivariant structure, and the obstructions spaces and tangent spaces are dual as $\mathbb{T}^2$-equivariant fiber bundles (but not as $\mathbb{T}^3$-equivariant fiber bundles). Hence d^-_π, the number of repelling weights in the tangent space is also the number of contracting weights in the obstruction space. Then Ind^s_π is the signed number of contracting weights in the tangent obstruction complex.

7.4.3 Derived Białynicki-Birula decomposition

Theorem 7.4.5. *i) For D a non-compact divisor of X, corresponding to the corner p of the toric diagram lying between the two sides z, z', and a generic slope s such that $l_z, l_{z'} \in L^{>0}$ (such slopes always exist, because the angle between l_z and $l_{z'}$ is smaller than π), we have:*

$$Z_D(x) = \sum_{\pi \in \Pi_D} \mathbb{L}^{\mathrm{Ind}^s_\pi/2} x^{d_\pi} \tag{7.4.19}$$

ii) For a generic slope s such that $l_{\tilde{z}} \in L^{<0} \iff \tilde{z} \in [z, z']$, one has:

$$Z_i(x) = S_{-i}[\mathrm{Exp}\left(\textstyle\sum_d \Delta^s \Omega_d \frac{\mathbb{L}^{d_i}-1}{\mathbb{L}^{1/2}-\mathbb{L}^{-1/2}} x^d\right)] \sum_{\pi \in \Pi_i} \mathbb{L}^{\mathrm{Ind}^s_\pi/2} x^{d_\pi} \tag{7.4.20}$$

Using the correction term:

$$\begin{aligned}\Delta^s\Omega(x) =& (\mathbb{L}^{3/2} + (\textstyle\sum_{\tilde{z}\in[z,z']} K_{\tilde{z}} - 2)\mathbb{L}^{1/2} - (\sum_{\tilde{z}\in[z,z']} K_{\tilde{z}} - 1)\mathbb{L}^{-1/2}) \sum_{n\geq 1} x^{n\delta} \\ &+ (\mathbb{L}^{1/2} - \mathbb{L}^{-1/2}) \sum_{\tilde{z}\in[z,z']} \sum_{k\neq k'} \sum_{n\geq 0} x^{n\delta + \alpha^{\tilde{z}}_{[k,k'[}}\end{aligned} \tag{7.4.21}$$

Proof. Consider the correspondence coming from the $\mathbb{C}^*$ action on the smooth scheme $\mathcal{M}_{Q_f,d}$:

$$\mathcal{M}_{Q_f,d} \xleftarrow{p^+} \mathcal{M}^+_{Q_f,d} \xrightarrow{\eta^+} \mathcal{M}^0_{Q_f,d}$$

Consider the connected component $\mathcal{M}^0_{Q_f,\pi}$ of $\mathcal{M}^0_{Q_f,d}$ containing the $\mathbb{C}^*$-fixed representation corresponding to the pyramid $\pi \in \Pi_f$. The tangent space of $\mathcal{M}_{Q_f,d}$ at $\mathcal{M}^0_{Q_f,\pi}$ has d^+_π contracting weights, d^0_π invariant weights and d^-_π repelling weights, with:

$$\begin{aligned} \dim(\mathcal{M}_{Q_f,d}) &= d^+_\pi + d^0_\pi + d^-_\pi \\ \dim(\mathcal{M}^0_{Q_f,\pi}) &= d^0_\pi \\ \mathrm{Ind}^s_\pi &= d^+_\pi - d^-_\pi \end{aligned} \tag{7.4.22}$$

then from Białynicki-Birula [BB73], $\mathcal{M}^+_{Q_f,d}$ is a disjoint union of affine fiber bundles $p^+_\pi : \mathcal{M}^+_{Q_f,\pi} \to \mathcal{M}^0_{Q_f,\pi}$ of dimension d^+_π, and the fixed components are smooth of dimension d^0_π, hence using the hyperbolic localization functor:

$$\begin{aligned} (p^+)_!(\eta^+)^*\mathcal{IC}_{\mathcal{M}_{Q_f,d}} &= \bigoplus_{\pi\in\Pi_f | d_\pi = d} (p^+_\pi)_! \mathbb{Q}_{\mathcal{M}^+_{Q_f,\pi}}[d^+_\pi + d^0_\pi + d^-_\pi] \\ &= \bigoplus_{\pi\in\Pi_f | d_\pi = d} \mathbb{Q}_{\mathcal{M}^0_{Q_f,d}}[-d^+_\pi + d^0_\pi + d^-_\pi] \\ &= \bigoplus_{\pi\in\Pi_f | d_\pi = d} \mathbb{L}^{\mathrm{Ind}^s_\pi/2}\mathcal{IC}_{\mathcal{M}^0_{Q_f,\pi}} \end{aligned} \tag{7.4.23}$$

Here we have used the fact that $\mathcal{M}_{Q_f,d}$ and $\mathcal{M}^0_{Q_f,\pi}$ are smooth in the first and last line, and the fact that p^+ is an affine fiber bundle in the second line. This isomorphism lift to an isomorphism of mixed Hodge modules. We denote now by ϕ_{W^0} the vanishing cycles functor of the restriction $\mathrm{Tr}(W)|_{\mathcal{M}^0_{Q_f,d}}$. The natural functoriality of the vanishing cycle functor gives a morphism $(p^+)_!(\eta^+)^*\phi_W \to \phi_{W^0}(p^+)_!(\eta^+)^*$, which lifts to a morphism of monodromic mixed Hodge modules. Then, because $\mathcal{IC}_{\mathcal{M}_{Q_f,d}}$ is $\mathbb{C}^*$-equivariant, [Ric16, theo 3.3] gives that:

$$(p^+)_!(\eta^+)^*\phi_W\mathcal{IC}_{\mathcal{M}_{Q_f,d}} \to \phi_{W^0}(p^+)_!(\eta^+)^*\mathcal{IC}_{\mathcal{M}_{Q_f,d}} \tag{7.4.24}$$

is an isomorphism at the level of perverse sheaves. Because the fact of being an isomorphism can be checked at the level of the underlying perverse sheaves, it is also an isomorphism of monodromic mixed Hodge modules. Hence one obtains, denoting by $q : \mathcal{M}^0_{Q_f,d} \to *$ the projection to a point:

$$\begin{aligned} [\mathcal{M}^+_{Q_f,d}]^{vir} &= H_c(\mathcal{M}^+_{Q_f,d}, \phi_W\mathcal{IC}_{\mathcal{M}_{Q_f,d}}) \\ &= q_!(p^+)_!(\eta^+)^*\phi_W\mathcal{IC}_{\mathcal{M}_{Q_f,d}} \\ &= q_!\phi_{W^0}(p^+)_!(\eta^+)^*\mathcal{IC}_{\mathcal{M}_{Q_f,d}} \\ &= \bigoplus_{\pi\in\Pi_f | d_\pi = d} \mathbb{L}^{\mathrm{Ind}^s_\pi/2} q_!\phi_{W^0}\mathcal{IC}_{\mathcal{M}^0_{Q_f,\pi}} \\ &= \bigoplus_{\pi\in\Pi_f | d_\pi = d} \mathbb{L}^{\mathrm{Ind}^s_\pi/2} H_c(\mathcal{M}^0_{Q_f,\pi}, \phi_{W^0}\mathcal{IC}_{\mathcal{M}^0_{Q_f,\pi}}) \end{aligned} \tag{7.4.25}$$

Here we have used (7.4.24) in the third line and (7.4.23) in the fourth line. The perverse sheaf $\phi_{W^0}\mathcal{IC}_{\mathcal{M}^0_{Q_f,\pi}}$ is supported on the critical locus of $\mathrm{Tr}(W)|_{\mathcal{M}^0_{Q_f,\pi}}$, which is just a single point, the representation associated to π. Hence the cohomology of the vanishing cycle on this point is just the Milnor number of this point, which is 1 from [BF08, Prop 3.3], i.e. :

$$[\mathcal{M}^+_{Q_f,d}]^{vir} = \bigoplus_{\pi\in\Pi_f|d_\pi=d} \mathbb{L}^{\mathrm{Ind}^s_\pi/2} \tag{7.4.26}$$

Now using the Lemma 7.4.1, one obtains in the case i):

$$\begin{aligned} Z_D(x) :&= \sum_d [\mathcal{M}^+_{Q_D,d}]^{vir} x^d \\ &= \bigoplus_{\pi\in\Pi_f} \mathbb{L}^{\mathrm{Ind}^s_\pi/2} x^{d_\pi} \end{aligned} \tag{7.4.27}$$

And in the case ii):

$$\begin{aligned} Z_i^{[z,z']:N}(x) :&= \sum_d [\mathcal{M}^+_{Q_i,d}]^{vir} x^d \\ &= \bigoplus_{\pi\in\Pi_f} \mathbb{L}^{\mathrm{Ind}^s_\pi/2} x^{d_\pi} \end{aligned} \tag{7.4.28}$$

Because $\sum_d \Delta^s\Omega_d x^d = \Omega_\theta(x) - \Omega_\theta^{[z,z']:N}(x)$ lies in the center of the quantum affine space, one has:

$$\mathcal{A}(x) = \mathrm{Exp}(\sum_d \frac{\Delta^s\Omega_d}{\mathbb{L}^{1/2}-\mathbb{L}^{-1/2}} x^d)\mathcal{A}^{[z,z']:N}(x) \tag{7.4.29}$$

And using Proposition 7.3.7:

$$\begin{aligned} Z_i(x) =& S_i(\mathcal{A}(x))S_{-i}(\mathcal{A}(x)^{-1}) \\ =& S_i(\mathrm{Exp}(\textstyle\sum_d \frac{\Delta^s\Omega_d}{\mathbb{L}^{1/2}-\mathbb{L}^{-1/2}} x^d)\mathcal{A}^{[z,z']:N}(x))S_{-i}((\mathrm{Exp}(\textstyle\sum_d \frac{\Delta^s\Omega_d}{\mathbb{L}^{1/2}-\mathbb{L}^{-1/2}} x^d)\mathcal{A}^{[z,z']:N}(x))^{-1}) \\ =& S_i(\mathrm{Exp}(\textstyle\sum_d \frac{\Delta^s\Omega_d}{\mathbb{L}^{1/2}-\mathbb{L}^{-1/2}} x^d))S_{-i}(\mathrm{Exp}(-\textstyle\sum_d \frac{\Delta^s\Omega_d}{\mathbb{L}^{1/2}-\mathbb{L}^{-1/2}} x^d))S_i(\mathcal{A}^{[z,z']:N}(x))S_{-i}(\mathcal{A}^{[z,z']:N}(x)^{-1}) \\ =& S_{-i}[\mathrm{Exp}\left(\textstyle\sum_d \Delta^s\Omega_d \frac{\mathbb{L}^{d_i}-1}{\mathbb{L}^{1/2}-\mathbb{L}^{-1/2}} x^d\right)] Z_i^{[z,z']:N}(x) \end{aligned} \tag{7.4.30}$$

Here we have used once more in the third line the fact that $\sum_d \Delta^s\Omega_d x^d$ lies in the center of the quantum affine space. □

7.4.4 Link with K-theoretic computations

The localization formula (7.4.26) is very similar to the localization formula for K-theoretic invariants defined in [NO16]. Those invariants are defined for projective spaces with symmetric obstruction theories, hence in particular for projective critical locus of a potential on a smooth space, and are expected to give the χ_y genus of the Hodge polynomial coming from cohomological invariants. Consider a moduli space M which is the critical locus of a potential, with a $\mathbb{C}^*$-action leaving the

potential invariant (the choice of such an action is called a choice of slope s in K-theoretic theory). We denote the attracting variety by M^+ and the fixed components of this $\mathbb{C}^*$-action by M^0_π for $\pi \in \Pi$, and denotes as before by Ind^s_π the signed number of contracting weight in the restriction of the tangent-obstruction complex of M at M^0_π. The same reasoning that leads to (7.4.26) gives:

$$[M^+]^{vir} = \bigoplus_{\pi\in\Pi} \mathbb{L}^{\mathrm{Ind}^s_\pi/2}[M^0_\pi]^{vir} \tag{7.4.31}$$

In fact, the author proved in [Des22] that this formula holds also when M is a [-1]-shifted symplectic scheme or stack, i.e. is locally described as the critical locus of a potential. If M is projective, $M^+ = M$, and then taking the χ_y-genus gives:

$$\chi_y([M]^{vir}) = \sum_{\pi\in\Pi} (-y)^{\mathrm{Ind}^s_\pi} \chi_y([M^0_\pi]^{vir}) \tag{7.4.32}$$

It is exactly the localization formula of K-theoretic invariants from [NO16, Sec 8.3]. It can be applied to cases of framed quiver with potential when the moduli space is projective, for example when the Empty Room Configuration has a finite number of atoms, as in [CKK14] and [Cir20]

It was proposed to define K-theoretic invariants by the formula (7.4.32) when M^0 is projective, but M is potentially non-projective. However this definition depends on the choice of slope, i.e. on the choice of $\mathbb{C}^*$ action. This dependency is explained by the formula (7.4.31), because the attracting variety depends on the slope. For toric Calabi-Yau threefolds, the dependency of K-theoretic invariants of framed sheaves was studied in [Arb19, Prop 3.3], and it was established that the K-theoretic invariants change only when a toric coordinates becomes attracting or repelling. Framed sheaves corresponds with D6-framed representations of the toric quiver with potential, and the cycles v^z are scaled as the toric coordinates of the quiver. Hence [Arb19, Prop 3.3] is coherent with the formula (7.4.31), because the attracting variety changes only when a weight λ_z becomes attracting or repelling. Hence Theorem 7.4.5 explains the discrepancy between K-theoretic and cohomological/motivic invariants observed for toric quivers, as we will check in several cases in Section 7.5.1.

7.5 Examples of toric quivers

In this section, we compare our results with the known BPS invariants for local curves, i.e. when the number i of internal lattice points in the toric diagram vanishes, and spell out our results and Conjecture 7.3.9 for local toric surfaces, i.e. for $i = 1$.

7.5.1 Local curves

In those cases, the quantum affine space is commutative, there is no wall crossing, i.e. the BPS invariants are independent of θ. The generating series of cohomological invariants were explicitly computed. Moreover, depending on the toric diagram, there can be 'preferred slope' as introduced in [IKV09], for which there is many cancellations in Ind^s_π: this index becomes then a sum of simple contributions for each atom of π, and the localization formula gives a closed expression. We show then the agreement between the cohomological computations and the localization computations of [IKV09], corrected as in Theorem 7.4.5.

Figure 7.9: Toric diagram and brane tiling for $\mathbb{C}^3/(\mathbb{Z}_2 \times \mathbb{Z}_2)$

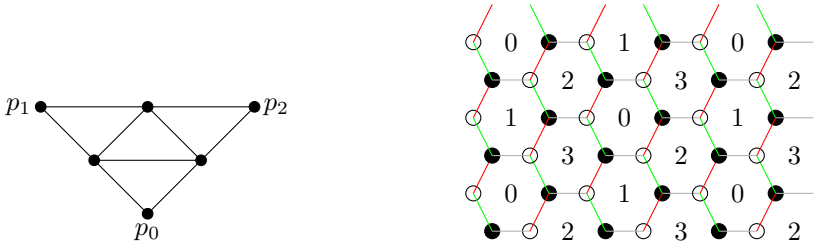

- $\mathbb{C}^3$

The toric diagram of $\mathbb{C}^3$ is given by Figure 7.1. We label by z, z', z'' the three edges of the toric diagram in the clockwise order, and consider a slope s such that $z \in L^{<0}$ and $z', z'' \in L^{>0}$. Then according to the discussion in Section 7.5.2, the refined generating series of framed invariant computed from K-theoretic localization in [NO16, sec 8.3] using the slope s (resp $-s$) correspond in our formalism to the generating series $Z_i^{z:N}$ (resp $Z_i^{z':N,z'':N}$). Then equation the result [NO16, sec 8.3] can be expressed as:

$$\begin{aligned}\Omega^{z:N}(x) &= \mathbb{L}^{1/2} \sum_{n\geq 1} x^{n\delta} \\ \Omega^{z':N,z'':N}(x) &= \mathbb{L}^{-1/2} \sum_{n\geq 1} x^{n\delta}\end{aligned} \tag{7.5.1}$$

Using the correction given in Proposition 7.3.7, one obtains for any of these two choices of slope:

$$\Omega(x) = \mathbb{L}^{3/2} \sum_{n\geq 1} x^{n\delta} \tag{7.5.2}$$

in perfect agreement with the result of [BBS13, Theo 2.7]. Note that the symmetric part vanishes in this case.

- $\mathbb{C}^3/(\mathbb{Z}_2 \times \mathbb{Z}_2)$

The toric diagram and perfect matchings are represented in the Figure 7.9. Each external edge of the toric diagram has two subdivisions. In green and red, we have written the zig-zag path corresponding with the edge $z_{3/2}$ between p_1 and p_2. It divides the quiver into two subquivers Q^0 and Q^1, with nodes $\{0,1\}$ and $\{2,3\}$. The two other external edges give zig-zag paths that are similar but rotated by an angle $\pm 2\pi/3$, dividing the quiver respectively into subquivers with nodes $\{0,3\}$ and $\{1,2\}$, resp. $\{0,2\}$ and $\{1,3\}$. Our computation of the anti-symmetric part of the attractor invariants gives (denoting $x_{i_1 i_2 \dots i_r} = x_{i_1} x_{i_2} \dots x_{i_r}$):

$$\Omega(x) = ((\mathbb{L}^{3/2} + 3\mathbb{L}^{1/2})x^\delta + \mathbb{L}^{1/2}(x_{01} + x_{23} + x_{03} + x_{12} + x_{02} + x_{13})) \sum_{n\geq 0} x^{n\delta} + \Omega^{sym}(x) \tag{7.5.3}$$

It agrees with the result of [MR21, Remark 5.2]:

$$\begin{aligned}\Omega(x) =&((\mathbb{L}^{3/2}+3\mathbb{L}^{1/2})x^{\delta}+\mathbb{L}^{1/2}(x_{01}+x_{23}+x_{03}+x_{12}+x_{02}+x_{13})\\&+1(x_0+x_1+x_2+x_3+x_{123}+x_{230}+x_{301}+x_{012}))\sum_{n\geq 0}x^{n\delta}\end{aligned} \tag{7.5.4}$$

• Other small crepant resolutions:

The other toric small crepant resolutions are resolutions of the zero locus of $XY-Z^{N_0}W^{N_1}$ in $\mathbb{C}^4$. The corresponding toric diagram has a trapezoidal shape with height 1, a lower edge of length N_0, and upper edge of length N_1. A noncommutative resolution of this threefold is determined by a triangulation σ of the toric diagram. The construction of the corresponding quiver and brane tiling is described in [Nag11, sec 1.1]. We enumerate triangles by T_i from the right to the left, for $i\in\mathcal{I}=\mathbb{Z}_N$, for $N=N_0+N_1$ (in particular $b=N+2$), cyclically identifying the right external edge of the toric diagram with the left external edge of the toric diagram. The triangulation defines a bijection:

$$\sigma=(\sigma_x,\sigma_y):I_N=\{0,...,N-1\}\to(I_{N_0}\times\{0\})\cup(I_{N_1}\times\{1\}) \tag{7.5.5}$$

We define:

$$\mathcal{J}=\{i\in\mathcal{I}|\sigma_y(i)=\sigma_y(i+1)\} \tag{7.5.6}$$

which enumerates $i\in\mathcal{I}$ such that triangles T_i and T_{i+1} have adjoint horizontal edges (we consider triangles T_{N-1} and T_0 for $i=N-1$.

We construct then a quiver with nodes $\mathcal{I}$, a pair of bidirectional arrows between successive nodes $i,i+1$, and an edge loop at nodes of $\mathcal{J}$. The corresponding brane tiling is obtained by stacking up layers of the form:

if $i\in\mathcal{I}-\mathcal{J}$, and of the form:

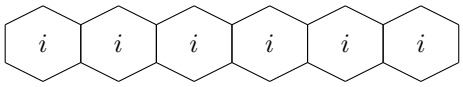

if $i\in\mathcal{I}$.

The zig-zag paths corresponding to the lower (resp. upper) edge of the toric diagram, denoted z^0 (resp. z^1) are given by the border between two successive layers $i-1,i$ such that $\sigma_y(T_i)=0$ (resp. $\sigma_y(T_i)=1$).

As an example, consider the triangulation of Figure 7.10, for $N_0=4$, $N_1=2$, $N=6$: We have $\sigma=((3,0),(2,0),(1,0),(1,1),(0,0),(0,1))$, $\mathcal{I}=\mathbb{Z}_6$, $\mathcal{J}=\{0,1\}$. The corresponding brane tiling is given by Figure 7.11, where we have drawn in red the zig-zag paths $z^1=z_{3/2}$ corresponding to the upper edge between p_1 and p_2, and in blue the the zig-zag paths $z^0=z_{-1/2}$ corresponding to the lower edge between p_3 and p_0.

We can use our evaluation of the anti-symmetric part of the attractor invariants. To this aim we must find all the dimension vectors that are of the form $\alpha^z_{[k,k'[}$, for z a side of the toric

Figure 7.10: Example of triangulation corresponding to a small crepant resolution

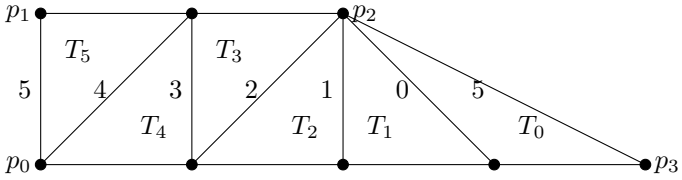

Figure 7.11: Corresponding brane tiling

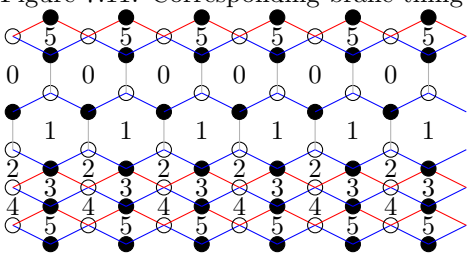

diagram and $k \neq k' \in \mathbb{Z}/K_z\mathbb{Z}$. The left and right external edges of the toric diagram have only one subdivision, i.e. they do not give such roots. According to our description of zig-zag paths corresponding to the above and below side of the toric diagram, such a dimension vector is of the form $d = e_j + e_{j+1} + ... + e_l$, $l+1 \neq j$, (in particular it is in the set of real root Δ_+^{re}), such that the corresponding layers of the brane tiling lie between two zig-zag paths of z^0 or two zig-zag paths of z^1, i.e. such that $\sigma_y(T_j) = \sigma_y(T_{l+1})$. According to our definition of $\mathcal{J}$, this holds if and only if $\sum_{i\notin\mathcal{J}} d_i$ is even. We obtain:

$$\Omega(x) = (\mathbb{L}^{3/2} + (N-1)\mathbb{L}^{1/2}) \sum_{d\in\Delta_+^{im}} x^d + \mathbb{L}^{1/2} \sum_{d\in\Delta_+^{re} | \sum_{i\notin\mathcal{J}} d_i \ even} x^d + \Omega^{sym}(x) \tag{7.5.7}$$

This is in agreement with [MN15, Theo 0.1], upon adding a suitable symmetric correction:

$$\Omega(x) = (\mathbb{L}^{3/2} + (N-1)\mathbb{L}^{1/2}) \sum_{d\in\Delta_+^{im}} x^d + \mathbb{L}^{1/2} \sum_{d\in\Delta_+^{re} | \sum_{i\notin\mathcal{J}} d_i \ even} x^d + 1 \sum_{d\in\Delta_+^{re} | \sum_{i\notin\mathcal{J}} d_i \ odd} x^d \tag{7.5.8}$$

- The conifold

It is a particular case of small crepant resolutions for $N_0 = N_1 = 1$. Then [MMNS12, Theo 1] gives:

$$\Omega(x) = (\mathbb{L}^{3/2} + \mathbb{L}^{1/2}) \sum_{n\geq 1} x^{n\delta} + \sum_{n\geq 0} (x_0 + x_1) x^{n\delta} \tag{7.5.9}$$

We label by z_1, z_2, z_3, z_4 the edges of the toric diagram. When one choose a generic slope, one can consider up to a circular permutation of the sides of the diagram that $z \in L^{<0} \iff z \in [z_1, z_2]$.

By toric localization, one access then to the BPS invariants $\Omega^{[z_1,z_2]:N}(x)$. Every edge has only one subdivision, hence the full and partially invertible invariants are related by:

$$\begin{aligned} \Omega(x) &= (\mathbb{L}^{3/2} - \mathbb{L}^{-1/2}) \sum_{n\geq 1} x^{n\delta} + \Omega^{[z_1,z_2]:N}(x) \\ \Longrightarrow \quad \Omega^{[z_1,z_2]:N}(x) &= (\mathbb{L}^{1/2} + \mathbb{L}^{-1/2}) \sum_{n\geq 1} x^{n\delta} + \sum_{n\geq 0} (x_0+x_1) x^{n\delta} \end{aligned} \tag{7.5.10}$$

It is in agreement with the computations of the refined topological vertex in [IKV09, Sec 5.1], as exposed in [MMNS12, Sec 4.3]. Namely, in [IKV09, Sec 5.1] the refined topological vertex is used to compute the 'PT partition function' which gives access to the invariants $\Omega^{[z_1,z_2]:N}_{(d_1,d_2)}$ for $d_1 > d_2$, hence using symmetries for all the invariants for $d \notin \mathbb{N}\delta$, and those invariants are in agreement with (7.5.10) (and coincide in fact with the motivic invariants Ω_d). The invariants $\Omega^{[z_1,z_2]:N}_{n\delta}$ and $\Omega_{n\delta}$ are different: it explains the observation of [MMNS12, p. 2] hat the motivic and refined computations agree 'up to a subtlety involving the Hilbert scheme of points', and the ambiguity in defining the refinement of the MacMahon function in [DG10].

- $\mathbb{C}^2/(\mathbb{Z}/2\mathbb{Z}) \times \mathbb{C}$

It is a particular case of small toric crepant resolution for $N_0 = 2$ and $N_1 = 0$. Then [MMNS12, Theo 0.1] gives:

$$\Omega(x) = (\mathbb{L}^{3/2} + \mathbb{L}^{1/2}) \sum_{n\geq 1} x^{n\delta} + \mathbb{L}^{1/2} \sum_{n\geq 0} (x_0+x_1) x^{n\delta} \tag{7.5.11}$$

We label by z, z', z'' the edges of the toric diagram, z being the edge with two subdivisions. The slope in [IKV09, Sec 5.3, Fig. 6)b)] gives $z'' \in L^{<0}$ and $z, z' \in L^{>0}$, hence the refined topological gives access to the BPS invariants $\Omega^{[z_1,z_2]:N}$. The edge z'' has only one subdivision, hence:

$$\begin{aligned} \Omega(x) &= (\mathbb{L}^{3/2} - \mathbb{L}^{1/2}) \sum_{n\geq 1} x^{n\delta} + \Omega^{[z_1,z_2]:N}(x) \\ \Longrightarrow \quad \Omega^{[z_1,z_2]:N}(x) &= 2\mathbb{L}^{1/2} \sum_{n\geq 1} x^{n\delta} + \mathbb{L}^{1/2} \sum_{n\geq 0} (x_0+x_1) x^{n\delta} \end{aligned} \tag{7.5.12}$$

It is in agreement with the computations of the refined topological vertex in [IKV09, Sec 5.3].

7.5.2 Toric threefolds with one compact divisors

- Canonical bundle over toric Fano surfaces:

In this case, the toric diagram has one internal lattice point and the only points on the boundary are the corners, i.e. external edges have only one subdivision. Our result gives then:

$$\Omega_*(x) = (\mathbb{L}^{3/2} + (b-2)\mathbb{L}^{1/2} + \mathbb{L}^{-1/2}) \sum_{n\geq 1} x^{n\delta} + \Omega_*^{sym}(x) \tag{7.5.13}$$

The arguments of [BMP20], and explicit computations for small dimension vectors done in [MP20, sec 6], support our Conjecture 7.3.9:

$$\Omega_*(x) = \sum_i x_i + (\mathbb{L}^{3/2} + (b-2)\mathbb{L}^{1/2} + \mathbb{L}^{-1/2}) \sum_{n\geq 1} x^{n\delta} \tag{7.5.14}$$

• Canonical bundle over toric weak Fano surfaces:

In those cases, the toric diagram has one internal lattice point, and its external edges can have various number of subdivisions. For completeness, we will give here our conjectural formula 7.3.9 (which is proven up to a symmetric correction) for those various geometries, using the notations of [HS12] (when there is some misprint in this reference, we use the label of the nodes given in the brane tiling):

∗ F_2 (model 13 of [HS12])

$$\Omega_* = \sum_i x_i + ((\mathbb{L}^{3/2} + 2\mathbb{L}^{1/2} + \mathbb{L}^{-1/2})x^\delta + \mathbb{L}^{1/2}(x_{13} + x_{24})) \sum_{n\geq 0} x^{n\delta} \tag{7.5.15}$$

∗ PdP_2 (model 11 of [HS12])

$$\Omega_* = \sum_i x_i + ((\mathbb{L}^{3/2} + 3\mathbb{L}^{1/2} + \mathbb{L}^{-1/2})x^\delta + \mathbb{L}^{1/2}(x_{12} + x_{345})) \sum_{n\geq 0} x^{n\delta} \tag{7.5.16}$$

∗ PdP_{3b} (model 9 of [HS12])

$$\begin{aligned}
&\textit{phase } a: \quad \Omega_* = \sum_i x_i + ((\mathbb{L}^{3/2} + 4\mathbb{L}^{1/2} + \mathbb{L}^{-1/2})x^\delta + \mathbb{L}^{1/2}(x_{12} + x_{3456})) \sum_{n\geq 0} x^{n\delta} \\
&\textit{phase } b: \quad \Omega_* = \sum_i x_i + ((\mathbb{L}^{3/2} + 4\mathbb{L}^{1/2} + \mathbb{L}^{-1/2})x^\delta + \mathbb{L}^{1/2}(x_{126} + x_{345})) \sum_{n\geq 0} x^{n\delta} \\
&\textit{phase } c: \quad \Omega_* = \sum_i x_i + ((\mathbb{L}^{3/2} + 4\mathbb{L}^{1/2} + \mathbb{L}^{-1/2})x^\delta + \mathbb{L}^{1/2}(x_{1246} + x_{35})) \sum_{n\geq 0} x^{n\delta}
\end{aligned} \tag{7.5.17}$$

∗ PdP_{3c} (model 8 of [HS12])

$$\begin{aligned}
&\textit{phase } a: \quad \Omega_* = \sum_i x_i + ((\mathbb{L}^{3/2} + 4\mathbb{L}^{1/2} + \mathbb{L}^{-1/2})x^\delta + \mathbb{L}^{1/2}(x_{126} + x_{345} + x_{1234} + x_{56})) \sum_{n\geq 0} x^{n\delta} \\
&\textit{phase } b: \quad \Omega_* = \sum_i x_i + ((\mathbb{L}^{3/2} + 4\mathbb{L}^{1/2} + \mathbb{L}^{-1/2})x^\delta + \mathbb{L}^{1/2}(x_{156} + x_{234} + x_{1345} + x_{26})) \sum_{n\geq 0} x^{n\delta}
\end{aligned} \tag{7.5.18}$$

∗ PdP_{3a} (model 7 of [HS12])

$$\begin{aligned}
\Omega_* = \sum_i x_i + ((\mathbb{L}^{3/2} + 4\mathbb{L}^{1/2} + \mathbb{L}^{-1/2})x^\delta + \mathbb{L}^{1/2}(x_{124} + x_{356} + x_{15} + x_{34} + x_{26} \\
+ x_{15}x_{34} + x_{34}x_{26} + x_{26}x_{15})) \sum_{n\geq 0} x^{n\delta}
\end{aligned} \tag{7.5.19}$$

$*$ PdP_{4a} (model 6 of [HS12])

$$\begin{aligned}
&\textit{phase } a: \quad \Omega_* = \sum_i x_i + ((\mathbb{L}^{3/2} = 5\mathbb{L}^{1/2} + \mathbb{L}^{-1/2})x^\delta + \mathbb{L}^{1/2}(x_{137} + x_{2456} + x_{1345} + x_{267}))\sum_{n\geq 0} x^{n\delta} \\
&\textit{phase } b: \quad \Omega_* = \sum_i x_i + ((\mathbb{L}^{3/2} + 5\mathbb{L}^{1/2} + \mathbb{L}^{-1/2})x^\delta + \mathbb{L}^{1/2}(x_{12345} + x_{67} + x_{1237} + x_{456}))\sum_{n\geq 0} x^{n\delta} \\
&\textit{phase } c: \quad \Omega_* = \sum_i x_i + ((\mathbb{L}^{3/2} + 5\mathbb{L}^{1/2} + \mathbb{L}^{-1/2})x^\delta + \mathbb{L}^{1/2}(x_{167} + x_{2345} + x_{1456} + x_{237}))\sum_{n\geq 0} x^{n\delta}
\end{aligned} \tag{7.5.20}$$

$*$ PdP_{4b} (model 5 of [HS12])

$$\begin{aligned}
\Omega_* = &\sum_i x_i + ((\mathbb{L}^{3/2} + 5\mathbb{L}^{1/2} + \mathbb{L}^{-1/2})x^\delta + \mathbb{L}^{1/2}(x_{1234} + x_{567} + x_{17} + x_{26} + x_{345} + x_{17}x_{26} \\
&+ x_{26}x_{345} + x_{345}x_{17}))\sum_{n\geq 0} x^{n\delta}
\end{aligned} \tag{7.5.21}$$

$*$ PdP_5 (model 4 of [HS12])

$$\begin{aligned}
&\textit{phase } a: \quad \Omega_* = \sum_i x_i + ((\mathbb{L}^{3/2} + 6\mathbb{L}^{1/2} + \mathbb{L}^{-1/2})x^\delta + \mathbb{L}^{1/2}(x_{1234} + x_{5678} + x_{1638} + x_{2745} \\
&\qquad + x_{1674} + x_{2385} + x_{1278} + x_{3456}))\sum_{n\geq 0} x^{n\delta} \\
&\textit{phase } b: \quad \Omega_* = \sum_i x_i + ((\mathbb{L}^{3/2} + 6\mathbb{L}^{1/2} + \mathbb{L}^{-1/2})x^\delta + \mathbb{L}^{1/2}(x_{46} + x_{123578} + x_{28} + x_{134567} \\
&\qquad + x_{1568} + x_{2347} + x_{1245} + x_{3678}))\sum_{n\geq 0} x^{n\delta} \\
&\textit{phase } c: \quad \Omega_* = \sum_i x_i + ((\mathbb{L}^{3/2} + 6\mathbb{L}^{1/2} + \mathbb{L}^{-1/2})x^\delta + \mathbb{L}^{1/2}(x_{234} + x_{15678} + x_{368} + x_{12457} \\
&\qquad + x_{278} + x_{13456} + x_{467} + x_{12358}))\sum_{n\geq 0} x^{n\delta} \\
&\textit{phase } d: \quad \Omega_* = \sum_i x_i + ((\mathbb{L}^{3/2} + 6\mathbb{L}^{1/2} + \mathbb{L}^{-1/2})x^\delta + \mathbb{L}^{1/2}(x_{1678} + x_{2345} + x_{1247} + x_{3568} \\
&\qquad + x_{1346} + x_{2578} + x_{1238} + x_{4567}))\sum_{n\geq 0} x^{n\delta}
\end{aligned} \tag{7.5.22}$$

∗ $L_{1,3,1}/\mathbb{Z}_2(0,1,1,1)$ (model 3 of [HS12])

$$\begin{aligned}
\textit{phase a}: \quad \Omega_* = &\sum_i x_i + ((\mathbb{L}^{3/2} + 6\mathbb{L}^{1/2} + \mathbb{L}^{-1/2})x^\delta + \mathbb{L}^{1/2}(x_{1453} + x_{2786} + x_{1756} + x_{2483} \\
&+ x_{18} + x_{37} + x_{2456} + x_{18}x_{37} + x_{37}x_{2456} + x_{2456}x_{18}))\sum_{n\geq 0} x^{n\delta} \\
\textit{phase b}: \quad \Omega_* = &\sum_i x_i + ((\mathbb{L}^{3/2} + 6\mathbb{L}^{1/2} + \mathbb{L}^{-1/2})x^\delta + \mathbb{L}^{1/2}(x_{14253} + x_{678} + x_{17256} + x_{348} \\
&+ x_{18} + x_{237} + x_{456} + x_{18}x_{237} + x_{237}x_{456} + x_{456}x_{18}))\sum_{n\geq 0} x^{n\delta}
\end{aligned} \tag{7.5.23}$$

$\mathbb{C}^3/(\mathbb{Z}_4 \times \mathbb{Z}_2)(1,0,3)(0,1,1)$ (model 2 of [HS12])

$$\begin{aligned}
\Omega_* = &\sum_i x_i + ((\mathbb{L}^{3/2} + 6\mathbb{L}^{1/2} + \mathbb{L}^{-1/2})x^\delta + \mathbb{L}^{1/2}(x_{1458} + x_{2367} + x_{2864} + x_{1753} + x_{12} + x_{34} + x_{56} + x_{78} \\
&+ x_{12}x_{34} + x_{34}x_{56} + x_{56}x_{78} + x_{78}x_{12} + x_{12}x_{34}x_{56} + x_{34}x_{56}x_{78} + x_{56}x_{78}x_{12} + x_{78}x_{12}x_{34}))\sum_{n\geq 0} x^{n\delta}
\end{aligned} \tag{7.5.24}$$

∗ $\mathbb{C}^3/(\mathbb{Z}_3 \times \mathbb{Z}_3)(1,0,2)(0,1,2)$ (model 1 of [HS12])

$$\begin{aligned}
\Omega_* = &\sum_i x_i + ((\mathbb{L}^{3/2} + 7\mathbb{L}^{1/2} + \mathbb{L}^{-1/2})x^\delta + \mathbb{L}^{1/2}(x_{153} + x_{678} + x_{294} + x_{153}x_{678} + x_{678}x_{294} \\
&+ x_{294}x_{153} + x_{189} + x_{237} + x_{456} + x_{189}x_{237} + x_{237}x_{456} + x_{456}x_{189} + x_{126} \\
&+ x_{597} + x_{348} + x_{126}x_{597} + x_{597}x_{348} + x_{348}x_{126}))\sum_{n\geq 0} x^{n\delta}
\end{aligned} \tag{7.5.25}$$

Chapter 8

On the existence of scaling multi-centered black holes

Joint work with Boris Pioline

For suitable charges of the constituents, the phase space of multi-centered BPS black holes in $\mathcal{N} = 2$ four-dimensional supergravity famously exhibits scaling regions where the distances between the centers can be made arbitrarily small, so that the bound state becomes indistinguishable from a single-centered black hole. In this note we establish necessary conditions on the Dirac product of charges for the existence of such regions for any number of centers, generalizing the standard triangular inequalities in the three-center case. Furthermore, we show the same conditions are necessary for the existence of multi-centered solutions at the attractor point. We prove that similar conditions are also necessary for the existence of self-stable Abelian representations of the corresponding quiver, as suggested by the duality between the Coulomb and Higgs branches of supersymmetric quantum mechanics.

8.1 Introduction

In string theory vacua with $\mathcal{N} = 2$ supersymmetry in 3+1 dimensions, determining the exact number of single-particle BPS states with total electromagnetic charge γ and arbitrary values of the moduli z is still a daunting problem. Much progress has been made on computing the BPS index $\Omega(\gamma, z)$, which counts the same states weighted by a sign $(-1)^{2J_3}$, where J_3 is the angular momentum. As a result, $\Omega(\gamma, z)$ becomes independent of the hypermultiplet moduli (in particular, of the string coupling in type II string theories compactified on a Calabi-Yau threefold), but it may still jump across certain codimension-one walls in vector moduli space – a phenomenon known as wall-crossing [DM11a], first identified in the context of supersymmetric gauge theories [SW94] and studied independently in the mathematical literature on Donaldson-Thomas invariants [KS, JS12].

At strong coupling, the jumps of $\Omega(\gamma, z)$ reflect the appearance or disappearance of multi-centered black hole solutions, where the total charge $\gamma = \sum_{i=1}^{n} \gamma_i$ is distributed over n centers with charge γ_i [Den00, DM11a]. The number of configurational bound states of such constituents can be determined by quantizing the phase space of such solutions [dBESMVdB09], providing

a transparent derivation of the wall-crossing formula [MPS11b]. More generally, the knowledge of the number of configurational bound states allows to express the total index $\Omega(\gamma, z)$ in terms of more elementary indices $\Omega_{\rm S}(\gamma_i)$ which count single-centered black holes [MPS11a], or in the context of quiver quantum mechanics, pure-Higgs states [BBdB+12, LWY12, MPS12]. However, this procedure is complicated by the fact that for certain configurations of charges $\{\gamma_i\}$, the space of solutions is non-compact, due to the existence of 'scaling regions' where some of the centers become arbitrarily close to each other, and hard to distinguish from single-centered black holes. The modest goal of this note is to establish some necessary conditions on the charges γ_i for such a scaling region to arise.

The distances between the centers of a multi-centered black hole solution are constrained by Denef's equations [Den00]

$$\forall i = 1 \dots n, \qquad \sum_{j\neq i} \frac{\kappa_{ij}}{r_{ij}} = \zeta_i \tag{8.1.1}$$

where $r_{ij} = |\vec{r}_i - \vec{r}_j|$ and $\kappa_{ij} = \langle \gamma_i, \gamma_j \rangle$ is the Dirac-Schwinger-Zwanziger product of electromagnetic charges, and ζ_i are real parameters determined by the vector multiplet moduli. In order to analyze solutions to (8.1.1), it is useful to introduce the quiver Q, obtained by associating one node i to each center $\vec{r}_i$, and κ_{ij} arrows from node i to node j whenever $\kappa_{ij} > 0$. Indeed, the same equations (8.1.1) describe supersymmetric solutions on the Coulomb branch of the supersymmetric quantum mechanics specified by the quiver Q [Den02]. We assume that the quiver Q is connected, since otherwise the n-body problem reduces to the same problem for each connected component.

When non-empty, the space of solutions to (8.1.1) modulo overall translations, which we denote by S_Q^ζ, is a real symplectic space of dimension $2n-2$ [dBESMVdB09]. For generic non-zero values of ζ_i away from walls of marginal stability, it is easy to see that the maximal distance $r_+ = \sup\{r_{ij}, i<j\}$ is bounded from above, as appropriate for a classical bound state. In contrast, the minimal distance $r_- = \inf\{r_{ij}, i<j\}$ may vanish, due to some regions in S_Q^ζ where a subset of the centers become arbitrarily close to each other [Den02, BWW06, DM11a]. The existence of such 'scaling regions' requires certain conditions on the signs of the Dirac products κ_{ij}, as well as on their magnitude. For example, if the i-th center satisfies $\kappa_{ij} \geq 0$ for all $j \neq i$, or $\kappa_{ij} \leq 0$ for all $j \neq i$, then it is clear from (8.1.1) that the distances r_{ij} cannot be arbitrarily small. Thus, in order for all centers to coalesce at one point, the quiver Q must have no source nor sink. In particular, scaling solutions never exist for $n = 2$ centers. For $n = 3$ centers, it is well-known [BWW06, DM11a] that scaling solutions exist whenever $\kappa_{12}, \kappa_{23}, \kappa_{31}$ have the same sign (say positive) and moreover satisfy the triangular inequalities,

$$\kappa_{12} \leq \kappa_{23} + \kappa_{31}, \quad \kappa_{23} \leq \kappa_{31} + \kappa_{12}, \quad \kappa_{31} \leq \kappa_{12} + \kappa_{23} \tag{8.1.2}$$

In that case, the equations (8.1.1) are solved by setting $r_{ij} = \lambda \kappa_{ij} + \dots$ with $\lambda \to 0$, with the dots corresponding to ζ-dependent corrections which become irrelevant as $\lambda \to 0$.

In general, the existence of scaling regions where all centers coalesce is independent of the parameters ζ_i, and can be analyzed by setting $\zeta_i = 0$ in (8.1.1), obtaining the 'conformal Denef equations'

$$\forall i = 1 \dots n, \qquad \sum_{j\neq i} \frac{\kappa_{ij}}{r_{ij}} = 0 \tag{8.1.3}$$

We refer to solutions of (8.1.3) as 'scaling solutions'. The case where only a subset of the n centers coalesce can be analyzed by restricting (8.1.3) to those centers. We shall also be interested

in solutions of (8.1.1) at the special point $\zeta_i = -\sum_{j\neq i}\kappa_{ij}$, which, as argued in [MPS, AP19a], corresponds to the attractor point z_γ for a black hole with total charge $\gamma = \sum_i \gamma_i$ [FKS95]. At that point, one obtains the 'attractor Denef equations'

$$\forall i = 1\dots n, \qquad \sum_{j\neq i}\kappa_{ij}\left(1+\frac{1}{r_{ij}}\right) = 0 \tag{8.1.4}$$

We denote by S^0_Q and $S^\star_Q$ the set of solutions to (8.1.3) and (8.1.4) modulo overall translations.

We shall now state a set of necessary conditions on κ_{ij} for the existence of solutions to (8.1.3). These conditions follow from geometric constraints on the centers, similarly to the three-center case, and are slightly more general than the conditions that were conjectured (and proven in some special cases) in [BMP21b, §2.3]. Quite remarkably, we shall see that the same conditions follow from the existence of solutions to (8.1.4) at the attractor point. This is in agreement with the expectation that the only multi-centered solutions allowed at the attractor point are scaling solutions [AP19a]. We anticipate that these conditions will prove useful in further studies of black hole micro-states in Calabi-Yau compactifications (see [AP19a, AP19b, AMP20, CMM22] for recent progress in this direction).

The first condition constrains the signs of the Dirac product κ_{ij}, and is easily stated in terms of the quiver Q: the quiver should be *strongly connected*, which means that for any pair of vertices i, j, there should be a path going from i to j and a path going from j to i. In particular, it implies that the n centers cannot be separated into two disjoint groups S and $\bar{S}$ such that all arrows go from S to $\bar{S}$ [MPS] (in particular Q should have no source nor sink).

The second condition constrains the magnitude of the Dirac products κ_{ij}, but requires some additional terminology and notation. Given a quiver Q, let Q_0 be the set of vertices, Q_1 the set of arrows and Q_2 the set of simple oriented cycles. A cut (respectively, a weak cut) is a subset $I \subset Q_1$ of the set of arrows such that each simple oriented cycle $w \in Q_2$ contains exactly (respectively, at most) one arrow. The second condition is that, for any weak cut I, the 'generalized triangular inequalities'

$$|I| \leq |Q_1 - I| \tag{8.1.5}$$

are satisfied, where $|I|$ denotes the number of arrows $i \to j$ in the weak cut I (counted with multiplicity κ_{ij}), and similarly for the complement $Q_1 - I$. In the case where one of these inequalities is saturated, there are no attractor solutions, and if furthermore Q is biconnected (also known as non-separable, see §8.2.2 for the relevant definitions), the only scaling solutions are collinear.

For example, in the special case of a cyclic quiver $v_1 \to v_2 \to \cdots \to v_n \to v_{n+1} = v_1$, each set of arrows $i \to i+1$ provides one possible cut, and the condition (8.1.5) reduces to the well-known conditions

$$\kappa_{n1} \leq \kappa_{12} + \kappa_{23} + \cdots + \kappa_{n-1,n} \tag{8.1.6}$$

and cyclic permutations thereof [MPS12]. More generally, if the quiver admits a cut as well as a cycle passing through all the nodes (which can be taken to be $v_1 \to v_2 \to \cdots \to v_n \to v_1$ at the expense of relabeling the nodes), then the condition (8.1.5) reduces to the conditions $\sum_{i<j}\kappa_{ij} \geq 0$ (and cyclic permutations thereof) conjectured in [BMP21b, §2.3]. We also study a natural generalization of these inequalities in the non-Abelian case, but we show that they cannot hold in full generality.

We further observe that the conditions stated above have a simple interpretation in terms of the Higgs branch of the supersymmetric quantum mechanics associated to the quiver Q with generic

potential W. In that description, BPS states correspond to cohomology classes of the moduli space of stable representations Q satisfying the potential equations $\partial_a W = 0$ for each arrow $a \in Q_1$, where the stability condition is determined by the parameters ζ_i [Den02]. In the attractor (or self-stability) chamber $\zeta^i = -\sum_{j\neq i} \kappa_{ij}$, it is immediate to show that stable representations cannot exist unless Q is strongly connected. Moreover, for a quiver (Q, W) with a cut and a generic potential, every cycle vanishes in any Abelian representation, hence each cycle contains a vanishing arrow. Let I be the set of arrows such that the corresponding chiral fields vanish, and suppose I is a cut [1]. The dimension of the moduli space of stable Abelian representations is then given by

$$\dim_{\mathbb{C}} \mathcal{M}^{\zeta,s}_{Q,W} = |Q_1 - I| - |I| - (|Q_0| - 1) \tag{8.1.7}$$

where the first term corresponds to the non-vanishing chiral fields, the second to the potential constraints induced by the vanishing chiral fields (which can be proven to be independent), and the last term to the quotient by the complexified gauge group $(\mathbb{C}^*)^{Q_0}$ modulo the diagonal $\mathbb{C}^*$ subgroup (which acts trivially). Requiring that the moduli space is not empty for some cut I, hence has positive dimension, we arrive at the inequality

$$|I| \leq |Q_1 - I| - |Q_0| + 1 \tag{8.1.8}$$

In §8.3 we show that the only cut which is compatible with the stability parameters $\zeta^i = -\sum_{j\neq i} \kappa_{ij}$ (corresponding to the attractor or self-stability condition) is the one which minimizes the expected dimension (8.1.7).[2] In that case, the condition (8.1.8) holds for any cut, and produces a stronger[3] version of the condition (8.1.5) on the Coulomb branch. Moreover, we prove Proposition 8.4.10 which says that the same inequality continues to holds when I is a weak cut, as on the Coulomb branch side. We also examine a natural non-Abelian generalization of these inequalities, but conclude that it cannot hold in full generality.

The remainder of this note is organized as follows. In Section 8.2, we derive general constraints for the existence of scaling or attractor solutions on the Coulomb branch of Abelian quivers, and conjecture similar constraints in the non-Abelian case. In Section 8.3 we discuss similar conditions for the existence of self-stable representations, which arise on the Higgs branch of the quiver quantum mechanics at the attractor point. Mathematical proofs of some technical results are relegated to the Appendix.

8.2 Existence of scaling and attractor solutions

In this section, we derive general conditions for the existence of scaling or attractor solutions. The main idea is to reinterpret Denef's equations as current conservation, decompose each current into a sum of positive currents running around the simple cycles, and enforce generalized triangular inequalities on each cycle. In order to implement this idea, we need the notions of biconnectedness, strong connectedness, cuts and R-charge, which we introduce along the way.

[1] In the appendix, we adapt the proof of the final inequalities when this condition is not satisfied, i.e. when there are more vanishing arrows than necessary: in this case, there are less than $|I|$ independent potential constraints

[2] This minimization property was first observed in examples of quivers associated to non-compact Calabi-Yau threefolds in [BMP21a].

[3] The fact that the inequalities for the existence of self-stable representations are stronger than the one for the existence of scaling solutions is consistent with the fact that the contribution of scaling solutions may cancel against the contribution of regular collinear solutions when computing the equivariant Dirac index of the phase space of multi-centered configurations using localisation [MPS13].

8.2.1 Denef's equations as current conservation

Consider a quiver $Q = (Q_0, Q_1)$. Here Q_0 denotes the set of nodes of the quiver, and Q_1 denotes the set of arrows $a : i \to j$ of sources $s(a) = i \in Q_0$ and target $t(a) = j \in Q_0$. Let Q_2 be the set of simple oriented cycles of Q, i.e. oriented cycles passing at most once through each node of Q. Consider the sequence:

$$\mathbb{R}^{Q_2} \xrightarrow{\partial_2} \mathbb{R}^{Q_1} \xrightarrow{\partial_1} \mathbb{R}^{Q_0} \xrightarrow{\partial_0} \mathbb{R} \tag{8.2.1}$$

with ∂_2, ∂_1 and ∂_0 defined by

$$\partial_2(w) = \sum_{a \in w} a \ , \qquad \partial_1(a) = t(a) - s(a) \ , \qquad \partial_0(i) = 1 \tag{8.2.2}$$

It is immediate to check that $\partial_1 \circ \partial_2 = 0$ and $\partial_0 \circ \partial_1 = 0$, so (8.2.1) is a complex[4]. We refer to elements of $\mathbb{R}^{Q_1}$ as 'currents', and elements of $\ker(\partial_1)$ as 'conserved currents'. The complex (8.2.1) is exact at $\mathbb{R}^{Q_0}$ if and only if Q is connected: we shall assume that Q is connected unless otherwise specified.

The Denef equations (8.1.1) for general stability parameters ζ_i can be recast as current conservation by rewriting them as follows:

$$\begin{aligned} \forall\, i \in Q_0 \qquad & \sum_{(a:i\to j)\in Q_1} \frac{1}{r_{ij}} - \sum_{(a:j\to i)\in Q_1} \frac{1}{r_{ij}} = \zeta_i \\ \iff \ & \partial_1 \left((\frac{1}{r_{ij}})_{(a:i\to j)\in Q_1} \right) = (\zeta_i)_{i\in Q_0} \end{aligned} \tag{8.2.3}$$

Assuming (without loss of generality) that the quiver Q is connected, and summing over $i \in Q_0$, it is clear that solutions only exist if $\partial_0((\zeta_i)_{i\in Q_0}) = \sum_{i\in Q_0} \zeta_i = 0$. We can therefore choose $(\chi_a)_{a\in Q_1}$ such that $\partial_1((\chi_a)_{a\in Q_1}) = (-\zeta_i)_{i\in Q_0}$. We define the current λ^χ_a running along the arrow $a : i \to j$ as

$$\lambda^\chi_a := \chi_a + \frac{1}{r_{ij}} \tag{8.2.4}$$

The equations (8.2.3) then amount to conservation $\partial_1(\lambda^\chi) = 0$ of the current λ^χ. For given ζ_i, the χ_a are in general not unique, but for the conformal (resp. attractor) Denef equations there is a canonical choice, namely

$$\lambda^0_a := \frac{1}{r_{ij}} \ , \qquad \lambda^\star_a := 1 + \frac{1}{r_{ij}} \tag{8.2.5}$$

such that the conserved current λ^0 and $\lambda^\star$ are strictly positive. This positivity will be crucial for deriving constraints on the existence of scaling and attractor solutions. This property is preserved for a small perturbation of the attractor stability parameters, obtained by replacing $\lambda^\star_a$ by $1+\delta_a+\frac{1}{r_{ij}}$ with $|\delta_a| \ll 1$.

[4]This complex is related to the cellular homology complex $0 \to \mathbb{R}^{Q_1} \xrightarrow{\partial_1} \mathbb{R}^{Q_0} \to 0$ of the graph considered as a cellular space. The cellular homology group H^0 gives the number of connected components of the graph, see [Hat02, Sec 2.2].

8.2.2 Biconnectedness and strong connectedness

In order to study the existence of conformal or attractor solutions, it will be convenient to decompose the connected quiver Q in two steps: first into biconnected components, and then into strongly connected components.[5]

For the first step, a quiver is said to be biconnected if it cannot be disconnected by removing one node. In general, a quiver can be decomposed into maximal biconnected subquivers called biconnected components joined by a shared node (see Figure 8.1). Consider the unoriented graph K with one node for each biconnected component and one node for each node of the quiver shared between different biconnected components, and an edge between the node i and the biconnected component b if $i \in b$. In lemma 8.4.2 we show that K is a connected tree, i.e. has no cycle. Given a solution of Denef's equations at any stability for each biconnected component, one can join these solutions at shared nodes by identifying the corresponding centers: the fact that K has no cycle ensures that this can be done consistently. According to lemma 8.4.3, a conserved current running on a connected quiver is also conserved on each of its biconnected components, and the converse is also true: a solution of Denef's equations on a connected quiver is obtained by gluing together solutions for each of the biconnected components. The gluing at a common point in $\mathbb{R}^3$ freezes the relative translational degrees of freedom. Denoting by B the set of biconnected components, one has:

$$S_Q^\zeta = \prod_{b \in B} S_{Q^b}^\zeta \tag{8.2.6}$$

One can also decompose Q into strongly connected components, defined as follows. A quiver is strongly connected if for each pair of nodes $i, j \in Q_0$ there is an oriented path from i to j and from j to i. We define an equivalence relation between nodes by writing $i \sim j$ if there is a path from i to j and from j to i: this relation is automatically symmetric, reflexive by considering the trivial path, and transitive by concatenation of paths. The equivalence classes under this relation are called strongly connected components. Let us now draw an arrow from a strongly connected component to another if there is an arrow in Q from one node in the first equivalence class to a node of the second equivalence class. The resulting graph Γ is connected and has no cycle because there cannot exists paths going both ways between two strongly connected components. Thus Γ defines a poset. In Figure 8.2, we show an example of a quiver with its graph Γ of strongly connected components.

From lemma 8.4.1, a strictly positive conserved current can exist on a quiver Q only if Q is strongly connected, therefore:

Proposition 8.2.1. *A quiver which admits scaling or attractor solutions must be strongly connected.*

Notice that by i) of lemma 8.4.4, a quiver is strongly connected if and only if its biconnected components are strongly connected. The biconnected components of a strongly connected quiver Q have an alternative description as follows. Consider the equivalence relation $\sim$ on the arrows of Q generated by $a \sim b$ if they are in a simple oriented cycle $w \in Q_2$. From ii) of lemma 8.4.4, the equivalence classes of $\sim$ are identical to the biconnected components of Q, therefore Q is biconnected if and only if $\sim$ has a single equivalence class.

[5] The notions of biconnected graph (also known as 'non-separable'), biconnected components of a graph (also known as 'blocks'), strongly connected directed graph and strongly connected components are standard in graph theory, see for example [Har99, Sec 3,6].

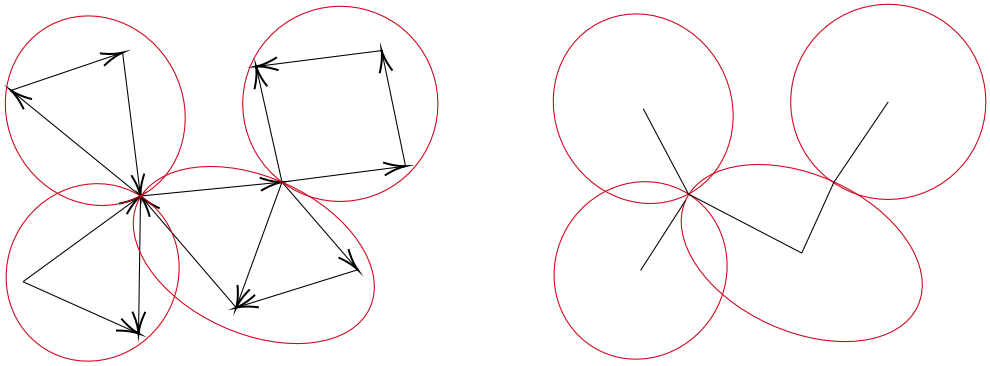

Figure 8.1: Constructing the unoriented graph of biconnected components.

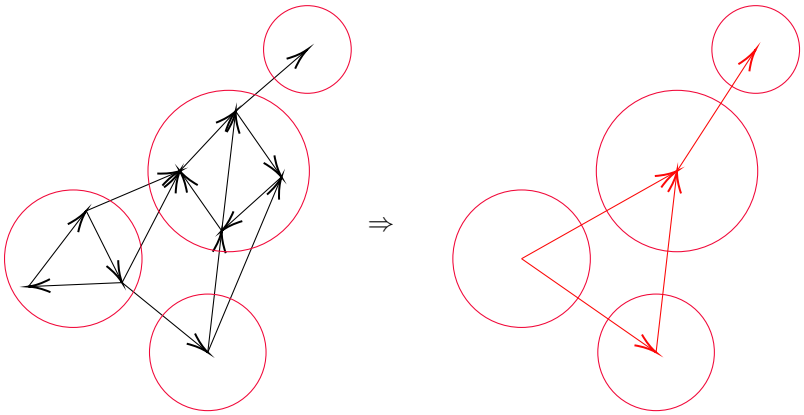

Figure 8.2: Constructing the graph of strongly connected components.

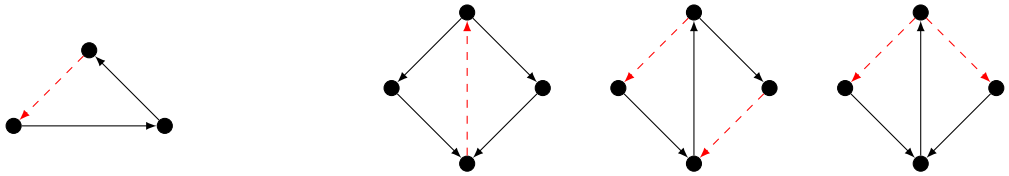

Figure 8.3: Two examples of quivers with cuts. Arrows in the cut are drawn in dashed red.

8.2.3 Cuts, weak cuts and R-charge

Consider a map $R : \mathbb{R}_1^Q \to \mathbb{R}$ assigning a charge $R(a)$ to each arrow $a \in Q_1$. For any simple cycle $w \in Q_2$, one consider the charge of the cycle $R \circ \partial_2(w) = \sum_{a \in w} R(a)$. We say that R is an R-charge if all simple cycles have charge $R \circ \partial_2(w) = 2$. For any subset $I \subset Q_1$ of arrows of Q, we define the charge R_I by $R_I(a) = 2$ if $a \in I$, and $R_I(a) = 0$ if $a \in Q_1 - I$.

We define a cut (resp. a weak cut, a strong cut) as a subset I of arrows of the quiver such that each simple oriented cycle $w \in Q_2$ contains exactly (resp. at most, at least) one arrow of I, or equivalently $R_I \circ \partial_2(w) = 2$ (resp. $R_I \circ \partial_2(w) \leq 2$, $R_I \circ \partial_2(w) \geq 2$). We shall consider maximal weak cuts, i.e. weak cuts which are maximal for the inclusion. There are two possibilities, as proven in lemma 8.4.5:

- either Q admits a cut, and then all maximal weak cuts are cuts, and Q admits an R-charge,
- or Q admits no R-charge and in particular no cut.

While quivers with few arrows typically have cuts (see Fig. 8.3), it is easy to find examples of quivers which do not have any cuts. Our main examples are the 'pentagram' and 'hexagram' quivers, shown in Figure 8.4 and 8.5. In both cases, the relations between the cycles forbids the existence of an R-charge, and therefore of a cut (see Figures 8.4 and 8.5). Each of these quivers nonetheless admits maximal weak cuts, as shown in dashed red in the respective figure.

Remark 8.2.2. The notion of R-charge is standard in the physics literature on quiver gauge theories, but the details may vary. Here we do not impose any condition on the total R-charge of the arrows ending or starting at a given node. The notion of cut is also standard in the mathematical and physic literature about quivers with potential. The notions of weak and strong cut introduced here appear to be new. R-charges and cuts are usually defined with respect to all cycles appearing in the potential, not only the simple cycles. Here we always assume that the potential is a generic sum of simple cycles, so this distinction is unessential.

The cuts of a quiver are particularly easy to describe when Q contains a cycle w_0 passing through all the nodes, and admits an R-charge. In particular Q is strongly connected in this case, and also biconnected: if one removes a node i of the quiver, two other nodes are still connected by the path on the cycle w_0 avoiding i. One can then label the nodes using w_0, such that this cycle passes by the nodes $1 \to 2 \to ... \to n \to 1$. According to lemma 8.4.6, the cuts are then given by $I = \{a : i \to j | i > j\}$ and circular permutations thereof (i.e. when we choose the order $r < r+1 < ... < n < 1 < ... < r-1$ on $\{1, ..., n\}$). Said differently, the cuts consist of the arrows 'going the wrong way' according to one of the n choices of circular ordering on the nodes. An example is shown in Figure 8.6.

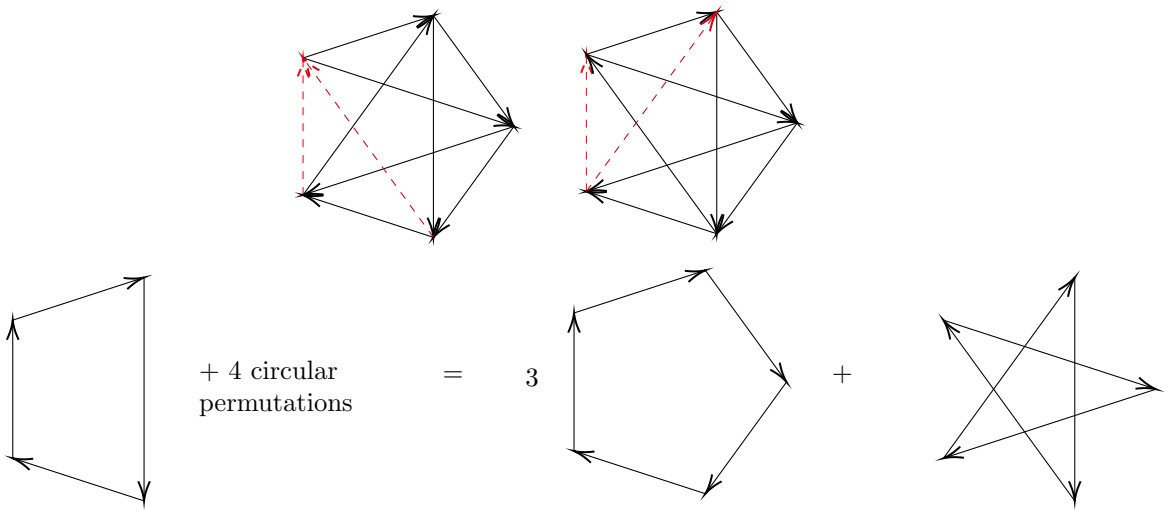

Figure 8.4: The pentagram quiver does not admit any cut, due to a relation between simple cycles. The maximal weak cuts are shown in red, up to cyclic permutation of the nodes.

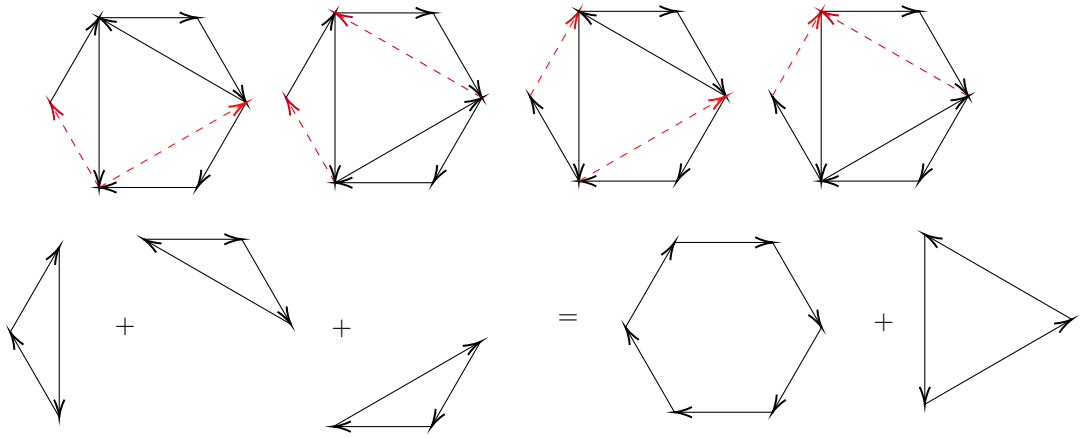

Figure 8.5: The hexagram quiver does not admit any cut, due to a relation between simple cycles. The maximal weak cuts are shown in red, up to cyclic permutation of the nodes.

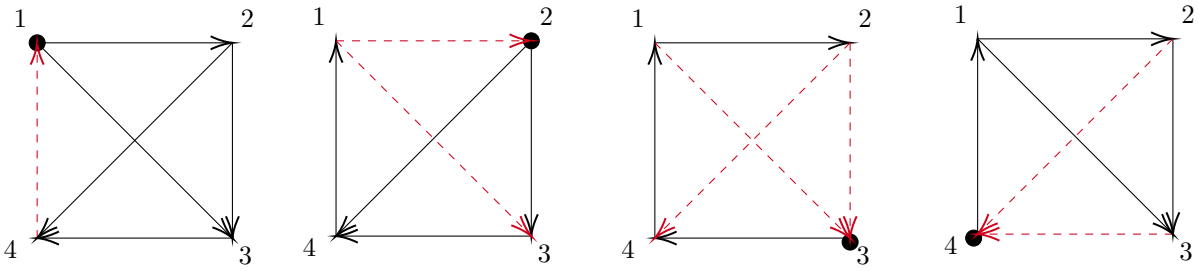

Figure 8.6: Structure of the cuts for a quiver with a cycle w_0 passing through all the nodes. For each choice of origin along the cycles, (marked by a black node), arrows in the cut (which are dashed) are those which go backward along the cycle.

8.2.4 Constraints on the existence of scaling and attractor solutions

Having introduced the necessary notions, we are now ready to derive necessary conditions for the existence of scaling and attractor solutions. The key point is the positivity of the currents $\lambda^\bullet$ in (8.2.5), whose conservation corresponds with the conformal ($\bullet = 0$) or attractor ($\bullet = \star$) Denef equation. We can then apply part *ii)* of lemma 8.4.1, to conclude that $\lambda^\bullet$ is a sum of positive currents circulating on simple cycles of the quiver, namely there exists $(\mu_w)_{w\in Q_2}$ such that

$$\lambda^\bullet_a = \sum_{w\ni a} \mu_w \ , \qquad \mu_w > 0 \quad \forall\ w \in Q_2 \tag{8.2.7}$$

Now, for each simple cycle w, and every arrow $(a : i \to j) \in w$, we have the (generalized) triangular inequality

$$r_{ij} \leq \sum_{(b:k\to l)\in w | b\neq a} r_{kl} \tag{8.2.8}$$

Since the function $f : x \mapsto (1 + \frac{1}{x})^{-1}$ is increasing on $\mathbb{R}^\star_+$, we deduce

$$\begin{aligned}\left(1+\frac{1}{r_{ij}}\right)^{-1} &\leq \left(1+\frac{1}{\sum_{(b:k\to l)\in w|b\neq a} r_{kl}}\right)^{-1} = \frac{\sum_{(b:k\to l)\in w|b\neq a} r_{kl}}{1+\sum_{(b:k\to l)\in w|b\neq a} r_{kl}} \\ &< \sum_{(b:k\to l)\in w|b\neq a} \frac{r_{kl}}{1+r_{kl}} = \sum_{(b:k\to l)\in w|b\neq a} \left(1+\frac{1}{r_{kl}}\right)^{-1}\end{aligned} \tag{8.2.9}$$

Thus, we have

$$\frac{1}{\lambda^\bullet_a} \leq \sum_{b\in w|b\neq a} \frac{1}{\lambda^\bullet_b} \tag{8.2.10}$$

both for $\bullet = 0$ and $\bullet = \star$. The data of a (weak) cut I allow one to choose consistently an arrow in each simple cycle (resp. in a set of cycles). One denotes for convenience:

$$\epsilon^I_a = \begin{cases} -1 & \text{if } a \in I \\ 1 & \text{if } a \in Q_1 - I \end{cases} \tag{8.2.11}$$

It then follows from (8.2.10) that, for any weak cut,

$$\sum_{a\in w} \frac{\epsilon_a^I}{\lambda_a^\bullet} \geq 0 \tag{8.2.12}$$

the inequality being strict when w contains no arrow of I. One can then take a linear combination of the inequalities (8.2.12) with the same strictly positive coefficients μ_w appearing in (8.2.7), obtaining

$$0 \leq \sum_{w\in Q_2} \mu_w \sum_{a\in w} \frac{\epsilon_a^I}{\lambda_a^\bullet} = \sum_{a\in Q_1} \frac{\epsilon_a^I}{\sum_{w\ni a}\mu_w} \left(\sum_{w\ni a} \mu_w\right) = \sum_{a\in Q_1} \epsilon_a^I = |Q_1 - I| - |I| \tag{8.2.13}$$

Hence, the existence of scaling or attractor solutions implies, for every weak cut, the inequality

$$|I| \leq |Q_1 - I| \tag{8.2.14}$$

A few remarks are in order:

- The inequality (8.2.14) can only be saturated for scaling solutions ($\bullet = 0$), and if each simple cycle contains an arrow of I, i.e. I is a cut. In that case, (8.2.8) is an equality for each $w \in Q_2, a \in I \cap w$. In particular, the centers along each oriented cycle of the scaling solution must be collinear. One has in particular that (8.2.8) is a strict inequality for $a \in w - (I \cap w)$, and therefore $|J| < |Q_1 - J|$ for all cuts J distinct from I. Moreover, two arrows contained in the same cycle w are necessarily collinear. If Q is biconnected and strongly connected, from lemma 8.4.4 one can connect any two arrows by a sequence of arrows such that two consecutive arrows are contained in a common cycle, and in that case the whole scaling solution is collinear.
- For a small perturbation of the attractor stability condition, such that the current is perturbed to $\lambda_a = 1 + \delta_a + 1/r_{ij}$ with $|\delta_a| \ll 1$, the inequality (8.2.9) remains true up to small corrections of order $\delta_a(1 + 1/r_{kl})^{-2}$. After multiplying by $\mu_w^\star$, which is of order $1 + 1/r_{kl}$, the resulting correction to (8.2.14) remains small even for $r_{kl} \to 0$. Since the leading terms are integer, this correction does not affect the inequality (8.2.14), although it affects the analysis of the cases where the inequality is saturated.

We thus obtain the main result of this note:

Proposition 8.2.3. *If a quiver Q admits attractor or scaling solutions, then for each weak cut I one has:*

$$|I| \leq |Q_1 - I| \tag{8.2.15}$$

If scaling solutions exist, the inequality can be saturated for at most one cut. When this is the case and if Q is biconnected, then the scaling solutions are collinear.

We shall now compare our result to the conjecture put forward (and proven for some simple cases) in [BMP21b]. In that reference, it was assumed that Q admits an R-charge and contains a cycle $w_0 \in Q_2$ passing through all the nodes, giving a cyclic ordering $Q_0 \simeq \mathbb{Z}/n\mathbb{Z}$. As show in lemma 8.4.6, all the cuts of Q are then of the form $I = \{a : i \to j | j > i\}$ and cyclic permutations. The conjecture in [BMP21b] is therefore a consequence of Proposition 8.2.3,

Proposition 8.2.4. *For a quiver with an R-charge and a cycle passing through all the nodes, scaling or attractor solutions can only exist if*

$$\sum_{i<j} \kappa_{ij} \geq 0 \qquad \textit{and cyclic permutations} \tag{8.2.16}$$

8.2.5 Non-Abelian scaling and attractor solutions

We now consider a non-Abelian quiver Q with dimension vector $(d_i)_{i\in Q_0}$, supposing $d_i \geq 1$ for $i \in Q_0$. On the Coulomb branch, the gauge group $\prod_{i\in Q_0} U(d_i)$ is broken to a Cartan subgroup $\prod_{i\in Q_0} U(1)^{d_i}$, and the scalar fields in the vector multiplets associated to this subgroup satisfy similar equations (8.1.1) as in the Abelian case with $n = \sum_{i\in Q_0} d_i$ centers, with d_i of them carrying the same charge γ_i and stability parameter ζ_i for each $i \in Q_0$. Labeling by (i,k) the k-th center with charge γ_i, for $1 \leq k \leq d_i$, the distances between centers satisfy a non-Abelian version of Denef's equations:

$$\forall i = 1 \dots n, \quad \forall k = 1 \dots d_i, \quad \sum_{j\neq i} \sum_{k'=1}^{d_j} \frac{\kappa_{ij}}{|\vec{r}_{(i,k)} - \vec{r}_{(j,k')}|} = \zeta_i \tag{8.2.17}$$

As before, solutions may only exist if $\sum_{i\in Q_0} \zeta_i d_i = 0$. The same equations arise from the 'totally Abelianized quiver' Q^d with nodes $Q_0^d := \{(i,k) | i \in Q_0, 1 \leq k \leq d_i\}$, and arrows $Q_1^d := \{(a,k,k') : (i,k) \to (j,k'))|(a : i \to j) \in Q_1, 1 \leq k \leq d_i, 1 \leq k' \leq d_j\}$. On special loci where m of the centers attached to the same node $i \in Q_0$ coincide, the gauge factor $U(1)^{d_i}$ is enhanced to $U(m)\times U(1)^{d_i-m}$, leading to partially Abelianized quivers with one node carrying charge $m\gamma_i$ and $d_i - m$ nodes carrying charge γ_i [MPS11b]. We can focus on the Denef equations associated to the totally Abelianized quiver Q^d, since solutions relevant for partially Abelianized quivers arise as special cases.

It is clear from this construction that the Abelianized quiver Q^d is connected (resp. strongly connected) if and only if Q is. In particular, if Q admits a non-Abelian d-dimensional scaling or attractor solution, then Q^d is strongly connected, and therefore also Q:

Proposition 8.2.5. *A non-Abelian quiver which admits scaling or attractor solutions must be strongly connected.*

If Q is biconnected, then Q^d is biconnected too, but the converse is not true: if i is a node shared between two biconnected components of Q, those two components merge into a single biconnected component in Q^d when $d_i \geq 2$ (see the example of the butterfly quiver with dimension vector $(2,1,1,1,1)$, Figure 8.8). In particular, the decomposition into biconnected components of the solutions to Denef's equations does not hold in the non-Abelian case, because biconnected components of Q are not in correspondence with those of Q^d.

We shall now attempt to derive constraints on the magnitude of the Dirac products κ_{ij} for the existence of non-Abelian scaling or attractor solutions. Let $\lambda^\bullet$ be the corresponding strictly positive conserved current on Q^d. For a an arrow on Q^d, we denote by $p(a)$ its projection to Q; similarly, for a path v on Q^d, we denote by $p(v)$ its projection to Q. For I a weak cut of Q, each cycle of $p^{-1}(Q_2)$ (i.e. projecting on a simple cycle of Q) contains at most one arrow of $p^{-1}(I)$. By the same argument as in the proof of proposition 8.2.3, the triangular inequality in the corresponding

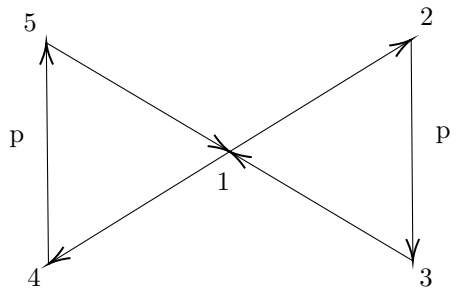

Figure 8.7: An example of non biconnected quiver: the butterfly quiver.

polygon in the non-Abelian scaling or attractor solutions gives:

$$\sum_{a\in w} \frac{\epsilon_a^{p^{-1}(I)}}{\lambda_a^\bullet} \geq 0 \tag{8.2.18}$$

Now, suppose that the current could be expressed as a sum $\lambda_a^\bullet = \sum_{w\in p^{-1}(Q_2)|w\in a} \mu_w$ of positive currents μ_w circulating on simple cycles of Q^d which project to simple cycles of Q. By taking the linear combination of the inequalities (8.2.18) with coefficients μ_w, one would conclude that $|p^{-1}(I)| \leq |Q_1^d - p^{-1}(I)|$, or equivalently

$$\sum_{(a:i\to j)\in I} d_i d_j \leq \sum_{(a:i\to j)\in Q_1 - I} d_i d_j \tag{8.2.19}$$

In the special case where $p^{-1}(Q_2) = Q_2^d$, i.e. when each cycle of Q^d projects to a simple cycle of Q, the existence of the positive currents μ_w follows directly from *ii)* of lemma 8.4.1, and the therefore the condition (8.2.19) must hold. This the case for example for the triangular quiver where one of the entries in the dimension vector is equal to one, as in the cases considered in [MPS12, §6][LWY14, §3] [KLY15, §4] [MVdB20]. More generally, when the quiver Q is biconnected, lemma 8.4.7 allows to express $\lambda^\bullet$ as a sum of (possibly negative) currents circulating on the cycles of $p^{-1}(Q_2)$. While we are not able to show that these currents can be taken to be positive, it seems plausible to propose that for a biconnected quiver, the existence of a d-dimensional scaling or attractor solution implies that for each weak cut I, the condition (8.2.19) is satisfied.

We can construct a counterexample to the inequalities (8.2.19) for a non biconnected quiver, namely the 'butterfly' quiver shown in Figure 8.7. We choose multiplicities $\kappa_{23} = \kappa_{45} = p \geq 1$, and multiplicity 1 for other arrows, and dimension vector $(2, 1, 1, 1, 1)$. The corresponding Abelianized quiver Q^d is obtained by splitting the central node 1 into two nodes which we denote by 1 and $1'$. In particular for the simple cycle $w : 1 \to 2 \to 3 \to 1' \to 4 \to 5 \to 1$, its projection on Q $p(w) := 1 \to 2 \to 3 \to 1 \to 4 \to 5 \to 1$ is not simple, and w cannot be expressed as a linear combination of cycles projection to a simple cycle of Q. We consider solutions inscribed in a rectangle with height y and length $2x$ as shown in Figure 8.8. The scaling (resp. attractor) Denef equations are trivially verified at the node 1 and $1'$, and require

$$\frac{p}{y} = \frac{1}{x} + \frac{1}{\sqrt{x^2+y^2}}\,, \qquad \text{resp.} \qquad p\left(1+\frac{1}{y}\right) = 2 + \frac{1}{x} + \frac{1}{\sqrt{x^2+y^2}} \tag{8.2.20}$$

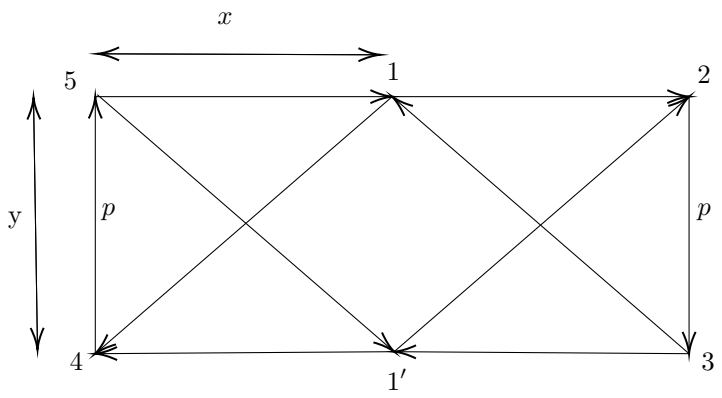

Figure 8.8: Scaling solution for the butterfly quiver with $d = (2, 1, 1, 1, 1)$.

at the other nodes. Solutions manifestly exist for any $p \geq 1$. In contrast, the inequalities (8.2.19) for the cut $I = \{2 \to 3, 4 \to 5\}$ would require

$$\sum_{(a:i\to j)\in I} d_i d_j = 2p \leq \sum_{(a:i\to j)\in Q_1 - I} d_i d_j = 8 \tag{8.2.21}$$

which is false. This shows that the assumption of biconnectedness is important for the inequalities (8.2.19) to hold. Whether the inequalities are verified in the biconnected case is left as an interesting problem for future work.

8.3 Existence of self-stable representations

In this section, we discuss constraints for the existence of vacuum solutions on the Higgs branch at the attractor point, which mathematically correspond to self-stable representations. Physically, we expect that such solutions only exist when the Coulomb branch admits scaling solutions (except for simple representations associated to the nodes of the quiver, which exist for arbitrary stability condition). Indeed, we shall demonstrate that for quivers with generic potential, the existence of self-stable Abelian representations requires similar but slightly stronger conditions as for existence of scaling solutions on the Coulomb branch.

8.3.1 Conserved current on the Higgs branch

We consider the quiver quantum mechanics associated to a connected quiver Q, dimension vector $(d_i) \in (\mathbb{N}^\star)^{Q_0}$, Fayet-Iliopoulos parameters $(\zeta_i) \in \mathbb{R}^{Q_0}$ and a generic potential W. On the Higgs branch, the expectation value of the chiral multiplets associated to the arrows $a \in Q_1$ breaks the gauge group $\prod_{i\in Q_0} U(d_i)$ to the center $U(1)^{Q_0}$. After integrating out the vector multiplets one is left with an effective quantum mechanics for the chiral multiplet scalars $(\phi_a)_{a\in Q_1}$. Supersymmetric

vacua are given by solutions of the D-term and F-term equations,

$$\sum_{(a:i\to j)\in Q_1} \phi_a^\dagger \phi_a - \sum_{(a:j\to i)\in Q_1} \phi_a \phi_a^\dagger = \zeta_i \,\mathrm{Id}_{d_i} \quad \forall\, i \in Q_0 \tag{8.3.1}$$

$$\partial_{\phi_a} W = 0 \tag{8.3.2}$$

modulo the action of the gauge group. From [Kin94a, Prop 6.5], such solutions are in one-to-one correspondence with polystable representations of the quiver, i.e. direct sums of stable representations, where the stability condition is determined by the slope $\sum_{i\in Q_0} d_i\zeta_i / \sum_{i\in Q_0} d_i$. For primitive dimension vector and generic stability parameters, polystable representations are automatically stable.

Summing up the relations (8.3.1) over $i \in Q_0$, it is clear that solutions only exist when $\partial_0((d_i\zeta_i)_{i\in Q_0} = \sum_{i\in Q_0} d_i\zeta_i = 0$. Thus, one can choose $(\chi_a)_{a\in Q_1} \in \mathbb{R}^{Q_1}$ such that $\partial_1((\chi_a)_{a\in Q_1} = (-d_i\zeta_i)_{i\in Q_0}$. The trace of the D-term equations (8.3.1) then implies the conservation at each node of Q of the current:

$$\lambda_a := \chi_a + \mathrm{Tr}(\phi_a\phi_a^\dagger) \tag{8.3.3}$$

The choice of χ_a is non unique, unless Q has no oriented cycle. For the attractor stability condition (also known as self-stability), one may choose $\chi_a = d_i d_j$ such that the current λ is strictly positive (arrows $a : i \to j$ such that $d_i d_j = 0$ do not support any chiral multiplet and may be removed from the quiver Q). By applying i) of lemma 8.4.1, it then immediately follows that, similarly to the Coulomb branch case,

Proposition 8.3.1. *A quiver which admits self-stable representation of dimension $(d_i) \in (\mathbb{N}^\star)^{Q_0}$ must be strongly connected.*

We note that for Abelian representations, the D-terms equations are equivalent to the conservation of the current λ. As on the Coulomb branch, one has then, according to lemma (8.4.3), that an Abelian representation of Q satisfies the D-term equations at the attractor stability condition if and only if the induced representations on the biconnected components of Q satisfy the induced D-terms equations. Moreover, by definition, the F-term equations $\partial_a W = 0$ constrain only the arrows which share a cycle with a, and therefore are in the same biconnected component as a. Thus, a representation satisfies the F-terms equations if and only if the induced representations satisfy the induced F-terms equations on each biconnected component. To summarize, stable Abelian representations of the quiver with potential (Q, W) at any stability condition are obtained by gluing such representations for the biconnected components of Q. As we shall see below, the example of the 'butterfly quiver' shows that this is no longer true in the non-Abelian case.

8.3.2 Stronger constraints in the Abelian case

In order to obtain conditions on the number of chiral fields, we shall rely on lemma 8.4.8, which applies to any quiver with potential (Q, W) such that $W = \sum_{w\in C} \nu_w w$ is a linear combination of a subset of simple cycles $C \subset Q_2$ with generic coefficients, and such that there exists a subset of arrows $I \subset Q_2$ such that each cycle of C contains exactly one arrow of I. Under these assumptions, any Abelian representation of (Q, W) is such that every each cycle in C vanishes when evaluated on

this representation. The proof relies on Bertini's theorem for linear systems on algebraic varieties, and generalizes the informal argument outlined in [DM11a, §5.2.3] in the case of a triangular cyclic quiver.

Now, consider a quiver Q with a cut I with potential $W = \sum_{w\in Q_2} \nu_w w$ which is generic in the sense of definition 8.4.9, and ϕ an Abelian representation of (Q, W). From lemma 8.4.8, it follows that there is a strong cut J such that the arrows of J vanish in ϕ while no other arrows vanish: for simplicity, we consider here the case where J is a cut, the general case being treated in the appendix. The representation ϕ is therefore a representation of the quiver with relations $(Q_J, \partial_J W)$, where Q_J is the subquiver of Q where one has removed the arrows of J, and the relations are $\partial_a W = 0$ for $a \in J$.

Suppose that ϕ is ζ-stable. The moduli space $M^{\zeta,s}_{Q_J}$ of ζ-stable representations of Q_J is smooth of dimension $|Q_1 - J| - |Q_0| + 1$. Since the moduli space $M^{\zeta,s}_{Q_J,\partial_J W_J}$ of ζ-stable Abelian representations of $(Q_J, \partial_J W)$ is given by the zero locus of the $|J|$ relations $\partial_a W$ in $M^{\zeta,s}_{Q_J}$, one expects then that its complex dimension is given by

$$d_J = |Q_1 - J| - |Q_0| + 1 - |J| \ , \tag{8.3.4}$$

unless there are linear relations between the relations. We shall now prove that there a no relation between the relations infinitesimally near ϕ.

For a cycle w of W, we denote its arrows by $w = b^w_1 ... b^w_{r_w}$. The linearization of $\partial_a W$ on the tangent space at ϕ gives:

$$\delta(\partial_a W) : (\delta\phi_b)_{b\in Q_1} \mapsto \sum_{w,i|b^w_i = a} \nu_w \sum_{i+1\le j\le i-1} \phi_{b^w_{i+1}} \cdots \phi_{b^w_{j-1}}\, \delta\phi_{b^w_j}\, \phi_{b^w_{j+1}} \cdots \phi_{b^w_{i-1}} \tag{8.3.5}$$

Here we use the cyclic ordering of the cycle. Consider a linear relation $(\tilde\phi_a)_{a\in Q_1}$ between these relations such that:

$$\sum_{a\in Q_1} \tilde\phi_a \delta(\partial_a W) = 0 \tag{8.3.6}$$

One computes:

$$\begin{aligned} 0 = \sum_{a\in Q_1} \tilde\phi_a \delta(\partial_a W) &= \sum_{w\in Q_2} \nu_w \sum_{1\le i\ne j\le r_w} \tilde\phi_{b^w_i} \phi_{b^w_{i+1}} \cdots \phi_{b^w_{j-1}}\, \delta\phi_{b^w_j}\, \phi_{b^w_{j+1}} \cdots \phi_{b^w_{i-1}} \\ &= \sum_{w\in Q_2} \nu_w \sum_{1\le i\ne j\le r_w} \phi_{b^w_{j+1}} \cdots \phi_{b^w_{i-1}} \tilde\phi_{b^w_i} \phi_{b^w_{i+1}} \cdots \phi_{b^w_{j-1}}\, \delta\phi_{b^w_j} \end{aligned} \tag{8.3.7}$$

Consider now the representation of Q $\bar\phi = \phi + \epsilon\tilde\phi$ with $\epsilon^2 = 0$ (hence it is a representation over the ring $\mathbb{C}[\epsilon]/\epsilon^2$). Because ϕ satisfies the equation of the potential, one has, multiplying by ϵ:

$$\begin{aligned} 0 &= \sum_{w\in Q_2} \nu_w \sum_{1\le j\le r_w} (\phi + \epsilon\tilde\phi)_{b^w_{j+1}} \cdot\cdots\cdot (\phi + \epsilon\tilde\phi)_{b^w_{j-1}}\, \delta\phi_{b^w_j} \\ &= \sum_{b\in Q_1} \partial_b W|_{\bar\phi} \delta\phi_b \end{aligned} \tag{8.3.8}$$

Now we consider a linear relation between the relations $\sum_{a\in J}\tilde{\phi}_a\delta(\partial_a W)=0$ where one restricts to deformations with vanishing arrows of J, hence $\delta\phi_b=0$ for $b\in J$. One obtains in this case $\bar{\phi}=(\epsilon\tilde{\phi}_a,\phi_b)_{a\in J,b\in Q_1-J}$, and $\partial_b W|_{\bar{\phi}}$ for $b\in Q_1-J$. Moreover, for $a\in J$, $\partial_a W_J|_{\bar{\phi}}=\partial_a W|_{\phi}=0$, hence $\bar{\phi}$ is a representation of (Q,W). Because W is generic, according to Lemma 8.4.8, the cycles of Q_2 vanish in $\bar{\phi}$. Each cycle in Q_2 contains exactly one arrow in J and other arrows in Q_1-J: because the arrows of Q_1-J do not vanish in ϕ, it follows that the arrows of J vanish in $\tilde{\phi}$. Hence there are no nontrivial linear relations between the $|J|$ differential forms, and the dimension of the tangent space at ϕ in $M^{\zeta,s}_{Q_J,\partial_I W_J}$ is:

$$0\leq d=|Q_1-J|-|Q_0|+1-|J| \tag{8.3.9}$$

Now $R_J\circ\partial_2=R_I\circ\partial_2$. Suppose that ζ is the attractor stability condition: the positive conserved current $\lambda=(1+|\phi_a|^2)_{a\in Q_1}$ can then be written as $\lambda=\sum_w\mu_w\partial_2(w)$ with $\mu_w>0$ from $ii)$ of lemma 8.4.1, and then because the arrows of J vanish on ϕ:

$$2|I|\leq R_I(\lambda)=R_J(\lambda)=2|J| \tag{8.3.10}$$

hence

$$2|I|\leq|Q_1|-|Q_0|+1 \tag{8.3.11}$$

We show in the appendix how to remove the assumption that J is a cut, and how to generalize the above argument when I is only a weak cut, and obtain finally an equivalent of Proposition 8.2.3 on the Higgs branch:

Proposition 8.3.2. *(Proposition 8.4.10) If a quiver with generic potential (Q,W) admits a self-stable Abelian representation, then for each weak cut I:*

$$|I|\leq|Q_1-I|-|Q_0|+1 \tag{8.3.12}$$

The case were I is a cut but J is not necessarily a cut is easy to deal with. Namely, because there is too much arrows vanishing, some relations of the potential $\delta_a W=0$ for $a\in J$ can become trivial, but this is counterpoised exactly by the fact that there is more relations of the form $\phi_a=0$ for $a\in J$. The case where I is only a weak cut and not a cut case is more subtle, because for a quiver without cut and generic potential, the cycles do not necessarily vanish in an Abelian representation, hence the first part of the proof does not work. One must set some arrows to zero to apply a similar argument, but one must ensure that the quiver stays connected during this procedure (such that the action of the gauge group up to global scaling is still free), and that it is done in a consistent way (such that one does not lose too many relations of the quiver). We refer to the proof in the Appendix for all the details.

8.3.3 Stronger constraints in the non-Abelian case

One can try to obtain stronger constraints for the existence of non-Abelian self-stable representations, by assuming that non-Abelian analogue of Lemma 8.4.8:

Assumption 8.3.3. In a stable representation ϕ of a quiver with potential (Q,W) with W generic, each cycle contains an arrow which vanishes on ϕ.

If this assumptions was true, one could generalize the inequalities for cuts from proposition 8.4.10 to the non-Abelian setting as follows. Let ϕ be a d-dimensional self-stable representation of a quiver Q with generic potential W, and I a cut of Q: under assumption 8.3.3, the arrows of a strong cut J of Q vanish in ϕ. We consider the simpler situation where J is a cut, the general case being treated as in 8.4.10. ϕ is a d-dimensional stable representation of the quiver with relation $(Q_J, \partial_J W)$. The moduli space $M^{\zeta,s}_{Q_J,d}$ of d-dimensional representations of Q_J is smooth of dimension $\sum_{(a:i\to j)\in Q_1-J} d_i d_j - \sum_{i\in Q_0} d_i^2 + 1$, and the space $M^{\zeta,s}_{Q_J,\partial_J W,d}$ of stable representations of $(Q, \partial_J W)$ is the zero set of $\sum_{(a:i\to j)\in J} d_i d_j$ equations inside $M^{\zeta,s}_{Q_J,d}$. Using the cyclicity of the trace, one can derive non-Abelian analogues of equations 8.3.7, giving that a linear relation $(\tilde{\phi}_a)_{a\in J}$ between these equations at the tangent space of ϕ gives a representation $\bar{\phi} = (\phi_a, \epsilon\tilde{\phi}_b)_{a\in Q_1-J, b\in J}$ of (Q_J, W) over $\mathbb{C}[\epsilon]/\epsilon^2$, which is still self-stable because some vanishing arrows in the self-stable representation ϕ have been set to a non-vanishing value. Then under the assumption 8.3.3, the cycles of Q_2 contain an arrow vanishing in $\bar{\phi}$, hence $\tilde{\phi}_a = 0$ for $a \in J$, hence there are no relations between the relations. The dimension of the tangent space at ϕ inside $M^{\zeta,s}_{Q_J,\partial_J W,d}$ is therefore:

$$0 \leq d = \sum_{(a:i\to j)\in Q_1} d_i d_j - \sum_{i\in Q_0} d_i^2 + 1 - \sum_{(a:i\to j)\in J} d_i d_j - \sum_{(a:i\to j)\in J} d_i d_j \tag{8.3.13}$$

Applying the same arguments as in the proof of Proposition 8.4.10 using the conserved current $(d_i d_j + \mathrm{Tr}(\phi_a^\dagger \phi_a))_{(a:i\to j)\in Q_1}$, one obtains

$$2 \sum_{(a:i\to j)\in I} d_i d_j \leq 2 \sum_{(a:i\to j)\in J} d_i d_j \tag{8.3.14}$$

hence for any cut I:

$$\sum_{(a:i\to j)\in I} d_i d_j \leq \sum_{(a:i\to j)\in Q_1-I} d_i d_j - \sum_{i\in Q_0} d_i^2 + 1 \tag{8.3.15}$$

However, Assumption 8.3.3 fails for non-Abelian quivers which are not biconnected. Consider as in subsection 8.2.5 the 'butterfly' quiver with p arrows $2 \to 3$ and $p \geq 2$ arrows $4 \to 5$, and dimension vector 2 on the central node 1, and 1 on the other nodes. For a generic potential W, the p equations corresponding with the arrows $2 \to 3$ (resp. $4 \to 5$) impose that $\phi_{12}\phi_{31} = 0$ (resp. $\phi_{14}\phi_{51} = 0$). Denote w^i (resp. $\bar{w}^i$) the cycle $a_{31}a^i_{23}a_{12}$ (resp. $a_{51}a^i_{45}a_{14}$), and $W = \sum_{i=1}^p \nu_i w_i + \sum_{i=1}^p \bar{\nu}_i \bar{w}_i$. Take $(\phi^i_{23})_{1\leq i\leq p}$ (resp. $(\phi^i_{45})_{1\leq i\leq p}$) as a generic vector satisfying $\sum_i \nu_i \phi^i_{23} = 0$ (resp. $\sum_i \nu_i \phi^i_{45} = 0$), in particular all these arrows are non-vanishing because W is generic. We fix then:

$$\phi_{51} = \begin{pmatrix} 1 \\ 0 \end{pmatrix} \ , \ \phi_{12} = (1,0) \ , \ \phi_{31} = \begin{pmatrix} 0 \\ 1 \end{pmatrix} \ , \ \phi_{14} = (0,1) \tag{8.3.16}$$

The resulting representation ϕ satisfies the F-term relations for the potential W. As can be seen on Figure 8.9, where the arrows correspond to nonzero matrix elements and the points $1, 1'$ correspond to the two elements of the basis of the two dimensional vector space of the node 1, each vector generates the whole representation, i.e. the only subobjects of ϕ are the trivial ones, and then ϕ is stable for any stability condition. We have therefore constructed a self-stable representation of a quiver with generic potential (Q, W) admitting a cut such that all the arrows are non-vanishing.

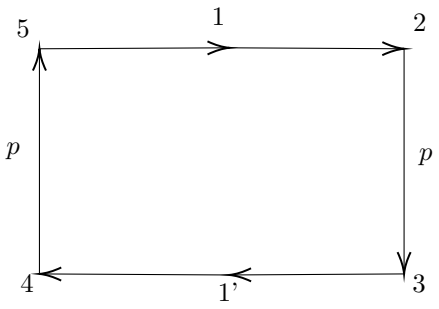

Figure 8.9: A stable representation of the butterfly quiver with dimension vector $(2,1,1,1,1)$.

Moreover, considering the cut I containing the arrows $2 \to 3$ and $4 \to 5$: for $p \geq 1$, one has:

$$\sum_{(a:i\to j)\in I} d_i d_j = 2p > 1 = \sum_{(a:i\to j)\in Q_1 - I} d_i d_j - \left(\sum_{i\in Q_0} d_i^2 - 1 \right) \tag{8.3.17}$$

i.e. the stronger triangular inequalities are not necessarily true for non biconnected quivers. Notice the similarity of this construction with the counterexample discussed in §8.2.5.

We leave it as an interesting problem to study if the assumption 8.3.3, and then also the stronger inequalities (8.3.15) in the non-Abelian case, hold when one restricts to biconnected quivers.

Acknowledgments: We are grateful to Guillaume Beaujard, Jan Manschot, Swapnamay Mondal and Olivier Schiffmann for useful discussions, and to the anonymous referees for their careful reading and valuable suggestions. The research of BP is supported by Agence Nationale de la Recherche under contract number ANR-21-CE31-0021.

8.4 Proofs

In this section, we provide mathematical proofs for some of the technical results used in the body of the chapter.

8.4.1 Conserved currents and graph homology

A strictly positive conserved current is an element of $\ker(\partial_1) \cap (\mathbb{R}_+^\star)^{Q_1}$. A quiver is strongly connected if and only if for any two nodes $i, j \in Q_0$, there is an oriented path from i to j and from j to i. The key result which allows us to derive constraints on the existence of scaling or attractor solutions is the following:

Lemma 8.4.1. *i) If Q admits a strictly positive conserved current, then Q is strongly connected.*

ii) A strictly positive conserved current λ can be expressed as a sum of strictly positive conserved currents circulating on all simple oriented cycles of the quiver, i.e. $\lambda = \sum_{w\in Q_2} \mu_w \partial_2(w)$, with $\mu_w > 0$.

Proof:

i) Suppose that Q is not strongly connected. The strongly connected components of Q form a connected tree with at least two nodes: one has then a nontrivial partition $Q_0 = Q_0' \sqcup Q_0''$ such that there is at least one arrow $Q_0' \to Q_0''$, and no arrow $Q_0'' \to Q_0'$. Consider $\lambda \in \ker(\partial_1) \cap \mathbb{R}^{Q_1}$: by summing the conservation of λ at each node of Q_0', one has $\sum_{(a:Q_0' \to Q_0'') \in Q_1} \lambda_a = 0$, and then $\lambda \notin (\mathbb{R}_+^\star)^{Q_1}$.

ii) Suppose now that Q is strongly connected. We must show that $\ker(\partial_1) \cap (\mathbb{R}_+^\star)^{Q_1} \subset \partial_2((\mathbb{R}_+^\star)^{Q_2})$. We begin by showing $\ker(\partial_1) \cap (\mathbb{R}_+)^{Q_1} \subset \partial_2((\mathbb{R}_+)^{Q_2})$: for this we reason inductively on the number of arrows which carry a non-vanishing current. For $\lambda \in \ker(\partial_1) \cap (\mathbb{R}_+)^{Q_1}$, we consider $Q^\lambda = (Q_0, \{a \in Q_1 | \lambda_a > 0\})$, the (possibly non connected) quiver where we keep only the arrows with a non-vanishing current. If $Q_1^\lambda \neq \emptyset$, take $(a : i \to j) \in Q_1^\lambda$ such that $\lambda_a > 0$ is minimal. One has $\lambda \in \ker(\partial_1) \cap (\mathbb{R}_+^\star)^{Q_1^\lambda}$, and then each connected component of Q^λ is strongly connected from i): there is then a path $v : j \to i$ in Q^λ, and then a simple oriented cycle $w := av \in Q_2$ containing a, such that the arrows of w are in Q^λ. One has $\lambda' := \lambda - \partial_2(\lambda_a w) \in \ker(\partial_1)$, and, because λ_a is minimal, $\lambda' \in (\mathbb{R}_+)^{Q_1}$. Moreover, $\lambda'_a = 0$, and then $Q_1^{\lambda'} \subsetneq Q_1^\lambda$: by induction on the number of arrows of Q^λ, one has $\lambda' \in \partial_2((\mathbb{R}_+)^{Q_2})$, and then $\lambda \in \partial_2((\mathbb{R}_+)^{Q_2})$. We have then $\ker(\partial_1) \cap (\mathbb{R}_+)^{Q_1} \subset \partial_2((\mathbb{R}_+)^{Q_2})$. Consider $\lambda \in \ker(\partial_1) \cap (\mathbb{R}_+^\star)^{Q_1}$: one has $0 < \epsilon \ll 1$ such that $\lambda - \partial_2(\epsilon \sum_{w \in Q_2} w) \in \ker(\partial_1) \cap (\mathbb{R}_+)^{Q_1}$, and then $\lambda = \partial_2 \sum_{w \in Q_2} (\mu_w + \epsilon) w$ with $\mu_w \in \mathbb{R}_+$, i.e. $\lambda \in \partial_2((\mathbb{R}_+^\star)^{Q_2})$.

□

8.4.2 Biconnected components of a quiver

A quiver is biconnected if there is no node i of the quiver such that removing i (and then also the arrows with source or target i) disconnects the quiver. On a quiver Q, the biconnected components are defined as the maximal subquivers of Q being biconnected. We prove the following fact about biconnected components:

Lemma 8.4.2. *i) The biconnected components give a partition of the arrows of the quiver Q, and two different biconnected components of a quiver can share at most one node.*

ii) Define K as the unoriented graph with one node for each biconnected component and one node for each node of the quiver shared between different biconnected components, and an edge between the node i and the biconnected component b if $i \in b$. Then K is a connected tree, i.e. has no loops.

Proof: This result can be deduced from [Har99, Prop 3.5], but we prove it here from clarity and completeness. Suppose that there is a sequence of distinct biconnected components $b_1, ..., b_p$ and a sequence of distinct nodes $i_1, ..., i_p$ such that $i_k \in b_k \cup b_{k+1}$, $i_p \in b_p \cup b_1$, with $p \geq 2$. Consider the subquiver $b_1 \cup ... \cup b_p$ of Q, and remove a node i: one can consider up to a circular permutation that $i \neq i_1$,..., $i \neq i_{p-1}$. Consider two nodes j, j' such that $j \in b_k$, $j' \in b_{k'}$, and suppose up to exchanging j and j' that $k \leq k'$. Because the $b_{k''}$ are biconnected, there is an unoriented path between j and i_k in b_k avoiding i, unoriented paths between $i_{k''}$ and $i_{k''+1}$ in $b_{k''}$ avoiding i for $k \leq k'' \leq k'$ and an unoriented path between $i_{k'}$ and j' in $b_{k'}$ avoiding i. By concatenation, these give an unoriented path between j and j' in $b_1 \cup ... \cup b_p$ avoiding i, i.e. $b_1 \cup ... \cup b_p$ is still connected when one has

removed i. One obtains then that $b_1 \cup ... \cup b_p$ is biconnected, but it is strictly bigger that the b_k, which were assumed to be maximal biconnected subquivers of Q, giving a contradiction.

In particular, for $p = 2$, one obtains that two different biconnected components can share at most one node: because an arrow is adjacent to two nodes, two different biconnected components cannot share an arrow, proving i). The argument above for general p gives exactly that K has no cycle, i.e. is a tree. Consider two biconnected components b, b', and two nodes $i \in b, i' \in b'$: because Q is connected, there is an unoriented path in Q between i and i': by denoting $b, b_1, ..., b_n, b'$ the biconnected components crossed by these paths, b and b' are then connected by a sequence of biconnected components sharing a node, i.e. the graph K is connected. This concludes the proof of ii). □

Denote by B the set of biconnected components of a quiver, and Q^b the quiver associated to a biconnected component. Two biconnected components have distinct arrows, and then one has a decomposition $\mathbb{R}^{Q_1} = \bigoplus_{b\in B} \mathbb{R}^{Q_1^b}$. Consider a simple unoriented cycle of Q: it cannot pass through different biconnected components, since otherwise it would project to a cycle in K, which is forbidden by the above lemma, i.e. it is included in a single biconnected component. In particular this applies to simple oriented cycles, and then one has $\mathbb{R}^{Q_2} = \bigoplus_{b\in B} \mathbb{R}^{Q_2^b}$, giving a decomposition of the complex:

$$\bigoplus_{b\in B} \mathbb{R}^{Q_2^b} \xrightarrow{\sum_{b\in B} \partial_2^b} \bigoplus_{b\in B} \mathbb{R}^{Q_1^b} \xrightarrow{\sum_{b\in B} \partial_1^b} \mathbb{R}^{Q_0} \xrightarrow{\partial_0} \mathbb{R} \to 0 \tag{8.4.1}$$

The cellular homology group H^1 of the graph gives the loops of the quiver (see [Hat02, Sec 2.2]), hence $\ker(\partial_1)$ is generated by the simple unoriented cycles of Q, each one lying in a single biconnected component. It gives then the decomposition $\ker(\partial_1) = \bigoplus_{b\in B} \ker(\partial_1^b)$:

Lemma 8.4.3. *A current on a quiver is conserved if and only if its restriction to each biconnected component is a conserved current.*

Lemma 8.4.4. *i) A quiver is strongly connected if and only if all its biconnected components are strongly connected.*

ii)Suppose that Q is strongly connected. Consider the equivalence class $\sim$ on the arrows of Q generated by $a \sim b$ if $a, b \in w$ for $w \in Q_2$. The equivalence classes of $\sim$ correspond to the biconnected components of Q.

Proof:

i) Suppose that Q is strongly connected. Consider i, i' in a biconnected component b. There is an oriented path $v : i \to i'$ in Q, giving a cycle $\bar{v} : b \to b$ on the graph K. If this cycle is trivial, then v stays in the biconnected component b. If it is not trivial, since K is a tree, the cycle $\bar{v}$ must be of the form $b \to j \to ... \to j \to b$, i.e. the path v can be decomposed as $i \xrightarrow{v_1} j \xrightarrow{v_2} j \xrightarrow{v_3} i'$, with v_3 and v_1 oriented paths in b. One obtains then an oriented path $v_3 v_1 : i \to i'$ in b, i.e. b is strongly connected.

Suppose that each biconnected component of Q is strongly connected. Consider i, i' two nodes of Q, with $i \in b, i' \in b'$. The graph K is connected, consider a path $b \ni i_1 \in b_1 ... i_{n-1} \in b_{n-1} \ni i_n \in b'$. Because b, b_k, b' are strongly connected, consider oriented paths $v : i \to i_1, v_k : i_k \to i_{k+1}, v' : i_n \to i'$ respectively in b, b_k, b'. This gives an oriented path $v' v_{n-1} ... v_1 v : i \to i'$ in Q, i.e. Q is strongly connected.

ii) Because a simple oriented cycle $w \in Q_2$ is contained in a single biconnected component of Q, an equivalence class of $\sim$ is contained in a single biconnected component of Q. One has then to show that a biconnected quiver contains only one single class of $\sim$. Two equivalence classes do not share any arrows by definition: one can construct an unoriented graph $\tilde{K}$ with a node corresponding to each equivalence class s of $\sim$, and a node for each node $i \in Q_0$ shared between different equivalence classes, and an edge between i and s when $i \in s$.

Considering two nodes i, j, there is a path between i and j in Q: the sequence of equivalence classes of $\sim$ crossed by this path gives a path in $\tilde{K}$ between i and j, i.e. $\tilde{K}$ is connected. Consider a cycle $i_1 \in s_1 \ni i_2 ... i_n \in s_n \ni i_1$ with no node or edge repeated in $\tilde{K}$. Because each equivalence class is strongly connected, one can choose an oriented path $v_k : i_k \to i_{k+1}$ with no node repeated in each equivalence class s_k, the concatenation giving an oriented cycle $v_n ... v_1$ in Q. Because each v_k contains no repeated node, there is a subcycle w of $v_n ... v_1$ which is simple and contains arrows of different equivalence classes of $\sim$, giving a contradiction. The graph $\tilde{K}$ is then a connected tree. If there were more than one equivalence classes of $\sim$, then there would be a node $i \in \tilde{K}$ such that removing i disconnects $\tilde{K}$, and then disconnects the quiver Q, a contradiction because Q was assumed to be biconnected. There is therefore a single equivalence class of $\sim$ in a biconnected quiver Q.

□

8.4.3 Cuts and R-charge

Lemma 8.4.5. *The following assertions are equivalent:*
i) *Q admits a cut.*
ii) *Q admits an R-charge.*
iii) *Each maximal weak cut of Q is a cut.*

Proof: *iii*) $\Rightarrow$ *i*): $\emptyset$ is a weak cut, and the poset of weak cuts is finite, then Q admits a maximal weak cut, which is a cut by assumption.

i) $\Rightarrow$ *ii*) Consider a cut I of Q. Recall that we have defined the homomorphism $R_I : \mathbb{R}^{Q_1} \mapsto \mathbb{R}$ by $R_I(a) = 2$ if $a \in I$ and $R_I(a) = 0$ otherwise. Each cycle $w \in Q_2$ contains exactly one arrow $a \in I$, and $R_I \circ \partial_2(w) = R_I(a) = 2$, i.e. R_I is a R-charge.

ii) $\Rightarrow$ *iii*). Consider a maximal weak cut I, and $R : \mathbb{R}^{Q_1} \to \mathbb{R}$ such that $R \circ \partial_2 \geq R_I \circ \partial_2$, and $R_I \circ \partial_2(w) = 2 \Rightarrow R \circ \partial_2(w) = 2$. We must show that $R \circ \partial_2 = R_I \circ \partial_2$. Consider $(w = a_n ... a_1) \in Q_2$ such that $R_I \circ \partial_2(w) = 0$ i.e. $a_k \notin I$ for each k (see Figure 8.10): in particular one has $R \circ \partial_2(w) \geq 0$. Because I is maximal, each arrow $a_k \in w$ is contained in a simple cycle $w_k = v_k a_k \in Q_2$ such that v_k contains exactly one arrow of I (since otherwise $I \cup \{a_k\}$ would be a larger weak cut). The oriented cycle $\bar{w} = v_1 ... v_n$ is a product of simple oriented cycles, and satisfies:

$$\begin{aligned} & R \circ \partial_2(\bar{w}) \geq R_I \circ \partial_2(\bar{w}) = 2n \\ & \partial_2(w) = \sum_k \partial_2(w_k) - \partial_2(\bar{w}) \\ \Rightarrow & R \circ \partial_2(w) = 2n - R \circ \partial_2(\bar{w}) \leq 0 \\ \Rightarrow & R \circ \partial_2(w) = 0 = R_I \circ \partial_2(w) \end{aligned} \tag{8.4.2}$$

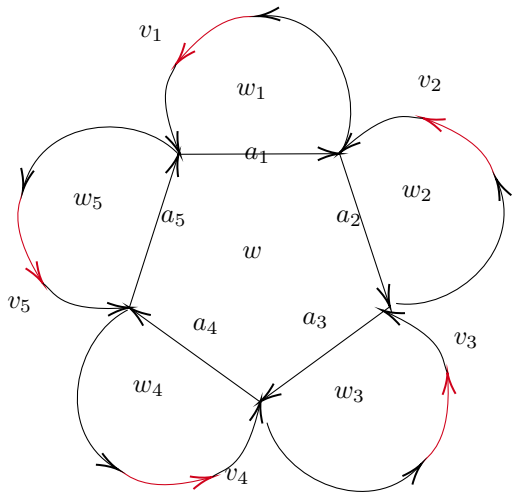

Figure 8.10: If Q admits an R-charge, then each maximal weak cut is a cut.

where the third line holds because $R_I \circ \partial_2(w_k) = 2$. By disjunction of cases, one has then $R \circ \partial_2 = R_I \circ \partial_2$. When R is an R-charge, one obtains then that R_I is a R-charge, i.e. I is a cut. □

Lemma 8.4.6. *For a quiver with an R-charge and a cycle w_0 passing through all the nodes, the cuts are given by $I = \{a : i \to j | i > j\}$ for each labeling of the nodes such that $w_0 : 1 \to 2 \to ... \to n \to 1$.*

Consider a cut I of Q: it contains exactly one arrow $a \in w_0$: we choose the labeling of Q_0 such that $a : n \to 1$ (see Figure 8.11). Consider an arrow $(b : i \to j) \in Q_1$, and denote by v_{ji} the minimal path going from j to i on the cycle w_0: v_{ji} contains an arrow of I if and only if $i < j$, and the simple oriented cycle $v_{ji}b \in Q_2$ contains exactly one arrow of the cut I, i.e. $b \in I$ if and only if $j < i$. One concludes that each cut of Q is of the form $I = \{b : i \in j | j < i.$ for a specific cyclic ordering of w_0.

Conversely, consider the set $I = \{b : i \to j | j < i\}$, and a cycle $w : i_1 \xrightarrow{a_1} i_2 ... i_r \xrightarrow{a_r} i_1 \in Q_2$, such that $R \circ \partial_2(w) = 2$ (see Figure 8.12). We will show that w contains exactly one arrow of I. The cycle $v_{i_1 i_r} ... v_{i_2 i_1}$ is equal to the m-th iteration w_0^m, for some $m \in \mathbb{N}$. Since $2 = R \circ \partial_2(w) = \sum_{k=1}^{r} R \circ \partial_2(v_{i_{k+1} i_k} a_k) - mR \circ \partial_2(w_0) = 2r - 2m$, the number of iterations is $m = r - 1$. But $w_0 \in Q_2$ contains exactly one arrow of I, and each cycle $v_{i_{k+1} i_k} a_k \in Q_2$ contains exactly one arrow of I. Indeed, there are two options: a) either $i_k > i_{k+1}$, and then $a_k \in I$ but $v_{i_{k+1} i_k}$ does not contain any arrow of I, or b) $i_k < i_{k+1}$, and then $a_k \notin I$ but $v_{i_{k+1} i_k}$ contains the arrow $n \to 1 \in I$. Evaluating the R-charge, we get $R_I \circ \partial_2(w) = \sum_{k=1}^{r} R_I \circ \partial_2(v_{i_{k+1} i_k} a_k) - (r-1) R_I \circ \partial_2(w_0) = 2$. Therefore $w \in Q_2$ contains exactly one arrow of I, i.e. I is a cut. □

When Q admits no R-charge (see Figures 8.5, 8.4 for examples), the set $I = \{b : i \in j | j < i\}$ is a minimal strong cut of Q which is not a cut: each simple oriented cycle contains at least one arrow of I, but there must be a cycle $w \in Q_2$ containing more that one arrow of Q. In particular, if Q has another cycle w_1 passing through all the nodes in a different order than w_0, then it has no R-charge. Indeed, for a labeling of the nodes such that $w_0 : 1 \to 2 \to ... \to n \to 1$, the cycle w_1

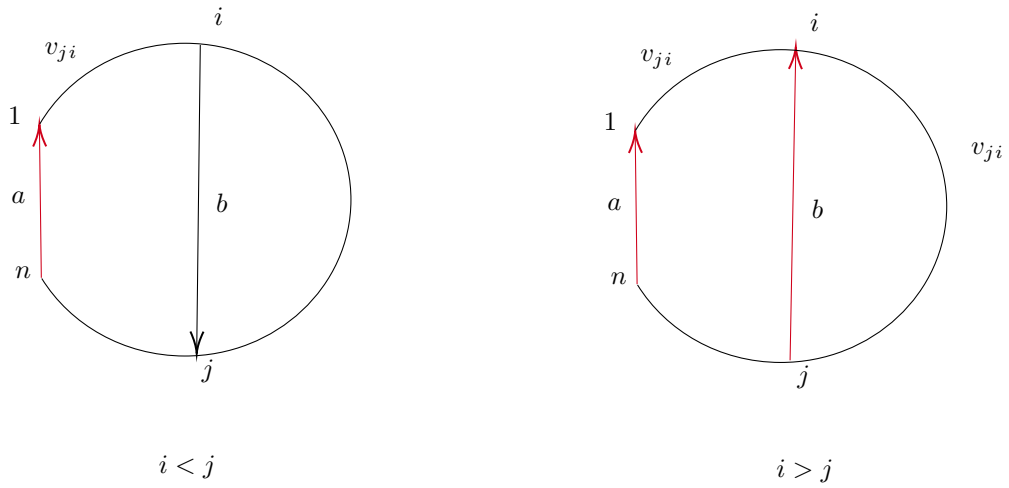

Figure 8.11: Under assumptions of lemma 8.4.6, all cuts are of the form $I = \{a : i \to j | i > j\}$

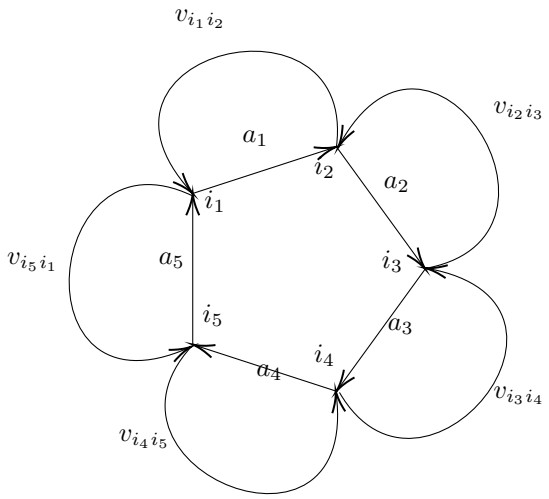

Figure 8.12: Under assumptions of lemma 8.4.6, the set $I = \{a : i \to j | i > j\}$ is a cut.

is of the form $1 = \sigma(1) \to \sigma(2) \to ... \to \sigma(n) \to \sigma(1)$, with σ a permutation of $\{1, ..., n\}$ different from the identity. There must then be at least two arrows of w_1 such that $\sigma(i) > \sigma(i+1)$, and then w_1 contains at least two arrows of $I = \{a : i \to j | i > j\}$, i.e. I is not a cut, and then Q has no R-charge. More generally, the criterion of the above lemma gives a simple algorithm to check if a quiver with a cycle passing through all the nodes has an R-charge.

8.4.4 Current decomposition for Abelianized quivers

Lemma 8.4.7. *For Q a biconnected quiver and d a dimension vector with $d_i \geq 1$ for $i \in Q_0$, a strictly positive conserved current on Q^d can be expressed as a sum of (not necessarily positive) currents circulating on the cycles in $p^{-1}(Q_2)$.*

Proof: Consider a strictly positive conserved current λ on Q^d: in particular Q^d, and therefore Q, is strongly connected from i) of lemma 8.4.1, and λ can be expressed as a sum of positive currents circulating on the cycles in Q_2^d. One must then show that for Q a biconnected strongly connected quiver each cycle in Q_2^d can be expressed as a linear combination of cycles in $p^{-1}(Q_2)$, i.e. $\partial_2(\mathbb{R}^{Q_2^d}) \subset \partial_2(\mathbb{R}^{p^{-1}(Q_2)})$. One can construct the Abelianized quiver by using a finite sequence of elementary steps, where one node is split into two nodes at each step. Each of these steps preserves the fact that the quiver is biconnected and strongly connected, thus it suffices to prove the statement for an elementary step.

Consider a biconnected strongly connected quiver Q, a node $i \in Q_0$ and the dimension vector d such that $d_i = 2$ and $d_j = 1$ for $j \neq i$. Consider a cycle $w \in Q_2^d - p^{-1}(Q_2)$: it necessarily passes through the two nodes $(i,1), (i,2)$, i.e. it is of the form[6] $(d,1)v(c,2)(b,2)u(a,1)$, where a, c are arrows of Q with source i, b, d arrows of Q with target i, and u and v paths of Q avoiding i, such that $dvc, bua \in Q_2$ (see Figure 8.13). We claim that there is a sequence of arrows $b_0 = b, b_1, ..., b_n$ with target i, a sequence of arrows $c_0, ..., c_n = c$ with source i, and sequences of paths $u_1, ..., u_n$ and $v_1, ..., v_{n-1}$ in Q, such that $b_k u_k c_k$ and $b_{k+1} v_k c_k$ are simple oriented cycles in Q_2 for $1 \leq k \leq n-1$. Then:

$$\begin{aligned}\partial_2\left((d,1)v(c,2)(b,2)u(a,1)\right) =& \partial_2\left((d,1)v(c,1) + (b,1)u(a,1)\right.\\ &+ \sum_{k=0}^{n-1}\left((b_k,2)u_k(c_k,2) - (b_k,1)u_k(c_k,1) + (b_{k+1},1)v_k(c_k,1) - (b_{k+1},2)v_k(c_k,2)\right) \qquad (8.4.3)\end{aligned}$$

where each of the cycles appearing on the right belongs to $p^{-1}(Q_2)$, i.e. project to a simple cycle of Q. Thus $\partial_2((d,1)v(c,2)(b,2)u(a,1)) \in \partial_2(\mathbb{R}^{p^{-1}(Q_2)})$, and then $\partial_2(\mathbb{R}^{Q_2^d}) \subset \partial_2(\mathbb{R}^{p^{-1}(Q_2)})$ which concludes the proof.

Proof of the claim: Consider a strongly connected biconnected quiver Q, and a node $i \in Q_0$. Consider the equivalence $\sim$ on the arrows of Q with source or target i, generated by $a \sim b$, with a (resp. b) with source (resp. target) i if there is a path v in Q such that bva is a simple oriented cycle in Q_2. We need to show that there is a single equivalence class under $\sim$. Let S be the set of equivalence classes. To each $s \in S$ of $\sim$ one can associate the subquiver $Q^s \subset Q - \{i\}$ whose nodes are the nodes j such that there is a path $v : j \to i$ passing only once through i and ending by an arrow in the given equivalence class.

[6] Since i is the only non-Abelian node, we abuse notation and denote by (a,k) and (b,k) the lift of the arrows $a : i \to j$ and $b : j \to i$ on Q to the k-th copy of the node i on Q^d.

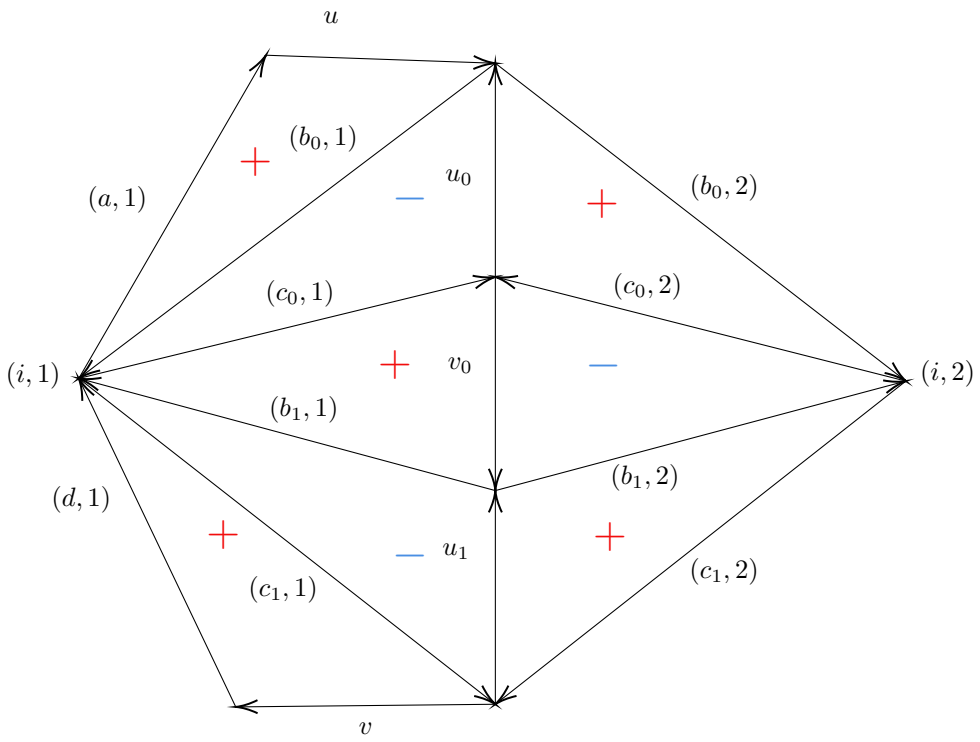

Figure 8.13: Proof of the fact that a simple cycle of Q^d can be expressed as a signed sum of cycles in $p^{-1}(Q_2)$.

Since Q is strongly connected, for each $j \in Q_0 - \{i\}$ there is a path from j to i, which up to truncating the path, can be considered as passing only once through i, i.e. $j \in Q_0^s$ for at least one $s \in S$. Consider $j \in Q_0^s$, $j' \in Q_0^{s'}$ and $u : j \to j'$ an oriented path of Q avoiding i. Consider paths $v : j \to i$, $v' : j' \to i$ passing only once through i and ending respectively by $b \in s$, $b' \in s'$. Because Q is strongly connected, there is a path $u' : i \to j$ beginning by an arrow a with source i: the two cycles vu' (resp. $v'uu'$) contain a simple cycle containing ba (resp. $b'a$), and then $b \sim a \sim b'$, i.e. $s = s'$. For $j = j'$ and u the trivial path at j, one obtains that the Q_0^s form a partition of $Q_0^s - \{i\}$, and for $u = a : j \to j'$ an arrow of Q one obtains that Q^s and $Q^{s'}$ are disconnected in $Q - \{i\}$. If there were different equivalence classes under $\sim$, $Q - \{i\}$ would be disconnected, contradicting the assumption that Q is biconnected. Thus there is a single equivalence class under $\sim$, which proves the claim. □

8.4.5 Higgs branch

Lemma 8.4.8. *Let Q be a quiver, $C \subset Q_2$ a set of cycles of Q such that there exists a subset $I \subset Q_1$ of arrows such that each cycle of C contains exactly one arrow of I. For any dimension vector $d \in \mathbb{N}_0^Q$, there exists a dense open subset $U_{C,d} \subset \mathbb{C}^C$ such that for any $(\nu_w)_{w\in C} \in U_{c,d}$ and any d-dimensional representation ϕ of the quiver Q with potential $W = \sum_{w\in C} \nu_w w$, the trace $\mathrm{Tr}(w)$ vanishes on the representation ϕ for all cycles $w \in C$ appearing in the potential.*

Proof: We follow an argument of Kontsevich quoted in the proof of [Efi11, Prop. 3.1]. For $d \in \mathbb{N}^{Q_0}$, denote by M_d the smooth quasi-projective connected space of d-dimensional representations of Q. Now, consider a potential cut I of W, such that $\mathrm{Tr}(W) = \sum_{a\in I} \mathrm{Tr}(a\partial_a W)$: by homogeneity, the critical points of $\mathrm{Tr}(W)$ on M_d necessarily have $\mathrm{Tr}(W) = 0$. Let $f : M_d \to \mathbb{C}^C$ be the map which associates to any d-dimensional representation of Q the vector $(\mathrm{Tr}(w)_{w\in C}$. Away from the locus $f^{-1}(0)$, the image of this map descends to the projective space $\mathbb{P}^{|C|-1}$. The trace of the potential $W = \sum_{w\in C} \nu_w w$ is obtained by composing f with a linear form, corresponding to a hyperplane section of $\mathbb{P}^{|C|-1}$. By applying Bertini's theorem to the complete linear system $\mathrm{Tr}(W)^{-1}(0)$, one finds that, for $(\nu_w)_{w\in C}$ in a dense open subset $U_{C,d} \subset \mathbb{C}^C$, $\mathrm{Tr}(W)^{-1}(0)$ is a smooth connected strict sub-variety of M_d away from the zero locus $f^{-1}(0)$. In particular, its tangent space at any point $x \in \mathrm{Tr}(W)^{-1}(0) - f^{-1}(0))$ is strictly included in the tangent space of M_d,

$$T_x(\mathrm{Tr}(W)^{-1}(0)) \subsetneq T_x(M_d) \tag{8.4.4}$$

hence $\delta(\mathrm{Tr}(W))|_x \neq 0$. It follows that the critical points of $(\mathrm{Tr}(W)$ lie in $f^{-1}(0)$, hence $\mathrm{Tr}(w) = 0$ for $w \in C$ on a d-dimensional representation of (Q, W). Specializing to the dimension vector $d = (1, ..., 1)$, one obtains that for $(\nu_w)_{w\in C} \in U_C$ a dense open subset of $\mathbb{C}^C$, and for any Abelian representation of (Q, W), the cycles w vanish for all $w \in C$. □.

Now, for any weak cut $I \subset Q_1$, we denote by Q_2^I the set of cycles containing exactly one arrow of I, and for $W = \sum_{w\in Q_2} \nu_w w$, we define $W_I := \sum_{w\in Q_2^I} \nu_w w$. Let $p_I : \mathbb{C}^{Q_2} \to \mathbb{C}^{Q_2^I}$ be the natural projection.

Definition 8.4.9. A potential $W = \sum_{w\in Q_2} \nu_w w$ is said to be generic if $(\nu_w)_{w\in Q_2}$ is in the dense open subset $\bigcap_I p_I^{-1}(U_{Q_2^I})$.

Proposition 8.4.10. *Consider a quiver with generic potential (Q, W). If there exists a self-stable Abelian representation of (Q, W), then for each weak cut I:*

$$|I| \leq |Q_1 - I| - |Q_0| + 1 \tag{8.4.5}$$

Proof: Let ϕ be a ζ-stable representation of (Q,W), with ζ, W generic, and I a weak cut of Q. Denote by J the set of arrows of Q vanishing in ϕ. The representation ϕ gives a ζ-stable representation of Q_J, the quiver where the arrows of J have been removed: in particular, the stability of ϕ implies that Q_J is connected (otherwise, ϕ would be a direct sum of representations supported on the connected components). Consider the set $K \subset I-J$ of arrows $(a : i \to j) \in I-J$ such that i and j are connected in $Q_{J\cup I}$. The quiver $Q_{J\cup K}$ obtained by removing all arrows in K is then still connected. Sending the arrows of K to 0 in ϕ, one obtains a representations ψ of $Q_{J\cup K}$ without vanishing arrows. Because $Q_{J\cup K}$ is connected, the gauge group $(\mathbb{C}^*)^{Q_0}$ scaling the nodes acts on the space $(\mathbb{C}^*)^{Q_1-J-K}$ of representations of $Q_{J\cup K}$ without vanishing arrows with stabilizer $\mathbb{C}^\star$, giving a smooth moduli space of dimension $|Q_1-J-K|-|Q_0|+1$.

Consider the potential W_I obtained from the generic potential W by keeping only the cycles $w \in Q_2$ which contain an arrow of I. Consider $L \subset J\cup K$ the set of arrows contained in a cycle $w \in Q_2$ such that $R_{J\cup K}\circ\partial_2(w) = R_I\circ\partial_2(w) = 2$. Consider $a \in L$:

- If $a \in I$, because I is a weak cut, any cycle $w \in Q_2$ which contains a is a cycle of W_I, and contains no other arrow of I, and in particular no other arrows of K, i.e. :
$$\partial_a W_I|_\psi = \partial_a W|_\psi = \partial_a W|_\phi = 0 \tag{8.4.6}$$
- Suppose $a \in J-I$. There is a cycle $w \in Q_2$ containing a such that $R_{J\cup K}\circ\partial_2(w) = R_I\circ\partial_2(w) = 2$. Hence w contains an arrow $b \in I$ different from a, which cannot be in K, hence $b \in I-K$. Denote by $i \sim j$ the equivalence relation identifying vertices i and j which are connected in $Q_{J\cup I}$: one has $t(b) \sim s(a)$ and $t(a) \sim s(b)$ because w contains no other arrows of $J\cup I$. Consider an other cycle w' containing a.
  - If w' contains an other arrow of J, then $0 = \partial_a w'|_\psi = \partial_a w'|_\phi$.
  - If w' contains no other arrow of J and an arrow $c \in K \subset I-J$, by definition, $s(c) \sim t(c)$: using $t(a) \sim s(c)$ and $t(c) \sim s(a)$ because w' contains no other arrows of $J\cup I$, one obtains $t(b) \sim s(b)$, a contradiction because $b \in I-K$.
  - If w' contains no other arrow of J and no arrow of I, then $t(a) \sim s(a)$, and then $t(b) \sim s(b)$, a contradiction because $b \in I-K$.
  - In the remaining case w' contains one arrow of J and one arrow of $I-K$, then w' is a cycle of W_I and $\partial_a w'|_\psi = \partial_a w'|_\phi$

  By disjunction of cases one has $\partial_a W|_\psi = \partial_a W|_\phi = 0$, and because the only cycles contributing to $\partial_a W|_\psi$ are cycles of W_I, one has $\partial_a W_I|_\psi = \partial_a W|_\psi = 0$.

By disjunction on cases, $\partial_a W_I|_\psi = 0$ for $a \in L$, hence ψ is a representation of the quiver with relations $(Q_{J\cup K}, \partial_L W_I)$ without vanishing arrows. The tangent space of the moduli space of representations of $(Q_{J\cup K}, \partial_L W_I)$ at ψ is given by the intersection of the kernel of the $|L|$ differential forms $\delta(\partial_a W_I)$ for $a \in L$.

As in (8.3.8), a linear relation $\sum_{a\in L}\tilde{\psi}_a\delta(\partial_a W_I) = 0$ between these differential forms yields a representation $\bar{\psi} = (\psi_a, \epsilon\tilde{\psi}_b)_{a\in Q_1-L, b\in L}$ over $\mathbb{C}\epsilon/\epsilon^2$ such that $\delta_b W|_{\bar{\psi}} = 0$ for $b \in Q_1 - J\cup K$. For an arrow $b \in J\cup K$, because $\partial_b|_\psi = 0$, $\partial_b|_{\bar{\psi}}$ is at most of order ϵ, and $\bar{\psi}_b$ is at most of order ϵ, hence $\bar{\psi}_b\partial_b|_{\bar{\psi}} = 0$. Then $\bar{\psi}_b\partial_b|_{\bar{\psi}} = 0$ for $b \in Q_1$. Since the each cycle of the potential W_I contains exactly one arrow of I, Lemma 8.4.8 implies that the cycles of W_I vanish in $\bar{\psi}$. By definition, each

arrow $a \in L \subset J \cup K$ is contained in a cycle w of W_I in which it is the only arrow of $J \cup K$. In particular all the other arrows are in $Q_1 - J - K$ and are non-vanishing: then $\epsilon\tilde{\psi}_a \prod_{a \neq b \in w} \psi_b = 0$, hence $\tilde{\psi}_a = 0$. The $|L|$ differential forms $\delta(\partial_a W_I)$ for $a \in L$ are then independent, hence:

$$|Q_1 - J - K| - |Q_0| + 1 - |L| \geq 0 \tag{8.4.7}$$

Defining

$$R(a) = \begin{cases} 0 & \text{if } a \in Q_1 - J \\ 1 & \text{if } a \in J - L \\ 2 & \text{if } a \in L \cap J \end{cases} \qquad R'(a) = \begin{cases} 0 & \text{if } a \in Q_1 - K \\ 1 & \text{if } a \in K - L \\ 2 & \text{if } a \in K \cap L \end{cases} \tag{8.4.8}$$

one finds

$$\sum_{a \in Q_1} (R + R')(a) \leq |Q_1| - |Q_0| + 1 \tag{8.4.9}$$

We will now show that the following inequality holds for all $w \in Q_2$:

$$R_I \circ \partial_2(w) \leq (R + R') \circ \partial_2(w) \tag{8.4.10}$$

By disjunction of cases,

- If w contains no arrow of I, one has directly $R_I \circ \partial_2(w) = 0 \leq (R + R') \circ \partial_2(w)$.

- Suppose that w contains an arrow $a \in I$. If w contains no arrow of J, then $t(a)$ and $s(a)$ are connected in $Q_{J \cup I}$, hence $a \in K$. Then in any cases, w contains an arrow of $J \cup K$. If it contains a single arrow of $J \cup K$, then by definition it is an arrow of L, contributing to $R + R'$ by 2. If it contains at least two arrows of $J \cup K$, then each of them contributes to $R + R'$ by 1. By disjunction of cases $R_I \circ \partial_2(w) = 2 \leq (R + R') \circ \partial_2(w)$.

The inequality (8.4.10) follows, and can be rewritten:

$$(R_I - R') \circ \partial_2(w) \leq R \circ \partial_2(w) \quad \forall\, w \in Q_2 \tag{8.4.11}$$

We now assume that ζ is a self-stability condition. Because the positive conserved current $\lambda = (1 + \delta_a + |\psi_a|^2)_{a \in Q_1}$ (with $\delta_a \ll 1$) corresponding with the self-stable representation ψ is a sum of positive currents supported of cycles in Q_2 from Lemma 8.4.1, it follows that:

$$(R_I - R')(\lambda) \leq R(\lambda) \tag{8.4.12}$$

We deduce then:

$$\begin{aligned}
2|I| + \sum_{a\in Q_1} (R_I - R')(a)\delta_a &\le \sum_{a\in Q_1} (R_I - R')(a)(1+\delta_a + |\phi_a|^2) + \sum_{a\in Q_1} R'(a) \\
&= (R_I - R')(\lambda) + \sum_{a\in Q_1} R'(a) \\
&\le R(\lambda) + \sum_{a\in Q_1} R'(a) = \sum_{a\in Q_1} R(a)(1+\delta_a + |\phi_a|^2) + \sum_{a\in Q_1} R'(a) \\
&= \sum_{a\in Q_1} (R+R')(a) + \sum_{a\in Q_1} \delta_a R(a) \\
&\le |Q_1| - |Q_0| + 1 + \sum_{a\in Q_1} \delta_a R(a) \\
\implies 2|I| &\le |Q_1| - |Q_0| + 1
\end{aligned} \tag{8.4.13}$$

Here we have used the facts that $(R_I - R')(a) \ge 0$ in the first line, $\phi_a = 0$ when $R(a) \neq 0$ in the fourth line, (8.4.9) in the fifth line, and $\delta \ll 1$ in the last line. □

Chapter 9

BPS Dendroscopy on Local $\mathbf{P^2}$

Joint work with Pierrick Bousseau, Bruno Le Floch, and Boris Pioline

The spectrum of BPS states in type IIA string theory compactified on a Calabi-Yau threefold famously jumps across codimension-one walls in complexified Kähler moduli space, leading to an intricate chamber structure. The Split Attractor Flow Conjecture posits that the BPS index $\Omega_z(\gamma)$ for given charge γ and moduli z can be reconstructed from the attractor indices $\Omega_\star(\gamma_i)$ counting BPS states of charge γ_i in their respective attractor chamber, by summing over a finite set of decorated rooted flow trees known as attractor flow trees. If correct, this provides a classification (or dendroscopy) of the BPS spectrum into different topologies of nested BPS bound states, each having a simple chamber structure. Here we investigate this conjecture for the simplest, albeit non-compact, Calabi-Yau threefold, namely the canonical bundle over $\mathbb{P}^2$. Since the Kähler moduli space has complex dimension one and the attractor flow preserves the argument of the central charge, attractor flow trees coincide with scattering sequences of rays in a two-dimensional slice of the scattering diagram $\mathcal{D}_\psi$ in the space of stability conditions on the derived category of compactly supported coherent sheaves on $K_{\mathbb{P}^2}$. We combine previous results on the scattering diagram of $K_{\mathbb{P}^2}$ in the large volume slice with an analysis of the scattering diagram for the three-node quiver valid in the vicinity of the orbifold point $\mathbb{C}^3/\mathbb{Z}_3$, and prove that the Split Attractor Flow Conjecture holds true on the physical slice of Π-stability conditions. In particular, while there is an infinite set of initial rays related by the group $\Gamma_1(3)$ of auto-equivalences, only a finite number of possible decompositions $\gamma = \sum_i \gamma_i$ contribute to the index $\Omega_z(\gamma)$ for any γ and z, with constituents γ_i related by spectral flow to the fractional branes at the orbifold point. We further explain the absence of jumps in the index between the orbifold and large volume points for normalized torsion free sheaves, and uncover new 'fake walls' across which the dendroscopic structure changes but the total index remains constant.

9.1 Introduction and summary

Determining the spectrum of BPS states at generic points in the moduli space in string theory models with $\mathcal{N} = 2$ supersymmetry in four dimensions is an important problem, with far reaching

implications both for physics and mathematics. On the physics side, it challenges our understanding of black holes at the microscopic level; on the mathematics side, it connects to deep questions in algebraic and symplectic geometry.

In the context of type IIA string theory compactified on a Calabi-Yau (CY) threefold $\mathfrak{Y}$, BPS states correspond to objects in the bounded derived category of coherent sheaves $\mathcal{C} = D^b\,\mathrm{Coh}(\mathfrak{Y})$ which are stable for a particular Bridgeland stability condition determined by the complexified Kähler moduli, known as Π-stability [Kon95, Dou01, DFR05a, Bri07]. For a general compact CY threefold, the construction of the space of Bridgeland stability conditions $\mathrm{Stab}(\mathcal{C})$ is a difficult mathematical problem, and the identification of the submanifold $\Pi \subset \mathrm{Stab}(\mathfrak{Y})$ corresponding to Π-stability depends on the symplectic geometry of $\mathfrak{Y}$ (namely, its genus-zero Gromov-Witten invariants). For fixed charge $\gamma \in K(\mathfrak{Y})$ and central charge[1] Z (determined by the Kähler moduli), stable objects are counted by the generalized Donaldson-Thomas (DT) invariant $\Omega_Z(\gamma)$ [Tho98, KS, JS12]. The latter, being integer valued, is locally constant but discontinuous across real-codimension one walls in $\mathrm{Stab}(\mathfrak{Y})$ (hence also on Π), due to the (dis)appearance of destabilizing sub-objects, leading to an intricate chamber structure. While the jump is determined in terms of the invariants on one side of the wall by a universal wall-crossing formula [KS, JS12], it is desirable to develop a global understanding of the BPS spectrum which allows to identify stable objects at any point z in $\Pi \subset \mathrm{Stab}(\mathfrak{Y})$.

9.1.1 The Split Attractor Flow Conjecture

The physical picture of BPS states as multi-centered black holes suggests one way to achieve this goal, namely to decompose stable BPS states of charge γ into bound states of elementary constituents of charge γ_i, with a hierarchical structure determined by attractor flow trees [Den00, DGR01]. As we review in more detail in §9.3.4, the latter are rooted trees decorated with charges γ_e along the edges, embedded in $\Pi \subset \mathrm{Stab}(\mathfrak{Y})$ such that the root vertex is mapped to the desired point $z \in \Pi$, edges follow the gradient flow (also known as attractor flow [FKS95]) for the modulus of the central charge $|Z(\gamma_e)|^2$ along the slice Π, and split at vertices on walls of marginal stability where the central charges of the incoming and descending charges become aligned. The aforementioned constituents γ_i arise as the end points (or leaves) of the tree, where the central charge is attracted to a local minimum of $|Z(\gamma_i)|$ along Π, or to a conifold point where $Z(\gamma_i) = 0$. We denote by $Z_{\gamma_i}(\gamma)$ the central charge at this local minimum, and by $\Omega_\star(\gamma_i) := \Omega_{Z_{\gamma_i}}(\gamma_i)$ the corresponding value of the DT invariant, known as attractor index.

The Split Attractor Flow Conjecture (SAFC), originally proposed in [Den00, DGR01] and sharpened in [DM11a], posits that for any $\gamma \in \Gamma$ and $z \in \Pi$, the BPS index $\Omega_Z(\gamma)$ can be computed by summing over a finite number of such attractor flow trees, weighted by the product of attractor indices $\Omega_\star(\gamma_i)$ and by some combinatorial factor obtained by applying the wall-crossing formula at each vertex.[2] If correct, this picture provides a categorization (which we like to call dendroscopy) of the BPS spectrum at $z \in \Pi$ into different types, each having a simple region of stability delimited by the first splitting at the root of the tree, and reduces the determination of the BPS spectrum to the computation of the attractor invariants $\Omega_\star(\gamma_i)$. Unfor-

[1] As we recall in §9.2.3, a stability condition $\sigma = (Z, \mathcal{A})$ on $\mathcal{C}$ also involves a choice of Abelian subcategory $\mathcal{A} \subset \mathcal{C}$ (the heart). We omit it here for brevity since it is locally determined by the central charge Z.

[2] The original formulation of the conjecture relied on the primitive wall-crossing formula and overlooked issues arising when some of the constituents carry non-primitive or identical charges. In §9.3.4, using insights from [DM11a, Man11b, MPS11b, AP19a] we give a more precise version of the conjecture in terms of the rational DT invariants $\bar{\Omega}(\gamma)$ defined in (9.1.1).

tunately, for a compact CY threefold $\mathfrak{Y}$, the computation of these invariants seems very difficult and the Split Attractor Flow Conjecture is still wide open, despite some encouraging results [DM11a, CW10, VHW10, Man11b, KS13, Gad16, AGMP22].

The problem however becomes more tractable for certain non-compact CY threefolds, such that the category $D^b\,\mathrm{Coh}(\mathfrak{Y})$ is isomorphic to the derived category $D^b\,\mathrm{Rep}(Q,W)$ of representations of a certain quiver with potential (Q,W). In particular, in the vicinity of an orbifold point where the central charges associated to the nodes of the quiver all lie in a common half-plane, the heart of the stability condition reduces to the category of quiver representations (or some tilt of it) and the notion of attractor index has a simple definition using King stability for the (suitably perturbed) 'self-stability' parameter $\theta_\star(\gamma) = \langle -, \gamma\rangle$ [MP20]. In that context, the enumeration of attractor flow trees becomes straightforward and precise versions of the Split Attractor Flow Conjecture have been proposed [AP19a, MP20] and then established rigorously [Moz21, AB21] using the mathematical framework of operads and scattering diagrams, respectively. As already anticipated in [KS13] and as will become apparent shortly, scattering diagrams turn out to be the mathematical incarnation of split attractor flows (at least for non-compact CY threefolds), while the physical interpretation of the trees in the operadic approach of [Moz21] remains obscure at present.

9.1.2 The Attractor Conjecture

As for the attractor indices which enter these formulae, it was conjectured in [BMP21a], that for quivers (Q,W) associated to a non-compact CY threefolds of the form $\mathfrak{Y} = K_S$ (namely, the total space of the canonical bundle over a Fano surface S), the attractor invariants $\Omega_\star(\gamma)$ take a very simple form: $\Omega_\star(\gamma) = 0$ except when γ corresponds to a dimension vector supported on one node of the quiver (in which case $\Omega_\star(\gamma) = 1$), or $\gamma = k\delta$ with $k \geq 1$ and δ the charge vector for the skyscraper sheaf (in which case $\Omega_\star(k\delta) = -\chi_{\mathfrak{Y}}$, the Euler number of $\mathfrak{Y}$). This Attractor Conjecture (AC) was arrived at by comparing the quiver indices with the counting of Gieseker-semistable sheaves on S, and supported by an analysis of the expected dimension of the moduli space of quiver representations in the self-stability chamber. Further evidence and an extension of AC to all toric CY three-folds was presented in [MP20, Des21]. In this work, we focus on the simplest case $\mathfrak{Y} = K_{\mathbb{P}^2}$ (also known as local $\mathbb{P}^2$), which is a crepant resolution of the orbifold singularity $\mathbb{C}^3/\mathbb{Z}_3$ and whose derived category of (compactly supported) coherent sheaves is isomorphic to the derived category of a three-node quiver (Q,W) shown in Figure 9.4. Combining ideas from [BMP21a, DP22], we prove Theorem 9.1.1, which states that the Attractor Conjecture holds for this quiver, thereby providing the attractor invariants relevant in the vicinity of the orbifold point.

Our main goal in this work is to extend this picture away from the orbifold point, and connect it to the scattering diagram for the derived category of sheaves on $\mathbb{P}^2$ constructed by one of the authors in [Bou19]. Before presenting our results in more detail however, we need to pause and explain the relation between scattering diagrams and flow trees.

9.1.3 Scattering diagrams and attractor flow trees

Scattering diagrams were first introduced in the context of the Strominger-Yau-Zaslow approach to mirror symmetry [KS06, GS11], and applied to DT invariants of quivers with potential in [Bri17]. More generally, as we explain in §9.3.3, for a given triangulated category $\mathcal{C}$ and phase[3] $\psi \in \mathbb{R}/2\pi\mathbb{Z}$,

[3]The scattering diagram $\mathcal{D}_\psi$ is invariant under $(\psi,\gamma,Z) \mapsto (\psi+\pi,-\gamma,Z)$ and $(-\psi,\gamma^\vee,Z^\vee)$ where $\gamma^\vee$ is the image of γ under derived duality, and $Z^\vee(\gamma) := -\overline{Z(\gamma^\vee)}$. For most of this work we restrict to the interval $(-\frac{\pi}{2},\frac{\pi}{2}]$.

the scattering diagram $\mathcal{D}_\psi$ is supported on a set of real-codimension one loci (or active rays) $\mathcal{R}_\psi(\gamma)$ in the space of stability conditions $\operatorname{Stab}\mathcal{C}$ where the central charge has fixed argument $\arg Z(\gamma) = \psi + \frac{\pi}{2}$ and supports semi-stable objects, in the sense that the rational DT index

$$\bar{\Omega}_Z(\gamma) := \sum_{m|\gamma} \frac{y - y^{-1}}{m(y^m - y^{-m})} \Omega_Z(\gamma/m)|_{y\to y^m} \tag{9.1.1}$$

is non-zero. Each point along $\mathcal{R}_\psi(\gamma)$ is equipped with an automorphism

$$\mathcal{U}_Z(\gamma) = \exp\big(\bar{\Omega}_Z(\gamma)\mathcal{X}_\gamma/(y^{-1} - y)\big) \tag{9.1.2}$$

of the quantum torus algebra spanned by formal variables $\mathcal{X}_\gamma$ satisfying $\mathcal{X}_\gamma\,\mathcal{X}_{\gamma'} = (-y)^{\langle\gamma,\gamma'\rangle}\mathcal{X}_{\gamma+\gamma'}$. The set $\mathcal{D}_\psi$ of all active rays $\mathcal{R}_\psi(\gamma)$ equipped with $\mathcal{U}_Z(\gamma)$ then forms a consistent scattering diagram, which informally means that the product of the automorphisms $\mathcal{U}_Z(\gamma)$ around each codimension-two intersection must equal one. This property uniquely specifies the invariants $\bar{\Omega}_Z(\gamma)$ on outgoing[4] rays in terms of those on incoming rays. In the context of quivers with potential, one can further restrict the scattering diagram from the space $(\mathbb{H}_B)^n$ of Bridgeland stability conditions (where $\mathbb{H}_B$ is the upper half-plane $\{z \in \mathbb{C} : \Im z > 0 \text{ or } (\Im z = 0 \text{ and } \Re z < 0)\}$ and n denotes the number of nodes in the quiver) to the space $\mathbb{R}^n$ of King stability conditions, such that $\mathcal{D}_\psi$ becomes a complex of convex rational polyhedral cones [Bri17].

In order to understand the relation between scattering diagrams and attractor flow trees, the key observation (elaborated upon in §9.3.5) is that for a local CY threefold, the central charge $Z(\gamma)$ is a holomorphic function of complexified Kähler moduli $z \in \Pi$, which implies that

1. The argument of $Z(\gamma)$ is constant along the gradient flow of $|Z(\gamma)|$

2. Local minima of $|Z(\gamma)|$ can only occur on the boundary of Π or at points $z \in \Pi$ where $|Z(\gamma)| = 0$

When Π has complex dimension 1 (as is the case for $K_{\mathbb{P}^2}$), the first observation implies that lines of gradient flow of $|Z(\gamma)|$ must lie along active rays $\mathcal{R}_\psi(\gamma)$, for a suitable value of ψ determined by the initial value of the flow. Since vertices in the attractor flow tree have to lie on walls of marginal stability where the central charges of the parent edge $Z(\gamma_v)$ and descendant edges $Z(\gamma_e), e \in \mathrm{ch}(v)$ become aligned, they must also must lie at the intersection of the corresponding rays $\mathcal{R}_\psi(\gamma_v)$ and $\mathcal{R}_\psi(\gamma_e), e \in \mathrm{ch}(v)$. Since stable BPS states of charge γ are ruled out at stability conditions where their central charge vanishes (a consequence of the support property for stability conditions), the second observation shows that the attractor points can only occur at the boundary of Π, corresponding to the initial rays of the scattering diagram. Starting from the leaves and going up towards the root, one can therefore view a split attractor flow as a sequence of scatterings of a set of initial rays $\mathcal{R}_\psi(\gamma_i)$, such that the final ray carries the desired charge $\gamma = \sum\gamma_i$ and passes through the desired point $z \in \Pi$ in the space of Π-stability conditions. When $\dim_{\mathbb{C}}\Pi > 1$, the connection between attractor flow trees and scattering diagrams is less direct, since the edges are real-dimension one trajectories embedded in real-codimension one rays. Nonetheless, in the vicinity of real-codimension two loci where active rays intersect, one can always take a two-dimensional transverse section such that the previous picture applies.

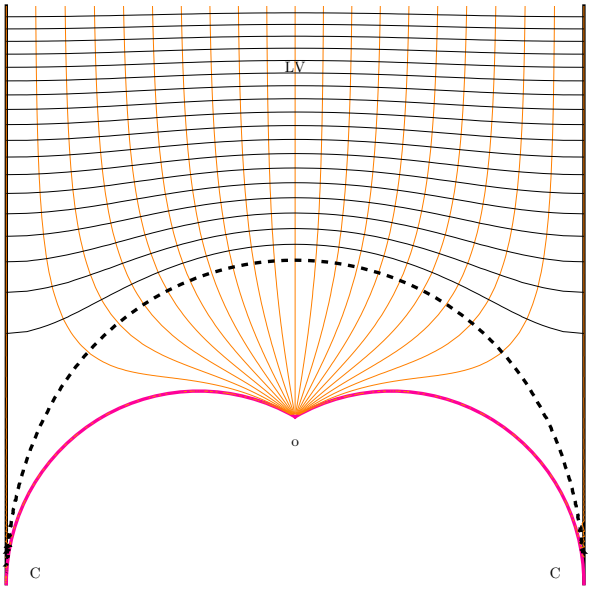

Figure 9.1: The fundamental domain $\mathcal{F}_o$ (9.7.1) depicted here is centered around the orbifold point $\tau_o = \frac{1}{\sqrt{3}} e^{5\pi \mathrm{i}/6} = -\frac{1}{2} + \frac{\mathrm{i}}{2\sqrt{3}}$. The domain $\mathcal{F}_C$ (9.7.2) is shifted horizontally by $+1/2$ and centered around the conifold point $\tau = 0$. The orange and black thin lines correspond to the contours of constant s and $t = \sqrt{2w - s^2}$, respectively, where (s, w) are defined in (9.1.7). In the region $\mathbb{H}^{\mathrm{LV}}$ above the dashed line (corresponding to $t = 0$), the exact central charge (9.1.3) along the Π-stability slice is related to the central charge on the large volume slice (9.1.6) by a $\widetilde{GL^+}(2, \mathbb{R})$ action.

9.1.4 The physical slice of Π-stability conditions

Returning to the special case of the local projective plane, the space $\mathrm{Stab}(K_{\mathbb{P}^2})$ of stability conditions on $D^b \mathrm{Coh}(K_{\mathbb{P}^2})$ was analyzed in detail in [Bri06, BM11]. Using the $\mathbb{C}^\times$ subgroup of the $\widetilde{GL^+}(2, \mathbb{R})$ action on the real and imaginary part of the central charge function, there is no loss of generality in assuming that $Z(\delta) = 1$, where $\delta = [0, 0, -1]$ is the Chern vector of the (anti)D0-brane, corresponding to the skyscraper sheaf $\mathcal{O}_x[1]$ (the homological shift [1] is for later convenience). The central charge for a general Chern vector $\gamma = [r, d, \mathrm{ch}_2]$ therefore takes the form

$$Z(\gamma) = -rT_D + dT - \mathrm{ch}_2 \tag{9.1.3}$$

where r is the rank (or D4-brane charge), d the first Chern class (or D2-brane charge) and ch_2 the second Chern class (or D0-brane charge), and $(T, T_D) \in \mathbb{C}^2$ parametrize the quotient $\mathrm{Stab}(K_{\mathbb{P}^2})/\mathbb{C}^\times$. Mirror symmetry selects a particular complex one-dimensional slice

$$Z_\tau(\gamma) = -rT_D(\tau) + dT(\tau) - \mathrm{ch}_2 \tag{9.1.4}$$

[4] We postpone the definition of incoming and outgoing rays to §9.3.3. For the present discussion, it suffices to orient the restriction of the rays along a transverse plane in the vicinity of a codimension-two intersection, according to the gradient of the central charge $|Z(\gamma)|$.

parametrized by τ in the Poincaré upper half-plane $\mathbb{H}$, such that T and T_D are given by periods on a family of elliptic curves with $\Gamma_1(3)$ level structure. The modulus τ of the elliptic curve parametrizes the universal cover of the modular curve $X_1(3) = \mathbb{H}/\Gamma_1(3)$, and $\Gamma_1(3)$ is the index 4 congruence subgroup of $SL(2,\mathbb{Z})$ generated by $T\colon \tau \mapsto \tau+1$ and $V\colon \tau \mapsto \tau/(1-3\tau)$ such that $(VT)^3 = 1$. The modular curve has two cusps at images of $\tau = \mathrm{i}\infty$ and $\tau = 0$, corresponding to the large volume and conifold points, respectively, and one elliptic point of order 3 at images of $\tau_o = \frac{1}{\sqrt{3}}e^{5\pi\mathrm{i}/6} = -\frac{1}{2}+\frac{\mathrm{i}}{2\sqrt{3}}$, corresponding to the orbifold point $\mathbb{C}^3/\mathbb{Z}_3$. A fundamental domain $\mathcal{F}_o$ (9.7.1) centered around the orbifold point τ_o is shown in Figure 9.1. Due to monodromies around these singular points, the periods $T(\tau), T_D(\tau)$ are not modular functions of $\Gamma_1(3)$. Rather, we show in Appendix 9.7.1 that they are given by Eichler-type integrals

$$\begin{pmatrix} T \\ T_D \end{pmatrix} = \begin{pmatrix} -\frac{1}{2} \\ \frac{1}{3} \end{pmatrix} + \int_{\tau_o}^{\tau} \begin{pmatrix} 1 \\ u \end{pmatrix} \, C(u)\mathrm{d}u \tag{9.1.5}$$

where $C(\tau) = \frac{\eta(\tau)^9}{\eta(3\tau)^3}$ is a weight 3 Eisenstein series for $\Gamma_1(3)$, which has neither poles nor zeros in the Poincaré upper half plane. This representation will play a central role in this work, as it gives a global and numerically efficient[5] formula for the analytic continuation of $Z_\tau(\gamma)$ to the universal cover $\mathbb{H}$ of the complexified Kähler moduli space $X_1(3)$. Near the large volume limit $\Im\tau \gg 1$, one finds that the central charge function reduces to a quadratic polynomial,

$$Z^{\mathrm{LV}}_{(s,t)}(\gamma) \coloneqq -\frac{r}{2}(s+\mathrm{i}t)^2 + d(s+\mathrm{i}t) - \mathrm{ch}_2 \tag{9.1.6}$$

with $\tau \simeq s + \mathrm{i}t$. In fact, observing that the variables $(s,w) \in \mathbb{R}^2$ defined by

$$s \coloneqq \frac{\Im T_D}{\Im T}\ , \quad w \coloneqq -\Re T_D + \frac{\Im T_D}{\Im T}\Re T = -\frac{\Im(T\bar{T}_D)}{\Im T}\ , \tag{9.1.7}$$

are invariant under the action of $\widetilde{GL^+}(2,\mathbb{R})$ on $\mathrm{Stab}(K_{\mathbb{P}^2})$ (after fixing $Z(\delta) = 1$), one easily checks that in the domain $\mathbb{H}^{\mathrm{LV}}$ defined by the condition $w > \frac{1}{2}s^2$ (keeping only the connected component containing the cusp at $\tau = \mathrm{i}\infty$), the central charge charge function (9.1.3) can be brought to the large volume form (9.1.6) with $t = \sqrt{2w - s^2}$. As shown in Figure 9.1, the domain $\mathbb{H}^{\mathrm{LV}}$ only covers a proper subset of the fundamental domain $\mathcal{F}_o$, in particular it does not include a neighborhood of the orbifold point.

As explained in [BM11] and reviewed in §9.2.4 below, for any point $\tau \in \mathbb{H}$ there exists a stability condition on $D^b\,\mathrm{Coh}(K_{\mathbb{P}^2})$ with central charge function given by the mirror symmetry prescription (9.1.3). In the fundamental domain $\mathcal{F}_C$ and its translates, the heart $\mathcal{A}(\tau)$ is constructed using the usual tilting pair construction (built from the subcategories of sheaves with slope $\mu = \frac{d}{r}$ less or greater than $s = \frac{\Im T_D}{\Im T}$). This construction is then extended to the full Poincaré upper half-plane using the group $\Gamma_1(3)$ of auto-equivalences of the derived category $D^b\,\mathrm{Coh}(K_{\mathbb{P}^2})$ generated by tensor product with $\mathcal{O}_{\mathfrak{Y}}(1)$ (corresponding to $T\colon \tau \mapsto \tau+1$) and by the spherical twist $\mathrm{ST}_{\mathcal{O}}$ with respect to the structure sheaf $\mathcal{O}$ of the zero section (corresponding to $V\colon \tau \mapsto \tau/(1-3\tau)$). The interior of the fundamental domain $\mathcal{F}_C$ and its translates are singled out by the condition that the stability condition is geometric, i.e. the skyscraper sheaves $\mathcal{O}_x$ are stable with fixed phase.

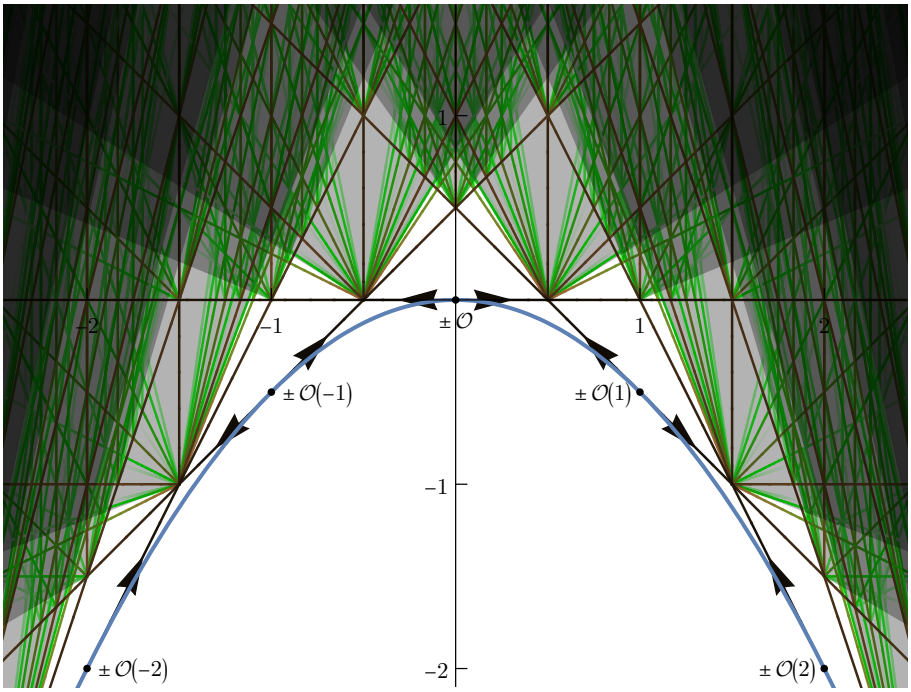

Figure 9.2: Large volume scattering diagram in (x, y) plane. The initial rays $\mathcal{R}_0(\mathcal{O}(m))$ and $\mathcal{R}_0(\mathcal{O}(m)[1])$ are tangent to the parabola $y = -\frac{1}{2}x^2$ at $(x, y) = (m, -\frac{1}{2}m^2)$ and move away from this point leftward and rightward, respectively. The gray areas indicate regions containing a dense set of rays. Ray colors encode the electric potential $2(d - rx)$, with lighter colors corresponding to larger values.

9.1.5 The scattering diagram at large volume

In [Bou19], the stability scattering diagram for $\mathcal{C} = D^b \operatorname{Coh}_c(\mathbb{P}^2)$ was constructed for the one-parameter family of stability conditions of the form (9.1.6), assuming the special value $\psi = 0$ for the phase. The construction was performed using a different set of coordinates $(x, y) = (s, \frac{1}{2}(t^2 - s^2))$ with $y > -\frac{1}{2}x^2$, such that the rays $\mathcal{R}_0(\gamma)$ become segments of straight lines $ry + dx - \mathrm{ch}_2 = 0$, similar to standard affine scattering diagrams in the context of mirror symmetry [KS06, GS11]. The main result of this analysis is that the initial rays of the resulting diagram, which we denote by $\mathcal{D}_0^{\mathrm{LV}}$, consist of a pair of rays $\mathcal{R}_0(\mathcal{O}(m))$ and $\mathcal{R}_0(\mathcal{O}(m)[1])$ emitted from every integer points $(x, y) = (m, -\frac{1}{2}m^2) \in \mathbb{Z}$ tangent to the parabola $y = -\frac{1}{2}x^2$, where the central charge of the coherent sheaf $\mathcal{O}(m)$ vanishes[6], see Figure 9.2.

In §9.4, we recast this construction in (s, t) coordinates, explain it in more physical terms and demonstrate its usefulness for computing the BPS indices. In particular, we observe that in these

[5]This formula is implemented in the Mathematica package `P2Scattering.m` along with many other routines for plotting scattering diagrams, scanning possible flow trees, etc, see Appendix 9.7.19 for details.

[6]Indeed, $Z^{\mathrm{LV}}_{(s,t)}(\gamma) = -\frac{1}{2}(s + \mathrm{i}t - m)^2$ for $\gamma = [1, m, \frac{1}{2}m^2]$.

coordinates, the ray $\mathcal{R}_0(\gamma)$ for $\gamma = [r, d, \mathrm{ch}_2]$ is either included in a vertical straight line (when $r = 0$), in a branch of hyperbola asymptoting to the 'light-cone' $|t - s| = \mathrm{cst}$ (when $r \neq 0$ and $\Delta := \frac{1}{2}d^2 - \frac{\mathrm{ch}_2}{r} \neq 0$) or in a branch of the said light-cone (when $r \neq 0$ and $\Delta = 0$). Thus, a useful analogy is to view the ray $\mathcal{R}(\gamma)$ as the worldline of a particle of global charge γ and electric charge r, propagating in the two-dimensional (half) Minkowski space spanned by the space and time coordinates (s, t), immersed in a constant electric field. The objects $\mathcal{O}(m)$ and $\mathcal{O}(m)[1]$ correspond physically to a D4-brane with m units of flux, and its anti-particle, carrying electric charge ± 1. These objects are pair-produced at $t = 0$ and $s \in \mathbb{Z}$, scatter against each other and produce an infinite set of outgoing rays, that in turn collide *ad infinitum*, producing the complete set of BPS states at large volume (i.e. late time). The resulting diagram is shown in Figure 9.3. The attractor flow trees can be thought of as sequences of scatterings producing a particle of desired charge γ and going through a desired point (s, t) in Minkowski spacetime.

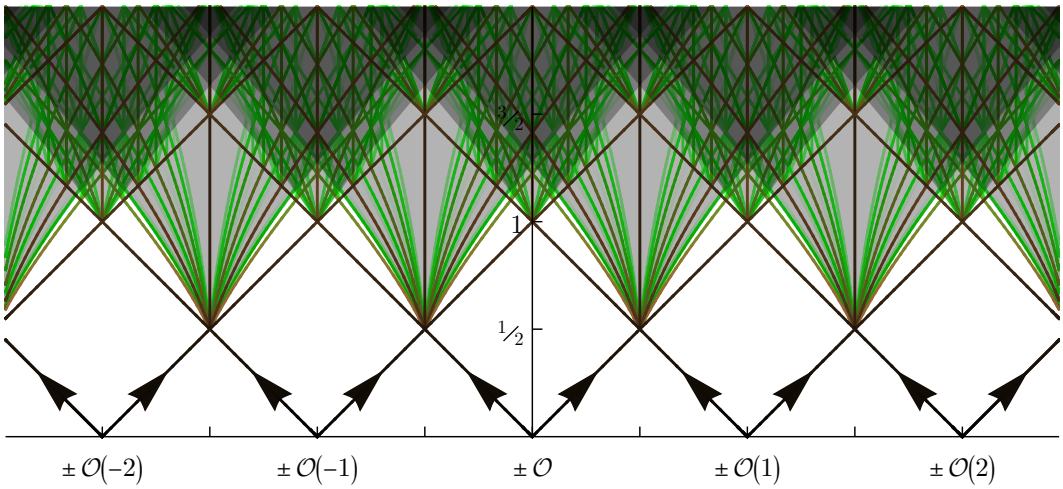

Figure 9.3: Large volume scattering diagram in (s, t) plane. The initial rays $\mathcal{R}_0(\mathcal{O}(m))$ and $\mathcal{R}_0(\mathcal{O}(m)[1])$ are emitted at $(s, t) = (m, 0)$ and moving leftward and rightward, respectively.

While this electromagnetic analogy has some peculiarities, e.g. the fact that pair production only takes place at $t = 0$ and integer spatial positions (unlike standard Schwinger pair production), it does provide valuable insight. In particular, it makes it obvious that rays can only propagate inside the forward light-cone (a property which we refer to as *causality*)[7], and that the (conveniently normalized) electric potential $\varphi_s(\gamma) = 2(d - rs)$ can only increase along a trajectory (a property which played an important role in the construction of *loc. cit.*) In §9.4.2, we combine these two properties to derive a bound on the number and charges of possible constituents $\mathcal{O}(m_i)$ and $\mathcal{O}(m'_j)[1]$ that contribute to the index $\Omega_{(s,t)}(\gamma)$ at any point (s, t) such that $\Re[Z^{\mathrm{LV}}_{(s,t)}(\gamma)] = 0$. This bound shows that the SAFC holds along the large volume slice for trees rooted on such loci, and gives an effective (if not particularly efficient) algorithm for determining the finite list of attractor flow trees (or scattering sequences) contributing to the index $\Omega_{(s,t)}(\gamma)$.

[7] In (x, y) coordinates, rays are contained in a cone tangent to the parabola $y = -\frac{1}{2}x^2$.

Using this algorithm, we reproduce the well known chamber structure for DT invariants along the large volume slice [ABCH13, BMW14, Mac14], consisting of a finite nested sequence of walls of marginal stability, such that the index vanishes inside the innermost wall and is equal to the index $\Omega_\infty(\infty)$ counting Gieseker-semistable sheaves outside the outermost wall. For illustration, in §9.4.3 and §9.4.4 we determine the trees contributing to $\Omega_\infty(\gamma)$ for $\gamma = [1, 0, 1-n]$ and $\gamma = [0, d, \mathrm{ch}_2]$ for low values of n and d. In the first case, the moduli space of Gieseker semi-stable sheaves coincides with the Hilbert scheme of n points on $\mathbb{P}^2$, the index of which is well-known [Göt90] (higher rank examples are considered in Appendix §9.7.16). In the second case $r = 0$, we recover the genus zero Gopakumar-Vafa invariants $N_d^{(0)}$ in the unrefined limit[8] $y \to 1$. We further match the contributing trees with the known stratification of the moduli space of Gieseker stable sheaves, extending the observations in [Bou19].

Although the choice $\psi = 0$ has the advantage (exploited in [Bou19]) that the geometric rays $\mathcal{R}_\psi^{\mathrm{geo}}(\gamma)$ become straight lines in (x, y) coordinates, it does not give access to the index $\Omega_{(s,t)}(\gamma)$ away from loci where $Z^{\mathrm{LV}}_{(s,t)}(\gamma)$ is purely imaginary. In §9.4.5, we generalize the scattering diagram $\mathcal{D}_0^{\mathrm{LV}}$ to a diagram $\mathcal{D}_\psi^{\mathrm{LV}}$ valid for any $\psi \in (-\frac{\pi}{2}, \frac{\pi}{2})$. While the walls of marginal stability are by construction independent of ψ, it turns out that the ψ-dependence of the rays $\mathcal{R}_\psi(\gamma)$ can be absorbed by a linear coordinate transformation $(s, t) \mapsto (s + t\tan\psi, t/\cos\psi)$ which preserves the walls and the boundary at $t = 0$. Thus, the topology of the trees contributing to the index at large volume for any charge γ is independent of ψ, the only change being in the location of the vertices along the walls of marginal stability. As we shall see momentarily, this is no longer true for the exact scattering diagram involving the exact central charge function (9.1.3).

9.1.6 The orbifold scattering diagram

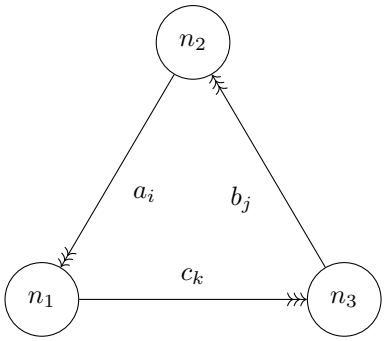

Figure 9.4: Quiver describing the BPS spectrum around the orbifold point τ_o. The potential is $W = \sum_{i,j,k} \epsilon_{ijk}\mathrm{Tr}(a_i b_j c_k)$, and the dimension vector (n_1, n_2, n_3) is related to the Chern vector $[r, d, \mathrm{ch}_2]$ via $(n_1, n_2, n_3) = (-\frac{3}{2}d - \mathrm{ch}_2 - r, -\frac{1}{2}d - \mathrm{ch}_2, \frac{1}{2}d - \mathrm{ch}_2)$.

In the vicinity of the orbifold point, the geometry of $K_{\mathbb{P}^2}$ degenerates into the orbifold singularity

[8] More generally, the refined Gieseker index computes the character $\sum_{j_L, j_R} N_d^{(j_L, j_R)} \chi_{j_L}(y_L)\chi_{j_R}(y_R)$ on the diagonal $y_L = y_R = y$, where $N_d^{(j_L, j_R)}$ are the refined BPS invariants [KKV99, CvGKT20]. It is an interesting open question to generalize the scattering diagram away from the Nekrasov-Shatashvilii limit $y_L = y_R$.

$\mathbb{C}^3/\mathbb{Z}_3$, and the BPS spectrum is instead described by stable objects in the derived category of representations $D^b\,\mathrm{Rep}(Q,W)$ of the quiver with potential shown in Figure 9.4, which we refer to as the orbifold quiver. This quiver arises from the tilting sequence in $D^b\,\mathrm{Coh}_c(K_{\mathbb{P}^2})$ obtained from the Ext-exceptional collection

$$E_1 = i_*(\mathcal{O})[-1], \quad E_2 = i_*(\Omega(1)), \quad E_3 = i_*(\mathcal{O}(-1))[1] \tag{9.1.8}$$

where Ω is the cotangent bundle of $\mathbb{P}^2$, i_* denotes the lift from $\mathbb{P}^2$ to $K_{\mathbb{P}^2}$ and $[k]$ denotes the cohomological shift by k units. Importantly, the central charges $Z_\tau(E_i)$ of the three objects are aligned at the orbifold point τ_o, and they remain in a common half-plane in an open region $\mathbb{H}^o$ around τ_o defined by the inequality $w < -\frac{1}{2}s$ in the fundamental domain $\mathcal{F}_o$ (9.7.1), along with the images of that region under the $\mathbb{Z}_3$ symmetry around τ_o. This ensures that the heart of the stability condition coincides with the Abelian category of quiver representations in the region $\mathbb{H}^o$, up to a $\widetilde{GL^+}(2,\mathbb{R})$ transformation.

Following Bridgeland [Bri17], the DT invariants for the quiver (Q,W) are determined by a scattering diagram $\mathcal{D}_Q$ defined in the affine space $\mathbb{R}^3$ spanned by King stability (also known as Fayet-Iliopoulos) parameters $(\theta_1,\theta_2,\theta_3)$. For any dimension vector $\gamma=(n_1,n_2,n_3)\in\mathbb{Z}^3$, the active ray $\mathcal{R}_o(\gamma)$ is defined as the locus where $\bar\Omega_\theta(\gamma)\neq 0$ inside the hyperplane $\{\theta\in\mathbb{R}^3 : n_1\theta_1+n_2\theta_2+n_3\theta_3=0\}$, where $\bar\Omega_\theta(\gamma)$ is the rational DT invariant associated to the moduli space of θ-semistable representations of (Q,W) with dimension vector γ (in particular, $\mathcal{R}_o(\gamma)$ is empty unless the n_i's are all positive). In §9.5.2, building on earlier arguments [BMP21a, MP20, DP22], we prove that the only initial rays are those for $\gamma\in\{\gamma_1,\gamma_2,\gamma_3,k\delta\}$ with $\gamma_1=(1,0,0),\gamma_2=(0,1,0),\gamma_3=(0,0,1),\delta=(1,1,1),k\geq 1$.

Theorem 9.1.1 (Attractor Conjecture for the $\mathbb{C}^3/\mathbb{Z}_3$ orbifold quiver)**.** *For the quiver with potential (Q,W) shown in Figure 9.4, the attractor invariant $\Omega_\star(\gamma)$ vanishes for all dimension vectors $\gamma=(n_1,n_2,n_3)$ except for*

$$\Omega_\star(k\gamma_i)=\delta_{k,1}\ , \quad \Omega_\star(k\delta)=-y^3-y-1/y \tag{9.1.9}$$

The complete scattering diagram $\mathcal{D}_Q$ is then determined from this initial data by consistency using the flow tree formula of [AP19a, AB21]. By scaling invariance, the scattering diagram can be restricted to the hyperplane $\theta_1+\theta_2+\theta_3=1$ with no loss of information, except for the rays $\mathcal{R}_o(\delta)$ associated to D0-branes which are no longer visible. The resulting two-dimensional scattering diagram $\mathcal{D}_o$ is shown in Figure 9.24, including only the initial rays and a few secondary rays.

Since the dimension vectors of the initial rays lie in the positive octant of $\mathbb{Z}^3$, the enumeration of all possible scattering trees for fixed total dimension vector $\gamma=(n_1,n_2,n_3)$ is straightforward, unlike for the large volume scattering diagram discussed previously. This gives an efficient algorithm to determine the quiver indices $\Omega_\theta(\gamma)$ for arbitrary dimension vector γ and stability parameters θ. The latter are in turn equal to the DT invariants $\Omega_\tau(\gamma)$ in the region $\mathbb{H}^o$ around the orbifold point τ_o, upon relating the Chern vectors and dimension vectors, as in the caption of Figure 9.4, and equating the King stability parameters θ_i with $\Re[e^{-\mathrm{i}\psi}Z_\tau(\gamma_i)]$ (up to overall rescaling). In §9.5, we show that the restriction of the orbifold scattering diagram $\mathcal{D}_Q$ to the hyperplane $\theta_1+\theta_2+\theta_3=1$ agrees with the exact scattering diagram $\mathcal{D}^\Pi_\psi$ (to be defined below) in a region around the orbifold point τ_o.

9.1.7 The exact scattering diagram

For the exact central charge function (9.1.3) and associated Bridgeland stability conditions, one can likewise define the scattering diagram $\mathcal{D}^\Pi_\psi$ as the set of active rays $\mathcal{R}_\psi(\gamma)$ in the Poincaré upper

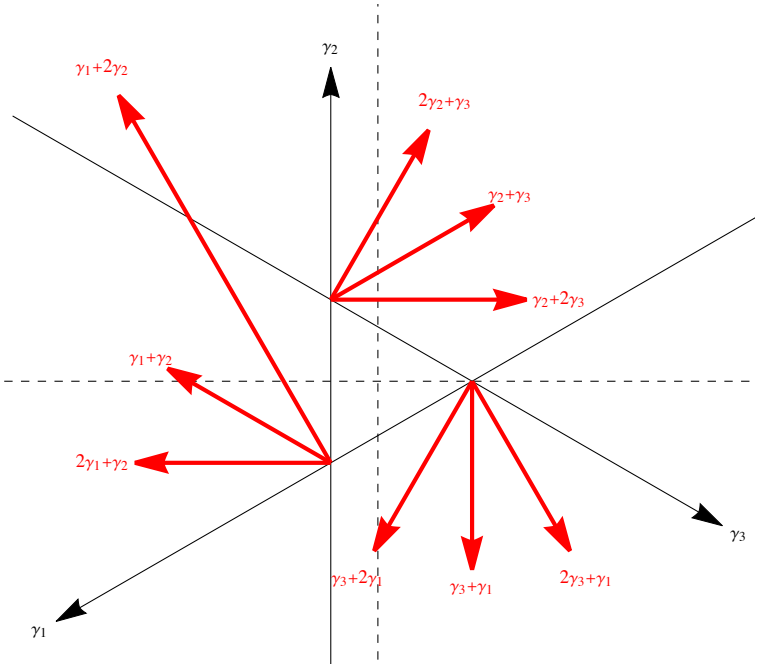

Figure 9.5: Two-dimensional section $\mathcal{D}_o$ of the orbifold scattering diagram $\mathcal{D}_Q$ along the hyperplane $\theta_1+\theta_2+\theta_3=1$. The initial rays associated to $\gamma_1,\gamma_2,\gamma_3$ are drawn in black, a few secondary rays are plotted in red. This diagram is embedded in the exact scattering diagram $\mathcal{D}^{\Pi}_{\psi}$ around $\tau=\tau_o$ by identifying the horizontal and vertical axis with the coordinates (u,v) defined in (9.6.27).

half-plane such that $Z_\tau(\gamma)$ has fixed argument $\psi+\frac{\pi}{2}$ and $\bar{\Omega}_\tau(\gamma)\neq 0$. Since the conifold points $\tau=m\in\mathbb{Z}$ lie on the boundary of the domain $\mathbb{H}^{\rm LV}$ (defined below (9.1.7)) covered by the large volume scattering diagram $\mathcal{D}^{\rm LV}_{\psi}$, the initial data must include the rays associated to $\mathcal{O}(m)$ and $\mathcal{O}(m)[1]$, along with their images under $\Gamma_1(3)$. In particular, since the spherical twist $\mathrm{ST}_{\mathcal{O}}$ maps $\mathcal{O}(0)[n]\mapsto\mathcal{O}(0)[n+2]$, there are now an infinite set of rays emitted from each point $\tau=m$, as shown in Figure 9.6. Similarly, there is an infinite set of rays emitted from every rational $\tau=\frac{p}{q}$ with $q\neq 0$ mod 3 which are in the same orbit under $\Gamma_1(3)$, where objects of charge $\pm\gamma_C$ become massless (the relevant objects are computed in §9.7.8 and shown in Table 9.1 for $0\leq p<q\leq 5$). In particular, this includes the initial rays associated to the exceptional objects E_i in (9.1.8), emanating from $\tau=0,-\frac{1}{2},-1$, as well as translates of those.

In order to analyze the structure of the resulting scattering diagram, it is convenient to introduce affine coordinates[9]

$$x:=\frac{\Re\left(e^{-\mathrm{i}\psi}T\right)}{\cos\psi}\ ,\quad y:=-\frac{\Re\left(e^{-\mathrm{i}\psi}T_D\right)}{\cos\psi} \tag{9.1.10}$$

such that the geometric rays in the (x,y)-plane are contained in straight lines $\{ry+dx=\mathrm{ch}_2\}$,

[9]Note that the map $\tau\mapsto(x,y)$ is not injective on $\mathbb{H}$, but its restriction to the fundamental domain $\mathcal{F}_C$ and its translates is, see Figure 9.26.

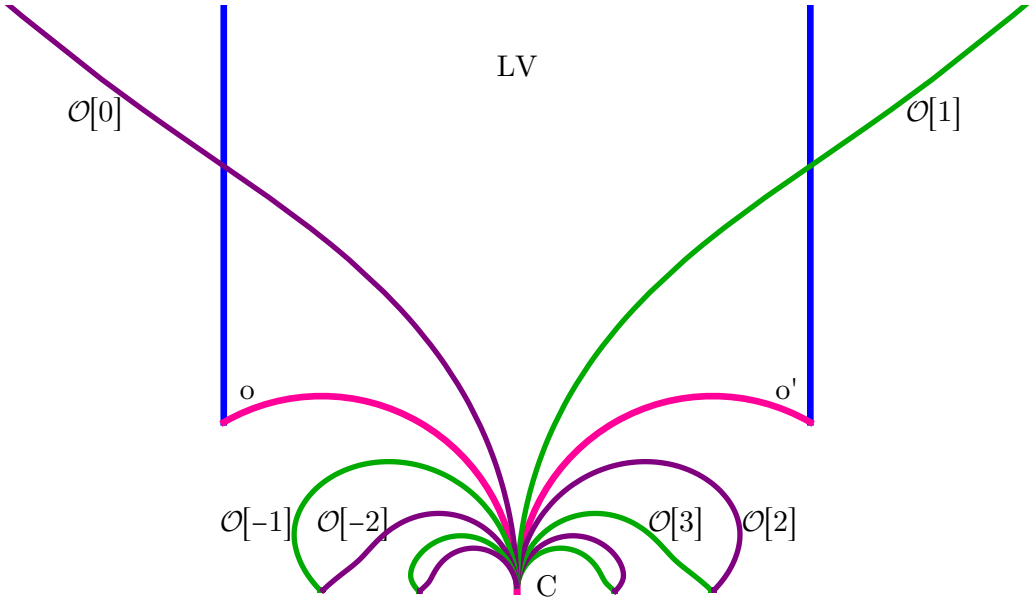

Figure 9.6: Rays $\mathcal{R}_\psi(\mathcal{O}[n])$ emitted from $\tau = 0$ for $\psi = 0$. The same picture holds near all conifold points at $\tau = \frac{p}{q}$ with $q \neq 0 \mod 3$. For each k, the rays corresponding to the D4-brane $\mathcal{O}[2k]$ (in purple) and anti-brane $\mathcal{O}[2k+1]$ (in green) end at the same large-volume point: $\tau = 1/(3k)$ for $k \neq 0$ and $\tau = \mathrm{i}\infty$ for $k = 0$. As ψ increases, the rays $\mathcal{R}_\psi(\mathcal{O}[n])$ move counterclockwise.

oriented along the vector $(-r, d)$. In these coordinates, the conifold point $\tau = m$ is mapped to

$$(x_{\mathcal{O}(m)}, y_{\mathcal{O}(m)}) = \left(m + \mathcal{V}\tan\psi, -\frac{1}{2}m^2 - m\mathcal{V}\tan\psi\right) \tag{9.1.11}$$

where $\mathcal{V}$ is the *quantum volume*[10]

$$\mathcal{V} := \Im T(0) = \frac{27}{4\pi^2}\Im\left[\mathrm{Li}_2\left(e^{2\pi\mathrm{i}/3}\right)\right] \simeq 0.462758 \tag{9.1.12}$$

In particular, just as in the large volume scattering diagram of [Bou19], the initial rays associated to $\mathcal{O}(m)$ and $\mathcal{O}(m)[1]$ are straight lines tangent to the parabola $y = -\frac{1}{2}x^2$ at $x = m$, but their starting point is displaced by a horizontal distance $\mathcal{V}_\psi := \mathcal{V}\tan\psi$ along that tangent.

For small enough ψ, namely $|\mathcal{V}_\psi| < \frac{1}{2}$, this displacement does not affect the structure of the scattering diagram, so that the exact scattering diagram $\mathcal{D}^{\Pi}_{\psi}$ coincides with the large volume scattering diagram $\mathcal{D}^{\mathrm{LV}}_0$ in the region above the parabola in the (x, y) plane, up to shifting the starting points of the initial rays. In the original coordinate τ, the only initial rays which escape towards the large volume region $\tau = \mathrm{i}\infty$ are those associated to $\mathcal{O}(m)$ and $\mathcal{O}(m)[1]$ (see Figure 9.7), and

[10] This quantum volume was first computed in [KZ01, (4.1)] in terms of Barnes' G-function, and turns out to be a special value of the L-function associated to the Eisenstein series $C(\tau)$, as noted independently in [BKSZ22], see (9.7.37) and (9.7.42) for the explicit relations.

Table 9.1: The object E of charge γ_C which becomes massless at $\tau = \frac{p}{q}$ with $q \neq 0 \mod 3$ is obtained by acting on $\mathcal{O}$ by an auto-equivalence g mapping $\tau = 0$ to $\tau = \frac{p}{q}$. Here T, U, V denote the generators $\tau \mapsto \tau + 1, \tau \mapsto \frac{\tau}{1+3\tau}$ and $\tau \mapsto \frac{\tau}{1-3\tau}$.

τ	g	γ_C	$\Delta(\gamma_C)$	E
0	$\mathbb{1}$	$[1,0,1)$	0	$\mathcal{O}$
1/5	U^2T^{-1}	$-[5,1,6)$	3/25	$E \to \Omega(2)[-1] \to \mathcal{O}^{\oplus 3}[2] \xrightarrow{+1}$
1/4	UT	$[4,1,6)$	$-3/32$	$E \to \mathcal{O}(1) \to \mathcal{O}^{\oplus 3}[3] \xrightarrow{+1}$
2/5	UT^{-2}	$-[5,2,6)$	12/25	$E \to \mathcal{O}(-2) \to \mathcal{O}^{\oplus 6} \xrightarrow{+1}$
1/2	TVT	$-[2,1,3)$	3/8	$\Omega(2)[1]$
3/5	TVT^2	$-[5,3,8)$	12/25	$\mathcal{O}(1)^{\oplus 6} \to \mathcal{O}(3) \to E \xrightarrow{+1}$
3/4	TVT^{-1}	$[4,3,10)$	$-3/32$	$\mathcal{O}(1)^{\oplus 3}[-3] \to \mathcal{O} \to E \xrightarrow{+1}$
4/5	TV^2T	$-[5,4,12)$	3/25	$\mathcal{O}(1)^{\oplus 3}[-2] \to \Omega(2)[1] \to E \xrightarrow{+1}$
1	T	$[1,1,3)$	0	$\mathcal{O}(1)$

their intersections patterns are identical to those of the large volume scattering diagram $\mathcal{D}_0^{\mathrm{LV}}$ in (s,t) plane, up to a change of variable $\tau \mapsto (s,t)$ obtained by equating the coordinates (x,y) on both sides. In particular, the topology of the trees contributing to the index $\Omega_\infty(\gamma)$ along the rays $\mathcal{R}_0(\gamma)$ is unchanged, and the SAFC for $\mathcal{D}_\psi^\Pi$ follows from the SAFC for $\mathcal{D}_0^{\mathrm{LV}}$.

In contrast, for $|\mathcal{V}_\psi| > \frac{1}{2}$, the displacement of the starting points of the initial rays associated to $\mathcal{O}(m)$ and $\mathcal{O}(m)[1]$ is large enough that the first collision no longer involves two consecutive rays $\mathcal{R}(\mathcal{O}(m-1)[1])$ and $\mathcal{R}(\mathcal{O}(m))$. Taking $\mathcal{V}_\psi < -\frac{1}{2}$ for definiteness, the ray $\mathcal{R}(\mathcal{O}(m-1)[1])$ interacts with two "new"[11] rays $\mathcal{R}(\mathcal{O}(m)[-1])$ and $\mathcal{R}(\Omega(m+1))$ in a region near the orbifold point $\tau_o + m$, in such a way that these three initial rays generate a portion (which grows with $|\mathcal{V}_\psi|$) of the orbifold scattering diagram $\mathcal{D}_o$ corresponding to the exceptional collection (9.1.8) tensored with $\mathcal{O}(m)$. The resulting outgoing rays escape towards the large volume points $\tau = \mathrm{i}\infty, -1/3, -2/3$, and those that escape towards $\mathrm{i}\infty$ collide further with the initial ray $\mathcal{R}(\mathcal{O}(m))$ and with rays for different values of $m \in \mathbb{Z}$. In fact, as ψ approaches the critical value $\mathcal{V}_\psi = -\frac{1}{2}$, the ray $\mathcal{R}(\mathcal{O}(m)[1])$ emitted at $\tau = m$ approaches arbitrary close to the conifold point $\tau = m+1$, and it escapes to the large volume point $\tau = m + \frac{2}{3}$ (respectively, $\tau = \mathrm{i}\infty$) as ψ approaches the critical value $\mathcal{V}_\psi = -\frac{1}{2}$ from below (respectively, from above as in Figure 9.8). More generally, we find that the topology of the scattering diagram jumps at a countable set of critical phases values where some ray $\mathcal{R}_\psi(\gamma)$ ends up at a conifold point.

Definition 9.1.2. The phase $\psi \in (-\pi/2, \pi/2)$ is **critical** if any of four equivalent conditions holds:

1. an active ray $\mathcal{R}_\psi(\gamma)$ ends at $\tau = 0$ (or any other conifold point);
2. an (initial) active ray $\mathcal{R}_\psi(\gamma)$ with $\gamma \notin [1,0,0)\mathbb{Z}$ starts at $\tau = 0$;
3. the point $(x,y) = (\mathcal{V}_\psi, 0)$ is the intersection of $\mathcal{R}_0^{\mathrm{LV}}(\mathcal{O})$ and another active ray of $\mathcal{D}_0^{\mathrm{LV}}$;
4. $\theta = (0, \frac{1}{2} + |\mathcal{V}_\psi|, \frac{1}{2} - |\mathcal{V}_\psi|)$ is the intersection of $\mathcal{R}^o(\gamma_1)$ and another active ray of $\mathcal{D}_o$.

[11] For small phases these rays escape towards other large volume limits.

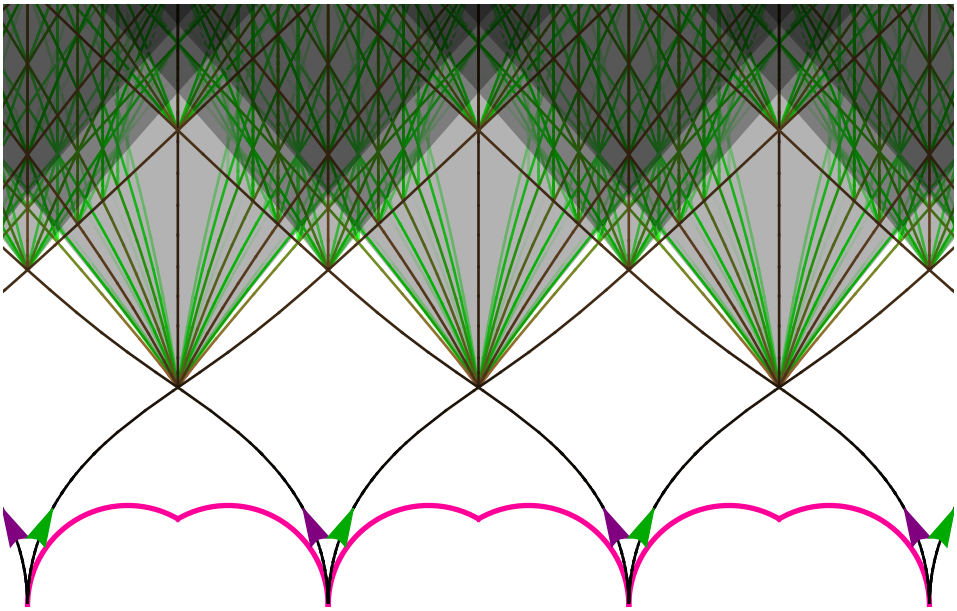

Figure 9.7: Scattering diagram $\mathcal{D}_\psi^\Pi$ for $\psi = 0$, restricted to the fundamental domain and its translates. The initial rays are $\mathcal{R}_\psi(\mathcal{O}(m))$ and $\mathcal{R}_\psi(\mathcal{O}(m)[1])$. The gray areas indicate regions where the scattering diagram is dense.

The equivalence of the four characterizations is proven by mapping DT invariants along rays of the exact diagram near $\tau = 0$ to rays of the large volume diagram $\mathcal{D}_0^{\rm LV}$ in §9.7.12 and orbifold diagram $\mathcal{D}_o$ in §9.7.13 and §9.7.14. As ray intersections in $\mathcal{D}_0^{\rm LV}$ (or $\mathcal{D}_o$) have rational coordinates (x, y) (or rational θ up to scaling, respectively), critical phases have rational values of $\mathcal{V}_\psi$. In detail, critical phases take the form

$$\psi_\alpha^{\rm cr} = \arctan(\alpha/\mathcal{V}) \tag{9.1.13}$$

or equivalently $\mathcal{V}_\psi = \alpha$, where $|\alpha|$ belongs to a dense set of rational values in the range $(\frac{1}{2}\sqrt{5}, \infty)$, or to the discrete series

$$\left\{ \frac{F_{2k} + F_{2k+2}}{2F_{2k+1}}, k \geq 0 \right\} = \{\tfrac{1}{2}, 1, \tfrac{11}{10}, \tfrac{29}{26}, \tfrac{19}{17}, \ldots\} \tag{9.1.14}$$

with F_p the p-th Fibonacci number (with $F_0 = 0$, $F_1 = 1$), converging to $\frac{1}{2}\sqrt{5} \simeq 1.11803$. This discrete series and dense set can be read off along the $y = 0$ line in the large volume diagram of Figure 9.2. In Figures 9.30 and 9.31, we show examples of trees contributing to $\gamma = \mathrm{ch}(\mathcal{O})$ and $\gamma = \mathrm{ch}(\mathcal{O}_C)$, with discontinuities occuring only on a subset of critical phases, specifically at half-integer values of $\mathcal{V}_\psi$.

Away from critical values of $\mathcal{V}_\psi$, we show that for any total charge γ, flow trees rooted in the large volume region admit a two-stage structure, with a 'trunk' inside the region $\diamondsuit_\psi$ lying above a certain piecewise linear region $y \geq \mathsf{p}(x)$ in the (x, y) plane (defined in (9.6.30)), and subtrees (or 'shrubs') inside triangular regions $\Delta_\psi(m)$ in the (x, y) plane containing the image of the orbifold

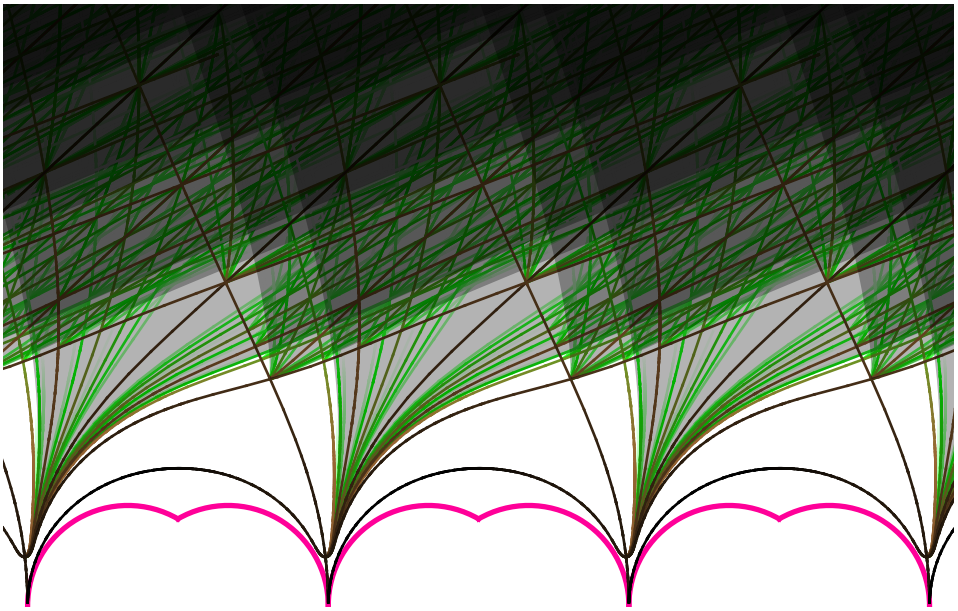

Figure 9.8: Scattering diagram $\mathcal{D}^{\Pi}_{\psi}$ for $\psi = -0.824$, slightly above $\psi^{\rm cr}_{-1/2} \simeq -0.82406$. As $\psi \to \psi^{\rm cr}_{-1/2}$, the rays $\mathcal{R}(\mathcal{O}(m)[1])$ emitted at $\tau = m$ approach arbitrary close to the conifold point $\tau = m+1$, before escaping to $\tau = \mathrm{i}\infty$.

point $\tau_o + m$ (see the example in Figure 9.9). Within each triangular region, the shrubs reduce to attractor flow trees for the orbifold quiver, with leaves given by initial rays of the exceptional collection (9.1.8) tensored with $\mathcal{O}(m)$. In addition to these shrubs, the trunk can also have leaves of type $\mathcal{R}(\mathcal{O}(m))$ for $\mathcal{V}_\psi < 0$ (or $\mathcal{R}(\mathcal{O}(m)[1])$ for $\mathcal{V}_\psi > 0$). We give effective bounds on the possible constituents which show that the SAFC holds for $\mathcal{D}^{\Pi}_{\psi}$ for any non-critical value of $\mathcal{V}_\psi$.

Finally, for $\psi = \pm\frac{\pi}{2}$, we find that the scattering diagram drastically simplifies. Indeed, the geometric rays $\Im[Z_\tau(\gamma)] = 0$ for $r \neq 0$ reduce to the contour lines $s = \frac{d}{r}$ of the function $s = \frac{\Im T_D}{\Im T}$ defined in (9.1.7) (for $r = 0$, the geometric rays $\mathcal{R}^{\rm geo}_{\pi/2}(\gamma)$ are empty). Hence, scattering can only take place at the orbifold point τ_o and its images under $\Gamma_1(3)$, where the function s is ill-defined. At each orbifold point, there are three incoming rays associated to the objects of corresponding exceptional collection, which scatter all at once according to the orbifold scattering diagram $\mathcal{D}_o$. In particular, a ray emitted from the orbifold point $\tau_o + m$ into the fundamental domain $\mathcal{F}_o(m)$ will escape to $\tau = \mathrm{i}\infty$ in the range $m-1 < \tau_1 < m$ without encountering any wall of marginal stability. For $m = 0$, this explains why the index for the orbifold quiver in the anti-attractor chamber $\Omega_c(\gamma)$ agrees with the Gieseker index $\Omega_\infty(\gamma)$ for normalized torsion free sheaves, as observed in [DFR05b, BMP21a]. We also prove the SAFC for that phase, which leads altogether to the following theorem:

Theorem 9.1.3 (Split Attractor Flow Conjecture for local $\mathbb{P}^2$)**.** *For any Π-stability condition $z \in \Pi \simeq \mathbb{H}$ of $K_{\mathbb{P}^2}$ and any charge vector γ such that $\psi = \arg(-\mathrm{i}Z_z(\gamma))$ is a non-critical phase in $(-\pi/2, \pi/2]$ in the sense of Definition 9.1.2, there are finitely many (maximally extended) split attractor flows starting from z whose leaves are active rays. All leaves are $\Gamma_1(3)$ images of the rays*

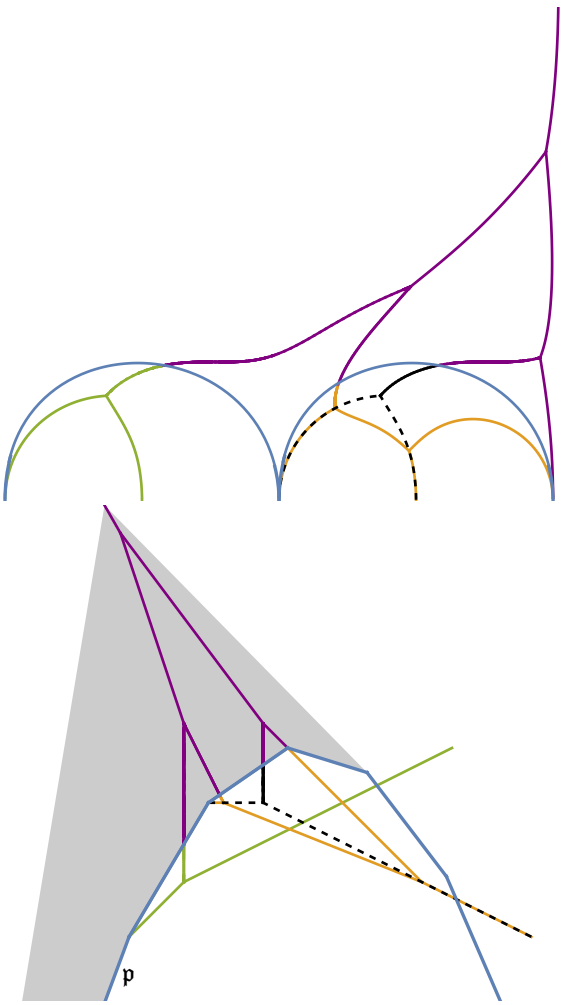

Figure 9.9: Left: Example of attractor flow tree $\mathcal{T}$ in the τ plane, for $|\mathcal{V}_\psi| > 1/2$ (specifically, $\mathcal{T} = \{\{\{2\mathcal{O}(-1)[1], \Omega(1)\}, \{4\mathcal{O}[1], \{3\Omega(2), \mathcal{O}(1)[-1]\}\}\}, \{3\mathcal{O}(1), \{\Omega(2), 2\mathcal{O}[1]\}\}\}$ and $\psi = -1.2$), in which the various subtrees (or shrubs) $\mathcal{T}_I$ corresponding to exceptional collections are given different colors (green, orange, black, partly dashed to make overlaps visible). Together with further initial rays, the rays entering the region $\diamondsuit_\psi$ (above the blue curves) participate in an attractor flow tree in that region, consisting only of outbound rays (solid purple curves). Right: same tree in the (x, y) plane; some initial rays in the orbifold regions appear to start in $\diamondsuit_\psi$, because $\tau \mapsto (x, y)$ is not injective. The intersection of $\diamondsuit_\psi$ with the convex hull of $\mathfrak{p}$ and of the tree's root is shaded in gray; it extends below the figure by a finite distance.

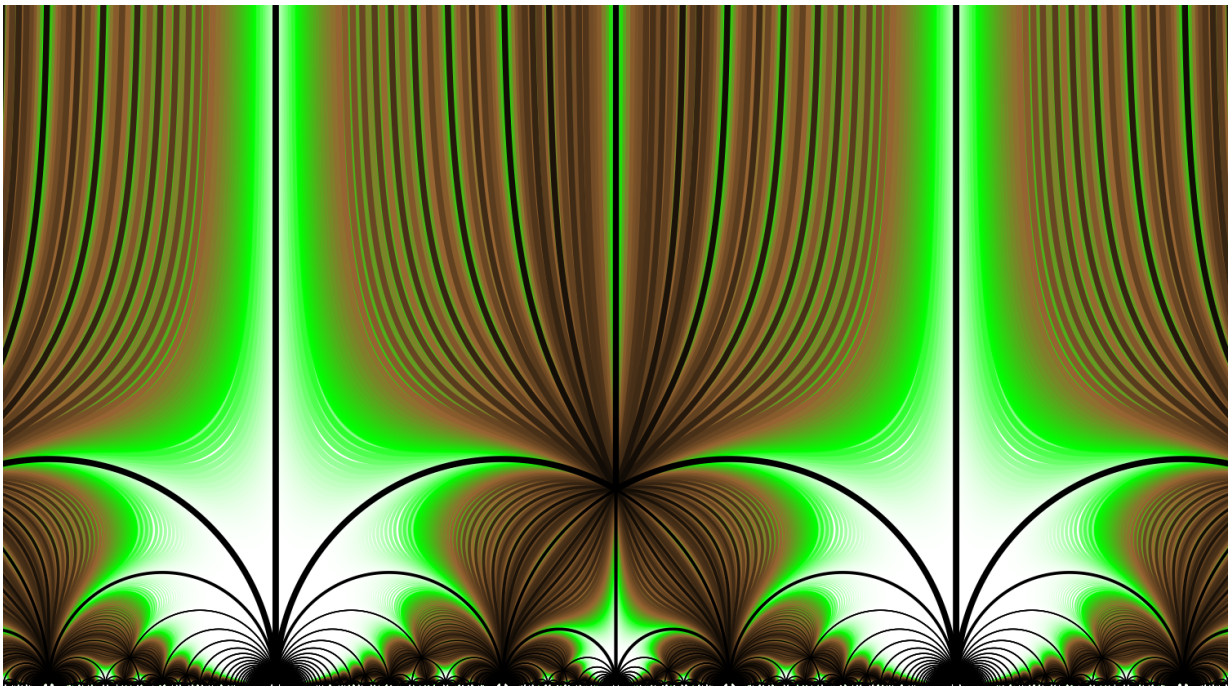

Figure 9.10: Scattering diagram for $\psi = \pm\frac{\pi}{2}$. Geometric rays coincides with contours of the function $s = \frac{\Im T_D}{\Im T}$. The orbifold scattering diagram is embedded in a infinitesimal neighborhood of all $\Gamma_1(3)$ images of τ_o, which shrinks as $\psi \to \pm\frac{\pi}{2}$.

$\mathcal{R}(\mathcal{O})$ and $\mathcal{R}(\mathcal{O}[1])$ that emanate from the conifold point $\tau = 0$. Moreover, if $|\psi| < \psi^{\mathrm{cr}}_{1/2}$, then such flows do not exist for $z \in \Delta_\psi$, while for $z \in \diamondsuit_\psi$ the leaves are $\mathcal{R}(\mathcal{O}(m))$ and $\mathcal{R}(\mathcal{O}(m)[1])$, $m \in \mathbb{Z}$. If $\psi^{\mathrm{cr}}_{1/2} < |\psi| < \pi/2$, then for $z \in \Delta_\psi$ the leaves are rays $\mathcal{R}(E_{j=1,2,3})$ corresponding to the exceptional collection (9.1.8), while for $z \in \diamondsuit_\psi$ the leaves are rays $\mathcal{R}(\mathcal{O}(m))$ and $\mathcal{R}(E_j(m))$ (for $j = 1, 2, 3$ and $m \in \mathbb{Z}$), emanating from conifold points at integer and half-integer values of τ. Finally, if $\psi = \pi/2$, then for z in the interior of $\mathcal{F}_o$ the leaves are $\mathcal{R}(E_{j=1,2,3})$.

9.1.8 Outline

This work is organized as follows. In §9.2 we recall some general facts about moduli spaces of sheaves on $\mathbb{P}^2$, the structure of the derived category $D^b\operatorname{Coh}(K_{\mathbb{P}^2})$ and the space of Bridgeland stability conditions associated to it. In §9.3 we recall the definition and main properties of the scattering diagram for quivers with potentials, extend this notion to general triangulated categories, and explain the relation between scattering rays and attractor flow trees. In §9.4, we revisit the scattering diagram $\mathcal{D}^{\mathrm{LV}}_\psi$ for the large volume central charge constructed in [Bou19], generalize it to arbitrary ψ, give an effective algorithm for determining the possible initial rays contributing to the index, and illustrate this procedure by computing the Gieseker index for various Chern vectors

of rank 0 or 1. In §9.5, we prove the Attractor Conjecture for the orbifold quiver, construct the corresponding scattering diagram $\mathcal{D}_o$ associated to the orbifold quiver, and determine the scattering sequences contributing to the quiver index for various dimension vectors. In §9.6, we determine the scattering diagram $\mathcal{D}^{\Pi}_{\psi}$ on the slice of Π-stability conditions, and show the SAFC in this case (Theorem 9.1.3). In Appendix 9.7.1 we derive the Eichler integral representation (9.1.5) of the periods T, T_D provided by local mirror symmetry, and use it to obtain expansions around the large volume, conifold and orbifold points. In §9.7.8 we determine the object in $D^b\,\mathrm{Coh}_c\,K_{\mathbb{P}^2}$ which becomes massless at the orbifold point $\tau = p/q$ for low values of p, q. In §9.7.9 we determine the possible end points of the flow to deduce the initial data of scattering diagrams for all phases ψ. In §9.7.15, we provide some details on the mathematical definition of DT invariants. In §9.7.16 we give further examples of scattering sequences for higher rank sheaves at large volume, complementing the examples in §9.5.4. Finally, in §9.7.19 we describe the main features of a Mathematica package which we have developed in the course of this investigation, which is freely available for further explorations.

9.2 Generalities

In this section, we first collect some basic facts about coherent sheaves on $\mathbb{P}^2$ and $K_{\mathbb{P}^2}$, Bridgeland stability conditions $\mathrm{Stab}\,\mathcal{C}$ on the derived category $\mathcal{C} = D^b(\mathrm{Coh}_c\,K_{\mathbb{P}^2})$ of compactly supported sheaves, and identify the slice $\Pi \subset \mathrm{Stab}\,\mathcal{C}$ of physical stability conditions.

9.2.1 Gieseker-stable sheaves on $\mathbb{P}^2$

Given a coherent sheaf E on $\mathbb{P}^2$, we denote its rank by $r(E)$, its degree by $d(E) = \int_{\mathbb{P}^2} c_1(E)\cdot H$ (where H is the hyperplane section generating $H^2(\mathbb{P}^2,\mathbb{Z})$), its second Chern character by $\mathrm{ch}_2(E)$, and by $\gamma(E)$ the Chern vector $[r, d, \mathrm{ch}_2]$ valued in $\mathbb{Z}\oplus\mathbb{Z}\oplus\frac{1}{2}\mathbb{Z}$. We denote by $\mathcal{O} = \mathcal{O}_{\mathbb{P}^2}(0)$ the structure sheaf, with Chern vector $[1,0,0]$, and by $\mathcal{O}_C$ the structure sheaf of the rational curve C in the hyperplane class, with Chern vector $[0,1,-\frac{1}{2}]$.

For any pair of coherent sheaves, the Euler form $\chi(E,E')$ is given the Riemann–Roch formula

$$\begin{aligned}\chi(E,E') &\coloneqq \dim\mathrm{Hom}(E,E') - \dim\mathrm{Ext}^1(E,E') + \dim\mathrm{Ext}^2(E,E')\\ &= rr' + \frac{3}{2}(rd' - r'd) + r\,\mathrm{ch}_2' + r'\mathrm{ch}_2 - dd'\end{aligned} \tag{9.2.1}$$

In particular for $E = \mathcal{O}$, the Euler characteristic

$$\chi(E) \coloneqq \chi(\mathcal{O},E) = \dim H^0(E) - \dim H^1(E) + \dim H^2(E) = r(E) + \frac{3}{2}d(E) + \mathrm{ch}_2(E) \tag{9.2.2}$$

is an integer. With some abuse of notation, we also denote by $\gamma(E)$ the vector $[r,d,\chi)$, valued in $\mathbb{Z}^3$ (note the round closing bracket, to distinguish it from the vector $[r,d,\mathrm{ch}_2]$). We denote the antisymmetrized Euler form by[12]

$$\langle\gamma,\gamma'\rangle \coloneqq \chi(\gamma,\gamma') - \chi(\gamma',\gamma) = 3\,(rd' - r'd) \tag{9.2.3}$$

[12]Our convention for the antisymmetrized Euler form is consistent with [Bri17, MP20] and opposite to that in [MPS11b, AP19a, BMP21a, AB21]

For a coherent sheaf E with $\mathrm{rk}(E) \neq 0$, we define the slope $\mu(E)$ and discriminant $\Delta(E)$ by

$$\mu(E) \coloneqq \frac{d(E)}{r(E)}, \quad \Delta(E) \coloneqq \frac{1}{2}\mu(E)^2 - \frac{\mathrm{ch}_2(E)}{r(E)} \tag{9.2.4}$$

and denote them by μ_γ and Δ_γ (when $r(E) = 0$ and $d(E) \neq 0$, we set $\mu(E) = +\infty$). Under tensoring with the m-th power of the line bundle $\mathcal{O}_C$, the Chern vector transforms as

$$\gamma \mapsto \gamma(m) \coloneqq [r, d + mr, \mathrm{ch}_2 + md + \frac{r}{2}m^2] \tag{9.2.5}$$

such that $\mu \mapsto \mu + m$ while Δ is invariant. In particular, the 'fluxed D4-brane' $\mathcal{O}(m)$ has Chern vector $[1, m, \frac{1}{2}m^2]$, slope m and vanishing discriminant. A sheaf with $r \neq 0$ is said to be normalized if its slope μ lies in the interval $(-1, 0]$.

A coherent sheaf E on $\mathbb{P}^2$ is said to be of pure dimension n if the dimension of the support of any non-zero subsheaf (including E itself) is of complex dimension n. A torsion-free sheaf E is said to be slope-semistable if it is of pure dimension 2 and if for any subsheaf $F \subset E$ one has $\mu(F) \leq \mu(E)$. It is Gieseker-semistable if it is of pure dimension 2 and if for any subsheaf $F \subset E$ one has $\mu(F) \leq \mu(E)$, with $\Delta(F) \geq \Delta(E)$ in case of equality. Gieseker stability is defined by requiring $\Delta(F) > \Delta(E)$ in case $\mu(F) = \mu(E)$, and slope stability by requiring $\mu(F) < \mu(E)$ for any proper subsheaf. In particular, slope-stability implies Gieseker stability, which implies Gieseker semistability, which implies slope-semistability.

Let $\mathcal{M}_\infty(\gamma)$ be the moduli space of Gieseker-semistable sheaves with Chern vector $\gamma = [r, d, \mathrm{ch}_2] = [r, d, \chi)$ (the rationale for the notation ∞ will become apparent in §9.4.1). If $\mathcal{M}_\infty(\gamma)$ is not empty, then it is a normal, irreducible, factorial projective variety of dimension

$$\dim_{\mathbb{C}} \mathcal{M}_\infty(\gamma) = \dim \mathrm{Ext}^1(E, E) = r^2(2\Delta - 1) + 1 \tag{9.2.6}$$

Moreover, it is smooth whenever $[r, d, \chi)$ is a primitive vector in $\mathbb{Z}^3$, such that semi-stable sheaves are automatically stable.

In order to state the condition for $\mathcal{M}_\infty(\gamma)$ to be non-empty, we consider exceptional stable sheaves, defined are those for which $\mathrm{Hom}(E, E) = \mathbb{C}, \mathrm{Ext}^1(E, E) = \mathrm{Ext}^2(E, E) = 0$. Such sheaves are then necessarily homogenous stable vector bundles, and have a trivial moduli space. They are entirely specified by their slope μ, which can take value in an infinite set $\mathcal{E} \subset \mathbb{Q}$, called the set of exceptional slopes. For $\mu = \frac{p}{r} \in \mathcal{E}$ with $r > 0$ and (p, r) coprime, the exceptional bundle of slope μ has rank r and discriminant $\Delta_\mu = \frac{1}{2}(1 - \frac{1}{r^2})$. The set $\mathcal{E}$ is the union of an increasing family $\mathcal{E}_n \subset \mathcal{E}_{n+1}$ obtained by the following recursive construction: $\mathcal{E}_0 = \mathbb{Z}$ and $\mathcal{E}_{n+1}$ is obtained from $\mathcal{E}_n$ by adjoining the slopes

$$\mu = \frac{1}{2}(\mu_1 + \mu_2) + \frac{\Delta_{\mu_2} - \Delta_{\mu_1}}{3 + \mu_1 - \mu_2} \tag{9.2.7}$$

between any consecutive slopes (μ_1, μ_2) in $\mathcal{E}_n$. For example, after four steps one gets

$$\mathcal{E} \supset \mathcal{E}_4 \cap [0, 1] = \left\{0, \frac{13}{34}, \frac{5}{13}, \frac{75}{194}, \frac{2}{5}, \frac{179}{433}, \frac{12}{29}, \frac{70}{169}, \frac{1}{2}, \frac{99}{169}, \frac{17}{29}, \frac{254}{433}, \frac{3}{5}, \frac{119}{194}, \frac{8}{13}, \frac{21}{34}, 1\right\} \tag{9.2.8}$$

The exceptional bundles of integer slope are the structure sheaves $\mathcal{O}(m)$, while the exceptional bundle of half-integer slope $m - \frac{3}{2}$ is the twisted cotangent bundle $\Omega(m)$, defined by the exact sequence

$$0 \to \Omega(m) \to \mathcal{O}(m-1)^{\oplus 3} \to \mathcal{O}(m) \to 0 \tag{9.2.9}$$

with Chern vector $\gamma = [2, 2m-3, m^2-3m+\frac{3}{2}]$.

For any Chern vector $\gamma = [r, d, \chi)$ with $r > 0$, $d \in \mathbb{Z}$, $\chi \in \mathbb{Z}$, the condition for $\mathcal{M}_\infty(\gamma) \neq \emptyset$ is then [DLP85]

$$\Delta(\gamma) \geq \delta_{\mathrm{LP}}(\mu(\gamma)) \qquad \text{or} \quad (\mu(\gamma) \in \mathcal{E} \text{ and } \Delta(\gamma) = \Delta_{\mu(\gamma)}) \tag{9.2.10}$$

where $\delta_{\mathrm{LP}}(\mu)$ is the 'Drézet–Le Potier curve'

$$\delta_{\mathrm{LP}}(\mu) \coloneqq \sup_{\mu' \in \mathcal{E},\, |\mu'-\mu|<3} [P(-|\mu'-\mu|) - \Delta_{\mu'}] \tag{9.2.11}$$

where $P(x) = \frac{1}{2}(x^2+3x+2)$ (see Figure 9.11). In particular, $\mathcal{M}_\infty(\gamma)$ is empty unless the Bogomolov bound $\Delta(\gamma) \geq 0$ is satisfied.

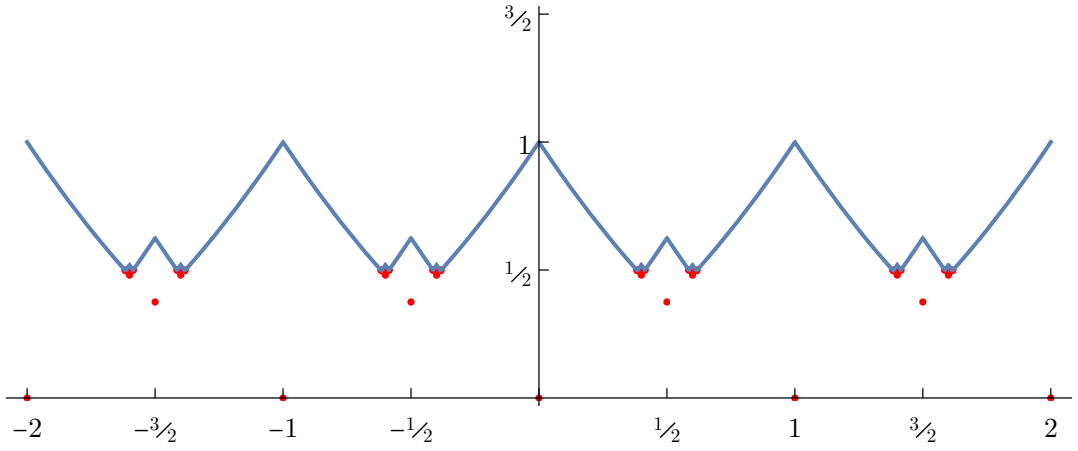

Figure 9.11: Drézet–Le Potier curve $\delta_{\mathrm{LP}}(\mu)$ (in blue) and discriminants Δ_μ of exceptional sheaves (in red).

We define the refined Gieseker index $\Omega_\infty(\gamma)$ as the Poincaré-Laurent polynomial for the moduli space $\mathcal{M}_\infty(\gamma)$,

$$\Omega_\infty(\gamma) = \sum_{p \geq 0} b_p(\mathcal{M}_\infty(\gamma))(-y)^{p-\dim_{\mathbb{C}} \mathcal{M}_\infty(\gamma)} \tag{9.2.12}$$

In the limit $y \to 1$, $\Omega_\infty(\gamma)$ reduces to the signed Euler characteristic $(-1)^{\dim_{\mathbb{C}} \mathcal{M}_\infty(\gamma)} e(\mathcal{M}_\infty(\gamma))$. When the inequality (9.2.10) is saturated, $\mathcal{M}_\infty(\gamma)$ has Picard rank $b_2(\mathcal{M}_\infty(\gamma)) = 1$, or 2 when the inequality is strict. The Gieseker index for sheaves on $\mathbb{P}^2$ with arbitrary rank was determined in [Man17], by relating it to the Gieseker index for sheaves on the Hirzebruch surface $\mathbb{F}_1$ (which coincides with the blow-up of $\mathbb{P}^2$ at one point) and using wall-crossing arguments. Quite remarkably, the generating series of Gieseker indices with fixed rank r and degree d are conjectured to transform as mock Jacobi forms of the parameters (τ, w) conjugate to the second Chern class ch_2 and Betti degree p in (9.2.12) [AMP20]. The simplest case is for rank 1, where the moduli space $\mathcal{M}_\infty([1,0,1-n))$ coincides with the Hilbert scheme of n points on $\mathbb{P}^2$, and the generating series is an actual Jacobi

form [Göt90],

$$\begin{aligned}\sum_{n\geq 0}\Omega_\infty([1,0,1-n])\,q^n &= \frac{\mathrm{i}q^{1/8}(y-1/y)}{\theta_1(q,y^2)}\\ &= 1+(y^2+1+1/y^2)q+(y^2+1+1/y^2)^2q^2+(y^6+2y^4+5y^2+6+\dots)q^3+\dots\\ &\overset{y\to 1}{\to} 1+3q+9q^2+22q^3+51q^4+108q^5+221q^6+429q^7+810q^8+1479q^9+\dots\end{aligned} \tag{9.2.13}$$

where $\theta_1(q,y)=\mathrm{i}\sum_{r\in\mathbb{Z}+\frac{1}{2}}(-1)^{r-\frac{1}{2}}q^{r^2/2}y^r$ is the Jacobi theta series (the dots in the middle line indicate the obvious additional terms required for invariance under $y\mapsto 1/y$). Further examples of generating series of Gieseker indices of rank $r>1$ can be found in [BMP21a, §A].

The notion of Gieseker semi-stable sheaves extends to vanishing rank as follows. A torsion sheaf E is Gieseker-semistable if it is of pure dimension 1 (hence $d(E)\neq 0$) and if for any proper subsheaf $F\subset E$ one has $\nu(F)\leq\nu(E)$, with $\nu(E)=\frac{\chi(E)}{d(E)}=\frac{\mathrm{ch}_2(E)}{d(E)}+\frac{3}{2}$. The moduli space $\mathcal{M}_\infty(\gamma)$ for $\gamma=[0,d,\chi)$ is non-empty for any $d>0$, and is invariant under $(d,\chi)\mapsto(d,d+\chi)$ and $(d,\chi)\mapsto(d,-\chi)$. As in the torsion-free case, it is a normal, irreducible, factorial projective variety of dimension

$$\dim_{\mathbb{C}}\mathcal{M}_\infty(\gamma)=\dim\mathrm{Ext}^1(E,E)=d^2+1 \tag{9.2.14}$$

and it is smooth whenever (d,χ) are coprime. For $\gamma=[0,1,1)$, corresponding to a D2-brane wrapped on a curve C in the linear system $|H|$, one has $\mathcal{M}_\infty(\gamma)=\mathbb{P}^2$. The Gieseker index, defined in the same way as in (9.2.12), turns out to be completely independent of χ [MS20], and related to the refined Gopakumar-Vafa invariants $N_d^{(j_L,j_R)}$ [KKV99, CvGKT20] via

$$\Omega_\infty([0,d,\chi))=\sum_{j_L,j_R}(-1)^{2j_L+2j_R}\chi_{j_L}(y)\chi_{j_R}(y)N_d^{(j_L,j_R)} \tag{9.2.15}$$

where $\chi_j(y)=\sum_{m=-j}^{j}y^{-2m}=\frac{y^{2j+1}-y^{-2j-1}}{y-1/y}$ is the character of the spin-j representation of $SU(2)$. The identification of the two fugacities y_L and y_R conjugate to j_L and j_R is natural in the Nekrasov-Shatashvilii limit of the refined topological string amplitude. Using the refined BPS invariants in [HKPK13, Table 2 p.61], we find for degree up to 6,

$$\begin{aligned}\Omega_\infty([0,1,\chi)) &= y^2+1+1/y^2\\ \Omega_\infty([0,2,\chi)) &= -y^5-y^3-y-1/y-1/y^3-1/y^5\\ \Omega_\infty([0,3,\chi)) &= y^{10}+2y^8+3y^6+3y^4+3y^2+3+\dots\\ \Omega_\infty([0,4,\chi)) &= -y^{17}-2y^{15}-6y^{13}-10y^{11}-14y^9-15y^7-16y^5-16y^3-16y-\dots\\ \Omega_\infty([0,5,\chi)) &= y^{26}+2y^{24}+6y^{22}+13y^{20}+26y^{18}+45y^{16}+68y^{14}+87y^{12}\\ &\quad +100y^{10}+107y^8+111y^6+112y^4+113y^2+113+\dots\\ \Omega_\infty([0,6,\chi)) &= -y^{37}-2y^{35}-6y^{33}-13y^{31}-29y^{29}-54y^{27}-101y^{25}\\ &\quad -169y^{23}-273y^{21}-401y^{19}-547y^{17}-675y^{15}-779y^{13}\\ &\quad -847y^{11}-894y^9-919y^7-935y^5-942y^3-945y+\dots\end{aligned} \tag{9.2.16}$$

In §9.4.3, §9.4.4 and §9.5.4 we reproduce some of the invariants (9.2.13) and (9.2.16) from attractor flow trees in the large volume and orbifold scattering diagrams.

9.2.2 Derived category of coherent sheaves on $K_{\mathbb{P}^2}$

The total space $X = K_{\mathbb{P}^2}$ of the canonical bundle over $\mathbb{P}^2$ is a non-compact, smooth Calabi-Yau threefold, obtained as a crepant resolution of the quotient $\mathbb{C}^3/\mathbb{Z}_3$ with diagonal action $z_i \mapsto e^{2\pi \mathrm{i}/3} z_i$, $i = 1, 2, 3$. We denote by $\mathrm{Coh}_c\, X$ the Abelian category of compactly supported coherent sheaves on X. A compactly supported coherent sheaf E is equivalent to a pair (F, ϕ) where $F = \pi_*(E) \in \mathrm{Coh}\, \mathbb{P}^2$ is the push forward of E, and $\phi\colon F \to F \otimes K_X$ is a morphism (see e.g. [Moz22, §8.1]). We abuse notation and denote by $\mathrm{ch}(E) = \mathrm{ch}(F) = [r, d, \chi)$ the Chern character of F. Physically, F describes the gauge field on a stack of r D4-branes wrapped on $\mathbb{P}^2$, while ϕ is the Higgs fields describing fluctuations in the fiber direction K_X. Given a sheaf F on $\mathbb{P}^2$, we denote by $i_\star(F) = (F, 0)$ its embedding along the zero section.

As explained for example in [Asp04], the category of BPS states in type IIA string theory on $\mathbb{R}^{3,1} \times X$ coincides with the bounded derived category $\mathcal{C} = D^b(\mathrm{Coh}_c\, X)$ of coherent sheaves on X with compact support. An object $E \in \mathcal{C}$ is a complex of coherent sheaves $\cdots \to E^{-1} \to E^0 \to E^1 \to \dots$ of arbitrary (but finite) length, where the component E^k in cohomological degree k is a coherent sheaf with compact support on X. We denote by $\mathcal{H}^k(E)$ the cohomology of the complex at the k-th place, and by $\mathrm{ch}(E) \coloneqq \sum_k (-1)^k \mathrm{ch}(E^k)$ the Chern character of the complex. The homological shift $E \mapsto E[1]$ taking the complex $(E^k)_{k\in\mathbb{Z}}$ to $(E^{k-1})_{k\in\mathbb{Z}}$ maps D-branes with charge $\gamma = \mathrm{ch}(E) = [r, d, \chi)$ to anti-D-branes with opposite charge $-\gamma$.

By Serre duality, the Euler form on X coincides with the antisymmetrized Euler form (9.2.3) on $\mathbb{P}^2$ [Moz22, Corollary 8.2],

$$\chi_X(E, E') \coloneqq \sum_{k=0}^{3} (-1)^k \dim \mathrm{Ext}^k_X(E, E') = 3(rd' - r'd) \tag{9.2.17}$$

where $\mathrm{ch}(E) = [r, d, \chi)$ and $\mathrm{ch}(E') = [r', d', \chi')]$. For $E = i_*(F)$ and $E' = i_*(F')$, the extension groups on X can be computed from those on $\mathbb{P}^2$ via (9.2.18),

$$\mathrm{Ext}^k_X(i_*F, i_*F') = \mathrm{Ext}^k_{\mathbb{P}^2}(F, F') \oplus \mathrm{Ext}^{3-k}_{\mathbb{P}^2}(F', F) \tag{9.2.18}$$

In particular, an exceptional sheaf F on $\mathbb{P}^2$ lifts to a spherical object $S = i_*(F)$ in $\mathcal{C}$, i.e. an object such that $\mathrm{Ext}^k_X(S, S) \simeq \mathbb{C}$ for $k = 0, 3$ and zero otherwise.

Starting from the Ext-exceptional collection on $\mathbb{P}^2$ given by

$$F_1 = \mathcal{O}[-1], \quad F_2 = \Omega(1), \quad F_3 = \mathcal{O}(-1)[1] \tag{9.2.19}$$

and embedding it along the zero section, one obtains a tilting sequence $\mathcal{S} = \bigoplus_{i=1}^3 E_i$ of objects $E_i = i_*(F_i)$ on X which generate the category $\mathcal{C}$ and such that $\mathrm{Ext}^k(\mathcal{S}, \mathcal{S}) = 0$ for $k \neq 0$. Physically, these objects correspond to the fractional branes of the superconformal field theory on the orbifold $\mathbb{C}^3/\mathbb{Z}_3$. The category $\mathcal{C}$ is then equivalent to the derived category of representations of the Jacobian algebra[13] $J(Q, W)$ for a quiver with potential (Q, W) associated to $\mathcal{S}$. The corresponding quiver (shown Figure 9.4) in has 3 nodes corresponding to each fractional brane, with 3 arrows $a_i\colon E_2 \to E_1$, $b_j\colon E_3 \to E_2$, $c_k\colon E_1 \to E_3$ in agreement with $\mathrm{Ext}^1(E_i, E_{i-1}) = \mathbb{Z}^3$ (with index i identified modulo 3). The potential $W = \sum_{i,j,k} \epsilon_{ijk} \mathrm{Tr}(a_i b_j c_k)$ can be determined by studying the

[13] Recall that the Jacobian algebra $J(Q, W)$ is the quotient of the path algebra by the ideal generated by relations $\{\partial_a W : a \in Q_1\}$.

A_∞ structure on the derived category of coherent sheaves [AK06], or read off from the associated brane tiling [FHK+06].

The derived category $\mathcal{C}$ admits a large group of auto-equivalences $\mathrm{Aut}(\mathcal{C})$, generated by the homological shift $E \mapsto E[1]$, by the translation $E \mapsto E(1) = E \otimes \mathcal{O}_X(1)$, by spherical twists $\mathrm{ST}_{\mathcal{O}}$ with respect to the spherical object $\mathcal{O}$, and by automorphisms of X itself (or rather, its formal completion at $\mathbb{P}^2$). For any spherical object S, the spherical twist ST_S acts on $E \in \mathcal{C}$ via [ST00]

$$\mathrm{ST}_S \colon E \mapsto \mathrm{Cone}\left(\mathrm{Hom}^\bullet_{K_{\mathbb{P}^2}}(S,E) \otimes S \xrightarrow{\mathrm{ev}} E\right) \tag{9.2.20}$$

where $\mathrm{Cone}(f)$ is defined by the exact triangle $A \xrightarrow{f} B \to \mathrm{Cone}(f) \to A[1]$. As a result ST_S maps the Chern vector

$$\mathrm{ch}\, E \mapsto \mathrm{ch}\, E - \langle \mathrm{ch}\, S, \mathrm{ch}\, E\rangle \,\mathrm{ch}\, S \tag{9.2.21}$$

As shown in [BM11], the translation $E \mapsto E(1)$ and the spherical twist $\mathrm{ST}_{\mathcal{O}}$ generate $\Gamma_1(3)$, the subgroup of $SL(2,\mathbb{Z})$ matrices defined below (9.1.4).

9.2.3 Stability conditions and Donaldson-Thomas invariants

A stability condition on a triangulated category $\mathcal{C}$ with Grothendiek group Γ consists of a pair $\sigma = (Z, \mathcal{A})$ such that [Bri07]

i) $\mathcal{A}$ is the heart of a bounded t-structure, in particular it is an Abelian subcategory of $\mathcal{C}$;

ii) $Z \colon \Gamma \to \mathbb{C}$ is a linear map, called the central charge;

iii) For any $0 \neq E \in \mathcal{A}$, $Z(E) = \rho(E) e^{\mathrm{i}\pi\phi(E)}$ where $\rho(E) > 0$ and $0 < \phi(E) \leq 1$; in other words, $Z(E)$ is contained in $\mathbb{H}_B = \mathbb{H} \cup (-\infty, 0)$;

iv) *(Harder-Narasimhan property)* Every $0 \neq E \in \mathcal{A}$ admits a finite filtration $0 \subset E_0 \subset E_1 \cdots \subset E_n = E$ by objects E_i in $\mathcal{A}$, such that each factor $F_i := E_i/E_{i-1}$ is σ-semistable and $\phi(F_1) > \phi(F_2) > \ldots > \phi(F_n)$;

v) *(Support property)* There exists a quadratic form Q on $\Gamma \otimes \mathbb{R}$ such that the kernel of Z in $\Gamma \otimes \mathbb{R}$ is negative definite with respect to Q, and moreover, for any σ-semistable object $E \in \mathcal{A}$, $Q(\gamma(E)) \geq 0$. Equivalently [KS], there exists a non-negative constant C such that, for all σ-semistable object $E \in \mathcal{A}$,

$$\|\gamma(E)\| \leq C\, |Z(E)| \tag{9.2.22}$$

where $\|\cdot\|$ is a fixed Euclidean norm on $\Gamma \otimes \mathbb{R}$.

In the last two items above, we define σ-semistability of an object $F \in \mathcal{A}$ by requiring that $\phi(F') \leq \phi(F)$ for every non-zero subobject of F. Unlike common practice, we do not declare that homological shifts $F[k]$ of a σ-semistable object F are also stable, but we compensate for this in the definition of the DT invariants below.

According to [Bri07], the space of stability conditions $\mathrm{Stab}(\mathcal{C})$ is a complex manifold of dimension $\mathrm{rk}\,\Gamma$, such that the map $\mathrm{Stab}(\mathcal{C}) \to \mathrm{Hom}(\Gamma, \mathbb{C})$ which sends $\sigma = (Z, \mathcal{A}) \mapsto Z$ is a local homeomorphism of complex manifolds. Moreover, it admits an action of $\widetilde{GL^+}(2,\mathbb{R}) \times \mathrm{Aut}(\mathcal{C})$ [Bri07,

Lemma 8.2], where $\widetilde{GL^+}(2,\mathbb{R})$ is the universal cover of the group of 2×2 real matrices with positive determinant. The group $GL(2,\mathbb{R})^+$ acts on the central charge Z via

$$\begin{pmatrix}\Re Z\\ \Im Z\end{pmatrix}\mapsto\begin{pmatrix}a & b\\ c & d\end{pmatrix}\begin{pmatrix}\Re Z\\ \Im Z\end{pmatrix}\ ,\quad ad-bc>0 \tag{9.2.23}$$

preserving the orientation on $\mathbb{R}^2$. Its universal cover acts on the stability condition $(Z,\mathcal{A})$ by suitably tilting the heart $\mathcal{A}$. The subgroup $\mathbb{C}^\times$ of matrices of the form $\lambda\left(\begin{smallmatrix}\cos\theta & \sin\theta\\ -\sin\theta & \cos\theta\end{smallmatrix}\right)$ with $\lambda>0$ preserves the complex structure and has trivial stabilizers, so the quotient $\mathrm{Stab}(\mathcal{C})/\mathbb{C}^*$ is still a complex manifold. When $\mathcal{C}$ is a category of coherent sheaves, there is a notion of derived duality $E\mapsto E^\vee$, and therefore an involution sending $(Z,\mathcal{A})\mapsto(Z^\vee,\mathcal{A}^\vee)$ where $\mathcal{A}^\vee$ is the derived dual of $\mathcal{A}$ (up to tilt) and $Z^\vee(E):=-\overline{Z(E^\vee)}$. This involution allows to extend $\widetilde{GL^+}(2,\mathbb{R})$ to the full group $\widetilde{GL}(2,\mathbb{R})$.

For any class $\gamma\in\Gamma$ and stability condition $\sigma\in\mathrm{Stab}(\mathcal{C})$, we denote by $\mathcal{M}_\sigma(\gamma)$ the moduli stack of σ-semistable objects of charge $\epsilon\gamma$ in $\mathcal{A}$, where $\epsilon=\pm1$ is chosen such that $Z(\epsilon\gamma)\in\mathbb{H}_B$. We further denote by $\Omega_\sigma(\gamma)$ the motivic Donaldson-Thomas invariant of $\mathcal{M}_\sigma(\gamma)$. Informally, one can think of $\Omega_\sigma(\gamma)$ as the Poincaré-Laurent polynomial of the cohomology with compact support of $\mathcal{M}_\sigma(\gamma)$, with a cohomological shift ensuring that

$$\Omega_\sigma(\gamma)=\sum_{p\geq 0}b_p(\mathcal{M}_\sigma(\gamma))(-y)^{p-\mathrm{virdim}_{\mathbb{C}}\mathcal{M}_\sigma(\gamma)} \tag{9.2.24}$$

where $\mathrm{virdim}_{\mathbb{C}}$ is the virtual dimension and $y^2=\mathbb{L}$ is the motive of the affine line (see Appendix 9.7.15 for a more precise mathematical definition). We further define the rational DT invariant $\bar\Omega_\sigma(\gamma)$ via (9.1.1). By construction, both $\Omega_\sigma(\gamma)$ and $\bar\Omega_\sigma(\gamma)$ are invariant under the action of $\widetilde{GL^+}(2,\mathbb{R})\times\mathrm{Aut}(\mathcal{C})$, in particular under $\gamma\mapsto-\gamma$, as well as derived duality acting on (σ,γ).

These invariants are locally constant on $\mathrm{Stab}\,\mathcal{C}$ but may jump when some object $E\in\mathcal{A}$ of charge γ goes from being stable to unstable. This may happen when the central charge $Z(\gamma')$ of a subobject $E'\subset E$ of charge γ' becomes aligned with $Z(\gamma)$, therefore along the real-codimension one *wall of marginal stability*

$$\mathcal{W}(\gamma,\gamma'):=\{\sigma=(Z,\mathcal{A})\in\mathrm{Stab}\,\mathcal{C}:\Im(Z(\gamma')\overline{Z(\gamma)})=0\} \tag{9.2.25}$$

The discontinuity across $\mathcal{W}(\gamma,\gamma')$ is determined from the invariants on either side of the wall by the wall-crossing formulae of [KS, JS12].

9.2.4 Stability conditions on $K_{\mathbb{P}^2}$ and Π-stability

The space of Bridgeland stability conditions $\mathrm{Stab}(\mathcal{C})$ on $\mathcal{C}=D^b(\mathrm{Coh}_c\,K_{\mathbb{P}^2})$ was studied in [Bri06, BM11]. After fixing the $\mathbb{C}^\times$ action such that skyscraper sheaves have central charge $Z_{[0,0,1]}=-1$, the central charge can be parametrized by the two complex coefficients (T,T_D) in (9.1.3),

$$Z(\gamma)=-rT_D+dT-\mathrm{ch}_2 \tag{9.2.26}$$

We define $s=\frac{\Im T_D}{\Im T}$, in such a way that $\Im Z(\gamma)=\Im T(d-rs)$. We then denote by

- $\mathrm{Coh}_c^{\leq s}$ the subcategory of $\mathrm{Coh}_c(X)$ generated (under extensions) by slope-semistable torsion-free sheaves of slope $\frac{d}{r}\leq s$

- $\mathrm{Coh}_c^{>s}$ the subcategory of $\mathrm{Coh}_c(X)$ generated by slope-semistable torsion-free sheaves of slope $\frac{d}{r} > s$ and by torsion sheaves
- $\mathrm{Coh}_c^{\sharp s}$ the subcategory of $\mathcal{C}$ of objects E such that $\mathcal{H}^i(E) = 0$ for $i \neq -1, 0$, $\mathcal{H}^{-1}(E) \in \mathrm{Coh}_c^{\leq s}$, $\mathcal{H}^0(E) \in \mathrm{Coh}_c^{>s}$

The Abelian category $\mathcal{A}(s) = \mathrm{Coh}_c^{\sharp s}$ is obtained by the standard tilt procedure from the torsion pair $(\mathrm{Coh}_c^{\leq s}, \mathrm{Coh}_c^{>s})$ and is the heart of a bounded t-structure on $\mathcal{C}$. For $\Im T > 0$, the construction ensures that $\Im Z(\gamma) \geq 0$ for any $E \in \mathcal{A}(s)$. In addition, if $\Im Z(\gamma) = 0$, namely $s = \mu$, we get

$$\Re Z(\gamma) = r\left(w - \frac{\mathrm{ch}_2}{r}\right) = r\left(w - \frac{1}{2}s^2 + \Delta\right) \tag{9.2.27}$$

where we defined $w = -\Re T_D + s\Re T$ as in (9.1.7). The coordinates (s, w) in fact parametrize the orbits of the action of $\widetilde{GL^+}(2,\mathbb{R})$ on $\mathrm{Stab}(\mathcal{C})$ in the region $\Im T > 0$, such that the central charge (9.2.26) is in the same orbit as the function used in [LZ19]

$$Z^{LJ}_{(s,w)}(\gamma) = (w - \mathrm{i}s)r + \mathrm{i}d - \mathrm{ch}_2 = (rw - \mathrm{ch}_2) + \mathrm{i}(d - sr) \tag{9.2.28}$$

The virtue of these coordinates is that walls of marginal stability become straight lines, given by the vanishing of

$$\Im\left[Z^{LJ}_{(s,w)}(\gamma')\overline{Z^{LJ}_{(s,w)}(\gamma)}\right] = (rd' - r'd)w + (r'\mathrm{ch}_2 - r\mathrm{ch}_2')s + (d\mathrm{ch}_2' - d'\mathrm{ch}_2) \tag{9.2.29}$$

Returning to (9.2.27), the Drézet–Le Potier bound $\Delta(E) \geq \delta_{\mathrm{LP}}(\mu(E))$ in (9.2.10) (which also holds for slope-semi-stable objects) implies that $\Re Z(\gamma) > 0$ (and therefore $\Re Z(-\gamma) < 0$ for the homologically shifted object $E[-1]$) in the region

$$\Im T > 0, \quad w \geq \frac{1}{2}s^2 - \hat{\delta}_{\mathrm{LP}}(s) \tag{9.2.30}$$

where we define $\hat{\delta}_{\mathrm{LP}}(\mu) = \delta_{\mathrm{LP}}(\mu)$ when $\mu \notin \mathcal{E}$, $\hat{\delta}_{\mathrm{LP}}(\mu) = \Delta_\mu$ otherwise. The region $w \geq \frac{1}{2}s^2 - \hat{\delta}_{\mathrm{LP}}(s)$ is the region above the blue jagged curve and red points in Figure 9.12 (the black and purple lines will be discussed momentarily). One can show that the remaining axioms for Bridgeland stability conditions (HN filtration and support property) are indeed satisfied by the pair $\sigma = (Z, \mathcal{A}(s))$ in this region. Moreover, the resulting stability condition turns out to exhaust the subset $U \subset \mathrm{Stab}(\mathcal{C})$ of geometric stability conditions, defined as those stability conditions for which all skyscraper sheaves $\mathcal{O}_x$ with $x \in \mathbb{P}^2$ are σ-stable with the same phase. The connected component of $\mathrm{Stab}(\mathcal{C})$ containing U, denoted by $\mathrm{Stab}^\dagger(\mathcal{C})$, is the union of the images of (the closure of) U under the group $\Gamma_1(3)$ of auto-equivalences of $\mathcal{C}$ generated by spherical twists, and is simply connected [BM11]. It is unknown whether $\mathrm{Stab}(\mathcal{C})$ might have other connected components.

Having identified the space of stability conditions $\mathrm{Stab}^\dagger \mathcal{C}$ inside the two-dimensional space of central charges parametrized by (T, T_D), it remains to determine which part of it is covered by the physical slice of Π-stability conditions. As mentioned in the introduction and further detailed in Appendix 9.7.1, the slice Π is isomorphic to the universal cover of the modular curve $X_1(3)$, and conveniently parametrized by τ in the Poincaré upper half-plane $\mathbb{H}$. As shown in [BM11], there is an embedding $\mathbb{H} \hookrightarrow \mathrm{Stab}^\dagger \mathcal{C}$ sending $\tau \mapsto (Z_\tau, \mathcal{A}_\tau)$ which is equivariant with respect to the action

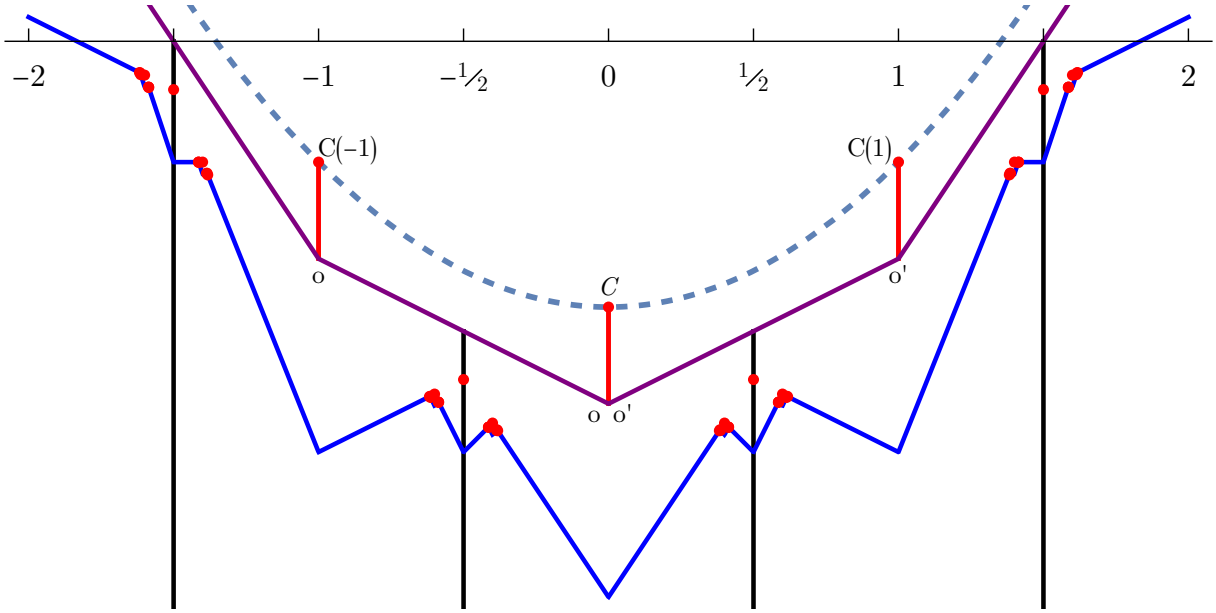

Figure 9.12: Image in the (s,w) plane of the fundamental domain $\mathcal{F}_C$ and some of its translates. The dotted line correspond to the parabola $w \geq \frac{1}{2}s^2$. The jagged blue curve corresponds to $w = \frac{1}{2}s^2 - \delta_{\rm LP}(s)$, and the red dots indicate the points $(\mu_\alpha, \frac{1}{2}\mu_\alpha^2 - \Delta_\alpha)$ corresponding to exceptional slopes. The vertical segments in red interpolate between the conifold point at $\tau = n$ and the orbifold point at $\tau = \tau_o + n$. The segments in purple are the images of infinitesimal arcs around the orbifold point τ_o (from $(-1, \frac{1}{6})$ to $(0, -\frac{1}{3})$), around $\tau_{o'}$ (from $(0, -\frac{1}{3})$ to $(1, \frac{1}{6})$), etc. These segments are connected at points with s integer along the parabola $w = \frac{1}{2}s^2 - \frac{1}{3}$. The vertical lines in black correspond to straight $\tau_1 = n + \frac{1}{2}$ lines connecting the orbifold point $\tau_o + n$ and conifold point $n - \frac{1}{2}$ in the τ plane.

of $\Gamma_1(3)$ on both sides. The central charge function Z_τ (9.1.4) is determined by the representation (9.1.5) for the periods,

$$T(\tau) = -\frac{1}{2} + \int_{\tau_o}^{\tau} C(u)\mathrm{d}u \ , \quad T_D(\tau) = \frac{1}{3} + \int_{\tau_o}^{\tau} C(u)\, u\mathrm{d}u \tag{9.2.31}$$

where $\tau_o = \frac{1}{\sqrt{3}} e^{5\pi \mathrm{i}/6}$ is a preimage of the orbifold point, and $C(\tau) = \frac{\eta(\tau)^9}{\eta(3\tau)^3}$ is a weight 3 modular form for $\Gamma_1(3)$. Indeed, one checks that the period vector $\Pi = (1, T, T_D)$ transforms under $\tau \mapsto \tau + 1$ and $\tau \mapsto -\frac{\tau}{3\tau - 1}$ with the same monodromy matrices $M_{\rm LV}, M_C$ (see (9.7.54)) as predicted by the translation $E \mapsto E(1)$ and spherical twist $E \mapsto \mathrm{ST}_{\mathcal{O}} E$ on the derived category side. It follows from the reality properties (9.7.18) of the periods T and T_D that the action of derived duality preserves the slice of Π-stability conditions,

$$Z_{-\bar\tau}(\gamma^\vee) = -\overline{Z_\tau(\gamma)} \tag{9.2.32}$$

where $[r, d, \mathrm{ch}_2]^\vee = [-r, d, -\mathrm{ch}_2] = [-r, d, 3d - \chi)$. Moreover, one can show that the periods

$T(\tau), T_D(\tau)$ satisfy the geometric stability conditions (9.2.30) in the fundamental domain $\mathcal{F}_C$ and its translates [BM11, §C].

In the limit $\tau \to \mathrm{i}\infty$, $C(\tau) = 1 + \mathcal{O}(q)$ with $q = e^{2\pi\mathrm{i}\tau}$, the central charge becomes a quadratic polynomial in τ,

$$Z_\tau(\gamma) = -\frac{r}{2}\left(\tau^2 + \tfrac{1}{8}\right) + d\tau - \mathrm{ch}_2 + \mathcal{O}\big(|\tau|q\big) \tag{9.2.33}$$

In fact, in the domain $\mathbb{H}^{\mathrm{LV}}$ defined below (9.1.7) as the preimage of the region above the the curve $w = \frac{1}{2}s^2$ inside the fundamental domain $\mathcal{F}_C$ and its translates (see Figure 9.1), the $\mathcal{O}(|\tau|q)$ corrections in (9.2.33) as well as the constant $\frac{1}{8}$ can be absorbed by an action of $\left(\begin{smallmatrix} 1 & (s-\Re T)/\Im T \\ 0 & t/\Im T \end{smallmatrix}\right) \in GL(2,\mathbb{R})^+$ with $t = \sqrt{2w - s^2}$, which maps $Z_\tau(\gamma)$ (note that $\Im T > 0$ throughout $\mathbb{H}^{\mathrm{LV}}$). The new central charge is then $Z^{\mathrm{LV}}_{(s,t)}(\gamma)$ in (9.1.6).

The heart $\mathcal{A}_\tau$ is more subtle. A natural choice is to set (with some abuse of notation) $\mathcal{A}_\tau = \mathcal{A}(s(\tau))$ where $s(\tau)$ is defined as usual by $s = \frac{\Im T_D}{\Im T}$ and $\mathcal{A}(s) = \mathrm{Coh}^{\sharp s}_c$. While this definition would a priori make sense in a larger domain where $\Im T(\tau) > 0$, we enforce it only in the fundamendal domain $\mathcal{F}_C$ and extend this definition to the full upper half-plane by $\Gamma_1(3)$ equivariance. Thus, the identification $\mathcal{A}_\tau = \mathcal{A}(s(\tau))$ holds in all translates of $\mathcal{F}_C$ under $\tau \mapsto \tau + 1$, in particular in the region $\mathbb{H}^{\mathrm{LV}}$ around the large volume point, and in a wedge of angle $2\pi/3$ above the orbifold point. However it no longer holds below the arcs which connect the conifold points $\tau \in \mathbb{Z}$ and orbifold points $\tau \in \tau_o + \mathbb{Z}$. In particular, near the real axis the objects in $\mathcal{A}_\tau$ may include complexes of arbitrary length. As a result, the slice of Π-stability conditions only covers a part of the space U of geometric stability conditions. This is best seen in Figure 9.12, where the image of the translates of $\mathcal{F}_C$ in the (s,w) plane lie above the purple line. While the image of the region $\Im T > 0$ in the upper half plane does extend below this line, the relevant heart no longer coincides with the one appropriate for geometric stability conditions.

9.3 Scattering diagrams and attractor flows

In this section, we recall the construction of stability scattering diagram for quivers with potential, generalize this notion to arbitrary triangulated categories, and explain its relation to the Split Attractor Flow Conjecture in the case of non-compact CY threefolds with one-dimensional Kähler moduli space.

9.3.1 Scattering diagram for quivers with potentials

Let (Q, W) be a quiver with potential. A representation R of (Q, W) is a set of finite dimensional vector spaces M_i for every node $i \in Q_0$, and linear maps $M_a \colon M_i \to M_j$ for every arrow $(a \colon i \to j) \in Q_1$ such that for any arrow $a \in Q_1$, the element $\partial W/\partial a$ in the path algebra of Q evaluates to zero on R. The set of representations R forms an Abelian category $\mathcal{A}$ graded by the lattice $\mathbb{Z}^{Q_0}$ of dimension vectors $\gamma = \dim R = (\dim M_i)_{i\in Q_0}$. For any set $(z_i)_{i\in Q_0}$ of points $z_i = -\theta_i + \mathrm{i}\rho_i$ in the upper half-plane $\mathbb{H}_B$, the pair $(Z, \mathcal{A})$ with central charge $Z(\gamma) = \sum_{i\in Q_0} n_i z_i$ defines a stability condition in the sense of §9.2.3. We denote by $\mathcal{M}_Z(\gamma)$ the moduli space of Z-semi-stable representations of dimension vector γ, by $\Omega_Z(\gamma)$ its motivic Donaldson-Thomas invariant (9.2.24) and by $\bar\Omega_Z(\gamma)$ its rational counterpart (9.1.1). These invariants vanish unless γ belongs to the positive quadrant $\Gamma_+ = \mathbb{N}^{Q_0}$.

As shown in [Bri17], the set of DT invariants is conveniently encoded in a stability scattering diagram $\mathcal{D}_Q$ in the space $\mathbb{R}^{Q_0}$ spanned by King stability parameters $\theta = (\theta_i)_{i\in Q_0}$. To define $\mathcal{D}$, we first introduce the hyperplane orthogonal to γ

$$\mathcal{R}_Q^{\rm geo}(\gamma) = \{\theta : (\theta,\gamma) = 0\} \tag{9.3.1}$$

which we call *geometric ray*[14]. At any point along $\mathcal{R}_Q^{\rm geo}(\gamma)$, the notion of Z-semi-stability coincides with the notion of θ-semi-stability (i.e. R is θ-semi-stable if and only if $(\theta,\gamma')\le 0$ for any subrepresentation $R'\subset R$ of dimension vector γ'). In particular, the index $\Omega_Z(\gamma) =: \Omega_\theta(\gamma)$ is independent of ρ. We then define the active ray $\mathcal{R}_Q(\gamma)$ as the subset of $\mathcal{R}_Q^{\rm geo}(\gamma)$

$$\mathcal{R}_Q(\gamma) = \{\theta : (\theta,\gamma) = 0, \quad \bar\Omega_\theta(\gamma)\neq 0\} \tag{9.3.2}$$

Since $\bar\Omega_\theta(\gamma)$ is invariant under rescaling $\theta\to\lambda\theta$ with $\lambda\in\mathbb{R}_{>0}$, and since it can only jump on a finite set of hyperplanes $\mathcal{R}_Q^{\rm geo}(\gamma')$ corresponding to the destabilization by a subobject of dimension vector $\gamma'<\gamma$, the set of rays $\{\mathcal{R}_Q(\gamma) : \gamma\in\Gamma_+\}$ decomposes into a complex of convex rational polyhedral cones in the space $\mathbb{R}^{Q_0}$ of King stability conditions.

Furthermore, to each point $\theta\in\mathcal{R}_Q(\gamma)$ we associate an automorphism $\mathcal{U}_\theta(\gamma)$ of the quantum torus algebra $\hat{\mathcal{T}}$ defined as follows. Let $\mathcal{T}$ be the algebra $\mathbb{C}(y)[[\mathcal{X}_{\Gamma_+}]]$ generated by formal variables $\mathcal{X}_\gamma$ for any $\gamma\in\Gamma_+$, with coefficients in $\mathbb{C}(y)$, subject to the relations

$$\mathcal{X}_\gamma\,\mathcal{X}_{\gamma'} = (-y)^{\langle\gamma,\gamma'\rangle}\mathcal{X}_{\gamma+\gamma'} \tag{9.3.3}$$

where

$$\langle\gamma,\gamma'\rangle = \sum_{a:(i\to j)\in Q_1}(n_i'n_j - n_in_j') \tag{9.3.4}$$

is the antisymmetrization of the Euler form $\chi_Q(\gamma,\gamma') = \sum_{i\in Q_0} n_in_i' - \sum_{a:(i\to j)\in Q_1} n_in_j'$. For any positive integer M, we denote by $\mathcal{T}_M$ the ideal spanned by generators $\mathcal{X}_\gamma$ with total dimension $\sum_{i\in Q_0} n_i > M$, and define the pro-nilpotent algebra $\hat{\mathcal{T}}$ as the inverse limit of $\mathcal{T}/\mathcal{T}_M$ as $M\to\infty$. We denote by $\hat{\mathcal{G}} = \exp(\hat{\mathcal{T}})$ the corresponding pro-unipotent group. The automorphism $\mathcal{U}_\theta(\gamma)$ is the element of $\hat{\mathcal{G}}$ defined by

$$\mathcal{U}_\theta(\gamma) = \exp\left(\frac{\bar\Omega_\theta(\gamma)\mathcal{X}_\gamma}{y^{-1}-y}\right) \tag{9.3.5}$$

The scattering diagram $\mathcal{D}_Q$ can be defined as the set of decorated rays $\{\mathcal{R}_Q(\gamma) : \gamma\in\Gamma_+\}$ equipped with the automorphism $\mathcal{U}_\theta(\gamma)$ at each point. The wall-crossing formula for DT invariants ensures that $\mathcal{D}_Q$ is consistent in the following sense [Bri17]: for any generic closed path $\mathcal{P}\colon t\in[1,0]\to\mathbb{R}^{Q_0}$ (where generic means that the intersection of $\mathcal{P}$ with a ray $\mathcal{R}(\gamma_i)$ at $t=t_i$ is transverse and does not meet any cone of codimension larger than one), the ordered product of automorphisms associated to each intersection is trivial

$$\prod_i \mathcal{U}_{\theta(t_i)}(\gamma_i)^{\epsilon_i} = 1\ , \quad \epsilon_i = \mathrm{sgn}\left(\frac{\mathrm{d}\theta}{\mathrm{d}t},\gamma_i\right) \tag{9.3.6}$$

[14] The rays are sometimes called walls of second kind or BPS walls. The word 'ray' avoids possible confusion with walls of marginal stability (or first kind), but admittedly is most adequate for two-dimensional scattering diagrams, where rays are in fact one-dimensional.

This consistency property ensures that all rays can be deduced from the knowledge othe initial rays, defined as those rays $\mathcal{R}(\gamma)$ which contain the self-stability condition $\theta(\gamma) = \langle -, \gamma\rangle$. The attractor tree formula of [Moz21] and the flow tree formula of [AB21] provide an algorithm to compute $\Omega_\theta(\gamma)$ on any ray in terms of the attractor invariants $\Omega_\star(\gamma)$ for the initial rays.

For a general quiver with potential (Q, W), the determination of the initial rays is a difficult problem. For an acyclic quiver however, it is easy to prove that the only initial rays are those associated to the simple representations at each node [Bri17, Theorem 1.5], with

$$\Omega_\star(\gamma_i) = 1, \quad \Omega_\star(k\gamma_i) = 0 \text{ for } k > 1 \tag{9.3.7}$$

More generally, one can show that $\Omega_\star(\gamma) = 0$ unless the support of γ (defined as the set of vertices $i \in Q_0$ such that $n_i \neq 0$) is strongly connected [MP20, Theorem 3.8]. For quivers associated to non-compact Calabi-Yau threefolds, it is conjectured in [BMP21a, MP20, Des21] that $\Omega_\star(\gamma) = 0$ unless γ belongs to the kernel of the antisymmetrized Euler form.

9.3.2 Scattering diagrams for Kronecker quivers

As an example which will play a central role later in this chapter, let us consider the Kronecker quiver with 2 nodes and κ arrows $a_i \colon 1 \to 2$. Since the quiver is acyclic, the only initial rays are those associated to $\gamma_1 = (1, 0)$ and $\gamma_2 = (0, 1)$, with $\Omega_\theta(\gamma_1)$ and $\Omega_\theta(\gamma_2) = 1$ along the axes $\theta_1 = 0$ and $\theta_2 = 0$, respectively. For other dimension vector (n_1, n_2), the moduli space $\mathcal{M}_\theta(\gamma)$ has virtual dimension

$$\operatorname{virdim}_{\mathbb{C}} \mathcal{M}_\theta(\gamma) = \kappa n_1 n_2 - n_1^2 - n_2^2 + 1 \tag{9.3.8}$$

It is empty unless $\theta_1 > 0, \theta_2 < 0$ and (9.3.8) is non-negative, in which case it coincides with the actual dimension. Note that the formula (9.3.8) is symmetric under the exchange $(n_1, n_2) \mapsto (n_2, n_1)$, and under $(n_1, n_2) \mapsto (n_1, \kappa n_2 - n_1)$, which corresponds to a mutation of the quiver. For the A_2 quiver ($\kappa = 1$), the only active ray in the quadrant $\theta_1 > 0, \theta_2 < 0$ is associated to $\gamma_1 + \gamma_2$, with $\Omega_\theta(\gamma_1 + \gamma_2) = 1$ along the diagonal $\theta_1 + \theta_2 = 0$. For the affine A_1 quiver ($\kappa = 2$), there is an infinity of active rays of the form $(k, k-1), (k-1, k)$ and (k, k) with $k \geq 1$, with DT invariant $1, 1$ and $-y - 1/y$, respectively. For the Kronecker quiver with $\kappa \geq 3$, arrows there is a discrete set of active rays (n_1, n_2) with unit DT invariant, obtained by successive mutations of $(1, 0)$ and $(0, 1)$, and a dense set of rays in the region $\kappa - \sqrt{\kappa^2 - 4} < \frac{2n_1}{n_2}, \frac{2n_2}{n_1} < \kappa + \sqrt{\kappa^2 - 4}$. For $\kappa = 3$, the discrete rays correspond to $(n_1, n_2) = (F_{2k}, F_{2k\pm 2})$ where F_{2k} are the even Fibonacci numbers $1, 3, 8, 21, \ldots$. In Table 9.2, we tabulate some of the DT indices $K_\kappa(n_1, n_2) \coloneqq \Omega_\theta(n_1, n_2)$ for low values of (κ, n_1, n_2), restricting to the case $\kappa = 0 \mod 3$ which is most relevant for the present work. It is worth noting that for $(n_1, n_2) = (1, 1)$, the moduli space of stable representations is $\mathbb{P}^{\kappa-1}$, hence

$$K_\kappa(1, 1) = (-1)^{\kappa+1} \frac{(y^\kappa - y^{-\kappa})}{y - 1/y} \overset{y\to 1}{\to} (-1)^{\kappa+1} \kappa \tag{9.3.9}$$

More generally, for $(n_1, n_2) = (1, n)$ or $(n, 1)$, the moduli space $\mathcal{M}_\theta(\gamma)$ is the Grassmannian of n-dimensional planes in $\mathbb{C}^\kappa$, hence $K_\kappa(1, n) = 0$ if $n > \kappa$. From the point of view of the flow tree or attractor tree formulae, this vanishing occurs as a result of cancellations between numerous different trees.

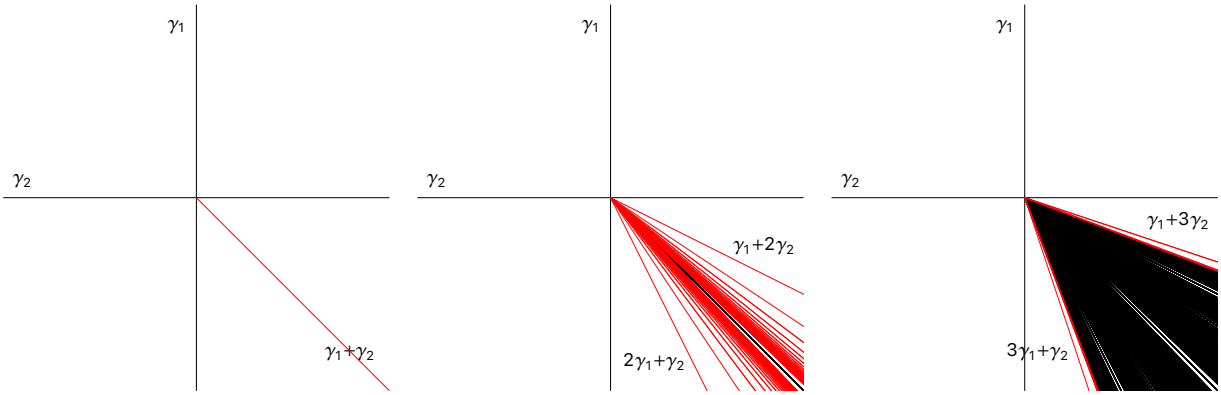

Figure 9.13: Scattering diagram for the Kronecker quiver with $\kappa = 1, 2, 3$ arrows

9.3.3 Stability scattering diagrams

The construction of the stability scattering diagrams in the space of King stability conditions for quivers with potential can be generalized to the space of Bridgeland stability conditions on any triangulated category $\mathcal{C}$ of CY3 type, at the cost of several complications.

The main complication is that charges γ such that $\Omega_Z(\gamma) \neq 0$ are no longer restricted to a fixed cone Γ_+, although they are still restricted by the condition $\Im Z(\gamma) \geq 0$. Secondly, there is no analog of King stability conditions, so no reason to restrict to rays where $\Re Z(\gamma) = 0$. In this subsection, we define a family of scattering diagrams $\mathcal{D}_\psi \subset \mathrm{Stab}\,\mathcal{C}$ labeled by a phase $\psi \in \mathbb{R}/2\pi\mathbb{Z}$, supported on active rays where semi-stable objects with $\arg Z(\gamma) = \psi + \frac{\pi}{2}$ exist.

We first need to properly define an analogue of the quantum torus algebra $\hat{\mathcal{T}}$. Let $\mathcal{T}_\Gamma$ be the algebra $\mathbb{C}(y)[\mathcal{X}_\Gamma]$ generated by formal variables $\mathcal{X}_\gamma$ for any $\gamma \in \Gamma = K(\mathcal{C})$, with coefficients in $\mathbb{C}(y)$, subject to the relations

$$\mathcal{X}_\gamma\, \mathcal{X}_{\gamma'} = (-y)^{\langle \gamma, \gamma' \rangle} \mathcal{X}_{\gamma+\gamma'} \tag{9.3.10}$$

For any stability condition $\sigma \in \mathrm{Stab}\,\mathcal{C}$, phase $\psi \in \mathbb{R}/(2\pi\mathbb{Z})$ and mass cut-off $M > 0$ we denote by $\mathcal{T}_{\sigma,\psi,M}$ the ideal spanned by generators $\mathcal{X}_\gamma$ with $\Im(e^{-\mathrm{i}\psi} Z_\sigma(\gamma)) > M$. We define the pro-nilpotent algebra $\hat{\mathcal{T}}_{\sigma,\psi}$ as the inverse limit of $\mathcal{T}/\mathcal{T}_{\sigma,\psi,M}$ as $M \to \infty$, and the pro-unipotent group $\hat{\mathcal{G}}_{\sigma,\psi} = \exp(\hat{\mathcal{T}}_{\sigma,\psi})$.

For any phase $\psi \in \mathbb{R}/(2\pi\mathbb{Z})$ and charge vector $\gamma \in \Gamma \backslash \{0\}$, we define the geometric ray as the codimension-one locus inside $\mathrm{Stab}(\mathcal{C})$

$$\mathcal{R}^{\mathrm{geo}}_\psi(\gamma) \coloneqq \{\sigma = (Z, \sigma) \in \mathrm{Stab}(\mathcal{C}) : \Re(e^{-\mathrm{i}\psi} Z(\gamma)) = 0, \Im(e^{-\mathrm{i}\psi} Z(\gamma)) > 0\} \tag{9.3.11}$$

along which the argument of the central charge $Z(\gamma)$ is equal to $\psi + \frac{\pi}{2}$ modulo 2π. We further define the active ray $\mathcal{R}_\psi(\gamma)$ as a subset of $\mathcal{R}^{\mathrm{geo}}_\psi(\gamma)$ along which the rational DT invariant $\bar{\Omega}_Z(\gamma)$ defined in (9.1.1) is not zero,

$$\mathcal{R}_\psi(\gamma) \coloneqq \{\sigma :\ \Re(e^{-\mathrm{i}\psi} Z(\gamma)) = 0, \Im(e^{-\mathrm{i}\psi} Z(\gamma)) > 0,\ \bar{\Omega}_\sigma(\gamma) \neq 0\} \tag{9.3.12}$$

Table 9.2: Table of indices $K_\kappa(n_1,n_2)$ for the Kronecker quiver with κ arrows, dimension vector (n_1,n_2) in the chamber $\theta_1>0,\theta_2<0$ with $n_1\theta_1+n_2\theta_2=0$. Negative powers of y omitted in the dots are determined by invariance under Poincaré duality $y\mapsto 1/y$.

$K_3(1,1)$	$y^2+1+\dots$
$K_3(1,2)$	$y^2+1+\dots$
$K_3(1,3)$	1
$K_3(2,2)$	$-y^5-y^3-y-\dots$
$K_3(2,3)$	$y^6+y^4+3y^2+3+\dots$
$K_3(2,4)$	$-y^5-y^3-y-\dots$
$K_3(2,5)$	$y^2+1+\dots$
$K_3(3,3)$	$y^{10}+y^8+2y^6+2y^4+2y^2+2+\dots$
$K_3(3,4)$	$y^{12}+y^{10}+3y^8+5y^6+8y^4+10y^2+12+\dots$
$K_3(3,5)$	$y^{12}+y^{10}+3y^8+5y^6+8y^4+10y^2+12+\dots$
$K_3(4,4)$	$-y^{17}-y^{15}-3y^{13}-4y^{11}-6y^9-6y^7-7y^5-7y^3-7y-\dots$
$K_3(4,5)$	$y^{20}+y^{18}+3y^{16}+5y^{14}+10y^{12}+14y^{10}+23y^8+30y^6+41y^4+46y^2+51+\dots$
$K_3(5,5)$	$y^{26}+y^{24}+3y^{22}+5y^{20}+9y^{18}+13y^{16}+18y^{14}+22y^{12}+26y^{10}+28y^8+30y^6$ $+30y^4+31y^2+31+\dots$
$K_6(1,1)$	$-y^5-y^3-y-\dots$
$K_6(1,2)$	$y^8+y^6+2y^4+2y^2+3+\dots$
$K_9(1,1)$	$y^8+y^6+y^4+y^2+1+\dots$
$K_9(1,2)$	$y^{14}+y^{12}+2y^{10}+2y^8+3y^6+3y^4+4y^2+4+\dots$

At any point σ along an active ray, we associate an automorphism

$$\mathcal{U}_\sigma(\gamma)=\exp\left(\frac{\bar\Omega_\sigma(\gamma)\mathcal{X}_\gamma}{y^{-1}-y}\right) \tag{9.3.13}$$

valued in $\mathcal{G}_{\sigma,\psi}$. Since the geometric ray (9.3.11) is invariant under rescaling γ by any positive real number, and since the automorphisms $\mathcal{U}_\sigma(\gamma)$ associated to collinear charges commute among each other, it is convenient to combine all active rays $\mathcal{R}_\psi(k\gamma)$ for a given primitive charge $\gamma\in\Gamma$ into a single 'effective' ray

$$\mathcal{R}^{\rm eff}_\psi(\gamma):=\{\sigma:\ \Re(e^{-\mathrm{i}\psi}Z(\gamma))=0,\Im(e^{-\mathrm{i}\psi}Z(\gamma))>0,\exists k\geq 1\ ,\Omega_\sigma(k\gamma)\neq 0\} \tag{9.3.14}$$

equipped with the automorphism

$$\mathcal{U}^{\rm eff}_\sigma(\gamma)=\exp\left(\sum_{k=1}^\infty\frac{\bar\Omega_\sigma(k\gamma)\mathcal{X}_{k\gamma}}{y^{-1}-y}\right)=\mathrm{Exp}\left(\sum_{k=1}^\infty\frac{\Omega_\sigma(k\gamma)\mathcal{X}_{k\gamma}}{y^{-1}-y}\right) \tag{9.3.15}$$

where Exp is the plethystic exponential. When γ is non-primitive, we set $\mathcal{U}^{\rm eff}_\sigma(\gamma)=\mathcal{U}^{\rm eff}_\sigma(\gamma/\ell)$ where ℓ is the largest integer which divides γ, so that both $\mathcal{R}^{\rm eff}_\psi(\gamma)$ and $\mathcal{U}^{\rm eff}_\sigma(\gamma)$ are invariant under rescaling γ by a non-negative rational number.

The stability scattering diagram $\mathcal{D}_\psi(\mathcal{C})$ is defined as the union of all active rays $\mathcal{R}_\psi(\gamma)$ with $\gamma\in\Gamma$, equipped with their respective automorphism $\mathcal{U}_\sigma(\gamma)$ (equivalently, the union of all effective rays $\mathcal{R}^{\rm eff}_\psi(\gamma)$ with γ primitive, equipped with $\mathcal{U}^{\rm eff}_\sigma(\gamma)$). We note that $\mathcal{D}_\psi(\mathcal{C})$ is invariant under

$\psi \mapsto \psi+\pi$ and $\psi \mapsto -\psi$, upon relabeling the charges γ into $-\gamma$ or $\gamma^\vee$, respectively. In the following, we shall restrict to $\psi \in (-\frac{\pi}{2}, \frac{\pi}{2}]$, such that the rays are supported on loci where semi-stable objects $\mathcal{A}$ exist in the heart.

As in the case of quivers, the wall-crossing formula for DT invariants again ensures that the scattering diagram $\mathcal{D}_\psi(\mathcal{C})$ is consistent, but in a more restricted sense than in the quiver context: rather than considering an arbitrary closed path $\mathcal{P}$, we pick any point σ on a codimension two intersection, and consider an infinitesimal path $t \in [1,0] \to \mathrm{Stab}\,\mathcal{C}$ circling counterclockwise[15] around σ in a two-dimensional plane containing σ and intersecting the rays $\mathcal{R}_\psi(\gamma_i)$ transversally (and away from cones of codimension greater than one). The consistency condition is then that the ordered product of automorphisms associated to each active ray $\mathcal{R}_\psi(\gamma_i)$ intersecting at σ is trivial:

$$\prod_i \mathcal{U}_{\sigma(t_i)}(\gamma_i)^{\epsilon_i} = 1 \tag{9.3.16}$$

Here, t_i are the intersection points of the path with all rays passing through σ and $\epsilon_i = \pm$ is given by

$$\epsilon_i = \mathrm{sgn}\Re\left(e^{-\mathrm{i}\psi}\frac{\mathrm{d}}{\mathrm{d}t}Z_{\sigma(t_i)}(\gamma_i)\right) \tag{9.3.17}$$

Rays such that $\epsilon_i = 1$ (respectively $\epsilon_i = -1$) are called outgoing (respectively incoming) at the point σ. Expanding out the exponential in each factor and using the algebra (9.3.10), the consistency property (9.3.16) allows to determine DT invariants on outgoing rays from the knowledge of DT invariants on incoming rays. The result takes the form

$$\bar\Omega^+_\sigma(\gamma) = \sum_{n\geq 1}\sum_{\gamma=\sum_{i=1}^n \gamma_i}\frac{g(\{\gamma_i\})}{\mathrm{Aut}(\{\gamma_i\})}\prod_i \bar\Omega^-_\sigma(\gamma_i) \tag{9.3.18}$$

where only a finite number of decompositions contribute (this follows from $\Im(e^{-\mathrm{i}\psi}Z_\sigma(\gamma_i)) = |Z(\gamma_i)|$ and the support condition). The coefficients $g(\{\gamma_i\})$ can be computed either using the attractor tree formula of [Moz21] or the flow tree formula of [AB21][16]. Both involve a sum over rooted trees decorated with charges γ_e along the edges and stability parameters θ_v at the vertices, valued in an auxiliary space $\mathbb{R}^n$. The former involves trees of arbitrary valency and stability parameters at the root vertex given by $\theta_i = \Re(e^{-\mathrm{i}\psi}Z_\sigma(\gamma_i))$, while the latter involves binary trees only, at the cost of perturbing the stability parameters at the root vertex.

Since the consistency condition (9.3.16) determines the outgoing rays from the incoming rays at each codimension-two intersection point of the scattering diagram, the full diagram is determined if one can identify a set of initial rays, from which all other rays originate by repeated scattering. In the context of quivers with potential, the initial rays in the space of King stability parameters are those which contain the self-stability condition $\theta(\gamma) = \langle -, \gamma\rangle$. We do not know a simple characterization of initial rays for a general scattering diagram, but in the context of scattering diagrams restricted to the slice of Π-stability condition, it is natural to conjecture that they either emanate from a boundary point of Π where the central charge $Z_\sigma(E)$ tends to zero, or from a regular attractor

[15] A change of orientation maps the product (9.3.16) to its inverse, so does not affect the consistency property, but it does exchange the notions of incoming and outgoing rays. In §9.3.5 we restrict to two-dimensional scattering diagrams where the rays inherit a global orientation from the complex structure.

[16] The Coulomb branch formula of [MPS11b, MPS17] gives yet another prescription, which gives the same coefficient $g(\{\gamma_i\})$ whenever all charges γ_i whose rays intersect σ lie in a common two-dimensional sublattice, such that scaling solutions do not occur.

point $\sigma_\star(E)$ such that central charge $|Z_{\sigma_\star(E)}(E)|$ attains a local minimum with $\arg Z_\sigma(E) = \psi + \frac{\pi}{2}$. Once such initial data has been fixed, by similar arguments as for standard scattering diagrams [Gro11], the scattering diagram $\mathcal{D}_\psi$ is expected to be uniquely determined, and the DT invariant $\Omega_\sigma(\gamma)$ at any point $\sigma \in \operatorname{Stab}\mathcal{C}$ can be read off from the automorphism $\mathcal{U}_\sigma(\gamma)$ along the ray $\mathcal{R}_\psi(\gamma)$ with $\psi = \arg Z_\sigma(\gamma) - \frac{\pi}{2}$ passing through the desired point σ.

9.3.4 Attractor flows and Split Attractor Flow Conjecture

We define the attractor flow $\mathrm{AF}(\gamma)$ as the flow on the physical slice of Π-stability conditions[17] induced by the gradient of the modulus square of the central charge $Z(\gamma)$ for a fixed charge $\gamma \in \Gamma\backslash\{0\}$. In local complex coordinates z^a on Π,

$$\frac{\mathrm{d}z^a}{\mathrm{d}\mu} = -g^{a\bar{b}}\partial_{\bar{b}}|Z(\gamma)|^2 \tag{9.3.19}$$

where μ is a coordinate parametrizing the flow, and $g^{a\bar{b}}$ is the inverse of the Kähler metric $g_{a\bar{b}}\mathrm{d}z^a\mathrm{d}\bar{z}^{\bar{b}}$ on Π specified by local mirror symmetry. Note that the flow depends only on the conformal class of the metric, up to reparametrization of μ.

A key property of (9.3.19) is that the modulus of the central charge necessarily decreases along the flow,

$$\frac{\mathrm{d}}{\mathrm{d}\mu}|Z(\gamma)|^2 = -2\partial_a|Z(\gamma)|^2 g^{a\bar{b}}\partial_{\bar{b}}|Z(\gamma)|^2 \leq 0 \tag{9.3.20}$$

and $z^a(\mu)$ must therefore reach a local minimum of $|Z(\gamma)|$ as $\mu \to \infty$, unless it encounters a singularity (or reaches the boundary) along the way. We denote by $z_\star(\gamma)$ the endpoint of the maximally extended flow; it is independent of the initial value of z^a at $\mu = 0$ within a given basin of attraction. If $Z_{z_\star(\gamma)}(\gamma) \neq 0$, the endpoint of the flow is said to be a regular attractor point, otherwise it is a singular attractor point. Following common lore, we define the attractor index as $\Omega_\star(\gamma)$ as the limit of $\Omega_z(\gamma)$ along the flow $z \to z_\star(\gamma)$, and similarly for the rational attractor index $\bar{\Omega}_\star(\gamma)$. This definition overlooks the possibility that a given charge may admit different attractor points (depending on the basin of attraction b), in which case one should attach an collection of attractor indices $\bar{\Omega}^{(b)}_\star(\gamma)$ to the same charge γ, but we shall gloss over this complication in this work.

An attractor flow tree is an oriented rooted tree T, decorated with charges $\gamma_e \in \Gamma\backslash\{0\}$ along each edge $e \in E_T$ and equipped with a continuous map $\pi\colon T \to \Pi$ such that

1. *(charge conservation)* At each vertex $v \in V_T$, $\gamma_v = \sum_{e\in\mathrm{ch}(v)}\gamma_e$ where γ_v is the charge along the edge ending at v and $\mathrm{ch}(v)$ the set of children edges leaving from v;

2. *(attractor flow along edges)* For each edge $e \in E_T$, the map $\pi|_e\colon e \to \Pi$ is an embedding and its image $\pi(e)$ follows the flow lines of $\mathrm{AF}(\gamma_e)$;

3. *(marginal stability at vertices)* At each vertex $v \in V_T$ and for each child edge $e \in \mathrm{ch}(v)$, the phase of the central charge $Z_{\pi(v)}(\gamma_e)$ is equal to that of $Z_{\pi(v)}(\gamma_v)$, and $\Im\big(Z_{\pi(v^+)}(\gamma_e)\overline{Z_{\pi(v^+)}(\gamma_v)}\big)\langle\gamma_e,\gamma_v\rangle > 0$, with v^+ a point infinitesimally close to v along the edge ending at v;

[17] More generally, one could consider the attractor flow along any complex subspace in the space of Bridgeland stability conditions, such as the large volume slice, equipped with a hermitean metric.

4. The leaves of the tree v_i are mapped to the attractor points $z_\star(\gamma_i)$, where γ_i is the charge along the edge ending at v_i.

The tree T is called active if $\bar\Omega_Z(\gamma_e)\neq 0$ along each edge. We denote by $\mathcal{T}_z(\{\gamma_i\})$ the set of attractor flow trees whose root vertex v_0 is mapped to $\pi(v_0)=z\in\Pi$, and whose leaves carry charge γ_i. For fixed charges $\{\gamma_i\}$, this set is obviously finite (most of the time empty).

The Split Attractor Flow Conjecture, originally proposed in [Den00, DGR01] and sharpened in [DM11a], amounts to the statement that for any $z\in\Pi$ and $\gamma\in\Gamma$, there exists only a finite number of decompositions $\gamma=\sum_i\gamma_i$ such that $\mathcal{T}_z(\{\gamma_i\})$ is non-empty; the rational index $\bar\Omega_z(\gamma)$ is then obtained by summing over all attractor flow trees,

$$\bar\Omega_z(\gamma)=\sum_{\gamma=\sum_i\gamma_i}\frac{1}{|\mathrm{Aut}(\{\gamma_i\})|}\sum_{T\in\mathcal{T}_z(\{\gamma_i\})}g_z(T)\prod_i\bar\Omega_\star(\gamma_i) \tag{9.3.21}$$

Here, $|\mathrm{Aut}(\{\gamma_i\})|$ is a symmetry factor, given by the order of the subgroup of permutations of n elements which preserves the ordered list of charges $\{\gamma_i\}$, and the prefactor $g_z(T)$ is obtained recursively by applying the wall-crossing formula at each of the vertices of the tree. In the case of a binary tree, such that each vertex v has two descendants edges $\mathrm{ch}(v)=\{L(v),R(v)\}$ (defined up to exchange), it is simply given by a product over all vertices,

$$g_z(T)=\prod_{v\in V_T}(-1)^{\langle\gamma_{L(v)},\gamma_{R(v)}\rangle+1}|\langle\gamma_{L(v)},\gamma_{R(v)}\rangle| \tag{9.3.22}$$

or in the case of refined invariants,

$$g_z(T,y)=\prod_{v\in V_T}(-1)^{\langle\gamma_{L(v)},\gamma_{R(v)}\rangle+1}\mathrm{sgn}(\langle\gamma_{L(v)},\gamma_{R(v)}\rangle)\,\frac{y^{\langle\gamma_{L(v)},\gamma_{R(v)}\rangle}-y^{-\langle\gamma_{L(v)},\gamma_{R(v)}\rangle}}{y-y^{-1}} \tag{9.3.23}$$

More generally, if the tree has vertices with higher valency, the prefactor $g_z(T)$ is given by the product of the local factors appearing in the formula (9.3.18), evaluated on the charges which descend from the vertex v:

$$g_z(T)=\prod_{v\in V_T}g(\mathrm{ch}(v)) \tag{9.3.24}$$

Alternatively, in cases where the Dirac pairing $\langle-,-\rangle$ is degenerate (as is the case for local CY threefolds) such that there exists a non-zero $\delta\in\Gamma$ with $\langle\delta,-\rangle=0$, one may perturb the charges $\gamma_i\to\gamma_i+\epsilon_i\delta$ where and ϵ_i are small parameters, such that the attractor flow tree is resolved into a union of binary trees, for which (9.3.22) or (9.3.23) can be applied. Such a perturbation is in fact a necessary step when applying the flow tree formula [AP19a, AB21] at each vertex, although it need not extend to a global perturbation of the full set of trees in $\mathcal{T}_z(\{\gamma_i\})$.

It is worth noting that there can be cancellations between different trees with the same embedding. This occurs for example for the Kronecker quiver with κ arrows and dimension vector $(1,n)$ with $n>\kappa$, as noted below (9.3.9), and can be viewed as a consequence of the Pauli exclusion principle for multi-centered black holes [Den02]. A *weak* version of the Split Attractor Flow Conjecture is then that the number of *active* attractor flow trees is finite.

While the formula (9.3.21) is largely a consequence of the wall-crossing formula, the main problem is to ensure that only a finite number of decompositions $\gamma=\sum\gamma_i$ can occur as leaves of

attractor flow trees, and to provide an algorithm for finding them in practice. The fact that the modulus of the central charge $|Z(\gamma_e)|$ decreases along each edge, and is additive at each vertex, implies that the central charges of the constituents are bounded by

$$\sum_i |Z_{z_\star(\gamma_i)}(\gamma_i)| \leq |Z_z(\gamma)| \tag{9.3.25}$$

This constraint was used in [DM11a, §C] to show that, in the context of compact CY threefolds at large radius, the number of attractor flow trees terminating in a fixed compact region of Kähler moduli space is finite. However, this constraint becomes less and less stringent in regions where $|Z_z(\gamma)|$ becomes large (e.g. in the large volume limit), and moot for constituents which are massless at their respective attractor points. As we demonstrate in §9.4.2, the Split Attractor Flow Conjecture (in its strong form) holds for $K_{\mathbb{P}^2}$ along the large volume slice defined by the quadratic central charge (9.1.6). In §9.6.4 we describe how the SAFC along the slice of Π-stability conditions is proven for $K_{\mathbb{P}^2}$ (Theorem 9.1.3).

9.3.5 From scattering sequences to attractor flow trees

The connection between the scattering diagram $\mathcal{D}_\psi(\mathcal{C})$ and the attractor flow is based on the observation that when $Z(\gamma)$ is a holomorphic function on Π, its argument is constant along $\mathrm{AF}(\gamma)$,

$$\frac{\mathrm{d}}{\mathrm{d}\mu} \arg Z(\gamma) = \Im\Big(\frac{\mathrm{d}}{\mathrm{d}\mu} \log Z(\gamma)\Big) = \Im\Big(-\partial_a Z(\gamma) g^{a\bar{b}} \partial_{\bar{b}} \bar{Z}(\gamma)\Big) = 0 \tag{9.3.26}$$

This property holds for any non-compact CY threefold [Den99], and is tied to the fact that the central charge of the D0-brane is independent of Kähler moduli[18]. A second important consequence of the holomorphy of Z is that minima of $|Z(\gamma)|$ can only occur when $Z(\gamma) = 0$ or at the boundary, hence regular attractor points never occur. Since $\bar{\Omega}_z(\gamma) = 0$ at a point z where $Z(\gamma) = 0$ by the support property (9.2.22), the endpoint of the flow must be a singular point in Kähler moduli space, hence belongs to the boundary of the space of stability conditions.

Since the argument of $Z(\gamma)$ is constant along the flow, the flow lines of $\mathrm{AF}(\gamma)$ must lie inside the geometric ray $\mathcal{R}_\psi^{\mathrm{geo}}(\gamma)$, where ψ is fixed in terms of the argument of the central charge at $\mu = 0$. Since the flow is only meaningful when $\bar{\Omega}(\gamma) \neq 0$, and can only split when the central charge of the descendants $Z(\gamma_e), e \in \mathrm{ch}(v)$ become aligned with that of the incoming charge γ_v at every vertex v, the whole attractor flow tree is in fact embedded inside the scattering diagram $\mathcal{D}_\psi(\mathcal{C})$, with each vertex v lying along the intersection of active rays along the wall of marginal stability $\mathcal{W}(\gamma_v, \gamma_e)$.

Specializing further to the case where the slice of Π-stability conditions has complex dimension 1, which is of main interest in this chapter, both the flow lines and the rays have real dimension one, so the intersection $\mathcal{D}_\psi(\mathcal{C}) \cap \Pi$ must in fact coincide with the set of all possible attractor flows carrying central charges of fixed argument $\psi + \frac{\pi}{2}$. Moreover, the complex structure on Π induces an orientation of the plane around each intersection point, such that the orientation of the rays defined locally by (9.3.17) extends to a global orientation, in which incoming and outgoing rays have decreasing and increasing values of $\Im(e^{-\mathrm{i}\psi} Z(\gamma_i)) = |Z(\gamma_i)|$, respectively. For a given charge $\gamma \in \Gamma$ and point $z \in \Pi$, the set of split attractor flows determines all possible scattering sequences, starting from initial rays $\mathcal{R}_\psi(\gamma_i)$ specified by the leaves of the tree and producing an active ray

[18] On a compact CY threefold, the physical central charge involves an extra factor $Z_{D0} = e^{-K} X_0$ equal to the D0-brane central charge, which is not holomorphic and cannot be trivialized by a Kähler transformation.

$\mathcal{R}_\psi(\gamma)$ going through the desired point $z \in \Pi$. In the (admittedly restrictive) context of local CY threefolds with a single Kähler modulus, the Split Attractor Flow Conjecture then amounts to the finiteness of the number of such scattering sequences.

9.4 The large volume scattering diagram

In this section, we determine the scattering diagram $\mathcal{D}^{\rm LV}_\psi$ for the category $\mathcal{C} = D^b(\mathrm{Coh}\, K_{\mathbb{P}^2})$ along the large volume slice $(Z^{\rm LV}_{(s,t)}, \mathcal{A}(s))$ with $(s,t) \in \mathbb{R} \times \mathbb{R}^+$, defined by the quadratic central charge (9.1.6)

$$Z^{\rm LV}_{(s,t)}(\gamma) = -\frac{r}{2}(s+\mathrm{i}t)^2 + d(s+\mathrm{i}t) - \mathrm{ch}_2 \tag{9.4.1}$$

and heart $\mathcal{A}(s) = \mathrm{Coh}^{\sharp s}$ defined in §9.2.4. For brevity we write (9.4.1) as $Z(\gamma)$ in this section. The scattering diagram $\mathcal{D}^{\rm LV}_\psi$ for $\psi = 0$ was analyzed in [Bou19], using adapted coordinates $(x = s, y = -\frac{1}{2}(s^2 - t^2))$ such that the rays $\Re Z(\gamma) = 0$ are straight lines $ry + dx - \mathrm{ch}_2 = 0$ lying above the parabola $y = -\frac{1}{2}x^2$. We shall recast the construction in coordinates (s,t), which have a more transparent relation to the coordinate τ on the physical slice, and generalize it to any phase $\psi \in (-\frac{\pi}{2}, \frac{\pi}{2})$. We shall also describe an algorithm for determining which scattering sequences can contribute to the index $\Omega_{(s,t)}(\gamma)$ for given charge γ and moduli (s,t), and apply it to compute the Gieseker index $\Omega_\infty(\gamma)$ for small Chern vectors. As a consequence of this algorithm, the Split Attractor Flow Conjecture holds along the large volume slice.

9.4.1 Scattering rays and walls of marginal stability

For simplicity we first consider the case $\psi = 0$. Evaluating the real and imaginary parts of (9.4.1),

$$\Re Z(\gamma) = -\frac{1}{2}r(s^2 - t^2) + ds - \mathrm{ch}_2\ , \quad \Im Z(\gamma) = t(d - sr) \tag{9.4.2}$$

we readily see that the geometric rays $\mathcal{R}^{\rm geo}_0(\gamma) = \{(s,t) : \Re(Z(\gamma)) = 0, \Im(Z(\gamma)) > 0\}$ are given as follows:[19]

- $r \neq 0$ and $\Delta > 0$: a branch of hyperbola intersecting the real axis at $s = \mu - \mathrm{sgn}(r)\sqrt{2\Delta}$ (where $Z(\gamma)$ vanishes) and asymptoting to $s = \frac{d}{r} - t\mathrm{sgn}r$ from below;
- $r \neq 0$ and $\Delta = 0$: the half-line $s = \frac{d}{r} - t\mathrm{sgn}r$;
- $r \neq 0$ and $\Delta < 0$: a branch of hyperbola starting at $(s,t) = (\mu, \sqrt{-2\Delta})$ (where $Z(\gamma)$ vanishes) and asymptoting to $s = \frac{d}{r} - t\mathrm{sgn}r$ from above;
- $r = 0$ and $d > 0$: a vertical line at $s = \mathrm{ch}_2/d$;
- $r = 0$ and $d \leq 0$: the geometric ray is empty.

Recall that the slope μ and discriminant Δ were defined in (9.2.4). Moreover, the rays are oriented in the direction of increasing t (or equivalently decreasing rs when $r \neq 0$), such that the modulus of the central charge $|Z(\gamma)| = \Im Z(\gamma)$ increases along the ray.

[19] Note that there are no rays associated to skyscraper sheaves with $r = d = 0$.

On the other hand, the walls of marginal stability $\mathcal{W}(\gamma,\gamma')$ where the phases of $Z(\gamma)$ and $Z(\gamma')$ align (or anti-align) are given by the vanishing of

$$W(\gamma,\gamma') := \frac{\Im(Z(\gamma')\overline{Z}(\gamma))}{t} := \frac{1}{2}(s^2+t^2)(rd'-r'd) - s(r\mathrm{ch}_2' - r'\mathrm{ch}_2) + (d\mathrm{ch}_2' - d'\mathrm{ch}_2) \tag{9.4.3}$$

When $rd'-r'd=0$, $\mathcal{W}(\gamma,\gamma')$ is a vertical line at $s_{\gamma,\gamma'}=\mu=\mu'$, otherwise, it is a semi-circle centered at $(s_{\gamma,\gamma'},0)$ of radius $R_{\gamma,\gamma'}$, with

$$s_{\gamma,\gamma'} := \frac{r\mathrm{ch}_2' - r'\mathrm{ch}_2}{rd'-r'd} = \frac{1}{2}(\mu+\mu') - \frac{\Delta-\Delta'}{\mu-\mu'} \tag{9.4.4}$$

$$R_{\gamma,\gamma'} := \sqrt{s_{\gamma,\gamma'}^2 - 2\frac{d\mathrm{ch}_2' - d'\mathrm{ch}_2}{rd'-r'd}} = \sqrt{(s_{\gamma,\gamma'}-\mu)^2-2\Delta} = \sqrt{(s_{\gamma,\gamma'}-\mu')^2-2\Delta'} \tag{9.4.5}$$

We shall denote this half-circle by $\mathcal{C}(s_{\gamma,\gamma'},R_{\gamma,\gamma'})$. Whenever distinct geometric rays $\mathcal{R}_0^{\mathrm{geo}}(\gamma)$ and $\mathcal{R}_0^{\mathrm{geo}}(\gamma')$ intersect, they do so at the highest point $(s_{\gamma,\gamma'},R_{\gamma,\gamma'})$ along the half-circle $\mathcal{W}(\gamma,\gamma')$, and bound states exist on the side of the wall where t is large, i.e. $(rd'-r'd)W(\gamma,\gamma')>0$. Assuming that $\Delta\geq 0$ and $\Delta'\geq 0$, the intersection is not empty provided $\mu\neq\mu'$ and, depending on the signs of r,r',

$$\begin{cases} i) & r>0, r'<0: & \mu'+\sqrt{2\Delta'} < \mu-\sqrt{2\Delta} \\ ii) & r>0, r'>0 \text{ and } \mu<\mu': & \mu'-\sqrt{2\Delta'} < \mu-\sqrt{2\Delta} \\ iii) & r<0, r'<0 \text{ and } \mu<\mu': & \mu'+\sqrt{2\Delta'} < \mu+\sqrt{2\Delta} \\ iv) & r>0, r'=0: & \frac{\mathrm{ch}_2'}{d'} < \mu-\sqrt{2\Delta} \\ v) & r=0, r'<0: & \mu'+\sqrt{2\Delta'} < \frac{\mathrm{ch}_2}{d} \end{cases} \tag{9.4.6}$$

The remaining cases ($r<0,r'>0$, or $r<0,r'=0$, or $r=0,r'>0$, or $r,r'\gtrless 0$ with $\mu>\mu'$) are given by exchanging γ and γ', while the intersection is evidently empty if $r=r'=0$. The case $i)$ is depicted in Figure 9.14, other cases can be understood similarly. It is interesting to note that whenever the intersection is not empty, one has

$$dd' - r\,\mathrm{ch}_2' - r'\mathrm{ch}_2 \geq 0 \tag{9.4.7}$$

In cases $i)-iii)$, this follows by writing $\mathrm{ch}_2=\frac{r}{2}s(2\mu-s)$, where $s=\mu-\mathrm{sgn}r\sqrt{2\Delta}$ is the point where the ray $\mathcal{R}_0^{\mathrm{geo}}(\gamma)$ crosses the real axis, and similarly for $\mathcal{R}_0^{\mathrm{geo}}(\gamma')$, such that

$$dd' - r\,\mathrm{ch}_2' - r'\mathrm{ch}_2 = \frac{rr'}{2}\left[(\mu-s)^2+(\mu-s')^2-(\mu-\mu)^2\right] \tag{9.4.8}$$

which is manifestly positive. Cases $iv)$ and $v)$ are obvious. If Δ or Δ' is negative, the conditions (9.4.6) for non-empty intersection continue to hold upon setting $\sqrt{2\Delta}\to 0$ or $\sqrt{2\Delta'}\to 0$, but the condition (9.4.7) no longer needs to hold.

The structure of the walls of marginal stability for fixed charge γ was analyzed in [ABCH13, BMW14, Mac14]. The main result is that for $r>0$, there is a finite number of walls, forming two sequences[20] of nested half-circles on either side of a vertical wall at $s=\frac{d}{r}$. For (s,t) outside the largest walls (sometimes called Gieseker walls) the index $\Omega_{(s,t)}(\gamma)$ agrees with the Gieseker index

[20] This duplication is due to our definition of DT invariants, which count semi-stable objects of charge $\epsilon\gamma$ where $\epsilon Z(\gamma)\in\mathbb{H}_B$.

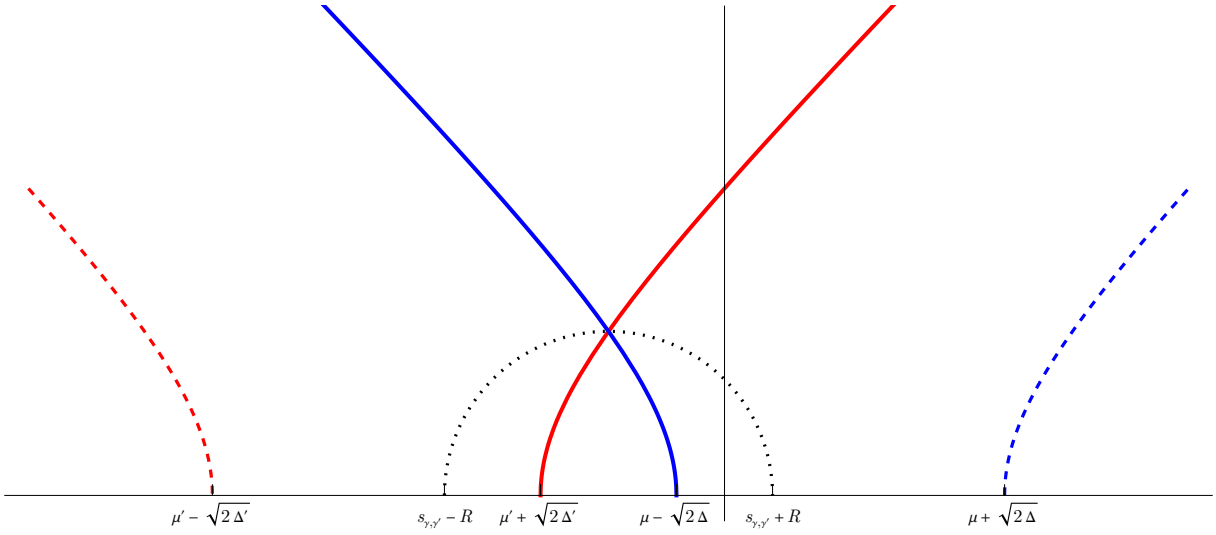

Figure 9.14: Assuming $r > 0, r' < 0, \mu' + \sqrt{2\Delta'} < \mu - \sqrt{2\Delta}$ with $\Delta, \Delta' > 0$, the rays $\mathcal{R}_0^{\rm geo}(\gamma)$ (in blue) and $\mathcal{R}_0^{\rm geo}(\gamma')$ (in red) intersect at the apex of the wall of marginal stability $\mathcal{W}(\gamma, \gamma')$ (in dotted black). The dashed rays corresponding to $\mathcal{R}_0^{\rm geo}(-\gamma)$ and $\mathcal{R}_0^{\rm geo}(-\gamma')$ do not intersect. Outgoing rays, not shown here, are emitted in the forward region between the blue and red lines. For $\psi \neq 0$ with $|\psi| < \frac{\pi}{2}$, the intersection point is displaced by an angle ψ along the dotted circle.

$\Omega_\infty(\gamma)$, justifying the notation. For $r = 0$ and $d \neq 0$, there is a single sequence of nested walls, and $\Omega_{(s,t)}(\gamma)$ similarly agrees with the Gieseker index $\Omega_\infty(\gamma)$ for outside the largest wall. When γ is a multiple of the Chern vector associated to $\mathcal{O}(m)$ for some $m \in \mathbb{Z}$, the chamber structure is actually trivial, with $\Omega_{(s,t)}(\gamma) = \delta_{r,1}$ for any $s < m$ and $t > 0$. As each wall in the nested sequence is crossed, the moduli space $\mathcal{M}_\sigma(\gamma)$ of σ-semistable objects undergoes a birational transformation contracting a particular nef divisor associated to the wall (but keeping the dimension $\dim_{\mathbb{C}} \mathcal{M}_\sigma(\gamma)$ unchanged), until the innermost wall (sometimes known as collapsing wall) is crossed, after which $\mathcal{M}_\sigma(\gamma)$ becomes empty. In particular, the index vanishes at the point $(\mu \pm \sqrt{2\Delta}, 0)$ or $(\mathrm{ch}_2/d, 0)$, respectively, where $Z(\gamma) = 0$, which always lies inside the innermost wall. In the rest of this section, we shall confirm this structure using the scattering diagram. Before doing so, we make a couple of remarks.

- Viewing (s, t) as 'space' and 'time' coordinates in a two-dimensional Minkovski space, one may think of the active ray $\mathcal{R}_0(\gamma) \subset \mathcal{R}_0^{\rm geo}(\gamma)$ as the worldline of a fictitious relativistic particle of mass-squared $m(\gamma)^2 = r^2\Delta = \frac{1}{2}d^2 - r\mathrm{ch}_2$, global charge γ and electric charge $q = r$ and immersed in a constant electric field. Indeed, when $r \neq 0$ the trajectory for such a particle is a branch of hyperbola asymptoting to the light cone $s \simeq t\mathrm{sgn}r$, while it is of course a straight line inside the light-cone when $r = 0$. When two such particles collide, their charges add up and their mass increases by

$$m^2(\gamma + \gamma') - m^2(\gamma) - m^2(\gamma') = dd' - r\,\mathrm{ch}_2' - r'\mathrm{ch}_2 \tag{9.4.9}$$

which is positive when $\Delta, \Delta' \geq 0$ by virtue of (9.4.7). This analogy is not perfect, since the initial position and velocity are fixed by the charge (in particular, the only allowed trajectory for $r = 0$ is a vertical line).

- Two key properties following from this analogy are that the rays remain within the forward lightcone $|\delta s| \leq \delta t$ (the *causality* property), and that the 'electric potential'

$$\varphi_s(\gamma) := 2(d - sr) \tag{9.4.10}$$

can only increase as t increases (for $r = 0$, it remains constant since the ray is vertical). The fact that $\Im Z(\gamma) = t\varphi_s(\gamma)$ increases with t is an obvious consequence of the monotonicity of $|Z(\gamma)|$ along the attractor flow, but the point is that $\Im Z(\gamma)$ increases faster than t. These properties will be instrumental in the next subsection for obtaining bounds on allowed constituents for a given total charge γ.

- In the simplest case of a collision of two incoming rays $\mathcal{R}_0^{\rm eff}(\gamma_1)$ and $\mathcal{R}_0^{\rm eff}(\gamma_2)$ with primitive vectors γ_i, each of them having $\Omega(k\gamma_i) = \delta_{k,1}$, there is an infinite fan of outgoing effective rays of the form $\mathcal{R}_0^{\rm eff}(n_1\gamma_1 + n_2\gamma_2)$, carrying an index $\Omega(n_1\gamma_1 + n_2\gamma_2) = K_\kappa(n_1, n_2)$ given by the DT invariant of a Kronecker quiver with $\kappa = |\langle\gamma_1, \gamma_2\rangle|$ arrows (a multiple of 3 due to (9.2.3)) and dimension vector (n_1, n_2) (see Table 9.2 for a table of some relevant values). More generally, the outgoing rays at each collision are determined from the incoming rays by requiring that the product (9.3.16) of automorphisms $\mathcal{U}(\gamma_i)^{\epsilon_i}$ around the collision point is equal to one, or equivalently by using the flow tree formula of [AP19a, AB21], with the indices associated to incoming rays playing the role of attractor indices.

9.4.2 Initial rays and scattering sequences

The main result of [Bou19] was to identify the initial rays of the scattering diagram $\mathcal{D}_0^{\rm LV}$. Namely, it was shown that the initial rays form two infinite families associated to $\mathcal{O}(m)$ and $\mathcal{O}(m)[1]$, with charge $\gamma_m = [1, m, \frac{1}{2}m^2]$ and $-\gamma_m$ respectively, emitted from the points $(m, 0)$ along the boundary, for any $m \in \mathbb{Z}$. Moreover, the automorphism $\mathcal{U}^{\rm eff}(\gamma)$ on each such ray is specified by

$$\Omega_\star(\pm k\gamma_m) = \delta_{k,1} \ , \quad \bar{\Omega}_\star(\pm k\gamma_m) = \frac{y - y^{-1}}{k(y^k - y^{-k})} \tag{9.4.11}$$

for every $k \geq 1$. The fact that initial rays can only emanate from integer points along the boundary follows by noting that in any triangle bounded by $t < \max(s - m, m + 1 - s)$ in the (s, t) plane, σ-semistable objects must be in the heart of the quiver associated to the tilting sequence $\langle E_1(m-1), E_2(m-1), E_3(m-1)\rangle$ (see (9.1.8)), but such objects necessarily have $\Re Z(\gamma) \neq 0$. The invariance of the initial rays under translations $(s, t) \mapsto (s+1, t)$ is a straightforward consequence of the action of auto-equivalences $E \mapsto E(1)$ on $\mathcal{C}$, while the invariance under $(s, t) \mapsto (-s, t)$ is consistent with the derived duality (9.2.32) in the large volume limit.

Given this simple structure for the initial rays, the consistency requirement (9.3.16) at any intersection determines in principle the automorphism $\mathcal{U}_\sigma^{\rm eff}(\gamma)$ at any point (s_0, t_0) along the geometric ray $\mathcal{R}_0^{\rm geo}(\gamma)$ for any primitive charge vector γ, and therefore the indices $\Omega_{(s,t)}(k\gamma)$ along the same ray. In particular, the invariance of initial rays under translations $(s, t) \mapsto (s+k, t)$ makes it obvious that the resulting indices will be invariant under the action of auto-equivalences $E \mapsto E(k)$,

$$\Omega_{(s,t)}\left([r, d, \chi)\right) = \Omega_{(s+k,t)}\left([r, d + kr, \chi + k(d + \tfrac{3}{2}r) + \tfrac{k^2}{2}r)\right) \ , \quad k \in \mathbb{Z} \tag{9.4.12}$$

while the invariance of initial rays under $(s,t)\mapsto(-s,t)$ implies the symmetry under derived duality

$$\Omega_{(s,t)}([r,d,\chi))=\Omega_{(-s,t)}([-r,d,3d-\chi)) \tag{9.4.13}$$

For $r\neq 0$ and $2d$ divisible by r, this can be combined with (9.4.12) to conclude that $\Omega_{(s,t)}([r,d,\chi))$ is invariant under $s\mapsto\frac{2d}{r}-s$. Similarly, for $r=0$ and 2χ divisible by d one concludes that $\Omega_{(s,t)}([0,d,\chi))$ is invariant under $s\mapsto\frac{2\chi}{d}-3-s$.

In order to compute the indices in practice, the difficulty is to determine which rays, among the infinite set of initial rays associated to $\mathcal{O}(m)$ and $\mathcal{O}(m)[1]$, can produce an outgoing ray with the desired charge γ passing through the desired point (s_0,t_0). The electromagnetic analogy mentioned in the previous subsection gives a way to tackle this apparently formidable problem. Indeed, the problem amounts to determining the set of all possible particles of charge $\gamma_i=k_i\,\mathrm{ch}\,\mathcal{O}(m_i)$ $(i=1,\dots n)$ and anti-particles of charge $\gamma'_j=-k'_j\,\mathrm{ch}\,\mathcal{O}(m'_j)$ $(j=1,\dots n')$, emitted from the boundary $t=0$ at spatial positions $s=m_i$ and $s=m'_j$, respectively, such that their scattering products contains a particle of charge γ going through (s_0,t_0).

A necessary condition is of course that all initial particles lie in the past light-cone of (s_0,t_0) and their global charges add up to the desired charge,

$$s_0-t_0\leq m_i,m'_j\leq s_0+t_0 \tag{9.4.14}$$

$$[r,d,\chi)=\sum_{i=0}^{n-1}k_i\left[1,m_i,1+\frac{m_i(m_i+3)}{2}\right)-\sum_{j=0}^{n'-1}k'_j\left[1,m'_j,1+\frac{m'_j(m'_j+3)}{2}\right) \tag{9.4.15}$$

but there can be cancellations between the charges of $k_i\mathcal{O}(m_i)$ and $k'_j\mathcal{O}(m'_j)[1]$ so these requirements alone do not yet give a finite set of decompositions. One can further reduce the set of possible decompositions to a finite list by exploiting the monotonicity of the 'electric potential' defined in (9.4.10). Indeed, since each of the initial particles and anti-particles is emitted along the 'light-cone' $t=|s-m_i|$ or $t=|s-m'_j|$ at the boundary, the first scattering can only take place after a time $t\geq\frac{1}{2}$, by which time the electric potential $\varphi_s(\gamma_i)$ has increased from 0 to k_i, and similarly for γ'_j. This immediately gives a bound

$$\sum_{i=0}^{n-1}k_i+\sum_{j=0}^{n'-1}k'_j\leq\varphi_{s_0}(\gamma) \tag{9.4.16}$$

In particular, since the multiplicities k_i and k'_j are ≥ 1, the number $n+n'$ of possible constituents is bounded by $\varphi_{s_0}(\gamma)$. Moreover, ordering the slopes m_i,m'_j such that

$$m'_0\leq m'_1\leq\cdots\leq m'_{n'-1}\ ,\quad m_{n-1}\leq\cdots\leq m_1\leq m_0 \tag{9.4.17}$$

with $k_i\leq k_{i-1}$ whenever $m_i=m_{i-1}$, and similarly $k'_j\leq k'_{j-1}$ whenever $m'_j=m'_{j-1}$, it is clear that the scattering between the left-moving particles $k_i\mathcal{O}(m_i)$ and right-moving anti-particles $k'_j\mathcal{O}(m'_j)[1]$ can only take place if $m'_{n'-1}<m_0$ and $m'_0<m_{n-1}$. Denoting by (s_1,t_1) the point where the last scattering takes place, such that $m'_0<s_1<m_0$, the left-most anti-particle must accumulate at least $2s_1-2m'_0-1$ electric potential in going from $m'_0+\frac{1}{2}$ to s_1, while the right-most particle must accumulate at least $2m_0-2s_1-1$ electric potential in going from $m_0-\frac{1}{2}$ to s_1. Thus, the bound (9.4.16) can be strengthened to

$$\sum_{i=0}^{n-1}k_i+\sum_{j=0}^{n'-1}k'_j+2(m_0-m'_0-1)\leq\varphi_{s_0}(\gamma) \tag{9.4.18}$$

This restricts the initial positions m_i, m'_j to a finite interval around s_1 that is typically tighter than the causality bound (9.4.14) for large t. At any rate, the set of allowed initial integer positions m_i, m'_j and multiplicities k_i, k'_j is finite. Thus, the list of possible decompositions having a particle of charge γ at position (s_0, t_0) among all their scattering products is finite, and the SAFC holds along the large volume slice, for trees rooted at a point where $\Re Z(\gamma) = 0$ (we relax this restriction in §9.4.5).

Unfortunately, many of decompositions $\gamma = \sum_{i=1}^{n} \gamma_i + \sum_{=1}^{n'} \gamma'_j$ which satisfy (9.4.15) and (9.4.18) turn out to not include γ among their scattering products, as the worldlines of the constituents may fail to intersect. To determine which of them do, one way is to construct all possible binary trees with constituents of charge γ_i and γ'_j, and retain those that satisfy the conditions (9.4.6) at each vertex. Identifying vertices connected by edges of vanishing length (i.e. mapped to the same point in (s,t) plane), one obtains a set of attractor flow trees associated to the decomposition. The contribution of each attractor flow tree to the total index $\Omega_{(s_0,t_0)}(\gamma)$ can then be computed by applying the (attractor or flow) tree formulae locally at each vertex, as explained in §9.3.4, or more globally by perturbing the charges of the initial constituents $\gamma_i \to \gamma_i + \epsilon_i \delta, \gamma'_j \to \gamma'_j + \epsilon'_j \delta$ where δ is the D0-brane charge vector and ϵ_i, ϵ'_j are small enough and generic.

While the resulting (unperturbed) attractor flow trees typically involve vertices of higher valency and tend to proliferate, it is sufficient to keep track of *scattering sequences*, where descendent edges whose charges are multiples of the same primitive charge γ_e are aggregated together as a single edge of charge $k\gamma_e$. Conversely, the original family of attractor flow trees can be recovered from the aggregated flow trees by replacing each edge of charge $k\gamma_e$ by edges of charge $\{k_1\gamma_e, k_2\gamma_e, \dots\}$ where $\{k_i\}$ runs over all integer partitions of k. We shall make use of this bookkeeping device in the next subsection, in order to keep the list of attractor flow trees (or rather, scattering sequences) within reasonable length.

9.4.3 Examples: Hilbert scheme of n points on $\mathbb{P}^2$

We now apply the procedure outlined above to the case of rank 1 sheaves with Chern vector $\gamma = [1, 0, 1-n)$. At large volume $t \to \infty$, the moduli space $\mathcal{M}_{(s,t)}(\gamma)$ reduces to the Hilbert scheme of n points on $\mathbb{P}^2$, for which the Poincaré polynomials are well-known (seee (9.2.13)). From the analysis in [ABCH13, CH14b], it follows that the chamber structure is given by a set of nested walls, the largest of which being the Gieseker wall corresponding to the destabilizing object $\mathcal{O}(-1)$. From the discussion below (9.4.3), this is the half-circle $\mathcal{C}(-n-\frac{1}{2}, n-\frac{1}{2})$. Thus it suffices to consider all scattering sequences which go through the points $(s,t) = (-n-\frac{1}{2}, n-\frac{1}{2})$, with constituents with slopes in the range $-2n \le m \le -1$, and electric potential bounded by $\varphi_{-n-\frac{1}{2}}(\gamma) = 2n+1$.

We find that for any n, there is indeed a scattering sequence whose first splitting lies on the Gieseker wall $\mathcal{C}(-n-\frac{1}{2}, n-\frac{1}{2})$, namely

$$T_{\text{Gieseker}} = \begin{cases} \{-\mathcal{O}(-2), 2\mathcal{O}(-1)\} & n = 1 \\ \{\{-\mathcal{O}(-n-1), \mathcal{O}(-n)\}, \mathcal{O}(-1)\} & n \ge 2 \end{cases} \tag{9.4.19}$$

For $n = 1$ the scattering sequence is a shorthand for two distinct attractor flow trees with a single splitting into either two or three descendants, namely $\{\gamma_1, 2\gamma_2\}$ and $\{\gamma_1, \gamma_2, \gamma_2\}$ with $\gamma_1 =$

$-\mathcal{O}(-2), \gamma_2 = \mathcal{O}(-1)$. The contributions of the two trees sum up to

$$\frac{1}{2}\kappa(\langle\gamma_1,\gamma_2\rangle)^2\bar{\Omega}(\gamma_1)\bar{\Omega}(\gamma_2)^2 + \kappa(\langle\gamma_1,2\gamma_2\rangle)\bar{\Omega}(\gamma_1)\bar{\Omega}(2\gamma_2) = \frac{1}{2}(y^2+1+y^{-2})^2 - \frac{y^6-y^{-6}}{y-y^{-1}}\frac{y-y^{-1}}{2(y^2-y^{-2})} \tag{9.4.20}$$

reproducing the index $K_3(1,2) = y^2+1+1/y^2$ of a Kronecker quiver with 3 arrows and dimension vector $(1,2)$ (see Table 9.2). For $n=2$, there is a single attractor flow tree with two vertices $\{\{\gamma_1,\gamma_2\},\gamma_3\}$ contributing

$$\kappa(\langle\gamma_1,\gamma_2\rangle)\kappa(\langle\gamma_1+\gamma_2,\gamma_3\rangle) = K_3(1,1)^2 = (y^2+1+1/y^2)^2 \tag{9.4.21}$$

For $n=1$ or $n=2$, there is a single wall of marginal stability associated to either of the two sequences, and the total index agrees with the prediction (9.2.13) for the Gieseker index outside the wall, and vanishes inside. This is consistent with the fact that the moduli space $\mathcal{M}_\infty(\gamma)$ for $n \leq 2$ has a single stratum.

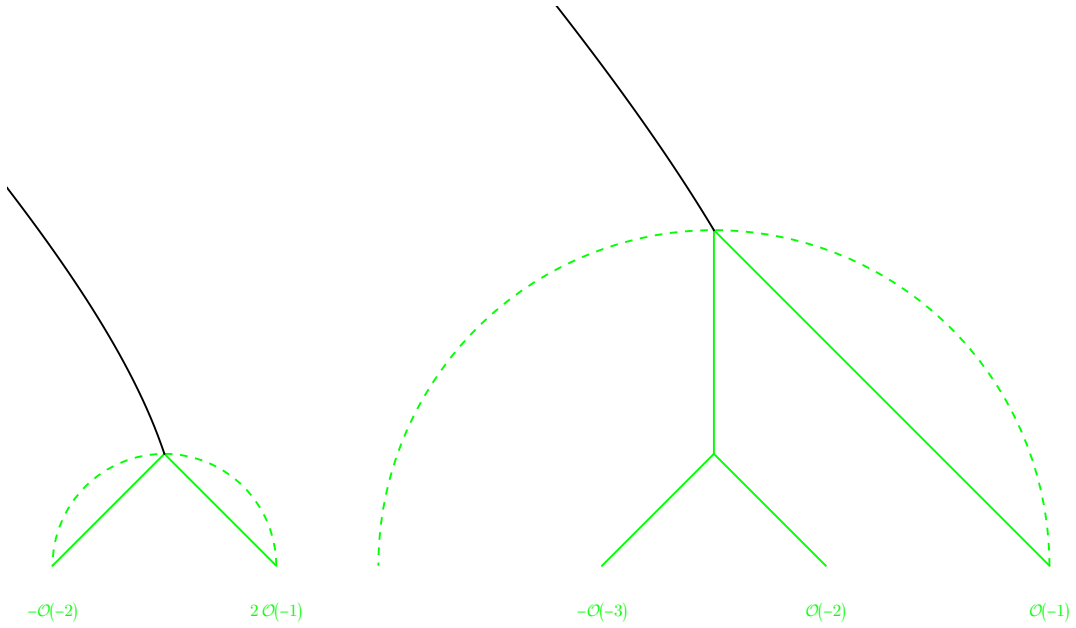

Figure 9.15: Scattering sequences for Hilbert scheme of 1 and 2 points on $\mathbb{P}^2$.

For $n \geq 3$, there are additional walls of the form $\mathcal{C}(s_{\gamma,\gamma'}, R_{\gamma,\gamma'})$, associated to scattering sequences with final vertex of the form $\gamma' + (\gamma-\gamma') \to \gamma$. Below we list the corresponding scattering sequences for $n \leq 7$, along with their respective contribution to the index in the region above the respective wall (for brevity, we only indicate the unrefined limit $y \to 1$, but the full refined index can be obtained from the Kronecker indices in Table 9.2). In all cases, we find agreement with (9.2.13):

- For $n = 3$, there are two nested walls, each of which is associated to one sequence,

$$\begin{array}{lll} \mathcal{C}(-\frac{7}{2}, \frac{5}{2}) & \{\{-\mathcal{O}(-4), \mathcal{O}(-3)\}, \mathcal{O}(-1)\} & K_3(1,1)^2 \\ \mathcal{C}(-\frac{5}{2}, \frac{1}{2}) & \{-2\mathcal{O}(-3), 3\mathcal{O}(-2)\} & K_3(2,3) \end{array}$$

  Again we stress that the scattering sequence $\{-2\mathcal{O}(-3), 3\mathcal{O}(-2)\}$ stands for 6 different attractor flow trees, corresponding to the 2×3 integer partitions of 2 and 3, which all split at the point and add up to the index of a Kronecker quiver with 3 arrows and dimension vector $(2, 3)$. In the Gieseker chamber, the contributions of the two sequences add up to $9 + 13 = 22$ as $y \to 1$.

- For $n = 4$ there are 3 nested walls, and correspondingly 3 sequences,

$$\begin{array}{lll} \mathcal{C}(-\frac{9}{2}, \frac{7}{2}) & \{\{-\mathcal{O}(-5), \mathcal{O}(-4)\}, \mathcal{O}(-1)\} & K_3(1,1)^2 \\ \mathcal{C}(-\frac{7}{2}, \frac{\sqrt{17}}{2}) & \{\{-\mathcal{O}(-4), \mathcal{O}(-3)\}, \{-\mathcal{O}(-3), 2\mathcal{O}(-2)\}\} & K_3(1,1)^2 K_3(1,2) \\ \mathcal{C}(-3, 1) & \{-\mathcal{O}(-4), 2\mathcal{O}(-2)\} & K_6(1,2) \end{array}$$

  In the Gieseker chamber, their contributions add up to $9 + 27 + 15 = 51$ as $y \to 1$.

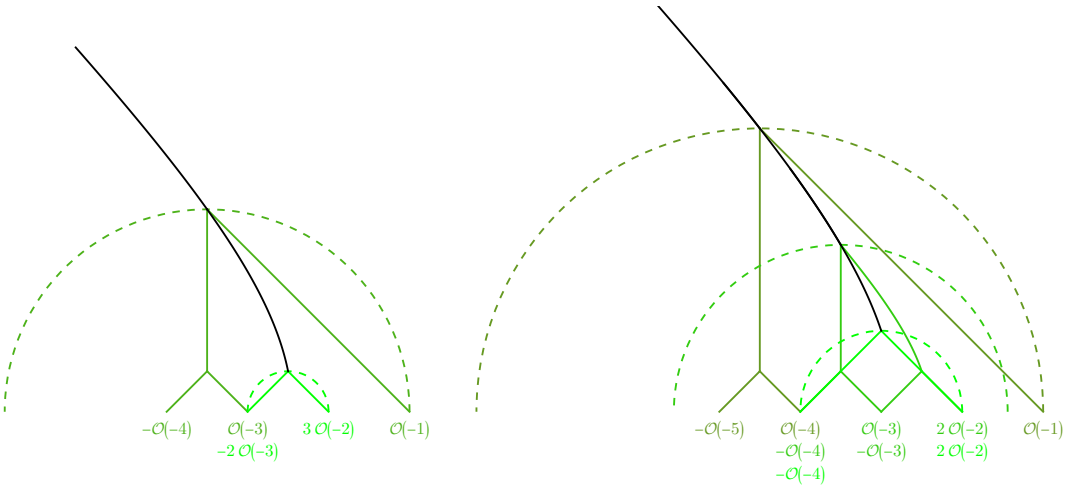

Figure 9.16: Scattering sequences for Hilbert scheme of 3 and 4 points on $\mathbb{P}^2$.

- For $n = 5$ there are 3 nested walls associated to 3 sequences,

$$\begin{array}{lll} \mathcal{C}(-\frac{11}{2}, \frac{9}{2}) & \{\{-\mathcal{O}(-6), \mathcal{O}(-5)\}, \mathcal{O}(-1)\} & K_3(1,1)^2 \\ \mathcal{C}(-\frac{9}{2}, \frac{\sqrt{41}}{2}) & \{\{-\mathcal{O}(-5), \mathcal{O}(-4)\}, \{-\mathcal{O}(-3), 2\mathcal{O}(-2)\}\} & K_3(1,1)^2 K_3(1,2) \\ \mathcal{C}(-\frac{7}{2}, \frac{3}{2}) & \{\{-2\mathcal{O}(-4), 2\mathcal{O}(-3)\}, \mathcal{O}(-2)\} & K_{-3,3,6}(2,2,1) \end{array}$$

  It is worth explaining in some detail the computation of the index associated to the last sequence $\{\{2\gamma_1, 2\gamma_2\}, \gamma_3\}$ with $\gamma_1 = -\mathcal{O}(-4), \gamma_2 = \mathcal{O}(-3), \gamma_3 = \mathcal{O}(-2)$ (which we have denoted

by $K_{a,b,c}(2,2,1)$ with $a=\langle\gamma_1,\gamma_2\rangle$, $b=\langle\gamma_2,\gamma_3\rangle$, $c=\langle\gamma_3,\gamma_1\rangle$). This sequence actually stands for 5 different attractor flow trees, namely

$$\begin{array}{ll} \{\{2\gamma_1,2\gamma_2\},\gamma_3\}, & \{\{\gamma_1,\gamma_1,2\gamma_2\},\gamma_3\}, \\ \{\{2\gamma_1,\gamma_2,\gamma_2\},\gamma_3\}, & \{\{\gamma_1,\gamma_1,\gamma_2,\gamma_2\},\gamma_3\}, \\ & \{\{\gamma_1,\gamma_2\},\{\{\gamma_1,\gamma_2\},\gamma_3\}\} \end{array} \tag{9.4.22}$$

The first four of those combine to produce the rational index $\overline{K}_3(2,2)\to-\frac{21}{4}$ of a Kronecker quiver with 3 arrows and dimension vector $(2,2)$. The fifth involves two copies of the Kronecker quiver with 3 arrows and dimension vector $(1,1)$. The total index is therefore

$$\begin{aligned} K_{-3,3,6}(2,2,1) &= \kappa(\langle 2\gamma_1+2\gamma_2,\gamma_3\rangle)\overline{K}_3(2,2)+\frac{1}{2}\kappa(\langle\gamma_1+\gamma_2,\gamma_3\rangle)^2K_3(1,1)^2 \\ &\to 6\frac{21}{4}+\frac{1}{2}3^2 3^2 = 72 \end{aligned} \tag{9.4.23}$$

Equivalently, this factor arises by applying the flow tree formula to a local scattering diagram with two incoming rays of charge $\alpha=\gamma_1+\gamma_2$ and $\beta=\gamma_3$ with $\Omega^-(\alpha)=K_3(1,2)=y^2+1+1/y^2, \Omega^-(2\alpha)=K_3(2,2)=-y^5-y^3-y-1/y-1/y^3-1/y^5$ and $\Omega^-(\beta)=1$, selecting the outgoing ray of charge $2\alpha+\beta$. In the Gieseker chamber, the contributions of the three sequences add up to $9+27+72=108$ as $y\to1$.

- For $n=6$ there are 5 nested walls associated to 5 sequences,

$\mathcal{C}(-\frac{12}{2},\frac{11}{2})$	$\{\{-\mathcal{O}(-7),\mathcal{O}(-6)\},\mathcal{O}(-1)\}$	$K_3(1,1)^2$
$\mathcal{C}(-\frac{11}{2},\frac{\sqrt{73}}{2})$	$\{\{-\mathcal{O}(-6),\mathcal{O}(-5)\},\{-\mathcal{O}(-3),2\mathcal{O}(-2)\}\}$	$K_3(1,1)^2K_3(1,2)$
$\mathcal{C}(-\frac{9}{2},\frac{\sqrt{33}}{2})$	$\{\{-\mathcal{O}(-5),\mathcal{O}(-4)\},\{\{-\mathcal{O}(-4),\mathcal{O}(-3)\},\mathcal{O}(-2)\}\}$	$K_3(1,1)^4$
$\mathcal{C}(-4,2)$	$\{\{-\mathcal{O}(-5),\mathcal{O}(-3)\},\mathcal{O}(-2)\}$	$K_6(1,1)^2$
$\mathcal{C}(-\frac{7}{2},\frac{1}{2})$	$\{-3\mathcal{O}(-4),4\mathcal{O}(-3)\}$	$K_3(3,4)$

In the Gieseker chamber, their contributions add up to $9+27+81+36+68=221$ as $y\to1$.

- For $n=7$ there are 6 nested walls, but one of them is associated to 2 sequences:

$\mathcal{C}(-\frac{15}{2},\frac{13}{2})$	$\{\{-\mathcal{O}(-8),\mathcal{O}(-7)\},\mathcal{O}(-1)\}$	$K_3(1,1)^2$
$\mathcal{C}(-\frac{13}{2},\frac{\sqrt{113}}{2})$	$\{\{-\mathcal{O}(-7),\mathcal{O}(-6)\},\{-\mathcal{O}(-3),2\mathcal{O}(-2)\}\}$	$K_3(1,1)^2K_3(1,2)$
$\mathcal{C}(-\frac{11}{2},\frac{\sqrt{65}}{2})$	$\{\{-\mathcal{O}(-6),\mathcal{O}(-5)\},\{\{-\mathcal{O}(-4),\mathcal{O}(-3)\},\mathcal{O}(-2)\}\}$	$K_3(1,1)^4$
$\mathcal{C}(-\frac{9}{2},\frac{5}{2})$	$\{\{-2\mathcal{O}(-5),2\mathcal{O}(-4)\},\mathcal{O}(-2)\}$	$K_{-3,6,9}(2,2,1)$
"	$\{\{-\mathcal{O}(-5),\mathcal{O}(-4)\},\{-2\mathcal{O}(-4),3\mathcal{O}(-3)\}\}$	$K_3(1,1)^2K_3(2,3)$
$\mathcal{C}(-4,\sqrt{2})$	$\{\{-\mathcal{O}(-5),\mathcal{O}(-3)\},\{-\mathcal{O}(-4),2\mathcal{O}(-3)\}\}$	$K_3(1,2)K_6(1,1)^2$
$\mathcal{C}(-\frac{39}{10},\frac{11}{10})$	$\{-\mathcal{O}(-5),\{-\mathcal{O}(-4),3\mathcal{O}(-3)\}\}$	$K_3(1,3)K_{15}(1,1)$

The index for the first tree associated to the wall $\mathcal{C}(-\frac{9}{2},\frac{5}{2})$ is computed in the same way as explained around (9.4.23). Note also that the scattering sequence associated to $\mathcal{C}(-4,\sqrt{2})$ is non-planar, as the ray $\mathcal{O}(-3)$ has to cross through $-\mathcal{O}(-4)$ before colliding with $-\mathcal{O}(-5)$. The contributions of the 7 sequences to the Gieseker index add up to $9+27+81+72+117+108+15=429$ as $y\to1$, in agreement with (9.2.13).

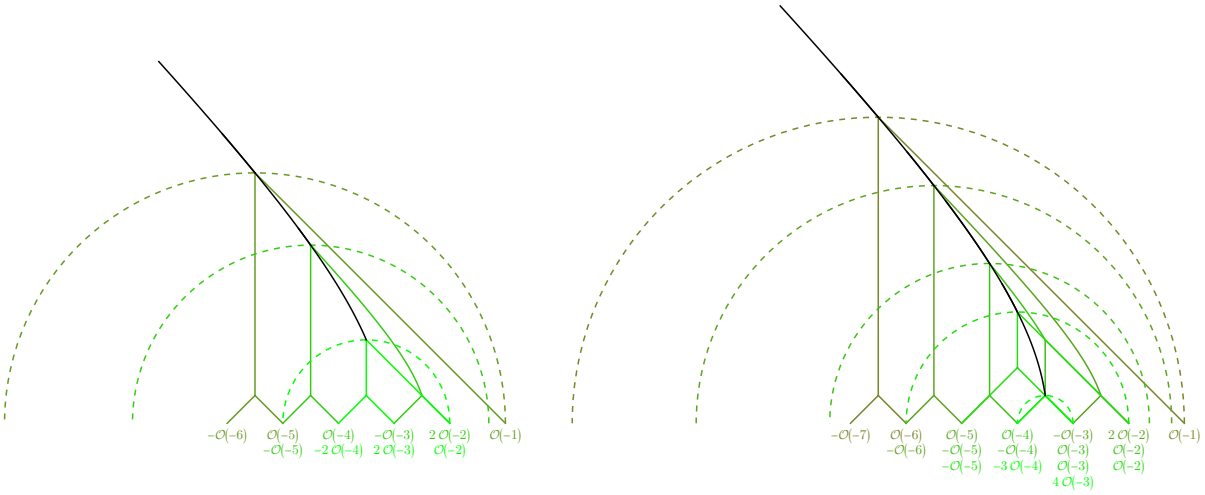

Figure 9.17: Scattering sequences for Hilbert scheme of 5 and 6 points on $\mathbb{P}^2$.

9.4.4 Examples: D2-D0 indices

We now turn to the case of rank 0 sheaves with Chern vector $\gamma = [0, d, \chi)$ with $d > 0$. At large volume $t \to \infty$, the index $\Omega_{(s,t)}(\gamma)$ is determined in terms of refined Gopakumar-Vafa invariants via (9.2.15), in particular it is independent of χ. This is in general no longer true for finite t, due to the existence of a sequence of nested walls of marginal stability. The outermost wall (or Gieseker wall) is determined as follows [Woo13, Proposition 7.5]. Let η be an integer in the range $-\frac{d}{2} \le \eta \le \frac{d}{2}$ such that $\chi + \frac{1}{2}d(d-3) = kd + \eta$ with $k \in \mathbb{Z}$. Then the Gieseker wall is the half-circle $\mathcal{C}(s_0, R_0)$ of radius $R_0 = \frac{d}{2} - \frac{|\eta|}{d}$ centered at $s_0 = \frac{\chi}{d} - \frac{3}{2} = k + \frac{\eta}{d} - \frac{d}{2}$. When $\eta \ge 0$, the destabilizing sub-object along the wall is $\mathcal{O}(k)$, whereas for $\eta \le 0$ it is the ideal sheaf $\mathcal{I}_{Z(-\eta)}(k)$ where $Z(w)$ is a scheme of dimension 0 and length w. For $\eta = 0$, these two notions agree, while for $|\eta| = \frac{d}{2}$ they do not, but destabilizing subobjects of both types may occur. It follows that all constituents of the trees contributing to $\Omega_\infty(\gamma)$ must be emitted in an interval of width $\frac{d}{2} - \frac{|\eta|}{d}$ centered around s_0, and electric potential bounded by $\varphi_{s_0}(\gamma) = 2d$.

We shall now discuss examples with low degree d, making use of the symmetry properties (9.4.12) and (9.4.13) to restrict the values of χ. In all cases, the wall structure matches with [BMW14] and the index outside the Gieseker wall agrees with the GV invariants in (9.2.16). The trees arising at each wall also agree with the stratification in [DM11b, Mai11, Mai13], with one exception for $(d, \chi) = (5, 3)$ mentioned below.

- For $(d, \chi) = (1, 1)$, such that $(k, \eta) = (0, 0)$, there is only one wall,

$$\chi = 1: \qquad \mathcal{C}(-\tfrac{1}{2}, \tfrac{1}{2}) \qquad \{-\mathcal{O}(-1), \mathcal{O}\} \qquad K_3(1,1)$$

  The tree corresponds to the fact that the structure sheaf of a curve $\mathcal{O}_C$ is given by the short exact sequence $0 \to \mathcal{O}(-1) \to \mathcal{O}_C \to \mathcal{O} \to 0$, and its index $K_3(1,1) = y^2 + 1 + 1/y^2$ reproduces the Poincaré polynomial of the linear system $[C] = \mathbb{P}^2$.

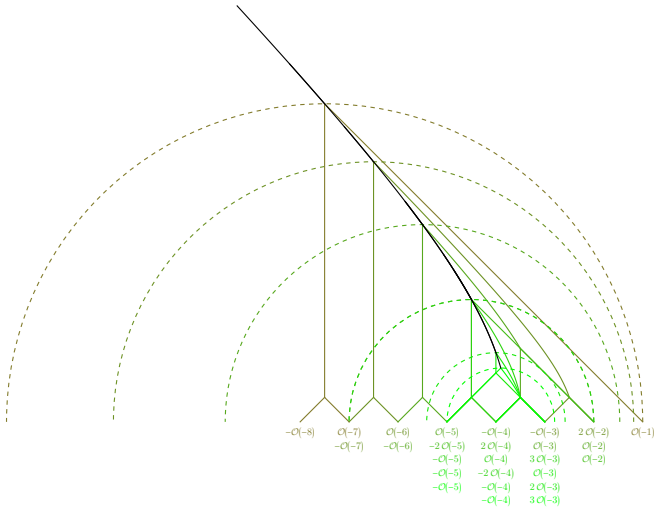

Figure 9.18: Scattering sequences for Hilbert scheme of 7 points on $\mathbb{P}^2$.

- For $(d,\chi) = (2,0),(2,1)$, such that $(k,\eta) = (0,-1),(0,0)$, respectively, there is a single wall

$$\begin{array}{lllll} \chi = 0: & & \mathcal{C}(-\frac{3}{2},\frac{1}{2}) & \{-2\mathcal{O}(-2), 2\mathcal{O}(-1)\} & K_3(2,2) \\ \chi = 1: & & \mathcal{C}(-1,1) & \{-\mathcal{O}(-2), \mathcal{O}\} & K_3(1,2) \end{array}$$

  giving the same index $-y^5 - y^3 - y - \dots$ in the Gieseker chamber in either case.

- For $(d,\chi) = (3,0),(3,1)$, such that $(k,\eta) = (0,0),(0,1)$, respectively, there are two walls in the first case, and a single wall in the second case,

$$\begin{array}{lllll} \chi = 0: & & \mathcal{C}(-\frac{3}{2},\frac{3}{2}) & \{-\mathcal{O}(-3), \mathcal{O}(0)\} & K_9(1,1) \\ \text{"} & & \mathcal{C}(-\frac{3}{2},\frac{1}{2}) & \{-3\mathcal{O}(-2), 3\mathcal{O}(-1)\} & K_3(3,3) \\ \chi = 1: & & \mathcal{C}(-\frac{7}{6},\frac{7}{6}) & \{\{-2\mathcal{O}(-2), \mathcal{O}(-1)\}, \mathcal{O}\} & K_3(1,2)K_9(1,1) \end{array}$$

  contributing $27 = 18 + 9$ as $y \to 1$ in the Gieseker chamber in either case.

- For $(d,\chi) = (4,0),(4,1),(4,2)$, such that $(k,\eta) = (0,2),(1,-1),(1,0)$, respectively, there are two walls in the first case, and three in the third case,

$$\begin{array}{lllll} \chi = 0: & & \mathcal{C}(-\frac{3}{2},\frac{3}{2}) & \{-\mathcal{O}(-3), \{\{-\mathcal{O}(-2), \mathcal{O}(-1)\}, \mathcal{O}\}\} & K_3(1,1)^2 K_{12}(1,1) \\ \text{"} & & \mathcal{C}(-\frac{3}{2},\frac{1}{2}) & \{-4\mathcal{O}(-2), 4\mathcal{O}(-1)\} & K_3(4,4) \\ \chi = 1: & & \mathcal{C}(-\frac{5}{4},\frac{7}{4}) & \{-\mathcal{O}(-3), \{-\mathcal{O}(-1), 2\mathcal{O}\}\} & K_3(1,2)K_{12}(1,1) \\ \text{"} & & \mathcal{C}(-\frac{5}{4},\frac{5}{4}) & \{\{-3\mathcal{O}(-2), 2\mathcal{O}(-1)\}, \mathcal{O}\} & K_3(2,3)K_{12}(1,1) \\ \chi = 2: & & \mathcal{C}(-1,2) & \{-\mathcal{O}(-3), \mathcal{O}(1)\} & K_{12}(1,1) \\ \text{"} & & \mathcal{C}(-1,\sqrt{2}) & \{\{-2\mathcal{O}(-2), \mathcal{O}(-1)\}, \{-\mathcal{O}(-1), 2\mathcal{O}\}\} & K_3(1,2)^2 K_{12}(1,1) \\ \text{"} & & \mathcal{C}(-1,1) & \{-2\mathcal{O}(-2), 2\mathcal{O}\} & K_6(2,2) \end{array}$$

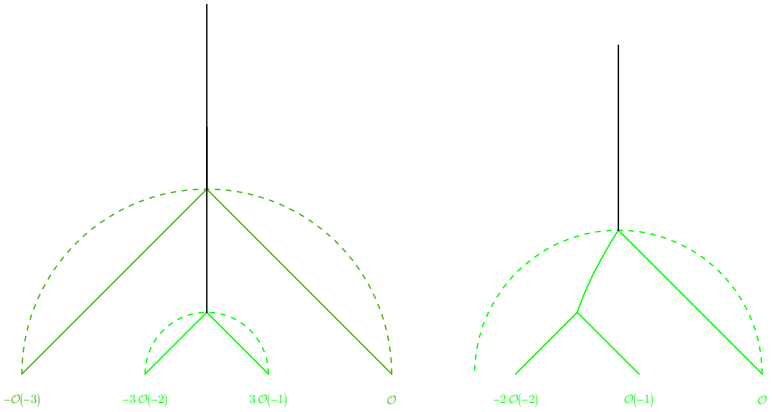

Figure 9.19: Scattering sequences for $(d, \chi) = (3, 0), (3, 1)$.

contributing $-108 - 84 = -36 - 156 = -108 - 72 - 12 = -192$ in the Gieseker chamber in each case. Note that for $\chi = 0$, the first wall involves three charges $-\mathcal{O}(-3), -\mathcal{O}(-2) + \mathcal{O}(-1)$ and $\mathcal{O}$ colliding at the same point, which can be resolved into two successive collisions by perturbing the incoming rays. For each value of χ, the sequences match with the stratification in [DM11b].

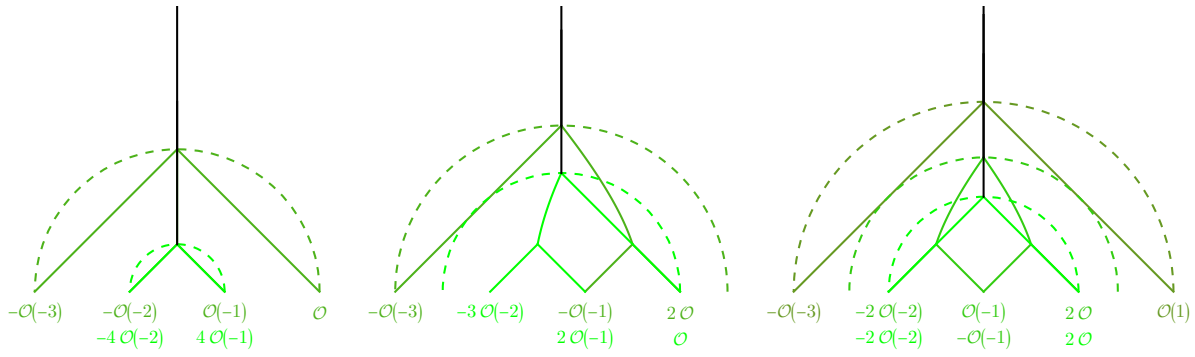

Figure 9.20: Scattering sequences for $(d, \chi) = (4, 0), (4, 1), (4, 2)$.

- For $(d,\chi) = (5,0),(5,1),(5,3)$, such that $(k,\eta) = (1,0),(1,1),(2,-2)$, we find

$\chi = 0$	$\mathcal{C}(-\frac{3}{2},\frac{5}{2})$	$\{-\mathcal{O}(-4),\mathcal{O}(1)\}$	$K_{15}(1,1)$
"	$\mathcal{C}(-\frac{3}{2},\frac{\sqrt{17}}{2})$	$\{\{-2\mathcal{O}(-3),\mathcal{O}(-2)\},\{-\mathcal{O}(-1),2\mathcal{O}\}\}$	$K_3(1,2)^2K_{15}(1,1)$
"	$\mathcal{C}(-\frac{3}{2},\frac{3}{2})$	$\{-\mathcal{O}(-3),\{\{-2\mathcal{O}(-2),2\mathcal{O}(-1)\},\mathcal{O}\}\}$	$K_{15}(1,1)K_{-3,3,6}(2,2,1)$
	$\mathcal{C}(-\frac{3}{2},\frac{1}{2})$	$\{-5\mathcal{O}(-2),5\mathcal{O}(-1)\}$	$K_3(5,5)$
$\chi = 1$	$\mathcal{C}(-\frac{13}{10},\frac{23}{10})$	$\{\{-2\mathcal{O}(-3),\mathcal{O}(-2)\},\mathcal{O}(1)\}$	$K_3(1,2)K_{15}(1,1)$
"	$\mathcal{C}(-\frac{13}{10},\frac{\sqrt{329}}{10})$	$\{\{-\mathcal{O}(-3),\{-\mathcal{O}(-2),\mathcal{O}(-1)\}\},\{-\mathcal{O}(-1),2\mathcal{O}\}\}$	$K_3(1,1)^2K_3(1,2)K_{15}(1,1)$
"	$\mathcal{C}(-\frac{13}{10},\frac{17}{10})$	$\{-\mathcal{O}(-3),\{-\mathcal{O}(-2),2\mathcal{O}\}\}$	$K_6(1,2)K_{15}(1,1)$
	$\mathcal{C}(-\frac{13}{10},\frac{13}{10})$	$\{\{-4\mathcal{O}(-2),3\mathcal{O}(-1)\},\mathcal{O}\}$	$K_3(3,4)K_{15}(1,1)$
$\chi = 3$	$\mathcal{C}(-\frac{9}{10},\frac{21}{10})$	$\{-\mathcal{O}(-3),\{\{-\mathcal{O}(-1),\mathcal{O}\},\mathcal{O}(1)\}\}$	$K_3(1,1)^2K_{15}(1,1)$
"	$\mathcal{C}(-\frac{9}{10},\frac{19}{10})$	$\{\{-3\mathcal{O}(-2),2\mathcal{O}(-1)\},\mathcal{O}(1)\}$	$K_3(2,3)K_{15}(1,1)$
"	$\mathcal{C}(-\frac{9}{10},\frac{\sqrt{241}}{10})$	$\{\{-2\mathcal{O}(-2),\mathcal{O}(-1)\},\{-2\mathcal{O}(-1),3\mathcal{O}\}\}$	$K_3(1,2)K_3(2,3)K_{15}(1,1)$
"	$\mathcal{C}(-\frac{9}{10},\frac{\sqrt{161}}{10})$	$\{\{-2\mathcal{O}(-2),\mathcal{O}\},\{-\mathcal{O}(-1),2\mathcal{O}\}\}$	$K_3(1,2)K_6(1,2)K_{15}(1,1)$
"	$\mathcal{C}(-\frac{9}{10},\frac{11}{10})$	$\{-2\mathcal{O}(-2),\{-\mathcal{O}(-1),3\mathcal{O}\}\}$	$K_3(1,3)K_{15}(1,2)$

contributing $15+135+1080+465 = 45+405+225+1020 = 135+195+585+675+105 = 1695$ in the Gieseker chamber. For $\chi = 0$, the third wall involves three charges $-\mathcal{O}(-3), -2\mathcal{O}(-2)+2\mathcal{O}(-1)$ and $\mathcal{O}$ colliding at the same point; it can be treated by perturbing in the same way as for $(d,\chi) = (4,0)$ and using the same reasoning as explained below (9.4.23). Note that the fourth sequence for $\chi = 3$ is non-planar, and corresponds to a codimension one stratum, which appears to be missing in [Mai11].

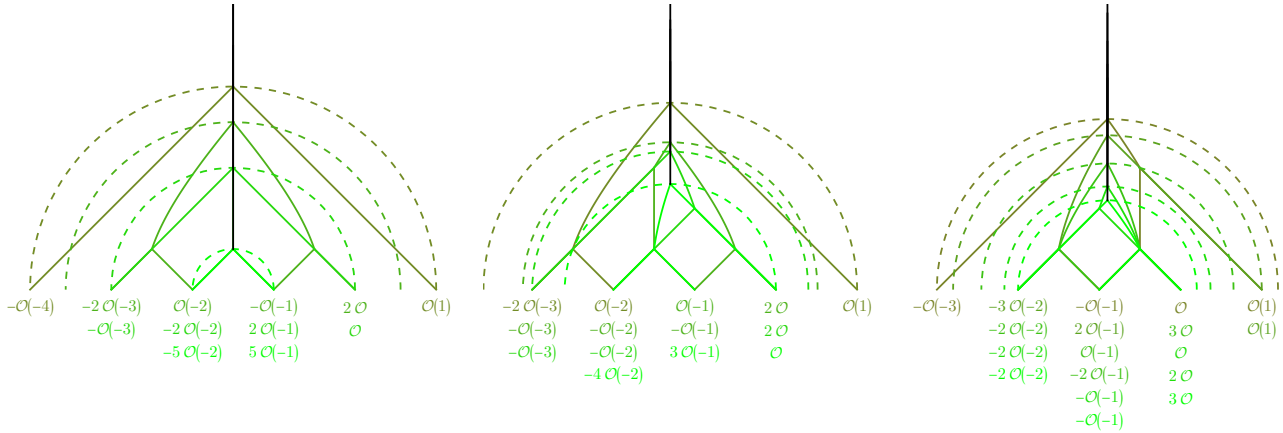

Figure 9.21: Scattering sequences for $(d,\chi) = (5,0),(5,1),(5,3)$

- For $(d,\chi)=(6,1)$, corresponding to $(k,\eta)=(2,-2)$,

$\mathcal{C}(-\frac{4}{3},\frac{8}{3})$	$\{-\mathcal{O}(-4),\{\{-\mathcal{O}(-1),\mathcal{O}\},\mathcal{O}(1)\}\}$	$K_3(1,1)^2K_{18}(1,1)$
$\mathcal{C}(-\frac{4}{3},\frac{7}{3})$	$\{\{\{-2\mathcal{O}(-3),\mathcal{O}(-2)\},\{-\mathcal{O}(-2),\mathcal{O}(-1)\}\},\mathcal{O}(1)\}$	$K_3(1,1)^2K_3(1,2)K_{18}(1,1)$
	$\{\{-2\mathcal{O}(-3),\mathcal{O}(-1)\},\mathcal{O}(1)\}$	$K_6(1,2)K_{18}(1,1)$
$\mathcal{C}(-\frac{4}{3},\frac{\sqrt{46}}{3})$	$\{\{-2\mathcal{O}(-3),\mathcal{O}(-2)\},\{-2\mathcal{O}(-1),3\mathcal{O}\}\}$	$K_3(1,2)K_3(2,3)K_{18}(1,1)$
$\mathcal{C}(-\frac{4}{3},\frac{\sqrt{31}}{3})$	$\{\{-\mathcal{O}(-3),\{-2\mathcal{O}(-2),2\mathcal{O}(-1)\}\},\{-\mathcal{O}(-1),2\mathcal{O}\}\}$	$K_{-3,6,3}(2,2,1)K_3(1,2)K_{18}(1,1)$
$\mathcal{C}(-\frac{4}{3},\frac{2\sqrt{7}}{3})$	$\{\{-\mathcal{O}(-3),\{-\mathcal{O}(-2),\mathcal{O}(-1)\}\},\{-\mathcal{O}(-2),2\mathcal{O}\}\}$	$K_3(1,1)^2K_6(1,2)K_{18}(1,1)$
$\mathcal{C}(-\frac{4}{3},\frac{5}{3})$	$\{-\mathcal{O}(-3),\{\{-2\mathcal{O}(-2),\mathcal{O}(-1)\},2\mathcal{O}\}\}$	$K_3(1,2)K_9(1,2)K_{18}(1,1)$
$\mathcal{C}(-\frac{4}{3},\frac{4}{3})$	$\{\{-5\mathcal{O}(-2),4\mathcal{O}(-1)\},\mathcal{O}\}$	$K_3(4,5)K_{18}(1,1)$

contributing $-162-270-486-702-2430-2430-1944-7182=-17064$ in the Gieseker chamber (here the factor $K_{-3,6,3}(2,2,1)$ in the fourth sequence can be computed as explained below (9.4.23), and still evaluates to 72). Note that the sequence associated to $\mathcal{C}(-\frac{4}{3},\frac{2\sqrt{7}}{3})$ is non-planar. We refrain from considering other values of χ in this case.

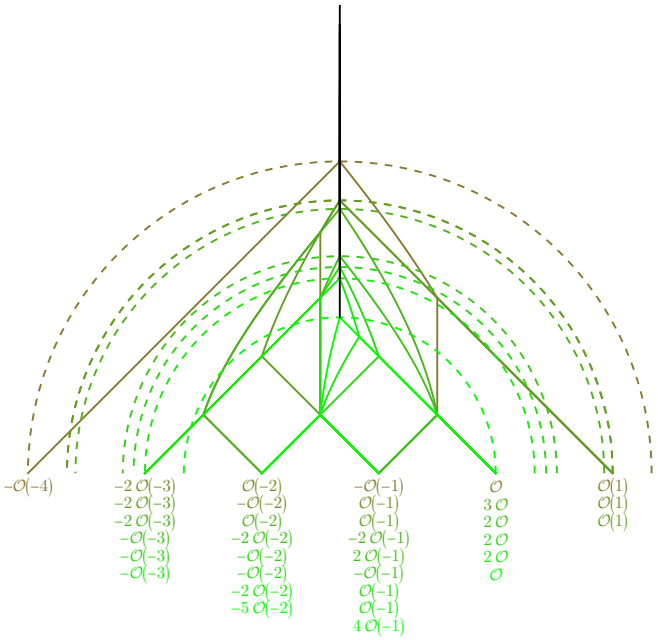

Figure 9.22: Scattering sequences for $(d,\chi)=(6,1)$

9.4.5 Generalization to $\psi\neq 0$

We now discuss how this picture generalizes to an arbitrary phase $\psi\in(-\frac{\pi}{2},\frac{\pi}{2})$. For $r\neq 0$, the geometric ray $\mathcal{R}_\psi^{\mathrm{geo}}(\gamma)$ is now a branch of hyperbola (degenerating to a straight line for vanishing

discriminant $\Delta = 0$)

$$s = \tfrac{d}{r} - t\tan\psi - \frac{\mathrm{sgn} r}{\cos\psi}\sqrt{t^2 + 2\Delta\cos^2\psi} \tag{9.4.24}$$

with $t > 0$, while for $r = 0$, it is the line $s = \frac{\mathrm{ch}_2}{d} - t\tan\psi$ when $d > 0$ (or the empty set when $d \leq 0$). In particular, the electromagnetic analogy of §9.4.1 breaks down for $\psi \neq 0$, since one of the two rays emanating from $s = m$ is no longer inside the light-cone (indeed, the angle between the two rays remains equal to $\frac{\pi}{2}$ independently of ψ).

Moreover, under the same conditions (9.4.6) two rays $\mathcal{R}^{\mathrm{geo}}_{\psi}(\gamma)$ and $\mathcal{R}^{\mathrm{geo}}_{\psi}(\gamma')$ still intersect on the same wall $\mathcal{W}(\gamma,\gamma')$, but at the point $(s_{\gamma,\gamma'} - R_{\gamma,\gamma'}\sin\psi, R_{\gamma,\gamma'}\cos\psi)$ at an angle ψ from the top of the half-circle $\mathcal{C}(s_{\gamma,\gamma'}, R_{\gamma,\gamma'})$. In fact, observing that

$$\Re\left(e^{-\mathrm{i}\psi} Z^{\mathrm{LV}}_{(s,t)}(\gamma)\right) = \cos\psi\,\Re\left(Z^{\mathrm{LV}}_{(s_\psi,t_\psi)}(\gamma)\right) \tag{9.4.25}$$

where (s_ψ, t_ψ) are related to (s,t) through

$$s_\psi = s + t\tan\psi, \quad t_\psi = \frac{t}{\cos\psi} \tag{9.4.26}$$

we see that the loci $\Re\left(e^{-\mathrm{i}\psi}Z(\gamma)\right) = 0$ in the (s,t) upper half-plane are mapped to the loci $\Re(Z(\gamma)) = 0$ in the (s_ψ, t_ψ) upper half-plane. The relation for the imaginary parts is however more complicated,

$$\Im\big(e^{-\mathrm{i}\psi} Z^{\mathrm{LV}}_{(s,t)}(\gamma)\big) = \Im\big(Z^{\mathrm{LV}}_{(s_\psi,t_\psi)}(\gamma)\big) - \sin\psi\,\Re\big(Z^{\mathrm{LV}}_{(s_\psi,t_\psi)}(\gamma)\big) + r(\sin\psi)t_\psi^2 \tag{9.4.27}$$

In particular, the transformation $e^{-\mathrm{i}\psi} Z^{\mathrm{LV}}_{(s,t)}(\gamma) \to Z^{\mathrm{LV}}_{(s_\psi,t_\psi)}(\gamma)$ is *not* a $\widetilde{GL^+}(2,\mathbb{R})$ transformation, due to the last term in (9.4.27). Rather, one should view (s_ψ, t_ψ) as variants of the affine coordinates (x,y) defined in (9.1.10), indeed $(x,y) = (s_\psi, \frac{1}{2}(t_\psi^2 - s_\psi^2))$.

Thus, we conclude that whenever $\psi \in (-\frac{\pi}{2}, \frac{\pi}{2})$, the scattering diagram $\mathcal{D}^{\mathrm{LV}}_{\psi}$ in the (s,t) upper half-plane coincides with the scattering diagram $\mathcal{D}^{\mathrm{LV}}_{0}$ in the (s_ψ, t_ψ) upper half-plane, and both have the same image in the (x,y) plane. Thus, the SAFC holds on the large volume slice, as long as $\cos\psi \neq 0$. For $\psi = \pm\frac{\pi}{2}$, the scattering diagram $\mathcal{D}^{\mathrm{LV}}_{\psi}$ becomes degenerate, as all loci $\Im Z(\gamma) = 0$ become either vertical lines $s = d/r$ for $r \neq 0$ or the horizontal line $t = 0$ on the boundary. As we shall see in §9.6, the scattering diagram $\mathcal{D}^{\Pi}_{\psi}$ along the slice of Π-stability conditions is better behaved in this limit.

9.5 The orbifold scattering diagram

In this section, we construct the scattering diagram $\mathcal{D}_Q$ for the orbifold quiver shown in Figure 9.4, following the general construction of §9.3.1. In §9.5.2, we identify the initial rays, giving a rigorous proof of the Attractor Conjecture for this case (Theorem 9.1.1 in the introduction). In §9.5.3, we restrict $\mathcal{D}_Q$ to a two-dimensional slice $\mathcal{D}_o$, which we shall identify later in §9.6.3 with a subset of the exact scattering diagram $\mathcal{D}^{\Pi}_{\psi}$. In §9.5.4 we illustrate the use of the diagram $\mathcal{D}_o$ for computing the index for small dimension vectors.

9.5.1 Quiver descriptions

As explained for example in [MP20, §4.2], any tilting sequence $\mathcal{S} = (E_1, E_2, E_3)$ in the derived category $\mathcal{C} = D^b\,\mathrm{Coh}(K_{\mathbb{P}^2})$ (in the sense that $\mathcal{S}$ generates $\mathcal{C}$ and $\mathrm{Ext}^k(E_i, E_j) = 0$ for $k \neq 0$ and all

$i,j)$ provides an isomorphism $\mathcal{C} \sim D^b(\mathrm{Rep}\, J(Q,W))$ with the derived category of representations of the Jacobian algebra $J(Q,W)$ of a certain quiver with potential (Q,W) associated to $\mathcal{S}$. A tilting sequence can be obtained from any strong exceptional collection (F_1,F_2,F_3) on $\mathbb{P}^2$ by setting $\mathcal{S} = (i_*(F_1[1]), i_*(F_2), i_*(F_3)[-1])$. Starting from the strong exceptional collection $(\mathcal{O}(-1),\Omega(1),\mathcal{O})$, one arrives at the tilting sequence in (9.1.8), associated to the quiver with potential depicted in Figure 9.4. All other strong exceptional collections are obtained by successive mutations of $(\mathcal{O}(-1),\Omega(1),\Omega)$, and similarly lead to 3-node quivers $(Q_{a,b,c}, W_{a,b,c})$ with a arrows from node 1 to node 2, b arrows from 2 to 3 and c arrows from 3 to 1, with (a,b,c) any set of positive integers satisfying the Markov condition $a^2+b^2+c^2 = abc$.

While the isomorphism $\mathcal{C} \simeq D^b(\mathrm{Rep}\, J(Q,W))$ holds for any choice of tilting sequence $\mathcal{S} = (E_1,E_2,E_3)$, the heart $\mathcal{A}_\sigma$ only coincides (up to the action of $\widetilde{GL^+}(2,\mathbb{R})$) with the Abelian category $\mathrm{Rep}\, J(Q,W)$ of representations of $J(Q,W)$ in a region $\mathbb{H}_{\mathcal{S}}$ of $\mathrm{Stab}\,\mathcal{C}$ where the objects E_i are stable and the phases of their central charges $Z(E_i)$ lie in a common half-space (see for example Lemma 3.16 in [Mac07]). In that case, the moduli space of σ-semistable objects E of Chern vector γ in $\mathcal{C}$ coincides with the moduli space of semi-stable representations of $J(Q,W)$, with dimension vector (n_1,n_2,n_3) and King parameters $(\theta_1,\theta_2,\theta_3)$ determined by

$$\gamma = \sum_{i=1}^{3} n_i \,\mathrm{ch}\, E_i \ , \quad \theta_i = \lambda\, \Re[e^{-\mathrm{i}\psi} Z(E_i)] \tag{9.5.1}$$

with $\psi = \arg Z(E) - \frac{\pi}{2}$ such that $n_1\theta_1 + n_2\theta_2 + n_3\theta_3 = 0$, and λ is an arbitrary non-negative factor. At the boundary of the region $\mathbb{H}_{\mathcal{S}}$, one of the objects E_i exits from the common half-space and one apply a left or right mutation so as to obtain a new quiver description.

Let us consider the exceptional collection in (9.1.8), corresponding to the fractional branes on the orbifold $\mathbb{C}^3/\mathbb{Z}_3$:

$$E_1 = i_*(\mathcal{O})[-1], \quad E_2 = i_*(\Omega(1)), \quad E_3 = i_*(\mathcal{O}(-1))[1] \tag{9.5.2}$$

with charges $\gamma_i = \mathrm{ch}\, E_i$ given by

$$\gamma_1 = [-1,0,0], \quad \gamma_2 = [2,-1,-\frac{1}{2}], \quad \gamma_3 = [-1,1,-\frac{1}{2}] \tag{9.5.3}$$

The corresponding quiver, shown in Figure 9.4, has 3 arrows $E_i \to E_{i-1}$ for each i modulo 3, consistently with $\langle \gamma_i, \gamma_{i-1}\rangle = -3$. Using the Eichler integral representation (9.1.5), it is easy to check that the central charges of the simple objects coincide at the orbifold point τ_o, namely $Z_{\tau_o}(\gamma_i) = 1/3$. Thus, this quiver description will be appropriate[21] in a region $\mathbb{H}^o$ around τ_o in the physical slice Π, which we identify in §9.6.3. The dimension vector associated to an object of charge $\gamma = [r,d,\mathrm{ch}_2]$ is given by

$$(n_1,n_2,n_3) = \left(-\frac{3}{2}d - \mathrm{ch}_2 - r, -\frac{1}{2}d - \mathrm{ch}_2, \frac{1}{2}d - \mathrm{ch}_2\right) = (-\chi, r+d-\chi, r+2d-\chi) \tag{9.5.4}$$

or conversely

$$r = 2n_2 - n_1 - n_3, \quad d = n_3 - n_2, \quad \mathrm{ch}_2 = -\frac{1}{2}(n_2+n_3) \tag{9.5.5}$$

[21] Note that the objects E_i are not stable at $\tau = \tau_o$ strictly, since their central charge is not in the half-plane $\mathbb{H}_B$; the objects $E_i[1]$ are stable, and lead to the same quiver but opposite dimension vector.

Abusing notation once again, we shall write $\gamma = (n_1, n_2, n_3)$, using round brackets on both sides to distinguish it from the other notations $\gamma = [r, d, \mathrm{ch}_2] = [r, d, \chi)$.

A similar quiver description holds true around any image of τ_o under an element $g \in \Gamma_1(3)$, with the tilting sequence being replaced by its image $(g(E_1), g(E_2), g(E_3))$. In particular, around $\tau = \tau_o + k$, the tilting sequence (9.1.8) is shifted to

$$E_1(k) = i_*(\mathcal{O}(k))[-1], \quad E_2(k) = i_*(\Omega(k+1)), \quad E_3(k) = i_*(\mathcal{O}(k-1))[1] \tag{9.5.6}$$

with Chern vectors $\gamma_1(k), \gamma_2(k), \gamma_3(k)$. The relevant dimension vector is then

$$\begin{cases} n_1(k) = n_1 - \frac{1}{2}k(3n_1 - 4n_2 + n_3) + \frac{1}{2}k^2(n_1 - 2n_2 + n_3) \\ n_2(k) = n_2 - \frac{1}{2}k(n_1 - n_3) + \frac{1}{2}k^2(n_1 - 2n_2 + n_3) \\ n_3(k) = n_3 - \frac{1}{2}k(4n_2 - n_1 - 3n_3) + \frac{1}{2}k^2(n_1 - 2n_2 + n_3) \end{cases} \tag{9.5.7}$$

where (n_1, n_2, n_3) denotes the value for $k = 0$, given in (9.5.4). We note that for fixed $\gamma = [r, d, \mathrm{ch}_2]$ and large k, the entries $n_i(k)$ grow like $-\frac{1}{2}k^2 r$ for $r \neq 0$, or like kd for $r = 0$, in particular they all have the same sign for large k.

9.5.2 Initial rays for the orbifold scattering diagram

In this subsection, we prove Theorem 9.1.1, which states that for the quiver with potential (Q, W) shown in Figure 9.4, the attractor invariant $\Omega_\star(\gamma)$ vanishes for all dimension vectors $\gamma = (n_1, n_2, n_3)$ except for

$$\gamma \in \big\{(1,0,0), (0,1,0), (0,0,1), (n,n,n) : n \geq 1\big\} \tag{9.5.8}$$

where it takes the values stated in (9.1.9). This result was conjectured in [BMP21a], but the proof outlined in that paper was not mathematically rigorous. Here we complete the proof, combining ideas from [BMP21a, §3.3] and [DP22, §3.2]. We denote by $a_i \colon 2 \to 1$, $b_i \colon 3 \to 2$ and $c_i \colon 1 \to 3$ the arrows of the quiver.

Proof of Theorem 9.1.1. Consider a representation ϕ of (Q, W) with dimension vector (n_1, n_2, n_3), assumed to be stable for a King stability condition $\theta = (\theta_1, \theta_2, \theta_3)$. Consider a cycle w of the quiver: because (Q, W) gives a noncommutative crepant resolution of $\mathbb{C}^3/\mathbb{Z}_3$ [Moz09, Proposition 3.13], the cycle w is a central element of the Jacobian algebra of (Q, W), hence it defines an endomorphism of ϕ. Because ϕ is stable, its only automorphisms are rescalings, hence w acts as a scalar on ϕ. Suppose now that ϕ is not of dimension vector (n, n, n) for $n \in \mathbb{N}^*$: w cannot be an automorphism (otherwise all its arrows would be isomorphisms, hence one would have $n_1 = n_2 = n_3$), hence w vanishes on ϕ.

We suppose now that the King stability parameters satisfy $\theta_1 < 0$, and $\theta_3 > 0$ (since $\theta_1 + \theta_2 + \theta_3 = 0$, other cases follow by circular permutation of the nodes). We now show by contradiction that ϕ_{c_j} vanishes for every arrow $c_j : 1 \to 3$. Suppose that there exists $x \in V_1$ and $j \in \{1, 2, 3\}$ such that $\phi_{c_j}(x) \in V_3$ does not vanish. Because $\theta_1 < 0$ and ϕ is stable, one must have $x \in \bigoplus_{k=1}^3 \mathrm{Im}(\phi_{a_k})$. Because $\theta_3 > 0$ and ϕ is stable, $\langle \phi_{c_j}(x) \rangle$ cannot be a sub-representation of ϕ, hence there must be an arrow $b_i \colon 3 \to 2$ such that $\phi_{b_i}\phi_{c_j}(x) \in V_2$ does not vanish. Because all the cycles of Q vanish on ϕ, one must have $\phi_{b_i}\phi_{c_j}(\bigoplus_{k=1}^3 \mathrm{Im}(\phi_{a_k})) = 0$, a contradiction. Hence the ϕ_{c_j} vanish on ϕ for all j. The set $I = \{c_1, c_2, c_3\}$ of vanishing arrows provides a cut of the potential W, in the sense that each cycle of W contains exactly one arrow of I.

The stable representation ϕ is then a representation of the quiver with relation $(Q_I, \partial_I W)$, where the arrows $c_j \in I$ have been traded for relations $\partial_{c_j} W = 0$ for $c_j \in I$. From general arguments of geometric invariant theory, the moduli $\mathcal{M}^{\theta,s}_{Q_I}$ of stable representations of Q_I is smooth of dimension $3n_3n_2+3n_2n_1-n_1^2-n_2^2-n_3^2+1$. The moduli space $\mathcal{M}^{\theta,s}_{Q_I,\partial_I W}$ of stable representations of $(Q_I, \partial_I W)$ is cut out by $3n_3n_1$ bilinear relations $\partial_{c_j} W = 0$ inside $\mathcal{M}^{\theta,s}_{Q_I}$. We denote the infinitesimal versions of these relations on the tangent space of ϕ by $\delta(\partial_{c_j} W)\colon V_3 \to V_1$. A linear dependence between these infinitesimal relations would be given by maps $\tilde{\phi}_{c_j}\colon V_1 \to V_3$ such that:

$$\mathrm{Tr}(\tilde{\phi}_{c_j}\delta(\partial_{c_j} W)) = 0 \tag{9.5.9}$$

As shown in [DP22, §3.2], this equation is equivalent to the fact that the representation $\bar{\phi} \coloneqq (\phi_a, \phi_b, \tilde{\phi}_c)$ of Q (which, like ϕ, satisfies the relations $\delta_{c_j} W = 0$) satisfies the relations $\delta_{a_i} W = 0$ and $\delta_{b_i} W = 0$. Hence $\bar{\phi}$ is a representation of (Q, W), which is θ-stable (because it has fewer subobjects than the θ-stable representation ϕ) of dimension $\gamma \neq (n, n, n)$. By the above arguments $\tilde{\phi}_{c_j} = 0$, therefore the relations $\partial_{c_j} W = 0$ are transverse, and $\mathcal{M}^{\theta,s}_{Q_I,\partial_I W}$ is smooth of dimension $3n_3n_2 + 3n_2n_1 - 3n_3n_1 - n_1^2 - n_2^2 - n_3^2 + 1$. In particular, because this dimension is positive, one has

$$n_1^2 + n_2^2 + n_3^2 - 3n_3n_2 - 3n_2n_1 - 3n_1n_3 + 6n_3n_1 \leq 1 \tag{9.5.10}$$

Now the proof proceeds exactly as in [BMP21a, §3.3]. Assume that θ is an attractor stability condition, hence a small deformation of the self-stability condition $\langle -, \gamma\rangle$ for some dimension vector $\gamma \neq (n, n, n)$. Then $\theta_1 < 0$ implies that $n_1 \geq n_2$, and $\theta_3 > 0$ implies that $n_3 \geq n_2$: hence $6n_3n_1 \geq 2n_3n_2 + 2n_2n_1 + 2n_1n_3$, and then, using (9.5.10):

$$\begin{aligned} q(\gamma) &\coloneqq \frac{1}{2}((n_1 - n_2)^2 + (n_2 - n_3)^2 + (n_3 - n_1)^2) = n_1^2 + n_2^2 + n_3^2 - n_1n_2 - n_2n_3 - n_3n_1 \\ &\leq n_1^2 + n_2^2 + n_3^2 - 3n_1n_2 - 3n_2n_3 - 3n_2n_3 + 6n_3n_1 \leq 1 \end{aligned} \tag{9.5.11}$$

The kernel of the quadratic form $q(\gamma)$ is given by dimensions vectors (n, n, n), but we have assumed that γ was not of this form. One has $q(\gamma) = 1$ only for $\gamma = (n + 1, n, n)$ and circular permutations thereof, but the inequality is strict in the second line of (9.5.11) unless $n = 0$. Hence, γ must be $(1, 0, 0)$, $(0, 1, 0)$, or $(0, 0, 1)$, with attractor invariants equal to 1. The DT invariants for $\gamma = (n, n, n)$ are independent of the stability conditions, and given by the shifted Poincaré polynomial $(-y)^{-3}P(K_{\mathbb{P}^2}, y) = -y^3 - y - 1/y$ by [MP20, Remark 5.2]. □

Having determined the initial rays for the orbifold quiver, it is now straightforward at least in principle to construct the stability scattering diagram $\mathcal{D}_Q$. The result is represented in Figure 9.23, including only initial and some secondary rays. The full diagram is dense except in a cone which includes the positive and negative octant, as will become clear shortly.

9.5.3 Restricted scattering diagram

Due to the rescaling symmetry in the space of King stability parameters, there is no significant loss of information[22] in restricting the scattering diagram $\mathcal{D}_Q$ to its intersection $\mathcal{D}_o$ with the hyperplane

[22] The price to pay is that the ray $\mathcal{R}^{\mathrm{eff}}_o(\delta)$ is no longer visible, but this causes no problem since the automorphism $\mathcal{U}^{\mathrm{eff}}(\delta)$ is central; moreover, the self-stability condition $\langle -, \gamma\rangle$ is now pushed to infinity in the direction opposite to the vector $\nu(\gamma)$ introduced below.

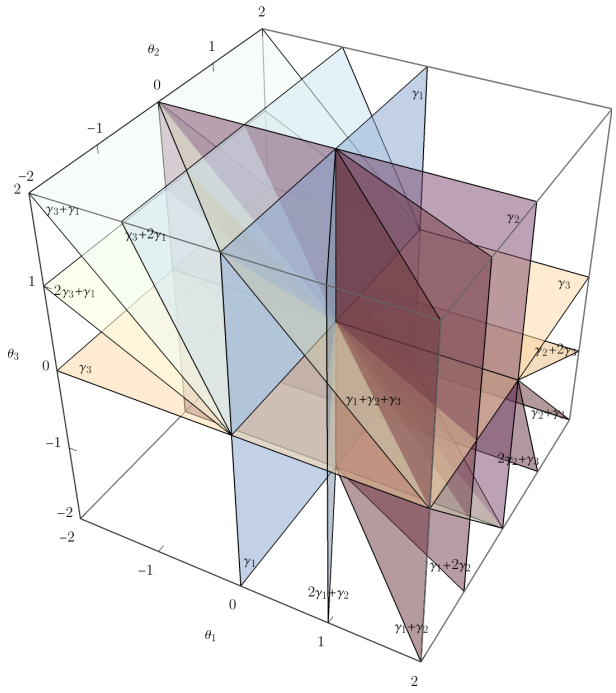

Figure 9.23: Quiver scattering diagram $\mathcal{D}_Q$, showing only the initial rays $\mathcal{R}_o(\gamma_i)$ and $\mathcal{R}_o(\delta)$ and secondary rays $\mathcal{R}_o(\gamma_j+\gamma_k)$.

$\mathcal{H}=\{\theta_1+\theta_2+\theta_3=1\}$. It is furthermore convenient to parametrize this hyperplane by $(u,v)\in\mathbb{R}^2$ such that

$$\theta_1=-u+v\sqrt{3}+\tfrac{1}{3},\quad \theta_2=2u+\tfrac{1}{3},\quad \theta_3=-u-v\sqrt{3}+\tfrac{1}{3} \tag{9.5.12}$$

In these coordinates, the $\mathbb{Z}_3$ symmetry permuting the nodes of the quiver cyclically acts by a rotation of angle $2\pi/3$ around the origin (see Figure 9.5). The geometric rays $\mathcal{R}_o^{\rm geo}(\gamma)=\{(u,v)\in\mathbb{R}^2:\sum_i n_i\theta_i(u,v)=0\}$ are given by straight lines

$$(n_1+n_3-2n_2)u+(n_3-n_1)v\sqrt{3}-\frac{1}{3}(n_1+n_2+n_3)=0 \tag{9.5.13}$$

oriented along the vector $\nu(\gamma)=(\sqrt{3}(n_3-n_1),2n_2-n_1-n_3)$ pointing from the attractor stability condition $\theta_i=\lambda(n_{i-1}-n_{i+1})$ towards the anti-attractor stability condition $\theta_i=\lambda(n_{i+1}-n_{i-1})$, with indices $i=1,2,3$ taken modulo 3. In particular, the initial rays intersect at $\mathcal{R}_o^{\rm geo}(\gamma_i)\cap\mathcal{R}_o^{\rm geo}(\gamma_{i+1})=\{p_i\}$ with

$$p_1=\left(-\frac{1}{6},-\frac{1}{2\sqrt{3}}\right),\quad p_2=\left(-\frac{1}{6},\frac{1}{2\sqrt{3}}\right),\quad p_3=\left(\frac{1}{3},0\right) \tag{9.5.14}$$

Interpreting the ray as the worldline of a fiducial particle traveling at point $r=(u,v)$ with velocity $\nu(\gamma)$, the condition (9.5.13) implies that the particle has angular momentum $r\wedge\nu(\gamma)=-\frac{1}{3}(n_1+n_2+n_3)$ with respect to the origin $(0,0)$ in the (u,v) plane, therefore rotates clockwise

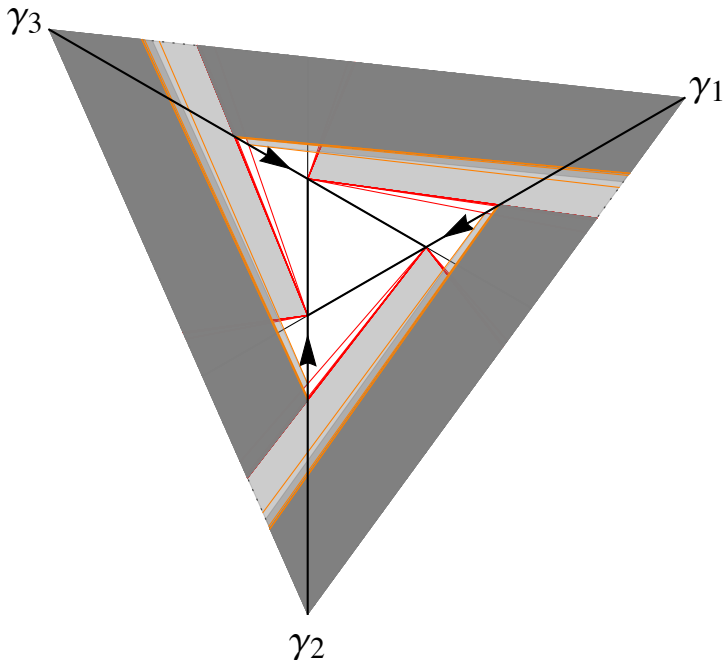

Figure 9.24: Two-dimensional section $\mathcal{D}_o$ of the orbifold scattering diagram $\mathcal{D}_Q$ along the hyperplane $\theta_1+\theta_2+\theta_3=1$. We show only the restriction to the triangle Δ_ψ (see §9.6.4) bounded by the points $p_i(\mathcal{V}_\psi)$ defined in (9.6.28) (with $\psi=-1.4$ for illustration), but the scattering diagram $\mathcal{D}_o$ in the space of King stability conditions is unbounded. Regions with a dense set of rays are shown in gray. The rays in red correspond to the discrete set of real roots of the Kronecker quiver with 3 arrows, with dimension vector $(F_{2k}, F_{2k+2}, 0)$ or permutations thereof, see §9.3.2.

around the origin (assuming that $n_i \geq 0$). In fact, (9.5.13) implies that the particle has angular momentum

$$(r-p_i)\wedge\nu(\gamma) = -n_{i-1} \tag{9.5.15}$$

with respect to any of the points p_i, so the particle rotates clockwise around each p_i, and can only pass through it if $n_{i-1}=0$ (this generalizes the previous statement since $p_1+p_2+p_3=0$).

Another consequence of (9.5.13) is that the linear function on Γ

$$\varphi_o(\gamma) = (n_3-n_1)u\sqrt{3} + (2n_2-n_1-n_3)v = (r,\nu(\gamma)) \tag{9.5.16}$$

increases monotonically along the ray and is additive at each vertex, similar to the electric potential (9.4.10) in the large volume scattering diagram. Unlike the latter however, the function (9.5.16) is not positive, in particular the first scattering between $\mathcal{R}_o(\gamma_i)$ and $\mathcal{R}_o(\gamma_{i+1})$ may take place at arbitrary negative values of $\varphi_o(\gamma_i), \varphi_o(\gamma_{i+1})$. Fortunately, we do not need to rely on such a cost function to define the quiver scattering diagram and enumerate all possible scattering sequences, instead we can use the fact that only positive dimension vectors support non-zero DT invariants.

In the next subsection, we use the orbifold scattering diagram to compute DT invariants for some simple dimension vectors.

9.5.4 Examples

We first consider the case $\gamma = [1, 0, 1-n)$, corresponding to the Hilbert scheme of n points on $\mathbb{P}^2$. The corresponding dimension vector is $\gamma = (n-1, n, n)$. As in §9.4.3 we find that the index in the anti-attractor chamber, which we denote by $\Omega_c(\gamma) \coloneqq \Omega_{\langle\gamma,-\rangle}(\gamma)$, agrees with the Gieseker index (9.2.13) for all cases considered, although the set of scattering sequences for the large volume and orbifold scattering diagrams may differ. As explained in §9.6.4, the absence of walls between the anti-canonical chamber and the large volume chamber is a general property of objects with slope $\mu \in [-1, 0]$.

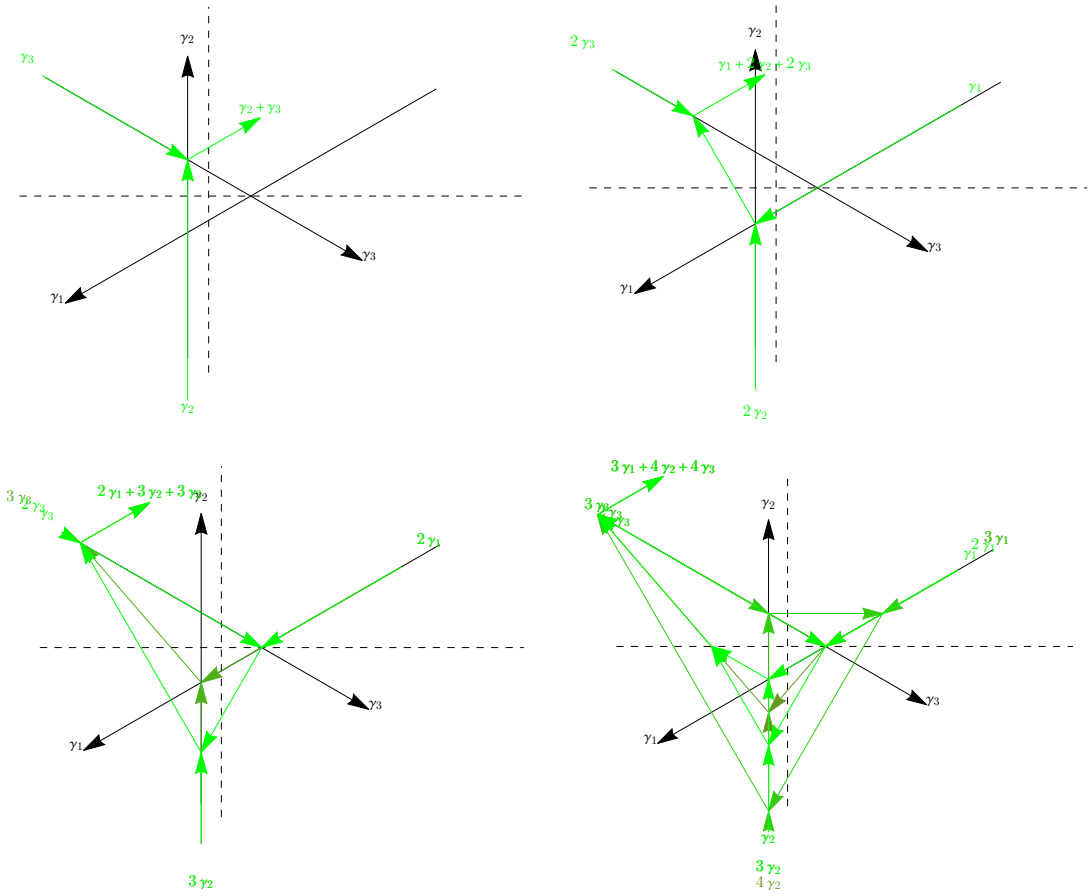

Figure 9.25: Scattering sequences for dimension vector $(n-1, n, n)$ corresponding the Hilbert scheme of n points on $\mathbb{P}^2$, with $n = 1, 2, 3, 4$

- For $n = 1$ we find a single scattering sequence $\{\gamma_2, \gamma_3\}$ contributing $K_3(1,1) = y^2+1+1/y^2 \to 3$ in the anti-attractor chamber.

- For $n = 2$, we find a single scattering sequence $\{\{\gamma_1, 2\gamma_2\}, 2\gamma_3\}\}$ contributing $K_3(1,2)^2 = (y^2 + 1 + 1/y^2)^2 \to 9$.

- For $n = 3$ we find two scattering sequences,

$$\begin{array}{ll} \{\{2\gamma_1, 3\gamma_2\}, 3\gamma_3\} & K_3(1,3)K_3(2,3) \to 13 \\ \{\{\{2\gamma_1, \gamma_3\}, 3\gamma_2\}, 2\gamma_3\} & K_3(1,2)^2K_3(1,3) \to 9 \end{array} \tag{9.5.17}$$

  for a total index of $y^6 + 2y^4 + 5y^2 + 6 + \cdots \to 22$.

- For $n = 4$ we find 3 scattering sequences,

$$\begin{array}{ll} \{\{\{3\gamma_1, \gamma_3\}, 4\gamma_2\}, 3\gamma_3\} & K_3(1,3)^2K_6(1,4) \to 15 \\ \{\{\{3\gamma_1, \{\gamma_2, 2\gamma_3\}\}, 3\gamma_2\}, 2\gamma_3\} & K_3(1,2)^2K_3(1,3)^2 \to 9 \\ \{\{\{\{2\gamma_1, \gamma_3\}, 3\gamma_2\}, \{\gamma_1, \gamma_2\}\}, 3\gamma_3\} & K_3(1,1)^2K_3(1,2)K_3(1,3)^2 \to 27 \end{array} \tag{9.5.18}$$

  for a total index of $y^8 + 2y^6 + 6y^4 + 10y^2 + 13 + \cdots \to 51$.

Next we consider $\gamma = [0, 1, 1-n)$, corresponding to a D2-brane bound to n anti-D0-branes. The corresponding dimension vector is $\gamma = (n, n+1, n+2)$. Unlike the Gieseker index at large volume, the index $\Omega_c(\gamma)$ in the anti-attractor chamber depends on n, though it is still invariant under $n \mapsto -n-2$. After a circular permutation, the dimension vector becomes $\gamma' = (n+1, n+2, n) = [3, -2, -1-n)$, and $\Omega_c(\gamma')$ agrees with the Gieseker index for rank 3 sheaves with $d = -2$ and $\chi = -1 - n$.

- For $n = -1$, the dimension vector $(-1, 0, 1)$ has mixed signs so the index vanishes.

- For $n = 0$, we find a single scattering sequence $\{\gamma_2, 2\gamma_3\}$ contributing $K_3(1,2) = y^2+1+1/y^2 \to 3$.

- For $n = 1$, we find 2 scattering sequences,

$$\begin{array}{ll} \{\gamma_1, \{2\gamma_2, 3\gamma_3\}\} & K_3(2,3)K_3(1,1) \to 39 \\ \{\{\gamma_1, 2\gamma_2\}, 3\gamma_3\} & K_3(1,2)K_3(1,3) \to 3 \end{array} \tag{9.5.19}$$

  giving a total index of $y^8 + 2y^6 + 5y^4 + 8y^2 + 10 + \cdots \to 42$.

- For $n = 2$, we find 3 scattering sequences,

$$\begin{array}{ll} \{2\gamma_1, \{3\gamma_2, 4\gamma_3\}\} & K_3(1,2)K_3(3,4) \to 204 \\ \{\{\{2\gamma_1, \gamma_3\}, 3\gamma_2\}, 3\gamma_3\} & K_3(1,2)K_3(1,3)^2 \to 3 \\ \{\{\{\gamma_1, 3\gamma_2\}, 4\gamma_3\}, \gamma_1\} & K_3(1,1)K_3(1,3)K_6(1,4) \to 45 \\ \{\{\{\gamma_1, 2\gamma_2\}, 3\gamma_3\}, \{\gamma_2, \gamma_3\}\}, \gamma_1\} & K_3(1,1)^3K_3(1,2)K_3(1,3) \to 81 \end{array} \tag{9.5.20}$$

  giving a total index of 333.

- For $n = 3$, we find 7 scattering sequences,

$\{3\gamma_1, \{4\gamma_2, 5\gamma_3\}\}$	$K_3(1,3)K_3(4,5) \to 399$
$\{2\gamma_1, \{\{\gamma_1, 3\gamma_2\}, 5\gamma_3\}, \gamma_2\}\}$	$K_3(1,2)K_3(1,3)K_6(1,5)K_{12}(1,1) \to 216$
$\{2\gamma_1, \{\{\gamma_1, 3\gamma_2\}, 4\gamma_3\}, \{\gamma_2, \gamma_3\}\}\}$	$K_3(1,1)^2K_3(1,2)K_3(1,3)K_6(1,4) \to 405$
$\{2\gamma_1, \{\{\gamma_1, 2\gamma_2\}, 3\gamma_3\}, \{2\gamma_2, 2\gamma_3\}\}\}$	$K_3(2,2,1)K_3(1,2)^2K_3(1,3) \to 648$
$\{\{\{3\gamma_1, \{\gamma_2, 2\gamma_3\}\}, 3\gamma_2\}, 3\gamma_3\}$	$K_3(1,2)K_3(1,3)^3 \to 3$
$\{\{\{2\gamma_1, 4\gamma_2\}, 5\gamma_3\}, \gamma_1\}$	$K_{6,6,3}(2,2,5)K_3(1,1) \to 216$
$\{\{\{\{2\gamma_1, \gamma_3\}, 3\gamma_2\}, 3\gamma_3\}, \{\gamma_2, \gamma_3\}\}, \gamma_1\}$	$K_3(1,1)^3K_3(1,2)K_3(1,3)^2 \to 81$

  giving a total index of 1968. Similar to the discussion below (9.4.23), the factor $K_{6,6,3}(2,2,5)$ for the penultimate sequence is computed by applying the flow tree formula to a local scattering diagram with two incoming rays of charge $\alpha = \gamma_1 + 2\gamma_2$ and $\beta = \gamma_3$ with $\bar{\Omega}^-(\alpha) = K_3(1,2) = y^2 + 1 + 1/y^2, \bar{\Omega}^-(2\alpha) = K_3(2,4) = -y^5 - y^3 - y - 1/y - 1/y^3 - 1/y^5$ and $\bar{\Omega}^-(k\beta) = \delta_{k,1}$, selecting the outgoing ray of charge $2\alpha + 5\beta$.

9.6 The exact scattering diagram

In this section, we determine the scattering diagram $\mathcal{D}^{\Pi}_{\psi}$ along the slice of Π-stability conditions, by combining results on the large volume and orbifold scattering diagrams constructed in §9.4 and §9.5 with invariance under $\Gamma_1(3)$. We start by analyzing the attractor flow for the exact central charge (9.1.4), first in the Poincaré upper half-plane (§9.6.1) and then in affine coordinates (§9.6.2). In §9.6.3 we then identify the orbifold scattering diagram $\mathcal{D}_o$ as a particular subset of $\mathcal{D}^{\Pi}_{\psi}$ in a region around the orbifold point. In §9.6.4 we describe the full diagram $\mathcal{D}^{\Pi}_{\psi}$ and prove the SAFC (Theorem 9.1.3).

9.6.1 Exact attractor flow

In this section, we study the attractor flow (9.3.19) for the central charge (9.1.4) along the slice of Π-stability conditions, equipped with an general hermitean metric $\mathrm{d}s^2 = g_{\tau\bar{\tau}}\mathrm{d}\tau\mathrm{d}\bar{\tau}$. Using the Eichler integral representation (9.1.5) for the coefficients T, T_D in the central charge, the attractor flow AF(γ) (9.3.19) reduces to

$$\frac{\mathrm{d}\tau}{\mathrm{d}\mu} = -g^{\tau\bar{\tau}}\partial_{\bar{\tau}}|Z_\tau(\gamma)|^2 = -g^{\tau\bar{\tau}}(d - r\bar{\tau})\,\overline{C(\tau)}Z_\tau(\gamma) \tag{9.6.1}$$

The flow is only meaningful in the region where the charge γ is populated, $\bar{\Omega}_\tau(\gamma) \neq 0$. As already noted in §9.3.5, the modulus $|Z_\tau(\gamma)| = \Im[e^{-\mathrm{i}\psi}Z_\tau(\gamma)]$ decreases along the flow while the argument of $Z_\tau(\gamma)$ is preserved, so the trajectories of (9.6.1) are included in the active ray $\mathcal{R}_\psi(\gamma)$ defined in (9.3.12) as the locus $\{\Re[e^{-\mathrm{i}\psi}Z_\tau(\gamma)] = 0, \Im(e^{-\mathrm{i}\psi}Z_\tau(\gamma)) > 0, \bar{\Omega}_\tau(\gamma) \neq 0\}$ inside $\mathbb{H}$, where the phase ψ is determined by the argument of $Z_{\tau_0}(\gamma)$ at the starting point τ_0. The attractor flow stops when either a) the flow crosses a wall of marginal stability, after which $\bar{\Omega}_\tau(\gamma)$ jumps, b) $|Z_\tau(\gamma)|$ reaches a local minimum in the interior of the upper half-plane, or c) τ reaches the boundary $\Im\tau = 0$. In §9.7.11 we rule out the possibility of an infinitely long flow.

Case a) arises at a point μ_1 where the quantity $\tilde{W}_\tau(\gamma,\gamma') := \Im[Z_\tau(\gamma')\overline{Z_\tau(\gamma)}]$ vanishes for some charge γ'. Since $\tilde{W}_\tau(\gamma,\gamma')$ varies along the flow according to

$$\frac{\mathrm{d}\tilde{W}_\tau(\gamma,\gamma')}{\mathrm{d}\mu} = -g^{\tau\bar{\tau}}|C|^2\left[2\tau_2(rd' - r'd)|Z_\tau(\gamma)|^2 + \tilde{W}_\tau(\gamma,\gamma')|d - r\tau|^2\right] \tag{9.6.2}$$

the sign of $(rd'-r'd)\tilde{W}_\tau(\gamma,\gamma')$ is positive for $\mu<\mu_1$ and negative for $\mu>\mu_1$. Thus, the flow crosses from the side of the wall where a two-particle bound state of charges γ and $\gamma-\gamma'$ is stable, into the side where the bound state decays. In particular, it follows from (9.6.2) that the flow cannot cross the same wall more than once, and that BPS states do not decay as one follows the attractor flow in reverse [DGR01].

As for case b), since $C(\tau)\neq 0$ for $\Im\tau>0$, $|Z_\tau(\gamma)|$ can only reach a local minimum at a point τ_i in the interior of $\mathbb{H}$ if $Z_{\tau_i}(\gamma)=0$, but this is ruled out by the assumption that $\bar\Omega_\tau(\gamma)\neq 0$ along the flow (and the support property). This leaves case c) with $\Im\tau_i=0$. Consider the image of the attractor flow on the quotient $\mathbb{H}/\Gamma_1(3)$. Since the quotient can be compactified by adding the large volume and conifold points, τ_i is either in the orbit of a large volume point or a conifold point, i.e. $\tau_i=p/q$ with (p,q) coprime, $q=0 \mod 3$ in the first case and $q\neq 0 \mod 3$ in the second case. Using suitable bounds on the central charge of semi-stable objects in the large volume region, we show in §9.7.10 that τ_i can only be a conifold point, where some spherical object E of charge γ_C becomes massless, $Z_{\tau_i}(\gamma_C)=0$.

To determine E, it suffices to find an element $g\in\Gamma_1(3)$ which maps $\tau=0$ to $\tau_i=p/q$, and act with the corresponding auto-equivalence on the object $\mathcal{O}$ which is massless at $\tau=0$. Since $(T,T_D)=(\mathrm{i}\mathcal{V},0)$ at $\tau=0$, where $\mathcal{V}$ is the quantum volume defined in (9.1.12), the periods at τ_i are then

$$T(\tau_i)=m+\mathrm{i}q\mathcal{V},\quad T_D(\tau_i)=m_D+\mathrm{i}p\mathcal{V} \tag{9.6.3}$$

where (m,m_D) are the off-diagonal elements of the monodromy matrix $M(g)$ in (9.7.50). The charge of the massless object E at $\tau=\tau_i$ is then $\gamma_C=[q,p,pm-qm_D]$ up to overall sign, see Table 9.1 for examples with $0\leq p\leq q\leq 5$.

Returning to the active ray $\mathcal{R}_\psi(\gamma)$, it follows from (9.6.3) that it can only reach the conifold point $\tau_i=p/q$ if

$$0=\Re[e^{-\mathrm{i}\psi}Z_{p/q}(\gamma)]=(dm-rm_D-\mathrm{ch}_2)\cos\psi+(dq-pr)\mathcal{V}\sin\psi \tag{9.6.4}$$

For generic ψ, this is only possible if γ is a multiple of γ_C, in which case $\mathcal{R}_\psi(\gamma)$ coincides with the ray $\mathcal{R}_\psi(\gamma_C)$ originating from $\tau_i=p/q$. For special values of ψ such that $\mathcal{V}_\psi:=\mathcal{V}\tan\psi$ is rational, namely

$$\mathcal{V}_\psi=\frac{\mathrm{ch}_2+rm_D-dm}{dq-pr} \tag{9.6.5}$$

it is possible that a ray $\mathcal{R}_\psi(\gamma)$ with $\langle\gamma_C,\gamma\rangle=dq-pr\neq 0$ originates from the point $\tau_i=\frac{p}{q}$, even though $Z_{\tau_i}(\gamma)\neq 0$. Conversely, for the same critical values of ψ there can also be rays which terminate at a conifold point, rather than escaping at a large volume point, as proven in Proposition 9.7.5 (this phenomenon occurs for instance in the $\psi\to\psi^{\mathrm{cr}}_{-1/2}$ limit of Figure 9.8). In the next subsection, we introduce adapted coordinates where these critical rays become much easier to detect.

9.6.2 Affine coordinates

While the attractor flow AF(γ) is complicated on the τ-plane, it becomes a straight line in affine coordinates (x, y) defined globally by[23]

$$x = \frac{\Re\left(e^{-\mathrm{i}\psi}T\right)}{\cos\psi}\ , \quad y = -\frac{\Re\left(e^{-\mathrm{i}\psi}T_D\right)}{\cos\psi} \tag{9.6.6}$$

It is useful to introduce the dual coordinates

$$\tilde{x} = \frac{\Im(e^{-\mathrm{i}\psi}T)}{\cos\psi}, \quad \tilde{y} = -\frac{\Im(e^{-\mathrm{i}\psi}T_D)}{\cos\psi} \tag{9.6.7}$$

such that the geometric ray $\mathcal{R}^{\rm geo}_\psi(\gamma)$, oriented along the direction of decreasing $\Im[e^{-\mathrm{i}\psi}Z(\gamma)] = r\tilde{y} + d\tilde{x}$, are given by oriented straight lines

$$ry + dx - \mathrm{ch}_2 = 0, \quad \frac{\mathrm{d}}{\mathrm{d}\mu}(r\tilde{y} + d\tilde{x}) < 0 \tag{9.6.8}$$

Notice that for the large volume central charge $Z^{\rm LV}_{(s,t)}$, the coordinates (x, y) coincide with $(s_\psi, \frac{1}{2}(t^2_\psi - s^2_\psi))$ defined in (9.4.26) and generalize the coordinates (x, y) of [Bou19] to any $\psi \in (-\frac{\pi}{2}, \frac{\pi}{2})$. Notably, the image of the upper half-plane $t > 0$ lies above the parabola $y = -\frac{1}{2}x^2$.

In contrast, for the exact central charge (9.1.4), the image of the fundamental domain $\mathcal{F}_C$ and its translates in the (x, y)-plane extend below the parabola $y = -\frac{1}{2}x^2$, while remaining above the parabola $y = -\frac{1}{2}x^2 - \frac{5}{24}$ passing through the images of the orbifold points at $\tau = \tau_o + n$ (see Figure 9.26)

$$(x_{o(n)}, y_{o(n)}) = \left(n - \tfrac{1}{2}, -\tfrac{1}{3} - \tfrac{1}{2}n(n-1)\right) \tag{9.6.9}$$

For $\psi = 0$, the preimage of the region $y > -\frac{1}{2}x^2$ includes the domain $\mathbb{H}^{\rm LV}$ defined by the condition $w > \frac{1}{2}s^2$ (or equivalently $t > 0$). In fact, the curves $t = 0$ and $y = -\frac{1}{2}x^2$ are tangent to the same point $\tau \simeq \frac{1}{2} + 0.559926\mathrm{i}$ corresponding to $(s, w) = (\frac{1}{2}, \frac{1}{8})$ or $(x, y) = (\frac{1}{2}, -\frac{1}{8})$, and are nearly indistinguishable for any τ_1, with the former lying below the latter. For general ψ, using (9.7.25) along the line $\tau_1 = \frac{1}{2}$ we get

$$y + \frac{1}{2}x = w - \frac{1}{2}s^2 + \frac{1}{2}\Im T \tan\psi(1 + \Im T \tan\psi) \tag{9.6.10}$$

so the relative position of the two curves depends on the sign of $\Im T \tan\psi$.

Geometrically, the coordinates (x, y) and $(\tilde{x}, \tilde{y})$ provide two systems of local Darboux coordinates for the Kähler form

$$\mathrm{d}x \wedge \mathrm{d}y = \mathrm{d}\tilde{x} \wedge \mathrm{d}\tilde{y} = -\frac{1}{4}(\mathrm{d}T \wedge \mathrm{d}\bar{T}_D + \mathrm{d}\bar{T} \wedge \mathrm{d}T_D) \tag{9.6.11}$$

Hence, locally there exists a function $H_\psi(x, y)$ such that $\tilde{x} = \partial_y H_\psi, \tilde{y} = -\partial_x H_\psi$, satisfying the Monge-Ampère type equation

$$(\partial^2_x H_\psi)(\partial^2_y H_\psi) - (\partial_x\partial_y H_\psi)^2 = 1 \tag{9.6.12}$$

[23] The affine coordinate y should not be confused with the refinement variable y in the definition of motivic DT invariants.

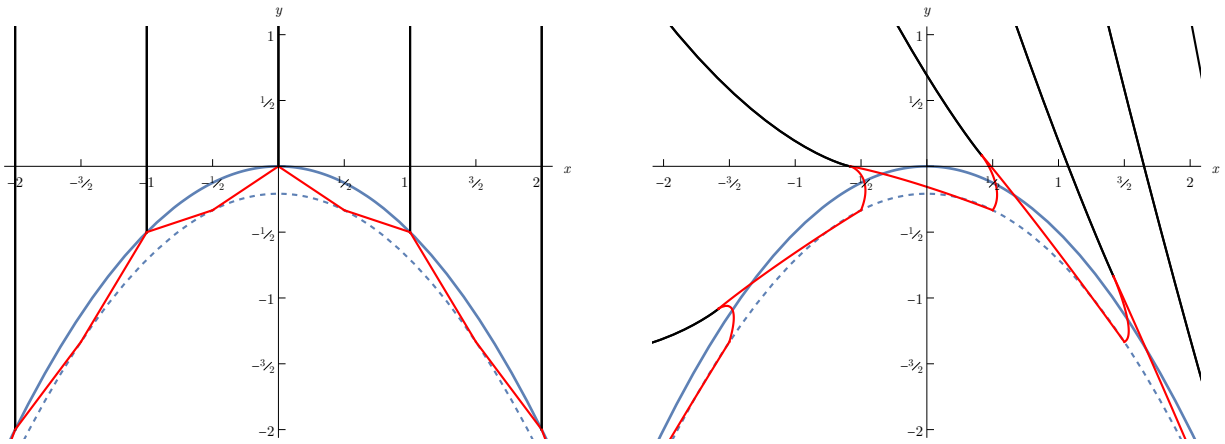

Figure 9.26: Image of the fundamental domain $\mathcal{F}_C$ and its translates $\mathcal{F}_C(m)$ in the (x,y)-plane for $\psi = 0$ (left) and $\psi = -0.9 < -\psi^{\rm cr}_{1/2}$ (right). The parabolas $y = -\frac{1}{2}x^2$ and $y = -\frac{1}{2}x^2 - \frac{5}{24}$ are shown for reference. For any $\psi \in (-\frac{\pi}{2}, \frac{\pi}{2})$, the map $\tau \mapsto (x,y)$ is injective in $\bigcup_{m\in\mathbb{Z}} \mathcal{F}_C(m)$.

One easily checks that the Legendre transform to the imaginary part of the tree-level prepotential (9.7.30), sometimes known as the Hesse potential [CdWM10], provides such a function,

$$H_\psi(x,y) = \langle \Im \left[-\frac{2\pi \mathrm{i}}{3} \frac{e^{-2\mathrm{i}\psi}}{\cos^2\psi} F_0\left(\cos\psi e^{\mathrm{i}\psi}(x+\mathrm{i}\tilde{x})\right)\right] + \tilde{x}y\rangle_{\tilde{x}} \tag{9.6.13}$$

where F_0 is normalized such that $T_D = -\frac{3}{2\pi\mathrm{i}}\partial_T F_0$ (see (9.7.30)). In the large volume limit, (9.6.13) evaluates to

$$\begin{aligned} H^{\rm LV}_\psi(x,y) &= \frac{1}{3\cos\psi}(x^2+2y)^{\frac{3}{2}} - \frac{1}{3}x(x^2+3y)\tan\psi \\ &= \frac{t^3}{3\cos\psi} + \frac{s}{6}(s^2-3t^2)\tan\psi - \frac{t}{6}(t^2-3s^2)\tan^2\psi \end{aligned} \tag{9.6.14}$$

An explicit computation shows that the Hessian matrix of H_ψ with respect to (x,y) coincides with that of $H^{\rm LV}_\psi$ (i.e. the Hessian is insensitive to the factor $C(u)$ appearing in the Eichler integral (9.1.5)), namely

$$\begin{pmatrix} \partial_{xx}H_\psi & \partial_{xy}H_\psi \\ \partial_{xy}H_\psi & \partial_{yy}H_\psi \end{pmatrix} = \frac{1}{\tau_2}\begin{pmatrix} |\tau|^2 & \tau_1 \\ \tau_1 & 1 \end{pmatrix} \tag{9.6.15}$$

In particular it is positive definite. This observation allows to write the orientation condition in (9.6.8) purely in terms of the coordinates (x,y): indeed, it becomes

$$-\frac{1}{r}\left[r^2\partial_x^2 H_\psi - 2dr\partial_x\partial_y H_\psi + d^2\partial_y^2 H_\psi\right]\frac{\mathrm{d}x}{\mathrm{d}\mu} < 0 \tag{9.6.16}$$

Thus we conclude that for $r \neq 0$ the ray is oriented such that $r\frac{\mathrm{d}x}{\mathrm{d}\mu} > 0$. In particular, the electric potential $\varphi_x(\gamma) = 2(d - xr)$ (generalizing (9.4.10) for the exact central charge) decreases along the

ray. When $r = 0$, we get instead $\frac{\mathrm{d}(d\tilde{x})}{\mathrm{d}\mu} = \frac{d}{\tau_2}\frac{\mathrm{d}y}{\mathrm{d}\mu} < 0$, so the vertical ray is oriented towards decreasing y for $d > 0$ (or increasing y for $d < 0$).

We now determine the images of the conifold points in the (x, y) plane. Using (9.6.3), we find that the point $\tau = p/q$ where the object of charge $\gamma_C = [q, p, pm - qm_D]$ becomes massless maps to

$$(x_C, y_C) = (m + q\mathcal{V}_\psi, -m_D - p\mathcal{V}_\psi) \tag{9.6.17}$$

where $\mathcal{V}_\psi = \mathcal{V}\tan\psi$. In particular, the conifold point $\tau = m$ where the object $\mathcal{O}(m)$ becomes massless is mapped to the point

$$(x_{\mathcal{O}(m)}, y_{\mathcal{O}(m)}) = \Big(m + \mathcal{V}_\psi, -\frac{1}{2}m^2 - m\mathcal{V}_\psi\Big) \tag{9.6.18}$$

on the parabola $y = -\frac{1}{2}x^2 + \frac{1}{2}\mathcal{V}_\psi^2$. Moreover, the associated rays $\mathcal{R}_\psi^{\mathrm{geo}}(\pm\mathcal{O}(m))$ are contained in the tangent to the parabola $y = -\frac{1}{2}x^2$ at $x = m$, just as for the large volume scattering diagram. Similarly, the point $\tau = n - \frac{1}{2}$ where $\Omega(n+1)$ becomes massless is mapped to

$$(x_{\Omega(n+1)}, y_{\Omega(n+1)}) = \Big(n - \frac{1}{2} - 2\mathcal{V}_\psi, -\frac{1}{2}(n^2 - n + 1) + (2n-1)\mathcal{V}_\psi\Big) \tag{9.6.19}$$

on the parabola $y = -\frac{1}{2}x^2 + 2\mathcal{V}_\psi^2 - \frac{3}{8}$, and the corresponding rays $\mathcal{R}_\psi^{\mathrm{geo}}(\pm\Omega(n+1))$ are contained in the tangent to the parabola $y = -\frac{1}{2}x^2 - \frac{3}{8}$ at $x = n - \frac{1}{2}$. The corresponding points are marked in Figure 9.27.

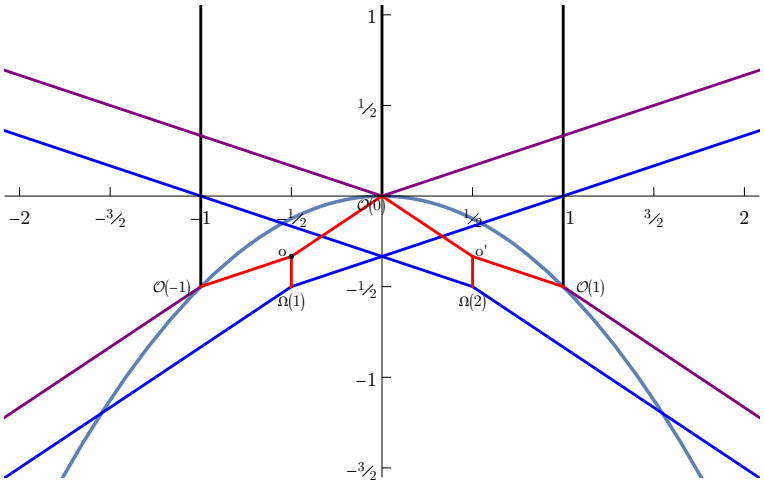

Figure 9.27: Images of the fundamental domains $\mathcal{F}_o$, $\mathcal{F}_{o'} = \mathcal{F}_o(1)$ and their $\mathbb{Z}_3$ images in the (x, y) plane for $\psi = 0$. The vertical black lines are the images of the semi-infinite lines $n + \frac{\mathrm{i}}{2\sqrt{3}} + \mathrm{i}\mathbb{R}^+$ for $n = -1, 0, 1$, while the blue and purple lines correspond to their images under $\mathbb{Z}_3$.

9.6.3 Orbifold region

We now discuss the domain of validity of the orbifold quiver description inside the space of Π-stability conditions, and how the two-dimensional scattering diagram constructed in §9.5.3 fits in

the scattering diagram for the exact central charge.

As explained in §9.5.1, the quiver description holds in the region $\mathbb{H}^o \subset \Pi$ where the central charges $Z_\tau(\gamma_i)$ of the simple objects belong to a common half-plane. In that region, the heart $\mathcal{A}(\tau)$ is equivalent under $\widetilde{GL^+}(2,\mathbb{R})$ to the Abelian category of representations of $J(Q,W)$, and the moduli space of semi-stable objects of phase $\arg Z_\tau(\gamma) = \psi + \frac{\pi}{2}$ in $\mathcal{A}(\tau)$ coincides with the moduli space of semi-stable representations for King stability parameters $\theta_i \propto \Re[e^{-\mathrm{i}\psi} Z_\tau(\gamma_i)]$. Choosing the scale such that $\theta_i(\gamma) = \Im[Z(\gamma_i)\bar{Z}(\gamma)] = \tilde{W}(\gamma,\gamma_i)$, we can apply the relation (9.6.2) to obtain the variation of θ_i along the attractor flow $\mathrm{AF}(\gamma)$,

$$\frac{\mathrm{d}\theta_i}{\mathrm{d}\mu} = -g^{\tau\bar{\tau}}|C|^2 \left[2\tau_2\langle\gamma,\gamma_i\rangle|Z(\gamma)|^2 + |d-r\tau|^2\theta_i\right] \tag{9.6.20}$$

The second term simply amounts to a rescaling of θ_i, while the first term shows that θ_i flows towards the self-stability condition $\langle\gamma_i,\gamma\rangle$. On the other hand, since $Z_\tau(\gamma_1)+Z_\tau(\gamma_2)+Z_\tau(\gamma_3) = Z_\tau(\delta) = 1$ for any $\tau \in \mathbb{H}$, it makes more sense to fix the scale by requiring

$$\theta_i = \frac{\Re[e^{-\mathrm{i}\psi} Z_\tau(\gamma_i)]}{\cos\psi} \tag{9.6.21}$$

such that $\theta_1+\theta_2+\theta_3 = 1$. The King stability parameters (9.6.21) are then linear combinations of the affine coordinates defined in (9.6.6), such that the lines of gradient flow (9.6.8) corresponds to straight lines $n_1\theta_1 + n_2\theta_2 + n_3\theta_1 = 0$.

Since the central charges $Z_\tau(\gamma_i)$ are all equal at the orbifold point $\tau_o = \frac{1}{\sqrt{3}}e^{5\pi\mathrm{i}/6}$, the region $\mathbb{H}^o \subset \Pi$ includes an open set around $\tau = \tau_o$. Using the Eichler integral representation (9.1.5), it is immediate to compute the central charge to first order in $\tau - \tau_o$,

$$Z_\tau(\gamma) \simeq Z^o_\tau(\gamma) \coloneqq -\frac{r}{3} - \frac{d}{2} - \mathrm{ch}_2 + C(\tau_0)(d - r\tau_o)\,(\tau - \tau_o) \tag{9.6.22}$$

leading to the central charges for the simple objects

$$\begin{cases} Z_\tau(\gamma_1) \simeq \frac{1}{3} + \tau_o\, C(\tau_o)\,(\tau-\tau_o) \\ Z_\tau(\gamma_2) \simeq \frac{1}{3} - (2\tau_o+1)\, C(\tau_o)\,(\tau-\tau_o) \\ Z_\tau(\gamma_3) \simeq \frac{1}{3} + (\tau_o+1)\, C(\tau_o)\,(\tau-\tau_o) \end{cases} \tag{9.6.23}$$

Computing the stability parameters via (9.6.21), one finds that the coordinates (u,v) on the two-dimensional section (9.5.12) are related to the distance away from the orbifold point via

$$\tau - \tau_o \simeq \frac{2\mathrm{i}\sqrt{3}}{C(\tau_o)} e^{\mathrm{i}\psi}(u + \mathrm{i}v)\cos\psi \tag{9.6.24}$$

In particular, as $\psi \to \pm\frac{\pi}{2}$, the scattering diagram $\mathcal{D}_o$ is mapped to an infinitesimal neighbourhood of τ_o (see Figure 9.10).

Going away from the orbifold point, the region $\mathbb{H}^o$ is bounded in the fundamental domain $\mathcal{F}_o$ by the condition

$$\Im(\overline{Z_\tau(E_1)}Z_\tau(E_3)) > 0 \tag{9.6.25}$$

and similarly by conditions $\Im(\overline{Z_\tau(E_2)}Z_\tau(E_1)) > 0$, $\Im(\overline{Z_\tau(E_3)}Z_\tau(E_2)) > 0$ in the images $M_o\mathcal{F}_o$ and $M_o^2\mathcal{F}_o$ under the $\mathbb{Z}_3$ symmetry. In terms of the variables (s,w) defined in (9.1.7), where walls of

(anti)marginal stability are straight lines (see (9.2.29)), the inequality (9.6.25) in $\mathcal{F}_o$ amounts to

$$w + \frac{1}{2}s < 0 \tag{9.6.26}$$

In that region, the coordinates (u, v) on the two-dimensional section of the quiver scattering diagram can be expressed in terms of the affine coordinates (9.6.6),

$$u = -\frac{1}{2}x + y + \frac{1}{12}, \quad v = -\frac{1}{2\sqrt{3}}\left(x + \frac{1}{2}\right) \tag{9.6.27}$$

such that the rays in the exact scattering diagram map to segments contained in the geometric rays (9.5.13).

However, while the initial rays $\mathcal{R}_o(\gamma_i)$ in the quiver scattering diagram extend to infinity inside the space of King stability conditions, they actually originate from conifold points at $\tau = 0, -\frac{1}{2}, -1$ in the slice of Π-stability conditions. Using the values of the periods in Table 9.3, one finds that these conifold points are mapped to points at finite distance in the coordinates defined by (9.6.27). To make this precise, let us parametrize the initial rays $\mathcal{R}_o(\gamma_i)$ in the quiver scattering diagram as

$$p_1(\lambda) = \left(\frac{1}{12} - \frac{\lambda}{2}, \frac{-2\lambda - 1}{4\sqrt{3}}\right), \quad p_2(\lambda) = \left(-\frac{1}{6}, \frac{\lambda}{\sqrt{3}}\right), \quad p_3(\lambda) = \left(\frac{1}{12} + \frac{\lambda}{2}, \frac{-2\lambda + 1}{4\sqrt{3}}\right) \tag{9.6.28}$$

with $\lambda \in \mathbb{R}$. In this parametrization, the ray $\mathcal{R}_o(\gamma_i)$ starts from $\lambda = -\infty$ and intersects $\mathcal{R}_o(\gamma_{i-1})$ and $\mathcal{R}_o(\gamma_{i+1})$ at $p_i(-1/2)$ and $p_i(1/2)$, respectively, reproducing the intersection points in (9.5.14).

In contrast to the rays $\mathcal{R}_o(\gamma_i)$ in the orbifold scattering diagram, the rays $\mathcal{R}_\psi(\gamma_i)$ in the slice of Π-stability conditions start from the images of the conifold points at $\tau = 0, -\frac{1}{2}, -1$ in the (u, v)-plane, given by the points $p_i(\mathcal{V}_\psi)$ with $\lambda = \mathcal{V}_\psi$. For $\psi = -\frac{\pi}{2} + \epsilon$ with $\epsilon \to 0^+$, these initial points recess to infinity, and one recovers the infinite two-dimensional scattering diagram constructed above. Similarly, for $\psi = \frac{\pi}{2} - \epsilon$ with $\epsilon \to 0^+$, the initial points of the rays $\mathcal{R}_\psi(-\gamma_i)$ associated to the exceptional collection $E_i[1]$ recess to infinity. On the contrary, for ψ small enough such that $|\mathcal{V}_\psi| < \frac{1}{2}$, the initial points are such that the initial rays $\mathcal{R}_\psi(\gamma_i)$ can no longer interact among themselves (see Figure 9.28).

In between these two regimes, there are critical phases ψ such that some ray in the scattering diagram $\mathcal{D}_o$ passes through one of the initial points $p_i(\mathcal{V}_\psi)$ (see Figure 9.24). The first of these critical values arise from the discrete series of rays $\mathcal{R}_\psi(F_{2k}\gamma_i + F_{2k+2}\gamma_{i+1})$ emitted in the scattering of γ_i and γ_{i+1}, where F_k are the Fibonacci numbers. As mentioned above (9.1.13) in the introduction, this leads to jumps in the topology of the scattering sequence contributing to the index $\Omega_\infty(\gamma)$ along the ray $\mathcal{R}_\psi(\gamma)$ as a function of the phase ψ.

9.6.4 Exact scattering diagram

Having identified the image of the large volume and orbifold region in affine coordinates, we are ready to describe the exact scattering diagram $\mathcal{D}^\Pi_\psi$ in the same coordinates. We prove the Split Attractor Flow Conjecture on the slice of Π-stability conditions, and give an algorithm to list the finite set of trees that contribute to a given (rational) DT invariant. Depending on the phase ψ, we find that $\mathcal{D}^\Pi_\psi$ has the following structure, modulo the action of $\Gamma_1(3)$:

- For small phases $|\psi| < \psi^{\rm cr}_{1/2}$ (where $\psi^{\rm cr}_\alpha$ was defined in (9.1.13)), $\mathcal{D}^\Pi_\psi$ coincides with the large volume diagram $\mathcal{D}^{\rm LV}_0$ in the (x, y) plane, except for a shift in the origin of the initial rays.

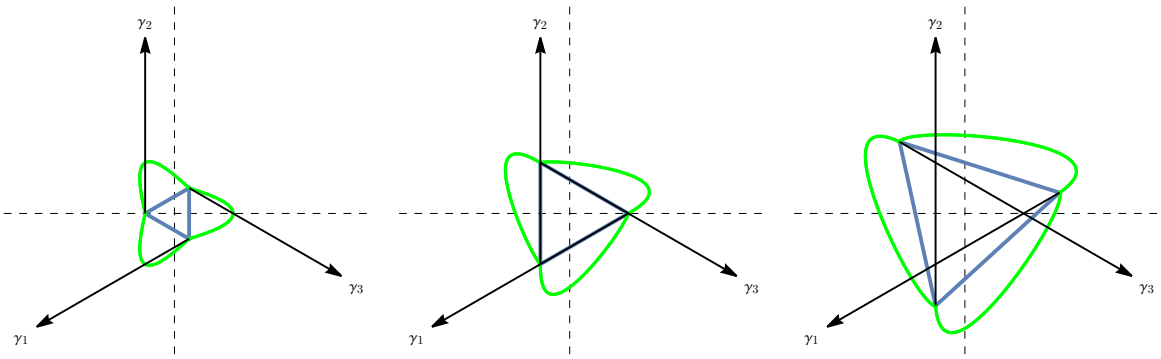

Figure 9.28: Initial rays around the orbifold point in (u, v) plane for $\psi = 0$ (left), $\psi = -\psi^{\rm cr}_{1/2}$ (middle) and $\psi < -\psi^{\rm cr}_{1/2}$ (right). The dashed lines represent the $u = 0$ and $v = 0$ axis. The green curves correspond to the boundary of the region $\mathbb{H}^o$ defined around (9.6.25). The blue triangle is the face Δ_ψ in a tesselation of $\mathbb{H}$ defined in §9.6.4. As $\psi \to -\frac{\pi}{2}$, the initial points recess to infinity, and the scattering diagram reduces to Figure 9.5.

- For large phases $\psi^{\rm cr}_{1/2} < |\psi| < \pi/2$ that are not critical (as defined at the end of §9.6.3), $\mathcal{D}^\Pi_\psi$ includes a triangular portion of the orbifold diagram, whose outbound rays seed scattering diagrams in the large volume region.

- For $\psi = \pi/2$, $\mathcal{D}^\Pi_\psi$ coincides with the $\theta_1 + \theta_2 + \theta_3 = 0$ slice of the quiver scattering diagram $\mathcal{D}_Q$ concentrated at the orbifold point τ_o in the τ-plane, supplemented with a vertical ray $\mathcal{R}(\mathcal{O}[1])$.

We refrain from discussing critical phases, since additional rays emanating from the conifold points complicate the analysis.[24]

Initial rays and a tessellation

A basic constraint on the scattering diagram $\mathcal{D}^\Pi_\psi$ is that it is invariant under the group $\Gamma_1(3)$ of auto-equivalences of $D^b\,\mathrm{Coh}(K_{\mathbb{P}^2})$, generated by tensor product by $\mathcal{O}_X(1)$ (acting by $T\colon \tau \mapsto \tau+1$) and by the spherical twist $\mathrm{ST}_\mathcal{O}$ (acting by $V\colon \tau \mapsto \frac{\tau}{1-3\tau}$). The quotient $\Pi/\Gamma_1(3)$ has two boundary points from which initial rays could emanate: the large volume point, which is ruled out because central charges grow without bound in this limit, and the conifold point. Without loss of generality, we can thus restrict to initial rays emanating from the point $\tau = 0$ in Π. The analysis in (9.6.4) (with $\tau = p/q = 0/1$ hence $m = m_D = 0$) shows a ray with charge $\gamma = [r, d, \mathrm{ch}_2]$ can only emanate from $\tau = 0$ if $d\mathcal{V}_\psi = \mathrm{ch}_2$. If $\mathcal{V}_\psi$ is irrational, this is only possible when $d = 0 = \mathrm{ch}_2$. In order to determine the associated attractor invariant, we use the fact that the orbifold and large volume descriptions valid in regions $\mathbb{H}^o$ and $\mathbb{H}^{\rm LV}$ that cover a neighborhood of $\tau = 0$. The outcome of this

[24] Our proof of the SAFC should go through for critical ψ, except that one must prove that the additional initial rays have positive values of the potential $\tilde\varphi_\tau(\gamma)$ defined in (9.6.34), a point which we have not investigated.

analysis in §9.7.12 is that the initial rays of the exact scattering diagram are[25]

$$\begin{aligned} \mathcal{R}^{\text{eff}}(\mathcal{O}): &\qquad \Omega([k,0,0]) = \delta_{k,1}, &&\text{and its } \Gamma_1(3) \text{ images},\\ \mathcal{R}^{\text{eff}}(\mathcal{O}[1]): &\qquad \Omega([-k,0,0]) = \delta_{k,1}, &&\text{and its } \Gamma_1(3) \text{ images}, \end{aligned} \tag{9.6.29}$$

provided ψ is *not critical* in a sense of Definition 9.1.2. In particular this holds for all small phases $|\psi| < \psi^{\text{cr}}_{1/2}$. Notably, since $V \in \Gamma_1(3)$ maps $\mathcal{O}(0)[n]$ to $\mathcal{O}(0)[n+2]$, the initial rays in $\mathcal{D}^{\Pi}_{\psi}$ include infinitely many effective rays starting from $\tau = 0$, which lie in images of $\mathcal{F}_C$ that border this point. By a mild abuse of notation we will denote by $\mathcal{R}^{\text{eff}}(\mathcal{O}(0)[n])$ these distinct rays, even though their charge vector only depends on the parity of n. More generally, there are an infinite set of rays emanating from every rational number $\tau = \frac{p}{q}$ with $q \neq 0 \mod 3$, corresponding to the images of $\mathcal{O}(0)[n]$ under $\Gamma_1(3)$. We denote by $\mathcal{R}^{\text{eff}}(\mathcal{O}(p/q)[n])$ the corresponding effective ray. For non-critical ψ, these images exhaust all initial rays. In particular, there are no rays emanating from the large volume points $\tau = \frac{p}{q}$ with $q = 0 \mod 3$, nor from points with $\tau \notin \mathbb{Q}$.

For any $\psi \in (-\pi/2, \pi/2)$ we introduce a $\Gamma_1(3)$-invariant tessellation of Π. Edges of the tiles consist of all $\Gamma_1(3)$ images of the straight line joining the conifold points $(x_{\mathcal{O}(-1)}, y_{\mathcal{O}(-1)})$ to $(x_{\mathcal{O}(0)}, y_{\mathcal{O}(0)})$ in the (x, y) plane. There are two types of tiles: an orbifold region around each $\Gamma_1(3)$ image of τ_o and a large volume region around each image of $\tau = \mathrm{i}\infty$. The orbifold region around τ_o is the aforementioned triangle Δ_ψ, whose corners are images of $\tau = 0, -1/2, -1$. The large volume region $\diamondsuit_\psi$ around $\tau = \mathrm{i}\infty$ maps in (x, y) coordinates to the region above the piecewise linear function (or 'jagged parabola', depicted in Figure 9.29)

$$y \geq \mathsf{p}(x) \coloneqq \Big(m + \mathcal{V}_\psi + \frac{1}{2}\Big)(\mathcal{V}_\psi - x) + \frac{m(m+1)}{2} \quad \text{with } m = \lfloor x - \mathcal{V}_\psi \rfloor \tag{9.6.30}$$

zigzaging between[26] the parabolas $y + \frac{1}{2}x^2 - \frac{1}{2}(\mathcal{V}_\psi)^2 \in \{0, \frac{1}{8}\}$. The boundary of $\diamondsuit_\psi$ joins consecutive conifold points $(x_{\mathcal{O}(m)}, y_{\mathcal{O}(m)})$, $m \in \mathbb{Z}$, so that $\diamondsuit_\psi$ borders all translates of Δ_ψ, while Δ_ψ borders three large volume regions. The initial rays (9.6.29) emanate from vertices of the tessellation by construction, and they enter different regions depending on ψ.

Small phases $|\psi| < \psi^{\text{cr}}_{1/2}$

Within Δ_ψ, the exact diagram $\mathcal{D}^{\Pi}_{\psi}$ coincides with a triangular region of the orbifold diagram $\mathcal{D}_o$. For our first case of interest, $|\mathcal{V}_\psi| < 1/2$, this region lies inside the empty central triangle of $\mathcal{D}_o$, thus Δ_ψ does not contain any ray, as depicted in Figure 9.28. The large volume regions are thus disconnected from each other in $\mathcal{D}^{\Pi}$, so that we can focus on $\diamondsuit_\psi$.

The initial rays in that region are $\mathcal{R}^{\text{eff}}(\mathcal{O}(m))$ and $\mathcal{R}^{\text{eff}}(\mathcal{O}(m)[1])$, emanating from integer conifold points $\tau = m \in \mathbb{Z}$. In (x, y) coordinates, the geometric ray $\mathcal{R}^{\text{geo}}(\pm[1, m, m^2/2])$ is contained in the line $y + mx = m^2/2$ tangent to the parabola $y + x^2/2 = 0$ at $x = m$. The active rays $\mathcal{R}^{\text{eff}}(\mathcal{O}(m))$ and $\mathcal{R}^{\text{eff}}(\mathcal{O}(m)[1])$ emanate leftwards/rightwards from the point $(x_{\mathcal{O}(m)}, y_{\mathcal{O}(m)}) = (m + \mathcal{V}_\psi, -m^2/2 - m\mathcal{V}_\psi)$ on this line: for $\psi = 0$ this coincides with the point of tangency with the parabola, while for $\psi \lessgtr 0$ it is moved left/right along the tangent line.

For $\psi = 0$, the initial rays $\mathcal{R}^{\text{eff}}(\mathcal{O}(m))$ and $\mathcal{R}^{\text{eff}}(\mathcal{O}(m)[1])$ for all $m \in \mathbb{Z}$ coincide with the initial rays for $\mathcal{D}^{\text{LV}}_0$. Under conditions that are fulfilled here, consistent scattering diagrams are uniquely

[25] To lighten the notation, we omit the ψ-dependence of the rays.

[26] To see this, rewrite $\mathsf{p}(x) = \frac{(\mathcal{V}_\psi)^2 - x^2}{2} + \frac{(2\{x - \mathcal{V}_\psi\} - 1)^2 - 1}{8}$ where $\{x\} = x - \lfloor x \rfloor$ denotes the fractional part.

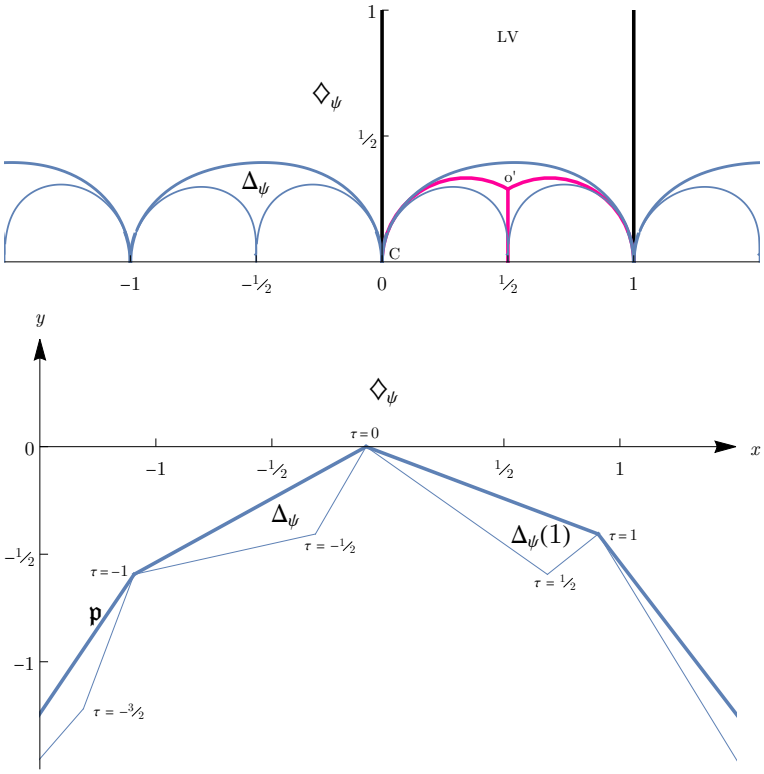

Figure 9.29: The upper half plane $\mathbb{H}$ is partitioned into regions $g \cdot \diamondsuit_\psi$ around images of the large volume point $i\infty$ and $g \cdot \Delta_\psi$ around images of the orbifold point τ_o. The region Δ_ψ and its translates $\Delta_\psi(k)$ map to triangles in the (x, y) plane, while the region $\diamondsuit_\psi$ above all blue curves maps to the region above the "jagged parabola" $\mathfrak{p}$ defined in (9.6.30). The figures are drawn for $\psi = -0.2$. While the figure in the τ plane is rather insensitive to the value of $\psi \in [0, 2\pi]$, the images of these regions in the (x, y) plane depend significantly on it: for instance the images of $\diamondsuit_\psi$ and Δ_ψ overlap for $\psi < -\psi^{\rm cr}_{1/2}$.

determined by the initial rays, so that $\mathcal{D}_0^{\Pi} \cap \diamondsuit_\psi$ coincides with $\mathcal{D}_0^{\mathrm{LV}}$ up to the map $\tau \mapsto (x, y)$. The rest of the exact diagram is completed by $\Gamma_1(3)$ invariance, namely $\mathcal{D}_{\psi=0}^{\Pi}$ consists of all images of $\mathcal{D}^{\mathrm{LV}}$ under $\Gamma_1(3)$, in which translations simply map $\mathcal{D}^{\mathrm{LV}}$ to itself.

In the large volume diagram $\mathcal{D}^{\mathrm{LV}}$, the first intersection along each initial ray is the intersection with the neighboring initial ray, with intersection points

$$\mathcal{R}^{\mathrm{geo}}(\mathcal{O}(m)) \cap \mathcal{R}^{\mathrm{geo}}(\mathcal{O}(m-1)) = \left\{(x,y) = \left(m - \tfrac{1}{2}, -\tfrac{1}{2}m(m-1)\right)\right\} \tag{9.6.31}$$

In other words, along each geometric ray there is a neighborhood of $(x, y) = (m, -m^2/2)$ in which there is no intersection. When ψ is varied away from zero, the initial point $(m+\mathcal{V}_\psi, -m^2/2 - m\mathcal{V}_\psi)$ remains in this intersection-free portion as long as $|\mathcal{V}_\psi| < 1/2$. We conclude that for small phases $|\psi| < \psi_{1/2}^{\mathrm{cr}}$, the exact diagram $\mathcal{D}_\psi^{\Pi}$ consists of disjoint copies (images under $\Gamma_1(3)$) of $\mathcal{D}^{\mathrm{LV}}$ with initial points shifted horizontally by $\mathcal{V}_\psi$ along the geometric rays.

To prove the (strong) SAFC for $\mathcal{D}_\psi^{\Pi}$ with $|\psi| < \psi_{1/2}^{\mathrm{cr}}$, we cannot rely on the absence of active rays in Δ_ψ and its $\Gamma_1(3)$ images, as only the leaves of attractor flow trees are required to be active. We must instead prove that edges of attractor flow trees cannot enter Δ_ψ. Recall that tree edges are straight line segment in (x, y) coordinates. We call such an edge 'outbound' if it lies in a large volume region $g \cdot \diamondsuit_\psi$ and if the line segment, prolonged in the attractor flow direction, intersects the boundary $\partial(g \cdot \diamondsuit_\psi) = g \cdot \mathfrak{p}$. In other words, an edge is outbound if it moves away from that boundary when following the scattering diagram direction. For instance, the initial rays $\mathcal{R}^{\mathrm{eff}}(\mathcal{O})$ and $\mathcal{R}^{\mathrm{eff}}(\mathcal{O}[1])$, supported on the line $y = 0$, are outbound: indeed, apart from the initial point $(x_{\mathcal{O}(0)}, y_{\mathcal{O}(0)}) = (\mathcal{V}_\psi, 0)$ of these rays, all other vertices $(x_{\mathcal{O}(m)}, y_{\mathcal{O}(m)})$ of the polygonal curve $\mathfrak{p}$ are below $y = 0$ since

$$y_{\mathcal{O}(m)} = -\tfrac{1}{2}m(m + 2\mathcal{V}_\psi) \leq 0 \tag{9.6.32}$$

thanks to m and $m + 2\mathcal{V}_\psi$ having the same sign for $m \in \mathbb{Z}$ and $|\mathcal{V}_\psi| < 1/2$. The leaves of an attractor flow tree are among the initial rays, which are $\Gamma_1(3)$ images of $\mathcal{R}^{\mathrm{eff}}(\mathcal{O})$ and $\mathcal{R}^{\mathrm{eff}}(\mathcal{O}[1])$, hence are outbound. Two outbound rays $\mathcal{R}(\gamma')$, $\mathcal{R}(\gamma'')$ can only intersect if they lie in the same large volume region, and any bound state $\mathcal{R}(n'\gamma' + n''\gamma'')$ lies in the angular sector between $\mathcal{R}(\gamma')$ and $\mathcal{R}(\gamma'')$ hence is outbound. We deduce that in an attractor flow tree all rays are outbound and must lie in the same large volume region. The SAFC for $\mathcal{D}_\psi^{\Pi}$ is then equivalent to the SAFC for $\mathcal{D}^{\mathrm{LV}}$ since trees contributing to a given $\bar{\Omega}_\tau(\gamma)$ are simply trees in one of the copies of $\mathcal{D}^{\mathrm{LV}}$. Assuming without loss of generality (up to $\Gamma_1(3)$ transformation of τ and γ) that $\tau \in \diamondsuit_\psi$, the electric potential $\varphi_\tau(\gamma) = 2(d - rx)$ bounds the number of leaves of the tree as in §9.4.2, while a causality argument (9.4.14) bounds the slope $m \in \mathbb{Z}$ of the initial rays which which can contribute. This establishes Theorem 9.1.3 for $|\psi| < \psi_{1/2}^{\mathrm{cr}}$.

Large phases $\psi_{1/2}^{\mathrm{cr}} < |\psi| < \pi/2$

More generally, the exact diagram combines aspects of the orbifold and large volume diagrams. For definiteness, we consider $-\pi/2 < \psi < -\psi_{1/2}^{\mathrm{cr}}$, namely $\mathcal{V}_\psi < -1/2$. Then, the $\Gamma_1(3)$ images of $\mathcal{R}^{\mathrm{eff}}(\mathcal{O})$ enter large volume regions while those of $\mathcal{R}^{\mathrm{eff}}(\mathcal{O}[1])$ enter orbifold regions. Specifically, $\mathcal{R}^{\mathrm{eff}}(\mathcal{O})$ enters $\diamondsuit_\psi$ while its homological shift $\mathcal{R}^{\mathrm{eff}}(\mathcal{O}[-1])$ enters Δ_ψ.[27] In the region Δ_ψ the exact scattering diagram coincides with the corresponding portion of $\mathcal{D}_o$, as argued in §9.6.3 on general

[27] For $\mathcal{V}_\psi > 1/2$, the situation is analogous: $\mathcal{R}^{\mathrm{eff}}(\mathcal{O}[1])$ enters $\diamondsuit_\psi$ while $\mathcal{R}^{\mathrm{eff}}(\mathcal{O})$ enters Δ_ψ.

grounds.[28] The initial ray $\mathcal{R}^{\text{eff}}(\mathcal{O})$, together with rays exiting from Δ_ψ to $\diamondsuit_\psi$, and all of their translates, then serve as incoming rays for the scattering diagram in the large volume region $\diamondsuit_\psi$.

By the same argument as for small ψ, all active rays in $\diamondsuit_\psi$ are outbound (point away from $\mathfrak{p}$ in the (x, y) plane), and more generally, the $\diamondsuit_\psi$ portion of any attractor flow tree consists only of outbound rays. In particular, none of these rays can ever re-enter Δ_ψ. The resulting picture for $\mathcal{D}^\Pi$ is that three initial rays scatter within Δ_ψ, producing some rays that leave Δ_ψ towards $\diamondsuit_\psi$; these rays further scatter with $\mathcal{R}^{\text{eff}}(\mathcal{O})$ and with translates of all of these rays so as to produce an ever denser set of outbound rays, similarly to the $|\psi| < \psi^{\text{cr}}_{1/2}$ case but with additional incoming rays from the orbifold regions. Throughout this process, only a limited set of initial rays participate in the construction of the scattering diagram in $\diamondsuit_\psi$:

$$\mathcal{R}^{\text{eff}}(\mathcal{O}(m)[-1]),\ \mathcal{R}^{\text{eff}}(\Omega(m+1)),\ \mathcal{R}^{\text{eff}}(\mathcal{O}(m-1)[1])\ \text{ and }\ \mathcal{R}^{\text{eff}}(\mathcal{O}(m)) \tag{9.6.33}$$

for each $m \in \mathbb{Z}$, which amount to one initial ray from each conifold point $\tau = m - 1/2$ and three from each integer conifold point.

Let us now prove the Split Attractor Flow Conjecture. As we have shown, edges of an attractor flow tree cannot exit the orbifold region Δ_ψ (in the attractor flow direction). Thus, for $\tau \in \Delta_\psi$ the problem reduces to the orbifold diagram, where the dimension vector $\gamma = (n_1, n_2, n_3)$ has a finite number of decompositions into elementary charges of the form $k\gamma_i$, and each decomposition leads to a finite number of trees with those leaves. This proves the conjecture for $\tau \in \Delta_\psi$.

For $\tau \in \diamondsuit_\psi$, infinitely many leaf rays (9.6.33) could in principle contribute. Since edges cannot exit orbifold regions, attractor flow trees ending at τ can be sawed into a *trunk* within $\diamondsuit_\psi$ rooted at τ, with leaves that are initial rays $\mathcal{R}(\mathcal{O}(m))$, and various *shrubs* in orbifold regions $\Delta_\psi(m)$. This is exemplified in Figure 9.9 on page 212. The trunk must lie in $H \cap \diamondsuit_\psi$, where H is the convex hull of $\mathfrak{p} = \partial\diamondsuit_\psi$ and of τ: this is easily seen by induction starting from the root, using the fact that all rays of the tree within $\diamondsuit_\psi$ are outbound. Since H has a finite extent in x, we learn that the set of orbifold regions that can be reached by the split attractor flow starting from τ is finite, therefore attractor flow trees have finitely many possible constituents.

This does not suffice for establishing finiteness however: as in the large volume diagram, some charges of possible constituents are opposite to each other, hence there are still infinitely many decompositions of γ. To deal with this, we introduce a variant of the electric potential of the large volume diagram, defined piecewise by

$$\tilde{\varphi}_\tau(\gamma) = \begin{cases} 2(d - r\lfloor x - \mathcal{V}_\psi \rfloor) & \text{in } \diamondsuit_\psi \\ c_\psi(n_1 + n_2 + n_3) & \text{in } \Delta_\psi \end{cases} \qquad \text{with } c_\psi := \frac{4(-2\mathcal{V}_\psi - 1)}{12\mathcal{V}_\psi^2 + 1} \tag{9.6.34}$$

extended to all of $\mathbb{H}$ by the action of $\Gamma_1(3)$.[29] We shall now prove that the potential is monotonically decreasing from the root to the (sum of) leaves of any attractor flow tree, as in the large volume diagram. It is manifestly additive in the charge γ, so that (the sum over all branches of) $\tilde{\varphi}_\tau(\gamma)$ does not jump at nodes of the tree. For a given edge in Δ_ψ, the potential $\tilde{\varphi}_\tau(\gamma)$ is constant. Next, we note that $\tilde{\varphi}_\tau(\gamma)$ is non-increasing along edges in $\diamondsuit_\psi$: if $r = 0$ this is immediate, while if $r \gtrless 0$ it follows from the monotonicity of x hence of $\lfloor x - \mathcal{V}_\psi \rfloor$ from (9.6.16).

It remains to check that $\tilde{\varphi}_\tau(\gamma)$ decreases when an edge $\{ry + dx = \text{ch}_2\}$ of the tree crosses from $\diamondsuit_\psi$ to Δ_ψ in the attractor flow direction. The boundary between these regions is the line segment

[28] An alternative proof of the matching is that the three $\mathbb{Z}_3$ images of $\mathcal{R}^{\text{eff}}(\mathcal{O}[-1])$ carry the same initial data as in the orbifold diagram and consistency allows for a unique diagram with that initial data.

[29] The definition in $\diamondsuit_\psi$ is consistent with $\Gamma_1(3)$ covariance: $\tau \to \tau + 1$ maps $x \to x + 1$ and $d \to d + r$.

between conifold points $(\mathcal{V}_\psi - 1, \mathcal{V}_\psi - 1/2)$ and $(\mathcal{V}_\psi, 0)$, namely $\{x - \mathcal{V}_\psi = y/(\frac{1}{2} - \mathcal{V}_\psi) \in (-1, 0)\}$. The intersection point of the two lines is easy to find, and must satisfy $x - \mathcal{V}_\psi \in (-1, 0)$. In addition, the tangents $(r, -d)$ and $(1, 1/2 - \mathcal{V}_\psi)$ must have the correct relative orientation for the attractor flow to enter Δ_ψ:

$$x - \mathcal{V}_\psi = \frac{\mathrm{ch}_2 - \mathcal{V}_\psi d}{d + r(\frac{1}{2} - \mathcal{V}_\psi)} \in (-1, 0), \qquad \begin{vmatrix} r & -d \\ 1 & \frac{1}{2} - \mathcal{V}_\psi \end{vmatrix} = d + r\Big(\frac{1}{2} - \mathcal{V}_\psi\Big) > 0 \tag{9.6.35}$$

Combining these inequalities yields $\mathcal{V}_\psi d - \mathrm{ch}_2 < d + r(\frac{1}{2} - \mathcal{V}_\psi)$, or equivalently $-\frac{d}{2} - \mathrm{ch}_2 < (d + r)(\frac{1}{2} - \mathcal{V}_\psi)$. We deduce

$$\begin{aligned} n_1 + n_2 + n_3 = -r - \frac{3}{2}d - 3\mathrm{ch}_2 &< -r + 3(d + r)\Big(\frac{1}{2} - \mathcal{V}_\psi\Big) \\ &< \Big[\frac{1}{-\mathcal{V}_\psi - 1/2} + 3\Big(\frac{1}{2} - \mathcal{V}_\psi\Big)\Big](d + r) \end{aligned} \tag{9.6.36}$$

In terms of the constant c_ψ spelled out in (9.6.34), this inequality reads $c_\psi(n_1 + n_2 + n_3) < 2(d + r)$, namely the potential $\tilde{\varphi}_\tau(\gamma)$ evaluated on the Δ_ψ side of the boundary is less than the potential evaluated on the $\diamondsuit_\psi$ side (to evaluate the latter we have used (9.6.35) to see that $\lfloor x - \mathcal{V}_\psi \rfloor = -1$). This establishes that the total electric potential is monotonically decreasing in any tree in the attractor flow direction.

The final step is to prove that the potential $\tilde{\varphi}_\tau(\gamma)$ is positive for all initial rays (9.6.33) at their starting point. Up to translations we only need to consider $\mathcal{R}(\mathcal{O})$ and the three initial rays of the orbifold diagram. The ray $\mathcal{R}(\mathcal{O})$ starts at $(\mathcal{V}_\psi - \epsilon, 0)$ with $\epsilon \to 0^+$, thus has a positive potential

$$\tilde{\varphi}(\mathcal{R}(\mathcal{O})) = 2(0 - \lfloor -\epsilon \rfloor) = 2 > 0 \tag{9.6.37}$$

The three initial rays of the quiver diagram have $(n_1, n_2, n_3) = (1, 0, 0)$ and permutations thereof, hence $\tilde{\varphi} = c_\psi > 0$. We conclude that the number of constituents participating in an attractor flow tree rooted at τ with total charge γ is at most $\tilde{\varphi}_\tau(\gamma)/\min(2, c_\psi)$.

The SAFC now follows by noting that trees contributing to $\bar{\Omega}_\tau(\gamma)$ are made of a bounded number of constituents taken among a finite set, hence there are finitely many possible lists of constituents. For each such list there are finitely many ways that these constituents can be arranged into a topological tree. For each topology there is at most one attractor flow tree in $\mathbb{H}$, constructed by following the attractor flow starting from the root. There is no ambiguity about where the flow should split: if some edge with charge γ' splits (in the topological tree) into $\gamma'_1 + \gamma'_2$, then the attractor flow must split when hitting the wall of marginal stability of γ' and γ'_1, which can only be crossed once according to (9.6.2). The flow may fail to hit that wall, in which case the topological tree does not correspond to any attractor flow tree. This establishes Theorem 9.1.3 for $\psi^{\mathrm{cr}}_{1/2} < |\psi| < \pi/2$.

Behavior in the limits $\psi \to \pm\pi/2$

For $\psi = \pi/2$, the scattering diagram $\mathcal{D}^{\Pi}_\psi$ drastically simplifies. In that case, geometric rays $\mathcal{R}^{\mathrm{geo}}(\gamma)_\psi$ satisfy

$$\Im Z_\tau(\gamma) = -r\Im T_D + d\Im T \tag{9.6.38}$$

thus are included in contours of constant slope $s = \frac{\Im T_D}{\Im T} = \frac{d}{r}$, independent of the value of ch_2 (see Figure 9.10). The contours only intersect at points where s is ill-defined, i.e. when $\Im T = \Im T_D = 0$.

These two curves intersect at the orbifold point τ_o and $\Gamma_1(3)$ images thereof. At τ_o, there are three incoming rays

$$\mathcal{R}^{\text{eff}}(\mathcal{O}),\ \mathcal{R}^{\text{eff}}(\Omega(1)[1]),\ \mathcal{R}^{\text{eff}}(\mathcal{O}(-1)[2]) \tag{9.6.39}$$

The first and last emanate from $\tau = 0$ and $\tau = -1$ and lie along the boundary of the fundamental domain $\mathcal{F}_o$, where $s = 0$ and $s = -1$, respectively while $\mathcal{R}^{\text{eff}}(\Omega(1)[1])$ is a vertical line emanating from $\tau = -1/2$, with slope $s = -1/2$. In addition, there are vertical rays $\mathcal{R}^{\text{eff}}(\mathcal{O}(m)[1])$ for any $m \in \mathbb{Z}$, which do not interact with the rays (9.6.39). Consistency at τ_o fixes uniquely the outgoing rays, which then continue on towards a large volume limit, either at $\tau \to -\frac{1}{2} + \mathrm{i}\infty$, $\tau \to -\frac{2}{3} + \mathrm{i}0$ or $\tau \to -\frac{1}{3} + \mathrm{i}0$. The rays (9.6.39) are associated to the homological shifts $E_i[1]$ of the objects E_i in the exceptional collection (9.1.8). Their scattering diagram around τ_o, which we denote by $\mathcal{D}_o^\vee$, is simply obtained from $\mathcal{D}_o$ by sending $(u, v) \mapsto (-u, -v)$ and reversing the direction of the arrows. Equivalently, we can send $(u, v) \mapsto (-u, v)$ and exchange γ_1 and γ_3, which amounts to applying the derived duality (9.2.32) and a suitable translation. Thus, the scattering diagram $\mathcal{D}^\Pi_{\pi/2}$ consists of the scattering diagram $\mathcal{D}_o^\vee$ concentrated at the point τ_o, the vertical ray $\mathcal{R}^{\text{eff}}(\mathcal{O}[1])$ and all $\Gamma_1(3)$ images thereof.

Similarly, for $\psi = -\pi/2 + \epsilon$ with $\epsilon \to 0^+$, the rays associated to the objects E_i in the exceptional collection (9.1.8).

$$\mathcal{R}^{\text{eff}}(\mathcal{O}[-1]),\ \mathcal{R}^{\text{eff}}(\Omega(1)),\ \mathcal{R}^{\text{eff}}(\mathcal{O}(-1)[1]) \tag{9.6.40}$$

intersect in a region of size ϵ around τ_o. As $\epsilon \to 0$, the scattering diagram $\mathcal{D}^\Pi_{-\pi/2+\epsilon}$ reduces to the orbifold scattering diagram $\mathcal{D}_o$ concentrated in a region of size ϵ at the point τ_o, the vertical ray $\mathcal{R}^{\text{eff}}(\mathcal{O})$ and all their $\Gamma_1(3)$ images.

In either case, the SAFC on $\mathcal{D}^\Pi_{\pi/2}$ reduces to the flow tree formula for quivers, which is proven in [AB21]. Moreover, the fact that rays do not intersect away from orbifold points makes it clear that the index $\Omega_c(\gamma)$ computed using the quiver associated to the exceptional collection $E_i(k)$ will coincide with the Gieseker index $\Omega_\infty(\gamma)$ along the ray $\mathcal{R}_{\pi/2}(\gamma)$ provided $k - 1 \leq \frac{d}{r} \leq k$ for $r \neq 0$, as observed in [DFR05b, BMP21a]. This concludes the proof of Theorem 9.1.3 for all non-critical phases $\psi \in (-\pi/2, \pi/2]$.

9.6.5 Case studies

In this final section, we study the scattering sequences which contribute to the Gieseker index $\Omega_\infty(\gamma)$ for two simple choices of charges, as function of the phase ψ. The initial rays in these sequences turn out to jump at a subset of the critical phases of Definition 9.1.2, while the index remains unaffected. This is reminiscent of the 'fake walls' encountered in earlier studies [ADJM12, CLSS13, AP19a], where the structure of the bound state changes while the index remains unchanged.

We first consider $\gamma = [0, 1, 1)$, corresponding to the Chern vector of the structure sheaf $\mathcal{O}_C$ of a rational curve in the hyperplane class. As noted below (9.2.14), the moduli space $\mathcal{M}_\infty(\gamma)$ is $\mathbb{P}^2$ itself, so $\Omega_\tau(\gamma)$ should equal $y^2 + 1 + 1/y^2$ for $\tau_2 \gg 1$ and arbitrary values of τ_1. Thus, for any $\psi \in (-\pi/2, \pi/2)$ the scattering diagram should contain a ray $\mathcal{R}^{\text{eff}}_\psi(\gamma)$ reaching $\tau_2 = \mathrm{i}\infty$ with the above index. The scattering sequences which contribute to this index however depend sensitively on the value of ψ (which we can assume to be negative, using the reflection symmetry of the scattering diagram):

- $-\psi^{\text{cr}}_{\frac{1}{2}} < \psi < \psi^{\text{cr}}_{\frac{1}{2}} \simeq 0.82406$: $T_0 = \{\mathcal{O}(-1)[1], \mathcal{O}(0)\}$ contributing $K_3(1, 1)$;

- $-\psi^{\rm cr}_{\frac{3}{2}} \simeq -1.27155 < \psi < -\psi^{\rm cr}_{\frac{1}{2}}$: $T_1 = \{2\mathcal{O}(0)[1], \Omega(2)\}$ contributing $K_3(1,2)$;
- $-\psi^{\rm cr}_{\frac{5}{2}} \simeq -1.38766 < \psi < -\psi^{\rm cr}_{\frac{3}{2}}$: $T_2 = \{3\mathcal{O}(1)[1], \{2\Omega(3), \mathcal{O}(2)[-1]\}\}$ contributing $K_3(1,2)K_3(1,3)$;
- $-\psi^{\rm cr}_{\frac{7}{2}} \simeq -1.43934 < \psi < -\psi^{\rm cr}_{\frac{5}{2}}$: $T_3 = \{3\mathcal{O}(2)[1], \{3\Omega(4), \{2\mathcal{O}(3)[-1], \mathcal{O}(2)[1]\}\}\}$ contributing $K_3(1,2)K_3(1,3)$;

In all cases, the tree produces the desired index $y^2 + 1 + 1/y^2$. More generally, when

$$-\psi^{\rm cr}_{n+1/2} < \psi < -\psi^{\rm cr}_{n-1/2} \ , \tag{9.6.41}$$

we find a single tree T_n with constituents in the positive cone spanned by the exceptional collection $\langle \mathcal{O}(n)[-1], \Omega(n+1), \mathcal{O}(n-1)[1] \rangle$ with Chern vectors $\gamma_1(n), \gamma_2(n), \gamma_3(n)$, obtained from (9.1.8) by n units of spectral flow (and homology shift $[-1]$). The tree T_n has $n+1$ constituents and is of the iterated form

$$T_n = \{k_1\gamma_3(n), \{k_2\gamma_2(n), \{k_3\gamma_1(n), \{k_4\gamma_3(n), \{k_5\gamma_2(n), \dots\}\}\}\}, \tag{9.6.42}$$

where $k_i = 3$ for $i = 1, \dots n-1$ and $k_n = 2, k_{n+1} = 1$. Equivalently, T_n is defined inductively by

$$T_n = \{3\gamma_3(n), \sigma_n^{-1} \cdot T_{n-1}(1)\} \ , \quad T_1 = \{2\gamma_3(1), \gamma_2(1)\} \tag{9.6.43}$$

where $T(1)$ is the tree T shifted by one unit of spectral flow, and σ_n acts by cyclic permutation

$$\sigma_n \colon \gamma_1(n) \mapsto \gamma_2(n) \ , \quad \gamma_2(n) \mapsto \gamma_3(n) \ , \quad \gamma_3(n) \mapsto \gamma_1(n) \tag{9.6.44}$$

The charges indeed add up to $(n-1)\gamma_1(n) + n\gamma_2(n) + (n+1)\gamma_3(n) = [0,1,1)$, and the index evaluates to $K_3(1,2)K_3(1,3)^{n-1} = y^2 + 1 + 1/y^2$. In Figure 9.30 we plot the scattering sequences for the first few values of n.

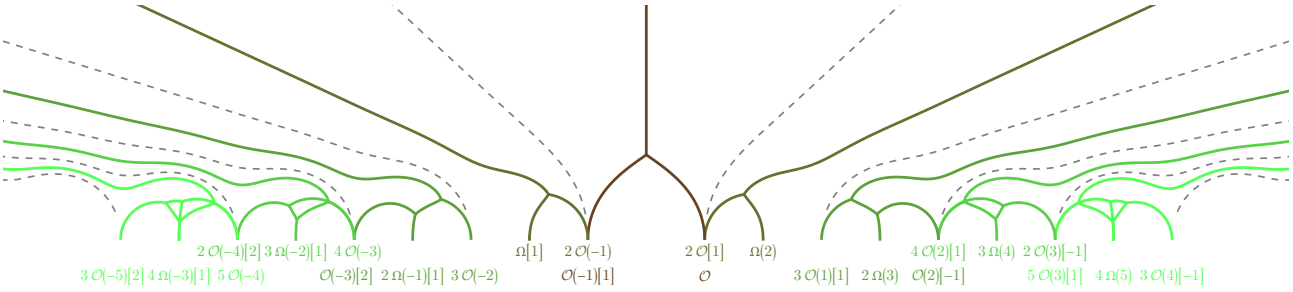

Figure 9.30: Attractor flow trees contributing to $\gamma = [0,1,-\frac{1}{2}] = [0,1,1)$ for ψ varying from $-\frac{\pi}{2}$ (right) to $\frac{\pi}{2}$ (left). The dashed lines corresponding to the incoming rays for $\psi = \psi^{\rm cr}_\alpha$ with $\alpha \in \{\pm\frac{1}{2}, \pm\frac{3}{2}, \pm\frac{5}{2}, \dots\}$.

We now consider $\gamma = [1,0,1)$, the Chern vector of the structure sheaf $\mathcal{O}$. This object is spherical and stable throughout the large volume region. In particular, for large τ_2 and any $\tau_1 < 0$, the index $\Omega_\tau(\gamma)$ should equal 1.

- In the range $-\frac{\pi}{2} < \psi < \psi^{\rm cr}_{1/2}$, there is a single ray originating from the conifold point $\mathcal{O}(0) = \gamma_1(0)[1]$;
- In the range $\psi^{\rm cr}_{\frac{1}{2}} < \psi < \psi^{\rm cr}_1$, we find a single sequence $\{3\mathcal{O}(-1), \Omega(0)[1]\}$ contributing $K_3(1,3) = 1$;
- In the range $\psi^{\rm cr}_1 < \psi < \psi^{\rm cr}_{\frac{3}{2}}$, we find a single sequence $\{6\mathcal{O}(-2), \{3\Omega(-1)[1], \mathcal{O}(-3)[2]\}\}$ contributing $K_3(1,3)K_6(1,6) = 1$;

More generally, for $\psi^{\rm cr}_{\frac{n}{2}} < \psi < \psi^{\rm cr}_{\frac{n+1}{2}}$ there is a sequence T_n obtained inductively through

$$T_n = \{(3n)\gamma_1(-n)[1], \sigma_{-n}\cdot T_{n-1}(-1)\}\ , \quad T_0 = \{\gamma_1(0)[1]\} \tag{9.6.45}$$

with total charge $[1,0,1)$ contributing 1 to the index. In Figure 9.31 we plot the scattering sequences for the first few values of n.

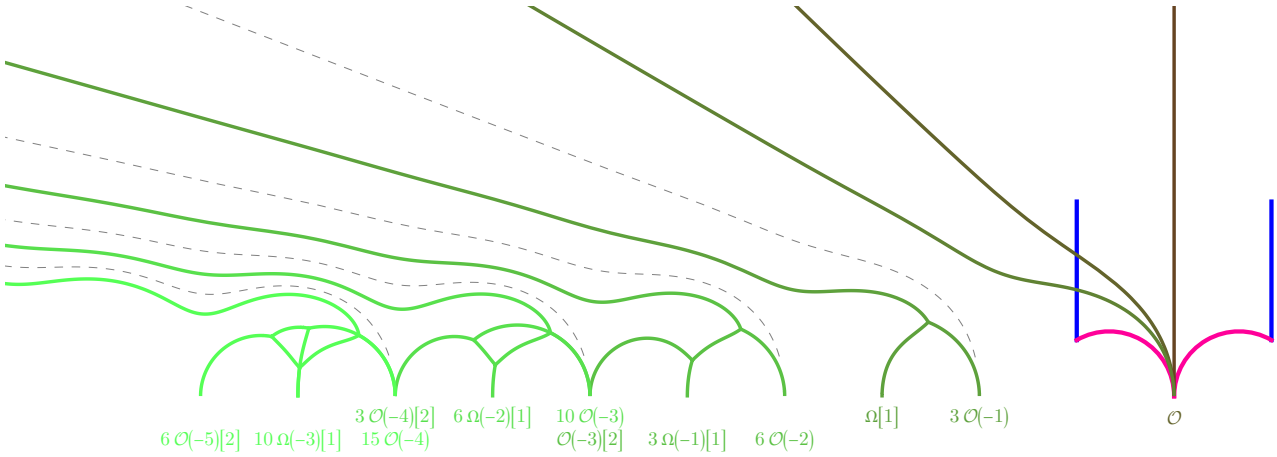

Figure 9.31: Attractor flow trees contributing to $\gamma = [1,0,0] = [1,0,1)$ for ψ varying from $-\frac{\pi}{2}$ (right) to $\frac{\pi}{2}$ (left). The dashed lines corresponding to the incoming rays for $\psi = \psi^{\rm cr}_\alpha$ with $\alpha \in \{\frac{1}{2}, 1, \frac{3}{2}, \dots\}$.

9.7 Appendix

9.7.1 Periods as Eichler integrals

In this section, we review the modular description of the Kähler moduli space of $K_{\mathbb{P}^2}$, derive the Eichler integral representation (9.1.5) of the periods (T, T_D), and use it to obtain asymptotic expansions around the large volume, conifold and orbifold points and the behavior under monodromies. We refer to [CKYZ99, DG00, Asp04, ABK08, HKR08, BM11, ASYZ14] for earlier studies in the literature.[30]

[30] We are grateful to Thorsten Schimannek for his help about the material in this section.

9.7.2 Kähler moduli space as the modular curve $X_1(3)$

Recall that the mirror of $K_{\mathbb{P}^2}$ is a family of genus-one curves $\Sigma(z) = x_1^3+x_2^3+x_3^3-z^{-1/3}x_1x_2x_3 = 0$ in $\mathbb{P}^2$ parametrized by the complex structure modulus $z \in \mathcal{M}_K = \mathbb{C}\backslash\{0,-\frac{1}{27}\}$, which is identified as the complexified Kähler moduli space of $K_{\mathbb{P}^2}$. The points $z = 0, -\frac{1}{27}, \infty$ then correspond to the large radius, conifold and orbifold points, respectively. Alternatively, we can consider the family of genus-one curves $\Sigma'(z')\colon x+y+1-z'x^3/y = 0$ in $\mathbb{C}_x^\times \times \mathbb{C}_y^\times$, related to $\Sigma(z)$ with $z' = -z-\frac{1}{27}$ by a 3-isogeny. The points $z' = 0, -\frac{1}{27}, \infty$ then correspond to the conifold, large radius and orbifold points, respectively.

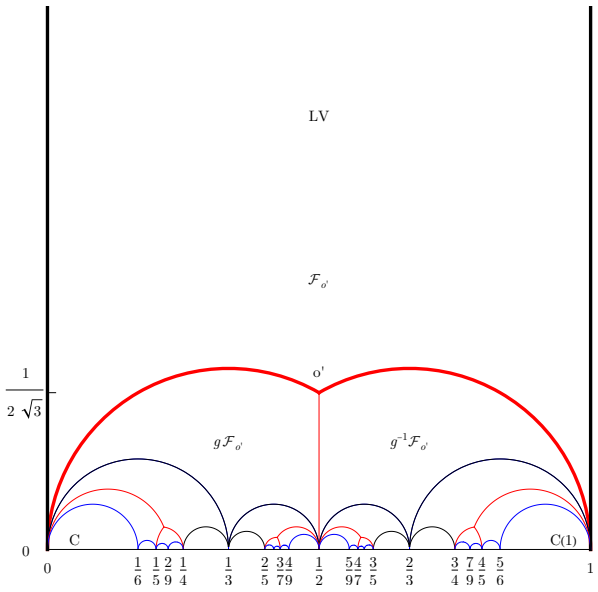

Figure 9.32: Fundamental domain $\mathcal{F}_{o'}$ centered around the orbifold point $\tau_{o'} = e^{\mathrm{i}\pi/6}/\sqrt{3}$, and some of its images. Here $g = ST^{-2}STS\colon \tau \mapsto \frac{\tau-1}{3\tau-2}$ and $g^{-1} = TST^3S\colon \tau \mapsto \frac{2\tau-1}{3\tau-1}$. The fundamental domain $\mathcal{F}_o$ is the same domain translated to the interval $[-1,0]$.

The space $\mathcal{M}_K$ is isomorphic to the modular curve $X_1(3) = \mathbb{H}/\Gamma_1(3)$, where $\Gamma_1(3)$ is the group of integer matrices $\left(\begin{smallmatrix} a & b \\ c & d \end{smallmatrix}\right)$ such that $a, d = 1 \mod 3$ and $c = 0 \mod 3$. This is an index 4 subgroup of $PSL(2,\mathbb{Z})$, with two cusps of width 1 and 3, corresponding to the large volume and conifold points, respectively, and one elliptic point of order 3 corresponding to the orbifold point. A convenient choice of fundamental domain is the domain centered around the orbifold point at $\tau_o = \frac{1}{\sqrt{3}}e^{5\pi\mathrm{i}/6} = (-\frac{1}{2}, \frac{1}{2\sqrt{3}})$, shifted horizontally by $-1/2$ compared to (9.7.2),

$$\mathcal{F}_o \coloneqq \left\{\tau :\ -1 \le \tau_1 < 0, (\tau_1+\frac{2}{3})^2+\tau_2^2 \ge \frac{1}{9}, (\tau_1+\frac{1}{3})^2+\tau_2^2 > \frac{1}{9}\right\} \tag{9.7.1}$$

This domain (or rather its translate $\mathcal{F}_{o'} \coloneqq \mathcal{F}_o(1)$ under $\tau \mapsto \tau+1$) is depicted in Figure 9.32, along with several of its images under $\Gamma_1(3)$. Alternatively, one may choose a fundamental domain

centered around $\tau = 0$,

$$\mathcal{F}_C := \Big\{\tau : -\frac{1}{2} \leq \tau_1 < \frac{1}{2}, (\tau_1 + \frac{1}{3})^2 + \tau_2^2 \geq \frac{1}{9}, (\tau_1 - \frac{1}{3})^2 + \tau_2^2 > \frac{1}{9}\Big\} \tag{9.7.2}$$

shown in Figure 9.6. It has the nice property of being invariant under the Fricke involution $\tau \to -1/(3\tau)$.

The isomorphism $\mathcal{M}_K \simeq X_1(3)$ is given explicitly by

$$J_3(\tau) = -15 - \frac{1}{z} = \frac{12 - 405z'}{1 + 27z'}, \tag{9.7.3}$$

where $J_3(\tau)$ is the normalized Hauptmodul of $\Gamma_1(3)$,

$$J_3 := \left(\frac{\eta(\tau)}{\eta(3\tau)}\right)^{12} + 12 = \frac{1}{q} + 54q - 76q^2 - 243q^3 + 1188q^4 - 1384q^5 - 2916q^6 + \dots \tag{9.7.4}$$

where $q = e^{2\pi i\tau}$. The latter maps the points $\tau = i\infty, 0$ and τ_o to $J_3 = \infty, 12$ and -15, corresponding to the large volume, conifold and orbifold points, respectively. One easily checks that the Fricke involution maps $J_3 \mapsto \frac{729}{J_3 - 12} + 12$ and $z \mapsto z'$. Plugging the q-expansion (9.7.4) into (9.7.3), we get

$$\begin{aligned} q &= -z + 15z^2 - 279z^3 + 5729z^4 - 124554z^5 + 2810718z^6 + \dots \\ z &= -q + 15q^2 - 171q^3 + 1679q^4 - 15054q^5 + 126981q^6 + \dots \end{aligned} \tag{9.7.5}$$

The Klein invariant is expressed in terms of J_3 via

$$J := \frac{E_4^3(\tau)}{\eta^{24}(\tau)} = J_3 + 744 + \frac{196830}{J_3 - 12} + \frac{19131876}{(J_3 - 12)^2} + \frac{387420489}{(J_3 - 12)^3} \tag{9.7.6}$$

leading to

$$J = \frac{(216z - 1)^3}{z(1 + 27z)^3} = -\frac{(1 + 24z')^3}{z'^3(1 + 27z')} \tag{9.7.7}$$

Using the isomorphism $\mathcal{M}_K \simeq X_1(3)$, the universal cover of $\mathcal{M}_K$ is therefore identified with the Poincaré upper half plane, tesselated by an infinite number of copies of the fundamental domain $\mathcal{F}_C$.

9.7.3 Periods as Eichler integrals

Under mirror symmetry, the central charges $(T(\tau), T_D(\tau))$ of the D2-brane and D4-brane are identified with periods $(\varpi, \varpi_D) = (\int_\ell \lambda, \int_{\ell_D} \lambda)$ of a suitable meromorphic differential λ over a basis of one cycles (ℓ, ℓ_D) on the mirror curve. Each of these periods satisfies the degree 3 Picard-Fuchs equation

$$\big[\Theta^2 + 3z(3\Theta + 2)(3\Theta + 1)\big]\Theta \cdot \begin{pmatrix} \varpi \\ \varpi_D \end{pmatrix} = 0 \tag{9.7.8}$$

where $\Theta = z\partial_z$. On the other hands, the periods $(\varpi', \varpi'_D) = (\int_\ell \omega, \int_{\ell_D} \omega)$ of the unique (up to scale) holomorphic differential ω on the mirror curve satisfy the degree 2 Picard-Fuchs equation

$$\big[\Theta^2 + 3z(3\Theta + 2)(3\Theta + 1)\big] \cdot \begin{pmatrix} \varpi' \\ \varpi'_D \end{pmatrix} = 0 \tag{9.7.9}$$

It follows that

$$\Theta \cdot \begin{pmatrix} \varpi \\ \varpi_D \end{pmatrix} = \begin{pmatrix} \varpi' \\ \varpi'_D \end{pmatrix} \tag{9.7.10}$$

Identifying the modular parameter as the ratio $\tau = \frac{\varpi'_D}{\varpi'}$, we find that ϖ'_D transforms as a modular form of weight 1 under $\Gamma_1(3)$, hence it is given (up to normalization) by the weight 1 Eisenstein series (denoted by A in [BFGW21]),

$$\varpi'(\tau) = 1 + 6\sum_{m\geq 1}\Big(\sum_{n|m}\chi(n)\Big)q^m = 1 + 6q + 6q^3 + 6q^4 + 12q^7 + \dots \tag{9.7.11}$$

where $\chi(n) = \left(\frac{n}{-3}\right)$ is the Dirichlet character equal to $+1$ for $n = 1 \mod 3$, -1 for $n = 2 \mod 3$ and 0 otherwise. Let C be the weight 3 Eisenstein series with the same character,

$$C(\tau) = 1 - 9\sum_{m\geq 1}\Big(\sum_{n|m} n^2\chi(n)\Big)q^m = 1 - 9\sum_{n\geq 1}\frac{\chi(n)q^n}{1-q^n} \tag{9.7.12}$$

This modular form can also be written as an eta product

$$C(\tau) := \frac{\eta(\tau)^9}{\eta(3\tau)^3} = \sum_{n=1}^{\infty} c_n q^n = 1 - 9q + 27q^2 - 9q^3 - 117q^4 + \dots \tag{9.7.13}$$

which makes it clear that it does not vanish anywhere in $\mathbb{H}$. The ratio $\frac{C-\varpi'^3}{27\varpi'^3}$ is a meromorphic function on $X_1(3)$, which can be shown coincides with z. Using the differential identities in $\frac{C-\varpi'^3}{27\varpi'^3}$, we obtain immediately that $z\partial_z = \frac{\varpi'}{C}\partial_\tau$. Substituting into (9.7.10), we get

$$\frac{d}{d\tau}\begin{pmatrix} T \\ T_D \end{pmatrix} = C\begin{pmatrix} 1 \\ \tau \end{pmatrix} \tag{9.7.14}$$

Using the values $(T, T_D) = (-\frac{1}{2}, \frac{1}{3})$ at the orbifold point τ_o [DG00] we can write the periods as a holomorphic Eichler integral

$$\begin{pmatrix} T \\ T_D \end{pmatrix} = \begin{pmatrix} -\frac{1}{2} \\ \frac{1}{3} \end{pmatrix} + \int_{\tau_o}^{\tau}\begin{pmatrix} 1 \\ u \end{pmatrix} C(u)\mathrm{d}u \tag{9.7.15}$$

Equivalently, using the identity

$$\int_{\tau_o}^{\tau_{o'}}\begin{pmatrix} 1 \\ u \end{pmatrix} C(u)\mathrm{d}u = \begin{pmatrix} 1 \\ 0 \end{pmatrix} \tag{9.7.16}$$

proven at the end of §9.7.7, one can also take $\tau_{o'} = \tau_o + 1$ as a base point and write

$$\begin{pmatrix} T \\ T_D \end{pmatrix} = \begin{pmatrix} \frac{1}{2} \\ \frac{1}{3} \end{pmatrix} + \int_{\tau_{o'}}^{\tau}\begin{pmatrix} 1 \\ u \end{pmatrix} C(u)\mathrm{d}u \tag{9.7.17}$$

This representation (or equivalently (9.7.15)) provides a global formula for the analytic continuation of T and T_D throughout the upper half-plane, which gives immediate access to the asymptotic expansions near all singular points and monodromies around them. It also proves to be very efficient for numerical evaluations. In Table 9.3 we record the values of the periods at some special points. Using $\overline{C(\tau)} = C(-\bar\tau)$ and (9.7.16), it is easy to establish the reality properties

$$\overline{T(\tau)} = -T(-\bar\tau)\ , \quad \overline{T_D(\tau)} = T_D(-\bar\tau)\ , \tag{9.7.18}$$

At the end of §9.7.7, we use (9.7.18) to conclude that $\Im T_D = 0$ on the semi-circle $\mathcal{C}(-\frac{1}{3}, \frac{1}{3})$ passing through the orbifold point τ_o. As a result, the slope $s = \Im T_D/\Im T$ vanishes on that semi-circle.

Table 9.3: Periods at some special points.

τ	z	j	J_3	T	T_D
$n \in \mathbb{Z}$	$-\frac{1}{27}$	∞	12	$n + \mathrm{i}\,\mathcal{V}$	$\frac{n^2}{2} + n\mathrm{i}\,\mathcal{V}$
$\frac{1}{2}$	$-\frac{1}{27}$	∞	12	$\frac{1}{2} - 2\mathrm{i}\,\mathcal{V}$	$\frac{1}{2} - \mathrm{i}\,\mathcal{V}$
$-\frac{1}{2}$	$-\frac{1}{27}$	∞	12	$-\frac{1}{2} - 2\mathrm{i}\,\mathcal{V}$	$\frac{1}{2} + \mathrm{i}\,\mathcal{V}$
$\frac{1}{4}$	$-\frac{1}{27}$	∞	12	$\frac{5}{2} + 4\mathrm{i}\,\mathcal{V}$	$\frac{1}{2} + \mathrm{i}\,\mathcal{V}$
$\frac{3}{4}$	$-\frac{1}{27}$	∞	12	$-\frac{3}{2} + 4\mathrm{i}\,\mathcal{V}$	$-\frac{3}{2} + 3\mathrm{i}\,\mathcal{V}$
$\frac{1}{5}$	$-\frac{1}{27}$	∞	12	$2 - 5\mathrm{i}\,\mathcal{V}$	$\frac{1}{2} - \mathrm{i}\,\mathcal{V}$
$\frac{2}{5}$	$-\frac{1}{27}$	∞	12	$4 - 5\mathrm{i}\,\mathcal{V}$	$2 - 2\mathrm{i}\,\mathcal{V}$
$\frac{3}{5}$	$-\frac{1}{27}$	∞	12	$-3 - 5\mathrm{i}\,\mathcal{V}$	$-\frac{3}{2} - 3\mathrm{i}\,\mathcal{V}$
$\frac{3}{7}$	$-\frac{1}{27}$	∞	12	$3 + 7\mathrm{i}\,\mathcal{V}$	$\frac{3}{2} + 3\mathrm{i}\,\mathcal{V}$
$\tau_o + n = \frac{e^{\mathrm{i}\pi/6}}{\sqrt{3}}$	∞	0	-15	$n - \frac{1}{2}$	$\frac{1}{3} + \frac{n(n-1)}{2}$
$\frac{9+\mathrm{i}\sqrt{3}}{42}$	∞	0	-15	$\frac{3}{2}$	$\frac{1}{3}$
$\frac{33+\mathrm{i}\sqrt{3}}{42}$	∞	0	-15	$-\frac{1}{2}$	$-\frac{2}{3}$
$\frac{33\mathrm{i}\sqrt{3}}{78}$	∞	0	-15	$\frac{5}{2}$	$\frac{4}{3}$
$\frac{45+\mathrm{i}\sqrt{3}}{78}$	∞	0	-15	$-\frac{3}{2}$	$-\frac{2}{3}$
$e^{2\pi\mathrm{i}/3}$	$\frac{1}{216}$	0	-231	$-\frac{1}{2} + 0.859778\,\mathrm{i}$	$-0.118598 - 0.429889\,\mathrm{i}$
$e^{\pi\mathrm{i}/3}$	$\frac{1}{216}$	0	-231	$\frac{1}{2} + 0.859778\,\mathrm{i}$	$-0.118598 + 0.429889\,\mathrm{i}$
i	$\frac{5-3\sqrt{3}}{108}$	1728	$255 + 162\sqrt{3}$	1.00267i	-0.378093

9.7.4 Expansion around large radius

In the large radius limit, integrating term-by-term the q-expansion of C, we get

$$\int_{\tau_o}^{\tau} \begin{pmatrix} 1 \\ u \end{pmatrix} C(u)\mathrm{d}u = \begin{pmatrix} \tau - \tau_o + \frac{1}{2\pi\mathrm{i}} \left(\bar{f}_1(\tau) - \bar{f}_1(\tau_o) \right) \\ \frac{1}{2}\tau^2 - \frac{1}{2}\tau_o^2 + \frac{1}{2\pi\mathrm{i}} \left(\tau\, \bar{f}_1(\tau) - \tau_o \bar{f}_1(\tau_o) \right) + \frac{1}{(2\pi\mathrm{i})^2} \left(\bar{f}_2(\tau) - \bar{f}_2(\tau_o) \right) \end{pmatrix} \tag{9.7.19}$$

where

$$\bar{f}_1(\tau) \coloneqq \sum_{n=1}^{\infty} \frac{c_n}{n} q^n \ , \quad \bar{f}_2(\tau) \coloneqq -\sum_{n=1}^{\infty} \frac{c_n}{n^2} q^n \tag{9.7.20}$$

We observe numerically that for $\tau = \tau_o$,

$$\tau_o + \frac{1}{2\pi\mathrm{i}} \bar{f}_1(\tau_o) = -\frac{1}{2} \ , \quad -\frac{1}{2}\tau_o^2 - \frac{\tau_o}{2\pi\mathrm{i}} \bar{f}_1(\tau_o) + \frac{1}{(2\pi\mathrm{i})^2} \bar{f}_2(\tau_o) = -\frac{1}{8} \tag{9.7.21}$$

we find that

$$T = \frac{f_1}{2\pi\mathrm{i}} - \frac{1}{2} \ , \quad T_D = \frac{f_2}{(2\pi\mathrm{i})^2} - \frac{f_1}{4\pi\mathrm{i}} + \frac{1}{4} \tag{9.7.22}$$

with

$$f_1 \coloneqq \log(-q) + \bar{f}_1 \ , \quad f_2 \coloneqq \frac{1}{2}[\log(-q)]^2 + \bar{f}_1 \log(-q) + \bar{f}_2 \ , \tag{9.7.23}$$

Consequently, we have

$$T = \tau + \frac{\bar{f}_1}{2\pi\mathrm{i}}\ , \quad T_D = \frac{1}{2}\tau^2 + \frac{1}{8} + \frac{\tau\,\bar{f}_1}{2\pi\mathrm{i}} + \frac{\bar{f}_2}{(2\pi\mathrm{i})^2} \tag{9.7.24}$$

In particular, on any vertical line with $2\tau_1 \in \mathbb{Z}$, we have

$$\Re T = \frac{\Im T_D}{\Im T} = \tau_1 \tag{9.7.25}$$

since $\bar{f}_1, \bar{f}_2$ are real. In the limit $\tau \to \mathrm{i}\infty$, $\bar{f}_1(\tau), \bar{f}_2(\tau)$ are exponentially suppressed hence $(T, T_D) \sim (\tau, \frac{1}{2}\tau^2)$. Substituting q in terms of z via (9.7.5), we find agreement with the usual representations in terms of Meijer G-functions [DG00]

$$f_1(z) = -\frac{1}{\Gamma(\frac{1}{3})\Gamma(\frac{2}{3})} G^{2,2}_{3,3}\left(\begin{smallmatrix}\frac{1}{3} & \frac{2}{3} & 1\\ 0 & 0 & 0\end{smallmatrix}\middle| 27z\right) \tag{9.7.26}$$

$$f_2(z) = \frac{1}{2}\left[G^{3,1}_{3,3}\left(\begin{smallmatrix}\frac{1}{3} & \frac{2}{3} & 1\\ 0 & 0 & 0\end{smallmatrix}\middle| 27z\right) + G^{3,1}_{3,3}\left(\begin{smallmatrix}\frac{2}{3} & \frac{1}{3} & 1\\ 0 & 0 & 0\end{smallmatrix}\middle| 27z\right)\right] - \frac{\pi^2}{3} \tag{9.7.27}$$

Expressing τ and T_D in terms of the flat coordinate T by inverting the q-expansions, we recover the usual expansion in terms of Gromov-Witten invariants,

$$T_D = (2\pi\mathrm{i})^2\left(\frac{T^2}{2} + \frac{1}{8}\right) - 9Q + \frac{135}{4}Q^2 + 244Q^3 + \frac{36999}{16}Q^4 + \frac{635634}{25}Q^5 + 307095Q^6 + \dots \tag{9.7.28}$$

where

$$Q := e^{2\pi\mathrm{i}T} = q + 9q^2 + 54q^3 + 246q^4 + 909q^5 + 2808q^6 + \dots \tag{9.7.29}$$

The expansion (9.7.28) can be integrated term-by-term to obtain the tree-level prepotential

$$F_0 = (2\pi\mathrm{i})^3\left(-\frac{T^3}{18} - \frac{T}{24} - \frac{1}{36}\right) + 3Q - \frac{45}{8}Q^2 + \frac{244}{9}Q^3 - \frac{12333Q^4}{64} + \frac{211878Q^5}{125} - \frac{102365Q^6}{6} + \dots \tag{9.7.30}$$

such that $T_D = -\frac{3}{2\pi\mathrm{i}}\partial_T F_0$.

9.7.5 Expansion around conifold point

The expansion near the conifold can be obtained by applying the Fricke involution $\tau \mapsto \tau' = -1/(3\tau)$ which maps τ_o to $\tau_{o'} = \tau_o + 1$ and C to

$$C'(\tau') := \frac{\eta(3\tau')^9}{\eta(\tau')^3} = \sum_{n=1}^{\infty} c'_n q'^n = q' + 3q'^2 + 9q'^3 + 13q'^4 + 24q'^5 + 27q'^6 + \dots \tag{9.7.31}$$

This is again recognized as an Eisenstein series,

$$C'(\tau') = \sum_{m\geq 1}\Big(\sum_{n|m} n^2\chi(m/n)\Big)q'^m = \sum_{n\geq 1}\chi(n)\frac{q'^n(1+q'^n)}{(1-q'^n)^2} \tag{9.7.32}$$

Changing variables $u \to u' = -1/(3u)$ in (9.7.15) and using $\eta(-1/\tau) = \sqrt{-\mathrm{i}\tau}\eta(\tau)$, we get

$$\begin{pmatrix} T \\ T_D \end{pmatrix} = \begin{pmatrix} -\frac{1}{2} \\ \frac{1}{3} \end{pmatrix} + \mathrm{i}\,3^{\frac{5}{2}}\int_{\tau_{o'}}^{\tau'} C'(u')\begin{pmatrix} 3u' \\ -1 \end{pmatrix}\mathrm{d}u' \tag{9.7.33}$$

Integrating terms by terms we get

$$\int_{\tau_{o'}}^{\tau} C'(u) \begin{pmatrix} 3u' \\ -1 \end{pmatrix} \mathrm{d}u = \begin{pmatrix} \frac{3}{2\pi \mathrm{i}} \left(\tau' f_1^c(\tau') - \tau_{o'} f_1^c(\tau_{o'})\right) + \frac{3}{(2\pi \mathrm{i})^2} \left(\bar{f}_2^c(\tau') - \bar{f}_2^c(\tau_{o'})\right) \\ -\frac{1}{2\pi \mathrm{i}} \left(f_1^c(\tau') - f_1^c(\tau_{o'})\right) \end{pmatrix} \tag{9.7.34}$$

where we defined

$$\begin{aligned} f_1^c(\tau') &\coloneqq \sum_{n=1}^{\infty} \frac{c'_n}{n} q'^n = q' + \frac{3}{2} q'^2 + 3q'^3 + \frac{13}{4} q'^4 + \dots \\ f_2^c(\tau') &\coloneqq f_1^c \log q' + \bar{f}_2^c(\tau') \\ \bar{f}_2^c(\tau') &\coloneqq -\sum_{n=1}^{\infty} \frac{c'_n}{n^2} q'^n = -q' - \frac{3}{4} q'^2 - q'^3 - \frac{13}{16} q'^4 - \dots \end{aligned} \tag{9.7.35}$$

We observe numerically that for $\tau = \tau_o$,

$$\kappa\, f_1^c(\tau_o) = -1, \quad \frac{\kappa}{2\pi \mathrm{i}} f_2^c(\tau_o) = \tfrac{1}{2} - \mathrm{i}\,\mathcal{V} \tag{9.7.36}$$

where

$$\kappa \coloneqq \frac{27\sqrt{3}}{2\pi}, \quad \mathcal{V} \coloneqq \frac{27}{4\pi^2} \Im \mathrm{Li}_2\left(e^{2\pi \mathrm{i}/3}\right) \simeq 0.462758 \tag{9.7.37}$$

we find that T, T_D can be expressed as

$$T = \frac{\kappa}{2\pi \mathrm{i}} f_2^c + \mathrm{i}\,\mathcal{V}\,, \quad T_D = -\frac{\kappa}{3} f_1^c \tag{9.7.38}$$

In particular, $(T, T_D) = (\mathrm{i}\mathcal{V}, 0)$ at the conifold point. Substituting q' in terms of z' using (9.7.5) (with $q \to q', z \to z'$), we recover the usual expression in terms of Meijer G-functions, and arrive at an alternative representation for the 'quantum volume' [CKYZ99],

$$\mathcal{V} = \frac{G_{3,3}^{2,2}\left(\begin{smallmatrix} \frac{1}{3} & \frac{2}{3} & 1 \\ 0 & 0 & 0 \end{smallmatrix} \middle| -1\right)}{2\pi\, \Gamma(\frac{1}{3})\Gamma(\frac{2}{3})} + \frac{\mathrm{i}}{2} \tag{9.7.39}$$

The value for $\mathcal{V}$ observed numerically in (9.7.37) can be determined exactly by evaluating (9.7.24) at $\tau = 0$ using zeta function regularization. Indeed, the L-series of $\bar{f}_1, \bar{f}_2$ easily evaluate to

$$L_{\bar{f}_1}(s) \coloneqq \sum_{m \geq 1} \frac{c_m}{m^{1+s}} = -9\zeta(s+1)\, L(s-1)\,, \quad L_{\bar{f}_2}(s) \coloneqq -\sum_{m \geq 1} \frac{c_m}{m^{2+s}} = 9\zeta(s+2)\, L(s) \tag{9.7.40}$$

where $L(s) \coloneqq \sum_{m \geq 1} \chi(m) m^{-s} = 3^{-s}\left(\zeta(s, \frac{1}{3}) - \zeta(s, \frac{2}{3})\right)$ is the Dirichlet L-series. Its completion

$$L^\star(s) = \left(\tfrac{3}{\pi}\right)^{\frac{s+1}{2}} \Gamma\left(\tfrac{s+1}{2}\right) L_s(s) \tag{9.7.41}$$

is analytic for $\Re(s) > 1$ and invariant under $s \mapsto 1 - s$, and so is the completed Riemann zeta function $\zeta^\star(s) = \pi^{-s/2}\Gamma(s/2)\zeta(s)$. Using this, one can evaluate the limit as $s \to 0$,

$$\bar{f}_1(0) = -9 \lim_{s \to 0} \zeta(s+1)\, L(s-1) = -\frac{27\sqrt{3} L(2)}{8\pi^2} \tag{9.7.42}$$

$$\bar{f}_2(0) = 9 \lim_{s \to 0} \zeta(s+2)\, L(s) = \frac{\pi^2}{2} \tag{9.7.43}$$

where we used $L(0) = 1/3$. This reproduces the expected value $(T, T_D) = (\mathrm{i}\,\mathcal{V}, 0)$ at $\tau = 0$.

9.7.6 Orbifold point

Near the orbifold point, integrating the Taylor expansion of C term by term we get

$$T = -\frac{1}{2} + C(\tau_o)(\tau-\tau_o) + \frac{1}{2}C'(\tau_o)(\tau-\tau_o)^2 + \dots \tag{9.7.44}$$

$$T_D = \frac{1}{3} + \frac{1}{2}C(\tau_o)(\tau^2-\tau_o^2) + \frac{1}{6}C'(\tau_o)(\tau-\tau_o)^2(2\tau+\tau_o) + \dots \tag{9.7.45}$$

We observe numerically that

$$C(\tau_o) = \frac{\Gamma(\frac{1}{3})^3}{\Gamma(\frac{2}{3})^6} \simeq 3.1185\ , \quad C'(\tau_o) = -\mathrm{i}\frac{729}{4\pi^{\frac{9}{2}}}\Gamma(\tfrac{1}{3})^3\Gamma(\tfrac{7}{6})^3 \simeq 16.2043\,\mathrm{i}\ , \tag{9.7.46}$$

$$J_3'''(\tau_o) = \frac{18\sqrt{3}\Gamma(\frac{1}{3})^9}{\mathrm{i}\Gamma(\frac{2}{3})^9} \simeq -14474\,\mathrm{i} \tag{9.7.47}$$

with the same values for $\tau = \tau_{o'}$. The flat coordinate $w = 1/z$ is obtained by expanding (9.7.3),

$$w = -J_3 - 15 = \frac{3\sqrt{3}\Gamma(\frac{1}{3})^9}{\mathrm{i}\,\Gamma(\frac{2}{3})^9}(\tau-\tau_o)^3 + \mathcal{O}((\tau-\tau_o)^6) \tag{9.7.48}$$

9.7.7 Monodromies

The monodromies around the three singular points can be computed by using the transformation property of the Eichler integral,

$$\begin{pmatrix} T+\frac{1}{2} \\ T_D-\frac{1}{3}\end{pmatrix}\left(\frac{a\tau+b}{c\tau+d}\right) = \begin{pmatrix} c & d \\ a & b\end{pmatrix}\begin{pmatrix} T+\frac{1}{2} \\ T_D-\frac{1}{3}\end{pmatrix}(\tau) + \int_{\frac{d\tau_o-b}{a-c\tau_o}}^{\tau_o}\begin{pmatrix} cu+d \\ au+b\end{pmatrix} C(u)\mathrm{d}u \tag{9.7.49}$$

whenever $ad-bc=1$, $c=0 \mod 3$. The last term is independent of τ, and is a degree 1 period polynomial for the weight 3 modular form C. It follows from (9.7.15) and (9.7.49) that the period vector $\Pi = (1, T, T_D)$ transforms as

$$\Pi^t \mapsto M\Pi^t \qquad M = \begin{pmatrix} 1 & 0 & 0 \\ m & d & c \\ m_D & b & a\end{pmatrix}\ , \tag{9.7.50}$$

where

$$\begin{pmatrix} m \\ m_D\end{pmatrix} = \begin{pmatrix} \frac{1}{2}(d-1)-\frac{c}{3} \\ \frac{1}{3}(1-a)+\frac{b}{2}\end{pmatrix} + \int_{\frac{d\tau_o-b}{a-c\tau_o}}^{\tau_o}\begin{pmatrix} cu+d \\ au+b\end{pmatrix} C(u)\mathrm{d}u \tag{9.7.51}$$

Consequently, the coordinates (s, w) defined in (9.1.7) transform as

$$s \mapsto \frac{as+b}{cs+d}, \quad w \mapsto \frac{w}{cs+d} + \frac{as+b}{cs+d}m - m_D \tag{9.7.52}$$

Under the $\Gamma_1(3)$ transformations

$$\tau \mapsto \tau+1\ , \quad \tau \mapsto -\frac{\tau}{3\tau-1}\ , \quad \tau \mapsto -\frac{\tau+1}{3\tau+2} \tag{9.7.53}$$

corresponding to monodromies around i∞, 0 and τ_o, we find, in agreement with [DFR05b][31]

$$M_{\rm LV} = \begin{pmatrix} 1 & 0 & 0 \\ 1 & 1 & 0 \\ \frac{1}{2} & 1 & 1 \end{pmatrix} \qquad M_C = \begin{pmatrix} 1 & 0 & 0 \\ 0 & 1 & -3 \\ 0 & 0 & 1 \end{pmatrix} \qquad M_o = \begin{pmatrix} 1 & 0 & 0 \\ -\frac{1}{2} & -2 & -3 \\ \frac{1}{2} & 1 & 1 \end{pmatrix} \tag{9.7.54}$$

satisfying $M_o = M_C M_{\rm LV}, M_o^3 = \mathbb{1}$.

In the remainder of this section, we prove the identity (9.7.16) and the statement below (9.2.32) by studying the action of the monodromy M_C. First, we observe that M_C maps τ_o to $\tau_{o'} = \tau_o + 1$, while preserving T_D. Thus, (9.7.15) implies the second equation in (9.7.16), namely

$$\int_{\tau_o}^{\tau_{o'}} u\, C(u) \mathrm{d}u = 0 \tag{9.7.55}$$

As a result, $T_D(\tau_{o'}) = T_D(\tau_o) = 1/3$. Similarly, M_C maps T to $T - 3T_D$, therefore $T(\tau_o) = T(\tau_{o'}) - 3T_D(\tau_{o'})$, which implies the first equation in (9.7.16),

$$\int_{\tau_o}^{\tau_{o'}} C(u) \mathrm{d}u = T(\tau_{o'}) - T(\tau_o) = 3T_D(\tau_{o'}) = 1 \tag{9.7.56}$$

Secondly, since M_C sends $\tau = \tau_1 + \mathrm{i}\tau_2$ to

$$-\frac{\tau}{3\tau - 1} = -\frac{3\tau_1^2 + 3\tau_2^2 - \tau_1}{3(3\tau_1^2 + 3\tau_2^2 - 2\tau_1) + 1} + \mathrm{i}\frac{\tau_2}{3(3\tau_1^2 + 3\tau_2^2 - 2\tau_1) + 1} \tag{9.7.57}$$

we see that on the half circle $\mathcal{C}(-1/3, 1/3)$ defined by $3\tau_1^2 + 3\tau_2^2 - 2\tau_1 = 0$, the action of M_C restricts to $\tau \mapsto -\bar\tau$. Since T_D is invariant under M_C, it follows that for any $\tau \in \mathcal{C}(-1/3, 1/3)$

$$T_D(\tau) = T_D(-\bar\tau) \tag{9.7.58}$$

Since $\overline{T_D(\tau)} = T_D(-\bar\tau)$ by (9.2.32), it follows that $\Im T_D = 0$ on the half circle $\mathcal{C}(-1/3, 1/3)$. □

9.7.8 Massless objects at conifold points

The structure sheaf $\mathcal{O}$ of $\mathbb{P}^2$ is a spherical object in the derived category $D^b(\mathrm{Coh}_c\, K_{\mathbb{P}^2})$, whose central charge vanishes at the conifold point $\tau = 0$. The action of the group $\Gamma_1(3)$ on the τ upper half-plane lifts to an action by auto-equivalences on the derived category of $K_{\mathbb{P}^2}$. Thus, for every $g \in \Gamma_1(3)$, $E = g(\mathcal{O})$ is a spherical object whose central charge vanishes at the conifold point $\tau = g(0) = p/q$ with $q \neq 0 \mod 3$. In this section we compute the object E for low values of p, q. The results are summarized in Table 9.1 on page 209.

For example, the element $V = \left(\begin{smallmatrix} 1 & 0 \\ -3 & 1 \end{smallmatrix}\right)$ (equal to the monodromy around the conifold point $\tau = 0$) acts on τ via $V\colon \tau \mapsto -\frac{\tau}{3\tau - 1}$, and on the derived category via the spherical twist $\mathrm{ST}_{\mathcal{O}}$ around the spherical object $\mathcal{O}$. The latter is given by the exact triangle (see (9.2.20) and [BM11, §9.1])

$$\mathrm{Hom}^\bullet_{K_{\mathbb{P}^2}}(\mathcal{O}, E) \otimes \mathcal{O} \xrightarrow{\mathrm{ev}} E \to \mathrm{ST}_{\mathcal{O}}(E) \xrightarrow{+1} \tag{9.7.59}$$

[31] This also agrees with [DG00] upon conjugating the matrices in by $\left(\begin{smallmatrix} 1 & 0 & 0 \\ 1/2 & 1 & 0 \\ 0 & 0 & 1 \end{smallmatrix}\right)$, due to a shift $T \to T + \frac{1}{2}$.

Similarly for $U = V^{-1}$ the action on the derived category is the inverse of the spherical twist $\mathrm{ST}_{\mathcal{O}}$ around the spherical object $\mathcal{O}$, which is given, following Proposition 2.10 of [ST00], by the exact triangle

$$\mathrm{ST}_{\mathcal{O}}^{-1}(E) \to E \xrightarrow{\mathrm{coev}} \mathrm{Hom}(\mathrm{Hom}^{\bullet}_{K_{\mathbb{P}^2}}(E,\mathcal{O}),\mathcal{O}) \xrightarrow{+1} \tag{9.7.60}$$

At the point $\tau = -1/2$, obtained by acting with VT on $\tau = 0$, the spherical object becoming massless is $\mathrm{ST}_{\mathcal{O}}(\mathcal{O}(1))$. We have $\mathrm{Hom}^0_{\mathbb{P}^2}(\mathcal{O},\mathcal{O}(1)) = \mathbb{C}^3$, $\mathrm{Hom}^k_{\mathbb{P}^2}(\mathcal{O},\mathcal{O}(1)) = 0$ for $k > 0$, and $\mathrm{Hom}^k_{\mathbb{P}^2}(\mathcal{O}(1),\mathcal{O}) = 0$ for $k \geq 0$. Hence, using (9.2.18),

$$\mathrm{Hom}^0_{K_{\mathbb{P}^2}}(\mathcal{O},\mathcal{O}(1)) = \mathrm{Hom}^0_{\mathbb{P}^2}(\mathcal{O},\mathcal{O}(1)) = \mathbb{C}^3 \ , \quad \mathrm{Hom}^{k\neq 0}_{K_{\mathbb{P}^2}}(\mathcal{O},\mathcal{O}(1)) = 0 \tag{9.7.61}$$

Finally, from the Euler exact sequence

$$0 \to \mathcal{O} \to \mathcal{O}(1)^{\oplus 3} \to T \to 0 \tag{9.7.62}$$

where T is the tangent bundle of $\mathbb{P}^2$, we obtain the exact sequence

$$0 \to \Omega(1) \to \mathcal{O}^{\oplus 3} \to \mathcal{O}(1) \to 0 \tag{9.7.63}$$

and so an exact triangle $\mathcal{O}^{\oplus 3} \to \mathcal{O}(1) \to \Omega(1)[1] \xrightarrow{+1}$. Hence the massless object at $\tau = -\frac{1}{2}$ is

$$\mathrm{ST}_{\mathcal{O}}(\mathcal{O}(1)) = \Omega(1)[1] \tag{9.7.64}$$

For the point $\tau = 4/5$, obtained by acting by TV on $\tau = -1/2$, the spherical object becoming massless is $\mathrm{ST}_{\mathcal{O}}(\Omega(1)[1])(1)$. Using (9.7.63) and the Bott vanishing theorem, we obtain $\mathrm{Hom}^0_{\mathbb{P}^2}(\Omega(1),\mathcal{O}) = \mathbb{C}^3$. On the other hand, using the Bott vanishing theorem and Riemann–Roch formula, we find that $\mathrm{Hom}^k_{\mathbb{P}^2}(\Omega(1),\mathcal{O}) = 0$ for all $k \neq 0$, and $\mathrm{Hom}^k_{\mathbb{P}^2}(\mathcal{O},\Omega(1)) = 0$ for all k. Hence, by (9.2.18),

$$\mathrm{Hom}^{\bullet}_{K_{\mathbb{P}^2}}(\mathcal{O},\Omega(1)) = \mathbb{C}^3[-3] \tag{9.7.65}$$

$$\mathrm{Hom}^3_{K_{\mathbb{P}^2}}(\mathcal{O},\Omega(1)) = \mathbb{C}^3 \ , \quad \mathrm{Hom}^{k\neq 3}_{K_{\mathbb{P}^2}}(\mathcal{O},\Omega(1)) \tag{9.7.66}$$

It follows that the exact triangle defining $E = \mathrm{ST}_{\mathcal{O}}(\Omega(1)[1])(1)$ is of the form

$$\mathcal{O}^{\oplus 3}(1)[-2] \to \Omega(2)[1] \to E \xrightarrow{+1} \tag{9.7.67}$$

Note in particular that E has rank -5 and degree -4, as expected.

It is important to remark that the map $\mathcal{O}^{\oplus 3}(1)[-2] \to \Omega(2)[1]$ in the derived category of $K_{\mathbb{P}^2}$ does not come from maps in the derived category of $\mathbb{P}^2$: indeed all extension groups $\mathrm{Hom}^3_{\mathbb{P}^2}$ between sheaves are zero since $\mathbb{P}^2$ is of dimension 2. As mentioned at the beginning of §9.2.2, in general, an object E in the derived category of coherent sheaves on $K_{\mathbb{P}^2}$ supported set-theoretically on the zero section can be viewed as a pair (F,ϕ) with F an object in the derived category of $\mathbb{P}^2$ and $\phi\colon F \to F \otimes K_{\mathbb{P}^2}$ a nilpotent Higgs field. For the object E defined by (9.7.67), since every map $\mathcal{O}^{\oplus 3}(1)[-2] \to \Omega(2)[1]$ in the derived category of $\mathbb{P}^2$ is zero, the underlying object F is simply the direct sum

$$F = \Omega(2)[1] \oplus \mathcal{O}^{\oplus 3}(1)[-1] \tag{9.7.68}$$

but there is a non-trivial nilpotent Higgs field on F coming from a map $\mathcal{O}^{\oplus 3}(1)[-1] \to \Omega(-1)[1]$ in $D^b(\mathrm{Coh}\,\mathbb{P}^2)$. Note that by Serre duality, we have

$$\mathrm{Hom}^2_{\mathbb{P}^2}(\mathcal{O}(1), \Omega(-1)) = \mathrm{Hom}_{\mathbb{P}^2}(\Omega(2), \mathcal{O}(1))^\vee \tag{9.7.69}$$

which is indeed non-zero.

The same type of analysis provides the exact triangles giving the following massless objects at other conifold points.

- $\tau = 1/5$, $g = U^2T^{-1}$. Because of the relations $(VT)^3 = 1$ and $U = V^{-1}$,

$$UT^{-1}(\mathcal{O}) = TVTV(\mathcal{O}) = TVT(\mathcal{O}[-2]) = \Omega(2)[-1] \tag{9.7.70}$$

  In the quiver associated to the exceptional collection $(\mathcal{O}, \Omega(2)[-1], \mathcal{O}(1)[-2])$ there are 3 relations and no arrows from the second to the first node, so we deduce successively

$$\mathrm{Hom}^\bullet_{K_{\mathbb{P}^2}}(\Omega(2)[-1], \mathcal{O}) = \mathbb{C}^3[-2] \tag{9.7.71}$$

$$\mathrm{Hom}(\mathrm{Hom}^\bullet_{K_{\mathbb{P}^2}}(\Omega(2)[-1], \mathcal{O}), \mathcal{O}) = \mathcal{O}^{\oplus 3}[2] \tag{9.7.72}$$

  The object $E = U(\Omega(2)[-1])$ is then given by the exact triangle

$$E \to \Omega(2)[-1] \to \mathcal{O}^{\oplus 3}[2] \xrightarrow{+1} \tag{9.7.73}$$

- $\tau = 1/4$, $g = UT$. One has $\mathrm{Hom}(\mathrm{Hom}^\bullet_{K_{\mathbb{P}^2}}(\mathcal{O}(1), \mathcal{O}), \mathcal{O}) = \mathrm{Hom}(\mathbb{C}^3[-3], \mathcal{O}) = \mathcal{O}^{\oplus 3}[3]$, thus the object $E = U(\mathcal{O}(1))$ is given by the exact triangle

$$E \to \mathcal{O}(1) \to \mathcal{O}^{\oplus 3}[3] \xrightarrow{+1} \tag{9.7.74}$$

- $\tau = 2/5$, $g = UT^{-2}$. One has $\mathrm{Hom}(\mathrm{Hom}^\bullet_{K_{\mathbb{P}^2}}(\mathcal{O}(-2), \mathcal{O}), \mathcal{O}) = \mathrm{Hom}(\mathbb{C}^6, \mathcal{O}) = \mathcal{O}^{\oplus 6}$, thus $E = U(\mathcal{O}(-2))$ is given by the exact triangle

$$E \to \mathcal{O}(-2) \to \mathcal{O}^{\oplus 6} \xrightarrow{+1} \tag{9.7.75}$$

- $\tau = 1/2$, $g = TVT$. This is a translate of (9.7.64), namely $E = \Omega(2)[1]$.
- $\tau = 3/5$, $g = TVT^2$. One has $\mathrm{Hom}^\bullet_{K_{\mathbb{P}^2}}(\mathcal{O}, \mathcal{O}(2)) = \mathbb{C}^6$, hence $E = TV(\mathcal{O}(2))$ is given by the exact triangle

$$\mathcal{O}(1)^{\oplus 6} \to \mathcal{O}(3) \to E \xrightarrow{+1} \tag{9.7.76}$$

- $\tau = 3/4$, $g = TVT^{-1}$. One has $\mathrm{Hom}^\bullet_{K_{\mathbb{P}^2}}(\mathcal{O}, \mathcal{O}(-1)) = \mathbb{C}^3[-3]$, hence $E = TV(\mathcal{O}(-1))$ is given by the exact triangle

$$\mathcal{O}(1)^{\oplus 3}[-3] \to \mathcal{O} \to E \xrightarrow{+1} \tag{9.7.77}$$

- $\tau = 1$, $g = T$. Trivially, $E = \mathcal{O}(1)$.

These results are summarized in Table 9.1 on page 209.

9.7.9 Endpoints of attractor flows for local $\mathbb{P}^2$

In this section we derive several bounds on the behaviour of the attractor flow on the slice of Π-stability conditions in the case $\mathfrak{Y} = K_{\mathbb{P}^2}$, which we used in §9.6.1. As explained there, the central charge $Z_\tau(\gamma)$ is a holomorphic function of $\tau \in \mathbb{H}$ with no critical point, so that the attractor flow can either end at a marginal stability wall, end at a conifold point, end at a large volume point, or continue indefinitely. In §9.7.10 and §9.7.11 we rule out the last two cases in turn. In §9.7.12, §9.7.13 and §9.7.14 we determine conditions for an attractor flow to end or start at a conifold point, which leads to the equivalent definitions of the critical phase ψ in Definition 9.1.2.

9.7.10 Attractor flows avoid large volume points

Let us assume that an attractor flow associated to some $\gamma \in \Gamma$ ends at a large volume point, which we take without loss of generality to be $\tau = \mathrm{i}\infty$. Such a flow $\mu \mapsto \tau(\mu) \in \mathbb{H}$ would at late times lie in the fundamental domain $\mathcal{F}_C$ centered around the conifold point $\tau = 0$, or its translates centered around $\tau = n$. By applying a transformation $g(\mu) \in \Gamma_1(3)$ (which depends discretely on the flow parameter μ), we can map $\tau(\mu)$ into $\tilde\tau = g \cdot \tau \in \mathcal{F}_C$, at the cost of also mapping γ to $\tilde\gamma = g \cdot \gamma$. The central charge is unchanged, and in particular the mass $|Z_{\tilde\tau(\mu)}(\tilde\gamma(\mu))| = |Z_{\tau(\mu)}(\gamma)|$ is monotonically decreasing, hence lower than its initial value. We now exclude such attractor flows by proving that this upper bound on $|Z_{\tilde\tau}(\tilde\gamma)|$ would translate into an upper bound on $\Im\tau$, regardless of the charge vector $\tilde\gamma$ (provided the corresponding DT invariant is nonzero). Passing to the contrapositive statement and dropping tildes,[32] we shall prove the following statement (recall that δ denotes the D0-brane charge vector).

Proposition 9.7.1. *For every $M > 0$, there exists $D > 0$ such that for every $\tau \in \mathcal{F}_C$ with $\Im(\tau) > D$, and every $\gamma \in \Gamma \setminus \mathbb{Z}\delta$ with $\Omega_\tau(\gamma) \neq 0$, one has $|Z_\tau(\gamma)| > M$.*

The proof relies on approximating the exact central charge Z by the large volume central charge (9.1.6) $Z^{\mathrm{LV}}_{(s,t)}(\gamma) = -\frac{r}{2}(s+\mathrm{i}t)^2 + d(s+\mathrm{i}t) - \mathrm{ch}_2$, and we begin by proving bounds on it. We denote

$$Y = \frac{1}{2}(t^2 - s^2) \tag{9.7.78}$$

Lemma 9.7.2. *For every (s,t) with $Y \geq 0$, and every $\gamma \in \Gamma$ such that $r \geq 0$ and $d^2 - 2r\mathrm{ch}_2 \geq 0$, one has*

$$|Z^{\mathrm{LV}}_{(s,t)}(\gamma)|^2 \geq r^2Y^2 + \frac{d^2}{2}Y \tag{9.7.79}$$

Proof. We have

$$\begin{aligned} |Z^{\mathrm{LV}}_{(s,t)}(\gamma)|^2 &= (rY + ds - \mathrm{ch}_2)^2 + (2Y + s^2)(d - rs)^2 \\ &\geq r^2Y^2 + 2rY(ds - \mathrm{ch}_2) + 2Y(d - rs)^2 \end{aligned} \tag{9.7.80}$$

If $r = 0$, this gives $|Z^{\mathrm{LV}}_{(s,t)}(\gamma)|^2 \geq 2d^2Y$ and so in particular (9.7.79). If $r > 0$, we rephrase the inequality in terms of the slope $\mu = d/r$ and use the assumption $-\mathrm{ch}_2/r \geq -\mu^2/2$ to obtain

$$|Z^{\mathrm{LV}}_{(s,t)}(\gamma)|^2 \geq r^2\big(Y^2 + Y(2\mu s - \mu^2) + 2Y(\mu - s)^2\big) \tag{9.7.81}$$

The coefficient of Y is $\mu^2 - 2s\mu + 2s^2 \geq \mu^2/2$, which yields (9.7.79). □

[32] Importantly, images of $\gamma \in \Gamma \setminus \mathbb{Z}\delta$ under $\Gamma_1(3)$ are in $\Gamma \setminus \mathbb{Z}\delta$ because δ is invariant.

Proof of Proposition 9.7.1. We write $\tau = \tau_1 + i\tau_2$ with $\tau_1 = \Re\tau$ and $\tau_2 = \Im\tau$. We denote by $\mathcal{O}(1)$ any function on $\mathcal{F}_C$ which is bounded for τ_2 large enough, uniformly in r and d. For instance, $1/\tau_2 = \mathcal{O}(1)$ and $\tau_1 = \mathcal{O}(1)$, as $-\frac{1}{2} \leq \tau_1 \leq \frac{1}{2}$ on $\mathcal{F}_C$. According to the large volume expansion of the periods in §9.7.4, $T = \tau + \mathcal{O}(1)$ and $T_D = \frac{\tau^2}{2} + \mathcal{O}(1)$, hence

$$\begin{aligned} \Re T &= \mathcal{O}(1), & \Re T_D &= -\tau_2^2/2 + \mathcal{O}(1) \\ \Im T &= \tau_2 + \mathcal{O}(1), & \Im T_D &= \tau_1\tau_2 + \mathcal{O}(1) = \mathcal{O}(1)\tau_2 \end{aligned} \tag{9.7.82}$$

As a result

$$\begin{aligned} s &= \frac{\Im T_D}{\Im T} = \tau_1 + \mathcal{O}(1)/\tau_2 = \mathcal{O}(1) \\ w &= -\Re T_D + s\Re T = \tau_2^2/2 + \mathcal{O}(1) \\ t &= \sqrt{2w - s^2} = \sqrt{\tau_2^2 + \mathcal{O}(1)} = \tau_2 + \mathcal{O}(1)/\tau_2 \\ Y &= w - s^2 = \tau_2^2/2 + \mathcal{O}(1) \end{aligned} \tag{9.7.83}$$

In particular, large enough τ_2, t or Y are synonymous within $\mathcal{F}_C$. Another consequence is

$$\tau = s + \mathrm{i}t + \mathcal{O}(1)/\tau_2, \qquad \tau^2 = (s + \mathrm{i}t)^2 + \mathcal{O}(1) \tag{9.7.84}$$

which implies that the large volume central charge is a good approximation of the central charge in the sense that

$$\begin{aligned} Z_\tau(\gamma) &= -rT_D + dT - \mathrm{ch}_2 \\ &= -\frac{r}{2}(s + \mathrm{i}t)^2 + d(s + \mathrm{i}t) - \mathrm{ch}_2 + |r|\mathcal{O}(1) + |d|\mathcal{O}(1) \\ &= Z^{\mathrm{LV}}_{(s,t)}(\gamma) + |r|\mathcal{O}(1) + |d|\mathcal{O}(1) \end{aligned} \tag{9.7.85}$$

Next, we seek to apply Lemma 9.7.2. For large enough τ_2, the point $\tau \in \mathcal{F}_C$ does not belong to the lower boundary of $\mathcal{F}_C$, thus τ defines a geometric stability condition. Hence, by [LZ19] (Corollary 1.33 in published version, or Corollary 1.30 in arXiv version), if $\Omega_\tau(\gamma) \neq 0$, then $\gamma = n\gamma'$ is a multiple $n \in \mathbb{Z} \setminus \{0\}$ of the class γ' of a Gieseker semistable sheaf. The latter obeys $r' \geq 0$ and $d'^2 - 2r'\,\mathrm{ch}_2' \geq 0$ (see for example [DLP85, Lemma 3.4]). Up to replacing γ by $-\gamma$, which does not change the mass $|Z_\tau(\gamma)|$, one can assume that $n > 0$, so that $r \geq 0$ and $d^2 - 2r\mathrm{ch}_2 \geq 0$. Lemma 9.7.2 thus applies (for large enough τ_2 to ensure $Y \geq 0$): for every $\gamma \in \Gamma \setminus \mathbb{Z}\delta$ such that $\Omega_\tau(\gamma) \neq 0$, we have

$$|Z^{\mathrm{LV}}_{(s,t)}(\gamma)| \geq \sqrt{r^2Y^2 + d^2Y/2} \geq |r|Y/2 + |d|\sqrt{Y}/2 \tag{9.7.86}$$

where we did not try to optimize the constants. As a result,

$$|Z_\tau(\gamma)| \geq |Z^{\mathrm{LV}}_{(s,t)}(\gamma)| - |r\mathcal{O}(1)| - |d\mathcal{O}(1)| \geq |r|Y/3 + |d|\sqrt{Y}/3 \tag{9.7.87}$$

for large enough Y. Since we restrict to $\gamma \notin \mathbb{Z}\delta$, one has $(r, d) \neq (0, 0)$, so that we have proven $|Z_\tau(\gamma)| \geq \sqrt{Y}/3$ for large enough Y, or equivalently for large enough τ_2. This ends the proof of Proposition 9.7.1, which confines any attractor flow away from all large volume points. □

9.7.11 Attractor flows end at walls or conifold points

We are now ready to prove that an attractor flow cannot continue indefinitely. We denote by $\overline{\mathbb{H}} = \mathbb{H} \cup \mathbb{R}$ the closed upper half plane.

Proposition 9.7.3. *For a charge vector $\gamma \in \Gamma \setminus \mathbb{Z}\delta$ and a starting point $\tau(\mu_0) \in \mathbb{H}$, consider the attractor flow $[\mu_0, \mu_\infty) \ni \mu \mapsto \tau(\mu)$ that is maximally extended subject to the condition $\Omega_{\tau(\mu)}(\gamma) \neq 0$. Then the limit $\tau(\mu_\infty) = \lim_{\mu\to\mu_\infty} \tau(\mu) \in \overline{\mathbb{H}}$ exists and lies either at a conifold point or on a wall of marginal stability of γ.*

Proof. The modular curve $X_1(3) = \Gamma_1(3)\backslash\mathbb{H}$ has a natural compactification $\overline{X_1(3)} \simeq \mathbb{P}^1$ obtained by adding the large volume point $z_{\rm LV}$ and the conifold point z_C. Let $\pi\colon \mathbb{H} \to X_1(3)$ be the quotient map. Then $\pi\circ\tau\colon [\mu_0, \mu_\infty) \to X_1(3)$ takes values in the compact space $\overline{X_1(3)}$ hence admits at least one limit point $z_\infty \in \overline{X_1(3)}$. In other words there exists a sequence $(\mu_n)_{n=1,2,\dots}$ that tends to μ_∞ and such that $\pi(\tau(\mu_n)) \to z_\infty$. For later purposes, it is useful to recall that the mass $|Z_{\tau(\mu)}(\gamma)|$ is monotonically decreasing hence has a limit as $\mu \to \mu_\infty$, which necessarily coincides with the limit of its subsequence $|Z_{\tau(\mu_n)}(\gamma)|$.

Consider the unique element $g_n \in \Gamma_1(3)$ that maps $\tau(\mu_n)$ to a point $\tau'_n = g_n \cdot \tau(\mu_n)$ in the fundamental domain $\mathcal{F}_C$ centered on the conifold point, and consider the corresponding charge $\gamma'_n = g_n \cdot \gamma$. By $\Gamma_1(3)$-equivariance,

$$\Omega_{\tau'_n}(\gamma'_n) = \Omega_{\tau(\mu_n)}(\gamma) \neq 0, \qquad |Z_{\tau'_n}(\gamma'_n)| = |Z_{\tau(\mu)}(\gamma)| \leq |Z_{\tau(\mu_0)}(\gamma)| \tag{9.7.88}$$

Proposition 9.7.1 applied with $M = |Z_{\tau(\mu_0)}(\gamma)|$ implies that the imaginary parts $\Im\tau'_n \leq D$ must be bounded above by some constant D. This bound excludes $\pi(\tau'_n) = \pi(\tau(\mu_n))$ from a neighborhood of the large volume point in $\overline{X_1(3)}$. Therefore, the large volume point cannot be a limit point z_∞ of $\pi\circ\tau$.

Next, assume that the limit point z_∞ lies in $X_1(3)$. Consider its lift $\tau_\infty \in \mathcal{F}_C$, and note that[33] $\tau'_n \to \tau_\infty$. By the support property, τ_∞ admits an open neighbourhood U on which there are finitely many classes $\gamma' \in \Gamma \setminus \mathbb{Z}\delta$ with non-zero DT invariants and with central charge less than the upper bound $|Z_{\tau(\mu_0)}(\gamma)|$. The point τ'_n lies in U for large enough n, hence γ'_n takes finitely many values. Up to passing to a subsequence we can assume that all $\gamma'_n = \gamma'$ are equal to the same charge vector. Fix an arbitrary (Euclidean) norm $\|\ \|\colon \Gamma \to [0, +\infty)$. The support property ensures that $\|\gamma'\| \lesssim |Z_\tau(\gamma')|$ whenever $\tau \in U$ and $\Omega_\tau(\gamma') \neq 0$, with an implied constant that is uniform in $\tau \in U$. This gives a positive lower bound on $|Z_{\tau'_n}(\gamma')|$, hence on its limit

$$m_\infty \coloneqq \lim_{\mu\to\mu_\infty} |Z_{\tau(\mu)}(\gamma)| = \lim_{n\to+\infty} |Z_{\tau(\mu_n)}(\gamma)| = \lim_{n\to+\infty} |Z_{\tau'_n}(\gamma')| = |Z_{\tau_\infty}(\gamma')| > 0 \tag{9.7.89}$$

We learn that the point $\tau_\infty \in \mathbb{H}$ is not a critical point of $Z_\tau(\gamma')$ and the gradient flow is smooth near τ_∞. Therefore, near τ_∞ there exists local coordinates $m = |Z_\tau(\gamma')|$ along attractor flow lines and ℓ parametrizing the different flow lines: the attractor flow keeps ℓ constant and decreases m. Consider a neighborhood that is rectangular in these coordinates,

$$V = (\ell_-, \ell_+) \times (m_-, m_+) \ni (\ell_\infty, m_\infty) = \tau_\infty \tag{9.7.90}$$

For large enough n we have $\tau'_n = (\ell_n, m_n) \in V$. The gradient flow of $|Z_\tau(\gamma')|$ starting from this point is (ℓ_n, m) with m decreasing from m_n all the way to m_- at the boundary of V. Since $m_- < m_\infty$, the

[33] Strictly speaking, if τ_∞ lies on the boundary of $\mathcal{F}_C$, it can have multiple $\Gamma_1(3)$ images in the closure $\overline{\mathcal{F}_C}$. Then τ'_n has a subsequence that converges to either of these images, which we then denote τ_∞.

attractor flow must stop before, and specifically (9.7.89) requires the attractor flow to stop precisely at $m = m_\infty$. Recall now that $\tau'_n = g_n \cdot \tau(\mu_n)$. The image $\{g_n^{-1} \cdot (\ell_n, m), m_\infty < m \leq m_n\}$ of the gradient flow of $|Z_\tau(\gamma')|$ is the gradient flow of $|Z_\tau(\gamma)|$ starting from $\tau(\mu_n)$, which is precisely the attractor flow. We have thus fully determined the end segment of the attractor flow: the end point $\tau(\mu_\infty) = g_n^{-1} \cdot (\ell_n, m_\infty)$ of the attractor flow exists. The gradient flow of $|Z_\tau(\gamma)|$ could continue unimpeded beyond $m = m_\infty$, hence what stops the attractor flow must be that $\Omega_\tau(\gamma) = 0$ for $\tau = g_n^{-1} \cdot (\ell_n, m)$ with $m < m_\infty$ (at least, close to m_∞). This means that $\tau(\mu_\infty)$ is on a wall of marginal stability.

It remains to treat the case where none of the limit points of $\pi \circ \tau$ are of the above type, in which case the only remaining possibility for the limit point is the conifold point $z_\infty = z_C \in \overline{X_1(3)}$. Since this is a unique limit point, we have $\lim_{\mu \to \mu_\infty} \pi(\tau(\mu)) = z_C$. For a constant $0 < D < \Im \tau_o$, consider the (connected) set $W_D = \{\tau \in \mathcal{F}_C, \Im \tau < D\}$, its projection $V_D = \pi(W_D) \subset X_1(3)$, and the union $U_D = \pi^{-1}(V_D) \subset \mathbb{H}$ of all of its $\Gamma_1(3)$ images. The sets V_D and U_D are manifestly open. In fact, $V_D \cup \{z_C\}$ is a neighborhood of z_C in $\overline{X_1(3)}$, hence for large enough μ, one has $\pi(\tau(\mu)) \in V_D$ thus $\tau(\mu) \in U_D$. We learn that $\tau(\mu)$ remains in a fixed connected component of U_D for large enough μ. For instance, the connected component of U_D containing W_D consists of the union of images $g \cdot W_D$ for all elements $g \in \Gamma_1(3)$ that leave $\tau = 0$ invariant, so if $\tau(\mu)$ lies in this connected component, it can only tend to the conifold point $\tau = 0$. Other connected components are $\Gamma_1(3)$ images of this one, which implies that $\tau(\mu)$ tends to a conifold point $\tau_C \in \mathbb{Q} \subset \partial\overline{\mathbb{H}}$. □

9.7.12 Initial data of the exact diagram from the large volume diagram

A key ingredient when building scattering diagrams is the initial data: DT invariants along the initial rays, which are rays that do not arise from the scattering of other rays. Initial rays correspond to attractor flows that do not end on a wall of marginal stability, hence that end at a conifold point by Proposition 9.7.3. In this subsection we identify the DT invariants of such a flow (near a conifold point) to some DT invariants in the large volume diagram. This establishes the equivalence of the characterizations (2) and (3) of critical phases in Definition 9.1.2. Using $\Gamma_1(3)$ invariance we take the conifold point to be $\tau = 0$. We assume $\psi \in (-\pi/2, \pi/2)$ in this section as the scattering diagram for $\psi = \pi/2$ is highly degenerate and best treated separately in §9.6.4. We recall $\mathcal{V}_\psi = \mathcal{V} \tan \psi$.

Proposition 9.7.4. *Consider an attractor flow that ends at the conifold point $\tau = 0$ and has $Z_\tau(\gamma) \in \mathrm{i}e^{\mathrm{i}\psi}[0, +\infty)$ with $\psi \in (-\pi/2, \pi/2)$. Then the point $(s,t) = (\mathcal{V}_\psi, |\mathcal{V}_\psi|)$ lies on (the closure of) an active ray $\mathcal{R}_0^{\mathrm{LV}}(\gamma)$ of charge γ in the large volume scattering diagram $\mathcal{D}_0^{\mathrm{LV}}$. Furthermore, each DT invariant $\Omega_\tau(k\gamma)$, $k \geq 1$, is eventually constant along the flow close to the conifold point, and coincides with the limit of $\Omega^{\mathrm{LV}}_{(s,t)}(k\gamma)$ as $(s,t) \to (\mathcal{V}_\psi, |\mathcal{V}_\psi|)$ along $\mathcal{R}_0^{\mathrm{LV}}(\gamma)$ in $\mathcal{D}_0^{\mathrm{LV}}$. In particular, either $\gamma = [r, 0, 0]$ with DT invariants $\Omega_\tau([k, 0, 0]) = \delta_{k, \mathrm{sgn} r}$, or ψ is a critical phase in the sense that $(\mathcal{V}_\psi, |\mathcal{V}_\psi|)$ is an intersection of active rays in $\mathcal{D}_0^{\mathrm{LV}}$.*

Proof. While the statement is expressed in a uniform way, we shall distinguish $d = 0$ from $d \neq 0$ momentarily as they require very different approaches.

There is a $\mathbb{Z}$-worth of fundamental domains meeting at this conifold point, acted upon by the monodromy $V \colon \tau \mapsto \frac{\tau}{1-3\tau}$ around $\tau = 0$. We use the coordinate $\tau' = -1/(3\tau)$, in which the conifold point lies at $\tau' \to +\mathrm{i}\infty$. and the monodromy acts as $V \colon \tau' \mapsto \tau' + 1$. In terms of $q' = e^{2\pi \mathrm{i} \tau'}$ (which vanishes at the conifold point), the expansion (9.7.38) reads

$$T = \mathrm{i}\mathcal{V} + \kappa \tau' q'(1 + o(1)), \qquad T_D = -\frac{\kappa}{3} q'(1 + o(1)) \tag{9.7.91}$$

where $o(1)$ denotes any function of τ' (such as $1/\tau'$ or q') that vanishes as $q' \to 0$. Within an attractor flow, the phase of $Z_\tau(\gamma)$ is fixed and its modulus is monotonically decreasing, hence $Z_\tau(\gamma) = -rT_D + dT - \mathrm{ch}_2$ has a limit as $q' \to 0$.

If $d = 0$ then $Z_\tau(\gamma) \to -\mathrm{ch}_2$, which does not belong to the half-line $\mathrm{i}e^{\mathrm{i}\psi}[0, +\infty)$ unless $\mathrm{ch}_2 = 0$, which corresponds to a charge $\gamma = [r, 0, 0]$, with $r \neq 0$ since $\gamma \neq 0$. Such a charge is a multiple of the class of sheaves $\mathcal{O}(0)[k]$ becoming massless at the conifold point. It is easy to see that $Z_\tau(\gamma) = -rT_D = (\kappa/3)rq'(1 + o(1)) \in \mathrm{i}e^{\mathrm{i}\psi}(0, +\infty)$ requires

$$\tau_1' = \Re\tau' = -n + (\mathrm{sgn}r)/4 + \psi/(2\pi) + o(1) \tag{9.7.92}$$

for some integer $n \in \mathbb{Z}$. Close enough to the conifold point, the $o(1)$ term is less than $1/2$, so along a given attractor flow n is eventually constant. Applying a $\Gamma_1(3)$ translation $V^n \colon \tau' \mapsto \tau' + n$ reduces the problem to the case $n = 0$, for which $|\tau_1'| < 1/2$ close enough to the conifold point. As the Fricke involution $\tau' = -1/(3\tau)$ maps the fundamental domain $\mathcal{F}_C$ to itself, we deduce that $\tau \in \mathcal{F}_C$ at late enough times along the flow. In addition,

$$\mathrm{sgn}(\Re\tau) = \mathrm{sgn}\Big(\frac{-\tau_1'}{3|\tau'|^2}\Big) = -\mathrm{sgn}(\tau_1') = -\mathrm{sgn}r \tag{9.7.93}$$

Let us determine the DT invariants along this attractor flow that eventually lies in $\mathcal{F}_C$ and ends at $\tau = 0$. It follows from [LZ19, Corollary 1.24] (Corollary 1.21 of the arXiv version) that $\Omega_\tau(\gamma)$ does not jump for γ proportional to $\gamma(\mathcal{O})$ and τ geometric (apart from $\gamma \mapsto -\gamma$ across the vertical axis). So it is enough to work at large volume, namely with Gieseker stability. Let E be a Gieseker-stable sheaf of class $\gamma = k\gamma(\mathcal{O})$ with $k \geq 1$. It is of slope $\mu = 0$ and of discriminant $\Delta = 0$. Hence, E is exceptional in the sense of [DLP85, Section 4.2]. By [DLP85, Lemma 4.3], there is a unique exceptional sheaf of given slope. As $\mathcal{O}$ is exceptional of slope 0, we obtain $E = \mathcal{O}$. The moduli space of stable objects is a point for $k = 1$ and empty for $k > 1$. So

$$\Omega_\tau(k\gamma(\mathcal{O})) = \delta_{k,1} \tag{9.7.94}$$

for $k \in \mathbb{Z}$ and for every $\tau \in \mathcal{F}_C$ with $\Re\tau < 0$, and likewise $\Omega_\tau(k\gamma(\mathcal{O})) = \delta_{k,-1}$ for $\Re\tau > 0$. Thanks to (9.7.93) this translates to the sign condition in the statement of the Proposition.

We henceforth assume that $d \neq 0$.

After proving that the phase must obey $\mathcal{V}_\psi = \mathrm{ch}_2/d$, our strategy is to show that the attractor flow (near $\tau = 0$) lies in the large volume region $\tau \in \mathbb{H}^{\mathrm{LV}}$, map this point to large volume coordinates (s, t), and finally use that the large volume scattering diagram for non-zero phase $\psi^{\mathrm{LV}} = \arg(-\mathrm{i}Z^{\mathrm{LV}}_{(s,t)}(\gamma))$ coincides with the diagram $\mathcal{D}_0^{\mathrm{LV}}$ with zero phase up to a further change of coordinates (9.4.26),

$$\Omega_\tau(\gamma) = \Omega^{\mathrm{LV}}_{(s,t)}(\gamma) = \Omega^{\mathrm{LV}}_{(\tilde{s},\tilde{t})}(\gamma), \qquad \tilde{s} = s + t\tan\psi^{\mathrm{LV}}, \qquad \tilde{t}^2 = t^2 + \big(t\tan\psi^{\mathrm{LV}}\big)^2 \tag{9.7.95}$$

Our calculations show that $(\tilde{s}, \tilde{t}) \to (\mathcal{V}_\psi, |\mathcal{V}_\psi|)$ as $\tau \to 0$ along the flow, which suffices to conclude.

We start by determining how the conifold point is approached. The central charge has a limit, hence T has a limit, and equivalently $\tau' q' \to c$ for some $c \in \mathbb{C}$. Decomposing $\tau' = \tau_1' + \mathrm{i}\tau_2'$, we see that $\tau_2' q' = \mathcal{O}(\tau_2' e^{-2\pi\tau_2'})$ vanishes at the conifold point so $\tau_1' q' \to c$. If $c \neq 0$ then $|\tau_1'| \sim |c|/|q'| = |c|e^{2\pi\tau_2'}$, which means that the phase of $\tau_1' q'$ diverges, contradicting $\tau_1' q' \to c$. Thus $c = 0$ and altogether $T \to \mathrm{i}\mathcal{V}$. We learn that

$$Z_\tau(\gamma) = \mathrm{i}\mathcal{V}d - \mathrm{ch}_2 + \kappa\tau' q'(d + o(1)) \tag{9.7.96}$$

with $\tau' q' \to 0$. Along the flow, the central charge is fixed to lie in $Z_\tau(\gamma) \in \mathrm{i}e^{\mathrm{i}\psi}[0,+\infty)$ and to move towards 0 along this half-line, hence $Z_\tau(\gamma) - (\mathrm{i}\mathcal{V}d - \mathrm{ch}_2)$ lies in the same half-line. This implies (using $-\pi/2 < \psi < \pi/2$ hence $\cos\psi > 0$)

$$d > 0, \qquad \frac{\mathrm{ch}_2}{d} = \mathcal{V}_\psi, \qquad 2\pi\tau_1' = -2\pi n + \psi + o(1) \tag{9.7.97}$$

where $\mathcal{V}_\psi = \mathcal{V}\tan\psi$ and $n \in \mathbb{Z}$ is eventually constant (as in (9.7.92), $\tau \in \mathcal{F}_C$ if and only if $n = 0$). We then evaluate the large-volume coordinates s, t,

$$\begin{aligned} s &= \frac{\Im T_D}{\Im T} = -\frac{\kappa}{3\mathcal{V}} e^{-2\pi\tau_2'}\big(\sin\psi + o(1)\big) \\ w &= -\Re T_D + s\Re T = \frac{\kappa}{3} e^{-2\pi\tau_2'}\big(\cos\psi + o(1)\big) \\ t^2 &= 2w - s^2 = \frac{2\kappa}{3} e^{-2\pi\tau_2'}\big(\cos\psi + o(1)\big) > 0 \end{aligned} \tag{9.7.98}$$

Therefore, close enough to the conifold point, the ray lies in the large volume region $2w > s^2$, and one has $\Omega_\tau(\gamma) = \Omega^{\mathrm{LV}}_{(s,t)}(\gamma)$.

Next we consider the phase $\psi^{\mathrm{LV}} = \arg(-\mathrm{i}Z^{\mathrm{LV}}_{(s,t)}(\gamma))$ of the large volume central charge at (s,t), and evaluate its tangent since this is what appears in the change of coordinates (9.7.95):

$$t\tan\psi^{\mathrm{LV}} = -t\frac{\Re Z^{\mathrm{LV}}_{(s,t)}(\gamma)}{\Im Z^{\mathrm{LV}}_{(s,t)}(\gamma)} = \frac{\mathrm{ch}_2 - ds + \frac{r}{2}(s^2 - t^2)}{d - rs} = \mathcal{V}_\psi + \mathcal{O}(e^{-\pi\tau_2'}) \tag{9.7.99}$$

Thus

$$\begin{aligned} \tilde{s} &= s + t\tan\psi^{\mathrm{LV}} = \mathcal{V}_\psi + \mathcal{O}(e^{-\pi\tau_2'}), \\ \tilde{t} &= \sqrt{t^2 + \big(t\tan\psi^{\mathrm{LV}}\big)^2} = |\mathcal{V}_\psi| + \mathcal{O}(e^{-\pi\tau_2'}) \end{aligned} \tag{9.7.100}$$

As announced, we learn that $(\tilde{s},\tilde{t})$ tends to the point $(\mathcal{V}_\psi, |\mathcal{V}_\psi|)$. By construction, $(\tilde{s},\tilde{t})$ moves along the geometric ray $\mathcal{R}_0^{\mathrm{geo,LV}}(\gamma)$ of the zero-phase large volume scattering diagram $\mathcal{D}_0^{\mathrm{LV}}$. DT invariants $\Omega_\tau(\gamma)$ near the end of the attractor flow are thus given by DT invariants along the ray $\mathcal{R}_0^{\mathrm{geo,LV}}(\gamma)$ near its intersection $(\mathcal{V}_\psi, |\mathcal{V}_\psi|)$ with the initial ray $\mathcal{R}_0^{\mathrm{LV}}([\mathrm{sgn}\mathcal{V}_\psi, 0, 0])$. The ray $\mathcal{R}_\psi^{\mathrm{geo}}(\gamma)$ is thus active close to $\tau = 0$ precisely when the ray $\mathcal{R}_0^{\mathrm{geo,LV}}(\gamma)$ is active close to $(\mathcal{V}_\psi, |\mathcal{V}_\psi|)$. We conclude that there are non-trivial initial rays at $\tau = 0$ if and only if $(\mathcal{V}_\psi, |\mathcal{V}_\psi|)$ is an intersection of active rays. □

9.7.13 Initial data of the exact diagram from the orbifold diagram

In the previous section we have mapped DT invariants along an attractor flow ending at $\tau = 0$ to DT invariants in the large volume scattering diagram. We now map the DT invariants to the orbifold diagram, thus proving the equivalence of the criteria (2) and (4) in Definition 9.1.2, in terms of attractor flows and of the orbifold diagram. The latter criterion involves the point $\theta = (0, \frac{1}{2} + |\mathcal{V}_\psi|, \frac{1}{2} - |\mathcal{V}_\psi|)$ whose (u,v) coordinates are determined from (9.5.12) to be

$$u = \frac{1}{12} + \frac{1}{2}|\mathcal{V}_\psi|, \qquad v = \frac{1}{4\sqrt{3}}(-1 + 2|\mathcal{V}_\psi|) \tag{9.7.101}$$

Recall the functions $p_j\colon \mathbb{R} \to \mathbb{R}^2$ given in (9.6.28) for $j = 1, 2, 3$ parametrizing the three initial rays of the orbifold diagram. The point (9.7.101) involved in Definition 9.1.2 is $p_1(-|\mathcal{V}_\psi|)$. By $\mathbb{Z}_3$-invariance (cyclic permutations of the θ_j) one can replace this point by $p_3(-|\mathcal{V}_\psi|)$, which will appear more naturally in this section. Rather than repeating what can already be learned about $\gamma = [k, 0, 0)$ from Proposition 9.7.4, we restrict our attention immediately to attractor flows with $\gamma \notin [1, 0, 0)$.

Proposition 9.7.5. *Consider an attractor flow that ends at the conifold point $\tau = 0$ and has $Z_\tau(\gamma) \in \mathrm{i}e^{\mathrm{i}\psi}[0, +\infty)$ with $-\pi/2 < \psi < \pi/2$ and with $\gamma \notin [1, 0, 0)\mathbb{Z}$. Then the point $p_3(-|\mathcal{V}_\psi|)$ is a ray intersection in $\mathcal{D}_o$.*

Proof. For $|\mathcal{V}_\psi| < 1/2$ there are no such ray intersections in $\mathcal{D}_o$, and we have shown as part of Proposition 9.7.4 that there is no such attractor flow. We thus concentrate on $\mathcal{V}_\psi \leq -1/2$, fixing the sign to be negative by using the $\psi \mapsto -\psi$ symmetry. In other words, $-\pi/2 < \psi \leq -\psi^{\mathrm{cr}}_{1/2}$.

A translation $V^n\colon \tau' \mapsto \tau' + n$ maps the attractor flow (9.7.97) to that with $n = 0$,

$$\tau'_1 = \psi/(2\pi) + o(1) \in (-1/2, 0) \tag{9.7.102}$$

As discussed below (9.7.92), this condition on τ' implies that $\tau \in \mathcal{F}_C$. Furthermore, the sign $\mathrm{sgn}(\Re\tau) = -\mathrm{sgn}(\tau'_1) = 1$ implies that $\tau \in \mathcal{F}_{o'} = \mathcal{F}_o(1)$. Within the orbifold fundamental domain $\mathcal{F}_o$, the region of validity $\mathbb{H}^o$ of the quiver description is described by the inequality (9.6.26) $2w + s < 0$, namely $t^2 < -s(1+s)$ for the point $\tau - 1 \in \mathcal{F}_o$. Since $s(\tau - 1) = s(\tau) - 1$ and t^2 is invariant under translations, this condition reduces to $t^2 < (1-s)s$, namely $2w < s$, for the point $\tau \in \mathcal{F}_{o'}$. Then, thanks to the asymptotics (9.7.98), we evaluate

$$s - 2w = \frac{\kappa \cos\psi}{3\mathcal{V}^2} e^{-2\pi\tau'_2}\big(-\mathcal{V}_\psi - 2\mathcal{V}^2 + o(1)\big) \tag{9.7.103}$$

Since $-\mathcal{V}_\psi \geq 1/2 > 2\mathcal{V}^2 \simeq 0.4283$, this is positive, which ensures that the attractor flow lies in $\mathbb{H}^{o'} = \mathbb{H}^o(1)$ and its DT invariants are correctly given by the quiver scattering diagram.

The translated attractor flow $\mu \mapsto \tau(\mu) - 1 \in \mathcal{F}_o$ tends to the $\tau = -1$ conifold point, hence

$$(x, y) \longrightarrow (x_{\mathcal{O}(-1)}, y_{\mathcal{O}(-1)}) = (\mathcal{V}_\psi - 1, \mathcal{V}_\psi - 1/2) \tag{9.7.104}$$

where coordinates of the conifold point were calculated in (9.6.18). The corresponding (u, v) coordinates are

$$(u, v) = \left(\frac{1}{12} - \frac{1}{2}x + y, -\frac{2x+1}{4\sqrt{3}}\right) \longrightarrow \left(\frac{1}{12} + \frac{1}{2}\mathcal{V}_\psi, \frac{1 - 2\mathcal{V}_\psi}{4\sqrt{3}}\right) = p_3(\mathcal{V}_\psi) = p_3(-|\mathcal{V}_\psi|) \tag{9.7.105}$$

where p_3 was defined in (9.6.28) and we used $\psi < 0$. Along the attractor flow, the quiver description is valid in a neighborhood of this point, so DT invariants of the exact ray $\mathcal{R}_\psi(\gamma)$ starting at $\tau = 0$ coincide with those of the ray $\mathcal{R}_o(\gamma)$ starting at $p_3(-|\mathcal{V}_\psi|)$ in the orbifold diagram. In particular, there exists an active ray (with $\gamma \notin [1, 0, 0]\mathbb{Z}$) ending at $\tau = 0$ if and only if $p_3(-|\mathcal{V}_\psi|)$ is a ray intersection. □

9.7.14 Attractor flows starting at conifold points

To complete our description of the neighborhood of the conifold point, we now also study the attractor flows that emanate from $\tau = 0$, namely $\mu \mapsto \tau(\mu)$ with $\mu \in (\mu_0, \mu_\infty)$ such that $\lim_{\mu\to\mu_0} \tau(\mu) = 0$.

We establish the equivalence of the characterizations (1) and (4) in Definition 9.1.2 by mapping such flows to rays passing through $p_1(-|\mathcal{V}_\psi|)$ in the quiver.

As before, the central charge must have a limit as $\mu \to \mu_0$, but now this limit must be non-zero (as its modulus should decrease along the flow). This rules out the case $d = 0$ because $Z_{\tau=0}(\gamma) = -\mathrm{ch}_2$ cannot be in the open half-line $\mathrm{i}e^{\mathrm{i}\psi}(0, +\infty)$. Thus, $d \neq 0$. By symmetry under $\psi \mapsto -\psi$, we focus on $\psi \in (-\pi/2, 0]$.

Returning to the expansion (9.7.96) of the central charge, we again find that $\tau' q'$ has a limit and that this limit must vanish to avoid a divergent phase. Thus, $Z_\tau(\gamma) \to \mathrm{i}\mathcal{V}d - \mathrm{ch}_2$ as $\mu \to \mu_0$. Along the flow, the central charge is fixed to lie in $Z_\tau(\gamma) \in \mathrm{i}e^{\mathrm{i}\psi}[0, +\infty)$ and to move towards 0 along this half-line, hence $(\mathrm{i}\mathcal{V}d - \mathrm{ch}_2) - Z_\tau(\gamma)$ lies in the same half-line. This implies (9.7.97) with a constant shift of τ'_1,

$$d > 0, \qquad \frac{\mathrm{ch}_2}{d} = \mathcal{V}_\psi, \qquad 2\pi\tau'_1 = -2\pi n + \psi + \pi + o(1) \tag{9.7.106}$$

The integer $n \in \mathbb{Z}$ can be eliminated by a $\Gamma_1(3)$ transformation $V^n \colon \tau' \to \tau' + n$. Then $\tau'_1 \in (1/4, 1/2]$, namely τ' is in the closure $\overline{\mathcal{F}}_C$, which is stable under the Fricke involution, so $\tau \in \overline{\mathcal{F}}_C$. In addition, the sign of τ'_1 yields $\Re\tau < 0$, so that τ lies in the closure $\overline{\mathcal{F}}_o$ of the orbifold fundamental domain.

The expansions of s and w are then the opposites of (9.7.98), so that for $\psi \in (-\pi/2, 0]$ we have $w, s \leq 0$ close to the conifold point, hence the inequality $2w \leq -s$ defining the orbifold region $\mathbb{H}^o$ within $\mathcal{F}_o$ is satisfied. DT invariants along the flow are thus correctly given by those of the orbifold diagram $\mathcal{D}_o$ at a suitable point (u, v). The affine coordinates (9.6.6) are

$$x = \frac{\Re(e^{-\mathrm{i}\psi}T)}{\cos\psi} = \mathcal{V}_\psi + o(1) = -|\mathcal{V}_\psi| + o(1), \quad y = -\frac{\Re(e^{-\mathrm{i}\psi}T_D)}{\cos\psi} = o(1). \tag{9.7.107}$$

Thus, (9.7.105) holds as well, and the attractor flow starts (in the conifold limit $\mu \to \mu_0$) at the point $p_1(-|\mathcal{V}_\psi|)$ lying on the initial ray $\mathcal{R}_o(\gamma_1)$ of the quiver scattering diagram.

As in the previous section, we find that flows with $\gamma \notin [1, 0, 0]\mathbb{Z}$ that start (rather than end) at $\tau = 0$ are given by rays of the quiver scattering diagram that end[34] (rather than start) at $(u, v) = p_1(-|\mathcal{V}_\psi|)$. By consistency of the orbifold scattering diagram, the points $p_1(-|\mathcal{V}_\psi|)$ of $\mathcal{R}_o$ with incoming rays or with outgoing rays are the same, and correspond by Proposition 9.7.5 to critical phases. This situation, in which both incoming and outgoing rays at $\tau = 0$ occur for a critical phase, is illustrated in Figure 9.8 for $\mathcal{V}_\psi \simeq -1/2$.

Since both incoming and outgoing rays at $\tau = 0$ are seen in the orbifold diagram, it should be interesting to translate the consistency of the orbifold scattering diagram at $p_1(-|\mathcal{V}_\psi|)$ into a notion of consistency of the exact diagram $\mathcal{D}^\Pi_\psi$ at the conifold point, which is a singular point in the moduli space.

9.7.15 On the mathematical definition of DT invariants

Here we provide mathematical details on the definition of the DT invariants $\Omega_\sigma(\gamma)$. These invariants are a direct generalisation of the integer BPS invariants of [DM16]. From [BD21], the objects of a smooth CY3 dg category $\mathcal{C}$ (like the dg category of perfect complexes with compact support on a smooth CY3-fold) form a -1-shifted symplectic derived stack $\mathcal{M}$ in the sense of [PTVV13]. We suppose that $\mathcal{M}$ admits an orientation, i.e. a square root of the line bundle $\det(\mathbb{L}_\mathcal{M})$ given by the

[34] We recall the opposite orientation of rays and of the attractor flow.

determinant of the cotangent complex of $\mathcal{M}$ (a canonical orientation was constructed in the case of sheaves with compact support on noncompact CY3-fold in [JU21b, Theorem 4.9]). For σ a stability condition on $\mathcal{C}$, σ-semistability is a Zariski open condition, hence from [STV11, Proposition 2.1] there is an open -1-shifted symplectic substack $\mathcal{M}_\sigma \hookrightarrow \mathcal{M}$ of σ-semistable objects. From the definition of semistability, $\mathrm{Ext}^i(E,E) = 0$ for any $E \in \mathcal{M}_\sigma$ and $i < 0$, hence by [BD21, Proposition 3.3] $\mathbb{T}_{\mathcal{M}_\sigma}|_E = \mathrm{Ext}(E,E)[1]$, $\mathcal{M}$ is a -1-shifted symplectic Artin–1 stack. We then define $\mathcal{M}_\sigma(\gamma)$ as the component of $\mathcal{M}_\sigma$ of objects of class γ in the Grothendieck group of $\mathcal{C}$. Suppose now that σ is generic, i.e. that two σ-semistable objects E, E' of the same phase have collinear charges. For γ primitive, we define the DT invariants $\Omega_\sigma(k\gamma), k \geq 1$ by:

$$\mathrm{Exp}\left(\sum_{k=1}^{\infty} \frac{\Omega_\sigma(k\gamma)}{y^{-1}-y} x^k\right) := \sum_{k=0}^{\infty} H_c(\mathcal{M}_\sigma(k\gamma), P_{\mathcal{M}_\sigma(k\gamma)}) x^k \tag{9.7.108}$$

where Exp denotes the plethystic exponential, $P_{\mathcal{M}_\sigma(k\gamma)}$ the monodromic mixed Hodge module on $\mathcal{M}_\sigma(k\gamma)$ constructed in [BBBBJ15, Theorem 4.4] using the orientation data, and $H_c(M,P)$ the Hodge polynomial of the cohomology with compact support on M with values in P. In the case of quiver with potentials and King stability conditions, these invariants are integer by [DM16], and we conjecture that this remains true in this more general framework. In particular, we conjecture that as in [DM16]:

$$\Omega_\sigma(k\gamma) = H_c\big(M_\sigma(k\gamma), \mathcal{H}^1(\mathrm{JH}_!\, P_{\mathcal{M}_\sigma(k\gamma)})\big) \tag{9.7.109}$$

where $\mathrm{JH}\colon \mathcal{M}_\sigma(k\gamma) \to M_\sigma(k\gamma)$ denotes the Jordan-Hölder map to the coarse moduli space, $\mathrm{JH}_!$ denotes the proper pushforward for the derived categories of monodromic mixed Hodge modules, and $\mathcal{H}^1$ denotes the first cohomology of a complex of monodromic mixed Hodge modules.

9.7.16 Gieseker indices for higher rank sheaves

In this section, we extend the list of examples in §9.4 and determine the trees contributing to the Gieseker index for some examples with higher rank. As explained in [CH14a, CH14b], for (r,d) coprime and discriminant $\Delta(\gamma) \geq \Delta_1(r,d)$ large enough, the Gieseker wall is $\mathcal{W}(\gamma,\gamma')$ due to a subobject with Chern vector $\gamma' = [r',d',\chi')$ uniquely determined by the following conditions:

- $0 < r' \leq r\ , \quad \mu(\gamma') < \mu(\gamma)$
- Every rational number in the interval $(\mu(\gamma'),\mu(\gamma))$ has denominator greater than r
- The discriminant of any stable bundle of slope $\mu(\gamma')$ and rank $\leq r$ is $\geq \Delta(\gamma')$
- the rank of any stable bundle of slope $\mu(\gamma')$ and discriminant $\Delta(\gamma')$ is $\geq r'$

The minimal value $\Delta_1(r,d)$ for which conditions are applicable and the rightmost point $x_+ = s_{\gamma,\gamma'} + R_{\gamma,\gamma'}$ of the Gieseker wall for the lowest discriminant $\Delta_0 \geq \Delta_1$ are tabulated in [CH14a, Table 3] for $r \leq 6$ and $0 < \mu(\gamma) \leq 1$.

9.7.17 Rank 2

We consider rank 2 sheaves with $\gamma = [2,-1,1-n)$, discriminant $\Delta = \frac{n}{2} - \frac{1}{8}$. The condition (9.2.10) gives $\Delta \geq \delta_{\mathrm{LP}}(-\frac{1}{2}) = \frac{5}{8}$ for non-exceptional sheaves. The generating function of Gieseker indices is

given by [Yos94] [BMP21a, (A.38)]

$$\begin{aligned} h_{2,-1} &= q + (y^2+1+1/y^2)^2 q^2 + (y^8+2y^6+6y^4+9y^2+12+\dots)q^3 \\ &\quad + \left(y^{12}+2y^{10}+6y^8+13y^6+24y^4+35y^2+41+\dots\right) q^4 + \dots \\ &\to q + 9q^2 + 48q^3 + 203q^4 + 729q^5 + 2346q^6 + \dots \end{aligned} \tag{9.7.110}$$

- For $n=1$, corresponding to the exceptional sheaf $\Omega(1)$, there is a single wall $\mathcal{C}(-\frac{3}{2},\frac{1}{2})$ associated to the scattering sequence $\{-\mathcal{O}(-2), 3\mathcal{O}(-1)\}$ contributing $K_3(1,3)=1$.

- For $n=2$ there is a single wall $\mathcal{C}(-\frac{5}{2},\frac{3}{2})$ associated to $\{\{-\mathcal{O}(-3),\mathcal{O}(-2)\}, 2\mathcal{O}(-1)\}$ contributing $K_3(1,1)K_3(1,2) = (y^2+1+1/y^2)^2$. The rightmost point on the wall is at $s=-1$, consistent with the entries $\Delta_0=\frac{7}{8}, x_+=0$ in [CH14a, Table 3].

- For $n=3$, there is a single wall associated to two scattering sequences

$$\begin{array}{lll} \mathcal{C}(-\frac{7}{2},\frac{5}{2}) & \{\{-\mathcal{O}(-4),\mathcal{O}(-3)\}, 2\mathcal{O}(-1)\} & K_3(1,1)K_3(1,2) \\ & \{\{-2\mathcal{O}(-3), 3\mathcal{O}(-2)\}, \mathcal{O}(-1)\} & K_3(1,1)K_3(2,3) \end{array}$$

  contributing $9+39=48$ in the unrefined limit.

- For $n=4$, there are 2 walls associated to four scattering sequences

$$\begin{array}{lll} \mathcal{C}(-\frac{9}{2},\frac{7}{2}) & \{\{-\mathcal{O}(-5),\mathcal{O}(-4)\}, 2\mathcal{O}(-1)\} & K_3(1,1)K_3(1,2) \\ & \{\{\{-\mathcal{O}(-4),\mathcal{O}(-3)\},\{-\mathcal{O}(-3),2\mathcal{O}(-2)\}\},\mathcal{O}(-1)\} & K_3(1,1)^2K_3(1,2) \\ & \{\{-\mathcal{O}(-4),2\mathcal{O}(-2)\},\mathcal{O}(-1)\} & K_3(1,1)K_6(1,2) \\ \mathcal{C}(-\frac{7}{2},\frac{1}{2}) & \{-3\mathcal{O}(-3),5\mathcal{O}(-2)\} & K_3(3,5) \end{array}$$

  contributing $9+81+45+68=203$ in the unrefined limit.

For $\gamma=[2,0,2-n)$, with discriminant $\Delta=n/2$, the expected generating function is

$$\begin{aligned} h_{2,0} &= -(y^5+y^3+y+\dots)q^2 - (y^9+2y^7+4y^5+6y^3+6y+\dots)q^3 \\ &\quad - \left(y^{13}+2y^{11}+6y^9+11y^7+19y^5+24y^3+27y+\dots\right) q^4 - \dots \\ &\to -6q^2 - 38q^3 - 180q^4 - 678q^5 - 2260q^6 - \dots \end{aligned} \tag{9.7.111}$$

The condition (9.2.10) gives $\Delta \geq \delta_{\mathrm{LP}}(0) = 1$ for non-exceptional sheaves.

- For $n=2$ there is a single wall $\mathcal{C}(-\frac{3}{2},\frac{1}{2})$ associated to $\{-2\mathcal{O}(-2), 4\mathcal{O}(-1)\}$ contributing $K_3(2,4)\to -6$.

- For $n=3$ there are two walls

$$\begin{array}{lll} \mathcal{C}(-\frac{5}{2},\frac{\sqrt{13}}{2}) & \{-\mathcal{O}(-3), 3\mathcal{O}(-1)\} & K_6(1,3) \\ \mathcal{C}(-2,1) & \{\{-\mathcal{O}(-3),\mathcal{O}(-2)\},\{-\mathcal{O}(-2),3\mathcal{O}(-1)\}\} & K_3(1,1)K_3(1,3)K_6(1,1) \end{array}$$

  contributing $-20-18=-38$ in the unrefined limit. The Gieseker wall has rightmost point at $s=-\frac{5}{2}+\frac{\sqrt{13}}{2}$, consistent with the values $\Delta_0=\frac{3}{2}, x_+\simeq 0,30$ in [CH14a, Table 3].

- For $n=4$ there are two walls

$$\begin{array}{lll} \mathcal{C}(-\frac{7}{2},\frac{\sqrt{33}}{2}) & \{\{-\mathcal{O}(-4),\mathcal{O}(-3)\},\{-\mathcal{O}(-2),3\mathcal{O}(-1)\}\} & K_3(1,1)K_3(1,3)K_6(1,1) \\ \mathcal{C}(-\frac{5}{2},\frac{3}{2}) & \{\{-2\mathcal{O}(-3),2\mathcal{O}(-2)\},2\mathcal{O}(-1)\} & K_{-3,3,6}(2,2,2) \end{array}$$

  The index for the second scattering sequence is obtained in the same way as in (9.4.23), i.e. by applying the flow tree formula for a local scattering diagram with two incoming rays of charge $\alpha=\gamma_1+\gamma_2$ and $\beta=\gamma_3$ with $\Omega^-(\alpha)=K_3(1,2)=y^2+1+1/y^2, \Omega^-(2\alpha)=K_3(2,2)=-y^5-y^3-y-1/y-1/y^3-1/y^5$ and $\Omega^-(\beta)=1$, and selecting the outgoing ray of charge $2\alpha+2\beta$. This leads to

$$K_{-3,3,6}(2,2,2)=-y^{13}-2y^{11}-6y^9-10y^7-17y^5-21y^3-24y-\cdots\to -162 \tag{9.7.112}$$

  Adding up the contributions of the two scattering sequences, we get $-18-162=-180$ in the limit $y\to 1$, in agreement with (9.7.111).

9.7.18 Rank 3

We now turn to rank 3 sheaves, with $\gamma=[3,-1,2-n)$, discriminant $\Delta=\frac{n}{3}-\frac{1}{9}$. The condition (9.2.10) gives $\Delta\geq\delta_{\rm LP}(-\frac{1}{3})=\frac{5}{9}$ for non-exceptional sheaves. The generating function is given by [Man11a, Table 1] [BMP21a, (A.40)]

$$\begin{aligned} h_{3,-1} &= (y+1+1/y^2)q^2+(y^8+2y^6+5y^4+8y^2+10+\dots)q^3+\dots \\ &\to 3q^2+42q^3+333q^4+1968q^5+9609q^6+\dots \end{aligned} \tag{9.7.113}$$

- For $n=2$ there is a single wall $\mathcal{C}(-\frac{3}{2},\frac{1}{2})$ associated to $\{-2\mathcal{O}(-2),5\mathcal{O}(-1)\}$ contributing $K_3(2,5)=y^2+1+1/y^2$.

- For $n=3$ there are three walls:

$$\begin{array}{lll} \mathcal{C}(-\frac{7}{2},\frac{33}{2}) & \{\{\{-\mathcal{O}(-3),\mathcal{O}(-2)\},\mathcal{O}(-1)\},\{-\mathcal{O}(-2),3\mathcal{O}(-1)\}\} & K_3(1,1)^3K_3(1,3) \\ \mathcal{C}(-\frac{5}{2},\frac{\sqrt{35}}{2\sqrt{3}}) & \{\{-\mathcal{O}(-3),\mathcal{O}(-2)\},\{-\mathcal{O}(-2),4\mathcal{O}(-1)\}\} & K_3(1,1)K_3(1,4)K_9(1,1) \\ \mathcal{C}(-2,1) & \{\mathcal{O}(-3),4\mathcal{O}(-1)\} & K_6(1,4) \end{array}$$

  contributing $27+0+15=42$ in the unrefined limit. The Gieseker wall $\mathcal{C}(-\frac{7}{2},\frac{33}{2})$ has rightmost point at $-\frac{5}{2}+\frac{1}{2}\sqrt{33}$, consistent with the values $\Delta_0=\frac{8}{9}, x_+\simeq 0,37$ quoted in [CH14a, Table 3].

For $\gamma=[3,1,5-n)$ with $\Delta=\frac{n}{3}-\frac{1}{9}$, we find instead the following scattering sequences (not related to the previous ones by reflection)

- For $n=1$, there is a scattering sequence $\{-\mathcal{O}(-1),4\mathcal{O}\}$ but its index $K_3(1,4)$ vanishes.

- For $n=2$ there is a single wall

$$\mathcal{C}(-\tfrac{3}{2},\tfrac{3}{2}) \quad \{\{-\mathcal{O}(-2),\mathcal{O}(-1)\},3\mathcal{O}(0)\} \quad K_3(1,3)K_3(1,1)$$

  contributing y^2+1+1/y^2.

- For $n = 3$ there is a single wall but two scattering sequences,

$$\begin{array}{lll} \mathcal{C}(-\frac{5}{2},\frac{5}{2}) & \{\{-2\mathcal{O}(-2),3\mathcal{O}(-1)\},2\mathcal{O}\} & K_3(1,2)K_3(2,3) \\ & \{\{-\mathcal{O}(-3),\mathcal{O}(-2)\},3\mathcal{O}\} & K_3(1,1)K_3(1,3) \end{array}$$

  The wall $\mathcal{C}(-\frac{5}{2},\frac{5}{2})$ has rightmost point at $x_+ = 0$, consistent with the values $\Delta_0 = \frac{8}{9}, x_+ = 0$ quoted in [CH14a, Table 3].

For $\gamma = [3,0,3-n)$ with discriminant $\Delta = n/3$, the generating function is [BMP21a, (A.40)]

$$\begin{aligned} h_{3,0} &= (y^{10}+y^8+2y^6+2y^4+2y^2+2+\dots)q^3 \\ &\quad + \left(y^{16}+2y^{14}+5y^{12}+9y^{10}+15y^8+19y^6+22y^4+23y^2+24+\dots\right)q^4+\dots \\ &\to 18q^3+216q^4+1512q^5+8109q^6\dots \end{aligned} \tag{9.7.114}$$

- For $n = 3$, there is a single wall $\mathcal{C}(-\frac{3}{2},\frac{1}{2})$ associated to $\{-3\mathcal{O}(-2),6\mathcal{O}(-1)\}$ contributing $K_3(3,6) \to 18$.

- For $n = 4$, there are two walls

$$\begin{array}{lll} \mathcal{C}(-\frac{5}{2},\frac{\sqrt{43}}{2\sqrt{3}}) & \{\{-\mathcal{O}(-3),\mathcal{O}(-2)\},\{-2\mathcal{O}(-2),5\mathcal{O}(-1)\}\} & K_3(1,1)K_3(2,5)K_9(1,1) \\ \mathcal{C}(-\frac{13}{6},\frac{\sqrt{73}}{6}) & \{\{-\mathcal{O}(-3),2\mathcal{O}(-1)\},\{-\mathcal{O}(-2),3\mathcal{O}(-1)\}\} & K_3(1,3)K_6(1,2)K_9(1,1) \end{array}$$

  contributing $81 + 135 = 216$ in the unrefined limit. The Gieseker wall has rightmost point $-\frac{5}{2}+\frac{1}{2}\sqrt{\frac{43}{3}} = x_+ - 1$, consistent with the values $\Delta_0 = \frac{4}{3}, x_+ \simeq 0,39$ quoted in [CH14a, Table 3].

9.7.19 Mathematica package `P2Scattering.m`

The MATHEMATICA package `P2Scattering.m`, available from

https://github.com/bpioline/P2Scattering

provides a suite of routines for analyzing the scattering diagrams considered in this work, both at large volume, around the orbifold and along the Π-stability slice. It was used extensively in order to generate the figures and arrive at the global picture presented in this article. A list of routines is provided in the documentation `P2Scattering.pdf` available in the GitHub repository, along with several demonstration worksheets. Here we simply give a taste of the package capabilities.

After copying file `P2Scattering.m` in the current directory, load the package via

```
In[1]:= SetDirectory[NotebookDirectory[]]; << P2Scattering`
Out[1]= P2Scattering 1.4 - A package for evaluating DT invariants on K_P2
```

For a given charge $\gamma = [r,d,\chi)$ and point (s,t) on the large volume slice, the scattering sequences contributing to the index $\Omega_{(s,t)}(\gamma)$ can be found by using the routine `ScanAllTrees`, for example for $\gamma = [3,0,0)$ through the point $(s,t) = (-\frac{3}{2},2)$,

```
In[2]:=  LiTrees = ScanAllTrees[{0, 3, 0}, {-3/2, 2}]
Out[2]:= {{-Ch[-3], Ch[0]}, {-3 Ch[-2], 3 Ch[-1]}}
```

```
In[3]:=  ScattDiagLV[LiTrees, 0]
```

Out[3]:=

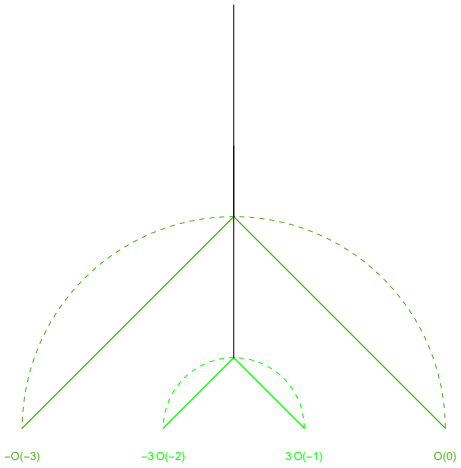


```
In[4]:=  Limit[EvaluateKronecker[ScattIndex[LiTrees]], y -> 1]
Out[4]:= {9,18}
```

reproducing the GV invariant $N_3^{(0)} = 27$ (compare with §9.4.4). Note that the current implementation of the routine `ScattIndex` assumes that the index associated to each scattering sequence is a product of Kronecker indices associated to each vertex, and may give the wrong result if some of the edges carry non-primitive charges (see (9.4.23) for an example). In the case above, it does produce the correct results for both scattering sequences, $\Omega_\infty(\gamma) = K_9(1,1) + K_3(3,3)$. More generally, the routine `IndexFromSequences`$[\{trees\},\{s,t\}]$ computes the total rational index $\bar\Omega_{s,t}(\gamma)$ by decomposing each scattering sequence into attractor flow trees as explained at the end of §9.4.2, and perturbing the charges of the constituents $\gamma_i \to \gamma_i + \epsilon_i\delta$ such that only binary splittings remain:

```
In[5]:=  Limit[Plus@@Flatten[IndexFromSequences[LiTrees, {-3/2, 2}]], y -> 1]
Out[5]:= 82/3
```

consistent with $\bar\Omega_{s,t}(3\gamma) = \Omega_{s,t}(3\gamma) + \frac{1}{9}\Omega_{s,t}(\gamma) = 27 + \frac{1}{3}$.

Similarly, one can find the scattering sequences contributing near the orbifold point using `McKayScanAllTrees`: for the same charge, corresponding to dimension vector $(0,3,6)$, a single scattering sequence contributes in the anti-attractor chamber, with index 18,

```
In[6]:= LiTrees = McKayScanAllTrees[chiton[{0, 3, 0}]]; LiTrees /.  McKayrep
Out[6]= {{3γ2, 6γ3}}
```

```
In[7]:= Limit[EvaluateKronecker[McKayScattIndex[LiTrees]], y ->1]
Out[7]= {18}
```

```
In[8]:= Show[McKayInitialRays[2], McKayScattDiag[LiTrees]]
```

Out[8]=

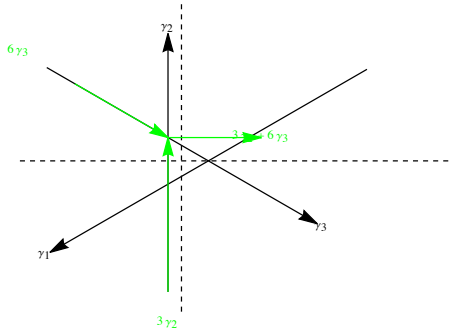

In this example, the index in the anti-attractor chamber differs from the one at large volume, due to wall-crossing along the circle $\mathcal{C}(-\frac{3}{2}, \frac{1}{2})$.

Bibliography

[AB21] Hülya Argüz and Pierrick Bousseau. The flow tree formula for Donaldson-Thomas invariants of quivers with potentials. 2021.

[ABCH13] Daniele Arcara, Aaron Bertram, Izzet Coskun, and Jack Huizenga. The minimal model program for the Hilbert scheme of points on $\mathbb{P}^2$ and Bridgeland stability. *Advances in Mathematics*, 235:580–626, 2013.

[ABK08] Mina Aganagic, Vincent Bouchard, and Albrecht Klemm. Topological Strings and (Almost) Modular Forms. *Commun. Math. Phys.*, 277:771–819, 2008.

[ADJM12] Evgeny Andriyash, Frederik Denef, Daniel L. Jafferis, and Gregory W. Moore. Bound state transformation walls. *JHEP*, 1203:007, 2012.

[AG60] Maurice Auslander and Oscar Goldman. Maximal orders. *Transactions of the American Mathematical Society*, 97(1):1–24, 1960.

[AGMP22] Sergei Alexandrov, Nava Gaddam, Jan Manschot, and Boris Pioline. Modular bootstrap for D4-D2-D0 indices on compact Calabi-Yau threefolds. 4 2022.

[AHK02] Paul S. Aspinwall, Richard Paul Horja, and Robert L. Karp. Massless d-branes on calabi–yau threefolds and monodromy. *Communications in Mathematical Physics*, 259:45–69, 2002.

[AHR19] Jarod Alper, Jack Hall, and David Rydh. The étale local structure of algebraic stacks. *arXiv: Algebraic Geometry*, 2019.

[AHR20] Jarod Alper, Jack Hall, and David Rydh. A luna étale slice theorem for algebraic stacks. *Annals of mathematics*, 191, 2020.

[AK06] Paul S. Aspinwall and Sheldon H. Katz. Computation of superpotentials for D-branes. *Commun. Math. Phys.*, 264:227–253, 2006.

[AKMV05] Mina Aganagic, Albrecht Klemm, Marcos Marino, and Cumrun Vafa. The Topological vertex. *Commun. Math. Phys.*, 254:425–478, 2005.

[AMP20] Sergei Alexandrov, Jan Manschot, and Boris Pioline. S-duality and refined BPS indices. *Commun. Math. Phys.*, 380(2):755–810, 2020.

[AMPP13] Sergei Yu. Alexandrov, Jan Manschot, Daniel Persson, and Boris Pioline. Quantum hypermultiplet moduli spaces in n = 2 string vacua: a review. volume 90, pages 181–211, 2013.

[AP19a] Sergei Alexandrov and Boris Pioline. Attractor flow trees, BPS indices and quivers. *Adv. Theor. Math. Phys.*, 23(3):627–699, 2019.

[AP19b] Sergei Alexandrov and Boris Pioline. Black holes and higher depth mock modular forms. *Commun. Math. Phys.*, 374(2):549–625, 2019.

[Arb19] Noah Arbesfeld. K-theoretic Donaldson-Thomas theory and the Hilbert scheme of points on a surface. 2019.

[Asp04] Paul S. Aspinwall. D-branes on Calabi-Yau manifolds. 2004.

[ASYZ14] Murad Alim, Emanuel Scheidegger, Shing-Tung Yau, and Jie Zhou. Special Polynomial Rings, Quasi Modular Forms and Duality of Topological Strings. *Adv. Theor. Math. Phys.*, 18(2):401–467, 2014.

[Aus62] Maurice Auslander. On the purity of branch locus. 1962.

[BB73] Andrzej Białynicki-Birula. Some theorems on actions of algebraic groups. *Annals of Mathematics*, 98:480–497, 1973.

[BBBBJ15] O. Ben-Bassat, Christopher Brav, Vittoria Bussi, and D. Joyce. A 'darboux theorem' for shifted symplectic structures on derived artin stacks, with applications. *Geometry & Topology*, 19, 2015.

[BBD+15] Christopher Brav, Vittoria Bussi, Delphine Dupont, Dominic Joyce, and Balázs Szendrői. Symmetries and stabilization for sheaves of vanishing cycles. *Journal of singularities*, 11, 2015.

[BBdB+12] Iosif Bena, Micha Berkooz, Jan de Boer, Sheer El-Showk, and Dieter Van den Bleeken. Scaling BPS Solutions and pure-Higgs States. *JHEP*, 1211:171, 2012.

[BBDG83] Alexander BEILINSON, Joseph BERNSTEIN, Pierre DELIGNE, and Ofer GABBER. Faisceaux pervers. *Astérisque*, 100, 1983.

[BBJ19] Christopher Brav, Vittoria Bussi, and D. Joyce. A 'darboux theorem' for derived schemes with shifted symplectic structure. *J. Amer. Math. Soc.*, 32, 2019.

[BBS07] Katrin Becker, Melanie Becker, and John Schwarz. *String theory and M-theory.* Cambridge University Press, 2007.

[BBS13] Kai Behrend, Jim Bryan, and Balazs Szendroï. Motivic degree zero Donaldson–Thomas invariants. *Inv. Math.*, 192, 2013.

[BCH73] James M. Bardeen, Brandon D. Carter, and Stephen William Hawking. The four laws of black hole mechanics. *Communications in Mathematical Physics*, 31:161–170, 1973.

[BD21] Christopher Brav and Tobias Dyckerhoff. Relative calabi–yau structures ii: shifted lagrangians in the moduli of objects. *Selecta Mathematica*, 27, 09 2021.

[BDLFP22] Pierrick Bousseau, Pierre Descombes, Bruno Le Floch, and Boris Pioline. Bps dendroscopy on local $\mathbb{P}^2$. 2022.

[Beh09] Kai Behrend. Donaldson-Thomas type invariants via microlocal geometry. *Ann. of Math. (2)*, 170(3):1307–1338, 2009.

[Bek19] Jacob David Bekenstein. Black holes and the second law. *Lettere al Nuovo Cimento (1971-1985)*, 4:737–740, 2019.

[BF96] Kai Behrend and Barbara Fantechi. The intrinsic normal cone. *Inventiones mathematicae*, 128:45–88, 1996.

[BF08] K. Behrend and B. Fantechi. Symmetric Obstruction Theories and Hilbert Schemes of Points on Threefolds, 2008.

[BFGW21] Pierrick Bousseau, Honglu Fan, Shuai Guo, and Long Wu. Holomorphic anomaly equation for $(\mathbb{P}_2, E)$ and the Nekrasov-Shatashvili limit of local $\mathbb{P}_2$. *Forum Math. Pi*, 9:e3, 2021.

[BJM19] Vittoria Bussi, Dominic Joyce, and Sven Meinhardt. On motivic vanishing cycles of critical loci. *Journal of Algebraic Geometry*, 2019.

[BK01] Tom Bridgeland and Alastair King. The mckay correspondence as an equivalence of derived categories. *Journal of the American Mathematical Society*, 14, 07 2001.

[BKSZ22] Kilian Bönisch, Albrecht Klemm, Emanuel Scheidegger, and Don Zagier. D-brane masses at special fibres of hypergeometric families of Calabi-Yau threefolds, modular forms, and periods. 3 2022.

[BM99] Tom Bridgeland and Antony Maciocia. Fourier-mukai transforms for k3 and elliptic fibrations. *Journal of Algebraic Geometry*, 11:629–657, 1999.

[BM11] Arend Bayer and Emanuele Macri. The space of stability conditions on the local projective plane. *Duke Math. J.*, 160:263–322, 2011.

[BM12] Arend Bayer and Emanuele Macrì. Projectivity and birational geometry of bridgeland moduli spaces. *Journal of the American Mathematical Society*, 27:707–752, 2012.

[BM22] Arend Bayer and Emanuele Macrì. The unreasonable effectiveness of wall-crossing in algebraic geometry. 2022.

[BMP20] Guillaume Beaujard, Jan Manschot, and Boris Pioline. Vafa-Witten invariants from exceptional collections. 4 2020.

[BMP21a] Guillaume Beaujard, Jan Manschot, and Boris Pioline. Vafa–Witten Invariants from Exceptional Collections. *Commun. Math. Phys.*, 385(1):101–226, 2021.

[BMP21b] Guillaume Beaujard, Swapnamay Mondal, and Boris Pioline. Multi-centered black holes, scaling solutions and pure-Higgs indices from localization. *SciPost Phys.*, 11(2):023, 2021.

[BMT11] Arend Bayer, Emanuele Macrì, and Yukinobu Toda. Bridgeland stability conditions on threefolds i: Bogomolov-gieseker type inequalities. *Journal of Algebraic Geometry*, 23:117–163, 2011.

[BMW14] Aaron Bertram, Cristian Martinez, and Jie Wang. The birational geometry of moduli spaces of sheaves on the projective plane. *Geometriae Dedicata*, 173(1):37–64, 2014.

[Boc11] R. Bocklandt. Consistency conditions for dimer models. *Glasgow Mathematical Journal*, 54:429 – 447, 2011.

[Bou19] Pierrick Bousseau. Scattering diagrams, stability conditions, and coherent sheaves on $\mathbb{P}^2$. 9 2019.

[Bra02] Tom Braden. Hyperbolic localization of intersection cohomology. *Transformation Groups*, 8:209–216, 2002.

[Bri98] Tom Bridgeland. Equivalences of triangulated categories and fourier–mukai transforms. *Bulletin of the London Mathematical Society*, 31, 1998.

[Bri00] Tom Bridgeland. Flops and derived categories. *Inventiones mathematicae*, 147:613–632, 2000.

[Bri03] Tom Bridgeland. Stability conditions on k3 surfaces. *Duke Mathematical Journal*, 141:241–291, 2003.

[Bri06] Tom Bridgeland. Stability conditions on a non-compact Calabi-Yau threefold. *Communications in mathematical physics*, 266(3):715–733, 2006.

[Bri07] Tom Bridgeland. Stability conditions on triangulated categories. *Ann. of Math. (2)*, 166(2):317–345, 2007.

[Bri10] Tom Bridgeland. Hall algebras and curve-counting invariants. *Journal of the American Mathematical Society*, 24, 2010.

[Bri17] Tom Bridgeland. Scattering diagrams, hall algebras and stability conditions. *Alg. Geo.*, 4:523–561, 2017.

[Bro11] Nathan Broomhead. Dimer models and calabi-yau algebras. *Memoirs of the American Mathematical Society*, 215:153–256, 04 2011.

[BSW08] R. Bocklandt, Travis Schedler, and Michael Wemyss. Superpotentials and higher order derivations. *Journal of Pure and Applied Algebra*, 214:1501–1522, 2008.

[BWW06] Iosif Bena, Chih-Wei Wang, and Nicholas P. Warner. Mergers and typical black hole microstates. *JHEP*, 11:042, 2006.

[CDM+14] Wu-yen Chuang, Diuliu-Emanuel Diaconescu, Jan Manschot, Gregory W. Moore, and Yan Soibelman. Geometric engineering of (framed) bps states. *Adv.Theor.Math.Phys*, 18, 2014.

[CdWM10] G. L. Cardoso, B. de Wit, and S. Mahapatra. BPS black holes, the Hesse potential, and the topological string. *JHEP*, 06:052, 2010.

[CH14a] Izzet Coskun and Jack Huizenga. The ample cone of moduli spaces of sheaves on the plane. 2014.

[CH14b] Izzet Coskun and Jack Huizenga. The birational geometry of the moduli spaces of sheaves on $\mathbb{P}^2$. In *Proceedings of the Gökova Geometry-Topology Conference*, volume 2015, pages 114–155. Citeseer, 2014.

[CI02] Alastair Craw and Akira Ishii. Flops of g-hilb and equivalences of derived categories by variation of git quotient. *Duke Mathematical Journal*, 124:259–307, 2002.

[Cir20] Michele Cirafici. Quantum Line Defects and Refined BPS Spectra. *Letters in Mathematical Physics*, 110, 2020.

[CKK14] Jinwon Choi, Sheldon Katz, and Albrecht Klemm. The refined BPS index from stable pair invariants. *Commun. Math. Phys.*, 328:903–954, 2014.

[CKYZ99] T. M. Chiang, A. Klemm, Shing-Tung Yau, and E. Zaslow. Local mirror symmetry: Calculations and interpretations. *Adv. Theor. Math. Phys.*, 3:495–565, 1999.

[CLSS13] Abhishek Chowdhury, Shailesh Lal, Arunabha Saha, and Ashoke Sen. Black Hole Bound State Metamorphosis. *JHEP*, 1305:020, 2013.

[CMM22] Aradhita Chattopadhyaya, Jan Manschot, and Swapnamay Mondal. Scaling black holes and modularity. *JHEP*, 03:001, 2022.

[CvGKT20] Jinwon Choi, Michel van Garrel, Sheldon Katz, and Nobuyoshi Takahashi. Local BPS Invariants: Enumerative Aspects and Wall-Crossing. *International Mathematics Research Notices*, 2020(17):5450–5475, 2020.

[CW10] Andres Collinucci and Thomas Wyder. The Elliptic genus from split flows and Donaldson-Thomas invariants. *JHEP*, 05:081, 2010.

[Dao10] Hailong Dao. Remarks on non-commutative crepant resolutions of complete intersections. *Advances in Mathematics*, 224(3):1021–1030, 2010.

[Dav16] Ben Davison. The integrality conjecture and the cohomology of preprojective stacks. *arXiv: Algebraic Geometry*, 2016.

[Dav17] Ben Davison. The critical CoHA of a quiver with potential. *Quart. J. Math. Oxford Ser.*, 68, 2017.

[Dav19] Ben Davison. Refined invariants of finite-dimensional Jacobi algebras. *arXiv*, 2019.

[dBESMVdB09] Jan de Boer, Sheer El-Showk, Ilies Messamah, and Dieter Van den Bleeken. Quantizing N=2 Multicenter Solutions. *JHEP*, 05:002, 2009.

[Den99] Frederik Denef. Attractors at weak gravity. *Nucl.Phys.*, B547:201–220, 1999.

[Den00] Frederik Denef. Supergravity flows and D-brane stability. *JHEP*, 08:050, 2000.

[Den02] Frederik Denef. Quantum quivers and Hall/hole halos. *JHEP*, 10:023, 2002.

[Des21] Pierre Descombes. Cohomological dt invariants from localization. *Journal of the London Mathematical Society*, 106, 2021.

[Des22] Pierre Descombes. Hyperbolic localization of the Donaldson-Thomas sheaf. 1 2022.

[DFR05a] Michael R. Douglas, Bartomeu Fiol, and Christian Romelsberger. Stability and BPS branes. *JHEP*, 0509:006, 2005.

[DFR05b] Michael R. Douglas, Bartomeu Fiol, and Christian Romelsberger. The Spectrum of BPS branes on a noncompact Calabi-Yau. *JHEP*, 0509:057, 2005.

[DG00] Duiliu-Emanuel Diaconescu and Jaume Gomis. Fractional branes and boundary states in orbifold theories. *JHEP*, 10:001, 2000.

[DG10] Tudor Dimofte and Sergei Gukov. Refined, Motivic, and Quantum. *Lett. Math. Phys.*, 91:1, 2010.

[DGR01] Frederik Denef, Brian R. Greene, and Mark Raugas. Split attractor flows and the spectrum of BPS D-branes on the quintic. *JHEP*, 05:012, 2001.

[DLP85] Jean-Mare Drezet and Joseph Le Potier. Fibrés stables et fibrés exceptionnels sur $\{P\}_2$. *Annales scientifiques de l'École Normale Supérieure*, 18(2):193–243, 1985.

[DM96] Michael R Douglas and Gregory Moore. D-branes, quivers, and ale instantons. *arXiv: High Energy Physics - Theory*, 1996.

[DM11a] Frederik Denef and Gregory W. Moore. Split states, entropy enigmas, holes and halos. *JHEP*, 1111:129, 2011.

[DM11b] Jean-Marc Drézet and Mario Maican. On the geometry of the moduli spaces of semi-stable sheaves supported on plane quartics. *Geometriae Dedicata*, 152(1):17–49, 2011.

[DM16] B. Davison and Sven Meinhardt. Cohomological Donaldson–Thomas theory of a quiver with potential and quantum enveloping algebras. *Inventiones mathematicae*, 2016.

[Dou01] Michael R. Douglas. D-branes, categories and N = 1 supersymmetry. *J. Math. Phys.*, 42:2818–2843, 2001.

[DP22] Pierre Descombes and Boris Pioline. On the existence of scaling multi-centered black holes. *Annales Henri Poincaré*, 23:3633 – 3665, 2022.

[Dri13] Vladimir Drinfeld. On algebraic spaces with an action of g_m. *arXiv preprint arXiv:1308.2604*, 2013.

[Efi11] Alexander I. Efimov. Quantum cluster variables via vanishing cycles. 2011.

[FHK+06] Sebastian Franco, Amihay Hanany, Kristian D. Kennaway, David Vegh, and Brian Wecht. Brane dimers and quiver gauge theories. *JHEP*, 01:096, 2006.

[FKS95] Sergio Ferrara, Renata Kallosh, and Andrew Strominger. $N = 2$ extremal black holes. *Phys. Rev.*, D52:5412–5416, 1995.

[Fre97] Daniel S. Freed. Special kähler manifolds. *Communications in Mathematical Physics*, 203:31–52, 1997.

[FT20] S. Feyzbakhsh and Richard P. Thomas. Curve counting and s-duality. *arXiv: Algebraic Geometry*, 2020.

[Ful98] William Fulton. Intersection theory, second edition. In *Ergebnisse der Mathematik und ihrer Grenzgebiete*, 1998.

[Gab72] Peter Gabriel. Unzerlegbare darstellungen i. *manuscripta mathematica*, 6:71–103, 1972.

[Gad16] Nava Gaddam. Elliptic genera from multi-centers. *JHEP*, 05:076, 2016.

[GHKK18] Mark Gross, Paul Hackinng, Sean Keel, and Maxim Kontsevich. Canonical bases for cluster algebras. *Jour. Amer. Math. Soc.*, 31(2):497–608, 2018.

[Göt90] Lothar Göttsche. The Betti numbers of the Hilbert scheme of points on a smooth projective surface. *Math. Ann.*, 286:193–207, 1990.

[GP97] Tom Graber and Rahul Pandharipande. Localization of virtual classes. *Inventiones mathematicae*, 135:487–518, 1997.

[Gro11] Mark Gross. *Tropical geometry and mirror symmetry.* Number 114. American Mathematical Soc., 2011.

[GS11] Mark Gross and Bernd Siebert. From real affine geometry to complex geometry. *Annals of mathematics*, pages 1301–1428, 2011.

[GY20] Dmitry Galakhov and Masahito Yamazaki. Quiver yangian and supersymmetric quantum mechanics. *Communications in Mathematical Physics*, 396:713 – 785, 2020.

[Har99] Franck Harary. *Graph Theory.* CRC Press, 1999.

[Hat02] Allen Hatcher. *Algebraic Topology.* Cambridge University Press, 2002.

[Haw75] Stephen William Hawking. Particle creation by black holes. *Communications in Mathematical Physics*, 43:199–220, 1975.

[HKPK13] Min-xin Huang, Amir-Kian Kashani-Poor, and Albrecht Klemm. The Ω deformed B-model for rigid $\mathcal{N} = 2$ theories. *Annales Henri Poincare*, 14:425–497, 2013.

[HKR08] Babak Haghighat, Albrecht Klemm, and Marco Rauch. Integrability of the holomorphic anomaly equations. *JHEP*, 10:097, 2008.

[Hor01] Richard Paul Horja. Derived category automorphisms from mirror symmetry. *Duke Mathematical Journal*, 127:1–34, 2001.

[HS12] Amihay Hanany and Rak-Kyeong Seong. Brane Tilings and Reflexive Polygons. *Fortsch. Phys.*, 60, 2012.

[HV07] Amihay Hanany and David Vegh. Quivers, tilings, branes and rhombi. *JHEP*, 10:029, 2007.

[IKV09] Amer Iqbal, Kan Kozçaz, and Cumrun Vafa. The refined topological vertex. *JHEP*, 10, 2009.

[IU09] Akira Ishii and Kazushi Ueda. Dimer models and the special mckay correspondence. *arXiv: Algebraic Geometry*, 2009.

[IU16] Akira Ishii and Kazushi Ueda. Dimer models and crepant resolutions. *Hokkaido Mathematical Journal*, 45:1–42, 2016.

[Jia17] Yunfeng Jiang. The moduli space of stable coherent sheaves via non-archimedean geometry. *arXiv preprint*, 2017.

[Joy03] Dominic Joyce. Special lagrangian submanifolds with isolated conical singularities. v. survey and applications. *Journal of Differential Geometry*, 63:279–347, 2003.

[Joy13] D. Joyce. A classical model for derived critical loci. *arXiv: Algebraic Geometry*, 2013.

[Joy14] Dominic Joyce. Conjectures on bridgeland stability for fukaya categories of calabi-yau manifolds, special lagrangians, and lagrangian mean curvature flow. *arXiv: Differential Geometry*, 2:1–62, 2014.

[JS12] Dominic Joyce and Yinan Song. A theory of generalized Donaldson-Thomas invariants. *Memoirs of the Am. Math. Soc.*, 217(1020), 2012.

[JU21a] Dominic Joyce and Markus Upmeier. Canonical orientations for moduli spaces of g_2-instantons with gauge group su(m) or u(m). *Journal of Differential Geometry*, September 2021.

[JU21b] Dominic Joyce and Markus Upmeier. Orientation data for moduli spaces of coherent sheaves over calabi–yau 3-folds. *Advances in Mathematics*, 381:107627, 2021.

[J19] Joachim Jelisiejew and Lukasz Sienkiewicz. Białynicki-birula decomposition for reductive groups. *Journal de Mathématiques Pures et Appliquées*, 131:290–325, 2019.

[Kin94a] Alastair King. Moduli of representations of finite dimensional algebras. *The Quarterly Journal of Mathematics*, 45:515–530, 1994.

[Kin94b] Alastair D. King. Moduli of representations of finite-dimensional algebras. *Quart. J. Math. Oxford Ser. (2)*, 45(180):515–530, 1994.

[KKV99] Sheldon H. Katz, Albrecht Klemm, and Cumrun Vafa. M theory, topological strings and spinning black holes. *Adv. Theor. Math. Phys.*, 3:1445–1537, 1999.

[KLY15] Heeyeon Kim, Seung-Joo Lee, and Piljin Yi. Mutation, Witten Index, and Quiver Invariant. *JHEP*, 07:093, 2015.

[KO95] S A Kuleshov and D O Orlov. Exceptional sheaves on del pezzo surfaces. *Russian Academy of Sciences. Izvestiya Mathematics*, 44:479 – 513, 1995.

[Kon95] Maxim Kontsevich. Homological algebra of mirror symmetry. In S. D. Chatterji, editor, *Proceedings of the International Congress of Mathematicians*, pages 120–139, Basel, 1995. Birkhäuser Basel.

[KS] Maxim Kontsevich and Yan Soibelman. Stability structures, motivic Donaldson-Thomas invariants and cluster transformations.

[KS06] Maxim Kontsevich and Yan Soibelman. Affine structures and non-archimedean analytic spaces. In *The unity of mathematics*, pages 321–385. Springer, 2006.

[KS10] M. Kontsevich and Y. Soibelman. Cohomological Hall algebra, exponential Hodge structures and motivic Donaldson-Thomas invariants. *arXiv: Algebraic Geometry*, 2010.

[KS13] Maxim Kontsevich and Yan Soibelman. Wall-crossing structures in Donaldson-Thomas invariants, integrable systems and Mirror Symmetry, 2013.

[KZ01] Albrecht Klemm and Eric Zaslow. Local mirror symmetry at higher genus. *AMS/IP Stud. Adv. Math.*, 23:183–207, 2001.

[Law89] Gary Reid Lawlor. The angle criterion. *Inventiones mathematicae*, 95:437–446, 1989.

[Li18] Chunyi Li. On stability conditions for the quintic threefold. *Inventiones mathematicae*, pages 1–40, 2018.

[Li22] Yang Li. Thomas-yau conjecture and holomorphic curves, 03 2022.

[LWY12] Seung-Joo Lee, Zhao-Long Wang, and Piljin Yi. Quiver Invariants from Intrinsic Higgs States. *JHEP*, 1207:169, 2012.

[LWY14] Seung-Joo Lee, Zhao-Long Wang, and Piljin Yi. Abelianization of BPS Quivers and the Refined Higgs Index. *JHEP*, 02:047, 2014.

[LZ19] Chunyi Li and Xiaolei Zhao. Birational models of moduli spaces of coherent sheaves on the projective plane. *Geometry & Topology*, 23(1):347–426, 2019.

[Mac07] Emanuele Macri. Stability conditions on curves. 2007.

[Mac12] Emanuele Macrì. A generalized bogomolov–gieseker inequality for the three-dimensional projective space. *Algebra & Number Theory*, 8:173–190, 2012.

[Mac14] Antony Maciocia. Computing the walls associated to Bridgeland stability conditions on projective surfaces. *Asian Journal of Mathematics*, 18(2):263–280, 2014.

[Mai11] Mario Maican. On the moduli spaces of semi-stable plane sheaves of dimension one and multiplicity five. *Illinois Journal of Mathematics*, 55(4):1467–1532, 2011.

[Mai13] Mario Maican. The classification of semistable plane sheaves supported on sextic curves. *Kyoto Journal of Mathematics*, 53(4):739–786, 2013.

[Man11a] Jan Manschot. The Betti numbers of the moduli space of stable sheaves of rank 3 on $\mathbb{P}^2$. *Lett.Math.Phys.*, 98:65–78, 2011.

[Man11b] Jan Manschot. Wall-crossing of D4-branes using flow trees. *Adv.Theor.Math.Phys.*, 15:1–42, 2011.

[Man17] Jan Manschot. Sheaves on $\mathbb{P}^2$ and generalized Appell functions. *Adv. Theor. Math. Phys.*, 21:655–681, 2017.

[Mas01] David B. Massey. The sebastiani–thom isomorphism in the derived category. *Compositio Mathematica*, 125, 2001.

[Mas16] David B. Massey. Natural commuting of vanishing cycles and the verdier dual. *Pacific Journal of Mathematics*, 284:431–437, 2016.

[MMNS12] Andrew Morrison, Sergey Mozgovoy, Kentaro Nagao, and Balazs Szendroi. Motivic Donaldson-Thomas invariants of the conifold and the refined topological vertex. *Advances in Mathematics*, 230, 2012.

[MN15] Andrew Morrison and Kentaro Nagao. Motivic Donaldson-Thomas invariants of toric small crepant resolutions. *Algebra and Number Theory*, 9, 2015.

[Mor12] Andrew Morrison. Motivic invariants of quivers via dimensional reduction. *Selecta Mathematica*, 18, 2012.

[Mou19] Lang Mou. Scattering diagrams of quivers with potentials and mutations. *arXiv: Representation Theory*, 2019.

[Moz09] Sergey Mozgovoy. Crepant resolutions and brane tilings I: Toric realization. 8 2009.

[Moz11] Sergey Mozgovoy. Motivic Donaldson-Thomas invariants and McKay correspondence. 7 2011.

[Moz13] Sergey Mozgovoy. Wall-crossing formulas for framed objects. *Quart. J. Math.*, 64:489–513, 2013.

[Moz21] Sergey Mozgovoy. Operadic approach to wall-crossing. 1 2021.

[Moz22] Sergey Mozgovoy. Wall-crossing structures on surfaces. 2022.

[MP20] S. Mozgovoy and B. Pioline. Attractor invariants, brane tilings and crystals. 2020.

[MPS] Jan Manschot, Boris Pioline, and Ashoke Sen. unpublished.

[MPS11a] Jan Manschot, Boris Pioline, and Ashoke Sen. A Fixed point formula for the index of multi-centered N=2 black holes. *JHEP*, 1105:057, 2011.

[MPS11b] Jan Manschot, Boris Pioline, and Ashoke Sen. Wall Crossing from Boltzmann Black Hole Halos. *JHEP*, 1107:059, 2011.

[MPS12] Jan Manschot, Boris Pioline, and Ashoke Sen. From Black Holes to Quivers. *JHEP*, 11:023, 2012.

[MPS13] Jan Manschot, Boris Pioline, and Ashoke Sen. On the Coulomb and Higgs branch formulae for multi-centered black holes and quiver invariants. *JHEP*, 05:166, 2013.

[MPS17] Jan Manschot, Boris Pioline, and Ashoke Sen. The Coulomb Branch Formula for Quiver Moduli Spaces. *Confluentes Mathematici*, 2:49–69, 2017.

[MR08] Sergey Mozgovoy and Markus Reineke. On the noncommutative Donaldson-Thomas invariants arising from brane tilings. *Adv. Math.*, 223(5):1521–1544, 9 2008.

[MR21] Sergey Mozgovoy and Markus Reineke. Donaldson-Thomas invariants for 3-Calabi-Yau varieties of dihedral quotient type. 2021.

[MS20] Davesh Maulik and Junliang Shen. Cohomological χ-independence for moduli of one-dimensional sheaves and moduli of Higgs bundles. 2020.

[MVdB20] I. Messamah and D. Van den Bleeken. Pure-Higgs states from the Lefschetz-Sommese theorem. *JHEP*, 11:161, 2020.

[Nag11] Kentaro Nagao. Non-commutative Donaldson–Thomas theory and vertex operators. *Geometry and Topology*, 15, 2011.

[Nak16] Hiraku Nakajima. Lectures on perverse sheaves on instanton moduli spaces. *arXiv: Representation Theory*, 2016.

[NO16] Nikita Nekrasov and Andrei Okounkov. Membranes and Sheaves. *Algebraic Geometry*, 3, 2016.

[NYY14] Takahiro Nishinaka, Satoshi Yamaguchi, and Yutaka Yoshida. Two-dimensional crystal melting and D4-D2-D0 on toric Calabi-Yau singularities. *JHEP*, 05, 2014.

[Per08] Markus Perling. Exceptional sequences of invertible sheaves on rational surfaces. *Compositio Mathematica*, 147:1230 – 1280, 2008.

[Pio06] Boris Pioline. Lectures on black holes, topological strings and quantum attractors. *Classical and Quantum Gravity*, 23:S981 – S1045, 2006.

[PTVV13] T. Pantev, B. Toën, M. Vaquié, and G. Vezzosi. Shifted Symplectic Structures. *Publ.math.IHES*, 117, 2013.

[PYK21] Pierre-Guy Plamondon, Toshiya Yurikusa, and Bernhard Keller. Tame algebras have dense g-vector fans. *International Mathematics Research Notices*, 2021.

[Ric16] Timo Richarz. Spaces with G_m-action, hyperbolic localization and nearby cycles. *arXiv: Algebraic Geometry*, 2016.

[RSYZ19] Miroslav Rapcak, Yan Soibelman, Yaping Yang, and Gufang Zhao. Cohomological Hall algebras, vertex algebras and instantons. *Commun. Math. Phys.*, 376, 2019.

[S+74] Hideyasu Sumihiro et al. Equivariant completion. *Journal of Mathematics of Kyoto University*, 14(1):1–28, 1974.

[ST00] Paul Seidel and Richard P. Thomas. Braid group actions on derived categories of coherent sheaves. *Duke Mathematical Journal*, 108:37–108, 2000.

[STV11] Timo Schürg, Bertrand Toën, and Gabriele Vezzosi. Derived algebraic geometry, determinants of perfect complexes, and applications to obstruction theories for maps and complexes. *Journal für die reine und angewandte Mathematik (Crelles Journal)*, 2015, 02 2011.

[SW94] N. Seiberg and Edward Witten. Electric - magnetic duality, monopole condensation, and confinement in N=2 supersymmetric Yang-Mills theory. *Nucl. Phys. B*, 426:19–52, 1994. [Erratum: Nucl.Phys.B 430, 485–486 (1994)].

[Sze01] Balázs Szendrői. Diffeomorphisms and families of fourier-mukai transforms in mirror symmetry. *arXiv: Algebraic Geometry*, pages 317–337, 2001.

[Sze15] Balazs Szendroi. Cohomological Donaldson-Thomas theory. 3 2015.

[Tho98] Richard P Thomas. A holomorphic Casson invariant for Calabi-Yau 3-folds, and bundles on K3 fibrations. *J. Differential Geom.*, (54):367–438, 1998.

[Tod18] Yukinobu Toda. Moduli stacks of semistable sheaves and representations of Ext-quivers. *Geometry & Topology*, 22:3083–3144, 2018.

[Toë14] Bertrand Toën. Derived algebraic geometry. 2014.

[TV05] Bertrand Toen and Michel Vaquié. Moduli of objects in dg-categories. *Annales Scientifiques De L Ecole Normale Superieure*, 40:387–444, 2005.

[TY01] Richard P. Thomas and Shing-Tung Yau. Special lagrangians, stable bundles and mean curvature flow. *Communications in Analysis and Geometry*, 10:1075–1113, 2001.

[VdB04] Michel Van den Bergh. Non-commutative crepant resolutions. In *The legacy of Niels Henrik Abel*, pages 749–770. Springer, Berlin, 2004.

[VHW10] Walter Van Herck and Thomas Wyder. Black Hole Meiosis. *JHEP*, 04:047, 2010.

[Wit82] Edward Witten. Supersymmetry and morse theory. *Journal of Differential Geometry*, 17:661–692, 1982.

[Woo13] Matthew Woolf. Nef and effective cones on the moduli space of torsion sheaves on the projective plane. 2013.

[xHKK20] Min xin Huang, Sheldon Katz, and Albrecht Klemm. Towards refining the topological strings on compact calabi-yau 3-folds. *Journal of High Energy Physics*, 2021:1–89, 2020.

[Yos94] Kota Yoshioka. The Betti numbers of the moduli space of stable sheaves of rank 2 on $\mathbb{P}^2$. *J. Reine Angew. Math*, 453:193–220, 1994.

[Zhu95] Yongchang Zhu. Modular invariance of characters of vertex operator algebras. *Journal of the American Mathematical Society*, 9:237–302, 1995.